

Environmentally Benign Synthetic Routes to Fused Heterocycles and Their Photophysical Studies

THESIS SUBMITTED FOR
THE DEGREE OF DOCTOR OF PHILOSOPHY (SCIENCE)
OF
JADAVPUR UNIVERSITY
JUNE, 2023



By

ANIRBAN BERA

INDEX NO.- 235/18/Chem./26

DEPARTMENT OF CHEMISTRY

JADAVPUR UNIVERSITY,

KOLKATA-700032, WEST BENGAL, INDIA

Dr. Amit Saha

Assistant Professor
Organic Chemistry Section
Department of Chemistry
Jadavpur University
Telephones: 033-24572981, 91-9433950204
Email: amit.saha@jadavpuruniversity.in

Dr. Shubhankar Samanta

Assistant Professor
Department of Chemistry
Bidhannagar College
Telephone: 91-9775550193
Fax: (9133) 2337 4782
Email: chemshubha@gmail.com

TO WHOM IT MAY CONCERN

This is to certify that the thesis entitled “*Environmentally benign synthetic routes to fused heterocycles and their photophysical studies*”, submitted by **Mr. Anirban Bera** who got his name registered on 12-10-2018 (**Index No.- 235/18/Chem./26**) for the award of Ph.D. (Science) degree, Jadavpur University, is absolutely based upon his own research work under our supervision and that neither this thesis nor any part of it has been submitted for either any degree or diploma or other academic award anywhere else before.

Research Supervisor (s)

Amit Saha
28.06.2023

Dr. Amit Saha

Supervisor

Dr. Amit Saha
Assistant Professor
Department of Chemistry
Jadavpur University
Kolkata-700032, India



Shubhankar Samanta
28/06/2023

Dr. Shubhankar Samanta

Joint-Supervisor

Dr. Shubhankar Samanta
Assistant Professor (WBES)
Department of Chemistry
Bidhannagar College
Salt Lake, Kol-64

*I would like to dedicate my thesis to Lord
Krishna and my beloved parents,*

Prasanta Kumar Bera

&

Manika Bera



FATHER OF GREEN CHEMISTRY

“Green chemistry is not about sacrifice. The new products of green chemistry not only perform as well, they almost always perform better than the incumbent technologies.”

- Paul Anastas



Acknowledgement

The complete thesis is not the result of one's effort but the cumulative outcome of a group of people. The direct and indirect contributions of these people make it possible to shape this great task.

I am fortunate enough to express my respectful regards and gratitude to my supervisors, Dr. Shubhankar Samanta and Dr. Amit Saha, for associating me with their research group. This work can't be shaped without their proper guidance and encouragement. I am highly grateful to them for their valuable suggestions and inspiring criticism throughout the course.

I am very grateful to all other faculty members of the Department of Chemistry, Jadavpur University, and the Department of Chemistry, Bidhannagar College, especially Dr. Madhumita Manna (ADPI, Govt. of West Bengal) and Dr. Saurabh Chakraborti (Principal, Bidhannagar College). I am expressing my gratitude to all the non-teaching staff and librarians of both institutions. I am very thankful to the NMR operator and all other technical staff of the Department of Chemistry, Jadavpur University, for providing spectral data.

I am grateful to Professor Subrata Nath Koner (HOD, Department of Chemistry, JU), Professor Chittaranjan Sinha (Department of Chemistry, JU), Prof. Subhash Chandra Bhattacharyya (Department of Chemistry, JU), Prof. Swapan Kumar Bhattacharya (Department of Chemistry, JU), and Dr. Ranjan Jana (Senior Principal Scientist, Organic and Medicinal Chemistry Division, CSIR-IICB) for their cooperation in various official works during these years.

I am very thankful to Dr. M. A. Mondal, Dr. S. Guha, Dr. U. C. Halder, Dr. A. Thakur, Dr. G. Maity, Dr. S. Bhar, Dr. U. Jana, Dr. T. Bhaumik, Dr. M. A. Mondal, and Prof. R. Ghosh for their kind help during my research work.

Special gratitude is offered to Prof. Saumen Kumar Mahapatra for his remarkable inspiration to bring me into the research field and for his constant support in my research career.

I am heartily thankful to Dr. Mijanur Rahaman Molla (Assistant Professor, University of Calcutta), Sourav Roy, Dr. Akash Jana, Subhra Kanti Bhoumik, Dr. Debabrata Maiti, Dr. Jayanta Samanta, and Sourav Dutta for providing an NMR facility and crystallographic data.

I am fortunate enough to get the support and fabulous company of my lab mates, especially Dr. Asraf Ali, Paritosh Barik, Sk. Abul Kalam Azad, Samim Sahaji, Sayan Bhadra, Chandan Kumar Pal, Soumitra Sau, Dr. Soumya Dutta, Mr. Manas Mondal, Mr. Debabrata Patra, Sourav Mondal, Dr. Susanta Kumar Manna, Dr. Arabinda Mondal, Dr. Arup Kumar Adak, Dr. Suresh Kumar Mondal, Sudipta Mondal, Pradip Shit, Murshed Ali, Arun, Soumya, Kasturi, Payel, and Sulogna.

I am thankful to Mrs. Nivedita Bera Samanta, Rajasmita Samanta, Anandita Samanta, Trishita Bera, and Ganga Rani Bera for their constant support and unconditional love and affection.

I would like to express my thanks to all the security guards at Bidhannagar College, especially Sumanta da and Rabin da for their kind cooperation.

The cooperation and friendly behaviour of my family members (mother, father, uncle, aunt, and sister) and relatives make my journey easy.

The journey wouldn't be easy without the help of my friends and colleagues, Rabi Sankar Das, Sudip Biswas, Soumya Chakraborty, Mr. Jagannath Koley, Mr. Asit Bhaumik, and Mr. Debanjan Gupta.

28th June, 2023

Anirban Bera

Anirban Bera

Department of Chemistry

Jadavpur University

188, Raja S. C. Mallick Road,

Jadavpur, Kolkata-700032

Preface

The research embodied in the present thesis, entitled “*Environmentally benign synthetic routes to fused heterocycles and their photophysical studies,*” was initiated in the period July, 2018 to June, 2023 under the joint supervision of **Dr. Amit Saha**, Assistant Professor, Organic Chemistry Section, Department of Chemistry, Jadavpur University, Kolkata-700032, India and **Dr. Shubhankar Samanta**, Assistant Professor, Department of Chemistry, Bidhannagar College, Saltlake, Sector 1, Kolkata-700064, India.

The prime focus of this research work is to explore the environmentally benign synthetic protocols of *N*-fused heterocycles and their application to photophysical studies. This thesis has been presented in six chapters:

Chapter 1 describes the origin of green chemistry, the requirements of green techniques for organic syntheses, a brief description of numerous bioactive natural products, their wide application in drug molecules, fluorescence probes, the dye industry, and the material science of fused quinazolinones, isothiazoles, pyrroles, pyrrolo lactam rings, and pyrroloquinoline moieties.

Chapter 2 explains all the chemicals and solvents utilised and the instrumental details required to complete the entire research work.

Chapter 3 describes “*A solvent- and catalyst-free tandem reaction: synthesis, and photophysical and biological applications of isoindoloquinazolinones*”.

Chapter 4 depicts “*Neat synthesis of isothiazole compounds, studies on their synthetic applications, and photophysical properties*”.

Chapter 5 deals with the “*Neat synthesis of c-fused pyrroles and its application to macrolactamization*”.

Chapter 6 elaborately describes “*Synthesis of multi-fused pyrrolo[1,2-a]quinoline systems by tandem aza-Michael-aldol reactions and their application to molecular sensing studies*”.

Anirban Bera
Anirban Bera

Abstract

Heterocyclic molecules are highly significant as they possess biological, pharmacological, and industrial applications. Even though a number of excellent synthetic pathways for heterocyclic compounds have been identified, further research is needed on greener synthesis techniques such as microwave, grinding, ultrasonic, photochemical, and conventional heating route maps. Furthermore, these techniques become more eco-compatible when they generate value-added products without the use of solvents. Herein, we have disclosed some synthetic routes for heterocycles, which have not only bioactive scaffolds but also photophysical applications. In their summarized form, these are listed chronologically.

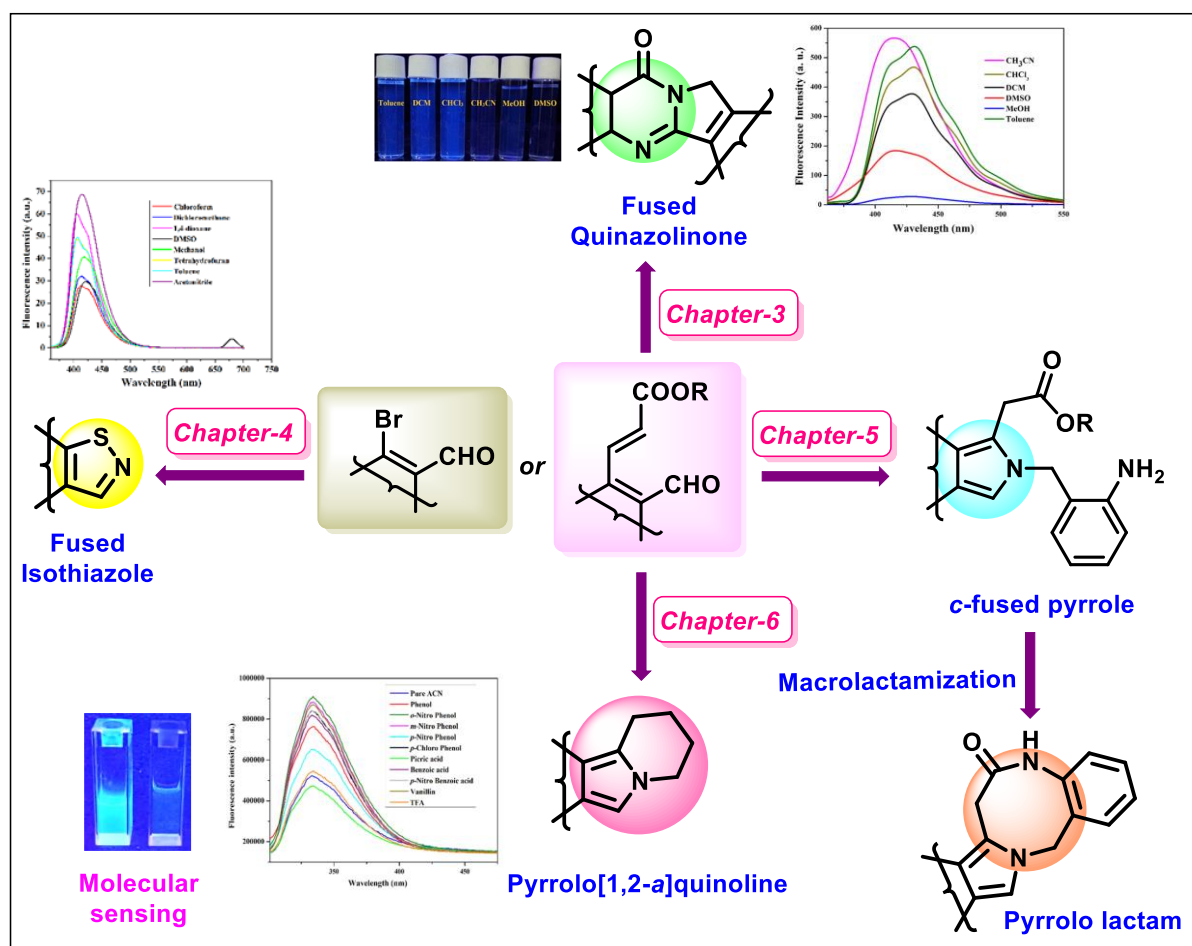
An easy green synthetic approach for fused isoindoloquinazolinones has been developed under neat reaction (yields up to 91%) condition. This new one-pot tandem methodology involves condensation of readily available anthranilamide with 3-(2-formylcycloalkenyl)-acrylic ester under solvent- and catalyst-free condition. This strategy avoids the use of oxidant, heavy metal catalyst and also free from work-up and generation of toxic by-products. A dramatic change of photophysical properties of dihydroisoindoloquinazolinones in basic and aqueous medium have also been documented in our study. Moreover, our model synthetic compound shows cytotoxic activity towards metastatic HepG2 and PC3 cancer cell lines.

Ammonium thiocyanate promoted simple, rapid and eco-friendly neat synthesis of isothiazoles has been developed for the first time. It is noteworthy that an instantaneous valuable synthetic route of β -enaminones has also been documented during the mechanistic investigation of isothiazole formation. Detail mechanistic explanation of isothiazole formation reaction is clearly explained by the control experiments. NBS promoted aromatisation of isothiazole derivatives and photophysical properties of an isothiazole-pyrene hybrid molecule have been investigated.

The current study describes an efficient environmental benign synthetic route of *N*-aryl substituted *c*-fused pyrrole derivatives *via* neat approach. It also provides base mediated intramolecular macrolactamization using amine ester amidation reaction and lead to fused diazocin-6(5*H*)-one with effective yields.

We have presented a weak acid promoted tandem aza-Michael-aldol strategy for the synthesis of diversely fused pyrrolo[1,2-*a*]quinoline (tricyclic to pentacyclic scaffolds) by the

construction of both pyrrole as well as quinoline ring in one-pot. The described protocol fabricated two C-N bonds and one C-C bond in the pyrrole-quinoline rings which have been sequentially formed under transition-metal-free conditions by the extrusion of eco-friendly water molecules. Ketorolac drug analogue has been synthesized following the current protocol and one of the synthesized tricyclic pyrrolo[1,2-*a*]quinoline fluorophore has been used to detect the highly toxic picric acid *via* fluorescent quenching effect.



Overall graphical abstract of my entire thesis.

Amit Saha
28.06.2023

Dr. Amit Saha
Supervisor

Shubhankar Samanta
28/06/2023

Dr. Shubhankar Samanta
Joint-Supervisor

Anirban Bera
28.06.2023

Signature of the Candidate

Dr. Amit Saha
Assistant Professor
Department of Chemistry
Jadavpur University
Kolkata-700032, India



Dr. Shubhankar Samanta
Assistant Professor (WBES)
Department of Chemistry
Bidhannagar College
Salt Lake, Kol-64

Contents

	Page No.
Title	I
Certificate from the supervisor (s)	II
Dedication	III
Acknowledgement	IV-VI
Preface	VII
Abstract	VIII-IX
Contents	X-XII
Abbreviations	XIII-XV
Chapter 1: General Introduction	1-39
1.1. Origins of Green Chemistry	1-6
1.2. Importance of heterocycles in daily life	6-7
1.3. Limitations of conventional approaches for the synthesis of bioactive <i>N</i> -fused heterocycles	7-12
1.4. Quinazolinone	13-19
1.5. Isothiazole	19-22
1.6. Fused Pyrroles and their family	22-29
1.7. Lactam ring	29-30
1.8. Pyrroloquinoline	31-33
1.9. Conclusion	34
1.10. References	35-39
Chapter 2: Methodologies and Materials	40-43
2.1. Chemicals and solvents	40-41
2.2. Methodologies	42-43

Chapter 3: A solvent- and catalyst-free tandem reaction: synthesis, and photophysical and biological applications of isoindoloquinazolinone	44-98
3.1. Introduction	45-49
3.2. Literature survey	50-62
3.3. Present work	63
3.4. Results & discussion	63-72
3.5. Conclusion	72
3.6. Experimental section	73-95
3.7. References	96-98
Chapter 4: Neat synthesis of isothiazole compounds, studies on their synthetic applications and photophysical properties	99-150
4.1. Introduction	100-103
4.2. Literature survey	103-110
4.3. Present work	110-111
4.4. Results and discussion	111-125
4.5. Conclusion	125
4.6. Experimental section	126-147
4.7. References	148-150
Chapter 5: Neat synthesis of <i>c</i>-fused pyrroles and its application to macrolactamization	151-198
5.1. Introduction	152-157
5.2. Literature survey	158-168
5.3. Present work	169
5.4. Results and discussion	169-173
5.5. Conclusion	174
5.6. Experimental section	174-195
5.7. References	196-198

Chapter 6: Synthesis of multi-fused pyrrolo[1,2-*a*]quinoline systems by tandem aza-Michael-aldol reactions and their application to molecular sensing studies 199-283

6.1.	Introduction	200-204
6.2.	Literature survey	205-216
6.3.	Present work	216-217
6.4.	Results and discussion	217-235
6.5.	Conclusion	235
6.6.	Experimental section	236-280
6.7.	References	281-283
Annexure I	List of Publications	284-285
Annexure II	Reprint of published papers	286-331
Annexure III	Copyright permission from Journals	332-334
Annexure IV	Presentation/Participation in International/National Symposium/Conferences	335-337

Abbreviations

Aq.	Aqueous
Ar	Aryl
AcOH	Acetic Acid
Bu ₃ SnH	Tertiary butyl tin hydride
°C	Degree centigrade
CDCl ₃	Deuteriated chloroform
DCM	Dichloromethane
dd	doublet of doublet
DMF	<i>N, N</i> -Dimethylformamide
DMSO	Dimethyl sulphoxide
DMSO- <i>d</i> ⁶	Deuteriated dimethyl sulphoxide
Equiv	Equivalent
Et	Ethyl
Et ₃ N	Triethylamine
EWG	Electron withdrawing group
hr / h	Hour (s)
HRMS	High Resolution Mass Spectroscopy
<i>i</i> PrOH	Isopropyl alcohol
<i>J</i>	Coupling constant
Me	Methyl
MHz	Megahertz
MDR	Multidrug resistant
mp.	Melting Point
Min	Minute
MS	Mass Spectroscopy
mmol	Milimole
<i>m</i>	meta
mL	Mililitre
MTT	3-(4,5-dimethylthiazol-2-yl) -2,5- diphenyltetrazolium bromide
MeOH	Methanol

M	Molar
mmol	Milimole
M ⁺	Molecular ion
MCPBA	meta chloro per benzoic acid
Na ₂ CO ₃	Sodium carbonate
Na ₂ HCO ₃	Sodium hydrogen carbonate
NBS	<i>N</i> -bromo succinamide
NMR	Nuclear Magnetic Resonance
NH ₂ -NH ₂ .H ₂ O	Hydrazine hydrated
<i>o</i>	ortho
OEt	Ethoxy
OMe	Methoxy
OLEDs	Organic light emitting diodes
ORTEP	Oak Ridge Thermal Ellipsoid Plot
<i>p</i>	para
PA	Picric Acid
PC	Photocatalyst
Pd	Palladium
Ph	Phenyl
Pd(OAc) ₂	Palladium(II) acetate
PBr ₃	Phosphorous tribromide
PPh ₃	Triphenyl phosphine
PE	Petroleum ether
PdCl ₂	Palladium chloride
<i>p</i> -TSOH	Para tolyl sulphonic acid
rt /RT	Room Temperature
RNA	Ribo Nuclic Acid
SOCl ₂	Thionil chloride
TLC	Thin Layer Chromatography
TBAB	Tetrabutylammonium bromide
TFA	Trifloro acetic acid
THF	Tetrahydrofuran
^t Bu	Tertiary butoxy
^t BuOK	Potassium tertiarybutoxide

UV

Ultra violet

VIS

Visible

μg

Microgram

μL

Microliter

λ_{max}

Absorption maximum

Chapter 1
General Introduction

1.1. Origins of Green Chemistry:

Everything we see, touch, and feel is a gift of chemistry. Chemistry brought about a revolution in human civilization up until roughly the middle of the 20th century. In this century, a multitude of potentially life-saving drug molecules, antibiotics, and pharmaceuticals came to light. The production of food and supply also rose significantly across the world as a result of the invention of hybrid varieties, novel farming methods, superior seeds, and the application of fertilizers, pesticides, and herbicides. According to the demands of modern civilization, the research community always continues their research in various types of chemical and pharmaceutical industries. As soon as chemistry became more advanced, its negative repercussions became apparent. Consequently, environmental pollution has escalated into a serious problem for our world. As a result, both aquatic and terrestrial life become damaged (**Figure 1.1**). Nowadays, people are very concerned about both their health and the environment. With a deep concern for the environment, chemists are introducing a new concept, “green chemistry”.¹

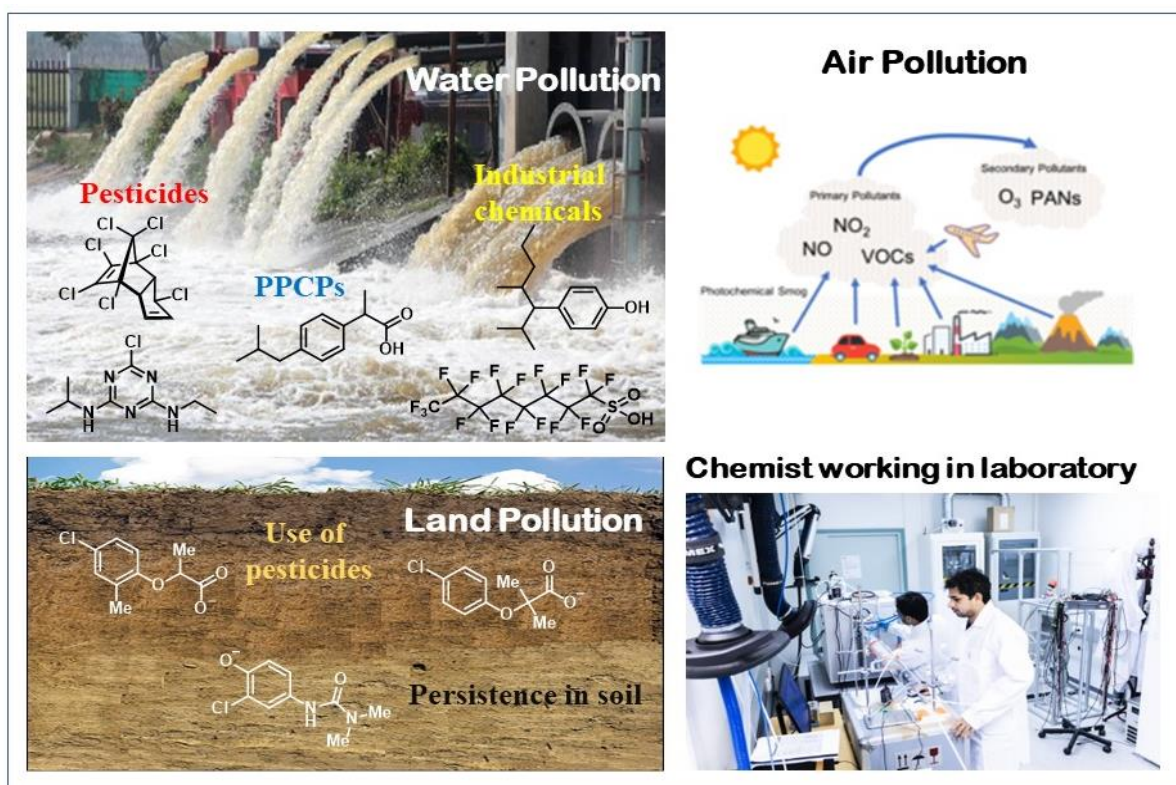


Figure 1.1. Advanced Chemistry: a big cause of environmental pollution.

1.1.1. Introducing a concept about green chemistry:

The initial development of the concept of "*green chemistry*" was sparked by the Pollution Prevention Act (1990), which mandated that U.S. national policy. Although the U.S. Environmental Protection Agency (EPA) is recognised for being a monitoring body, it departed from the "command and control" or "end of pipe" strategy when putting into place what would later be known as its "*green chemistry*" programme.

In 1991, a research grant was launched by the EPA's Office of Pollution Prevention and Toxics for redesigning the existing chemicals and procedures to lessen the adverse impacts on both human health and the environment. Earlier in the 1990s, the EPA continued to sponsor fundamental green chemistry research in collaboration with the American National Science Foundation (NSF).

Success stories in both academic and industrial green chemistry were brought to light in 1996 with the inaugural edition of the annual Presidential Green Chemistry Challenge Awards. The awards programme is the cornerstone of the educational curriculum in green chemistry.

In the mid-to-late 1990s, there was a rise in the number of international conferences on green chemistry, such as the Gordon Research Conferences, and green chemistry networks emerged in the United Kingdom, the United States, Italy, and Spain.

In 1998, after the publication of the 12 Principles of Green Chemistry, the emerging science received a precise set of criteria for future advancement. The Royal Society of Chemistry introduced a journal, "*Green Chemistry*", in 1999 to promote the green approach in the research field.

In the last decade, there have been an increasing number of national networks, prestigious journals have published special issues focused on green chemistry, and the popularity of the field has grown. In 2005, Chauvin, Grubbs, and Schrock were awarded the Nobel Prize in Chemistry for their commendable research work, which is convincing evidence of "a great step forward for green chemistry" (**Figure 1.2**).²

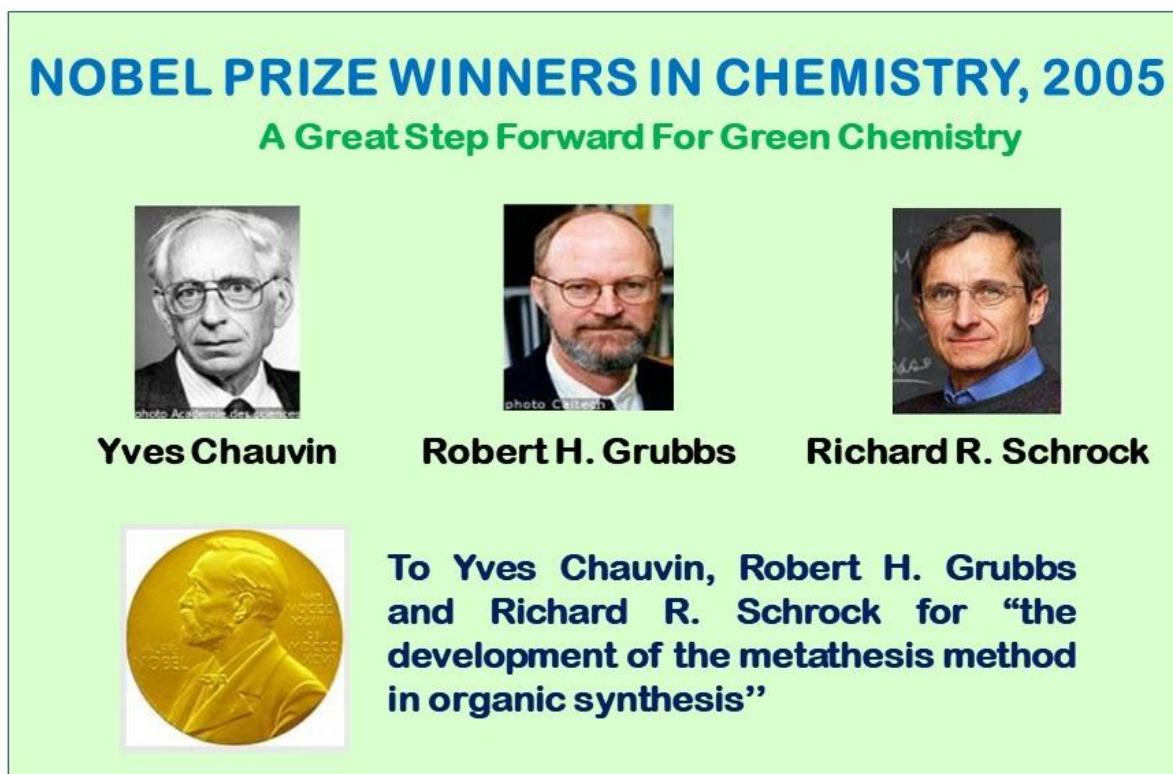


Figure 1.2. Nobel Prize winners in favour of Green Chemistry.

Green Chemistry is known as sustainable chemistry or clean chemistry. A question often arises how we can fulfil the demands of our society without disturbing our environment. It can only be possible by maintaining the green protocol everywhere. Utilization of environmentally benign solvents, renewable materials, and non-toxic chemicals are the main key factors in green synthesis. The 12 Principles about green synthesis are given below (**Figure 1.3**).³

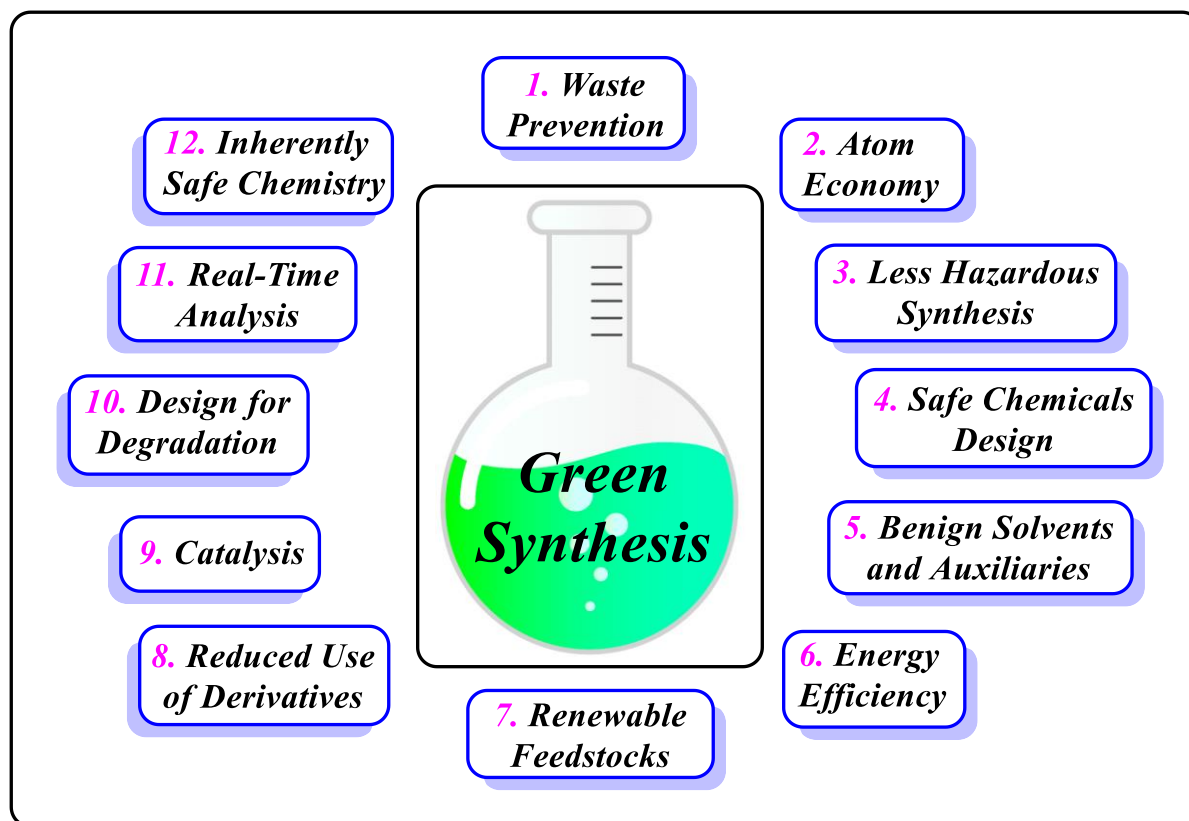


Figure 1.3. Twelve principles of Green Chemistry proposed by Paul Anastas.

1.1.2. A solvent selection guideline related to green synthesis:

Aristotle, an ancient Greek philosopher, stated, “*No Coopora nisi Fluida*”, which translates as “No reaction occurs in the absence of solvent”.⁴ It is remarkable statement and hence chemists execute their reactions in the solvent phase. But any suitable reason can’t be found behind this. Chemists use different classes of organic solvents to carry out their reactions. All the marketed organic solvents are not environmentally acceptable. Some of them are toxic and hazardous, and not acceptable for the environment as well as human health. For this purpose, a number of pharmaceutical companies have reported solvent selection guides; more recently, Fischer *et al.* elegantly describe a comprehensive approach to the environmental selection of solvents based on the environment, health, and safety issues (Figure 1.4).⁵

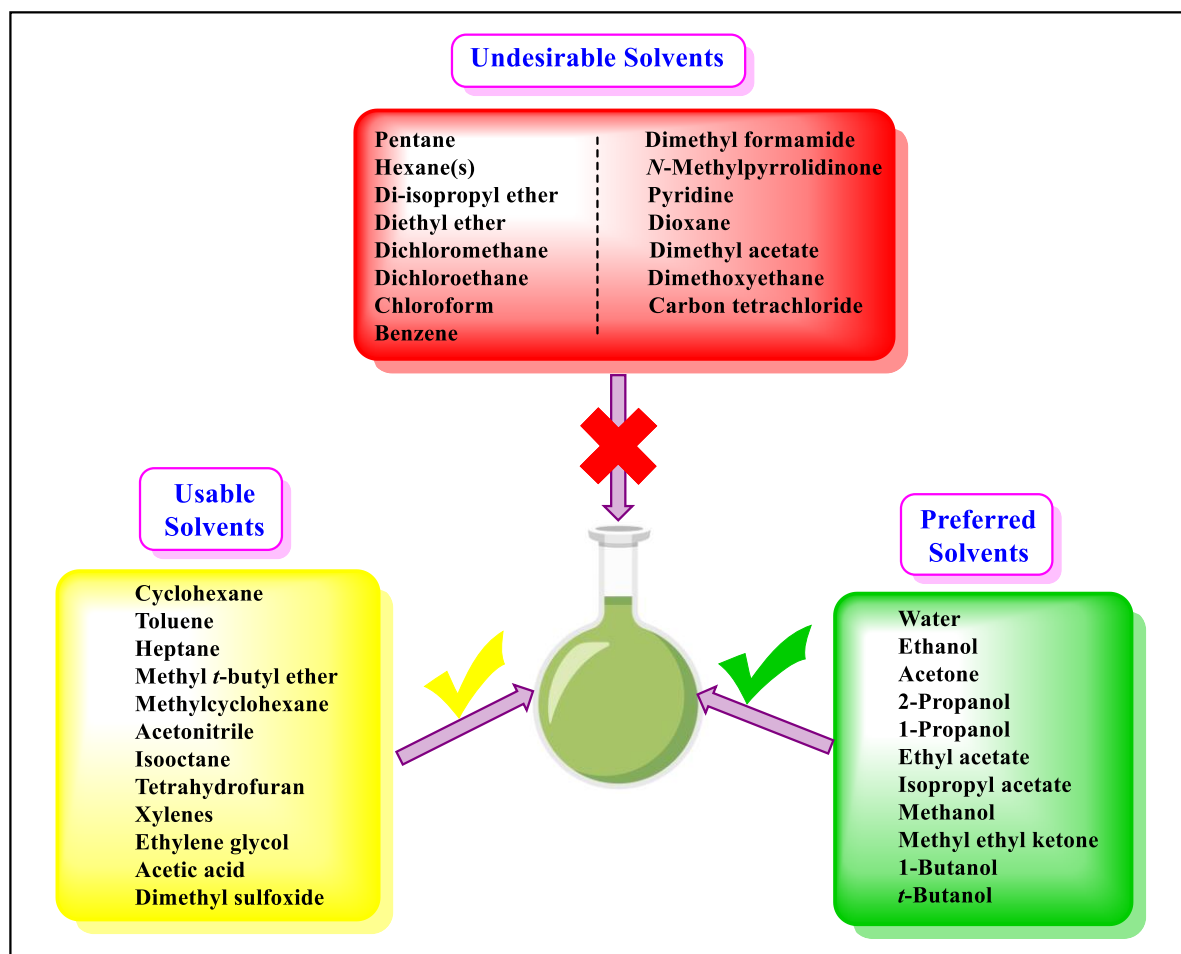


Figure 1.4. A table about solvent selection guideline.

Hexane, Benzene, Dimethyl Formamide (DMF), *N*-methyl pyrrolidinone (NMP), Pyridine etc. have been added to the "**red list**" in the industry due to their carcinogenicity, mutagenicity, nephrotoxicity, skin absorption/sensitization, and toxic properties. Pentane, Di-isopropyl ether, and Diethyl ether have high flammability, the potential for high emissions through high vapour pressure and static charge, the potential for peroxide formation, and odour issues; hence, they are also included in the "**red list**" of solvent safety categories. For environmental regulatory considerations such as ground water contamination, ozone depletion potential, and photo-reactive potential, the chlorinated solvents chloroform, dichloromethane, and carbon tetrachloride are also restricted. Toluene, acetonitrile, tetrahydrofuran, dimethyl sulfoxide, etc. are moderately usable. Water, methanol, ethanol, acetone, ethyl acetate, propanol, butanol, etc. are preferred solvents and acceptable for the environment. To fully meet the development of human civilization, researchers are always engaged in the synthesis of heterocyclic and carbocyclic molecules using different toxic organic solvents in various fields (pharmaceutical, biological, material, light-emitting, toxic

metal ion sensing, molecular sensing, etc.). Among them, pharmaceutical development flourishes more in heterocyclic molecules.

1.2. Importance of heterocycles in daily life:

More than 80 % commercially available life-saving drug molecules come from heterocycles, and the synthesis of these compounds directly involves the pharmaceutical industry. Heterocyclic compounds are generally five- or six-membered ring cycles and contain at least one or more heteroatoms such as nitrogen (*N*), oxygen (*O*), and sulphur (*S*). Heterocyclic compounds are found as the core moiety in several bio-active natural products, bio-molecules (DNA & RNA, hemoglobin, chlorophyll, and so on), amino acids (tryptophan, L-proline, histidine, and so on), and vitamins (vitamin B 12, vitamin C, folic acid, thiamine, riboflavin, and so on).⁶ Most of the bioactive compounds come from heterocycles, which are widely used as modifiers in photography, cosmetics, and information storage devices. The pharmaceutical and agrochemical industries are totally dependent on heterocyclic compounds. Due to the great abundance of fused heterocycles in everywhere, a new trend in synthetic organic chemistry research has been noticed globally.

Among them, *N*-fused heterocyclic frameworks such as fused quinazolinones, isothiazoles, pyrroles, pyrrolo lactam rings, and pyrroloquinoline moieties are the most celebrated organic molecules, which are all not abundant in nature but also found in non-naturally occurring compounds such as essential amino acids, vitamins, alkaloids, hormones, etc. All these nitrogen-containing heterocycles have a multitude of pharmacological activities, such as anticancer, antitumor, antifungal, antidiabetic, antiallergic, antiviral, antibacterial, anti-inflammatory, anti-HIV, and pain-killing properties (**Figure 1.5**).⁷

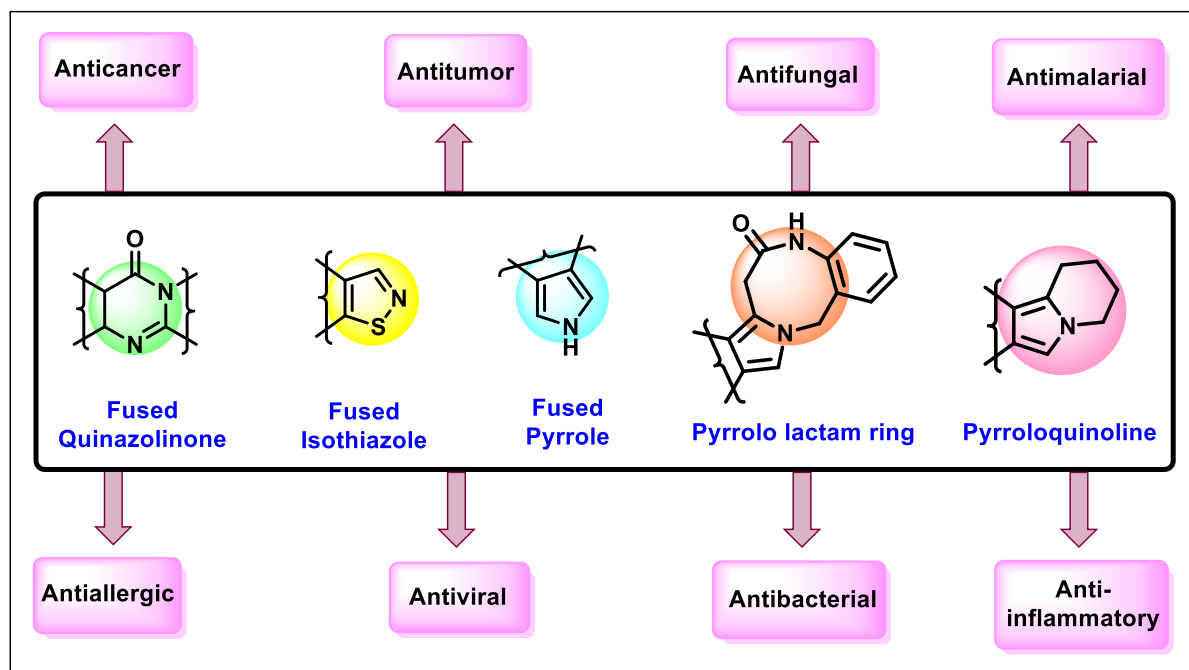
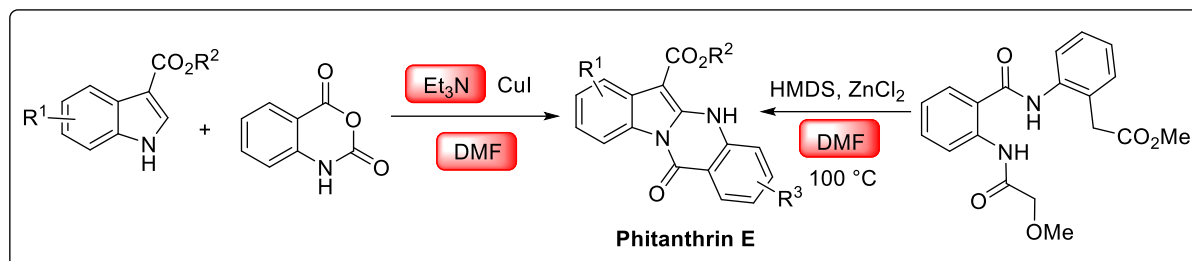


Figure 1.5. Several bioactive *N*-fused heterocycles.

We now turn our attention to a few *N*-fused alkaloids or bioactive molecules, such as Phaitanthrin E, Luotonin A, Ziprasidone, Ketorolac, and Crispine A, which contain fused quinazolinones, isothiazoles, pyrroles, pyrrolo lactam rings, and pyrroloquinoline moieties and were produced using conventional synthetic protocols.

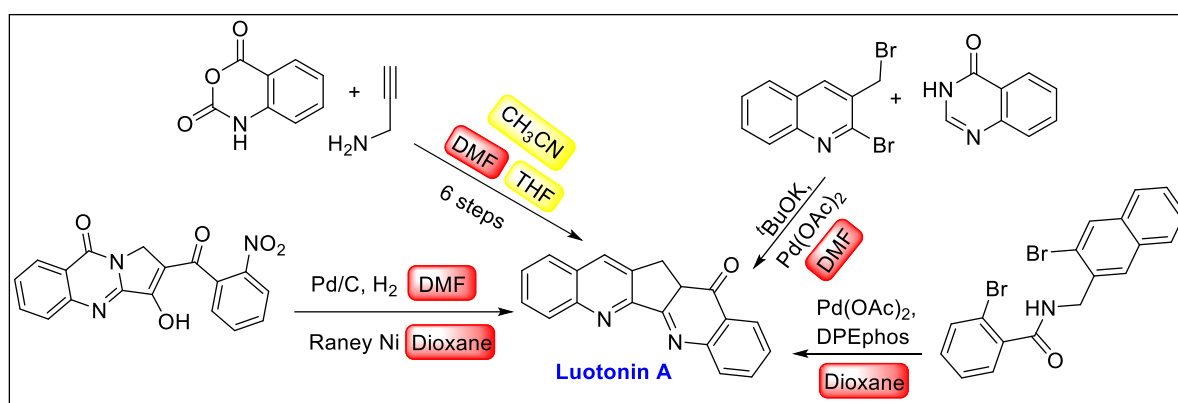
1.3. Limitations of conventional approaches for the synthesis of bioactive *N*-fused heterocycles:

Phaitanthrins E was isolated from the Taiwanese orchid *Phaius mishmensi* by Wu and co-workers. The synthesized derivatives of this natural alkaloid have antiproliferative effects against human colorectal cancer cells (DLD-1), and were found to have promising anticancer properties competitive with the natural Phaitanthrin E. Some synthetic protocols of Phaitanthrin E are presented in **Scheme 1.1**.⁸ Isoitic anhydride condenses with indole-3-carboxylate in presence of Cu (I) catalyst producing Phaitanthrin E. Another independent approach involves intramolecular dehydration of substrate followed by intramolecular nucleophilic addition and intramolecular substitution reactions in presence HMDS/ZnCl₂ furnished the alkaloid Phaitanthrin E (**Scheme 1.1**). However, all these cases red marked solvents are used to success the target and hence researchers are tried to develop solvent-free sustainable synthesis.



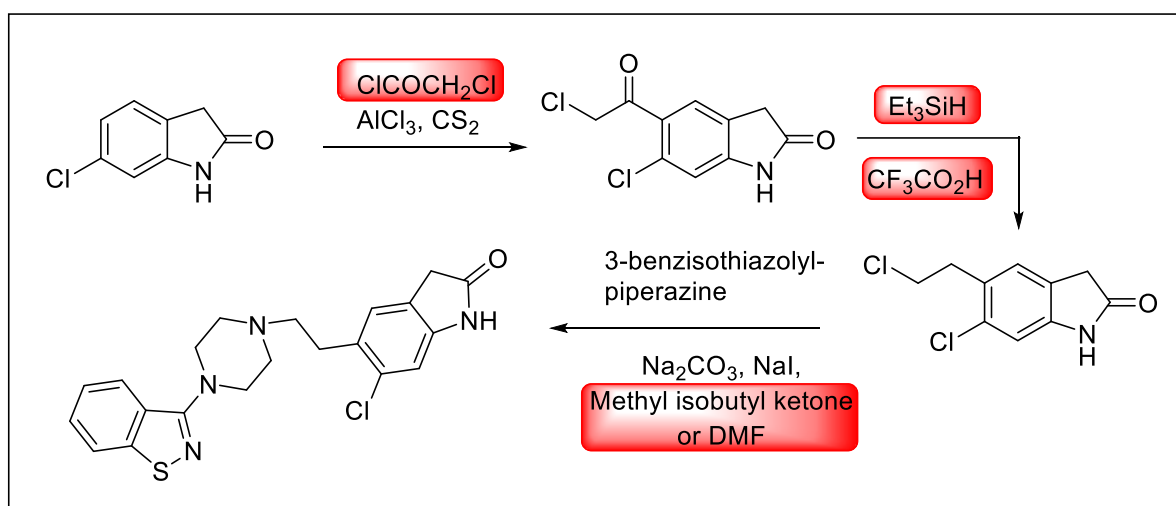
Scheme 1.1. Synthetic route of Phaitanthrin E.

Luotonins are quinazolinones fused alkaloids which display three major skeleton types, namely Luotonins A, B, and E which have shown bio-activity against leukemia P-388 cells. Luotonin A is the most effective one, with its activity stemming from topoisomerase I-dependent DNA-cleavage. Some of the synthetic processes are presented in **Scheme 1.2**.⁹ All these processes involved toxic solvents and synthetic chemist try to design new method to resolve pollutant issues.



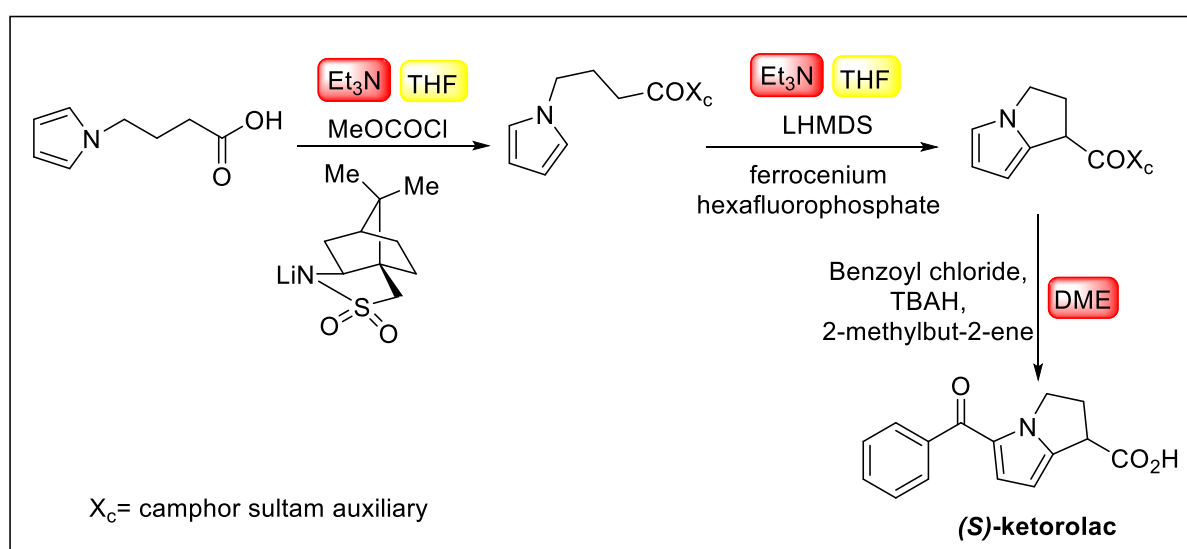
Scheme 1.2. Synthetic routes of Luotonin A.

Ziprasidone has been found to be an atypical antipsychotic potential agent. The outline for the synthetic route of benzisothiazolylpiperazine derivatives is mentioned here (**Scheme 1.3**).¹⁰ The entire protocol employs toxic chemicals and solvents such as chloroacetyl chloride, triethylsilane, trifluoroacetic acid, and methyl isobutyl ketone, or DMF. All these things make it troublesome. So, we are finding a pathway that can make the intended molecule in a sustainable way.



Scheme 1.3. Synthesis of Ziprasidone.

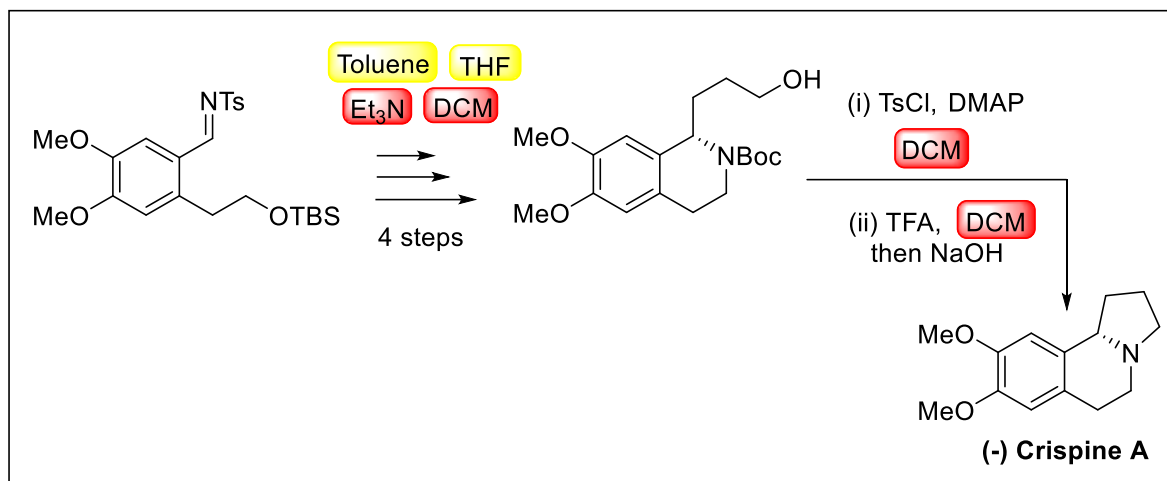
Numerous pharmaceuticals, natural products, and organic synthetic materials are built on the basis of pyrroles and indoles. (*S*)-ketorolac is a well-known NSAID-approved nonsteroidal anti-inflammatory drug molecule available on the market under the trade names Toradol and Biorolac. The synthetic route of ketorolac involving three steps is shown in **Scheme 1.4**.¹¹ In every step, various types of organic solvents are used, such as triethyl amine, tetrahydrofuran, and 1,2-dimethoxyethane. Most of these are not friendly to our environment. Therefore, we are going to construct a scaffold that can produce the desired molecule in a green manner.



Scheme 1.4. Synthesis of ketorolac.

Crispine A, a pyrroloisoquinoline alkaloid found in *Carduus crispus*, has been shown to have pharmacological activities against the human cell lines HeLa, KB, and SKOV3. A Rh-catalyzed asymmetric synthesis of it was presented here.¹² However, in this multistep

synthetic protocol, several hazardous carcinogenic solvents were used shown in **Scheme 1.5**, which are not friendlier for our environment. Therefore, finding a green synthetic protocol is essential.



Scheme 1.5. Synthetic route of Crispine A.

Despite the fact that numerous technologies for synthesising pharmacological molecules and pharmaceutical active ingredients have been discovered, these techniques have a number of negative environmental effects. In order to get around these traditional tactics, researchers are always coming up with new strategies to stop environmental pollution problems. Toxic reagents and red or yellow marking solvent, for example, not only produce dangerous pollutants but also offer extremely efficient pathways to achieve the goal. In this situation, modern science has started to pay more attention to green methodologies.

1.3.1. Requirement of green techniques towards the organic synthesis:

To meet the challenges of the development of organic chemistry, researchers and scientists devote their efforts to finding out how the synthetic conversion takes place while reducing environmental and health risks.¹³ Consequently, the researcher uses the non-toxic green solvents to perform the reaction. Besides this, it is also far better if it is possible to avoid the use of any solvent for chemical transformation, i.e., solvent-free synthesis. A solvent-free reaction reduces the multistep procedure, one of which is avoiding the aqueous work-up for purification purposes. Microwave irradiation (MW), ultrasound irradiation (US), conventional thermal heating, mechanochemistry (grinding), and ball milling techniques are mainly involved in the environmentally benign green synthesis. Photoinduced and

electrochemical methods are also the growing fields in the modern green chemistry scenario (Figure 1.6).

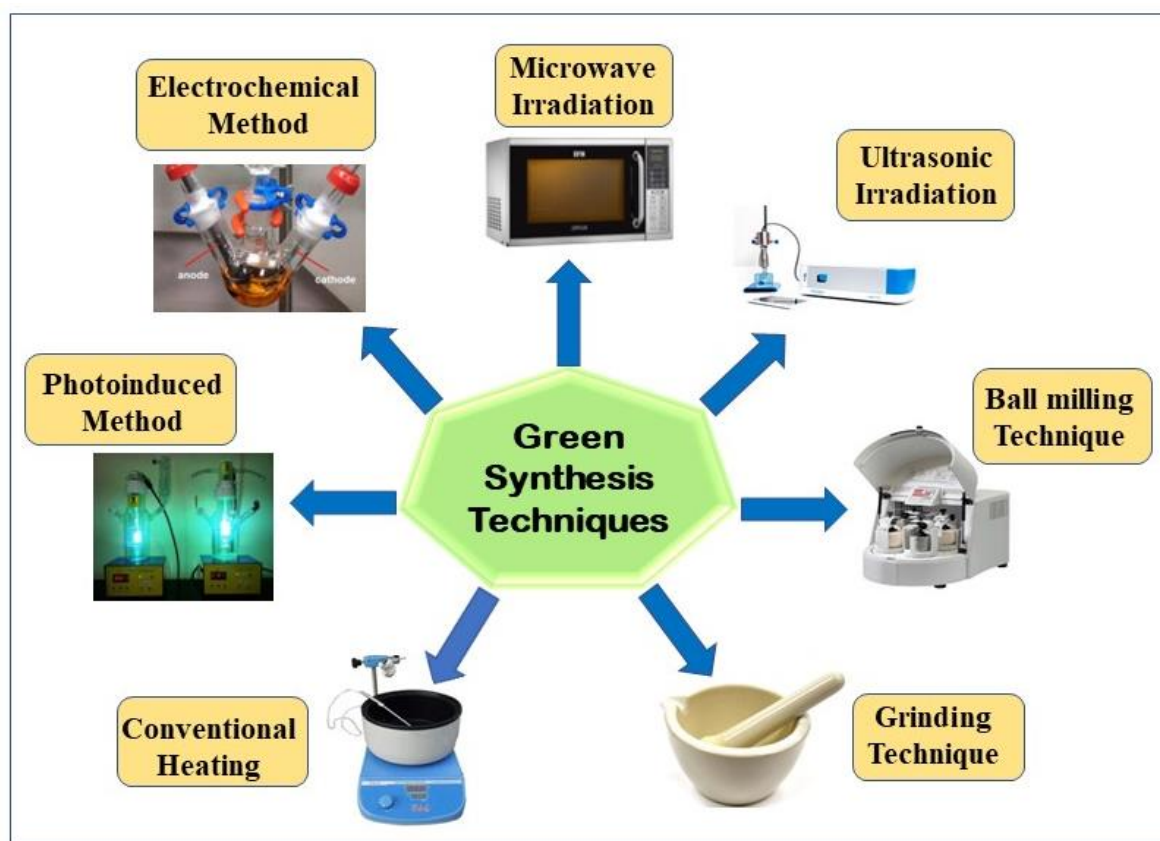


Figure 1.6. Different techniques for green synthesis.

Microwave heating,¹⁴ transfer energy directly to the reactant molecule in the reaction vessel and it reduces the reaction time compare to the conventional thermal heating. The chemical transformation under microwave irradiation takes place in faster rate, cost effective, gives the high yield product, and simplified the purification process in compare to the conventional heating. A new advanced technology, ultrasonic irradiation, creates cavitation bubbles of liquid molecules under spontaneous ultrasonic irradiation. The energy for chemical change is produced by the bubbles collapsing in subsequent compression cycles. As a result, the reaction proceeds at a faster rate and takes less time with high yields.¹⁵ Another mechanical technique, ball milling, is used to grind the powders into fine particles. In this technique, the reactant molecules are broken by mechanical forces.¹⁶ This technique has been attracted due to its simplicity, low cost, as well as its high yield. In the grinding technique, use of a grindstone facilitates safe, simple, solvent-free chemistry, as well as high yield, economic efficiency, and environmental friendliness.¹⁷ Photoinduced reaction is a modern field

involving a chemical transformation initiated by absorbing light radiation. In this method, organic substances get excited by absorbing heat energy, generating radicals or cations, and this radical helps to get the products.¹⁸ Another emerging technology, electrochemical synthesis, employs the transportation of electrons from the electrode to the chemical ingredients in the solution phase, either directly or in reverse, across the electrode/solution confluence, leading to chemical transformation. A galvanostat or potentiostat and an electrode-equipped electrochemical cell make up the straightforward equipment for electrochemical synthesis.¹⁹ The main benefits of electrochemical synthesis over other methods are not requiring chemical oxidants or reductants, mild reaction conditions, effective pollution control, higher selectivity, and higher yield percentages.

Hence, all things involving green synthesis or solvent-free synthesis are healthier for the environment. By inspiring these green techniques, we focused our research towards solvent-free synthesis or synthesis using green solvents towards fused quinazolinones, isothiazoles, pyrroles, pyrrolo lactam rings, and pyrroloquinoline moieties by conventional heating techniques in our laboratory (**Figure 1.7**). We have also explored our methodology using synthesized heterocyclic molecules to the natural products, biological activities, photophysical studies and molecular sensing properties.

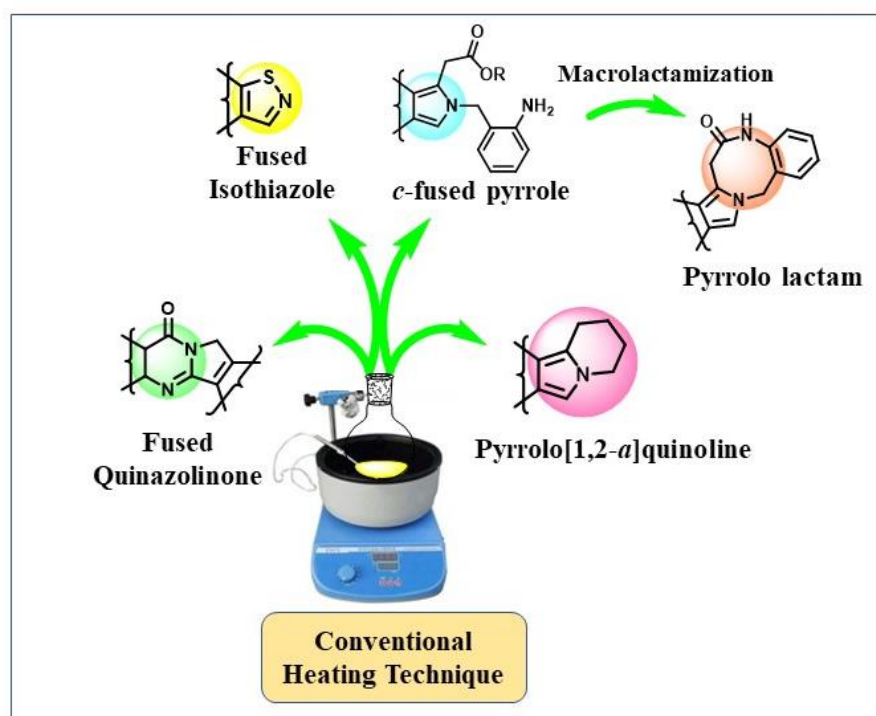


Figure 1.7. All compounds are synthesized using conventional heating techniques under green protocol.

1.4. Quinazolinone:

Quinazolinones are the most celebrated moiety in heterocyclic chemistry for their wide, and diverse biological activities. Presently, more than 200 naturally occurring bio-active quinazolinones are found in nature.²⁰ Quinazolinone moieties have drawn high attention due to their medicinal applicability, such as their anticancer therapeutic potential, antidiabetic, analgesic, antibacterial, and anticonvulsant activities.^{20a} Quinazolinone's skeleton is structurally similar to that of purine and pyrimidine bases (**Figure 1.8**).^{20b-d}

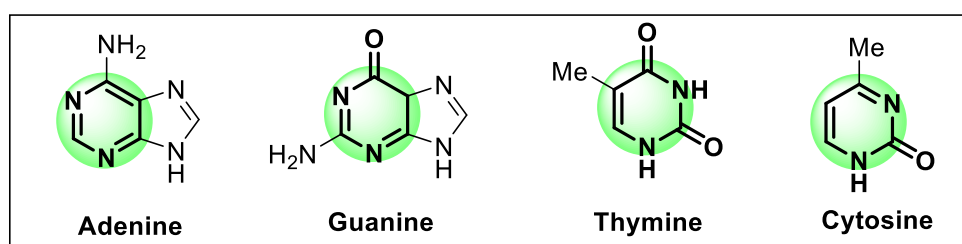


Figure 1.8. Purine and pyrimidine bases of nucleic acid.

1.4.1. Quinazolinone containing naturally occurring alkaloids:

Now, we introduce with few naturally occurring bio-active quinazolinone moieties (**Figure 1.9**). Penipanoid C was extracted from the *Penicillium oxalicum* 0312F₁, a marine fungus, and later on isolated from *Penicillium paneum* SD-44. Penipanoid C exhibits inhibitory activity moderately against replication of tobacco mosaic virus.^{21a} The first luciferase inhibitor, 2-(4-(methylamino)phenyl)quinazolin-4(3*H*)-one, was derived from *Streptomyces* sp. A496.^{21b} Recently, 2-(1*H*-indol-3-yl)quinazolin-4(3*H*)-one has been identified from *Streptomyces* sp. BCC 21795 and displays a cytotoxic effect against Vero cells.^{21c} (-)-Chaetominine, a new framework of tripeptide alkaloidal metabolites, was characterized from the solid-substrate culture of *Chaetomium* sp. IFBE015, an endophytic fungus on the apparently healthy *Adenophora axilliflora* leaves.^{21d} The cytotoxic assays of (-)-Chaetominine exhibits highly potential activity *in vitro* against human leukemia K562 and colon cancer SW1116 with IC₅₀ values 21 μ M and 28 μ M respectively.^{20a} Isochaetominines C was isolated recently from *Aspergillus* sp. and displayed weak inhibitory activity against Na⁺/K⁺-ATPase.^{21e} Aniquinazoline D was obtained from a marine mangrove leaf of *Rhizophora stylosa*., and exhibits effective potential against the brine shrimp with LD50 value 3.42 μ M.^{21f}

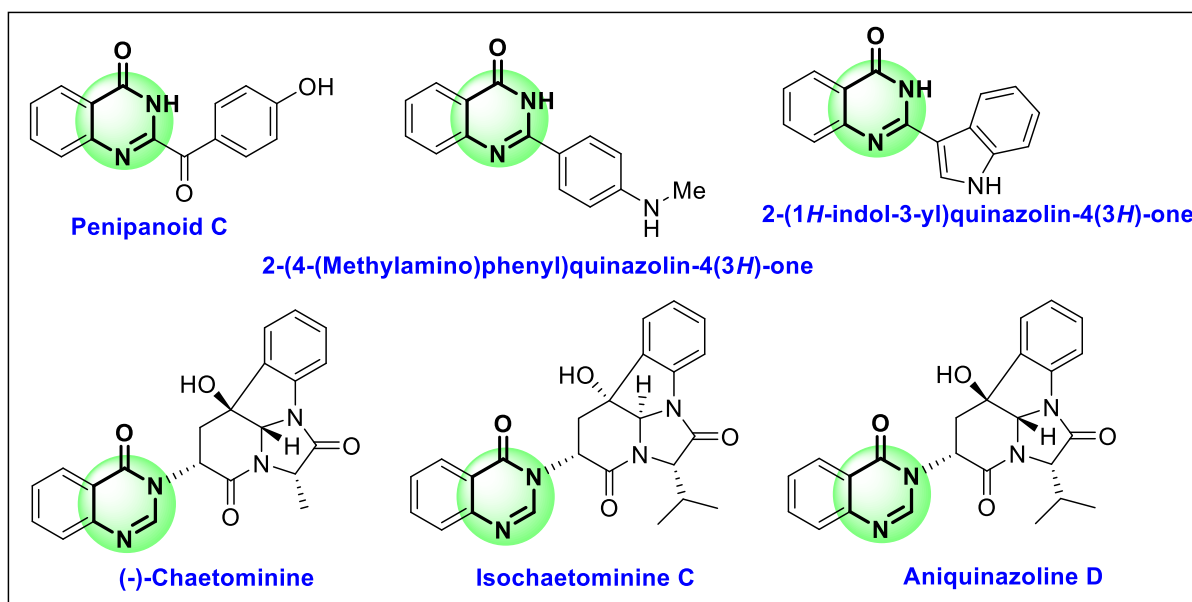


Figure 1.9. Naturally occurring bioactive quinazolinone moieties.

1.4.2. Quinazolinone containing drug molecules:

Besides these bio-active natural products, quinazolinones have great abundance in the medicinal world. Many prescribed drug molecules are found in which quinazolinones are present in the core skeleton (**Figure 1.10**). Albaconazole,^{22a-c} is an antifungal drug, has efficiency against vulvovaginal candidosis, a common infection in healthy women caused by *Candida albicans*. It also has potent *in vitro* activity against dermatophytes and some other filamentous and opportunistic fungi, such as *Paecilomyces spp.*, *Aspergillus spp.*, and *Chaetomium spp.* Febrifugine, a well-known prescribed drug used for the treatment of malaria, especially *P. falciparum* and *P. vivax*.^{22d-f} Quinethazone helps control blood pressure and is used as an antihypertensive agent.^{22e-f} Nolatrexed (NOL) is a commercially available novel quinazoline-based therapeutic drug and used for the treatment of hepatocellular carcinoma (HCC).^{22a, e, g} It also inhibits thymidylate synthase, which has been developed as an antitumor agent.^{22g} Raltitrexed is also a quinazoline-based prescribed drug, used as chemotherapy for cancer patients.^{22h} Fenquizone is a popular low-ceiling diuretic agent.^{22e, f}

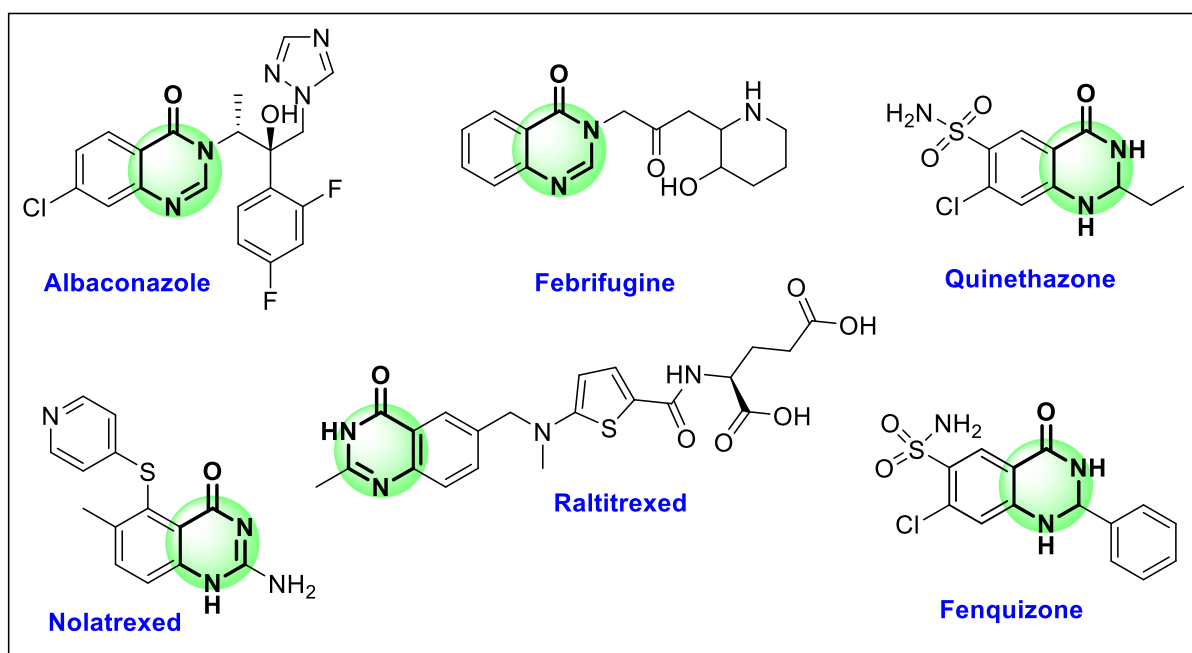


Figure 1.10. Useful prescribed drugs containing quinazolinone moieties.

1.4.3. Fused quinazolinone:

Like quinazolinone moieties, fused quinazolinones have great importance in our modern society. Quinazolinone is fused with the pyrrole, indole, and isoindole rings and gives more natural products and drug molecules. Some bioactive fused quinazolinone alkaloids are given below (**Figure 1.11**). Vasnetine is an analogous alkaloid of vasicinone and was isolated from the leaf extract of *Adhatoda visca*, commonly used as a bronchodilator and hypotensive medicine in India.^{23a, b} Auranthine, a white solid fungal metabolite isolated from *Penicillium aurantiogriseum*, has cytotoxic properties against both human kidney epithelial cells (IHKE), and human liver cancer cell lines (HepG2). However, its methylated derivative was found to be more sensitive to IHKE cell lines (IC₅₀ value is 25 μM).^{23c-e} Mackinazolinone, a quinazolino-carboline type alkaloids, exhibit diverse pharmacological activities such as anti-microbial, anti-inflammatory, and antidepressant activities etc.^{23f-h} Rutaecarpine, isolated from the dried fruits of *Evodia rutaecarpa*, is used for the treatment of headaches, dysentery, and gastrointestinal disorders.^{23i, j} Phaitanthrin A, a new optically active alkaloid, has been identified from an orchid *Phaius mishmensis* and exhibited moderate cytotoxic effect against NCI-H460, SF-268, and MCF-7 cell lines with IC₅₀ values of 27.0, 43.9, 33.8 μM respectively.^{20a}

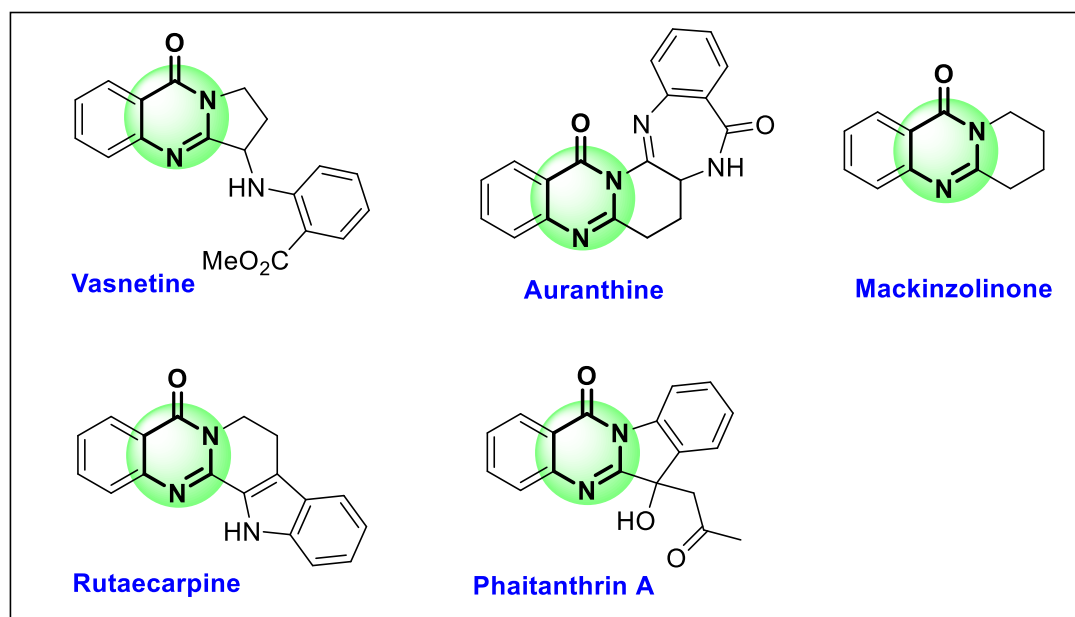


Figure 1.11. Some naturally occurring bio-active fused quinazolinone alkaloids.

1.4.4. Photophysical applications of fused quinazolinone:

Besides the availability of bioactive natural alkaloids, many novel quinazolinones have been found with excellent luminescence properties (**Figure 1.12**). The first batch of U.S. patents for newly formed fluorescent dyes containing an HPQ structure were requested by American Cyanamid Company in 1965. On the basis of this structure, further fluorescent materials and probes have now been invented. In 1992, PPQ, 2-(2'-phosphoryloxyphenyl)-4(3*H*)-quinazolinone was created as a fluorescent phosphatase probe. PPQ can be precisely hydrolyzed into the unsolvable product HPQ as a luminous precipitate in water using alkaline phosphatase and acid. A new kind of fluorescent probe, CPPCQ, is a precipitate that fluoresces brightly right away after enzymatic hydrolysis and is commercialized under the trade name "ELF™ 97 Phosphate".²⁴

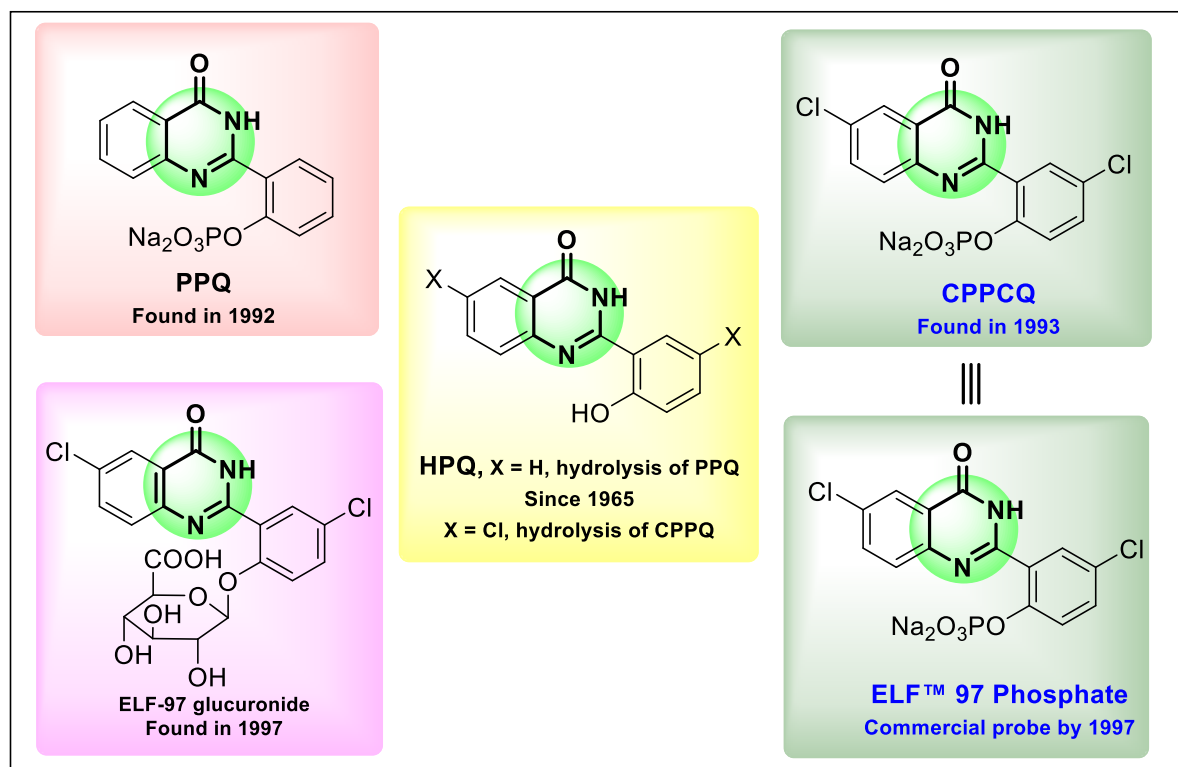
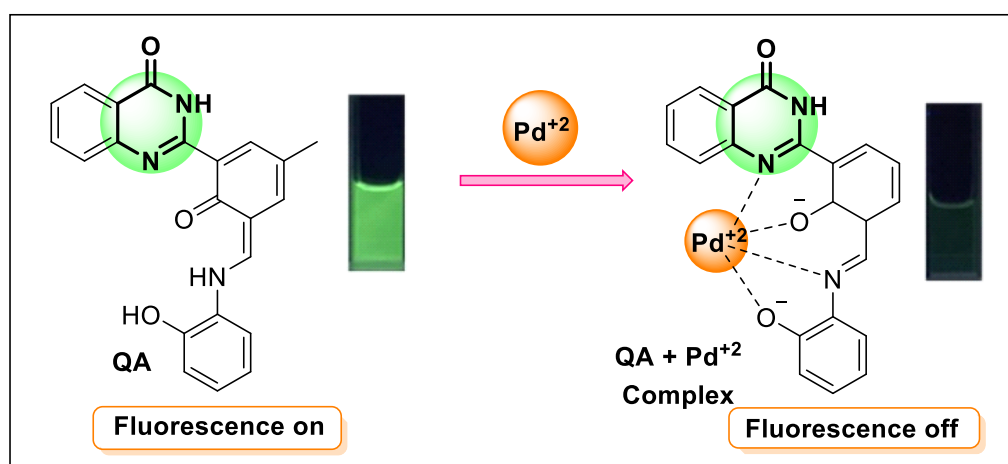


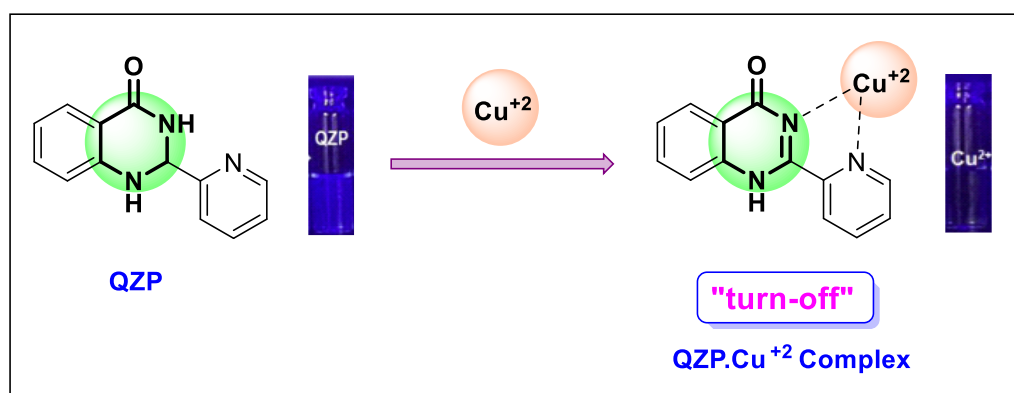
Figure 1.12. Various quinazolinone based fluorescence probes.

Another quinazolinone-based 2-(2'-hydroxyphenyl)quinazolin-4(3*H*)-one enaminone derivative, QA, emits green fluorescence in PBS buffer solution (pH = 7.4). QA shows high selectivity towards Pd²⁺ ions over the other metal ions, with complete quenching of fluorescence at 538 nm (**Scheme 1.6**).²⁵



Scheme 1.6. Fluorescence on-off mechanism of quinazolinone based probe.

To selectively find Cu^{2+} ions, the synthetic dihydroquinazolinone derivatives, QZP, employ a fluorescence "turn-off" mechanism. QZP can bind Cu^{2+} ions by quenching the fluorescence of its (Scheme 1.7).²⁶



Scheme 1.7. Quinazolinone-based fluorescence sensor.

1.4.5. Optoelectronic materials of quinazolinone:

A series of quinazolinone-based probes have been found to have inherent emissive properties and are used as optoelectronic materials in the broad spectrum (Figure 1.13). Compound **I**, 14H-quinazolino[3,2-*f*]phenanthridine-14-one derivatives, exhibited the emission of blue light in chloroform solvent.^{27a} Compound 11-Hydroxy-6-phenyl-11b,12-dihydro-13H-quinazolino[3,4-*a*]quinazolin-13-ones (**II**), displayed solid-state fluorescence in an orange-green colour.^{27b} Another compound, 6-Phenyl-5,6-dihydro-8H-quinazolino[4,3-*b*]quinazolin-8-ones (**III**), emits bright blue lights in the solution phase.^{27b} An efficient 1-H-spiro[isindoline-1,2'-quinazoline]-3,4'(3'*H*)-dione (**IV**), also emits fluorescence in the visible region from 413 nm to 436 nm with an effective stock shift value of 44-72 nm.^{27c}

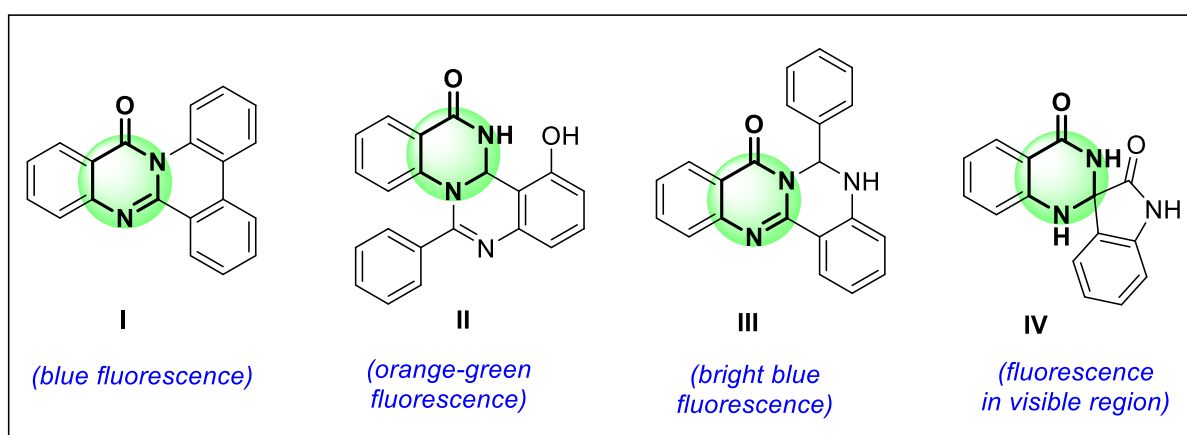


Figure 1.13. Optoelectronic material based on quinazolinone based probe.

1.4.6. Agrochemical applications of quinazolinone:

A major pest, the cotton leaf worm, *Spodoptera littoralis* (Boisd), destroys a variety of commercially significant cultivated crops, including cotton, tobacco, peanuts, soybeans, and vegetables. There is an approximate 26-100% yield loss in the crop as a consequence, according to research. Tetraactyl bis-quinazolin-4(3*H*)-one, a recently developed derivative, was effective against cotton leaf worm as an insecticide (**Figure 1.14**).²⁸

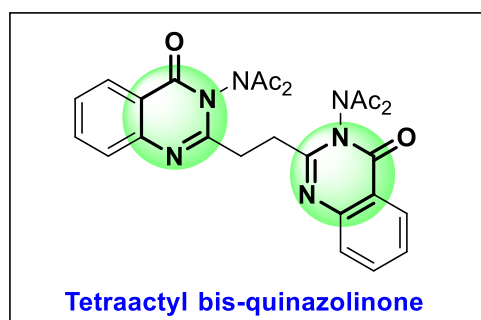


Figure 1.14. Insecticidal activity of quinazolinone derivative.

After a brief discussion about quinazolinones and fused quinazolinones, we are now discussing about isothiazole derivatives.

1.5. Isothiazole:

Five-membered heterocycles containing sulphur (S) and nitrogen (N), two hetero atoms in a 1,2-relationship, are known as isothiazole derivatives. Depending on the position of these heteroatoms, they may be classified in different classes (**Figure 1.15**).

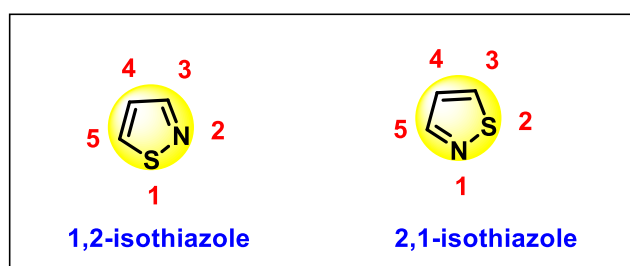


Figure 1.15. Classification of isothiazole derivatives.

Isothiazole draws special attention due to its broad applicability in the medicinal, agrochemical, and pharmaceutical fields, as well as in the electronic materials and synthesis fields. Some isothiazole scaffolds display a wide range of bioactivities, such as antiviral, anticancer, antidiabetic, etc. (**Figure 1.16**).^{29a}

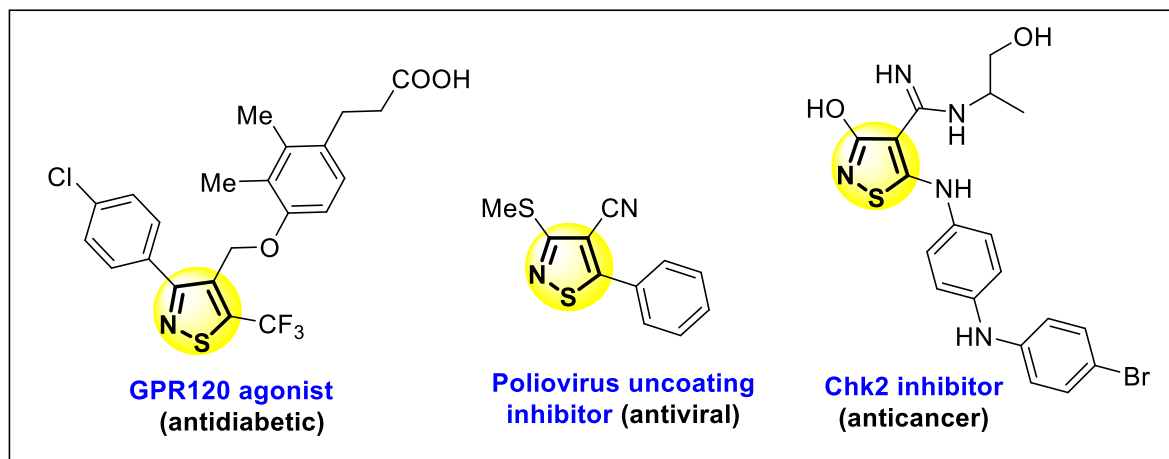


Figure 1.16. Selected isothiazole molecules with pharmacological activities.

Some isothiazole molecules are commercially available in the market as drug molecules, such as sulfamizole as an antibacterial sulfa drug, denotivir as antiviral drug, isotianil which is effective against rice blast, and methylchloroisothiazolone (MCIT), which is used as kathon preservatives (**Figure 1.17**).^{29a, b}

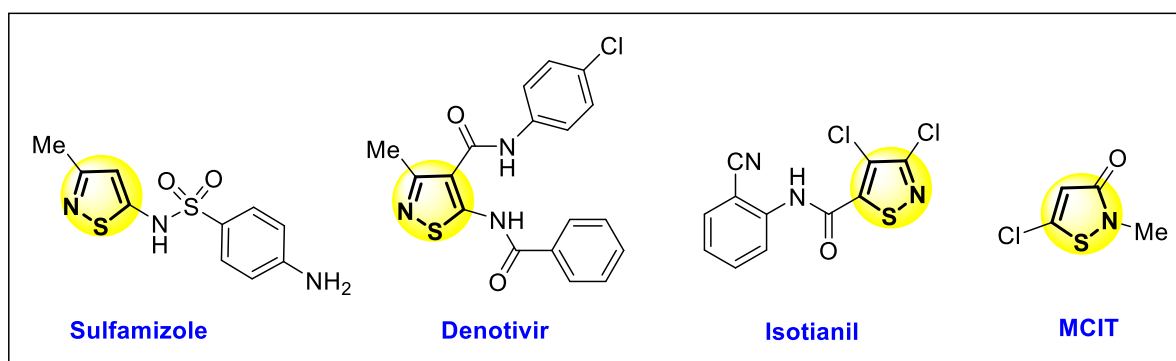


Figure 1.17. Commercially available important isothiazole moieties.

1.5.1. Fused isothiazole:

Fused isothiazole represents itself as an important five-membered heteroaromatic compound. Fused isothiazoles have various pharmacological activities in a broad spectrum, such as anticancer, antipsychotic, neuroprotective, and antitumor agents, etc. Selected fused isothiazole derivatives are displayed here with their pharmacological activities (**Figure 1.18**).²⁹ To treat solid tumours by inhibiting CAIX, benzo[*d*]isothiazol-3(2*H*)-one 1,1-dioxide is being developed as a therapeutic candidate.^{29c} Tiospirone was investigated as a potential novel atypical antipsychotic medication since it contains significant 5-HT_{2A} and D₂

antagonist action.¹⁰ Lurasidone has a wide range of therapeutic benefits and is characterized by its multi-receptor affinity.^{29d}

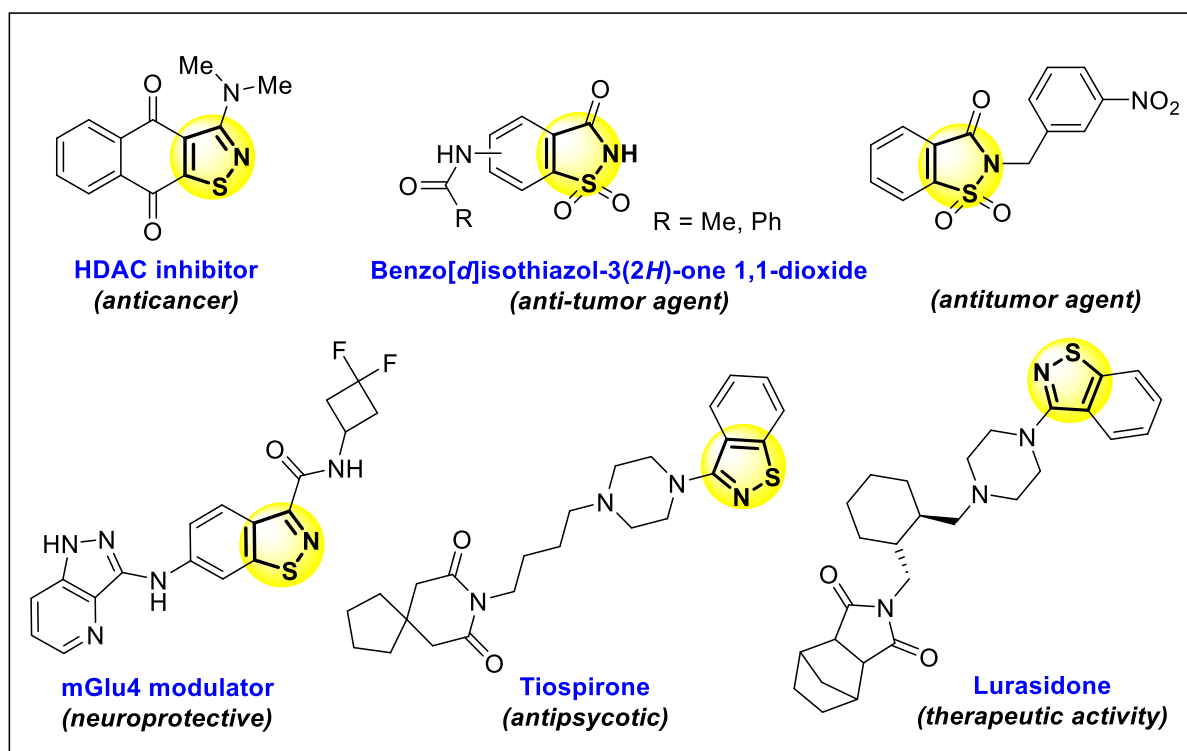


Figure 1.18. Selected fused isothiazole moieties with pharmacological activities.

1.5.2. Photophysical application of fused isothiazole derivatives:

Isothiazoles are not only important for their pharmacological activities; they also show excellent fluorescence behaviour. Two newly synthesized ester derivatives of isothiazole moieties have been developed, and their optical properties are also documented here (**Figure 1.19**). The absorption and emission spectra were recorded for both compounds in *n*-hexane and ethanol solvents. The emission properties depend on the solvent polarity. Solvent polarity influenced the intensity of the emission spectra. In an ethanol solution, $n \rightarrow \pi^*$ and $\pi \rightarrow \pi^*$ transitions take place for both the compounds, and the emission maxima move towards a red shift.³⁰

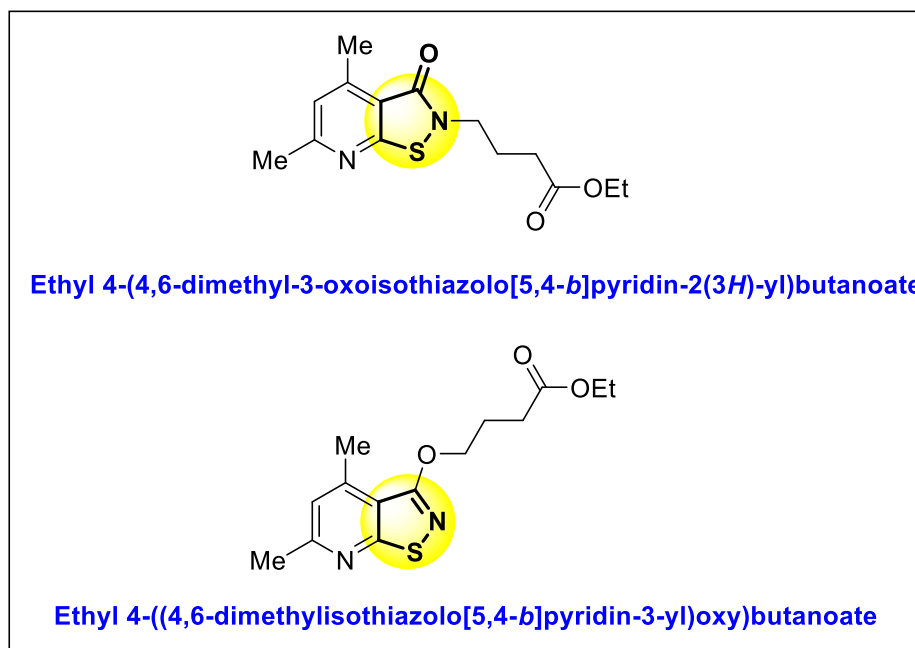


Figure 1.19. Isothiazole based fluorescence probe.

After the discussion about isothiazoles, we are now motivated towards another five membered heterocyclic molecule, fused pyrroles, and their family.

1.6. Fused Pyrroles and their family:

An important class of *N*-fused heterocycles includes pyrrole and its derivatives. Several bioactive natural compounds, such as porphyrins, bacteriochlorins, chlorophyll, porphyrinogens, vitamin B12, numerous cytochrome enzymes, bilirubin, and biliverdin derived from marine sources, have pyrrole as their primary structural component.^{31a-c} Pyrrole derivatives are extensively used in the organic synthesis of agrochemicals, pharmaceuticals, photographic chemicals, perfumes, dyes, and other organic compounds.^{31b} Pyrrole derivatives have exhibited diverse bioactivities such as antiviral, antifungal, antibacterial, antitumor, antioxidant, anti-inflammatory, anti-hyperlipidemic, antiparasitic, antimalarial, anti-HIV, anti-cancer, and analgesic effects.^{31a, c}

The cycloalkyl ring is fused with the pyrrole moiety at different positions, producing a different class of heterocyclic molecules, known as *a*, *b*, and *c*-fused pyrroles (**Figure 1.20**). The decoration of the pyrrole ring in the proper position *via* their important pharmacophore unit generated many natural and pharmaceutical active products.

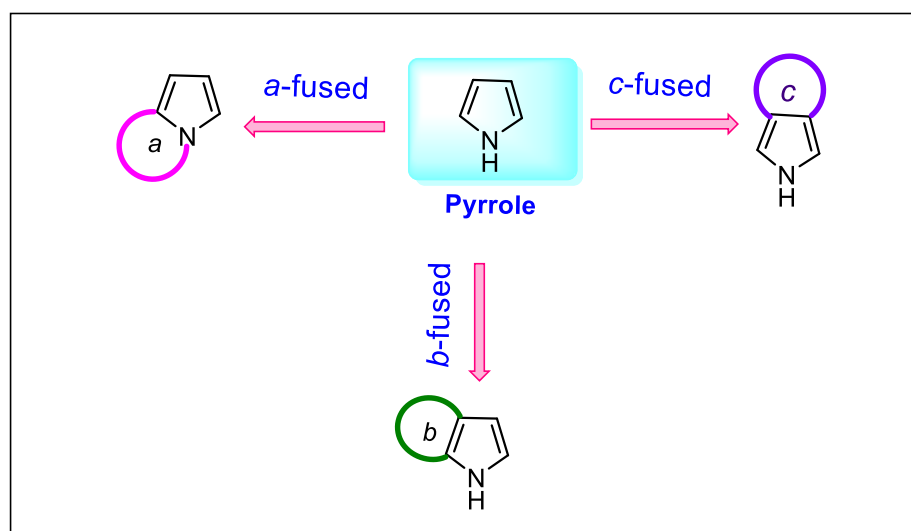


Figure 1.20. Schematic representation of various fused pyrroles.

1.6.1. *a*-fused Pyrrole:

Different kinds of *a*-fused pyrrole are produced when a heterocyclic or carbocyclic ring is fused at the *a*-position of the pyrrole molecule. Some of them are found in many natural products as well, and they show various bioactivities such as antitumor, anti-HIV activities, anti-inflammatory, analgesic, and antibacterial properties (**Figure 1.21**).^{32a} Ketorolac, a popularly prescribed drug, is utilized in cases of moderate to severe short-term pain.^{32b,c} Another naturally occurring substance with a six-membered ring is pilogotin A and pilogotin B, which were extracted from *Poliganotum sibiricum*.^{32d, e} Pyrrole-fused heterocycles pyrrolo-pyrimidine and pyrrolo-imidazole have been exhibited as antihypertensive agent with molluscicidal activity.^{32f}

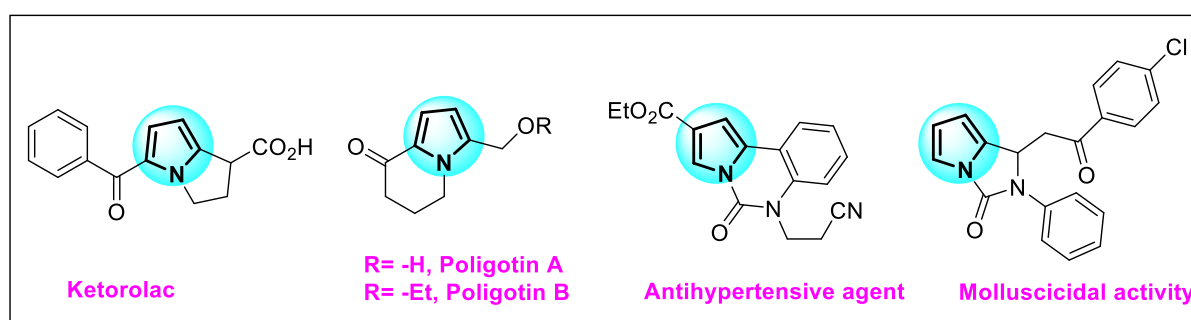


Figure 1.21. Few bio-active, natural products containing *a*-fused pyrrole moieties.

1.6.2. *b*-fused Pyrrole:

A heterocyclic or carbocyclic ring fused at the *b*-position of a pyrrole ring produces *b*-fused pyrrole, as for example in indole rings, which are bicyclic, planar, and aromatic in nature. Indole holds an important position in heterocyclic chemistry because of its bioactivities and medicinal applicability. The most familiar tryptophan is present in amino acids and protein chains.^{33a} Again, the drug molecules serotonin, indomethacin, bufotinine, etc. are available on the market and contain the indole moiety as the key nucleus. In the case of animals, the indole-based drug Serotonin was used as a critical neurotransmitter (anticholinesterase-monoamine oxidase inhibitor). Indomethacin, a non-steroidal anti-inflammatory drug, has been used to get relief from pain, fever, and inflammation. The Indole-containing natural product bufotenine isolated from the *Physostigma venenosum* seeds has been selected for the medication of Alzheimer's disease (**Figure 1.22**).^{33b, c}

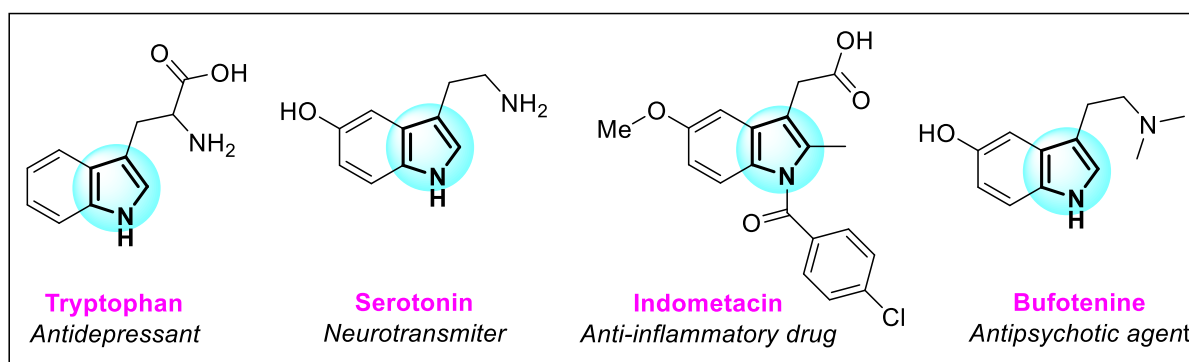


Figure 1.22. Some *b*-fused pyrrole containing bio-active natural alkaloids.

1.6.3. *c*-fused Pyrrole:

A novel family of pyrroles known as "*c*-fused pyrroles," including isoindole and isoindoline, is created when a carbocyclic or heterocyclic ring fuses at the *c*-position of a pyrrole. Again *c*-fused pyrrole can be obtained after fusion of saturated carbocyclic analogue (**Figure 1.23**).

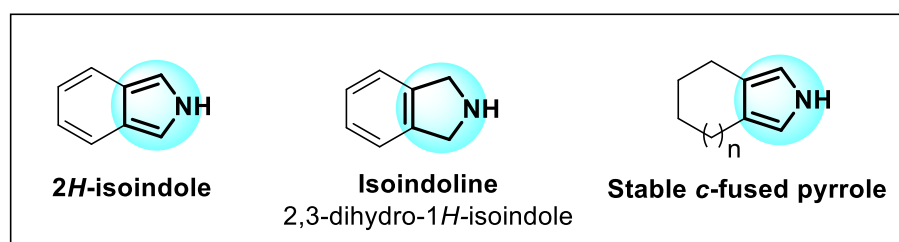


Figure 1.23. Schematic presentation of various types of *c*-fused pyrroles.

Pyrroles fused at the *c*-junction always get special priority as they are found in a broad range of various bioactive natural products. Here, we are basically focused on the isoindole moiety, as it is widely present in various bioactive natural products and pharmacophores (**Figure 1.24**). A natural product with prominent physiological properties is mostly composed of 1,2-substituted *c*-fused pyrrolonaphthoquinones. The examples are *Azamonosporascone* isolated from *Monosporascus cannonballus* and *Reniera isoindole alkaloid*, which showed antimicrobial activity.^{34a, b} The well-known natural products *Bhimamycin C* and *Bhimamycin D* displayed activity in human ovarian cancer cell lines.^{34a, b}

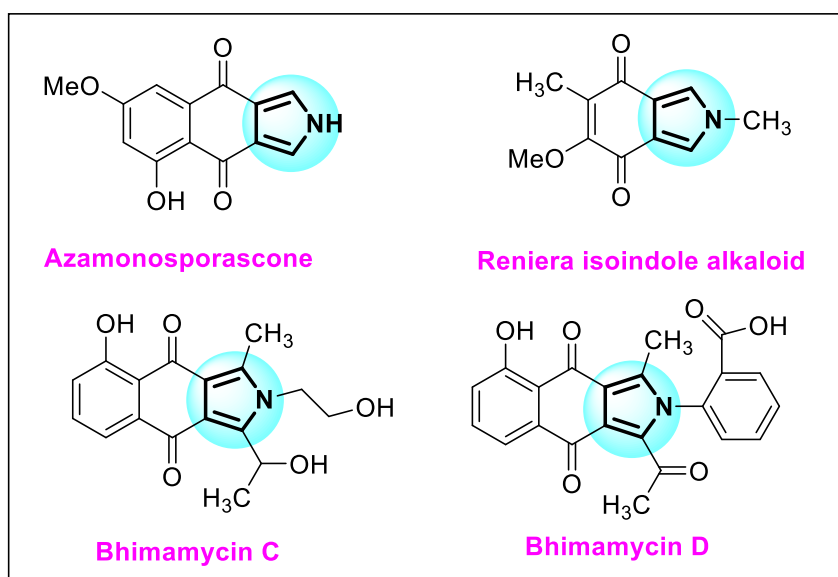
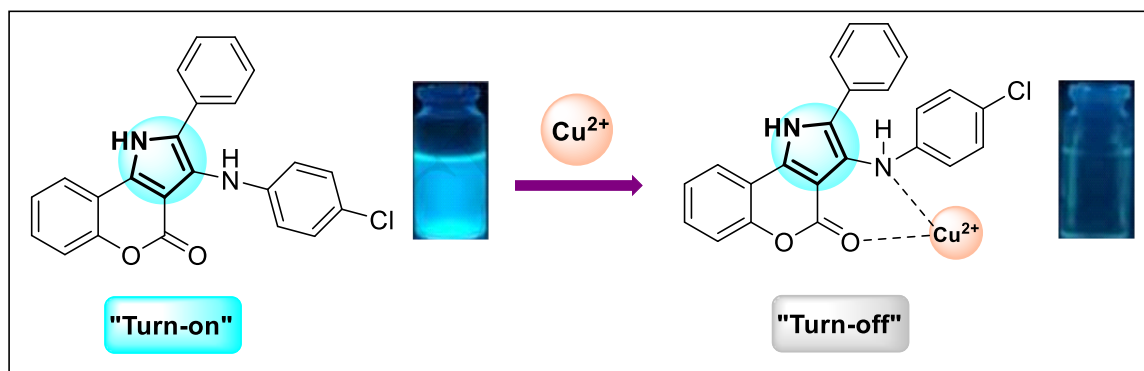


Figure 1.24. Selected examples of natural products containing *c*-fused pyrrole.

1.6.4. Photophysical applications of fused pyrrole:

1.6.4.1. Metal ion sensing properties:

Besides the availability of numerous bio-active natural products, fused pyrroles have diverse photophysical applications in a broad spectrum. Pyrrole-fused fluorophores can be widely used as chemosensors, dyes in textile industries, pigments, fluorescent makers, etc. Coumarin-based fused pyrrole is highly sensitive to the metal ions in living organisms. Although Cu^{+2} is an essential heavy metal for the human body, its irregular distribution can cause many crucial diseases like Parkinson's disease, Wilson's disease, Alzheimer's disease etc. Chromeno[4,3-*b*]pyrrol-4(1*H*)-one, coumarin-based fluorescent probe exhibited fluorescence "on-off" mechanism in the presence of metal ions. This synthesized probe selectively bound with Cu^{+2} , showing a quenching effect (**Scheme 1.8**).³⁵



Scheme 1.8. Coumarin based fused pyrrole containing chemosensor.

1.6.4.2. Pyrrole in dye and pigment industry:

Pyrrolo[3,4-*c*]pyridines are considered to be the most significant class of fluorophores. Both 1-imino-6,7-dimethyl-1,2-dihydro-3*H*-pyrrolo[3,4-*c*]pyridine-3,4(5*H*)-dione and 6,7-dimethyl-1*H*-pyrrolo[3,4-*c*]pyridine-1,3,4(2*H*,5*H*)-trione fluorophores emit light in the bluish-green region and are extensively used as dyes, pigments, fluorescent markers, and metal sensors (**Figure 1.25**).³⁶



Figure 1.25. Pyrrolo[3,4-*c*]pyridine-based dyes and pigments.

BODIPYs (4,4-difluoro-4-bora-3a,4a-diaza-s-indacene) has two isoindole units joined by methyne carbon. This is an example of a fluorophore, which was discovered by Kreuzer and Treibs in 1968. These astonishing photophysical activities, with their high fluorescence quantum yield and good photostability, made them very charming for their various utilizations, such as photosensitizers for organic photovoltaics and fluorescent markers in bio-imaging. The π -electron conjugation can be expanded also by the annulations of the aromatic rings into the pyrrole unit, resulting in a rigidified aromatic system and the fluorescent property (**Figure 1.26**).³⁷

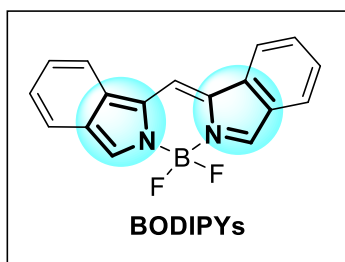


Figure 1.26. Fluorescent makers for bio-imaging.

1.6.4.3. Pyrroles in material science:

Organic materials having extensive π -conjugation with fused pyrroles are widely used as organic light-emitting diodes (OLEDs), organic field-effect transistors (OFETs), organic photovoltaics (OPVs), electrochromic materials, and sensors (**Figure 1.27**).^{38a, b} Extensive π -conjugation reduces the band gaps and also increases the charge transport mobilities due to more electronic coupling and systematic intermolecular π - π overlapping. Considering the vast applications in material science, fused pyrroles have gathered more attention recently.

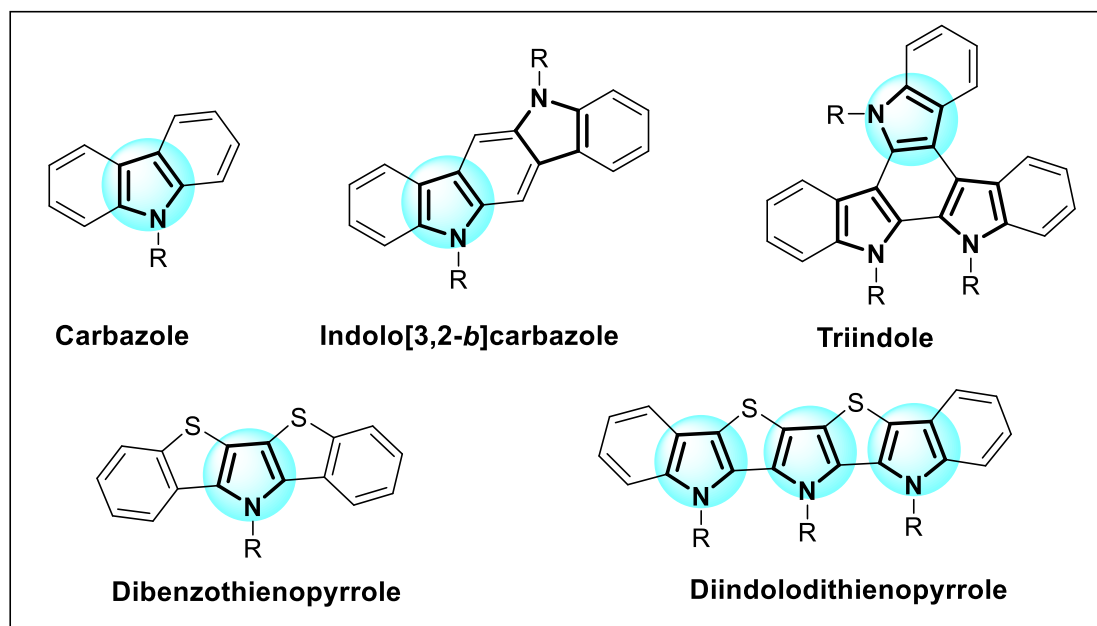


Figure 1.27. Multi-fused pyrroles used as OLEDs, OFETs and OPVs.

QBPBP and QFBPBP are a new class of pyrrolo[3,2-*b*]pyrrole-based *n*-channel organic field-effect transistors (OFETs). Recently, *n*-channel organic semiconductors have made great progress due to their high electron mobilities. Considering the crucial role of *n*-channel organic semiconductors in *p*-*n* junctions and complementary logic circuits, this is a challenging and significant aspect of organic transistors (**Figure 1.28**).³⁹

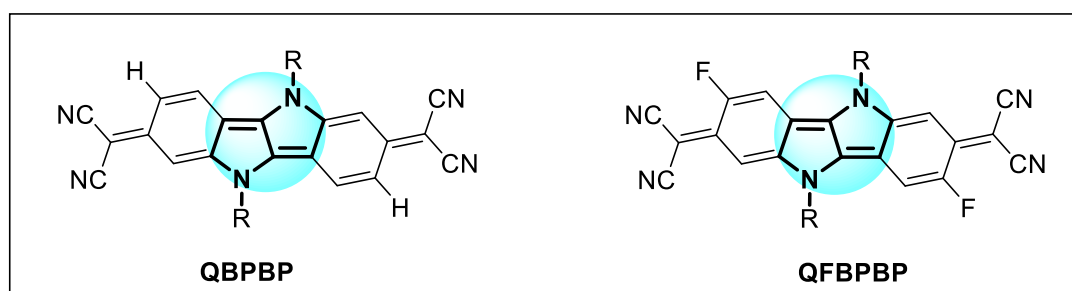


Figure 1.28. High performance *n*-channel Organic Field-Effect Transistors (OFETs).

Pyrrole-fused azacoronene exhibits good optoelectronic and electronic properties compared to polycyclic aromatic hydrocarbons and *p*-conjugated polymers. The introduction of nitrogen atoms into polycyclic aromatic hydrocarbons known as *N*-doped carbon materials used as semiconductors was formed by the intramolecular electrochemical oxidation coupling of pyrrole residues (**Figure 1.29**).⁴⁰

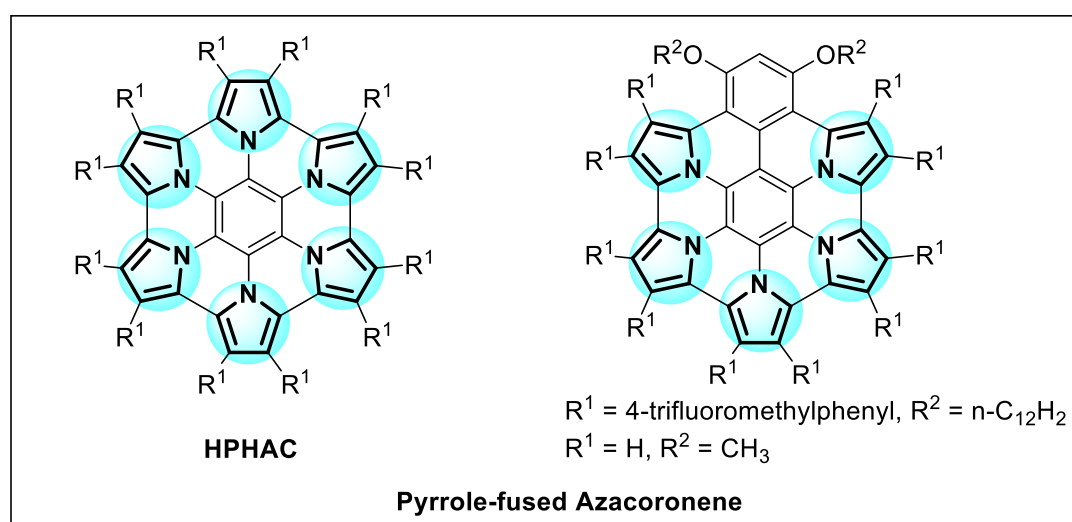


Figure 1.29. Pyrrole-fused azacoronene semiconductor.

Organic solar cells (OSCs) have drawn worldwide attention due to their several merits, such as their light weight, semitransparency, flexibility, and low toxicity. PPIC1 and PPIC2 are pyrrolo[3,2-*b*]pyrrole-based 8-fused-ring electron acceptors (FREAs) in organic solar cells (OSCs). Pyrrolo[3,2-*b*]pyrrole (PP)-based OSCs show better power conversion efficiency (PCE) than naphthalene, thiophene, and pyrrole-bearing FREAs. PDPP2FT and PDPP3F, which contain diketopyrrolopyrrole (DPP) units and structurally low-band gap polymers, are reported as organic solar cells (**Figure 1.30**).⁴¹

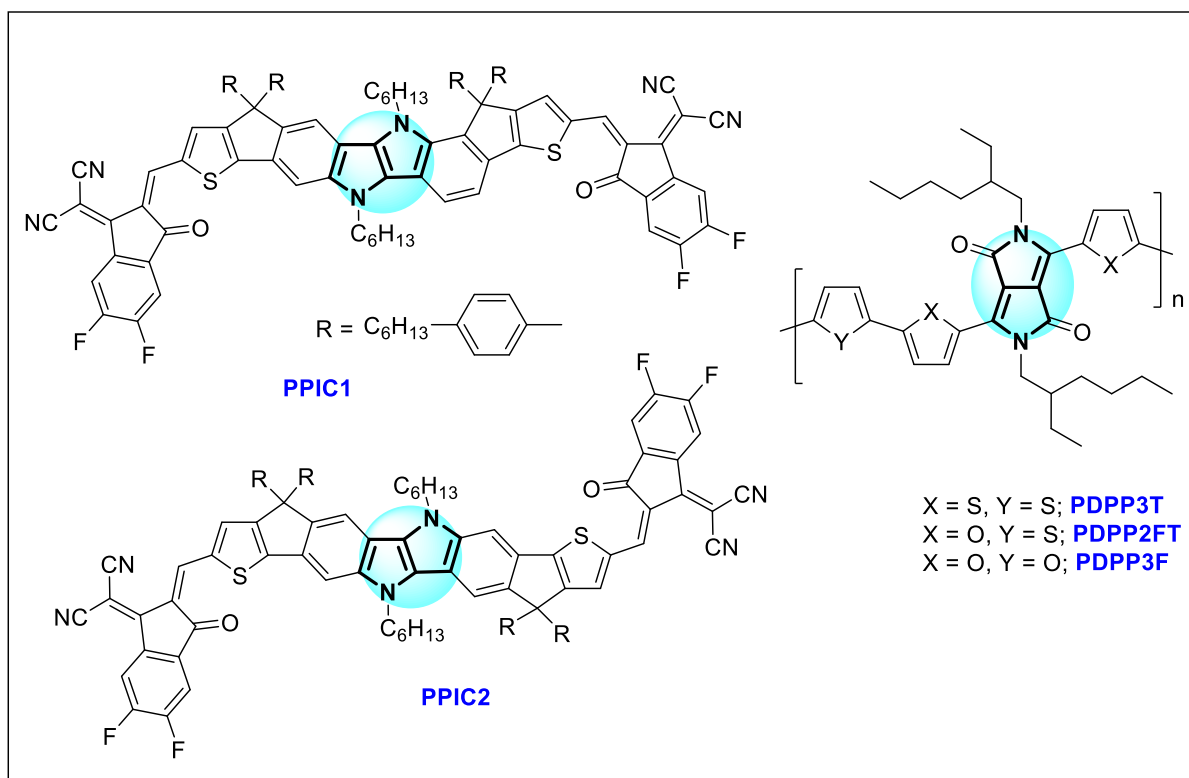


Figure 1.30. Pyrrolo[3,2-*b*]pyrrole (PP) based organic solar cells (OSCs).

1.7. Lactam ring:

Lactams are cyclic amides derived from amino alkanolic acids. Cyclic esters with different ring sizes are available in the literature (**Figure 1.31**). Medium sized ring lactams are prevalent in many bioactive compounds and natural products.

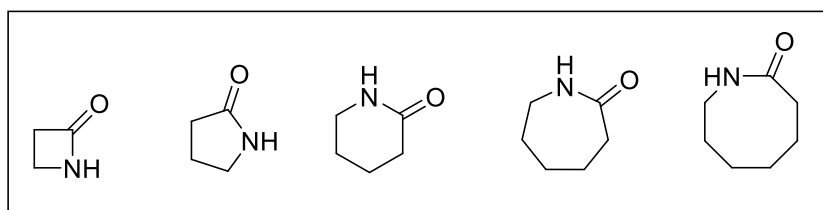


Figure 1.31. Different ring sizes using lactam scaffolds.

1.7.1. Pyrrolo lactam:

A number of biologically active natural molecules contain medium-sized ring lactams (8 - 11 members), which are also interesting scaffolds in medicinal chemistry.^{42a, g} Especially, medium-sized pyrrolo lactam rings are highly demandable molecules in light of their diverse bioactivities, such as anti-malarial, anti-cancer, and inflammatory properties, etc. (**Figure**

1.32). An alkaloid (+)-Balasubramide, containing an eight-membered ring lactam, was discovered in *Clausena indica*, a plant that thrives in SriLanka's central highland rainforests. It can help inhibit the neuroinflammation.^{42b, c} Rhazinilam, first identified from the leaf extract of *Rhazya stricta* in 1970. Later, it was also discovered in labs on *Aspidosperma quebrachoblanco* leaves with a 0.002% yield. It can be effective to inhibit tubulin formation.^{42a, d} Lyngbyatoxin A, a first-generation indole alkaloid, is a highly inflammatory and vesicatory substrate that has been extracted from the blue-green alga *Lyngbya majuscula* Gomont.^{42a, e} Decursivine, a novel alkaloid, was isolated from the stems and leaves of *Rhaphidophora decursiva* Schott. It exhibited moderate antimalarial activity against *Plasmodium falciparum*.^{42f} Another eight-membered lactam ring containing the natural product SM-406 displayed anti-cancer activity.^{42g, h}

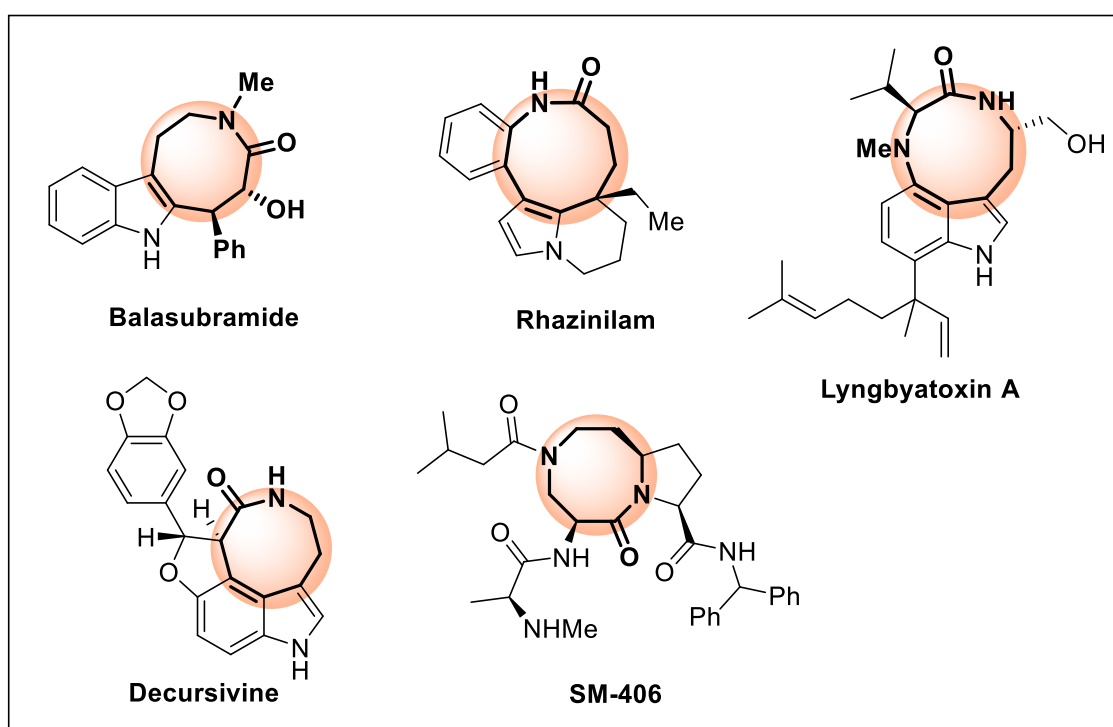


Figure 1.32. Natural products with medium-sized ring lactam.

After the discussion of fused pyrroles and pyrrole-fused lactam rings, we shifted our attention towards pyrroloquinoline.

1.8. Pyrroloquinoline:

Pyrroloquinoline introduced a new class to expand the fused pyrrole family. Pyrroloquinolines are widely present in a multitude of natural products, agrochemicals, and pharmaceutical substances, and additionally, the synthetic moieties of this class are capable of exhibiting the optical and electronic properties. The functionalized pyrroloquinolines have attracted a lot of synthetic interest because of their distinct biological activity and widespread use (**Figure 1.33**). *Tylophora indica* was the natural source of tylophorine, which has enormous bioactivities including anti-allergic, anti-inflammatory, antibacterial, anti-asthmatic, antiviral, and antifungal properties. It also has been demonstrated that it is a strong inhibitor of eukaryotic protein synthesis, RNA transcription, and the activity of many cyclins that control the cell cycle.⁴³ Gephyrotoxin, a substituted perhydropyrrolo[1,2-*a*]quinoline, was discovered in the secretions of the frog *Dendrobates histrionics*. Gephyrotoxin was discovered to have a variety of neurological effects, including a weak muscarinic antagonist.⁴⁴ Tricyclic pyrrolo[1,2-*a*]quinolines are display several bio-activities in a broad spectrum, such as apoptosis inducer, antioxidant, antiproliferative, antibacterial, and antileukemic ingredients against P388 leukaemia.^{44a, c, d}

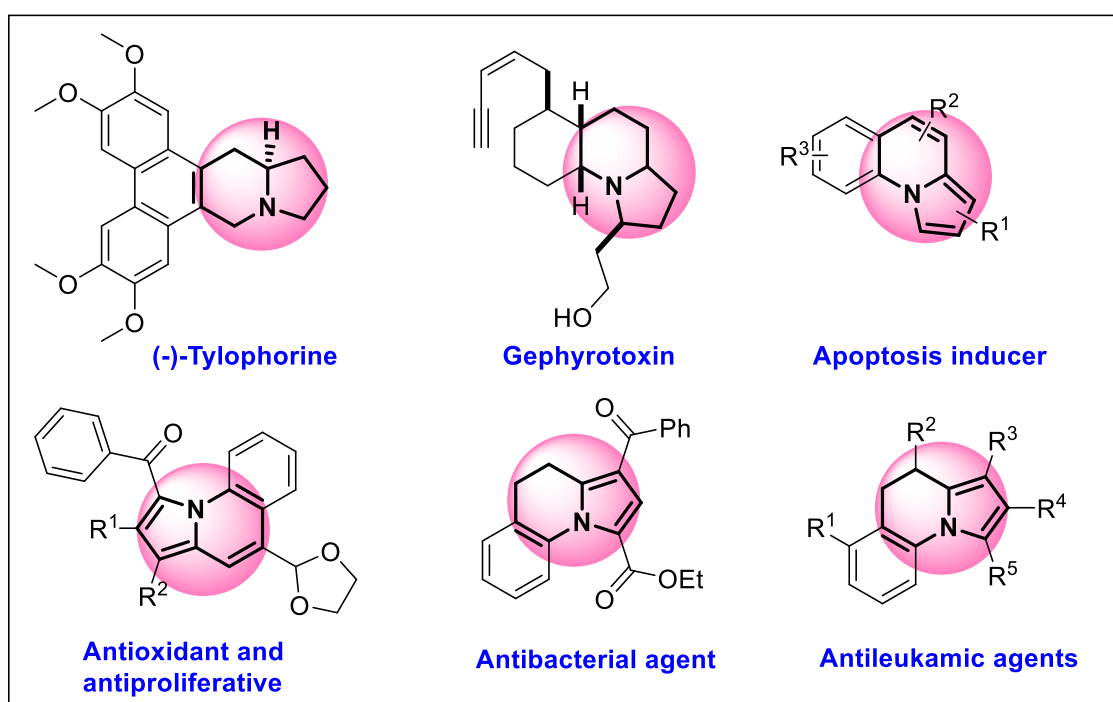
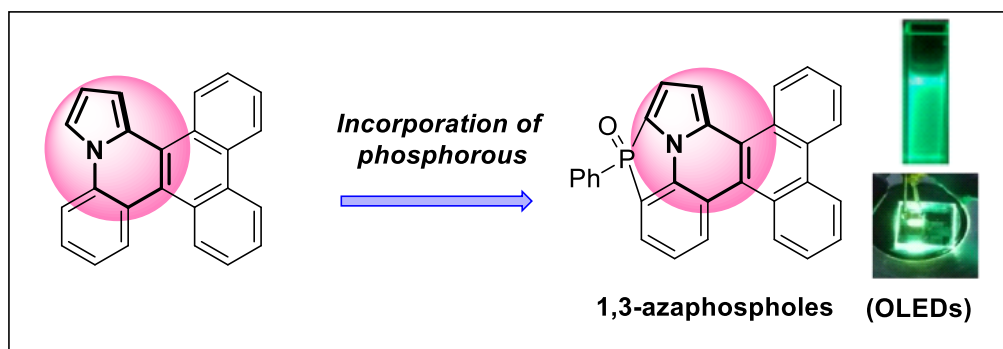


Figure 1.33. Numerous biological activities of naturally occurring pyrrolo[1,2-*a*]quinolines.

1.8.1. Pyrroloquinoline in material science:

Pyrrolo[1,2-*a*]quinoline, one of the fundamental fused rings in heterocyclic chemistry, finds extensive usage in the field of material science. Incorporating a phosphorus atom into the π -conjugated system of pyrrolo[1,2-*a*]quinoline produces new annulated 1,3-azaphospholes. This phosphorus-based annulated 1,3-azaphosphole is exclusively used as organic light-emitting diodes (OLEDs) (**Scheme 1.9**).⁴⁵



Scheme 1.9. Pyrrolo[1,2-*a*]quinoline embedded organic light-emitting diodes (OLEDs).

HSQ 1, HSQ 2, and HSQ 3, three novel pyrroloquinolines containing acceptor-donor-acceptor (A-D-A) type molecules, were extensively used as dyes (**Figure 1.34**). These dyes exhibited bright yellow to orange fluorescence in the solid state. The photophysical behaviour of these dyes showed viscosity-sensitive emission, i.e., the enhancement of emission intensity by 33-43 folds in glycerol.⁴⁶

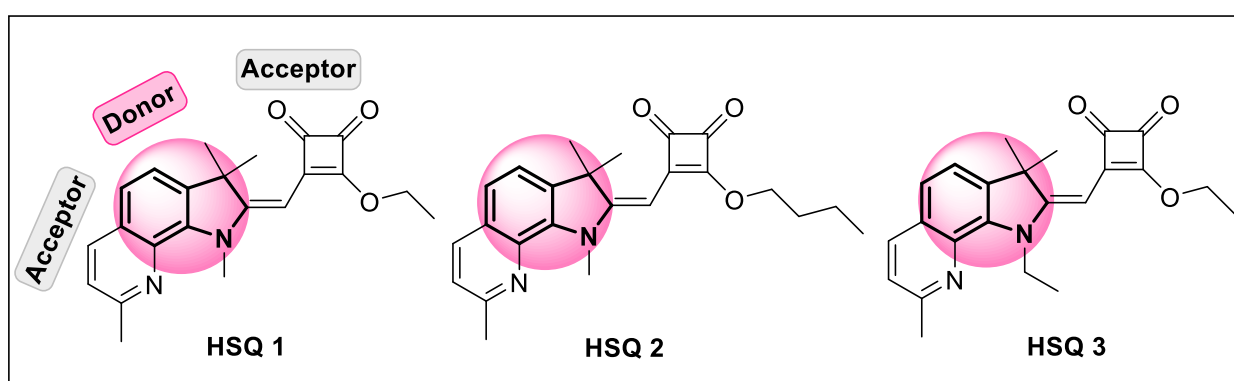
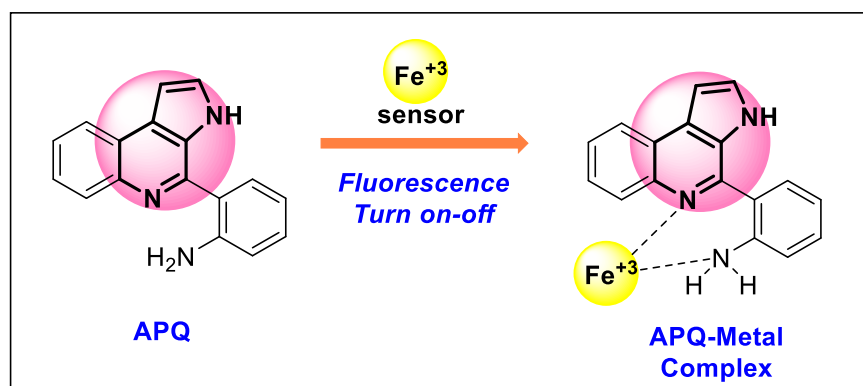


Figure 1.34. Pyrroloquinoline-based synthetic fluorescence dyes.

1.8.2. Sensing properties of Pyrroloquinoline:

APQ, a fluorophore based on pyrrolo[2,3-*c*]quinoline, has good sensing properties. It can effectively detect the Fe^{+3} ion by quenching the fluorescence intensity. By incubating the Fe^{+3} ion, it demonstrated significant fluorescence behaviour ("turn on-off") (Scheme 1.10).⁴⁷



Scheme 1.10. Iron sensing properties of pyrrolo[2,3-*c*]quinoline based fluorophore.

1.9. Conclusion:

Based on the discussion of the importance of numerous *N*-fused heterocycles, our primary goal was to synthesise *N*-fused heterocycles following environmentally friendly protocols. By avoiding toxic materials, employing benign solvents and auxiliaries, and simplifying reaction processes, we have developed inherently safe chemistry. The entire thesis consists of a green synthetic protocol, a solvent-free strategy, or using benign solvents for the synthesis of various *N*-fused heterocyclic molecules and their photophysical applications, and is entitled “*Environmentally benign synthetic routes to fused heterocycles and their photophysical studies*”.

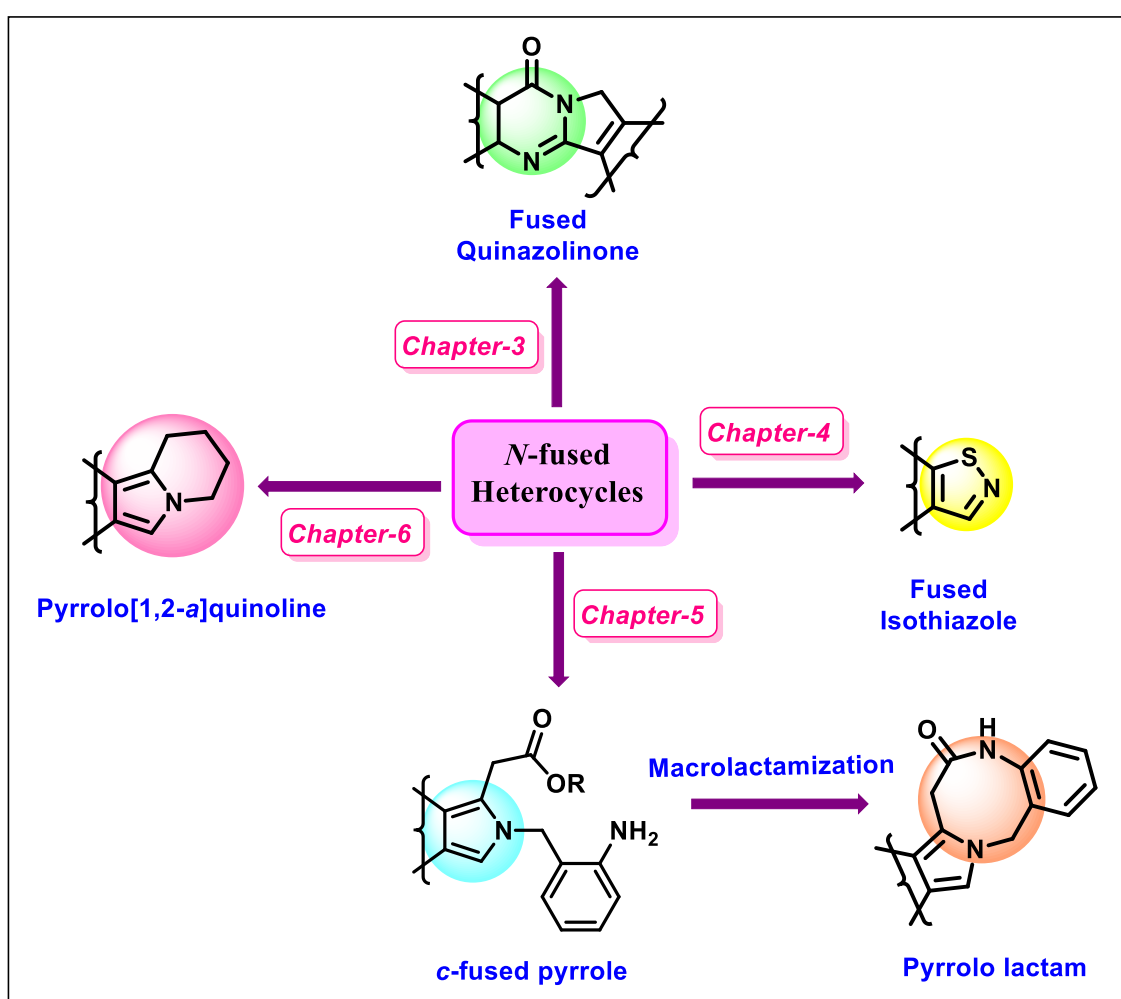


Figure 1.35. Chapter wise schematic representation of our synthesized scaffolds.

1.10. References:

1. M. Singhal, A. Singh, S. P. Khan, E. Sultan, N. K. Sachan, *Int. Res. J. Pharm.*, 2012, **3**, 31-36.
2. Paul T. Anastas, and Evan S. Beach, *Changing the Course of Chemistry*, 2009.
3. S. L. Y. Tang, R. L. Smithb and M. Poliakoff, *Green Chem.*, 2005, **7**, 761-762.
4. K. Tanaka and F. Toda, *Chem. Rev.*, 2000, **100**, 1025-1074.
5. (a) K. Alfonsi, J. Colberg, P. J. Dunn, T. Fevig, S. Jennings, T. A. Johnson, H. P. Kleine, C. Knight, M. A. Nagy, D. A. Perry, M. Stefaniak, *Green Chem.*, 2008, **10**, 31-36; (b) A. D. Curzons, D. C. Constable, V. L. Cunningham, *Clean Prod. Process.*, 1999, **1**, 82-90; (c) C. Jimenez-Gonzalez, A. D. Curzons, D. J. C. Constable, V. L. Cunningham, *Clean Technol. Environ. Pol.*, 2005, **7**, 42-50; (d) C. Capello, U. Fischer, K. Hungerbuhler, *Green Chem.*, 2007, **9**, 927-934.
6. (a) P. Fürst and P. Stehle, *J Nutr*, 2004, **134**, 1558S-1565S; (b) M. F Perutz. Brookhaven Symp Biol., 1960, **13**, 165-183; (c) M. S. Saini, A. Kumar, J. Dwivedi and R. Singh, *Int. J. Pharm. Sci. Res.*, 2013, **4**, 66-77.
7. (a) V. Sharma, V. Kumar and P. Kumar, *Curr Med Chem Anticancer Agents*, 2013, **13**, 422-432; (b) D. Mitrienko, G. I. *J. Am. Chem. Soc.*, 2007, **129**, 2726; (c) D. Deiddau, G. Lampis, C. Maullu, R. Pompei, F. Isaia, V. Lippolis and G. Verani, *Pharmacol. Res.*, 1997, **36**, 193-197; (d) P. A. Datar and T. A. Deokule, *Med chem.*, 2014, **4**, 390-399; (e) J. M. Quintela, C. Peinador, C. Veiga, L. Gonzalez, L. M. Botana, A. Alfonsob and R. Riguera, *Bioorg. Med. Chem.*, 1998, **6**, 191-1925; (f) S. M. Sondhi, M. Dinodia, J. Singh and R. Rani, *Curr. Bioact. Compd.*, 2007, **3**, 91-108; (g) Z. Li, Y. Cao, P. Zhan, C. Pannecouque, J. Balzarini and E. D. Clercq, X. Liu, *Lett. Drug Des Discov.*, 2013, **10**, 27-34.
8. (a) T. Itoh, T. Abe, T. Choshi, T. Nishiyama, M. Ishikura, *Heterocycles*, 2016, **92**, 1132-1136; (b) S. D. Vaidya and N. P. Argade, *Org. Lett.*, 2015, **17**, 6218-6221.
9. (a) J. L. Liang, H. C. Cha and Y. Jahng, *Molecules*, 2011, **16**, 4861-4883; (b) S. H. Kwon, H-A. Seo, and C-H, Cheon, *Org. Lett.*, 2016, **18**, 5280-5283.
10. H. R. Howard, J. A. Lowe, T. F. Seeger, P. A. Seymour, S. H. Zorn, P. R. Maloney, F. E. Ewing, M. E. Newman, A. W. Schmidt, J. S. Furman, G. L. Robinson, E. Jackson, C. Johnson, and J. Morrone, *J. Med. Chem.*, 1996, **39**, 143-148.
11. P. S. Baran, J. M. Richter, and D. W. Lin, *Angew. Chem. Int. Ed.*, 2005, **44**, 609-612.

12. P-F. Chiang, W-S. Li, J-H. Jian, T.-S. Kuo, P-Y. Wu, and H-L. Wu, *Org. Lett.*, 2018, **20**, 158-161.
13. G. Nagendrappa, *Resonance*, 2002, 59-68.
14. (a) V. Molteni and D. A. Ellis, *Curr. Org. Synth.*, 2005, **2**, 333-375; (b) A. Adhikari, S. Bhakta, and T. Ghosh, *Tetrahedron*, 2022, **126**, 133085.
15. (a) R. F. Martínez, G. Cravotto, and P. Cintas, *J. Org. Chem.*, 2021, **86**, 13833-13856; (b) S. S. Low, M. Yew, C. N. Lim, W. S. Chai, L. E. Low, S. Manickam, B. T. Tey, P. L. Show, *Ultrason. Sonochem.*, 2022, **82**, 105887.
16. S. Chaudhuri, A. Ghosh, S. K. Chattopadhyay, *Green Synthetic approaches for Biologically Relevant heterocycles*, 2021, **2**, 617-653.
17. A. F.M. Fahmy, A. A. El-Sayed, M. M. Hemdan, A. I. Hassaballah and A. F. Mabied, *Asian J. Chem.*, 2017, **29**, 2679-2686.
18. S. Dadashi-Silab, S. Doran, and Y. Yagci, *Chem. Rev.*, 2016, **116**, 10212-10275.
19. M. K. Sharma, *Synthesis of Advanced Materials by Electrochemical Methods*, 2021, 435-466.
20. (a) U. A. Kshirsagar, *Org. Biomol. Chem.*, 2015, **13**, 9336-9352; (b) J. Kaneti, M. Georgieva, M. Rangelov, I. Philipova, B. Vasileva, I. Angelov, D. Staneva, G. Miloshev, and S. Bakalova, *Biochim Biophys Acta Gen Subj BBA-GEN SUBJECTS*, 2021, **1865**, 129773; (c) B. K. Tiwary, K. Pradhan, A. K. Nanda, and R. Chakraborty, *J Chem Biol Ther*, 2015, **1**, 104; (d) L. He, H. Li, J. Chen, and X-F. Wu, *RSC Adv.*, 2014, **4**, 12065-12077.
21. (a) S. Shen, W. Li, and Jian Wang, *Nat. Prod. Res.*, 2013, **27**, 2286-2291; (b) B. Somanadhan, C. Leong, S. R. Whitton, S. Ng, A. D. Buss, and M. S. Butler, *J. Nat. Prod.*, 2011, **74**, 1500-1502; (c) J. Kornsakulkarn, S. Saepua, K. Srijomthong, P. Rachtawee, and C. Thongpanchang, *Phytochem. Lett.*, 2015, **12**, 6; (d) R. H. Jiao, S. Xu, J. Y. Liu, H. M. Ge, H. Ding, C. Xu, H. L. Zhu, and R. X. Tan, *Org. Lett.*, 2006, **8**, 5709-5712; (e) L. Liao, M. You, B. K. Chung, D-C. Oh, K-B Oh, and J Shin, *J. Nat. Prod.*, 2014, **78**, 349-354; (f) C-Y. An, X-M. Li, C-S. Li, M-H. Wang, G-M. Xu, and B-G. Wang, *Mar. Drugs*, 2013, **11**, 2682-2694.
22. (a) C. Bodhak, S. Hazra, and A. Pramanik, *ChemistrySelect*, 2018, **3**, 7707-7712; (b) C. Blyth, *J. Pediatr. Infect. Dis.*, 2011, **30**, 506-507; (c) G. M. Gonza'lez, E. Robledo, E. Garza-Gonza'lez, M. Elizondo, and J. G. Gonza'lez, *Antimicrob. Agents Chemother.*, 2009, **53**, 4540-4541; (d) S. Jiang, Q. Zeng, M. Gettayacamin, A. Tungtaeng, S. Wannaying, A. Lim, P. Hansukjariya, C. O. Okunji, S. Zhu, and D. Fang, *Antimicrob.*

- Agents Chemother.*, 2005, **49**, 1169-1176; (e) T. P. Selvam, and P. V. Kumar, *Research in Pharmacy*, 2011, **1**, 1-21; (f) P. S. Auti, G. George, and A. T. Paul, *RSC Adv.*, 2020, **10**, 41353-41392; (g) R. G. Gish, C. Porta, L. Lazar, P. Ruff, R. Feld, A. Croitoru, L. Feun, K. Jeziorski, J. Leighton, J. Knox, J. Gallo, and G. T. Kennealey, *J. Clin. Oncol.*, 2007, **25**, 3069-3075; (h) R-Z. Jin, W-T. Zhang, Y-J. Zhou, and X-S. Wang, *Tetrahedron Lett.*, 2016, **57**, 2515-2519.
23. (a) B. S. Joshi, Y. Bai, M. S. Puar, K. K. Dubose, and S. W. Pelletier, *J. Nat. Prod.*, 1994, **57**, 95-962; (b) Y. Zheng, W-B. Song, S-W. Zhang, and L-J. Xuan, *Org. Biomol. Chem.*, 2015, **13**, 6474-6478; (c) M. V. Madhubabu, R. Shankar, S. s. More, M. V. B. Rao, U. K. S. Kumar, and R. Akula, *RSC Adv.*, 2016, **6**, 36599-36601; (d) S. E. Yeulet, and P. G. Mantle, J. N. Bilton, H. S. Rzepa, and R. N. Sheppard, *J. Chem. Soc., Perkin Trans. 1*, 1986, 1891-1894; (e) S. A. Kalinina, D. V. Kalinin, Y. Hövelmann, C. G. Daniliuc, C. Mück-Lichtenfeld, B. Cramer, and H-U. Humpf, *J. Nat. Prod.*, 2018, **81**, 2177-2186; (f) J-F. Liu, P. Ye, K. Sprague, K. Sargent, D. Yohannes, C. M. Baldino, C. J. Wilson, and S-C. Ng, *Org. Lett.*, 2005, **7**, 3363-3366; (g) S. R. Johns, and J. A. Lambert, *Chem. Commun.*, 1965, 267a-267a; (h) W. R. Bowman, M. R. J. Elsegood, T. Stein, and G. W. Weaver, *Org. Biomol. Chem.*, 2007, **5**, 103–113; (i) M. Wang, W. Ye, N. Sun, W. Yu, and J. Chang, *J. Org. Chem.*, 2023, **88**, 1061-1074; (j) S. Malasala, A. Polomoni, S. M. Chelli, S. Kar, Y. V. Madhavia, and S. Nanduri, *Org. Biomol. Chem.*, 2021, **19**, 1854-1859.
24. Z. Xing, W. Wu, Y. Miao, Y. Tang, Y. Zhou, L. Zheng, Y. Fu, Z. Song, and Y. Peng, *Org. Chem. Front.*, 2021, **8**, 1867-1889.
25. L. Tang, S. Ding, and X. Yan, *Inorg. Chem. Commun.*, 2016, **74**, 35-38.
26. P. N. Borase, P. B. Thale, and G. S. Shankarling, *Dyes Pigm.*, 2016, **134**, 276-284.
27. (a) B. Banerji, S. Bera, S. Chatterjee, S. K. Killi, and S. Adhikary, *Chem. Eur. J.*, 2016, **22**, 3506-3512; (b) S. Chatterjee, R. Srinath, S. Bera, K. Khamaru, A. Rahman, and B. Banerji, *Org. Lett.*, 2019, **21**, 9028-9032; (c) M. M. Mane, and D. M. Pore, *J. Chem. Sci.*, 2016, **128**, 657-662.
28. (a) M. M. Elshahawi, A. K. EL-Ziaty, J. M. Morsy, and A. F. Aly, *J. Heterocyclic Chem.*, 2016, **53**, 1443-1448; (b) I. Khan, S. Zaib, S. Batool, N. Abbas, Z. Ashraf, and A. Saeed, *Bioorg. Med. Chem.*, 2016, **24**, 2361-2381.
29. (a) A. D. O. Silva, J. McQuade, and M. Szostak, *Adv. Synth. Catal.*, 2019, **361**, 3050-3067; (b) A. S. Kalogirou, I. C. Christoforou, H. A. Ioannidou, M. J. Manos, and P. A. Koutentis, *RSC Adv.*, 2014, **4**, 7735-7748; (c) V. Coviello, B. Marchi, S. Sartini, L.

- Quattrini, A. M. Marini, F. Simorini, S. Taliani, S. Salerno, P. Orlandi, A. Fioravanti, T. D. Desidero, D. Vullo, F. D. Settimo, C. T. Supuran, G. Bocci, and C. L. Motta, *J. Med. Chem.*, 2016, **59**, 6547-6552; (d) X-W. Chen, Y-Y. Sun, L. Fu, and J-Q. Li, *Eur. J. Med. Chem.*, 2016, **123**, 332-353.
30. E. Krzyżak, M. Śliwińska, and W. Malinka, *J Fluoresc*, 2015, **25**, 277-282.
31. (a) I. Azad, F. Hassan, M. Saquib, N. Ahmad, A. R. Khan, A. G. Al-Sehemi, and M. Nasibullah, *Orient. J. Chem.*, 2018, **34**, 1670-1700; (b) R. Kaur, V. Rani, V. Abbot, Y. Kapoor, D. Konar, and K. Kumar, *J Pharm Chem Chem Sci.*, 2017, **1**, 17-32; (c) F. R-Charati, Z. Hossaini, M. A. Khalilzadeh, and H. Jafaryan, *J. Heterocycl. Chem.*, 2012, **49**, 217-220.
32. (a) G. Murineddu, G. Loriga, E. Gavini, A. T. Peana, A. C. Mule, and G. A. Pinna, *Arch. Pharm. Pharm. Med. Chem.*, 2001, **334**, 393-398; (b) S. B. Etcheverry, D. A. Barrioa, A. M. Cortizoa, and P. A. M. Williams, *J. Inorg. Biochem.*, 2002, **88**, 94-100; (c) D. R. Artis, I-S. Cho, and J. M. Muchowski, *JAI Press Inc.*, 1992, **1**, 109-135; (d) L. R Sun, S. X. Wang, and X. J. Li, *Asian Nat. Prod. Res.*, 2005, **7**, 127-130; (e) A. Dinsmore, K. Mandy, and J. P. Michael, *Org. Biomol. Chem.*, 2006, **4**, 1032-1037; (f) Y. Zhang, J. Zheng, S. Cui, *J. Org. Chem.*, 2014, **79**, 6490-6500.
33. (a) V. Sharma, P. Kumar, and D. Pathak, *J. Het. Chem.*, 2010, **47**, 491-502; (b) T. V. Sravanthi, and S. L. Manju, *Eur. J. Pharm. Sci.*, 2016, **91**, 1-10; (c) S. Lal, and T. J. Snape, *Curr. Med. Chem.*, 2012, **19**, 4828-4837.
34. (a) S. Nandi, and J. K. Ray, *Tetrahedron Lett.*, 2011, **52**, 6203-6206; (b) H-M. Huang, J-R. Gao, L-F. Hou, J-H. Jia, L. Han, Q. Ye, and Y-J. Li, *Tetrahedron*, 2013, **69**, 9033-9037.
35. S. Mukherjee, S. Hazra, S. Chowdhury, S. Sarkar, K. Chattopadhyay, and A. Pramanik, *J. Photochem. Photobiol. A*, 2018, **364**, 635-644.
36. O. V. Ershov, S. V. Fedoseev, M. Y. Ievlev, and M. Y. Belikov, *Dyes Pigm.*, 2016, **134**, 459-464.
37. (a) A. Loudet and K. Burgess, *Chem. Rev.*, 2007, **107**, 4891-4932; (b) J. Wang, N. Boens, L. Jiao, and E. Hao, *Org. Biomol. Chem.*, 2020, **18**, 4135-4156.
38. (a) C. Bulumulla, R. Gunawardhana, P. L. Gamage, J. T. Miller, R. N. Kularatne, M. C. Biewer, and M. C. Stefan, *ACS Appl. Mater. Interfaces*, 2020, **12**, 32209-32232; (b) M-J. Jiang, W-J. Xiao, J-C. Huang, W-S. Li, and Y-Q. Mo, *Tetrahedron*, 2016, **72**, 979-984.

39. H. Wu, Y. Wang, X. Qiao, D. Wang, X. Yang, and H. Li, *Chem. Mater.*, 2018, **30**, 6992-6997.
40. M. Takase, T. Narita, W. Fujita, M. S. Asano, T. Nishinaga, H. Benten, K. Yoza, and K. Müllen, *J. Am. Chem. Soc.*, 2013, **135**, 8031-8040.
41. (a) Z. Wang, B. Jia, G. Cai, J. Wang, Y. Li, P. Xue, X. Lu, Y. Lin, G. Wang, and X. Zhan, *Dyes Pigm.*, 2021, **195**, 109705; (b) C. H. Woo, P. M. Beaujuge, T. W. Holcombe, O. P. Lee, and J. M. J. Fréchet, *J. Am. Chem. Soc.*, 2010, **132**, 15547-15549.
42. (a) N. Wang, Q-S. Gu, Z-L. Li, Z. Li, Y-L. Guo, Z. Guo, and X-Y. Liu, *Angew. Chem. Int. Ed.*, 2018, **57**, 14225-14229; (b) M. B. Johansen, A. B. Leduc, and M. A. Kerr, *Synlett*, 2007, **16**, 2593-2595; (c) L. Yang, G. Deng, D-X. Wang, Z-T. Huang, J-P. Zhu, and M-X. Wang, *Org. Lett.*, 2007, **9**, 1387-1390; (d) D. J. Abraham, R. D. Rosenstein, R. L. Lyon, and H. H. S. Fong, *Tetrahedron Lett.*, 1972, **10**, 909-912; (e) J. H. Cardellina, F-J. Marner, R. E. Moore, *Science*, 1979, **204**, 193-195; (f) H. Zhang, S. Qiu, P. Tamez, G. T. Tan, Z. Aydogmus, N. V. Hung, N. M. Cuong, C. Angerhofer, D. D. Soejarto, J. M. Pezzuto, and H. H. S. Fong, *Pharm. Biol.*, 2002, **40**, 221-224; (g) M. Choury, A. B. Lopes, G. Blond, and M. Gulea, *Molecules*, 2020, **25**, 3147; (h) R. L. Reyes, T. Iwai, and M. Sawamura, *Chem. Rev.*, 2021, **121**, 8926-8947.
43. (a) M. Baumann, and I. R. Baxendale, *J. Org. Chem.*, 2015, **80**, 10806-10816; (b) G. Lahm, A. Stoye, and T. Opatz, *J. Org. Chem.*, 2012, **77**, 6620-6623.
44. (a) U. C. Rajesh, U. Gulati, and D. S. Rawat, *ACS Sustainable Chem. Eng.*, 2016, **4**, 3409-3419; (b) M. C. Al-Matarneh, R-M. Amārandi, I. I. Mangalagiu, and R. Danac, *Molecules*, 2021, **26**, 2066; (c) F-s. Wu, H-y. Zhao, Y-l. Xu, K. Hu, Y-m. Pan, and X-l. Ma, *J. Org. Chem.*, 2017, **82**, 4289-4296; (d) C. Nanjappa, S. K. T. Hanumanthappa, N. Gopalpur, S. Ganapathy, S. D. Shruthi, S. More, G. Jose, H. B. V. Sowmya, and R. S. Kulkarni, *Synth. Commun.*, 2015, **45**, 2529-2545.
45. D. Wu, L. Chen, S. Ma, H. Luo, J. Cao, R. Chen, Z. Duan, and F. Mathey, *Org. Lett.*, 2018, **20**, 4103-4106.
46. S. Khopkar, M. Jachak, and G. Shankarling, *Dyes Pigm.*, 2019, **161**, 1-15.
47. T. U. Kumar, S. Pawar, A. Nag, and A. Bhattacharya, *J. Fluoresc.*, 2019, **29**, 271-277.

Chapter 2

Methodologies and Materials

This chapter explains the materials used during the entire research project and also described the analytical instrumental details related to the research work.

2.1. Chemicals and solvents:

All commercially available chemicals and solvents are used in this entire study which has been given in **Table 2.1.1** (chemicals) and **Table 2.1.2** (solvents).

2.1.1. Used chemicals with their manufacturers:

Name of Chemicals	Manufacturer
7-Methoxy-1-tetralone, 6-Methoxy-1-tetralone, 5-Methoxy-1-tetralone, 2-Bromobenzaldehyde, Cyclopentanone, Cycloheptanone, 1-Acetylpyrene, Anthranilamide, 5,8-Dimethoxy-1-tetralone, 5-Methoxy-2-tetralone, 8-Methoxy-2-tetralone, 2-Phenylacetophenone, Chroman-4-one, 6-Chloro-4-chromanone, 3'-Methylacetophenone, 2-Aminobenzylamine, 2-Acetylnaphthalin, tert-Butyl acrylate, 2'-Nitroacetophenone	Sigma-Aldrich
4-Methyl-1-tetralone, 7-Bromo-1-tetralone, 7-Chloro-1-tetralone, 7-Nitro-1-tetralone, 5-Chloro-2-nitrobenzaldehyde, Copper(II) trifluoromethanesulfonate, 4-Bromo-2-nitrobenzaldehyde	BLD pharm
Cyclohexanone, Cyclooctanone, Acetophenone, Trifluoroacetic acid, Ammonium chloride, Sodium carbonate, Acetic acid, Acrylonitrile, TLC Silica gel 60 F ₂₅₄ , Phenol, Vanillin, Potassium thiocyanate	MERCK

Name of Chemicals	Manufacturer
Ammonium thiocyanate, 4-Bromoaniline, Palladium(II) acetate, Palladium(II) chloride	HIMEDIA
Potassium-tert-butoxide, Sodium hydride, Phosphorous tribromide, 1-tetralone, Hydrazine hydrated, Methyl acrylate	SPECTROCHEM PVT. LTD.
4-Chloroaniline, <i>p</i> -toluidine, Sodium hydrogen carbonate, <i>p</i> -Chlorophenol, Picric acid	LOBA chemie
N-Bromo succinimide, <i>o</i> -Nitrophenol, Tetrabutylammoniumbromide, 3-Aminothiophene-2-carboxamide	SRL
Sodium dithionite, 2-Nitrobenzaldehyde, Aminoacetaldehyde dimethyl acetal	Avra Synthesis PVT. LTD.
Acrylonitrile, Sodium sulphate	RANKEM
Ethyl acrylate, Isatoic anhydride	SDFCL
<i>p</i> -Nitrophenol, <i>m</i> -Nitrophenol, Benzoic acid, <i>p</i> -Nitrobenzoic acid, Potassium carbonate	NICE CHEMICAL Pvt. Ltd.
MTT reagent for cell culture	SRL

2.1.2. Used solvents with their manufacturers:

Name of Solvents	Manufacturer
Methanol, Ethanol, Petroleum ether, Hexane, Ethyl acetate, Acetone, <i>N, N</i> -Dimethylformamide, Tetrahydrofuran, 1,4-Dioxane, Dimethyl sulphoxide, Triethyl amine, Diethyl ether	RANKEM
Acetonitrile, DMSO- <i>d</i> ⁶ , Chloroform- <i>d</i>	Sigma-Aldrich
Chloroform, Toluene, Dichloromethane	MERCK
1,2-Dichloroethane	SRL

2.2. Methodologies:

2.2.1. Crystallographic data analysis:

Single crystals of synthesized compounds were recorded on a CMOS based Bruker D8 Venture PHOTON 100 diffractometer at 298K equipped with a INCOATEC micro-focus source with graphite monochromatic Mo K α radiation ($\lambda = 0.71073 \text{ \AA}$) operation at 50 kV and 30 mA. Information of the Single crystal was obtained by sending the cif file to the Cambridge crystallographic data center (CCDC).

2.2.2. NMR spectra:

Bruker-Advanced Digital instruments were used for recording the ^1H NMR and ^{13}C NMR spectra. ^1H NMR spectra were recorded on 300 MHz, 400 MHz, and 500 MHz instruments using $\text{CDCl}_3/\text{DMSO-}d_6$ solvents, while tetramethylsilane (TMS) was used as an internal standard. Chemical shifts were recorded in ppm units. ^{13}C NMR (75 MHz, 100 MHz, and 125 MHz) spectral analysis was recorded on a 300 MHz, 400 MHz, and 500 MHz instrument with proton decoupling.

2.2.3. Mass spectra:

ESI-HRMS spectra were recorded on XEVO G2-XS QTOF and Waters Xevo G-2 S QTOF instrument with electrospray ionization mass spectrophotometer.

2.2.4. UV-Visible and Fluorescence spectroscopy:

The UV/Vis absorption spectral data were recorded on Shimadzu UV-2450 UV/vis spectrophotometer, Labtronics Model LT-291, and Shimadzu UV spectrophotometer UV-1800. The emission spectral data were recorded on Photon Technology International S/N-3201, PerkinElmer Fluorescence Spectrometer (Model LS 45), and Jobin Yvon Fluoromax spectrofluorometer.

2.2.5. Chromatography:

Chromatographic purifications were performed with 60–120 mesh or 100–200 mesh silica gel in SRL grade. For reaction monitoring, commercially available pre-coated silica gel 60 F254 TLC sheets were used. A fractional mixture of petroleum ether and ethyl acetate was used as an eluent. Molecular sieves (4 \AA) were used to distil and store the solvents.

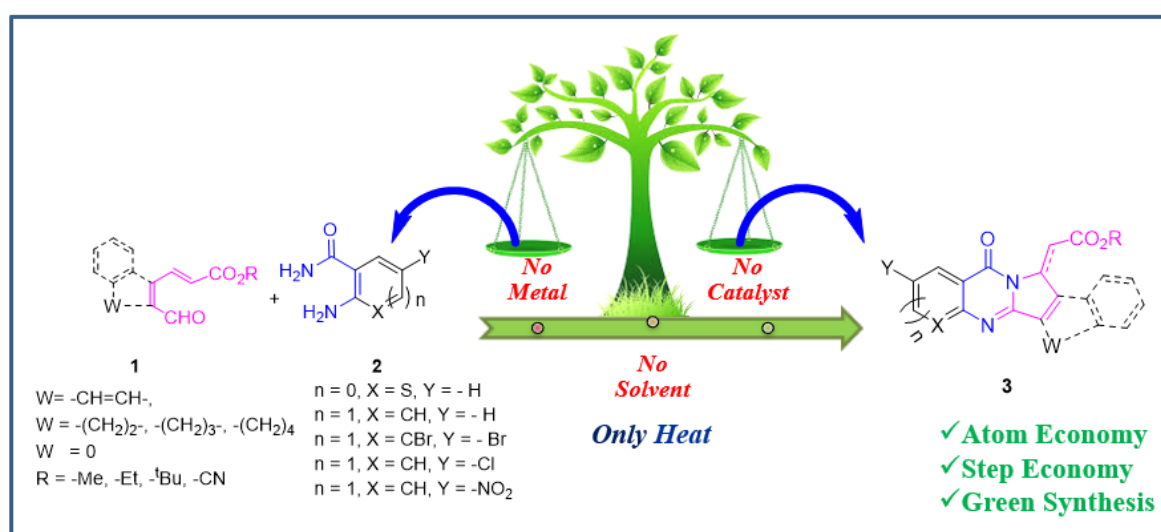
2.2.6. Cell culture:

PC3 and HepG2 cells were kept alive in RPMI containing 10% fetal bovine serum, $1 \times$ non-essential amino acid, L-glutamine (2 mM), streptomycin (100 U/mL), and penicillin (100 U/mL) at 37 °C, 5% CO₂, and 95% relative humidity (RH). After overnight cell germination, aphidicolin (6 μ M) was applied to the cells in an exponential phase.

Chapter 3

*A solvent- and catalyst-free tandem reaction:
synthesis, and photophysical and biological
applications of isoindoloquinazolinones*

A solvent- and catalyst-free tandem reaction: synthesis, and photophysical and biological applications of isoindoloquinazolines



(Contents of this chapter have been published in *New J. Chem.*, 2020, **44**, 4324-4331)

3.1. Introduction:

Quinazolinones always get a special honour due to their wide abundance in several biologically active natural products, pharmaceuticals, and agrochemicals.^{1a} Substituted quinazolinones have drawn our attention because of their significant bioactivities, such as anticancer, antidiabetic, anti-inflammatory, antimicrobial, antitubercular, and antiviral properties.¹

3.1.1. Quinazolinone based natural alkaloids:

Quinazolinone scaffolds are found in approximately more than 200 bioactive naturally occurring alkaloids isolated from various plants and various microorganisms.^{1e} Among various quinazolinone compounds, Luotonin A², a well-known alkaloid found in *Peganum nigellastrum*, displays significant cytotoxicity towards leukaemia P388 cells. Vasicione³, extracted from the leaves of *Adhatoda vasica* Nees, has inhibitory effects on bronchodilatory disease. Tryptanthrin,⁴ Isaindigotone,⁵ and Wuzhuyurutine A⁶ show potential activities against cancer cell lines, inflammatory condition and gastrointestinal disorders respectively (**Figure 3.1**).

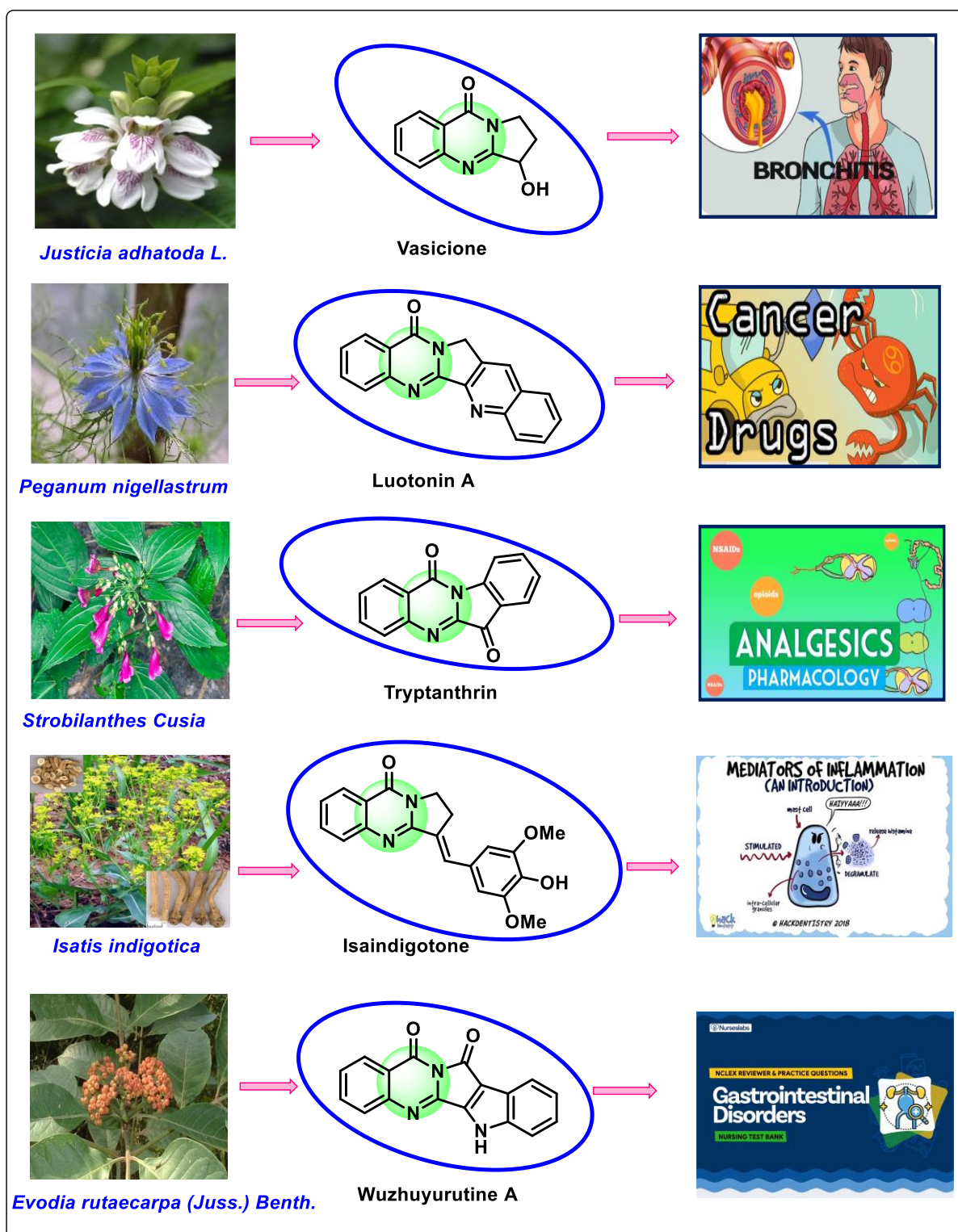


Figure 3.1. Isoindoloquinazolinone based naturally occurring bioactive alkaloids.

3.1.2. Application in pharmaceutical chemistry:

Besides their diverse and significant pharmacological activities, quinazolinones are ubiquitously found in many marketed drugs that are clinically used and prescribed for the treatment of various diseases (**Figure 3.2**).^{7a} Anagrelide is chemically known as 6,7-dichloro-1,5-dihydroimidazo(2,1-*b*)quinazolin-2(3*H*)-one and it is used for the treatment of thrombocytosis and chronic myeloid leukaemia.^{7b, c} Evodiamine, extracted from the *Evodia* plants, reduces the uptake of fat in animal models. It can also help inhibit the growth of cancer cells.^{1e, 7c} Afloqualone is prescribed as a sedative and muscle relaxant drug with the trade name Arofuto®.^{1e, 7c} The brand names of quazinone are dozonone and posicor, which is chemically known as (3*R*)-6-chloro-3-methyl-5,10-dihydroimidazo[2,1-*b*]quinazolin-2(3*H*)-one. It is very useful for the treatment of heart disease, especially as a vasodilator and cardiotoxic drug.^{7c}

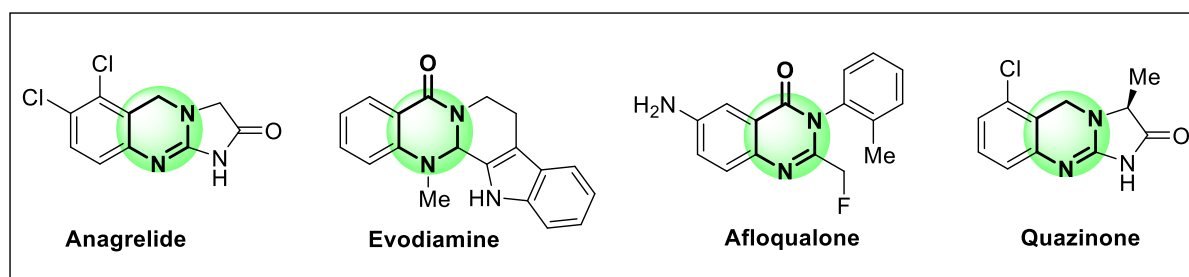


Figure 3.2. Some quinazolinone embedded marketed drug molecules.

3.1.3. Photophysical properties of quinazolinone scaffolds:

Since, quinazolinone scaffolds are widely distributed in nature and frequent application in biology, so researchers are continuously finding the application in photophysical properties for cell-imaging studies. Quinazolinone-based another probe, QBH involves fluorescence on-off mechanism in presence of HClO/ClO^- . This probe helps to cell imaging detection of hypochlorite in living cells and especially, it is effective to detect the hypochlorite in water sample (**Figure 3.3**).⁸

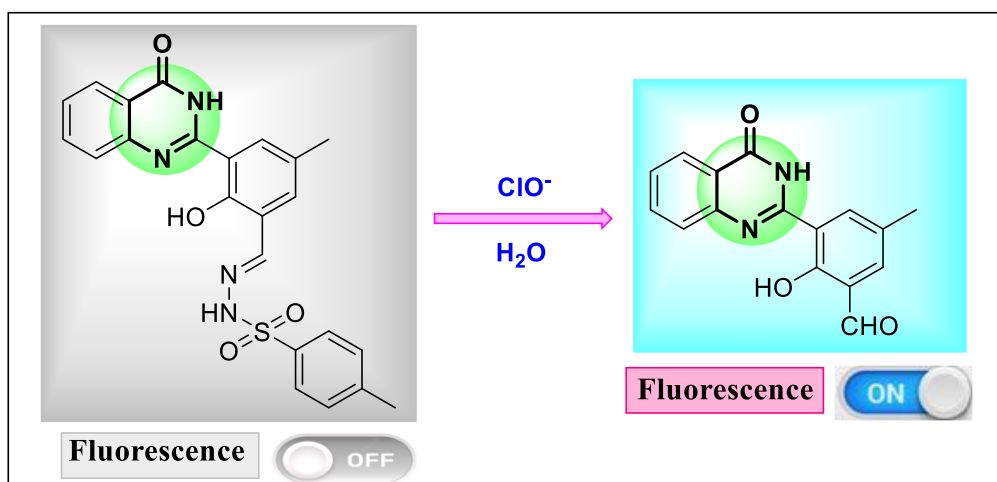


Figure 3.3. QBH probe displayed fluorescence quenching with hypochlorite.

3.1.4. Multiple properties of quinazolinone-based fluorescence dye:

A fluorescence probe is a very powerful tool in biological research. A quinazolinone-based novel dye, 6-dimethylamino-2-(quinolin-2-yl)-quinazolin-4(3*H*)-one (DMAQQ), exhibited bright green fluorescence in the presence of HeLa cells excited by one and two photons and offers a new platform for bio-imaging applications (**Figure 3.4**).⁹

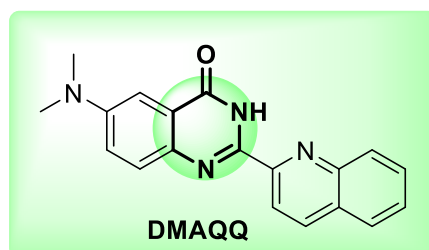


Figure 3.4. DMAQQ, quinazolinone based novel dye.

3.1.5. Application in material science:

The novel quinazolinone-containing chelating ligand 2,4-[bis-(2,4-dihydroxybenzylidene)]-dihydrazinoquinazolinone (DBHQ) can bind with the Ga^{3+} ion, forms a DBHQ- Ga^{3+} complex and hence, it has been used as an element in the semiconductor industry and electronic instruments. The fluorescence intensity of this complex is also increased by the addition of some phosphorylated compounds. When phosphorylated amino acids such as serine and tyrosine, glucose-6-phosphate (G6P), and pyridoxal-5-phosphate (PLP) were added to the DBHQ- Ga^{3+} complex, the fluorescence quantum yield of the complex increased many fold (1.38–1.59 times) (**Figure 3.5**).¹⁰

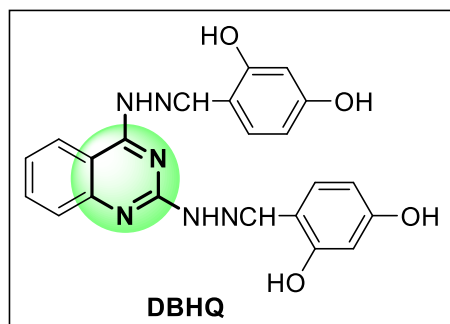


Figure 3.5. DBHQ, a quinazolinone embedded semiconductor.

3.1.6. Application in Co-ordination Chemistry:

Novel 3-aryl-4(3*H*)-quinazolinone-2-carboxaldehyde thiosemicarbazones usually react with metal ions and produce a chelating complex, where the ligand plays the role of a chelating agent. This thiosemicarbazone derivative of 4(3*H*)-quinazolinone-2-carboxaldehyde can easily bind with copper (II) and zinc (II) metal ions (**Figure 3.6**). The copper (II) chelating complexes have potential activity against cancer cells. The zinc complex is well-known to show various biological activities such as analgesic, anticonvulsant, antimicrobial, and cytotoxic activities towards Ehrlich Ascites Carcinoma cells.¹¹

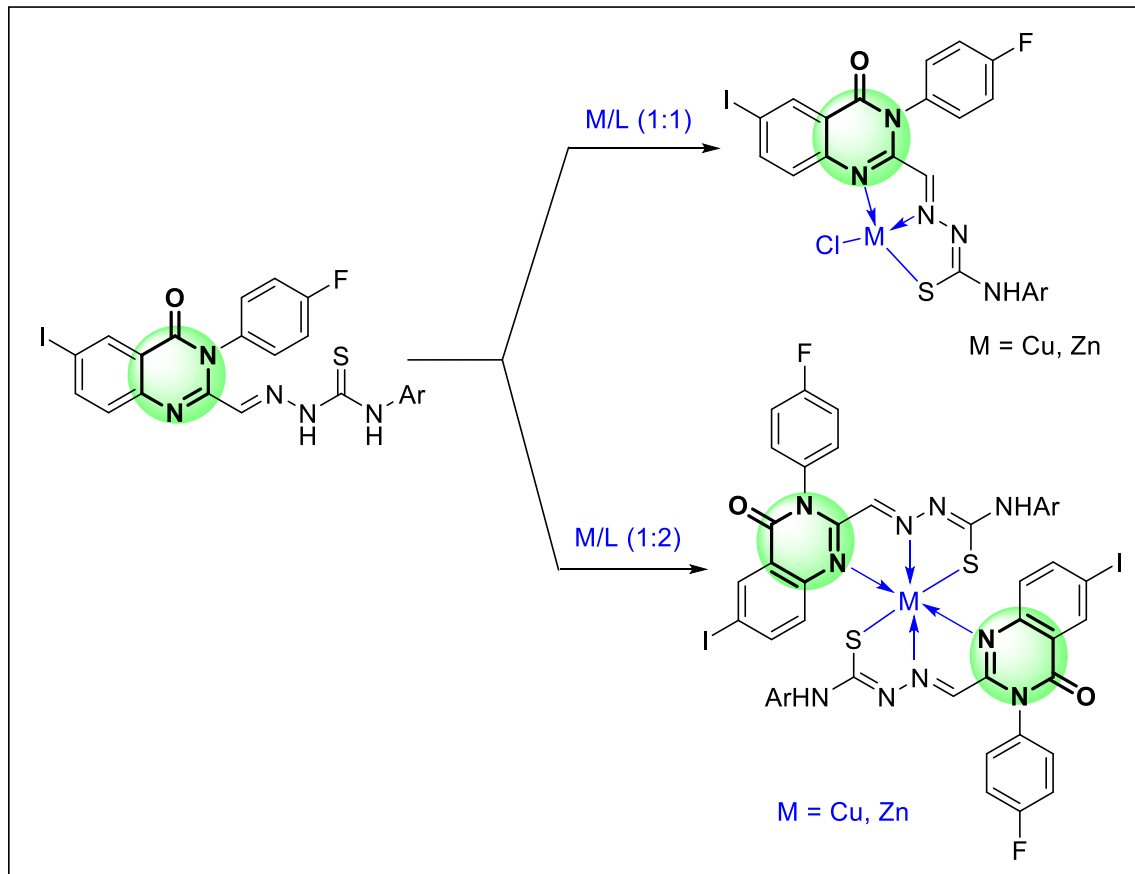


Figure 3.6. Quinazolinone based chelating complexes.

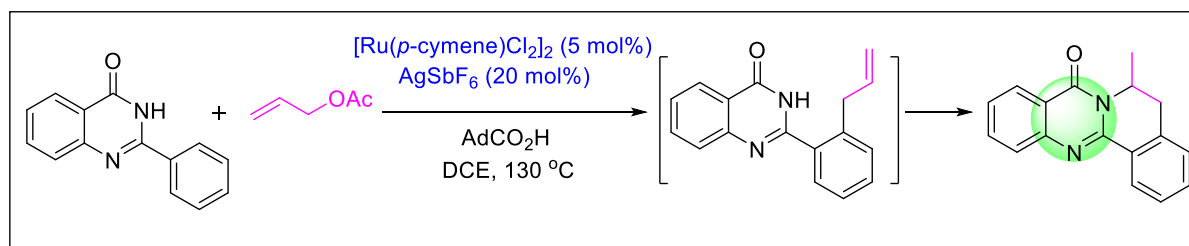
After a prolonged investigation on the applications of quinazolinones and fused quinazolinones, we are currently focused on the various synthetic methods of fused quinazolinones that have been developed using green and conventional approaches.

3.2. Literature Survey:

3.2.1. Traditional pathways towards quinazolinone synthesis:

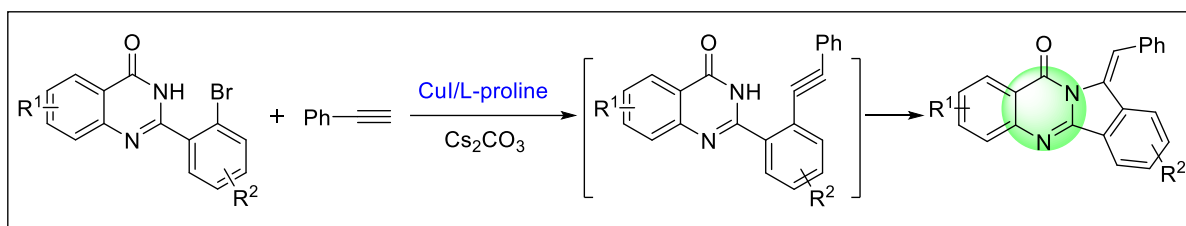
(i) Metal-catalyzed approaches:

R. Jana *et al.*^{1a} established ruthenium (II)-catalyzed neutral *C-H* allylation for the synthesis of dihydroisoquinolino[1,2-*b*]quinazolinones by using 2-arylquinazolinones and allyl acetate. This tandem protocol involves *C-H* allylation at first, then hydroamination takes place *via* intermolecular fashion with -CONH group present in close proximity. No external oxidant such as copper (II) or silver (I) salts are required; this reaction proceeds only in the presence of a ruthenium (II) catalyst *via* a redox-neutral protocol. The highly selective product can be achieved smoothly in a very short time and in a single operation (**Scheme 3.1**).



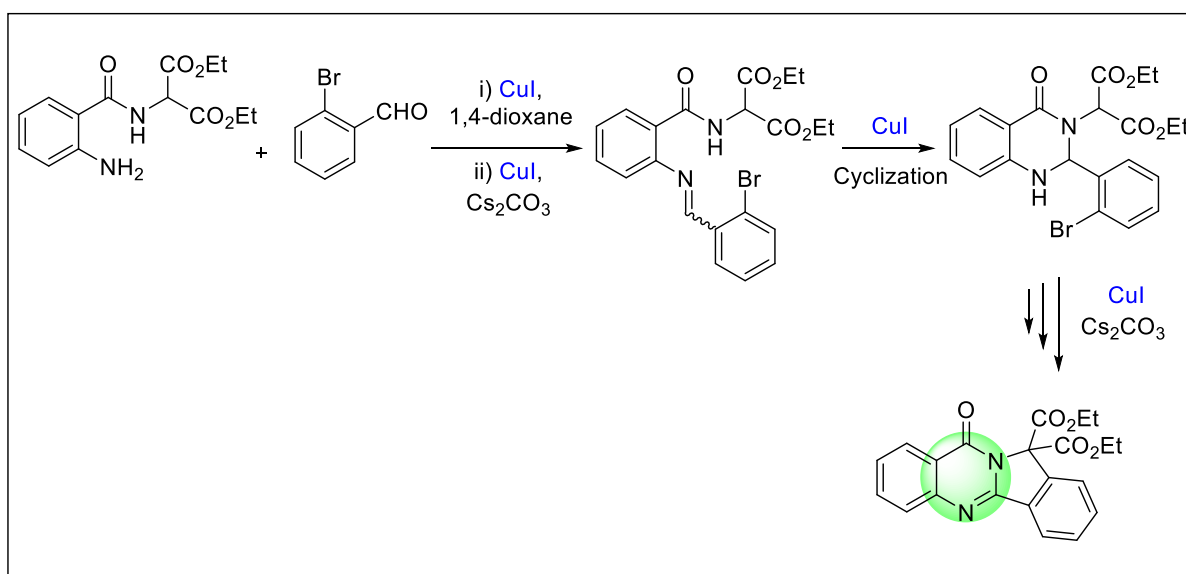
Scheme 3.1. Ruthenium (II)-catalyzed neutral *C-H* allylation/Hydroamination Cascade reaction access to dihydroisoquinolino[1,2-*b*]quinazolinones.

J. Q. Liu *et al.*¹² have reported consecutive Cu-catalyzed Sonogashira coupling and hydroamination protocols for the isoindolo[1,2-*b*]quinazolin-10(12*H*)-one synthesis. From retrosynthesis analysis, it was found that 2-(2-bromophenyl)quinazolin-4(3*H*)-one, a good precursor, was prepared from *o*-bromobenzaldehyde and 2-aminobenzamide. At first, 2-(2-bromophenyl)quinazolin-4(3*H*)-one involves Sonogashira coupling with phenylacetylene in the presence of CuI/L-proline and Cs₂CO₃ in dioxane solvent, and then intra-molecular hydroamination cyclization takes place as there -CONH group present in the intermediate. To enhance the substrate scope, they used electron-donating and electron-withdrawing substituents on the benzene ring, and they obtained moderate to excellent yield (**Scheme 3.2**).



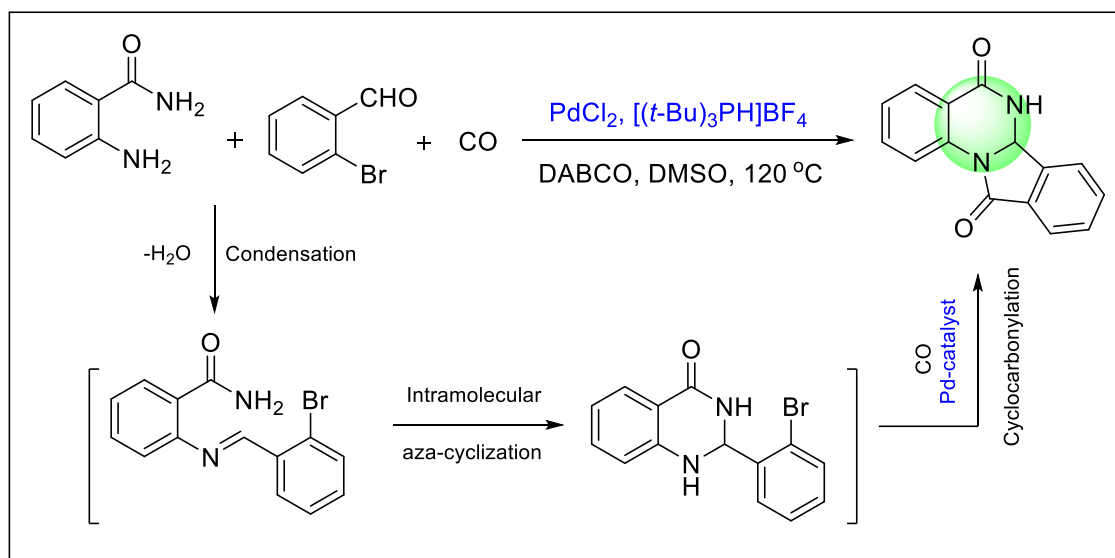
Scheme 3.2. Cu-catalyzed synthesis of isoindolo[1,2-*b*]quinazolin-10(12*H*)-one via Sonogashira coupling and hydroamination reaction.

X. S. Wang and his co-worker¹³ developed the first copper (I)-catalyzed synthetic protocol of isoindolo[1,2-*b*]quinazoline derivatives. For this transformation, they have selected 2-bromobenzaldehyde and diethyl 2-(2-aminobenzamido)malonates as reactant partners. These two reacting partners react with each other in the presence of CuI and Cs₂CO₃ by using 1,4-dioxane solvent, resulting in novel isoindolo[1,2-*b*]quinazoline derivatives with moderate to excellent yields (**Scheme 3.3**).



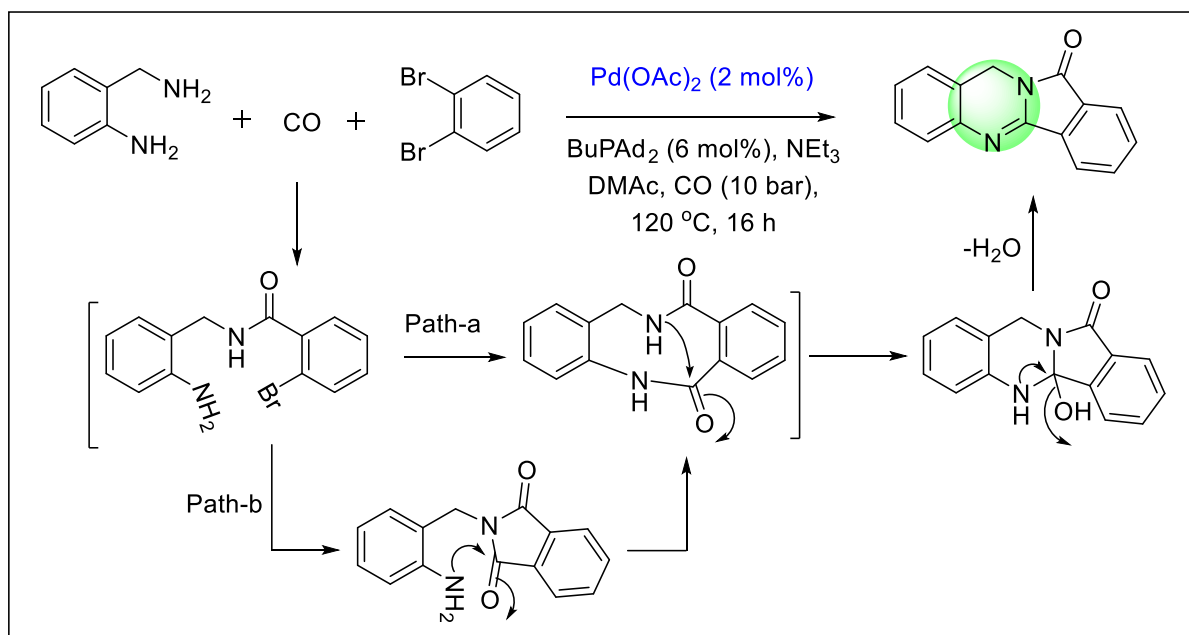
Scheme 3.3. Copper-catalyzed synthetic protocol of isoindolo[1,2-*b*]quinazoline.

X. Fan and his research group¹⁴ explained a highly efficient, one-pot, three-component palladium-catalyzed cascade pathway for the formation of isoindolo[2,1-*a*]quinazoline derivatives. Herein, they disclose the synthetic pathway starting with commercially available 2-bromobenzaldehydes, 2-aminobenzamides, and carbon monoxide. Here, 2-aminobenzamides underwent condensation reactions with 2-bromobenzaldehydes to form 2,3-dihydroquinazolin-4(1*H*)-ones which cyclocarbonylation in the presence carbon monoxide and Pd catalyst to form the desired ultimate fused product (**Scheme 3.4**).



Scheme 3.4. Palladium-catalyzed three-component cascade protocol of isoindolo[2,1-*a*]quinazoline.

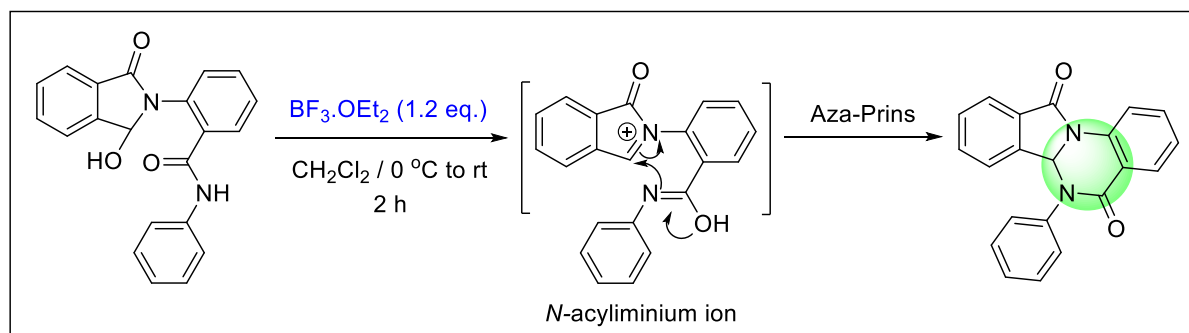
X. F. Wu and his co-workers¹⁵ described a palladium-catalyzed synthetic protocol for isoindoloquinazolinones starting from 2-aminobenzyl amine and 1,2-dibromobenzenes. In the presence of Pd (II) catalyst *via* dicarbonylation followed by the formation of 2-(2-aminobenzyl)isoindoline-1,3-dione and 12,13-Dihydro-5*H*-dibenzo[*b,g*][1,5]-diazonine-6,11-dione intermediate, the desired product isoindoloquinazolinone was obtained (**Scheme 3.5**).



Scheme 3.5. Palladium-catalyzed synthesis of isoindoloquinazolinones *via* dicarbonylation.

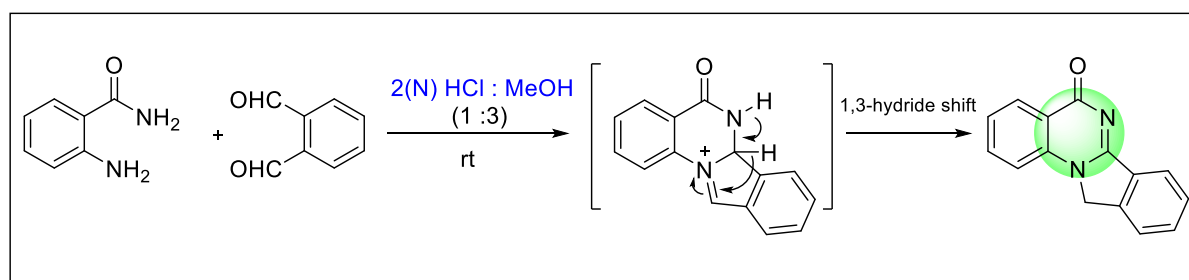
(ii) Metal-free approaches:

A. K. Saikia and his research group¹⁶ introduced a new direction for the synthesis of isoindolo[2,1-*a*]quinazolinones utilizing aza-Prins type intramolecular cyclization. In the presence of Lewis acid, the *N*-acyliminium ion will be generated, and simultaneously the enol form will occur for nucleophilic attack, very similar to aza-Prins type cyclization to produce isoindolo[2,1-*a*]quinazolinones with excellent yields. The major advantages of this strategy are metal-free synthesis, mild reaction conditions, and inexpensive reagents (**Scheme 3.6**).



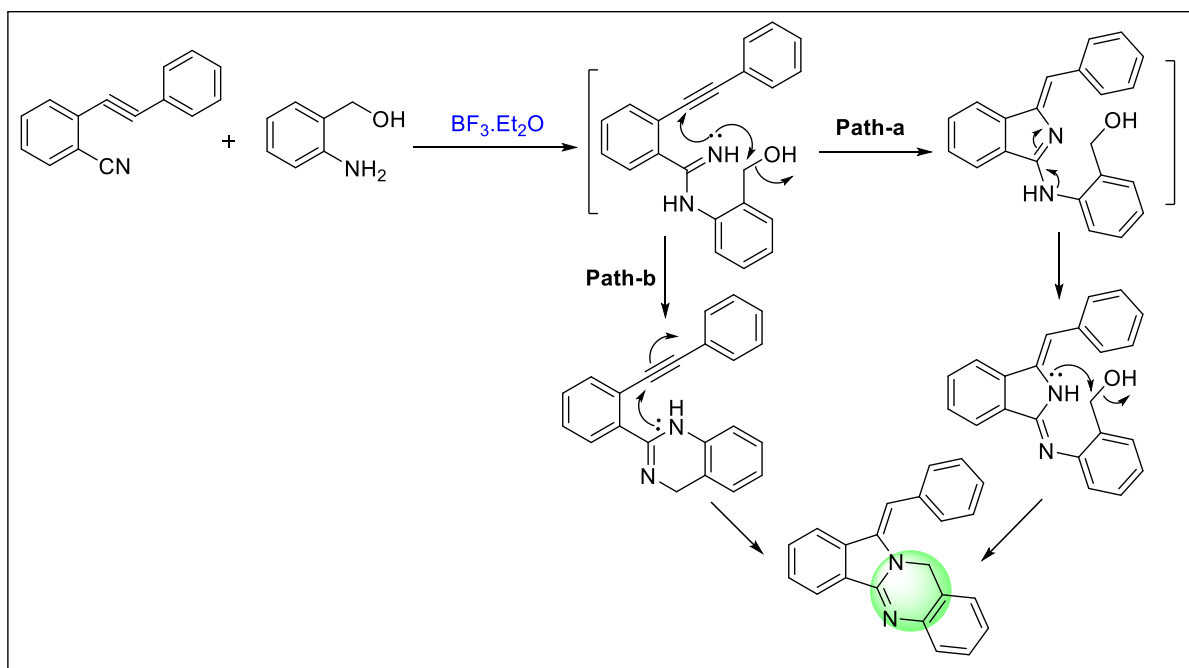
Scheme 3.6. Synthesis of isoindolo[2,1-*a*]quinazolinones *via* aza-Prins cyclization.

A. Mondal *et al.*¹⁷ reported a one-pot synthetic protocol of isoindole-fused quinazolin 4-ones. He has described an acid catalyzed condensation reaction between readily available anthranilamide and dialdehyde. This protocol involves intramolecular 1,3-hydride transfer (**Scheme 3.7**).



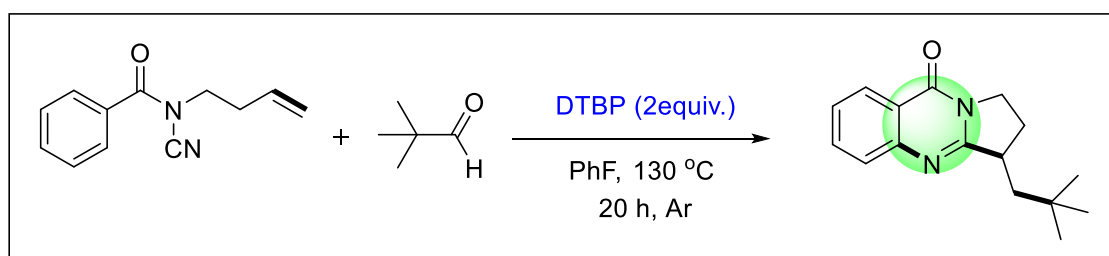
Scheme 3.7. One-pot, acid catalyzed synthesis of isoindole-fused quinazolin 4-ones.

R. Akula and his research group¹⁸ reported a simple, convenient, and efficient one-pot synthetic protocol of tetracyclic isoindoloquinazolinones. From retrosynthetic analysis, it was found that 2-(phenylethynyl) benzonitrile is a good starting material for the synthesis of isoindolo[1,2-*a*]quinazoline. This 2-(phenylethynyl) benzonitrile and (2-aminophenyl) methanol in the presence of Lewis acid, $\text{BF}_3 \cdot \text{Et}_2\text{O}$ involves the formation of two rings *via* the construction of a sequential *C-N* bond and produces 12-benzylidene-10,12-dihydroisoindolo[1,2-*b*]quinazoline derivatives (**Scheme 3.8**).



Scheme 3.8. A convenient one-pot synthetic protocol of tetracyclic isoindoloquinazolinones.

Y. Wang and his co-workers¹⁹ approach a convenient sequential pathway that describes the metal-free annulation of unactivated substituted *N*-cyanamide alkenes and aldehydes for the formation of dihydroisoquinolinones. This strategy involves oxidative cascade decarbonylation of aldehydes with *N*-cyanamide alkenes to construct the *C-C/C-N* bonds (**Scheme 3.9**).

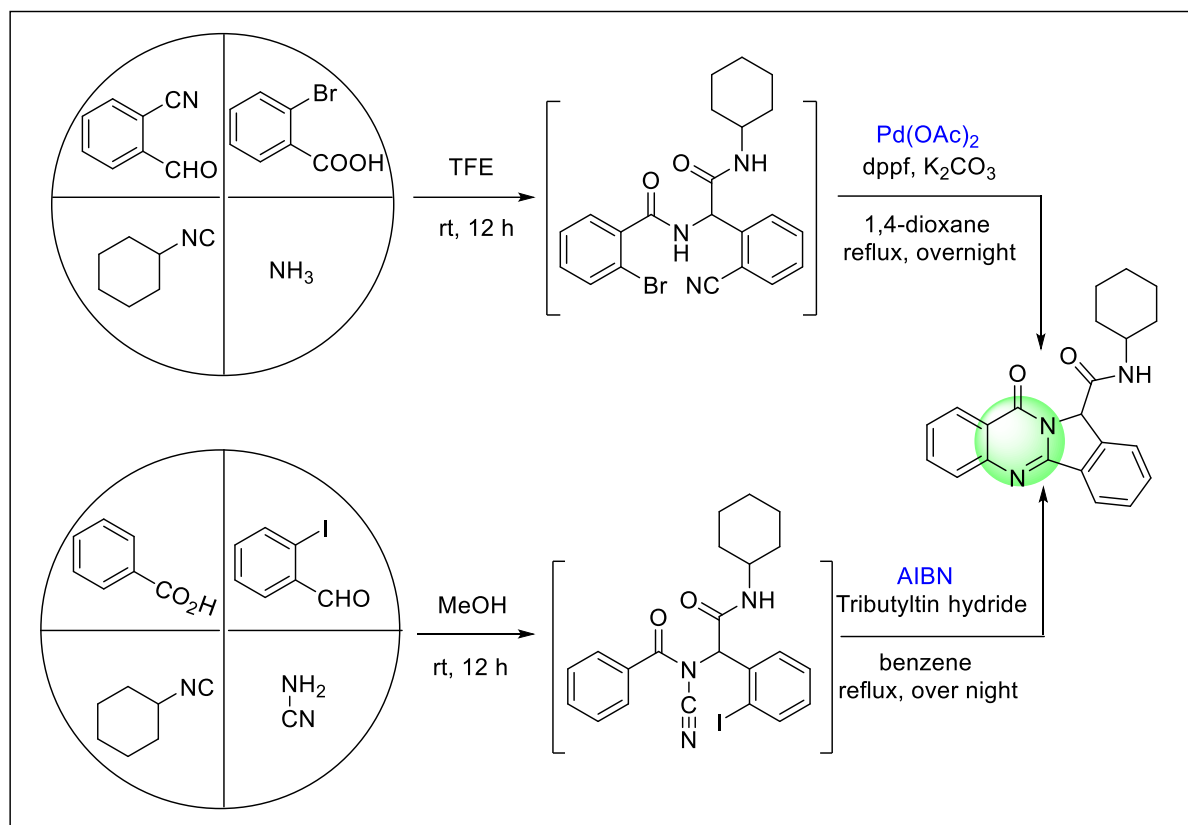


Scheme 3.9. A convenient metal-free decarbonylative annulation of alkenes for the synthesis of dihydroisoquinolinones.

(iii) Tandem approach:

A. Dömling and his co-workers²⁰ developed a multicomponent synthetic approach to diverse polycyclic quinazolinones. Here, the synthetic protocol of isoindolo[1,2-*b*]quinazolinones is described *via* two strategies: The first strategy involves a Pd-catalyzed Ugi four-component reaction (Ugi-4CR) of *o*-cyanobenzaldehyde, *o*-bromobenzoic acid, isocyanide, and ammonia

followed by intramolecular *N*-arylation to get the desired products. The second strategy also involves the Ugi four-component reaction (Ugi-4CR) using benzoic acid, *o*-iodobenzaldehyde, isocyanides, and cyanamide through radical cyclization in the presence of AIBN to construct the quinazolinones (**Scheme 3.10**).



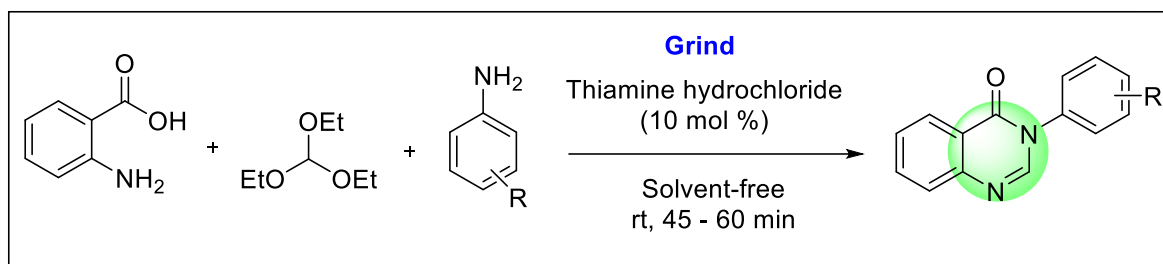
Scheme 3.10. Multicomponent synthetic protocol of polycyclic quinazolinones.

3.2.2. Green pathways towards quinazolinone synthesis:

(i) Synthetic approaches of grinding:

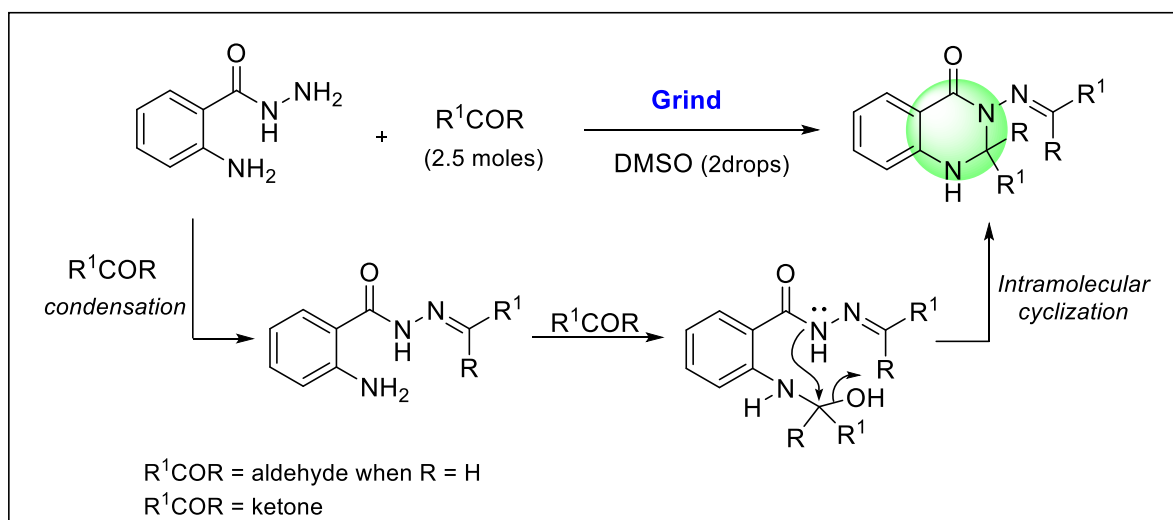
The grinding technique has various interesting benefits, including being an economically effective method, reducing reaction times, and providing high yields. So, it is very useful to us.

Kawade *et al.*²¹ accomplished a solvent-free grinding technique in creating quinazolinone derivatives. They combined anthranilic acid, aromatic amines, and triethyl orthoformate in a mortar for this synthetic purpose and then added an organocatalyst, thiamine hydrochloride (10 mol %). After that, they grind the reacting mixture well with a pestle for 45 to 60 minutes (**Scheme 3.11**).



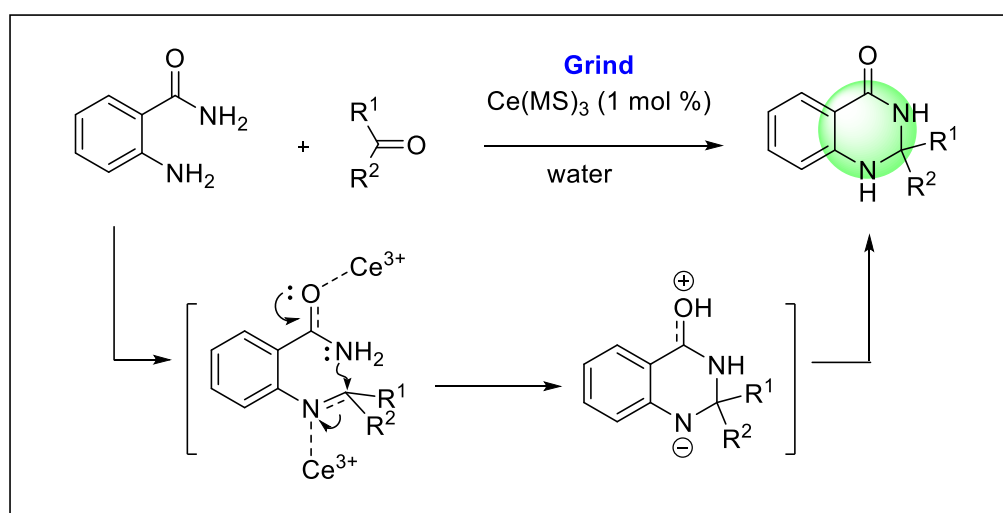
Scheme 3.11. Solvent-free grinding approach of quinazolinone.

A. Kumar and his worker²² described an innovative, green approach for the synthesis of 3-arylideneaminoquinazolin-4(1*H*)-ones by employing a "solvent-assisted grinding" process involving *o*-aminobenzhydrazide and aldehydes or ketones at ambient temperature. The necessary products were quickly created by simply pulverising the reacting particles in the absence of a solvent or using two drops of DMSO solvent (**Scheme 3.12**).



Scheme 3.12. Solvent-assisted grinding technique for the quinazolin-4(1*H*)-ones.

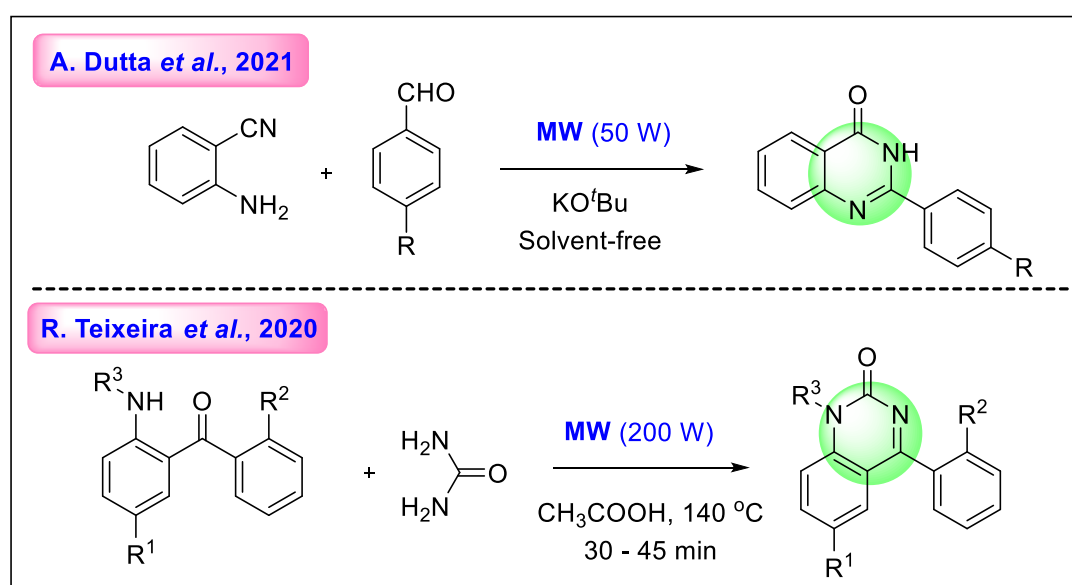
Another research group led by M. Wang²³ also reported a grinding protocol for 2-substituted-2,3-dihydro-4(1*H*)-quinazolinones that uses anthranilamide with aldehydes, or ketones, and cerous methanesulfonate as catalyst for condensation reactions in an aqueous environment (**Scheme 3.13**).



Scheme 3.13. Synthesis 2-substituted-2,3-dihydro-4(1H)-quinazolinones *via* grinding.

(ii) Microwave assisted synthetic approach:

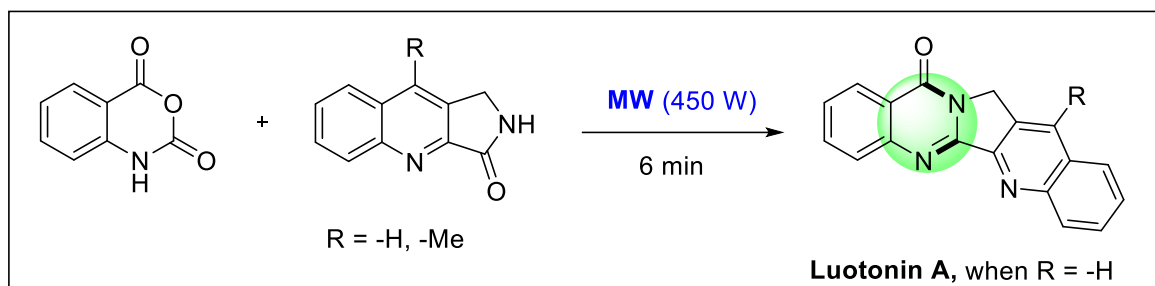
Microwave heating is a powerful tool in green synthesis. Herein, we describe different approaches to quinazolinones *via* microwave irradiation. A metal-, oxidant-, and solvent-free synthetic route has been recognized by D. Sarma *et al.* to make quinazolin-4(3H)-ones using 2-aminobenzonitrile and aldehydes heated in a microwave.²⁴ Another group led by R. Teixeira found a green approach to 4-phenylquinazolin-2(1H)-one derivatives.²⁵ They conducted the reaction in a sealed tube employing 2-aminobenzophenone and urea in acetic acid under microwave irradiation to get the desired product (**Scheme 3.14**).



Scheme 3.14. Various microwave-heating synthetic approach of quinazolinones.

➤ **Microwave assisted solvent-free synthesis of Luotonin:**

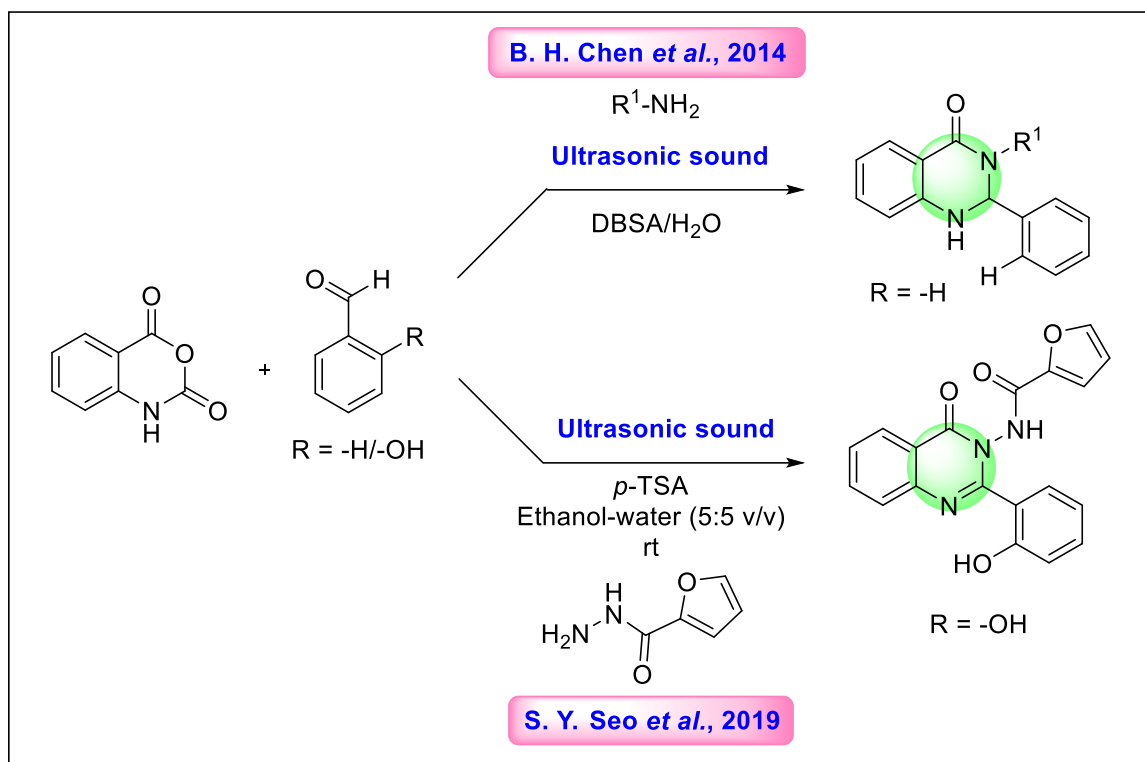
Yadav and Reddy²⁶ exposed the method for making Luotonin A, which is based on a microwave-heated reaction between isatoic anhydride and 3-oxo-1*H*-pyrrolo[3,4-*b*]quinoline under neat conditions. For the synthesis of Luotonin A, the reported protocol was a clean, simple, effective, and high-yielding procedure (**Scheme 3.15**).



Scheme 3.15. Microwave assisted solvent-free synthesis of Luotonin A.

(iii) Synthetic approaches of ultrasonic irradiation:

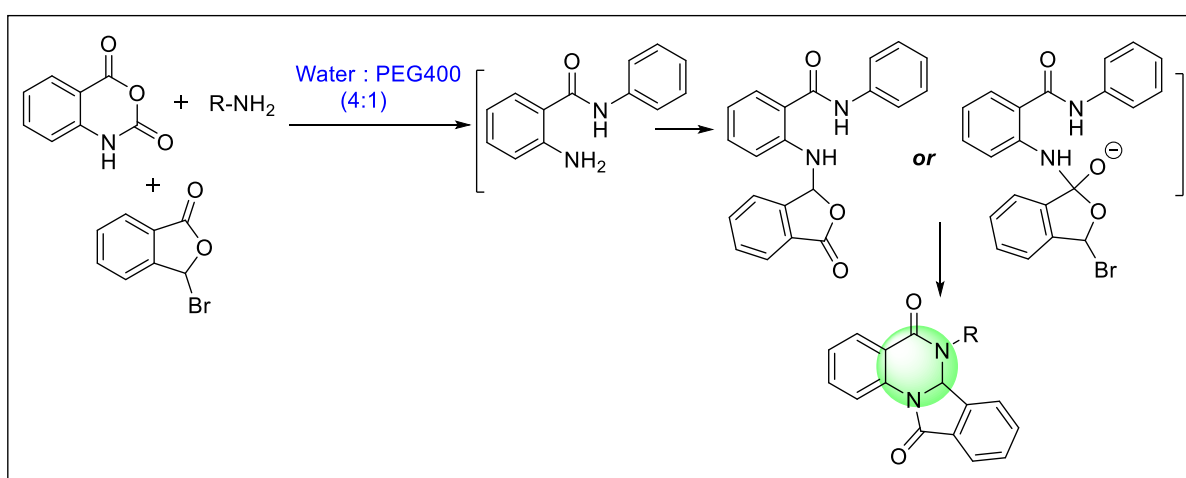
Chen *et al.*²⁷ depicted a three-component, one-pot protocol for the synthesis of 2,3-dihydroquinazolin-4(1*H*)-one by employing isatoic anhydride, amine, and aromatic aldehyde under ultrasonic irradiation. Another research team led by N. C. Dige²⁸ has shown an ultrasound-assisted synthetic route of 4-oxoquinazolin-3(4*H*)-yl)furan-2-carboxamide derivatives starting from isatoic anhydride, salicylaldehydes, and 2-furoic hydrazide using *p*-TSA in an ethanol-water medium. This superior technique reduces the reaction time, involves mild reaction conditions, and provides high yields (**Scheme 3.16**).



Scheme 3.16. Various synthetic approach of quinazolinones *via* ultrasound irradiation.

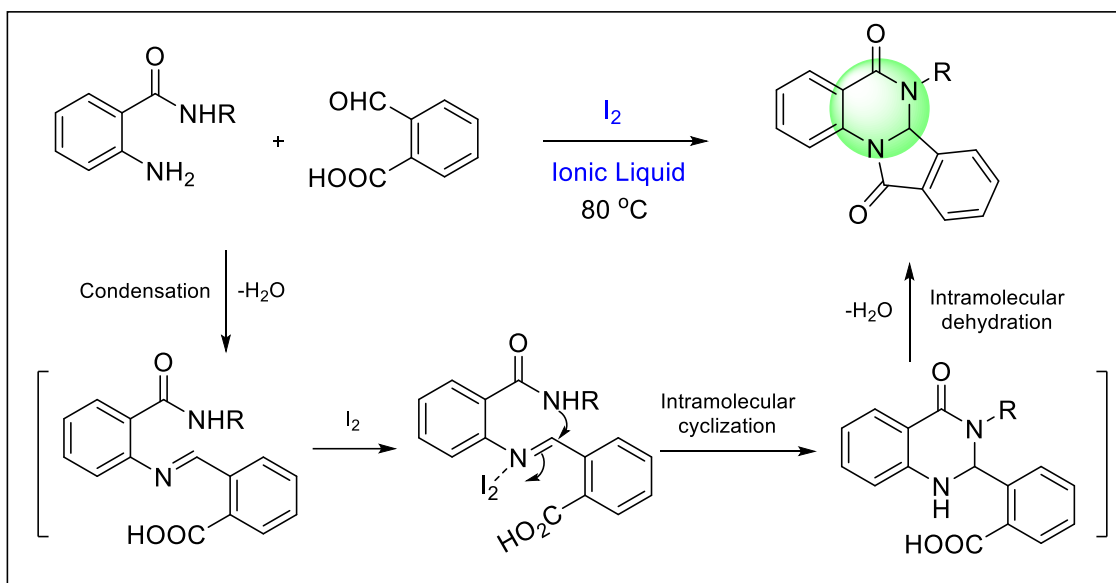
(iv) Synthetic approaches using green solvents:

R. Akula²⁹ also reported another pathway, i.e., a catalyst- and metal-free, green pathway for the synthesis of quinazoline derivatives starting from isatoic anhydride. At first, isatoic anhydride reacts with amine partners; decarboxylation occurs, then it reacts with 3-bromoisobenzofuran-1(3*H*)-one and produces dihydroisobenzofuranquinazolinone derivatives with good yields. The entire protocol involves the formation of two rings governed by the C-N bond (**Scheme 3.17**).



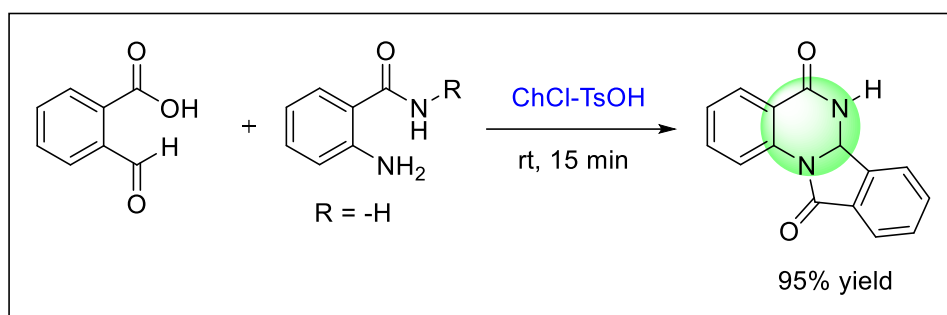
Scheme 3.17. Catalyst- and metal-free green protocol of fused quinazoline derivatives.

L. Lu *et al.*³⁰ depicted an ionic liquid-mediated green synthetic protocol of isoindolo[2,1-*a*]quinazoline derivatives based on an iodine-catalyzed reaction between 2-aminobenzamides and 2-formylbenzoic acid. At first, these two reacting partners underwent condensation reactions, then acylamino groups were attacked in intramolecular fashion in the iodine-activated intermediate, and finally, intramolecular cyclization took place by eliminating the water molecules to produce the isoindolo[2,1-*a*]quinazoline moieties (**Scheme 3.18**).



Scheme 3.18. Ionic liquid mediated synthetic protocol of isoindolo[2,1-*a*]quinazoline.

An environmentally acceptable, one-pot, highly efficient protocol was developed by R. V. Devi *et al.*³¹ for the synthetic purpose of isoindolo[2,1-*a*]quinazoline by using deep eutectic solvents. Recently, deep eutectic solvents have been recognized as green solvents due to their biodegradable, non-volatile, nontoxic, non-flammable, recyclable, and inexpensive properties. Herein is described a reaction between 2-formylbenzoic acid and various easily available 2-aminobenzamide derivatives in the presence of DESs (ChCl-TsOH) to obtain the isoindolo[2,1-*a*]quinazoline derivatives (**Scheme 3.19**).

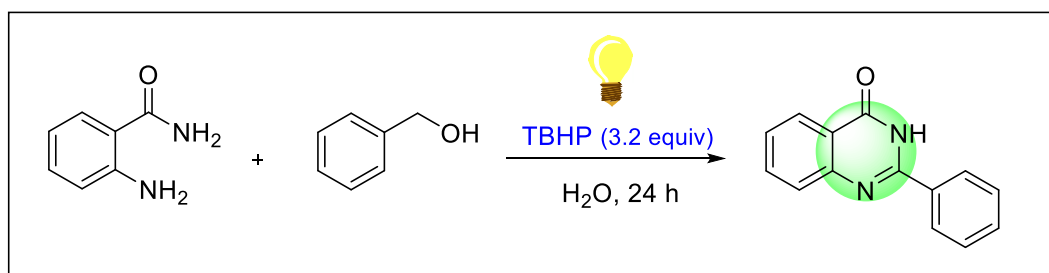


Scheme 3.19. Synthesis of isoindolo[2,1-*a*]quinazoline by deep eutectic solvents.

(v) Photoinduced synthetic approaches:

Photoinduced catalyst-free reactions give a clear indication of the advancement of green and sustainable chemistry in organic syntheses.

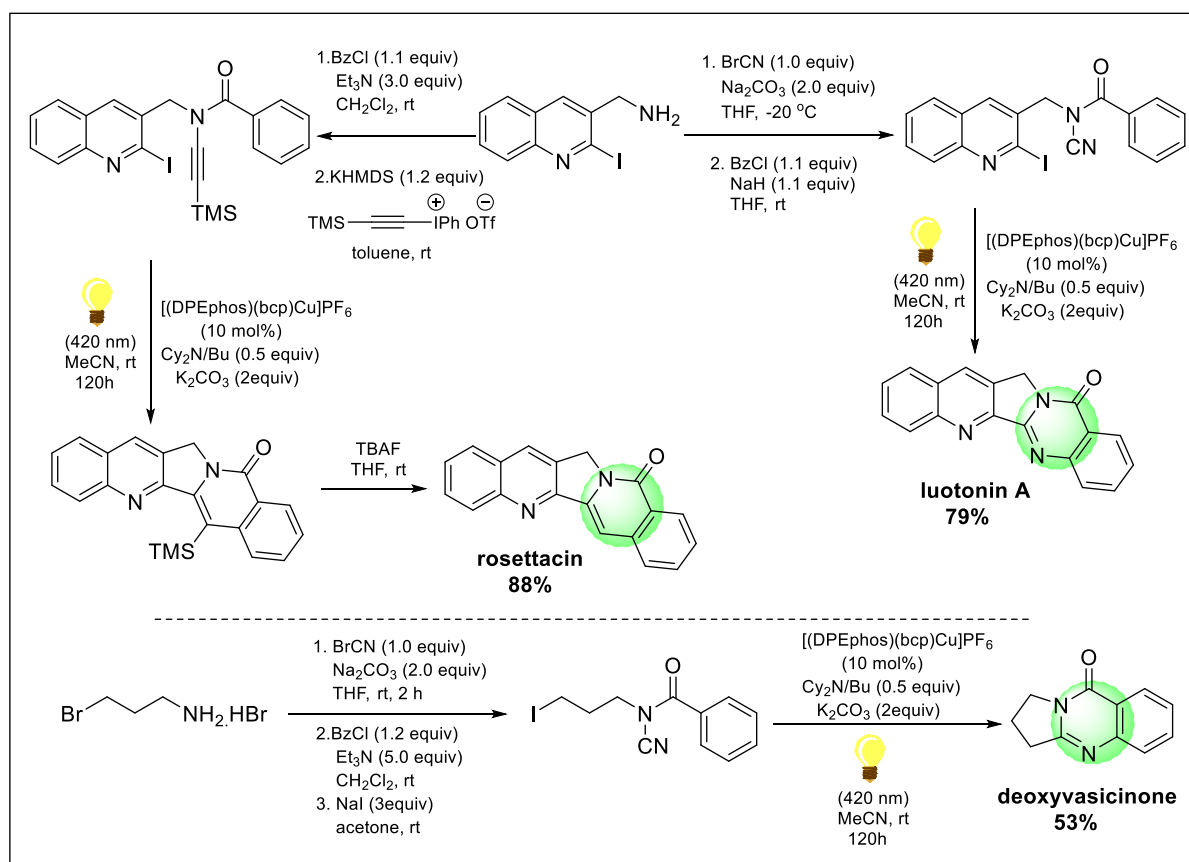
T. K. Sarma *et al.*³² reported a visible light-promoted, simple-to-use, environmentally friendly method for synthesising quinazolinone derivatives starting from inexpensive anthranilamide. *Tert*-butyl hydroperoxide (TBHP), an oxidising agent that is broken down into radicals, is used to carry out this reaction in an aqueous medium. This transition doesn't require a photocatalyst or an external catalyst. As TBHP decomposes more rapidly after being exposed to visible light irradiation, free radicals are generated, which act as a trigger for this domino reaction (**Scheme 3.20**).



Scheme 3.20. Visible light-promoted synthetic approach of quinazolinone.

3.2.3. Photoinduced total synthesis of quinazoline-based natural products:

An efficient photoinduced radical cyclization *via* copper-catalyzed domino-type reaction protocol was governed by H. Baguia *et al.*³³ for the synthesis of Luotonin A, Rosettacin, and Deoxyvasicinone. This photo redox transformation takes place smoothly starting from 2-iodo-3-aminomethylquinoline under visible light irradiation by using [(DPEphos)(bcp)Cu]PF₆ as a Cu-catalyst, and the radical cyclization of cyanamides and ynamides occurs to provide the desired products (**Scheme 3.21**).

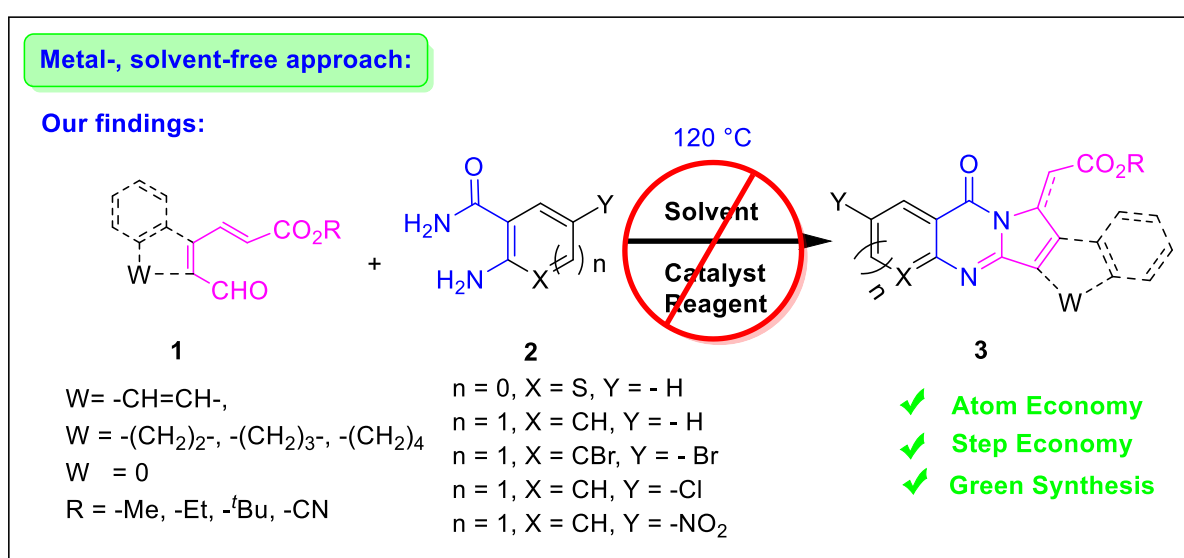


Scheme 3.21. Total synthesis of luotonin A, rosettacin, and deoxyvasicinone.

The above literature survey, shows a wide spectrum of methodologies developed by multiple groups by using various solvents, metals, and catalysts to synthesize the different fused quinazolinone derivatives. To the best of our knowledge, solvent-free synthesis of isoindoloquinazolinones *via* conventional heating process is still limited. So, it has been a challenging task to find an efficient and convenient solvent-free synthetic route from easily available starting materials. After a prolonged investigation and as a part of our ongoing studies devoted towards the development of new heterocycles,³⁴ we have successfully developed solvent-free protocol of pyrrolo/isoindolo quinazolinone derivatives using conventional thermal heating, which is discussed below.

3.3. Present work:

- ❖ Herein, we have disclosed an operatively simple, catalyst- and solvent-free synthesis of pyrrolo/isoindolo quinazolinone derivatives from 3-(2-formylcycloalkenyl)-acrylic ester derivatives **1** and anthranilamide **2** under conventional heating conditions (120 °C) with moderate to good yields (**Scheme 3.22**).
- ❖ The photophysical properties of dihydroisoindoloquinazolinones in basic and aqueous medium have also been documented in our study.
- ❖ Our model synthetic compound shows cytotoxic activity towards metastatic HepG2 and PC3 cancer cell lines.



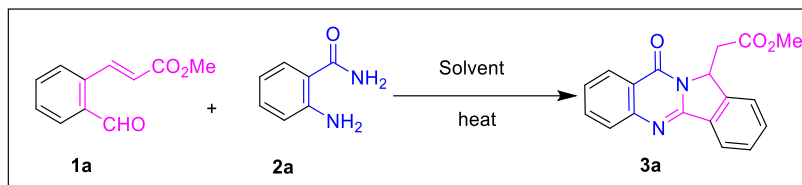
Scheme 3.22. Overall synthetic observations of fused quinazolinones.

3.4. Results & discussion:

At the outset of this investigation to synthesize highly condensed fused quinazolinone derivatives **3**, reaction was commenced with (*E*)-methyl 3-(2-formylphenyl)acrylate **1a** and anthranilamide **2a** in DMSO at room temperature, but no reaction occurred (**Table 3.1; entry 1**). However, the intermolecular condensation reaction followed by intramolecular aza-cyclization in one-pot succeeded by increasing the temperature up to 120 °C in DMSO (**entry 4**). It was found that cyclization was inefficient below 120 °C (**entries 2-3**). The two-component coupling reaction proceeds satisfactorily in toluene and ethanol (**entries 5-6**). However, no fruitful product was isolated in acetonitrile, THF and dioxane (**entries 7-9**). In order to increase the efficacy of our developed methodology, studies without any solvent were

carried out and the desired fused quinazolinones **3a** was obtained in very good yield (91%), (**entry 10**).

Table 3.1: Optimization of reaction conditions towards highly condensed quinazolinone^a



Entry	Solvent	T (°C)	Time (h)	Yield of 3a (%)
1.	DMSO	25	8	0
2.	DMSO	60	8	0
3.	DMSO	80	8	0
4.	DMSO	120	2	82
5.	Ethanol	78	2.5	73
6.	Toluene	110	3	85
7.	Acetonitrile	82	6	0
8.	THF	66	6	0
9.	Dioxane	101	6	0
10.	---	120	2	91^b

^a**Conditions:** (*E*)-methyl 3-(2-formylphenyl)acrylate **1a** (1 mmol), anthranilamide **2a** (1 mmol), solvent (2 ml); ^b Reaction performed without solvent.

With the optimal condition in hand, the scope of the new two-component neat reaction was evaluated with a variety of substrates as shown in **Table 3.2**. Methyl/ethyl/tertiary butyl of (*E*)-3-(2-formylphenyl)acrylates were smoothly converted to the corresponding isoindoloquinazolines **3a-3c** in moderate to high yields. The cyclized product **3b** was unambiguously confirmed by X-ray crystal structure shown in **Figure 3.7**.³⁵ With this encouraging result in hand, scope of the neat reaction was examined with different cycloalkenyl derivatives. Formation of the oxidized and reduced forms of the cyclized product depends on the nature of the ring. Aromatic moieties of ester derivatives were prone to air oxidation and

lead to **3a-3f**, whereas the corresponding cycloalkenyl ester derivatives **3i-3q** (7 and 8 membered rings) are reluctant to air oxidation. On the contrary, methyl/ethyl (*E*)-3-(2-formylcyclohexenyl)acrylates **3g** and **3h** smoothly transformed to their corresponding oxidized quinazolinones. The two component coupling reactions of 2-aminothiophene-3-carboxamide **2c** with (*E*)-3-(2-formylphenyl)acrylates under neat condition were well tolerated and delivers **3f**, **3m** and **3n**. We further extended the scope of the novel methodology to pentacyclic quinazolinones **3o** but the yield of the desired product was reduced to 55% for the highly steric constancy of the starting material. Notably, chloride and bromide substituted anthranilamide (**2b-2c**) were unable to produce cyclized products **3d** and **3e** at 120 °C under neat condition and the condensations were performed at 140 °C under solvent-free condition which resulted the formations of desired products (**3d** and **3e**) in good yields. Neat reaction of **1a** was unhappy for electron withdrawing substituent (-NO₂) in anthranilamide furnish very low yield of **3r** (23%) but two component coupling reaction was auspicated in DMSO at 120 °C and gave two isomeric quinazolinones **3r** & **3s** in moderate yield. Nevertheless, only one isomer **3p** was generated for cycloheptenyl system under equivalent conditions. Our green protocol was equally adequate to another acrylonitrile substituted aza-Michael acceptor and furnished good yield of quinazolinone derivative **3q**. Further, we have extended the scope of the reaction to the substrate (*2E,4E*)-methyl 6-oxo-4-phenylhexa-2,4-dienoate which furnished cyclized product **3t** with good yield 72%.

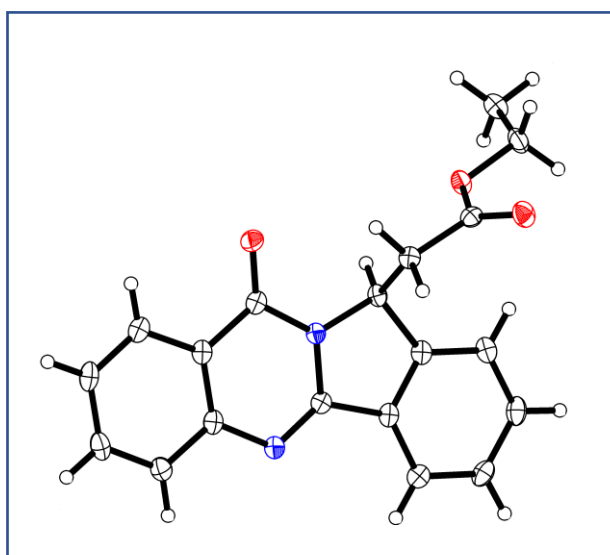
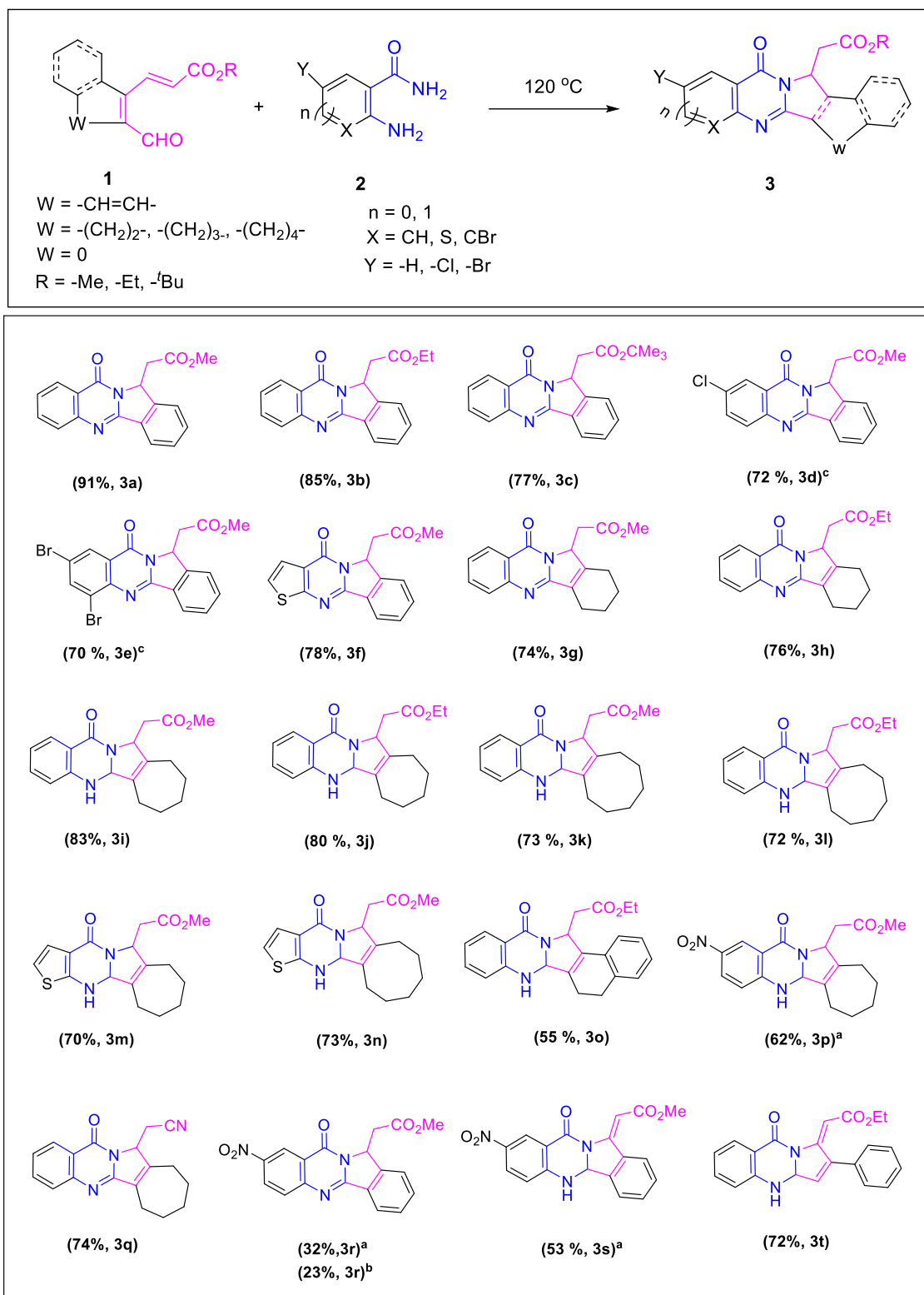
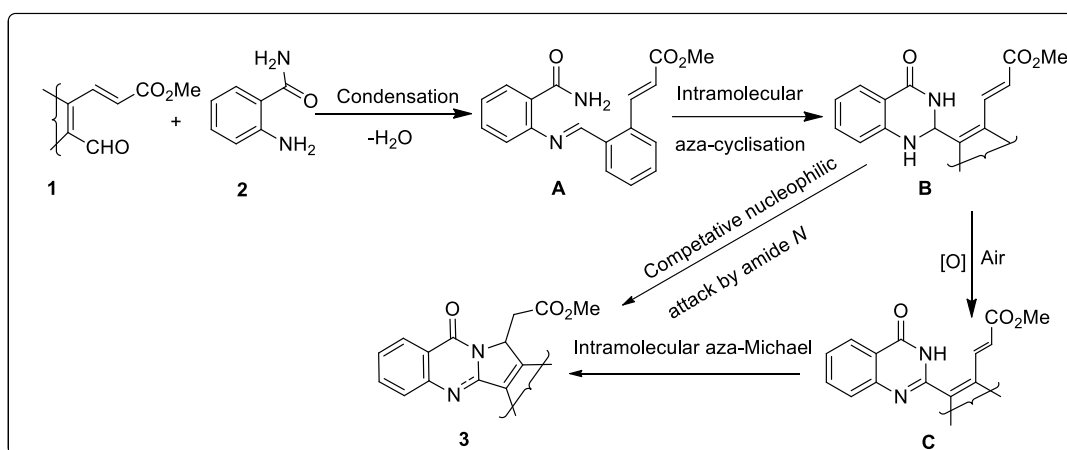


Figure 3.7. ORTEP diagram for **3b**.

Table 3.2: Substrate scope for tandem one-pot neat reaction^b

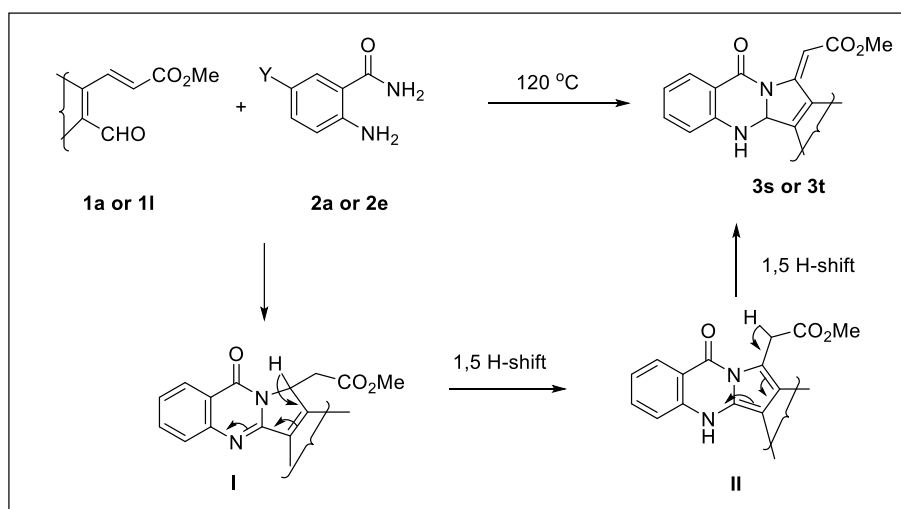
^b**Conditions:** (*E*)-methyl 3-(2-formylcycloalkenyl)acrylate **1a** (1 mmol), anthranilamide **2** (1 mmol); ^c reactions were performed at 140 °C; ^a reaction were performed in DMSO.

The mechanism of the reaction could be ascertained *via* four-step sequential process in one-pot (**Scheme 3.23**). The step-atom economical mechanistic pathway involves schiff base (**A**) formation followed by intramolecular aza-cyclization to produce intermediate **B**, which afford quinazolinone derivative after air oxidation.³⁶ The quinazolinone intermediate **C** undergoes intramolecular aza-Michael reaction provided fruitful condensed derivative **3a-3h** and **3q-3r**.³⁷ The product formation of **3i-3p** could be elucidate *via* competitive intramolecular aza-Michael reaction of more nucleophilic amide *N*-atom.



Scheme 3.23. Plausible mechanism for the synthesis of fused quinazolinone.

The formation of **3s** and **3t** could be explain *via* two step 1,5-H shift of **I** intermediate (**Scheme 3.24**).



Scheme 3.24. Synthetic route of isomerised quinazolinone.

Interestingly, it is noticed that the substrate **3j** poses high fluorescent property and hence investigation of photophysical property has also been discussed. The tolerance of these valuable functional groups would offer an opportunity for further transformation.

3.4.1. Photophysical Studies:

After successful synthetic studies, attention was drawn towards photophysical studies of synthesized dihydroquinazolinone molecule **3j**. The UV/Vis absorption spectra of degassed 2×10^{-6} M solution of **3j** in different solvents have been recorded (**Figure 3.8**), and the results are tabulated in **Table 3.3**.

Excited state properties of quinazolinone derivative **3j** were investigated by fluorescence emission spectroscopy. Like other quinazolinone derivatives, the fluorescence properties of **3j** were also found to be strongly dependent on solvent polarity.³⁸ The heterocyclic compound **3j** showed negative solvatochromatic emission (**Figure 3.9**) as a function of solvent polarity.³⁹ As the solvent polarity increases (from non-polar e.g., toluene to polar e.g., acetonitrile (MeCN)), a hypsochromic shift for **3j** was noticed and the emission maximum was found to shift from 431 to 416 nm. The above solvent effect observed is due to their close lying ($^1\pi-\pi^*$) and ($^1n-\pi^*$) singlet excited states.⁴⁰ Higher the dissolving ability of solvent with lower dielectric constant (non-polar solvent) favour, the $\pi-\pi^*$ interaction in quinazolinone unit and produce greater emission.⁴¹ Conversely, in polar protic solvent (e.g., MeOH) due to intermolecular H-bonding effect with quinazolinone unit, the $\pi-\pi^*$ transition is dominated which results shifting in the emission band to longer wave length.

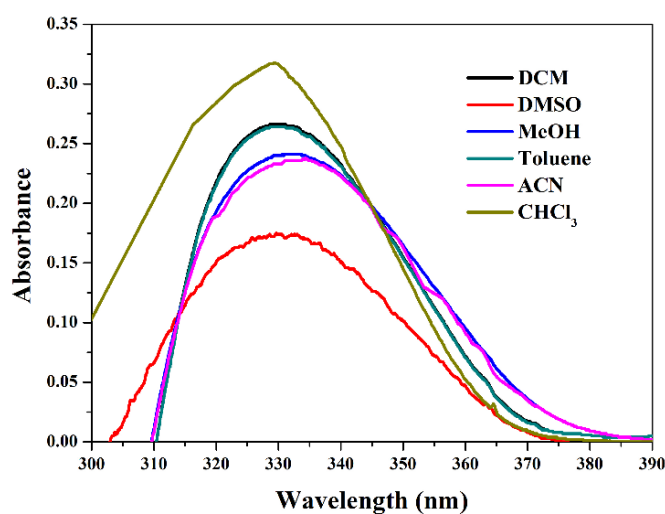


Figure 3.8. UV-Vis absorption spectra of **3j** in different solvents.

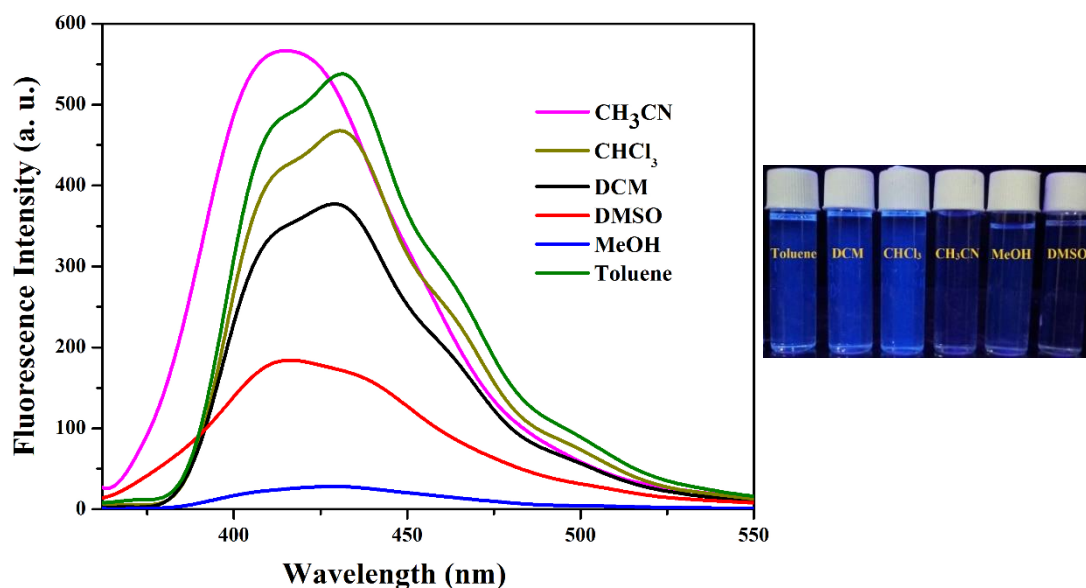


Figure 3.9. Fluorescence of quinazolinone derivative in different solvents.

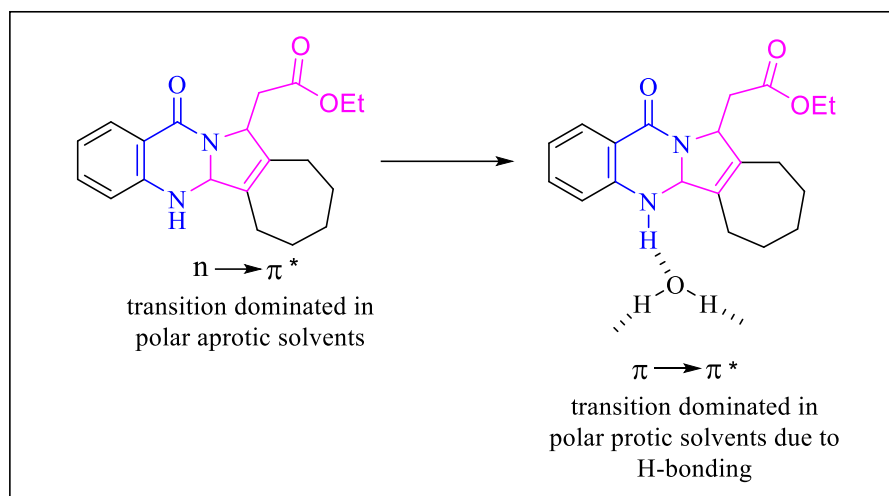
Table 3.3: UV-Vis absorption and fluorescence data of **3j** in different solvent

Solvent	$\epsilon^a(25\text{ }^\circ\text{C})$	δH hydrogen bonding ^b	$\lambda_{\text{max}}^c(\text{nm})$	ϵ_{max}^d	$\lambda_{\text{emi}}^e(\text{nm})$	stokes' shift ^f (nm)
Toluene	2.38	2.0	330	132000	431	101
Chloroform	4.81	7.1	329	159000	431	101
DCM	9.10	7.1	331	133000	429	98
MeOH	33.00	19.4	333	120500	430	97
ACN	37.50	6.1	331	119000	416	82
DMSO	46.70	7.8	329	87500	416	87

^aDielectric constant at 25 °C. ^bHydrogen bonding capability. ^cMaximum absorption wavelength. ^dMolar absorption coefficient at maximum absorption wavelength. ^eMaximum emission wavelength. ^fDifference between maximum absorption wavelength and maximum emission wavelength.

A fluorescence property of dihydroquinazolinone derivative **3j** was also investigated in an aqueous binary solvent system to understand the effect of hydrogen bonding interaction. The emission spectra (**Figure 3.10**) of **3j** in CH₃CN–H₂O binary mixtures were recorded and it was observed that increasing the amount of water in the CH₃CN–H₂O mixture, there is a bit of bathochromic shift with gradual decrease in fluorescence intensity. The above fact can be

attributed due to solute–solvent interactions through the formation of hydrogen-bonds between the solvent and the heterocyclic part of quinazolinone moiety (**Scheme 3.25**).⁴²



Scheme 3.25. Solvent-solute H-bonding interaction.

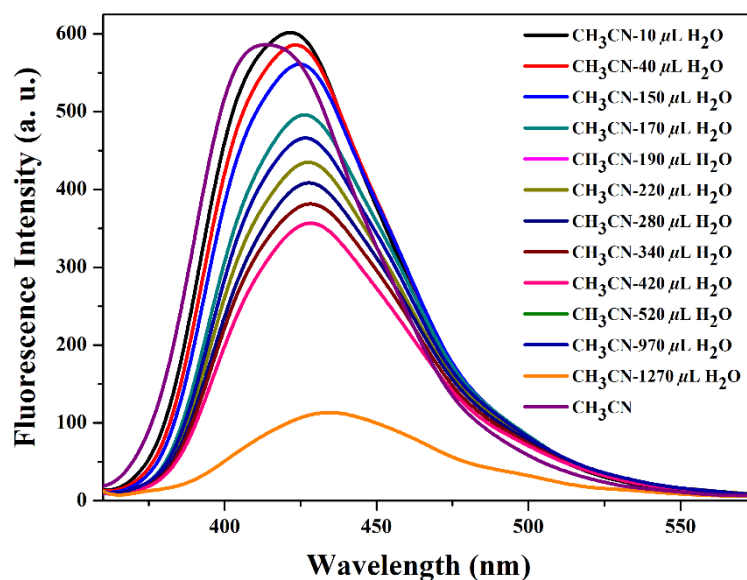
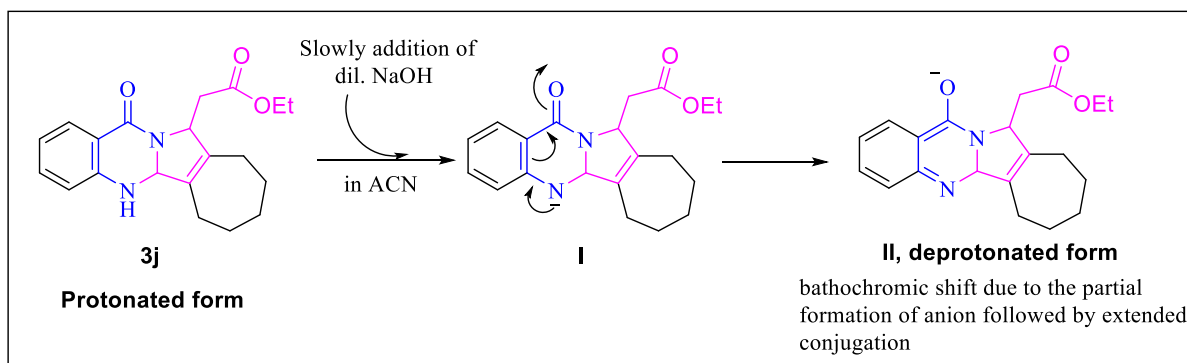


Figure 3.10. Fluorescence quenching of **3j** water % in MeCN-H₂O mixture.



Scheme 3.26. Solute-alkali interaction in excited state.

As the quinazolinone derivative contain base labile proton (NH) so it is quite interesting to check the emission spectral behaviour with increase of pH (**Figure 3.11**). The fluorescence maximum of **3j** in neutral CH_3CN is around 412 nm, which is red shifted to ≈ 437 nm by the successive addition of different concentration of NaOH (micro molar). This is because in pure CH_3CN , protonated **3j** is the predominant species. Thus, the fluorescence spectrum in pure CH_3CN is mainly due to protonated **3j** in the excited state. At higher pH , the bathochromic shift was obtained due to the deprotonation of **3j** followed by extended conjugation and decrease of fluorescence intensity may be explain by the lower solubility of the molecule in alkali solution (**Scheme 3.26**).

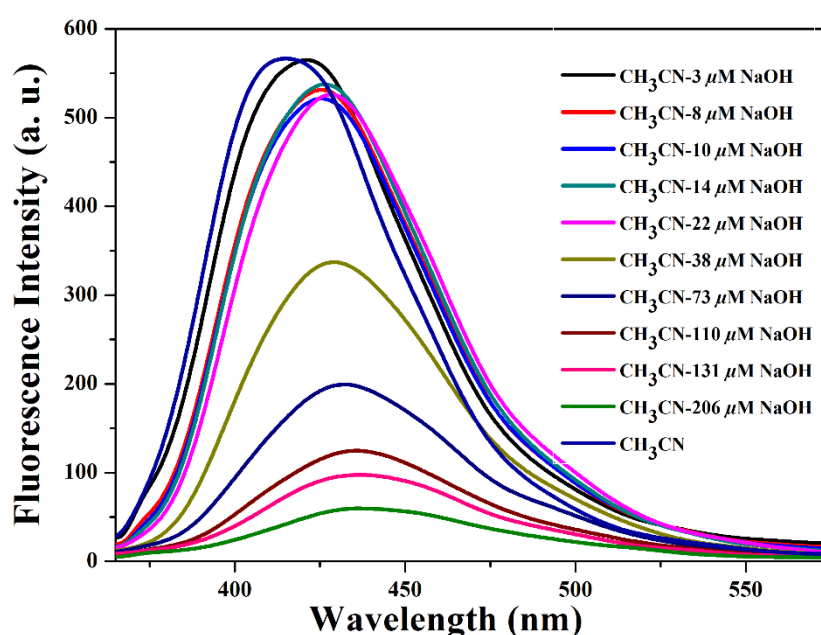


Figure 3.11. Fluorescence spectral change of **3j** by stepwise addition of NaOH in CH_3CN (λ_{max} shifted from 408 nm in pure CH_3CN to 438 nm in CH_3CN -206 μM NaOH).

3.4.2. Biological Study:

After successful investigation of the photophysical properties, our research turned towards biological application of our model compound **3j** using two different metastatic cancer cell lines; hepatocellular carcinoma (HepG2) and prostate cancer (PC3). HepG2 is a human liver cancer cell line, obtained from the liver tissue of a 15-year-old American adolescent boy of European ancestry.⁴³ The human prostate cancer cell line (PC3) is derived from bone metastasis of a grade IV prostatic adenocarcinoma from a 62-year-old male Caucasian which is used widely in research and drug development.⁴⁴ To examine the anticancer activity of the

compound **3j**, HepG2 and PC3 were seeded in 48 well plates at 1×10^4 cells per well in DMEM and RPMI (10% FBS) medium respectively and exposed to **3j** at different concentrations for 24 h (**Figure 3.12**). After incubation, cells were washed twice with PBS and incubated with MTT solution (450 $\mu\text{g}/\text{ml}$) for 3 h at 37 $^\circ\text{C}$. The resulting formazan crystals were dissolved in a MTT solubilising buffer and the absorbances were measured at 570 nm by using a microplate reader (Biotek, USA). Each point was assessed in triplicate. Untreated cells were considered as 100% viable. We found that this compound has significant anticancer activity against both of this cell lines. IC-50 value of this compound was found to be 134 $\mu\text{g}/\text{ml}$ for HepG2 cells and 112 $\mu\text{g}/\text{ml}$ for PC3 cells.

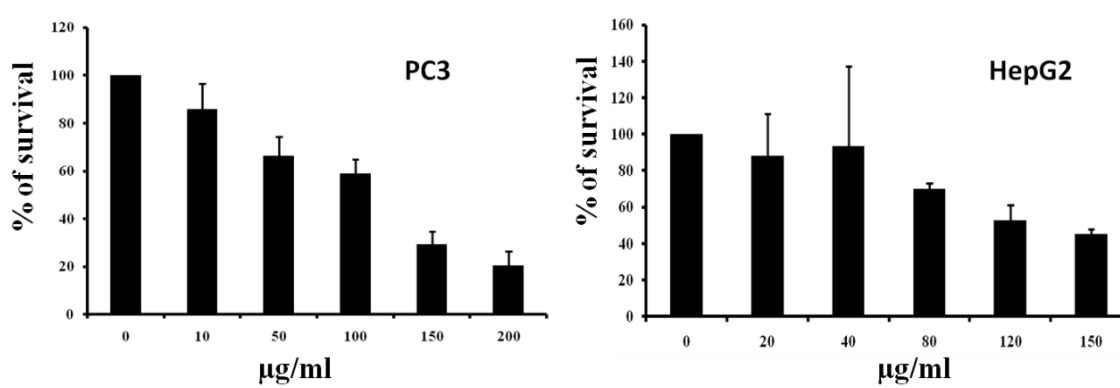


Figure 3.12. Cytotoxic effect of the compound **3j** on PC3 and HepG2 cells.

Cells were incubated with increasing concentrations of the compound for 24 h and their percentage of survivability was assessed by MTT assay. Data represented are means \pm SD of three identical experiments made in three replicates.

3.5. Conclusion:

To conclude, an environmentally benign catalyst- and solvent-free tandem approach for the synthesis of highly functionalized fused quinazolinones with good to excellent yields has been demonstrated. The designed substrate, 3-(2-formylcycloalkenyl)acrylic ester derivatives are effective coupling partners for anthranilamide compounds to synthesize highly fused quinazolinones under neat condition with wide substrate scope, step-atom economy and minimal work-up procedure. The synthesized compounds show good fluorescence property and hence of photophysical properties in different solvents and solvent-solute interaction in the excited state of synthesized fluorophore are also documented. Since our study compound chemosensitized to HepG2 and PC3 cells lines. So, we will use this compound in *in-vivo* mouse model for future research.

3.6. Experimental section:

General information:

^1H NMR (400 MHz) and ^1H NMR (500 MHz) spectra were recorded on a 400 MHz and 500 MHz spectrometer in CDCl_3 / $\text{DMSO}-d^6$ solvent using TMS as the internal standard. ^{13}C NMR was recorded in the same MHz instruments. HRMS was measured using a TOF analyzer. 60-120 or 100-200 mesh silica gels (SRL) were used for column chromatographic purification. Progress of the reaction was monitored by using precoated silica gel 60 F254 TLC sheets (Merck). Petroleum ether (boiling range 60-80 °C) or *n*-hexane was used as the eluent for column chromatographic separation. Solvents were distilled, dried and stored over molecular sieves (4 Å). The UV-Vis absorption spectra were recorded on a Shimadzu UV-2450 UV-Vis spectrophotometer and the fluorescence emission spectra were recorded on Photon Technology International S/N-3201.

General Procedure for the preparation of 1a – 1j:³⁴

β -Bromovinyl aldehyde or 2-Bromo Benzaldehyde **1** (1 mmol), Na_2CO_3 (4 mmol), Bu_4NBr (1 mmol), PdCl_2 (10 mol%), and H_2O (5 mL) were taken in a two-neck, round-bottom flask. Acrylic ester (4 mmol) was added, and the mixture stirred for 2 h in 50 °C, diluted with brine solution, and extracted with EtOAc (3 × 25 mL). The extracted solution was dried over Na_2SO_4 , and the solvent was evaporated. The product was purified by column chromatography using EtOAc–PE as eluent.

Preparation of (*E*)-3-(2-formylcyclohept-1-en-1-yl)acrylonitrile (**1k**):

2-bromocyclohept-1-ene-1-carbaldehyde (1 mmol), $\text{P}(o\text{-tolyl})_3$ (0.25 mmol), $\text{Pd}(\text{OAc})_2$ (10 mol%), triethyl amine (1 mL), methanol (1 mL), acetonitrile (1 mL) were placed in a two-neck, round-bottom flask. Acrylonitrile (2 mmol) was added and the mixture stirred in inert atmosphere for 2 h in 80 °C and extracted with EtOAc (3 × 25 mL). The extracted solution was dried over Na_2SO_4 , and the solvent was evaporated. The product was purified by column chromatography using EtOAc–PE as eluent.

Preparation of 2-amino-5-nitrobenzamide (2e):

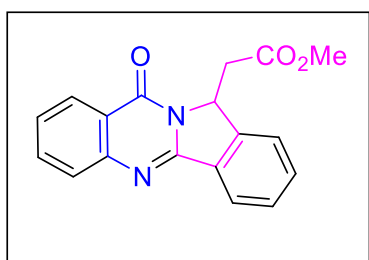
Isatoic anhydride (1 mmol) was dissolved in 5 mL conc. H_2SO_4 and it was placed in ice bath. NaNO_3 (1 mmol) was taken in another round-bottom flask and it also kept in ice bath. The acidic solution of isatoic anhydride was added drop wise to the ice cooled NaNO_3 and the resulting mixture stirred continuously for 1 h. After that, the reaction mixture was poured in ice cube, a yellow precipitation was obtained. This precipitation was collected by filtration and dried. This yellow precipitation was dissolved in 15 mL liq. NH_3 . This mixture was allowed to stir in reflux condition at $\sim 80^\circ\text{C}$ for 8 h. After, the filtration of this reaction mixture a yellow precipitation was collected and dried.

General Procedure for preparation of (3a – 3t):

Compound **1** (1.0 mmol) and **2** (1.0 mmol) were taken in a round-bottom flask and it was placed in a heating oil bath. The heating of the resulting mixture was carried out up to 2 h in open flask at 120°C under the neat condition. The progress of the reaction was monitored by TLC. The crude residue was purified by silica-gel (100-200 mesh) column chromatography using ethyl acetate and petroleum ether (1:2) as an eluent to get the desired product **3**.

3.6.1. Characterization of NMR data for (3a – 3t):**Methyl 2-(10-oxo-10,12-dihydroisindolo[1,2-b]quinazolin-12-yl)acetate: (3a)³⁷**

Yellow solid (278.5 mg, 91%), mp. 104°C . ^1H NMR (400 MHz, Chloroform-*d*): δ 8.36 – 8.32

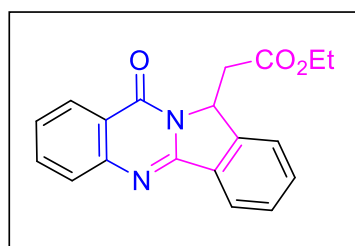


(m, 1H), 8.16 (d, $J = 7.0$ Hz, 1H), 7.83 – 7.68 (m, 2H), 7.62 – 7.51 (m, 3H), 7.47 (t, $J = 6.0$ Hz, 1H), 5.87 (dd, $J = 7.8, 3.6$ Hz, 1H), 3.72 – 3.67 (m, 1H), 3.66 (s, 3H), 2.98 (dd, $J = 16.5, 7.9$ Hz, 1H). ^{13}C NMR (125 MHz, Chloroform-*d*): δ 170.4, 160.8, 154.4, 149.2, 143.3, 134.4, 132.7, 131.9, 129.4, 127.4, 126.6,

126.5, 123.5, 123.2, 121.0, 58.5, 52.0, 35.8. HRMS calcd. for $\text{C}_{18}\text{H}_{15}\text{N}_2\text{O}_3$: $(\text{M}+\text{H})^+$ 307.1084, found : 307.1083.

Ethyl 2-(10-oxo-10,12-dihydroisoindolo[1,2-b]quinazolin-12-yl)acetate: (3b)

Off white solid (272.0 mg, 85%), mp. 132 °C. ¹H NMR (500 MHz, Chloroform-*d*): δ 8.34 (d,



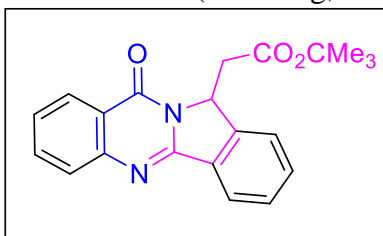
$J = 7.5$ Hz, 1H), 8.16 (d, $J = 7.5$ Hz, 1H), 7.82 – 7.64 (m, 2H), 7.63 – 7.50 (m, 3H), 7.48 (t, $J = 7.2$ Hz, 1H), 5.85 (dd, $J = 7.7$, 3.7 Hz, 1H), 4.08 (q, $J = 7.2$ Hz, 2H), 3.65 (dd, $J = 16.2$, 3.7 Hz, 1H), 3.04 (dd, $J = 16.2$, 7.7 Hz, 1H), 1.12 (t, $J = 7.2$ Hz, 3H).

¹³C NMR (125 MHz, Chloroform-*d*): δ 169.7, 160.7, 154.5,

149.2, 143.3, 134.3, 132.6, 131.9, 129.4, 127.8, 126.6, 126.5, 123.6, 123.3, 121.0, 60.6, 58.6, 35.9, 14.0. HRMS calcd. for C₁₉H₁₇N₂O₃: (M+H)⁺ 321.1241, found : 321.1239.

Tert-butyl 2-(10-oxo-10,12-dihydroisoindolo[1,2-b]quinazolin-12-yl)acetate: (3c)

Off white solid (268.0 mg, 77%), mp. 141 °C. ¹H NMR (500 MHz, Chloroform-*d*): δ 8.35 (d,

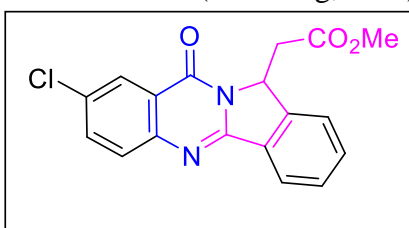


$J = 7.9$ Hz, 1H), 8.17 (d, $J = 7.4$ Hz, 1H), 7.82 – 7.74 (m, 2H), 7.61 – 7.56 (m, 3H), 7.48 (t, $J = 7.37$ Hz, 1H), 5.78 (dd, $J = 6.9$, 3.6 Hz, 1H), 3.46 (dd, $J = 15.8$, 3.6 Hz, 1H), 3.22 – 3.17 (m, 1H), 1.19 (s, 9H). ¹³C NMR (125 MHz, Chloroform-*d*): δ

168.7, 160.6, 154.6, 149.0, 143.2, 134.3, 132.5, 132.0, 129.3, 127.2, 126.5, 126.4, 123.5, 123.3, 121.0, 81.3, 58.8, 36.6, 27.6 (3C). HRMS calcd. for C₂₁H₂₁N₂O₃: (M+H)⁺ 349.1554, found : 349.1552.

Methyl 2-(8-chloro-10-oxo-10,12-dihydroisoindolo[1,2-b]quinazolin-12-yl)acetate: (3d)

Off white solid (244.8 mg, 72%), mp. 145 °C. ¹H NMR (500 MHz, Chloroform-*d*): δ 8.19 –

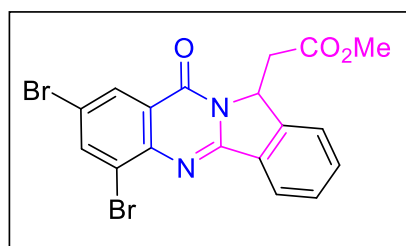


8.13 (m, 1H), 8.04 (d, $J = 6.8$ Hz, 1H), 7.75 (d, $J = 7.5$ Hz, 1H), 7.66 – 7.52 (m, 1H), 7.53 – 7.49 (m, 3H), 5.77 – 5.73 (m, 1H), 3.58 (s, 3H), 3.56 (dd, $J = 14.3$, 3.9 Hz, 1H), 2.96 – 2.89 (m, 1H). ¹³C NMR (125 MHz, Chloroform-*d*): δ

170.1, 159.5, 154.6, 147.5, 143.3, 134.7, 132.8, 131.5, 129.5, 128.8, 126.3, 125.9, 123.6, 123.2, 121.9, 58.7, 51.9, 35.5. HRMS calcd. for C₁₈H₁₄ClN₂O₃: (M+H)⁺ 341.0695, found : 341.0694.

Methyl 2-(6,8-dibromo-10-oxo-10,12-dihydroisoindolo[1,2-b]quinazolin-12-yl)acetate: (3e)

Off white solid (323.3 mg, 70%), mp. 168 °C. ¹H NMR (500 MHz, Chloroform-*d*): δ 8.37 (s, 1H), 8.18 (d, *J* = 7.5 Hz, 1H), 8.11 (s, 1H), 7.63 – 7.54 (m, 2H), 7.45 – 7.42 (m, 1H), 5.81 (dd, *J* = 7.5, 3.5 Hz, 1H), 3.65 (s, 3H), 3.63 – 3.60 (m, 1H), 3.00 (dd, *J* = 16.4, 7.7 Hz, 1H). ¹³C NMR (125 MHz, Chloroform-*d*): δ 170.0, 158.9, 155.2, 146.0, 143.2, 140.3, 133.1, 131.4, 129.5, 128.7, 124.1, 123.5, 123.1, 121.9, 119.3, 58.8, 52.0, 35.3. HRMS calcd. for C₁₈H₁₃Br₂N₂O₃: (M+H)⁺ 462.9295, found : 462.9294.

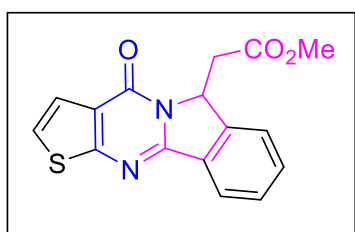


¹H NMR (500 MHz, Chloroform-*d*): δ 8.37 (s, 1H), 8.18 (d, *J* = 7.5 Hz, 1H), 8.11 (s, 1H), 7.63 – 7.54 (m, 2H), 7.45 – 7.42 (m, 1H), 5.81 (dd, *J* = 7.5, 3.5 Hz, 1H), 3.65 (s, 3H), 3.63 – 3.60 (m, 1H), 3.00 (dd, *J* = 16.4, 7.7 Hz, 1H). ¹³C NMR (125 MHz, Chloroform-*d*): δ 170.0, 158.9, 155.2, 146.0, 143.2, 140.3, 133.1, 131.4, 129.5, 128.7,

124.1, 123.5, 123.1, 121.9, 119.3, 58.8, 52.0, 35.3. HRMS calcd. for C₁₈H₁₃Br₂N₂O₃: (M+H)⁺ 462.9295, found : 462.9294.

Methyl 2-(4-oxo-4,6-dihydrothieno[2',3':4,5]pyrimido[2,1-*a*]isoindol-6-yl)acetate: (3f)

Off white solid (243.4 mg, 78%), mp. 167 °C. ¹H NMR (400 MHz, Chloroform-*d*): δ 8.11 (d, *J* = 6.9 Hz, 1H), 7.81 (d, *J* = 5.3 Hz, 1H), 7.62 – 7.57 (m, 3H), 7.42 (d, *J* = 5.2 Hz, 1H), 5.85 (dd, *J* = 7.9, 3.7 Hz, 1H), 3.73 (dd, *J* = 16.5, 3.7 Hz, 1H), 3.66 (s, 3H), 2.99 (dd, *J* = 16.5, 7.9 Hz, 1H). ¹³C NMR (100 MHz, Chloroform-*d*): δ 170.1, 168.2, 167.1, 155.7, 151.9, 143.4, 141.1, 133.8, 129.9, 128.7, 125.2, 117.4, 116.5, 61.3, 51.6, 46.4. HRMS calcd. for C₁₆H₁₃N₂O₃S: (M+H)⁺ 313.0649, found : 313.0647.

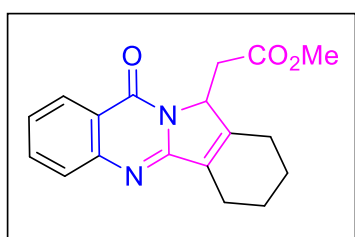


¹H NMR (400 MHz, Chloroform-*d*): δ 8.11 (d, *J* = 6.9 Hz, 1H), 7.81 (d, *J* = 5.3 Hz, 1H), 7.62 – 7.57 (m, 3H), 7.42 (d, *J* = 5.2 Hz, 1H), 5.85 (dd, *J* = 7.9, 3.7 Hz, 1H), 3.73 (dd, *J* = 16.5, 3.7 Hz, 1H), 3.66 (s, 3H), 2.99 (dd, *J* = 16.5, 7.9 Hz, 1H). ¹³C NMR (100 MHz, Chloroform-*d*): δ 170.1, 168.2, 167.1, 155.7, 151.9, 143.4, 141.1, 133.8, 129.9, 128.7, 125.2, 117.4,

116.5, 61.3, 51.6, 46.4. HRMS calcd. for C₁₆H₁₃N₂O₃S: (M+H)⁺ 313.0649, found : 313.0647.

Methyl 2-(10-oxo-1,2,3,4,10,12-hexahydroisoindolo[1,2-*b*]quinazolin-12-yl)acetate: (3g)

Yellow solid (229.4 mg, 74%), mp. 114 °C. ¹H NMR (400 MHz, Chloroform-*d*): δ 8.29 (d, *J* = 8.1 Hz, 1H), 7.72 – 7.71 (m, 2H), 7.43 – 7.42 (m, 1H), 5.18 (m, 1H), 3.63 (s, 3H), 3.35 (dd, *J* = 15.7, 3.4 Hz, 1H), 3.00 (dd, *J* = 15.1, 7.4 Hz, 1H), 2.51 (m, 2H), 2.36 (m, 2H), 1.85 – 1.74 (m, 2H), 1.32 – 1.24 (m, 2H). ¹³C NMR (100 MHz, Chloroform-*d*): δ 168.9, 160.8, 151.6, 149.3, 134.5, 134.2, 132.7, 127.6, 126.5, 126.0, 121.0, 59.6, 52.2, 38.2, 22.8, 21.9, 21.6, 21.1. HRMS calcd. for C₁₈H₁₉N₂O₃: (M+H)⁺ 311.1397, found : 311.1396.

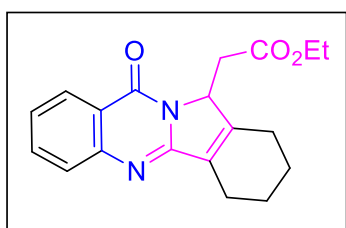


¹H NMR (400 MHz, Chloroform-*d*): δ 8.29 (d, *J* = 8.1 Hz, 1H), 7.72 – 7.71 (m, 2H), 7.43 – 7.42 (m, 1H), 5.18 (m, 1H), 3.63 (s, 3H), 3.35 (dd, *J* = 15.7, 3.4 Hz, 1H), 3.00 (dd, *J* = 15.1, 7.4 Hz, 1H), 2.51 (m, 2H), 2.36 (m, 2H), 1.85 – 1.74 (m, 2H), 1.32 – 1.24 (m, 2H). ¹³C NMR (100 MHz, Chloroform-*d*): δ 168.9, 160.8, 151.6, 149.3, 134.5, 134.2, 132.7, 127.6,

126.5, 126.0, 121.0, 59.6, 52.2, 38.2, 22.8, 21.9, 21.6, 21.1. HRMS calcd. for C₁₈H₁₉N₂O₃: (M+H)⁺ 311.1397, found : 311.1396.

Ethyl 2-(10-oxo-1,2,3,4,10,12-hexahydroisindolo[1,2-b]quinazolin-12-yl)acetate: (3h)

Yellow solid (246.3 mg, 76%), mp. 98 °C. ¹H NMR (400 MHz, Chloroform-*d*): δ 8.29 – 8.22

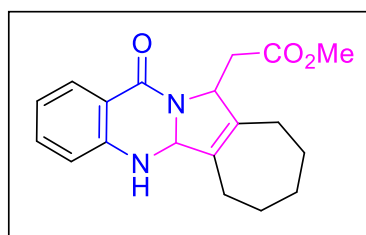


(m, 1H), 7.71 – 7.69 (m, 2H), 7.43 – 7.39 (m, 1H), 5.15 (m, 1H), 4.08 – 3.98 (m, 2H), 3.26 (dd, *J* = 15.4, 3.8 Hz, 1H), 3.10 (dd, *J* = 15.4, 6.9 Hz, 1H), 2.49 – 2.35 (m, 4H), 1.86 – 1.73 (m, 4H), 1.07 (t, *J* = 7.2 Hz, 3H). ¹³C NMR (100 MHz, Chloroform-*d*): δ 169.6, 160.3, 157.9, 152.3, 149.4, 134.5, 134.1, 131.8, 127.2,

126.5, 126.0, 61.3, 60.9, 33.6, 23.5, 22.1, 21.6, 20.4, 14.1. HRMS calcd. for C₁₉H₂₁N₂O₃: (M+H)⁺ 325.1554, found : 325.1552.

Methyl 2-(13-oxo-5,5a,7,8,9,10,11,13-octahydro-6H-cyclohepta[3,4]pyrrolo[2,1-b]quinazolin-11-yl)acetate: (3i)

Yellow solid (270.7 mg, 83%), mp. 133 °C. ¹H NMR (400 MHz, Chloroform-*d*): δ 7.99 (d, *J*

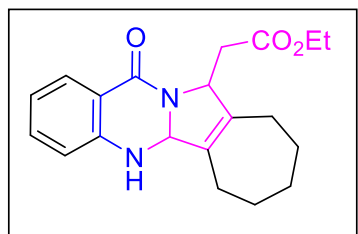


= 7.5 Hz, 1H), 7.38 (t, *J* = 7.4 Hz, 1H), 6.92 (t, *J* = 7.5 Hz, 1H), 6.59 (d, *J* = 8.3 Hz, 1H), 5.94 (s, 1H), 5.30 (s, 1H), 4.47 (d, *J* = 6.2 Hz, 1H), 3.70 (s, 3H), 2.92 – 2.87 (m, 1H), 2.50 (d, *J* = 17.0 Hz, 1H), 2.26 – 2.09 (m, 2H), 1.78 – 1.77 (m, 2H), 1.51 – 1.32 (m, 4H), 1.27 – 1.24 (m, 2H). ¹³C NMR (100 MHz, Chloroform-*d*): δ 172.4, 166.0, 148.2, 135.9, 133.9, 129.3, 129.1, 119.4, 118.1, 111.4, 67.1,

53.6, 52.3, 35.1, 33.8, 32.1, 31.0, 26.8, 25.4. HRMS calcd. for C₁₉H₂₃N₂O₃: (M+H)⁺ 327.1710, found : 327.1711.

Ethyl 2-(13-oxo-5,5a,7,8,9,10,11,13-octahydro-6H-cyclohepta[3,4]pyrrolo[2,1-b]quinazolin-11-yl)acetate: (3j)

Yellow solid (272.1 mg, 80%), mp. 130 °C. ¹H NMR (400 MHz, DMSO-*d*⁶): δ 8.09 (s, 1H),

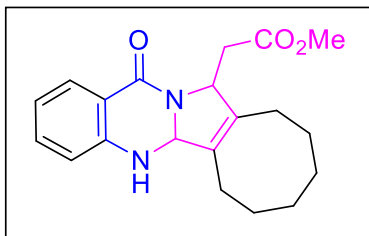


7.75 (d, *J* = 6.9 Hz, 1H), 7.38 (t, *J* = 7.8 Hz, 1H), 6.86 (t, *J* = 7.4 Hz, 1H), 6.80 (d, *J* = 8.3 Hz, 1H), 5.05 (s, 1H), 4.75 – 4.74 (m, 1H), 4.10 (q, *J* = 7.1 Hz, 2H), 2.79 – 2.76 (m, 1H), 2.46 (m, 1H), 2.42 – 2.25 (m, 3H), 2.04 – 1.98 (m, 1H), 1.94 – 1.88 (m, 1H), 1.81 – 1.78 (m, 1H), 1.61 – 1.55 (m, 4H), 1.15 (t, *J* = 7.0

Hz, 3H). ¹³C NMR (100 MHz, Chloroform-*d*): δ 171.9, 166.0, 148.3, 135.8, 133.8, 129.3, 129.1, 119.3, 118.1, 111.4, 67.1, 61.4, 53.7, 35.2, 33.8, 32.1, 31.0, 26.8, 25.4, 14.4. HRMS calcd. for C₂₀H₂₅N₂O₃: (M+H)⁺ 341.1867, found : 341.1866.

Methyl 2-(14-oxo-5,5a,6,7,8,9,10,11,12,14-decahydrocycloocta[3,4]pyrrolo[2,1-*b*]quinazolin-12-yl)acetate: (3k)

White solid (248.3 mg, 73%), mp. 159 °C. ^1H NMR (400 MHz, DMSO- d_6): δ 8.24 (s, 1H),

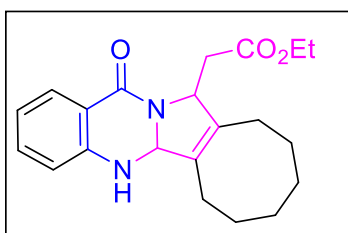


7.75 (d, $J = 7.5$ Hz, 1H), 7.37 (t, $J = 7.8$ Hz, 1H), 6.87 (t, $J = 7.4$ Hz, 1H), 6.80 (d, $J = 8.3$ Hz, 1H), 5.11 (s, 1H), 4.79 (d, $J = 5.2$ Hz, 1H), 3.61 (s, 3H), 2.67 (m, 1H), 2.50 (s, 1H), 2.39 – 2.31 (m, 2H), 2.16 (d, $J = 14.4$ Hz, 1H), 1.87 (d, $J = 12.2$ Hz, 1H), 1.64 – 1.53 (m, 2H), 1.34 (m, 4H), 1.23 – 1.21 (m, 2H).

^{13}C NMR (125 MHz, Chloroform- d): δ 172.4, 165.8, 148.3, 133.6, 133.4, 129.2, 126.3, 119.2, 118.2, 111.3, 64.9, 53.8, 52.2, 31.4, 31.3, 29.3, 27.8, 26.2, 25.9, 25.8. HRMS calcd. for $\text{C}_{20}\text{H}_{25}\text{N}_2\text{O}_3$: (M+H) $^+$ 341.1867, found : 341.1865.

Ethyl 2-(14-oxo-5,5a,6,7,8,9,10,11,12,14-decahydrocycloocta[3,4]pyrrolo[2,1-*b*]quinazolin-12-yl)acetate: (3l)

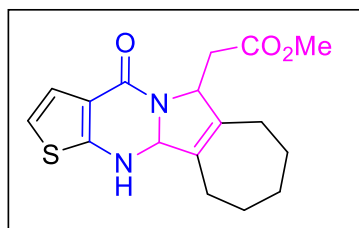
Yellow solid (255.0 mg, 72%), mp. 123 °C. ^1H NMR (400 MHz, Chloroform- d): δ 7.97 (dd, $J = 7.8, 1.6$ Hz, 1H), 7.37 (ddd, $J = 8.3, 7.3, 1.7$ Hz, 1H), 6.90 (t, $J = 8.0$ Hz, 1H), 6.58 (d, $J = 8.0$ Hz, 1H), 5.35 (s, 1H), 4.45 (d, $J = 8.2$ Hz, 1H), 4.19 – 4.10 (m, 2H), 2.61 (t, $J = 17.1$ Hz, 2H), 2.41 (t, $J = 9.9$ Hz, 2H), 2.12 (d, $J = 14.4$ Hz, 1H), 1.48 – 1.36 (m, 9H), 1.22 (t, $J = 7.1$ Hz, 3H). ^{13}C NMR (100 MHz, Chloroform- d): δ 172.0, 166.1, 148.5, 133.9, 133.5, 129.3, 126.2, 119.3, 118.1, 111.5, 65.0, 61.5, 53.9, 31.5, 31.3, 29.4, 27.9, 26.4, 26.0 (2C), 14.3. HRMS calcd. for $\text{C}_{21}\text{H}_{27}\text{N}_2\text{O}_3$: (M+H) $^+$ 355.2023, found : 355.2022.



^{13}C NMR (100 MHz, Chloroform- d): δ 172.0, 166.1, 148.5, 133.9, 133.5, 129.3, 126.2, 119.3, 118.1, 111.5, 65.0, 61.5, 53.9, 31.5, 31.3, 29.4, 27.9, 26.4, 26.0 (2C), 14.3. HRMS calcd. for $\text{C}_{21}\text{H}_{27}\text{N}_2\text{O}_3$: (M+H) $^+$ 355.2023, found : 355.2022.

Methyl 2-(4-oxo-6,7,8,9,10,11,11b,12-octahydro-4H-cyclohepta[3,4]pyrrolo[1,2-*a*]thieno[2,3-*d*]pyrimidin-6-yl)acetate: (3m)

Yellow solid (232.4 mg, 70%), mp. 148 °C. ^1H NMR (400 MHz, DMSO- d_6): δ 7.72 (d, $J = 5.3$

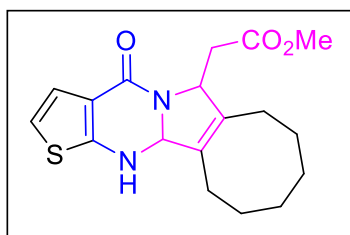


Hz, 1H), 7.56 (s, 1H), 6.89 (d, $J = 5.3$ Hz, 1H), 5.01 (s, 1H), 4.78 (d, $J = 5.4$ Hz, 1H), 3.62 (s, 3H), 2.73 (m, 1H), 2.49 – 2.22 (m, 3H), 2.04 – 1.91 (m, 2H), 1.78 (m, 1H), 1.61 – 1.59 (m, 3H), 1.20 – 1.13 (m, 2H). ^{13}C NMR (100 MHz, Chloroform- d): δ 172.0, 163.6, 154.0, 136.2, 133.7, 129.0, 114.7, 110.2, 68.5,

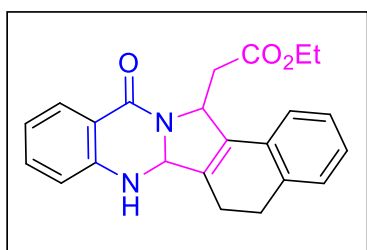
55.5, 52.5, 35.2, 33.5, 32.1, 29.2, 26.8, 25.4. HRMS calcd. for $C_{17}H_{21}N_2O_3S$: $(M+H)^+$ 333.1275, found : 333.1276.

Methyl 2-(4-oxo-4,6,7,8,9,10,11,12,12b,13-decahydrocycloocta[3,4]pyrrolo[1,2-a]thieno[2,3-d]pyrimidin-6-yl)acetate: (3n)

Off white solid (252.6 mg, 73%), mp. 139 °C. 1H NMR (400 MHz, Chloroform-*d*): δ 7.48 (d, $J = 5.3$ Hz, 1H), 6.53 (d, $J = 5.2$ Hz, 1H), 5.40 (s, 1H), 5.34 (s, 1H), 4.41 (d, $J = 5.0$ Hz, 1H), 3.70 (s, 3H), 2.79 (dd, $J = 16.8$, 5.9 Hz, 1H), 2.58 (d, $J = 16.8$ Hz, 1H), 2.41 – 2.37 (m, 2H), 2.15 – 2.12 (m, 1H), 2.01 – 1.97 (m, 1H), 1.70 – 1.60 (m, 2H), 1.56 – 1.37 (m, 6H). ^{13}C NMR (100 MHz, Chloroform-*d*): δ 172.0, 163.9, 154.7, 139.3, 134.6, 133.9, 125.8, 114.5, 66.6, 55.9, 52.5, 31.7, 31.2, 31.0, 27.8, 26.4, 26.2, 25.9. HRMS calcd. for $C_{18}H_{23}N_2O_3S$: $(M+H)^+$ 347.1431, found : 347.1430.

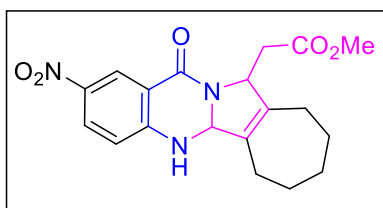


Yellow solid (205.7 mg, 55%), mp. 145 °C. 1H NMR (400 MHz, Chloroform-*d*): δ 8.02 (d, $J = 7.8$ Hz, 1H), 7.43 (t, $J = 7.6$ Hz, 1H), 7.37 – 7.17 (m, 3H), 6.97 (t, $J = 7.4$ Hz, 1H), 6.68 (d, $J = 8.0$ Hz, 1H), 6.04 (s, 1H), 5.69 (s, 1H), 4.71 – 4.70 (m, 1H), 4.20 – 4.08 (m, 2H), 3.15 – 3.00 (m, 2H), 2.85 – 2.83 (m, 2H), 2.52 – 2.39 (m, 1H), 2.20 – 2.16 (m, 1H), 1.18 (t, $J = 7.1$ Hz, 3H). ^{13}C NMR (125 MHz, Chloroform-*d*): δ 171.5, 168.1, 160.8, 149.3, 137.7, 134.5, 134.0, 130.9, 129.9, 128.5, 127.6, 127.1, 126.7, 126.4, 124.7, 122.5, 66.3, 60.9, 53.3, 29.7, 27.8, 18.2, 13.7. HRMS calcd. for $C_{23}H_{23}N_2O_3$: $(M+H)^+$ 375.1710, found : 375.1711.



Methyl 2-(2-nitro-13-oxo-5,5a,7,8,9,10,11,13-octahydro-6H-cyclohepta[3,4]pyrrolo[2,1-b]quinazolin-11-yl)acetate: (3p)^a

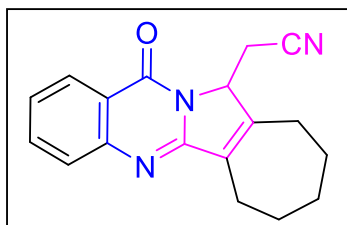
Yellow solid (230.1 mg, 62%), mp. 168 °C. 1H NMR (400 MHz, DMSO-*d*⁶) δ 8.50 (d, $J = 2.8$ Hz, 2H), 8.17 (dd, $J = 9.3$, 2.8 Hz, 1H), 7.10 (d, $J = 9.6$ Hz, 1H), 5.10 (s, 1H), 5.03 (d, $J = 5.6$ Hz, 1H), 3.61 (s, 3H), 2.79 – 2.74 (m, 1H), 2.38 – 2.23 (m, 3H), 2.04 – 1.96 (m, 1H), 1.87 (dd, $J = 15.1$, 6.5 Hz, 1H), 1.78 – 1.74 (m, 2H), 1.60 – 1.50 (m, 4H). ^{13}C NMR (75 MHz, DMSO-*d*⁶) δ 170.4, 169.3, 162.7, 155.4, 152.4, 129.3, 126.1,



123.9, 116.9, 113.1, 66.2, 53.8, 52.1, 34.1, 32.4, 31.0, 28.8, 26.0, 24.0. HRMS calcd. for $C_{19}H_{22}N_3O_5$: $(M+H)^+$ 372.1561, found : 372.1562.

2-(13-oxo-7,8,9,10,11,13-Hexahydro-6H-cyclohepta[3,4]pyrrolo[2,1-b]quinazolin-11-yl)acetonitrile: (3q)

Yellow solid (215.4 mg, 74%), mp. 134 °C. 1H NMR (400 MHz, Chloroform-*d*) δ 7.83 (dd, J

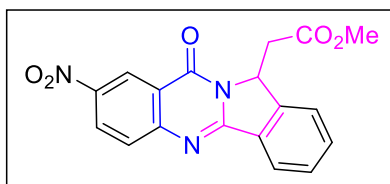


= 7.7, 1.3 Hz, 1H), 7.25 – 7.23 (m, 1H), 6.78 (t, J = 7.3 Hz, 1H), 6.60 (d, J = 8.0 Hz, 2H), 2.04 – 1.99 (m, 4H), 1.60 – 1.58 (m, 3H), 1.55 – 1.49 (m, 3H), 1.27 – 1.23 (m, 2H). ^{13}C NMR (101 MHz, Chloroform-*d*) δ 164.2, 145.7, 134.0, 132.0, 131.0, 128.9, 128.4, 118.8, 117.7, 115.2, 114.9, 72.6, 41.6 (2C), 29.1 (2C), 21.6

(2C). HRMS calcd. for $C_{18}H_{18}N_3O$: $(M+H)^+$ 292.1452, found : 292.1450.

Methyl 2-(8-nitro-10-oxo-10,12-dihydroisoindolo[1,2-b]quinazolin-12-yl)acetate: (3r)^a

Brown liquid (112.3 mg, 32%). 1H NMR (400 MHz, Chloroform-*d*) δ 9.19 (d, J = 2.6 Hz, 1H),

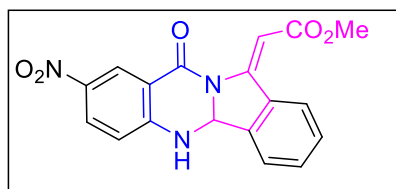


8.55 (dd, J = 9.3, 2.5 Hz, 1H), 8.22 (d, J = 7.7 Hz, 1H), 7.93 (d, J = 9.0 Hz, 1H), 7.70 – 7.63 (m, 3H), 5.87 (dd, J = 7.4, 3.6 Hz, 1H), 3.63 (s, 3H), 3.61 – 3.59 (m, 1H), 3.14 – 3.08 (m, 1H). ^{13}C NMR (101 MHz, Chloroform-*d*) δ 170.0, 159.6,

157.6, 153.3, 145.4, 143.8, 134.0, 129.9, 128.7, 128.6, 124.4, 123.4, 123.3, 121.6, 121.4, 59.2, 52.2, 35.3. HRMS calcd. for $C_{18}H_{14}N_3O_5$: $(M+H)^+$ 352.0935, found : 352.0937.

Methyl (E)-2-(8-nitro-10-oxo-5,10-dihydroisoindolo[1,2-b]quinazolin-12(4bH)-ylidene)acetate: (3s)^a

Off white solid (186.0 mg, 53%), mp. 152 °C. 1H NMR (500 MHz, 12% DMSO-*d*⁶ in



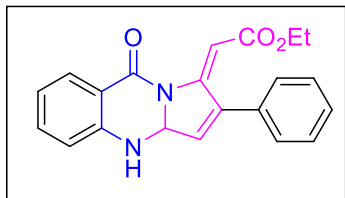
Chloroform-*d*) δ 8.61 (d, J = 2.5 Hz, 1H), 8.12 (d, J = 15.6 Hz, 1H), 8.00 (dd, J = 9.0, 2.6 Hz, 1H), 7.77 (s, 1H), 7.64 (d, J = 7.7 Hz, 1H), 7.55 (d, J = 7.0 Hz, 1H), 7.43 – 7.37 (m, 2H), 6.73 (d, J = 9.0 Hz, 1H), 6.28 (d, J = 4.9 Hz, 1H), 3.67 (s,

3H). ^{13}C NMR (126 MHz, 12% DMSO-*d*⁶ in Chloroform-*d*) δ 166.0, 162.1, 152.0, 140.4, 138.0, 137.2, 133.1, 129.8, 129.3, 128.5, 128.0, 126.9, 124.8, 121.0, 114.0, 112.4, 64.6, 51.2.

HRMS calcd. for $C_{18}H_{14}N_3O_5$: $(M+H)^+$ 352.0935, found : 352.0934.

Ethyl (E)-2-(9-oxo-2-phenyl-4,9-dihydropyrrolo[2,1-b]quinazolin-1(3aH)-ylidene)acetate:
(3t)

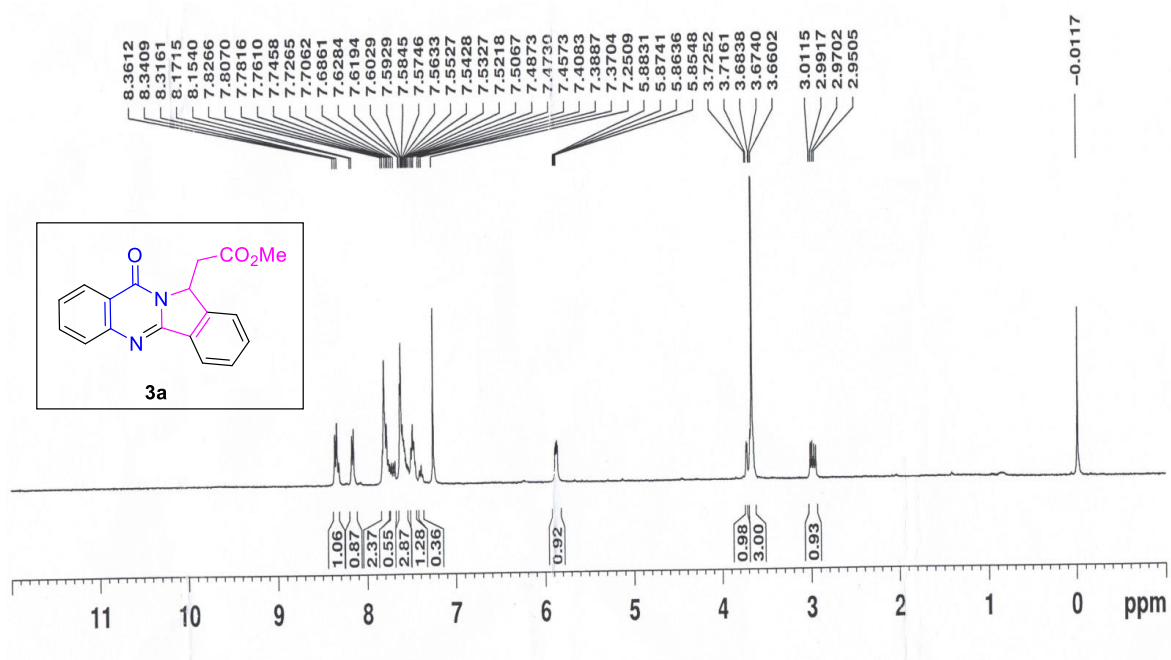
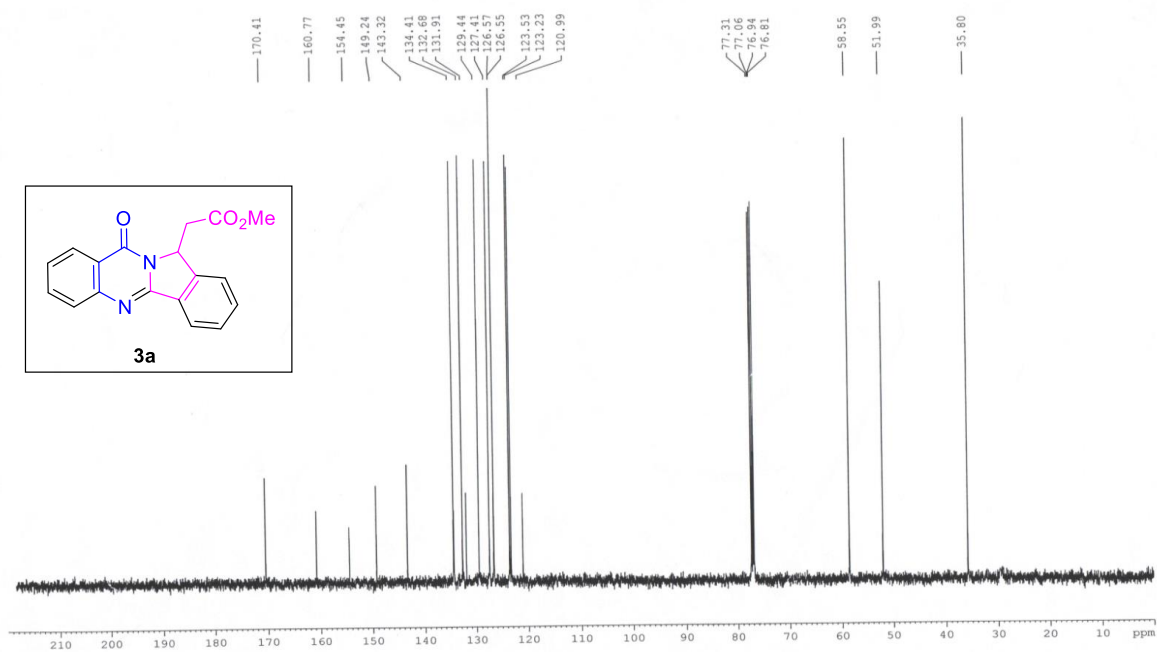
Yellow solid (249.2 mg, 72%), mp. 72 °C. ¹H NMR (400 MHz, DMSO-*d*⁶): δ 8.15 (s, 1H),

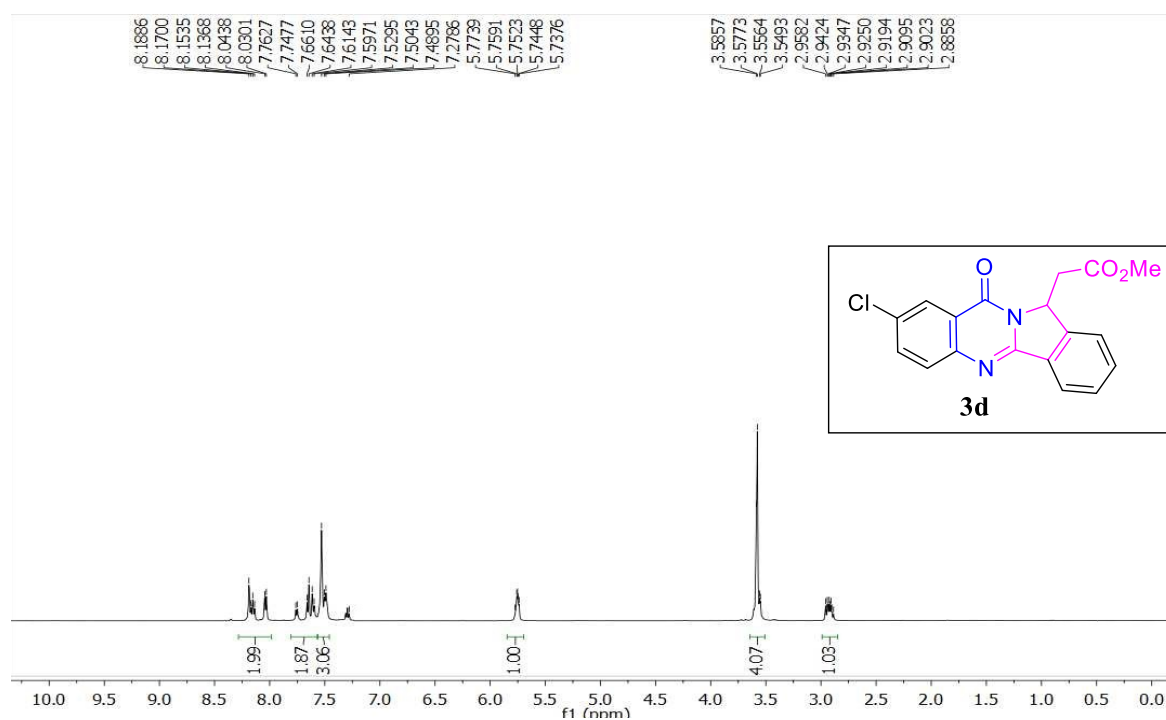
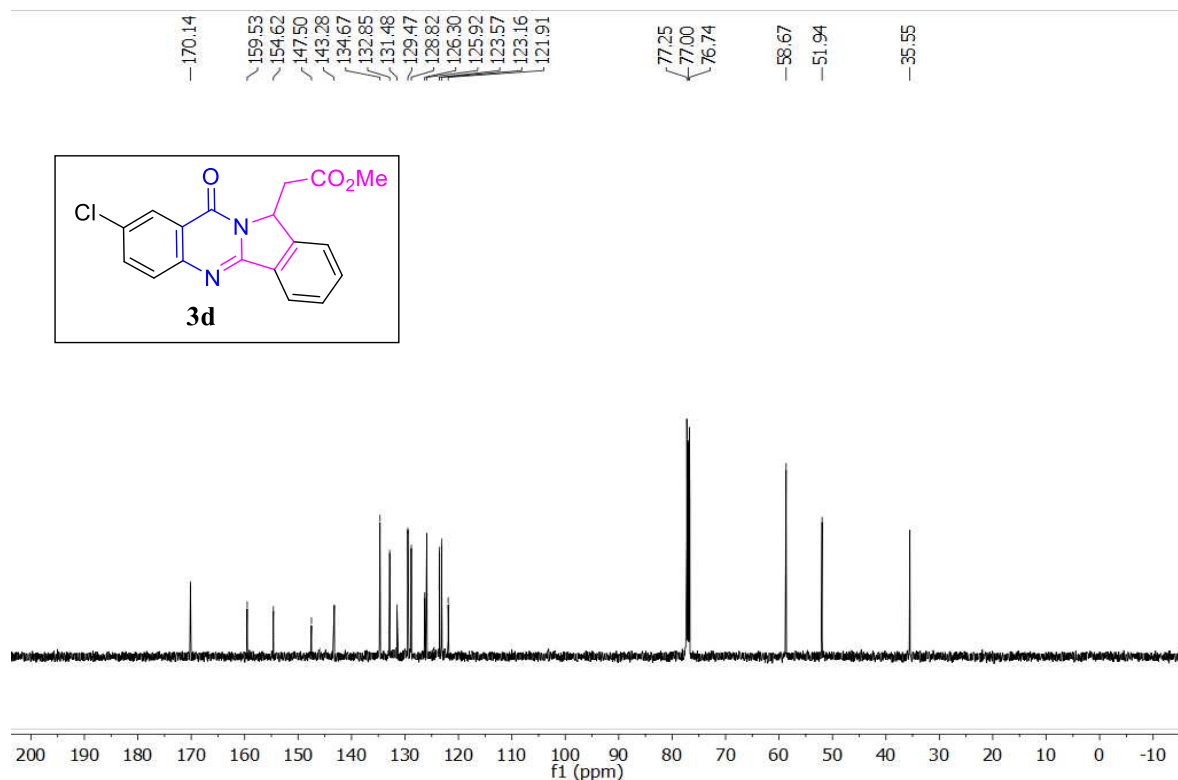


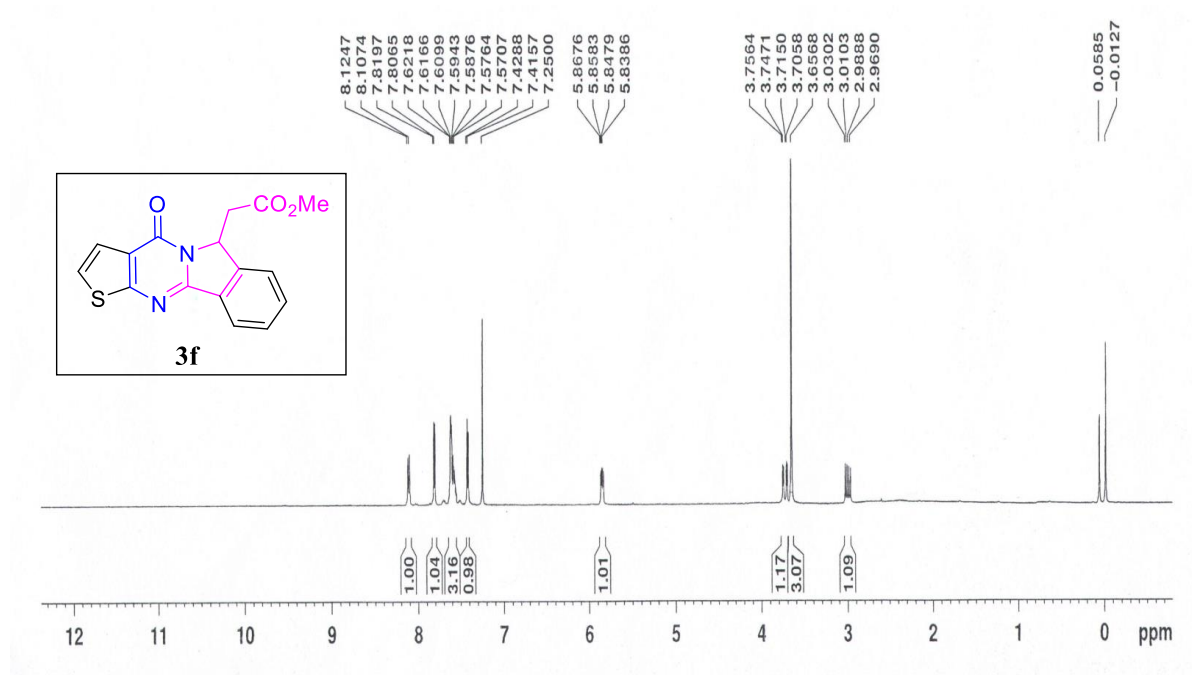
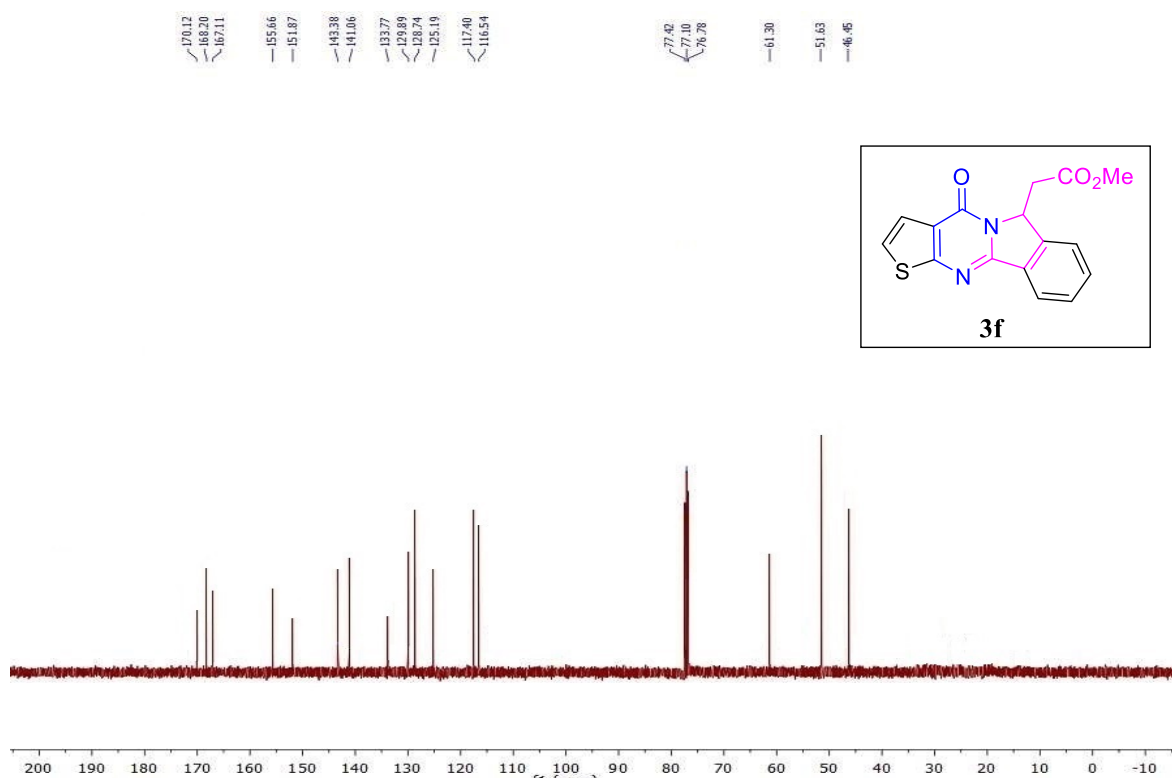
7.58 – 7.54 (m, 1H), 7.50 – 7.39 (m, 2H), 7.29 (d, *J* = 6.9 Hz, 2H),
7.24 (t, *J* = 7.1 Hz, 1H), 6.80 (s, 1H), 6.71 – 6.66 (m, 2H), 6.47
(d, *J* = 9.4 Hz, 1H), 5.33 (d, *J* = 15.6 Hz, 1H), 4.89 (d, *J* = 9.5 Hz,
1H), 4.08 (q, *J* = 7.2 Hz, 2H), 1.17 (td, *J* = 7.0, 3.2 Hz, 3H). ¹³C

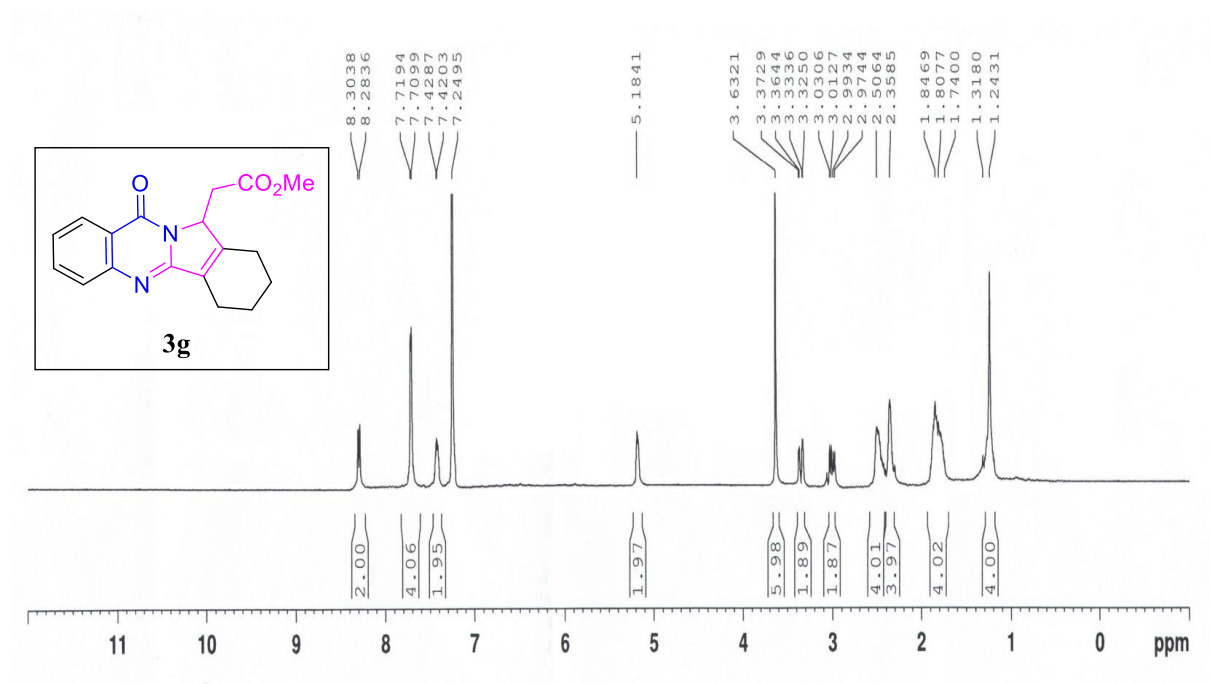
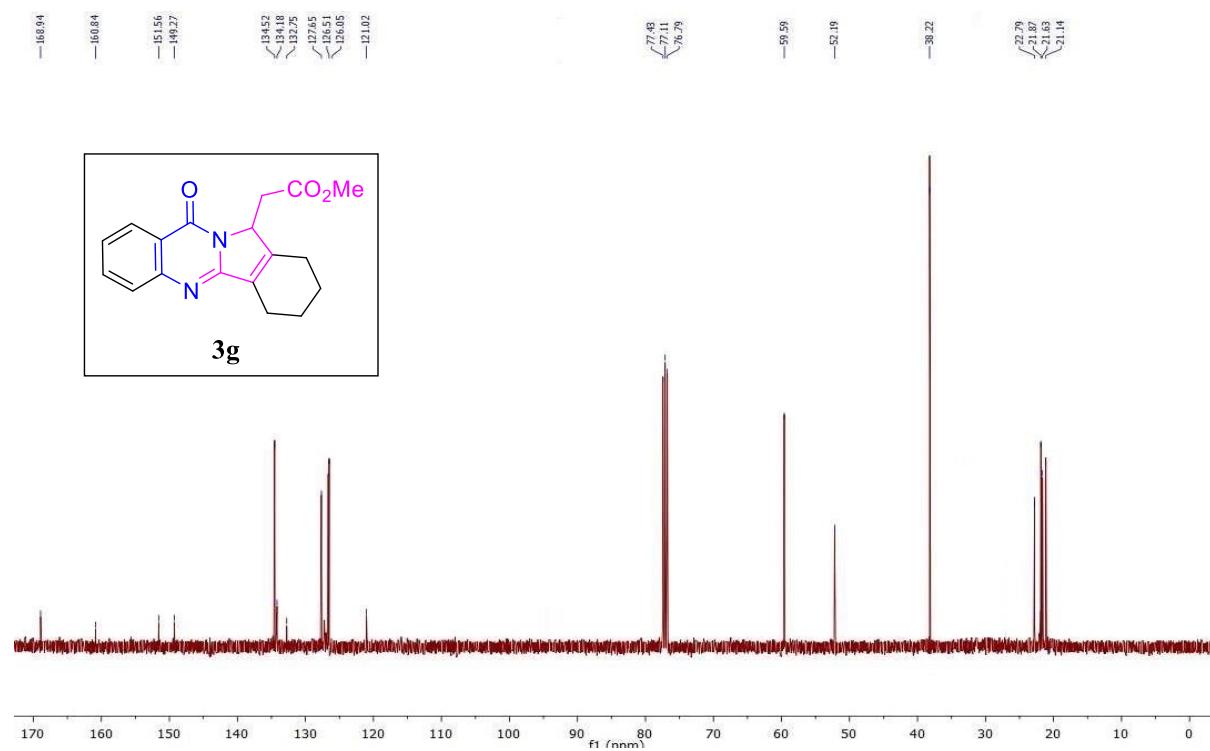
NMR (100 MHz, Chloroform-*d*): δ 166.6, 164.8, 146.6, 146.4, 143.3, 135.3, 134.5, 134.0,
129.0 (2C), 128.9 (2C), 128.7, 128.6, 123.9, 119.5, 115.5, 114.9, 63.2, 60.7, 14.3. HRMS calcd.
for C₂₁H₁₉N₂O₃: (M+H)⁺ 347.1397, found : 347.1396.

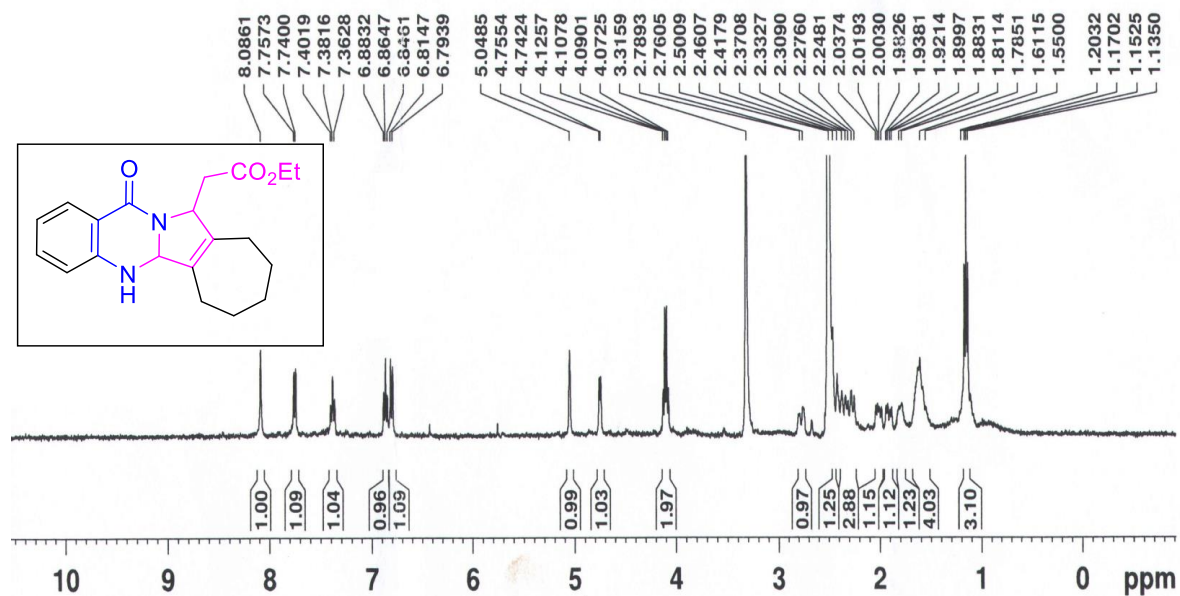
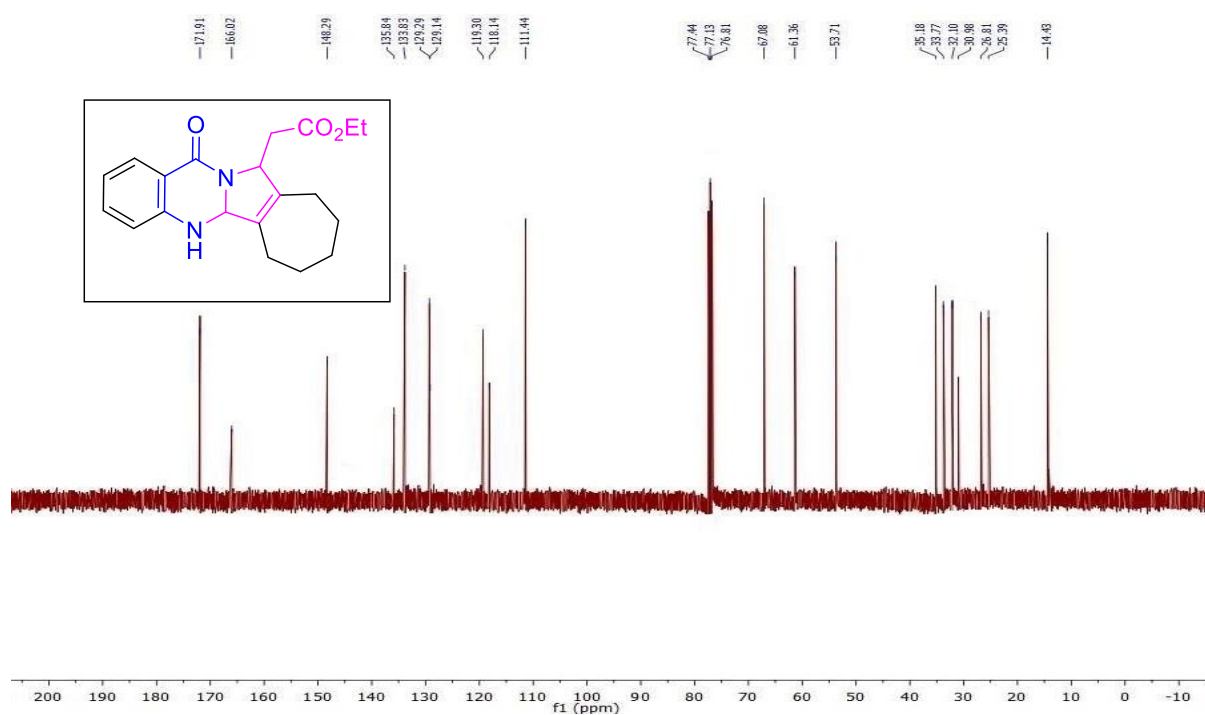
3.6.2. Representative NMR spectra:

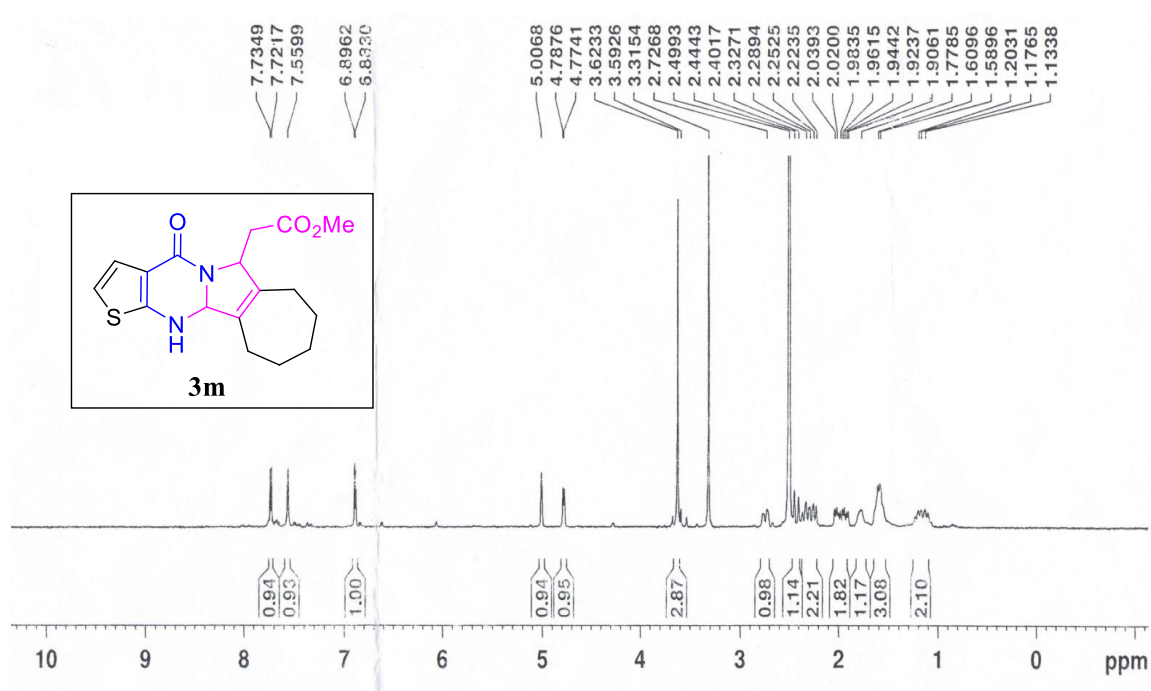
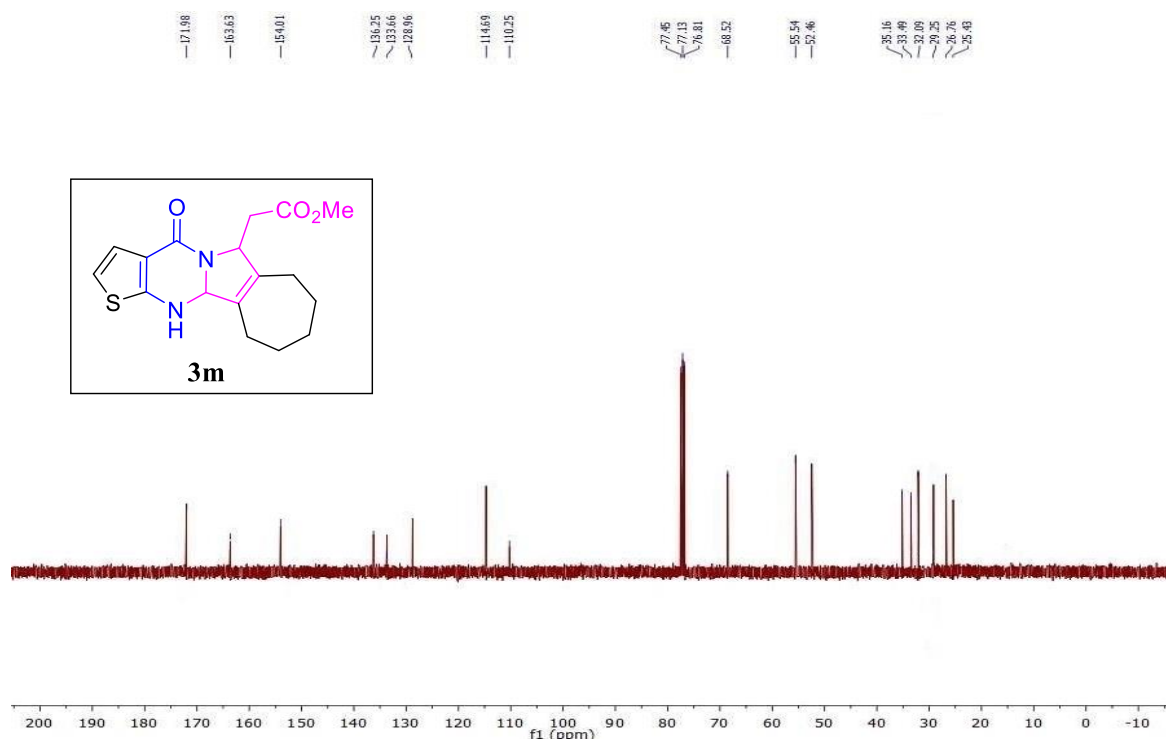
¹H NMR Spectra of 3a (400 MHz, Chloroform-*d*):¹³C NMR Spectra of 3a (125 MHz, Chloroform-*d*):

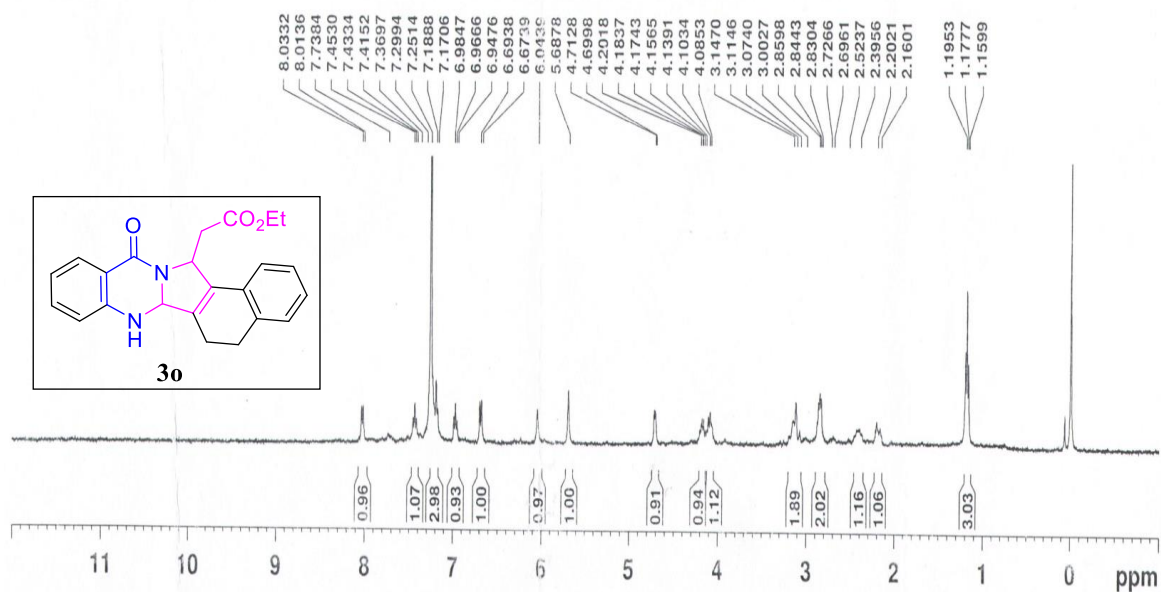
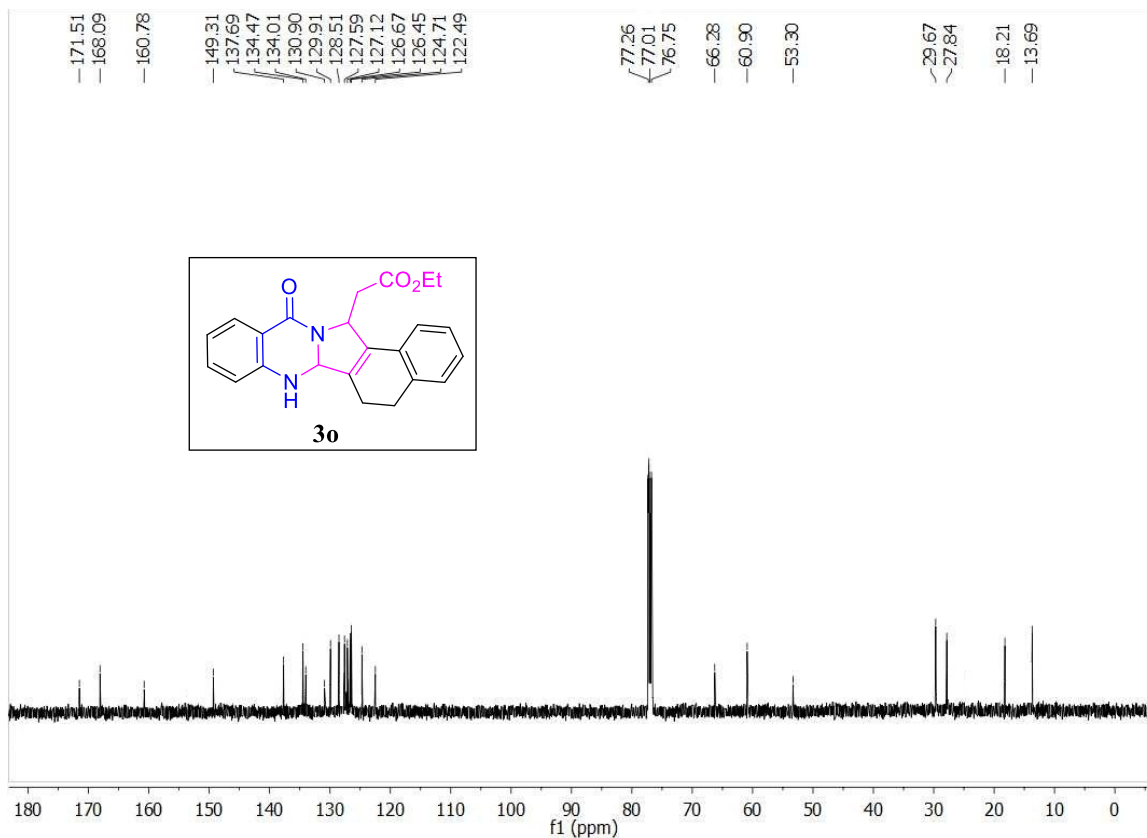
¹H NMR Spectra of 3d (500 MHz, Chloroform-*d*):**¹³C NMR Spectra of 3d (125 MHz, Chloroform-*d*):**

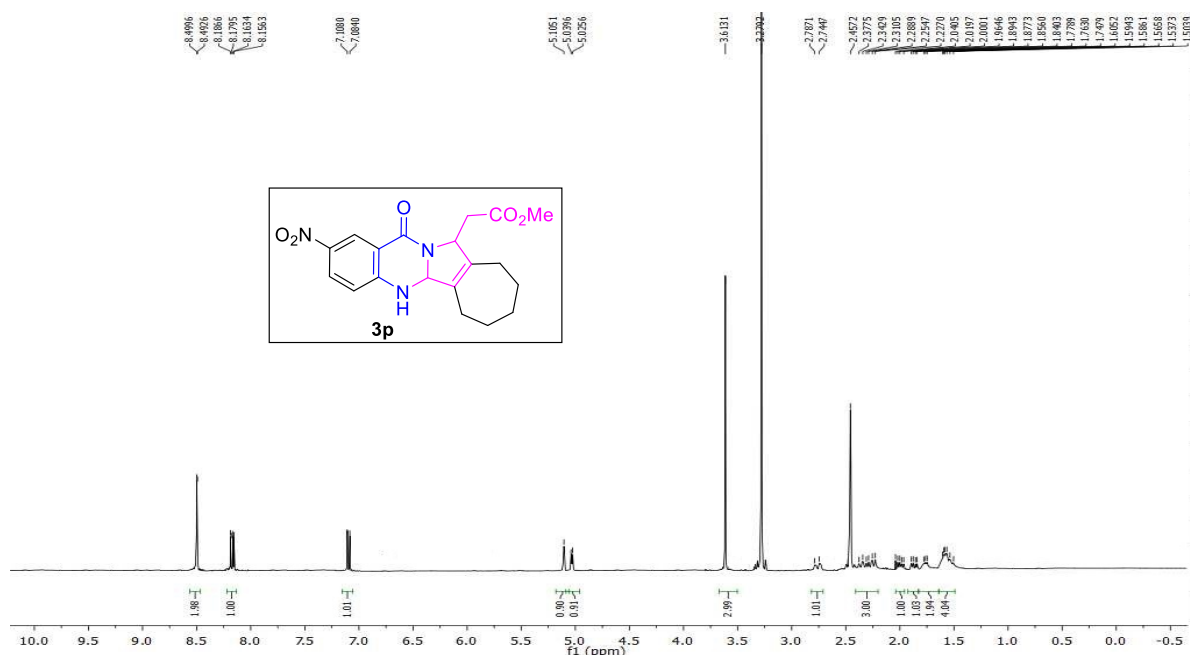
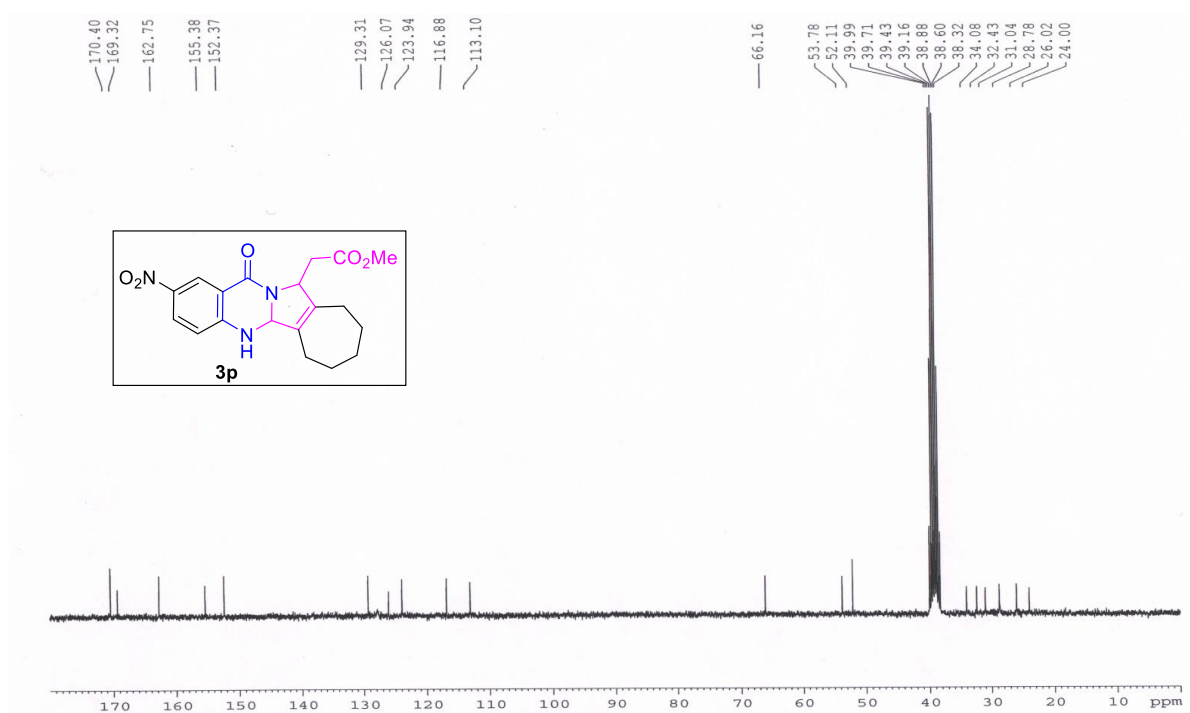
¹H NMR Spectra of 3f (400 MHz, Chloroform-*d*):**¹³C NMR Spectra of 3f (100 MHz, Chloroform-*d*):**

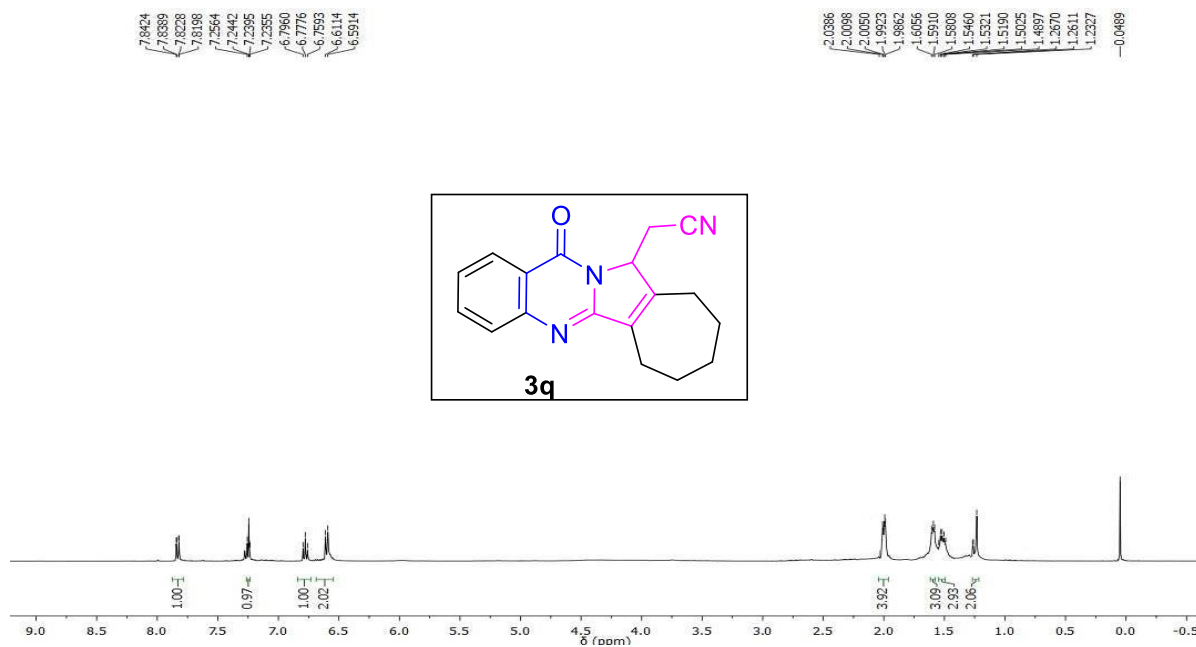
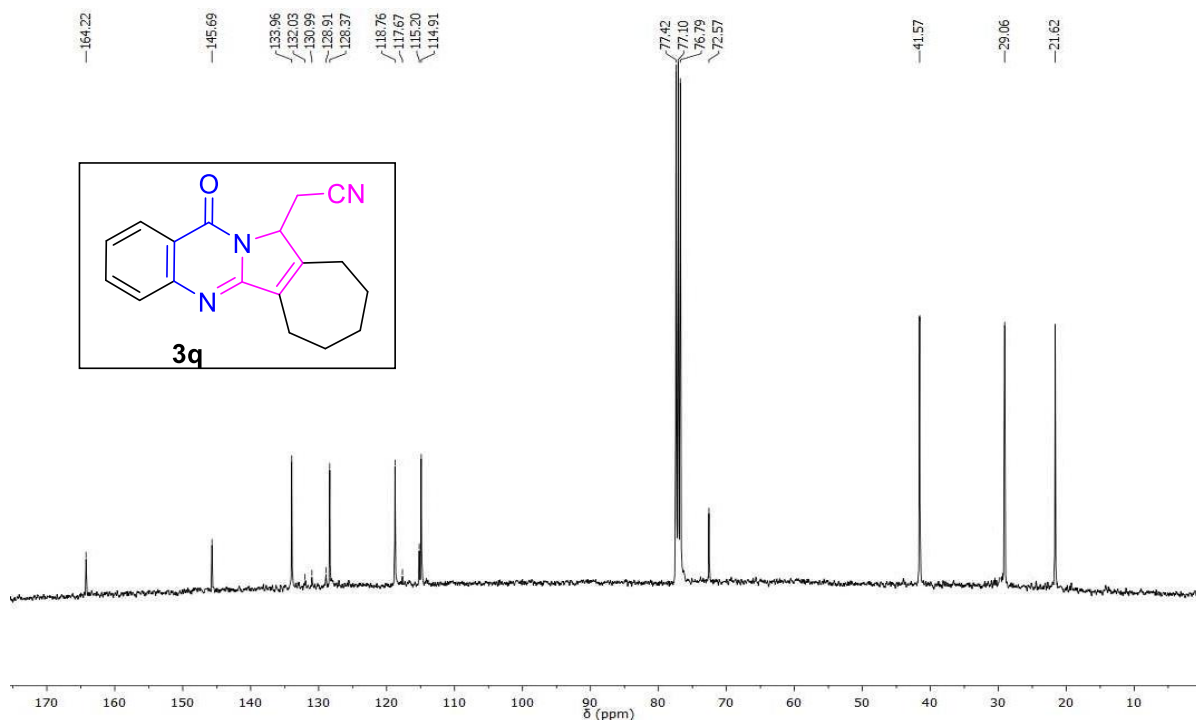
^1H NMR Spectra of 3g (400 MHz, Chloroform-*d*): **^{13}C NMR Spectra of 3g (100 MHz, Chloroform-*d*):**

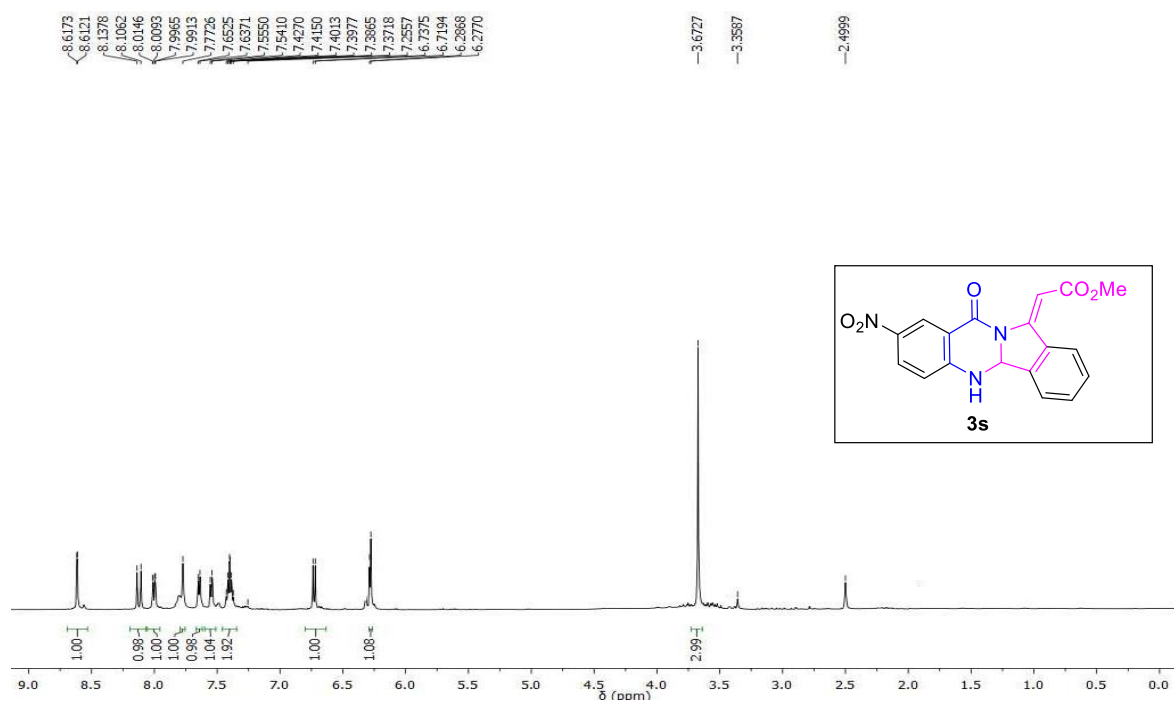
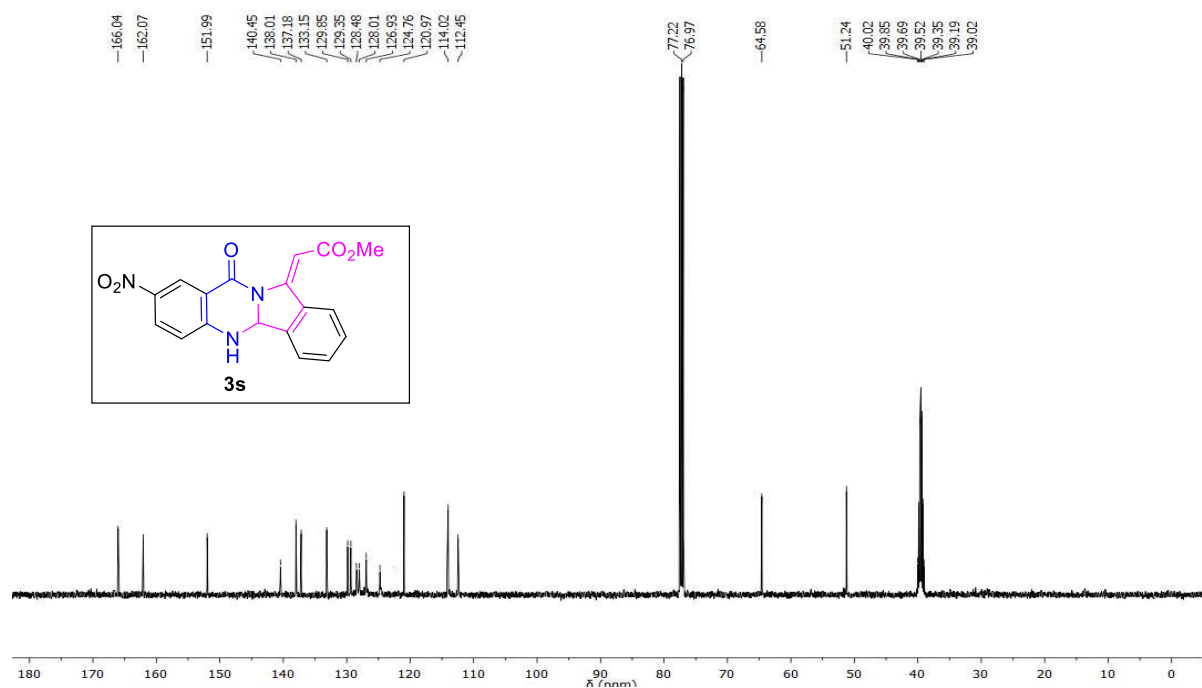
¹H NMR Spectra of 3j (400 MHz, DMSO-*d*⁶):**¹³C NMR Spectra of 3j (100 MHz, Chloroform-*d*):**

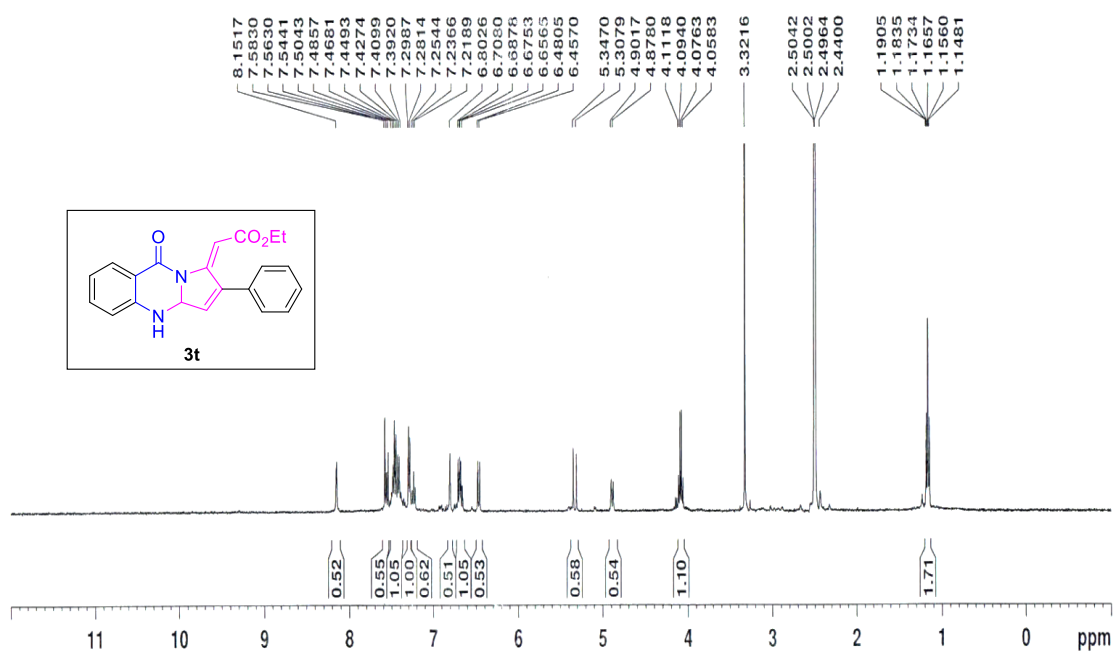
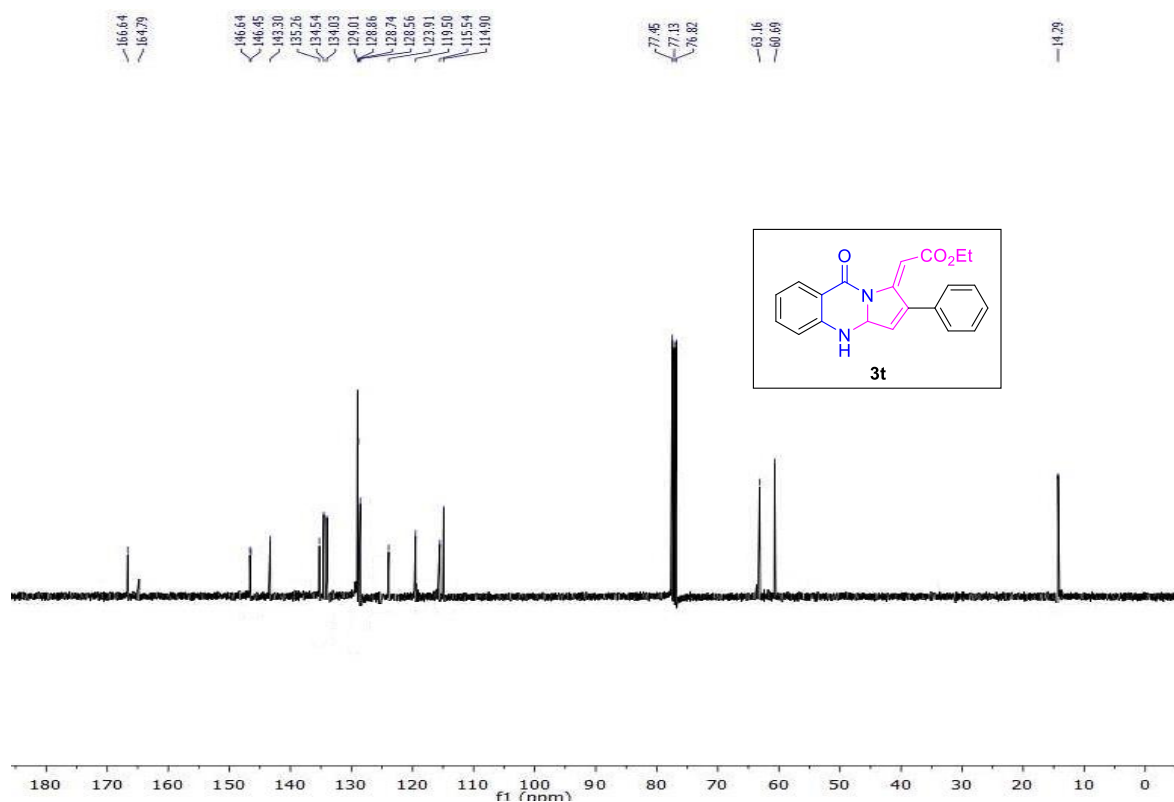
^1H NMR Spectra of 3m (400 MHz, DMSO- d_6): **^{13}C NMR Spectra of 3m (100 MHz, Chloroform- d):**

¹H NMR Spectra of 3o (400 MHz, Chloroform-d):**¹³C NMR Spectra of 3o (125 MHz, Chloroform-d):**

^1H NMR Spectra of 3p (400 MHz, $\text{DMSO-}d_6$): **^{13}C NMR Spectra of 3p (75 MHz, $\text{DMSO-}d_6$):**

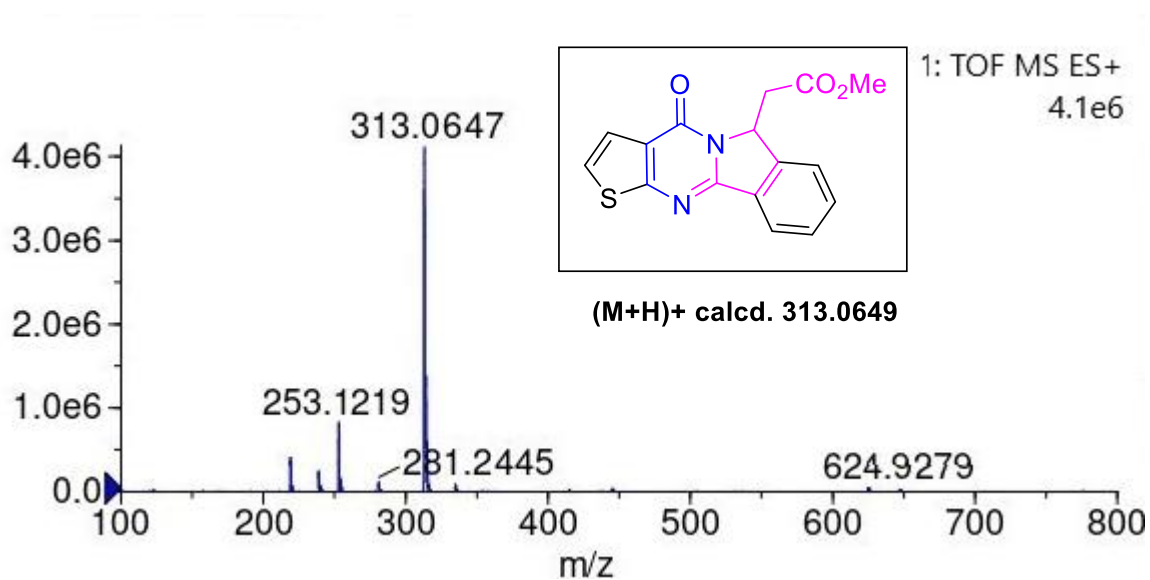
^1H NMR Spectra of 3q (400 MHz, Chloroform-*d*): **^{13}C NMR Spectra of 3q (101 MHz, Chloroform-*d*):**

^1H NMR Spectra of 3s (500 MHz, 12% DMSO- d_6 in Chloroform- d): **^{13}C NMR Spectra of 3s (126 MHz, 12% DMSO- d_6 in Chloroform- d):**

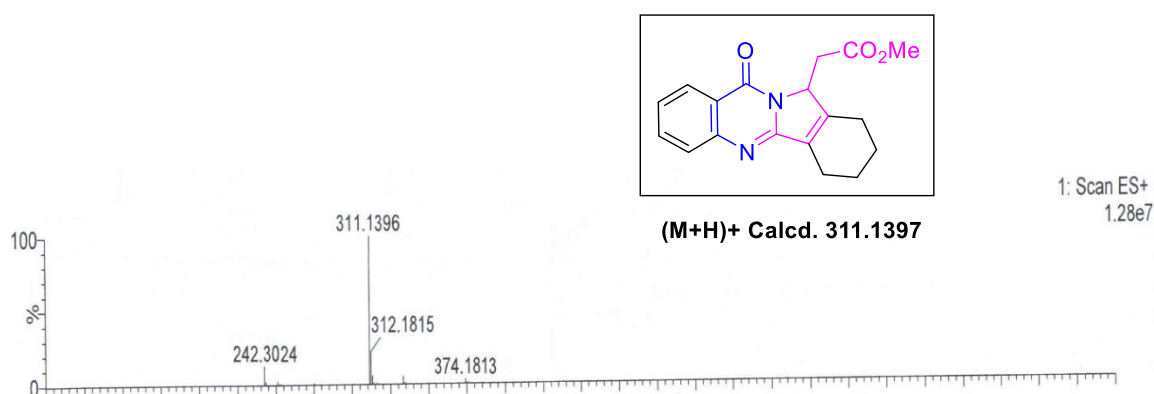
^1H NMR Spectra of 3t (400 MHz, DMSO- d_6): **^{13}C NMR Spectra of 3t (100 MHz, Chloroform- d):**

3.6.3. Representative HRMS spectra:

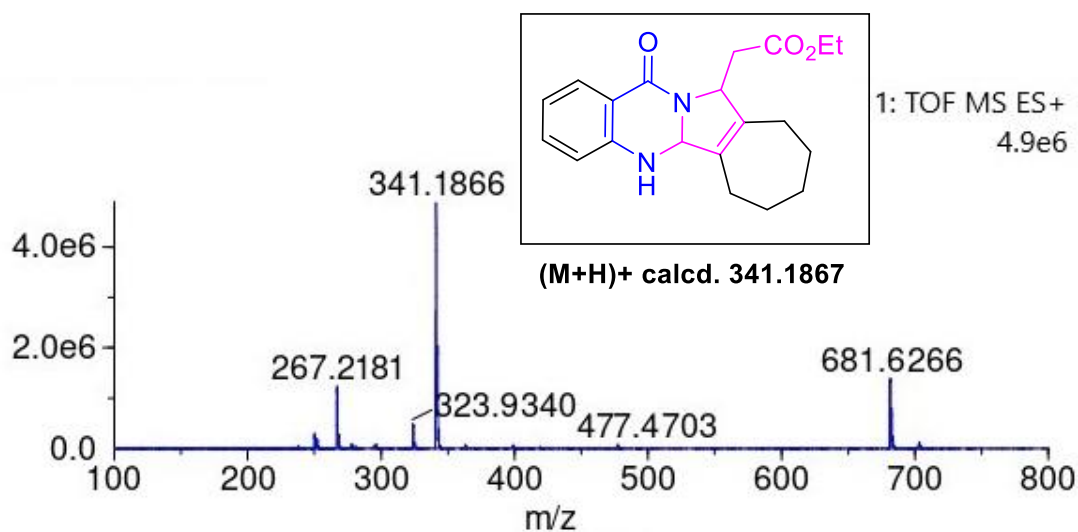
Methyl 2-(4-oxo-4,6-dihydrothieno[2',3':4,5]pyrimido[2,1-a]isoindol-6-yl)acetate: (3f)



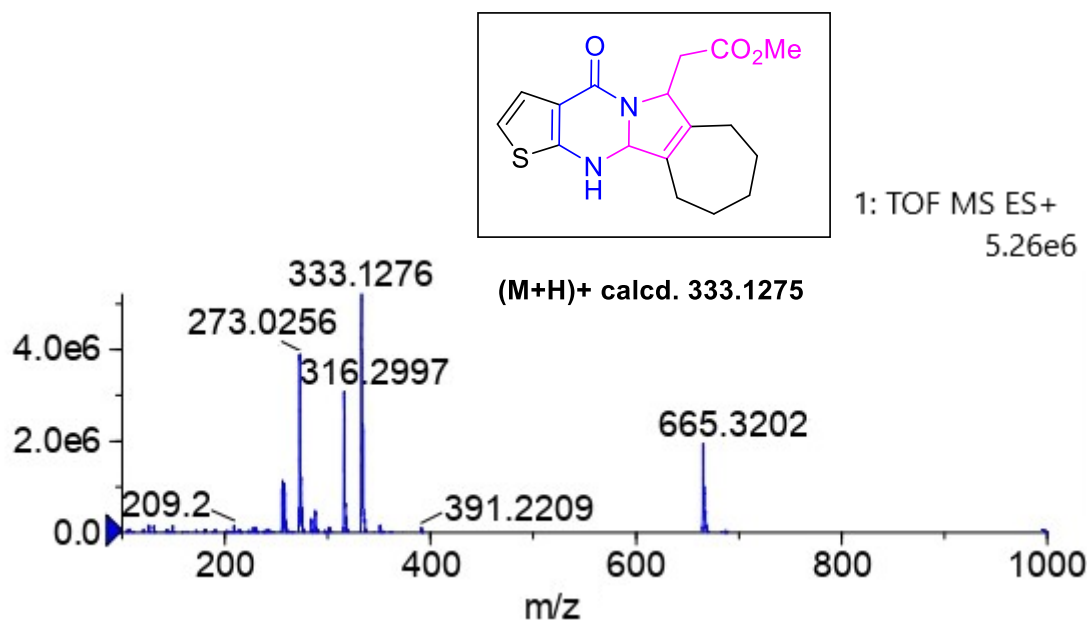
Methyl 2-(10-oxo-1,2,3,4,10,12-hexahydroisoindolo[1,2-b]quinazolin-12-yl)acetate: (3g)



Ethyl 2-(13-oxo-5,5a,7,8,9,10,11,13-octahydro-6H-cyclohepta[3,4]pyrrolo[2,1-b]quinazolin-11-yl)acetate: (3j)

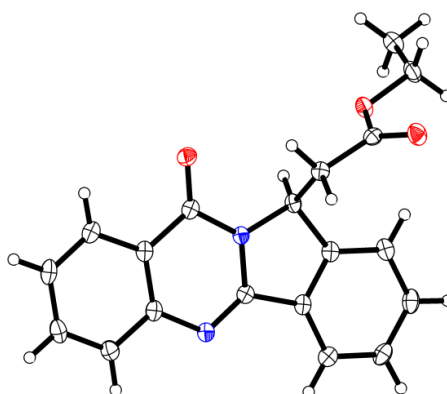


Methyl 2-(4-oxo-6,7,8,9,10,11,11b,12-octahydro-4H-cyclohepta[3,4]pyrrolo[1,2-a]thieno[2,3-d]pyrimidin-6-yl)acetate: (3m)



3.6.4. Crystallographic information:

Identification code	AB-14_a
Empirical formula	C ₁₉ H ₁₆ N ₂ O ₃
Formula weight	320.34
Temperature/K	293(2)
Crystal system	monoclinic
Space group	P2 ₁ /c
a/Å	8.90430(10)
b/Å	21.8459(3)
c/Å	7.86370(10)
α/°	90.00
β/°	100.695(2)
γ/°	90.00
Volume/Å ³	1503.09(3)
Z	4
ρ _{calc} /cm ³	1.416
μ/mm ⁻¹	0.792
F(000)	672.0
Crystal size/mm ³	0.1 × 0.05 × 0.05
Radiation	Cu Kα (λ = 1.54184)
2θ range for data collection/°	10.1 to 132.26
Index ranges	-10 ≤ h ≤ 10, -25 ≤ k ≤ 25, -8 ≤ l ≤ 9
Reflections collected	16614
Independent reflections	2624 [R _{int} = 0.0399, R _{sigma} = 0.0224]
Data/restraints/parameters	2624/0/218
Goodness-of-fit on F ²	1.048
Final R indexes [I ≥ 2σ (I)]	R ₁ = 0.0403, wR ₂ = 0.0996
Final R indexes [all data]	R ₁ = 0.0432, wR ₂ = 0.1019
Largest diff. peak/hole / e Å ⁻³	0.20/-0.28



Molecular structure of **3b** determined by SCXRD analysis. Thermal ellipsoids are shown in 50% probability level. (CCDC number of **3b** is 1945935).

Atom color code: Grey = Carbon atom, Blue = Nitrogen atom, Red = Oxygen atom, and White = Hydrogen atom.

3.7. References:

1. (a) G. Bairy, S. Das, H. M. Begam, and R. Jana, *Org. Lett.*, 2018, **20**, 7107-7112; (b) S. Chatterjee, R. Srinath, S. Bera, K. Khamaru, A. Rahman, and B. Banerji, *Org. Lett.*, 2019, **21**, 9028-9032; (c) U. A. Kshirsagar, *Org. Biomol. Chem.*, 2015, **13**, 9336-9352; (d) R. Cheng, L. Tang, T. Guo, D. Z-Negrerie, Y. Du, and K. Zhao, *RSC Adv.*, 2014, **4**, 26434-26438; (e) A. A. Radwan, and F. K. Alanazi, Biological Activity of Quinazolinones, 2020, 1-28 (DOI: 10.5772/intechopen.90621).
2. (a) J. L. Liang, H. C. Cha, and Y. Jahng, *Molecules*, 2011, **16**, 4861-4883; (b) M. B. Wagh, R. Shankar, U. K. S. Kumar, and C. H. Gill, *Synlett*, 2011, **1**, 84-88; (c) A. Cagir, S. H. Jones, R. Gao, B. M. Eisenhauer, and S. M. Hecht, *J. Am. Chem. Soc.*, 2003, **125**, 13628-13629; (d) M-C. Tseng, Y-W. Chu, H-P Tsai, C-M. Lin, J. Hwang, and Y-H. Chu, *Org. Lett.*, 2011, **13**, 920-923; (e) Z-Z. Ma, Y. Han, T. Nomu, and Y-J. Chen, *Heterocycles*, 1997, **46**, 541-546.
3. (a) V. Ziaee, H. Jalalizadeh, M. Iranshahi, and A. Shafiee, *Iran. J. Chem. & Chem. Eng*, 2004, **23**, 33-36; (b) S. Eguchi, T. Suzuki, T. Okawa, and Y. Matsushita, *J. Org. Chem.*, 1996, **61**, 7316-7319.
4. (a) R. Kaur, S. K. Manjal, R. K. Rawal, and K. Kumar, *Bioorg. Med. Chem.*, 2017, **25**, 4533-4552; (b) Y. Jahng, *Arch. Pharm. Res.*, 2013, **36**, 517-535; (c) H. Hou, H. Li, Y. Han, and C. Yan, *Org. Chem. Front.*, 2018, **5**, 51-54; (d) L. A. Onambele, H. Riepl, R. Fischer, G. Pradel, A. Prokop, and M. N. Aminake, *Int. J. Parasitol.: Drugs Drug Resist.*, 2015, **5**, 48-57; (e) A. M. Tucker, and P. Grundt, *ARKIVOC*, 2012, 546-569.
5. P. Molina, A. Ta ´rraga, A. G-Tejero, I. Rioja, A. Ubeda, M. C. Terencio, and M. J. Alcaraz, *J. Nat. Prod.*, 2001, **64**, 1297-1300.
6. J. Teng, and X. W. Yang, *Heterocycles*, 2006, **68**, 1691-1698.
7. (a) I. Khan, A. Ibrar, W. Ahmed, and A. Saeed, *Eur. J. Med. Chem*, 2015, **90**, 124-169; (b) P. S. Auti, G. George, and A. T. Paul, *RSC Adv.*, 2020, **10**, 41353-41392; (c) T. P. Selvam, and P. V. Kumar, *Research in Pharmacy*, 2011, **1**, 1-21.
8. X. Tang, Z. Zhu, Z. Wang, Y. Tang, L. Wang, and L. Liu, *Spectrochim. Acta A Mol. Biomol. Spectrosc.*, 2020, **228**, 117845.
9. L. Liua, Y. Zhang, J. Zhou, J. Yang, C. Zhong, Y. Zhang, Y. Luo, Y. Fu, J. Huang, Z. Song, and Y. Peng, *Dyes Pigm.*, 2019, **165**, 58-64.
10. J. Kimura, H. Yamada, T. Yajima, and T. Fukushima, *J. Lumin.*, 2009, **129**, 1362-1365.

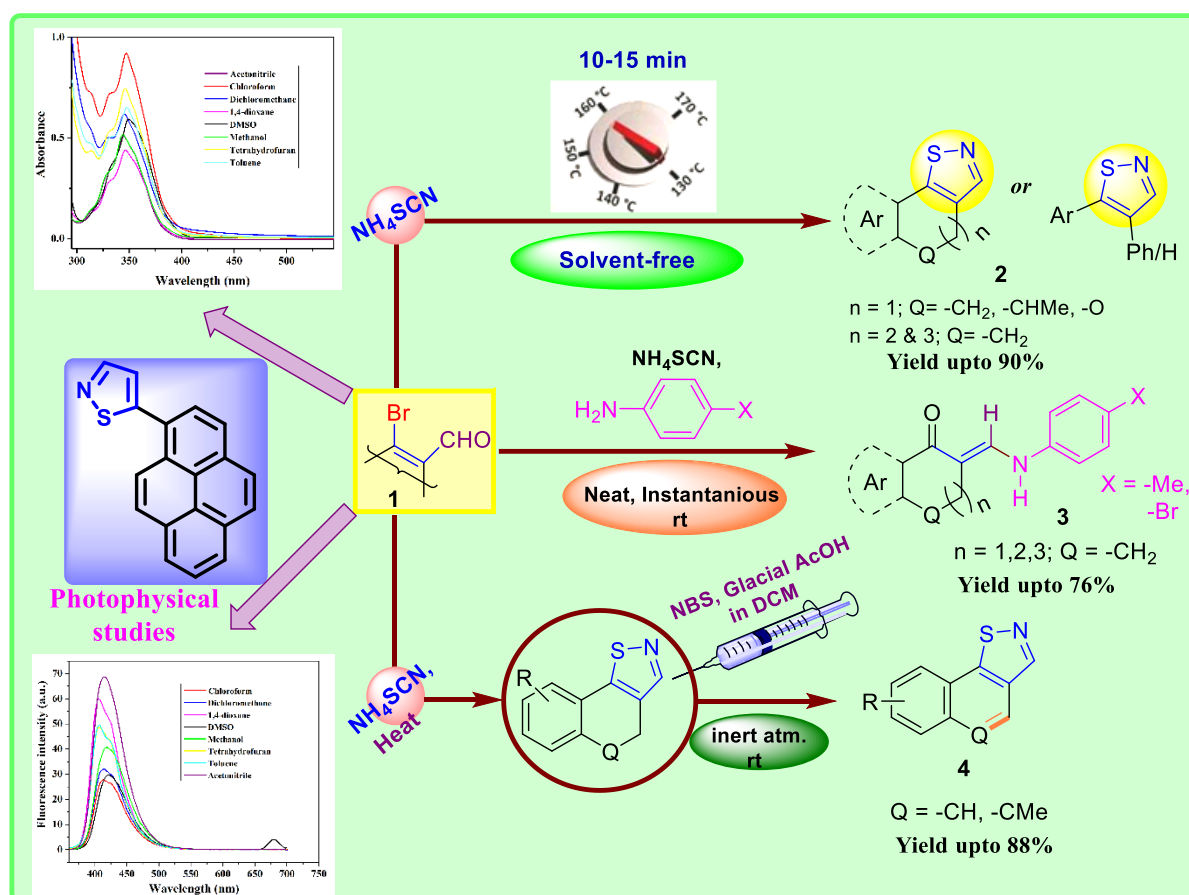
11. M. M. Aly, Y. A. Mohamed, K. A. M. El-Bayouki, W. M. Basyouni, and S. Y. Abbas, *Eur. J. Med. Chem.*, 2010, **45**, 3365-3373.
12. J-Q. Liu, Y-G. Ma, M-M. Zhang, and X-S Wang, *J. Org. Chem.*, 2017, **82**, 4918-4923.
13. Y. Zhang, J-Q. Liu, and X-S. Wang, *Tetrahedron Lett.*, 2020, **61**, 152508.
14. S. Guo, J. Zhai, F. Wang, and X. Fan, *Org. Biomol. Chem.*, 2017, **15**, 3674-3680.
15. J. Chen, H. Neumann, M. Beller, and X-F. Wu, *Org. Biomol. Chem.*, 2014, **12**, 5835-5838.
16. S. Biswas, B. Porashar, P. J. Arandhara, and A. K. Saikia, *Chem. Commun.*, 2021, **57**, 11701-11704.
17. M. A. Mondal, S. Mondal, and A. A. Khan, *J. Chem. Sci.*, 2020, **132**, 63.
18. M. V. Madhubabu, R. Shankar, S. s. More, M. V. B. Rao, U. K. S. Kumar, and R. Akula, *RSC Adv.*, 2016, **6**, 36599-36601.
19. X. Liu, P. Qian, Y. Wang, and Y. Pan, *Org. Chem. Front.*, 2017, **4**, 2370-2374.
20. R. Xu, Z. Wang, Q. Zheng, P. Patil, and A. Dömling, *J. Org. Chem.*, 2022, **87**, 13023-13033.
21. (a) B. Borah, S. Swain, M. Patat, and L. R. Chowhan, *Front. Chem.*, 2022, **10**, 991026; (b) D. S. Kawade, M. A. Chaudhari, J. B. Gujar, and M. S. Shingare, *Iran. J. Catal.*, 2016, **6**, 313-318.
22. S. Kuntikana, C. Bhat, M. Kongot, S. I. Bhat, and A. Kumar, *ChemSelect.*, 2016, **1**, 1723-1728.
23. M. Wang, J. Gao, Z. Song, and L. Wang, *J. Heterocycl. Chem.*, 2012, **49**, 1250-1253.
24. A. Dutta, and D. Sarma, *Sustain. Chem. Pharm.*, 2021, **20**, 100402.
25. R. Teixeira, T. Menengat, G. Andrade, B. Cotrim, C. Ponte, W. C. Santos, and G. Resende, *Molecules*, 2020, **25**, 1467.
26. J. S. Yadav, and B. V. S. Reddy, *Tetrahedron Lett.*, 2002, **43**, 1905-1907.
27. B-H. Chen, J-T. Li, G-F. Chen, *Ultrason. Sonochem.*, 2015, **23**, 59-65.
28. N. C. Dige, P. G. Mahajan, H. Raza, M. Hassan, B. D. Vanjare, H. Hong, K. H. Lee, J. latip, and S-Y. Seo, *Bioorg. Chem.*, 2019, **92**, 103201.
29. M. V. Madhubabu, R. Shankar, G. r. Reddy, T. S. Rao, M. V. B. Rao, and R. Akula, *Tetrahedron Lett.*, 2016, **57**, 5033-5037.
30. L. Lu, K. Yang, M-M. Zhang, and X-S. Wang, *J. Heterocyclic Chem.*, 2014, **51**, 630.
31. R. V. Devi, A. M. Garande, and P. M. Bhate, *Synlett*, 2016, **27**, 2807-2810.
32. D. Sarma, B. Majumdar, B. Deori, S. Jain, and T. K. Sarma, *ACS Omega*, 2021, **6**, 11902-11910.

33. H. Baguia, C. Deldaele, E. Romero, B. Michelet, and G. Evano, *Synthesis*, 2018, **50**, 3022-3030.
34. (a) S. K. Manna, A. Mandal, S. K. Mondal, A. K. Adak, A. Jana, S. Das, S. Chattopadhyay, S. Roy, S. K. Ghorai, S. Samanta, M. Hossain, and M. Baidya, *Org. Biomol. Chem.*, 2015, **13**, 8037-8047; (b) S. K. Manna, S. K. Mondal, A. Ahmed, A. Mandal, A. Jana, M. Iqbal, S. Samanta, and J. K. Ray, *RSC Adv.*, 2014, **4**, 2474-2481; (c) S. K. Mondal, S. K. Manna, A. Mandal, S. Samanta, and J. K. Ray, *Tetrahedron Lett.*, 2014, **55**, 6411-6415; (d) A. Jana, S. K. Manna, S. K. Mondal, A. Mandal, A. Jana, B. K. Senapati, M. Jana, and S. Samanta, *Tetrahedron Lett.*, 2016, **57**, 3722-3726; (e) S. K. Mondal, A. Mandal, S. K. Manna, Sk. A. Ali, M. Hossain, V. Venugopal, A. Jana, and S. Samanta, *Org. Biomol. Chem.*, 2017, **15**, 2411-2421; (f) S. K. Mondal, Sk. A. Ali, S. K. Manna, A. Mandal, B. K. Senapati, M. Hossain, and S. Samanta, *ChemSelect.*, 2017, **2**, 9312-9318.
35. CCDC number of **3b** is 1945935.
36. Y. N. Kim, and H. C. Cheon, *Tetrahedron Lett.*, **2014**, **55**, 2340-2344.
37. Y. Zheng, W-B. Song, S-W. Zhang, and L-J. Xuan, *Org. Biomol. Chem.*, 2015, **13**, 6474-6478.
38. A. Yuan, C. Zheng, Z. Zhang, L. Yang, C. Liu, and H. Wang, *J. Fluoresc.*, 2014, **24**, 557-561.
39. A. V. Kulinich, E. K. Mikitenko, and A. Ishchenko, *Phys. Chem. Chem. Phys.*, 2016, **18**, 3444-3453.
40. C. Reichardt, *Chem. Rev.*, 1994, **94**, 2319-2358.
41. A. S. Klymchenko, *Acc. Chem. Res.*, 2017, **50**, 366-375.
42. S. B. Wakshe, P. R. Dongare, A. H. Gore, U. R. Kondekar, G. B. Kolekar and B. D. Ajalkar, *Inorg. Nano-Met. Chem.*, 2018, **48**, 49-56.
43. (a) A. Jemal, R. Siegel, E. Ward, Y. Hao, J. Xu, and M. J. Thun, *CA Cancer J. Clin.*, 2009, **59**, 225-249; (b) R. Singh, and M. J. Czaja, *Cancer Biol. Ther.*, 2005, **4**, 1419-1421; (c) J. Song, Z. Qu, X. Guo, Q. Zhao, X. Zhao, L. Gao, K. Sun, F. Shen, M. Wu, and L. Wei, *Autophagy*, 2009, **5**, 1131-1144.
44. (a) S. Singh, D. Chitkara, R. Mehrazin, S. Behrman, R. Wake, and R. Mahato, *PLoS One.*, 2012, **7**, e40021; (b) Jr. Lee JT, LS. Steelman, and JA. McCubrey, *Cancer Res.*, 2004, **64**, 8397-8404.

Chapter 4

Neat synthesis of isothiazole compounds, studies on their synthetic applications and photophysical properties

Neat synthesis of isothiazole compounds, studies on their synthetic applications and photophysical properties



(Contents of this chapter have been published in *New J. Chem.*, 2022, **46**, 11685-11694)

4.1. Introduction:

Isothiazoles are five-membered nitrogen (N) and sulfur (S) containing heterocycles which had been ubiquitously found in various bio-active alkaloids, and synthetic intermediates as a key structure. Among aromatic heterocycles, isothiazoles are considered as a valuable tool for the synthetic purpose in agrochemicals and pharmaceuticals industries. Substituted isothiazoles have wide spread of biological applications, such as anticancer, antifungal, antidiabetic, and neuroprotective agents, HIV inhibitor, and anti-bacterial agent etc. (Figure 4.1).¹

4.1.1. Isothiazole in alkaloids:

Brassilexin, and Sinalexin are two highly important bio-active molecules which exhibit antifungal activity as phytoalexins. Brassilexin is found in identified by *Brassica* species, and sinalexin is obtained from *Sinapis alba*.² An isothiazolonaphthoquinone, aulosirazole, isolated from the blue-green algae *Aulosira fertilissima* Ghose, displayed cytotoxicity against selectively solid tumor cells. It can destroy the solid tumor cells in greater extent than the leukemia cells.^{2b,3} Pronqodine A is a quinone-embedded isothiazole analogue, which regulates the prostaglandin E₂ release from human synovial sarcoma SW982 cells.^{2b,4} Similar analogues, HDAC inhibitor shows anticancer activities.^{1b} GPR 120 agonist has antidiabetic properties. Benz-1,2-thiazole derivative, mGlu4 modulator has neuroprotective properties^{1b} (Figure 4.1).

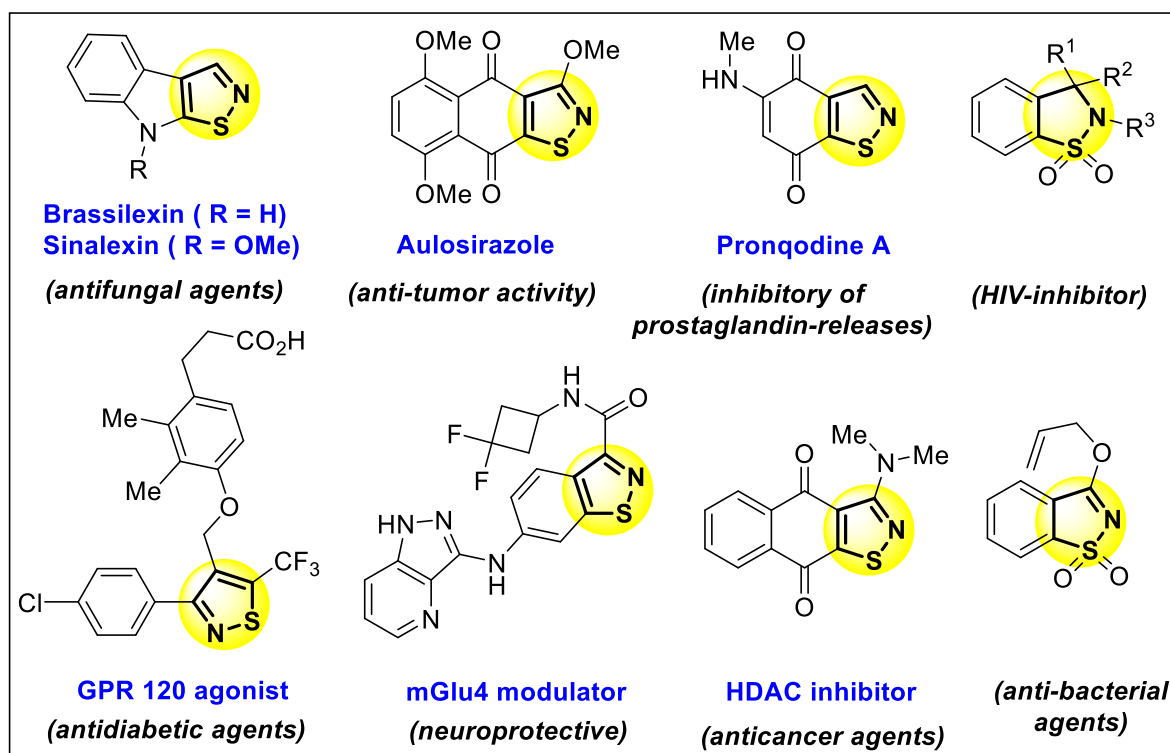


Figure 4.1. Some bio-active substituted isothiazole moieties.

4.1.2. Isothiazole in drug molecules:

Substituted isothiazoles have great abundance in medical world. Many commercially available drug molecules are directly related to the isothiazole moieties. So, it has broad spectrum in pharmaceutical industries. Zipracidone, a *d*-fused isothiazole based bio-active molecule, is used as antipsychotic drugs. The brand name of zipracidone is Geodon. It is also used for the treatment of bipolar disorder, and schizophrenia.⁵ Another atypical antipsychotic drug is perospirone with dopamine (DA) D₂-receptor antagonist.⁶ Monocyclic isothiazoles, such as denotivir and sulfasomizole are used as antiviral and antibacterial drug respectively^{1b, 5, 7} (Figure 4.2).

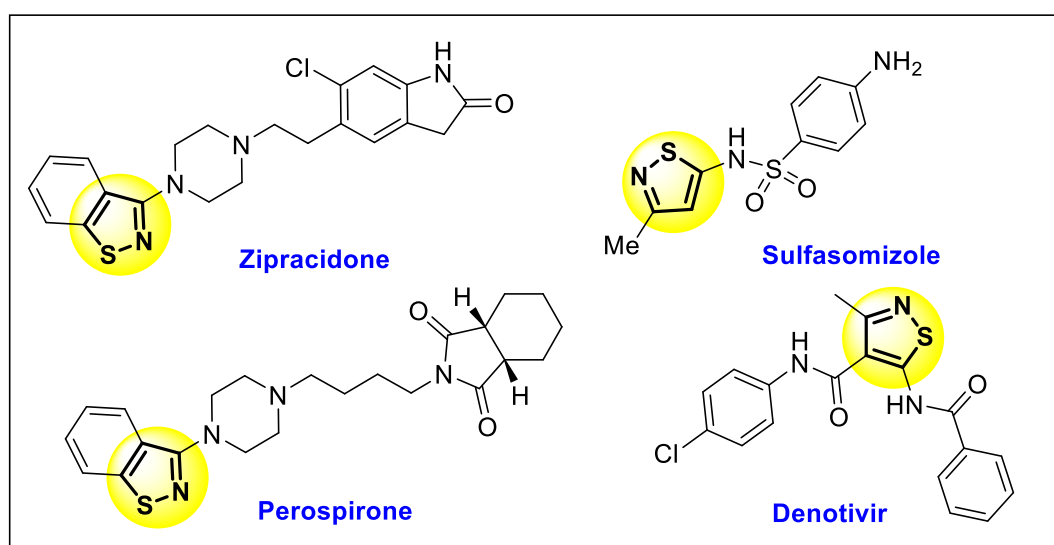


Figure 4.2. Drug molecules containing isothiazole moieties.

4.1.3. Agrochemical uses:

Besides the pharmacological activities substituted isothiazoles have extensively been used in agrochemical industries. Benzene-embedded isothiazole, Benclonthiaz has the insecticide composition and is used as pesticide.^{8a} Acylated aminoisothiazole is also used as insecticide^{8b} (Figure 4.3).

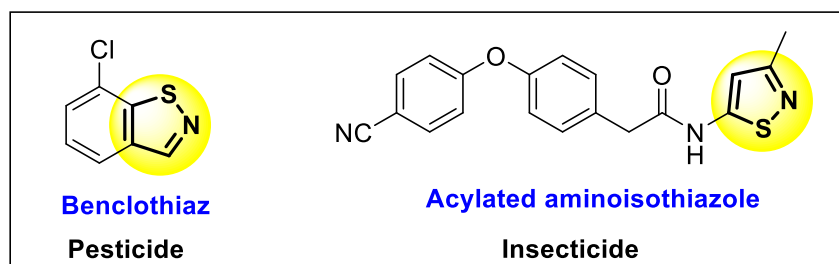


Figure 4.3. Application in agrochemical industries of isothiazole derivatives.

4.1.4. Application in consumer products:

After the remarkable applications in pharmaceuticals, and agrochemical industries, we observed that isothiazol-3-ones have a great contribution in cosmetic, paints, leather industries as a consumer product. The isothiazolinones such as, methylisothiazolinone (MI), benzisothiazolinone (BIT), octylisothiazolinone (OIT), methylchloroisothiazolinone (MCI), and dichlorooctylisothiazolinone (DCOIT) are commonly used in commercial purpose (**Figure 4.4**).⁹ Methylisothiazolinone is used in cosmetics, paints, and water treatment plant for purification of waste water. When it is combined with MCI in 3:1 proportion, it becomes Kathon, an active commercial biocide. OIT, and BIT are generally used in leather products and for cleaning purpose respectively. DCOIT is extensively used as antifouling agent to destroy the unwanted biofouling.

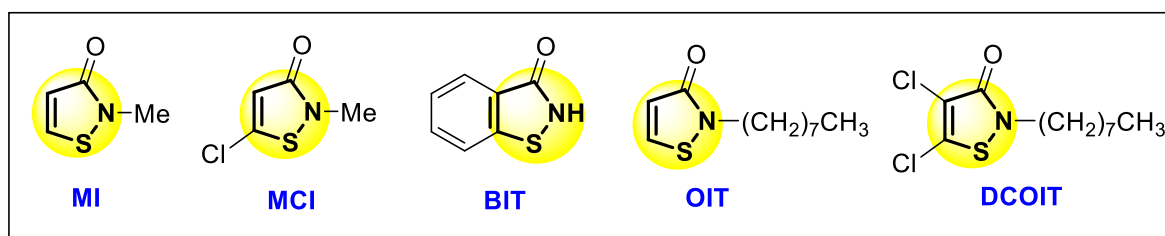


Figure 4.4. Chemical structures of common isothiazolinones consumer products.

4.1.5. Application as dye:

Recently, heterocyclic azo dyes snatch the great attention in modern textile world for their brilliant colour, and chromophoric strength. 3-Amino-5-nitro-[2,1]-benzisothiazole is very useful as diazonium component for the formation of disperse dye having high market value. As for example, it produces C.I. Disperse Blue 148, the best blue trichromatic azo dye (**Figure 4.5**).¹

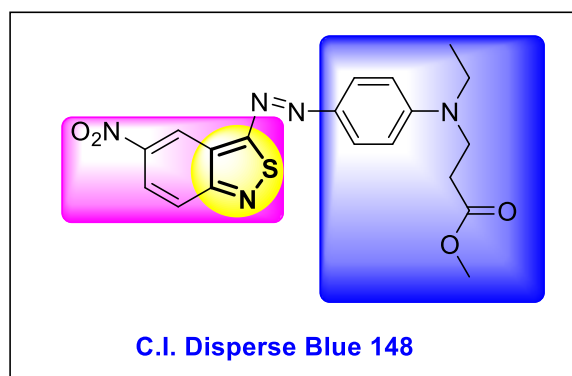


Figure 4.5. Benzisothiazole based azo-dye.

4.1.6. Isothiazole in nucleobases:

Generally, nucleobases present in DNA and RNA are nonemissive but it becomes emissive when it is attached with isothiazole scaffolds. The combination of ribonucleoside purine mimics with isothiazoles and construct an emissive isothiazolo analogues, isothiazolo[4,3-*d*]pyrimidine (**Figure 4.6**).¹¹

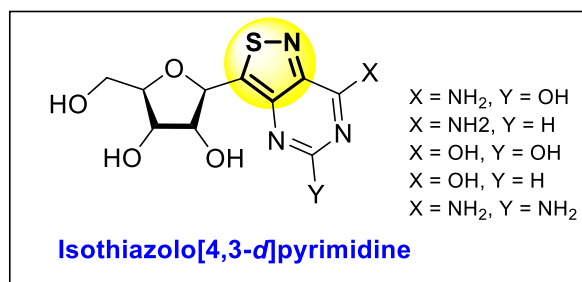


Figure 4.6. Isothiazole based fluorescent ribonucleoside.

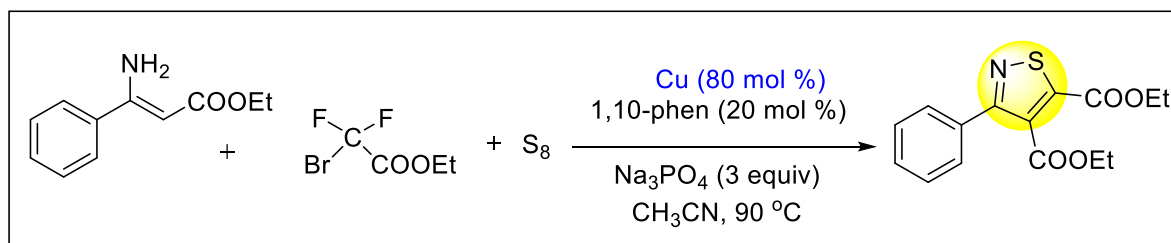
Following an in-depth study into the uses of fused isothiazoles, our present attention focuses on the synthetic approaches for preparing fused isothiazoles following both conventional and green methods.

4.2. Literature survey:

[A] Conventional approaches:

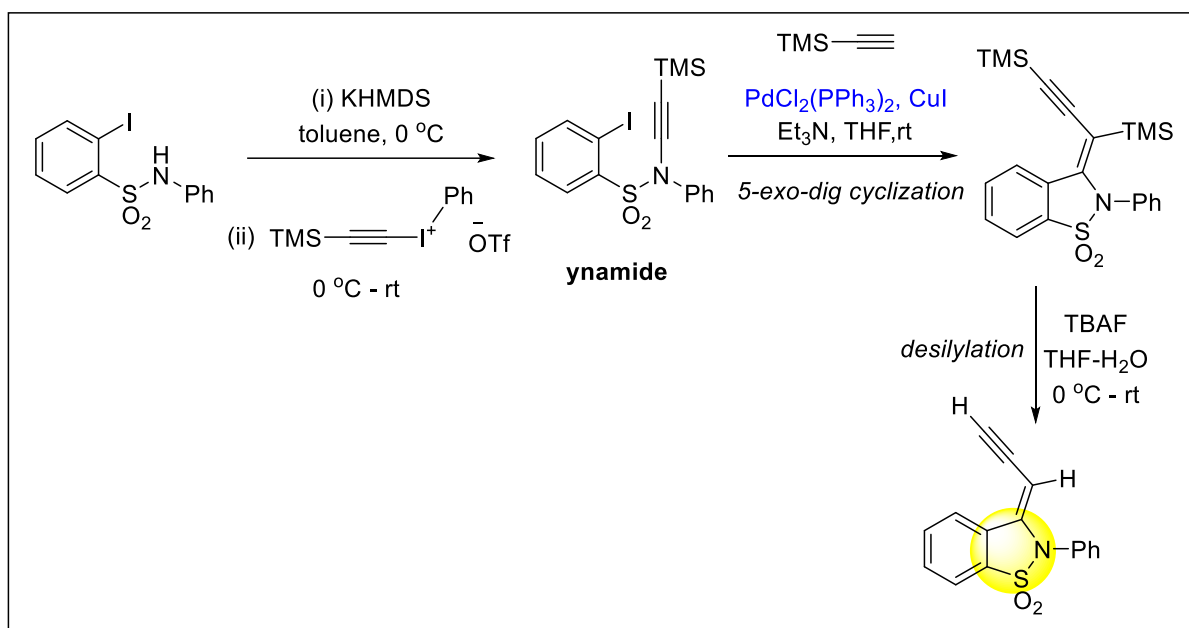
(i) Metal catalyzed synthetic approaches:

X. Ma *et al.*¹² described a Cu-catalyzed three-component protocol for the synthesis of isothiazoles. This synthetic protocol involving a reaction among the enaminoesters, bromodifluoroalkyl compounds, and sulphur with high selectivity. The isothiazoles were formed by breaking of two *C-F* bonds simultaneous creation of the new *C-S*, *C-N*, and *N-S* bonds (**Scheme 4.1**).



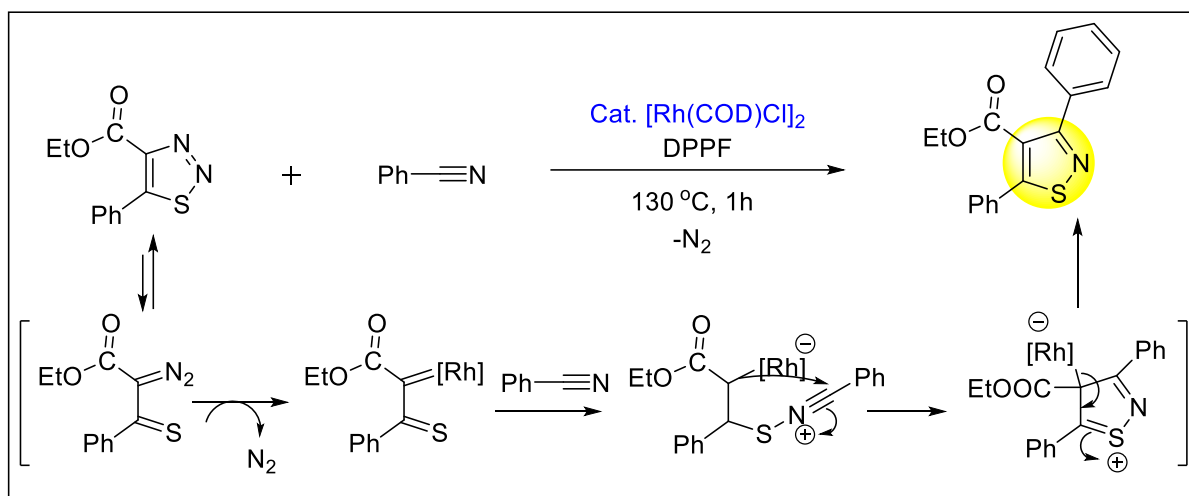
Scheme 4.1. Synthesis of isothiazoles *via* Cu-catalyzed three-component reaction.

A. Demonceau *et al.*¹³ developed a Pd/Cu-catalyzed, base-promoted one-pot synthetic protocol for enyne-substituted benzoisothiazole starting from 2-iodo-*N*-(trimethylsilylethynyl)benzenesulfonamides. Initially, ynamide was derived by performing a reaction with *N*-phenyl 2-iodobenzenesulfonamide and potassium hexamethyldisilazane in toluene, followed by the addition of trimethylsilylethynyliodonium triflate. After that, this ynamide underwent 5-*exo-dig* cyclization with trimethylsilylacetylene in the presence of Pd/Cu-catalyst and Et₃N. Finally, tetrabutylammonium fluoride is used for desilylation to produce enyne-substituted benzoisothiazole (**Scheme 4.2**).



Scheme 4.2. Pd/Cu-catalyzed synthetic protocol of enyne-substituted benzoisothiazole.

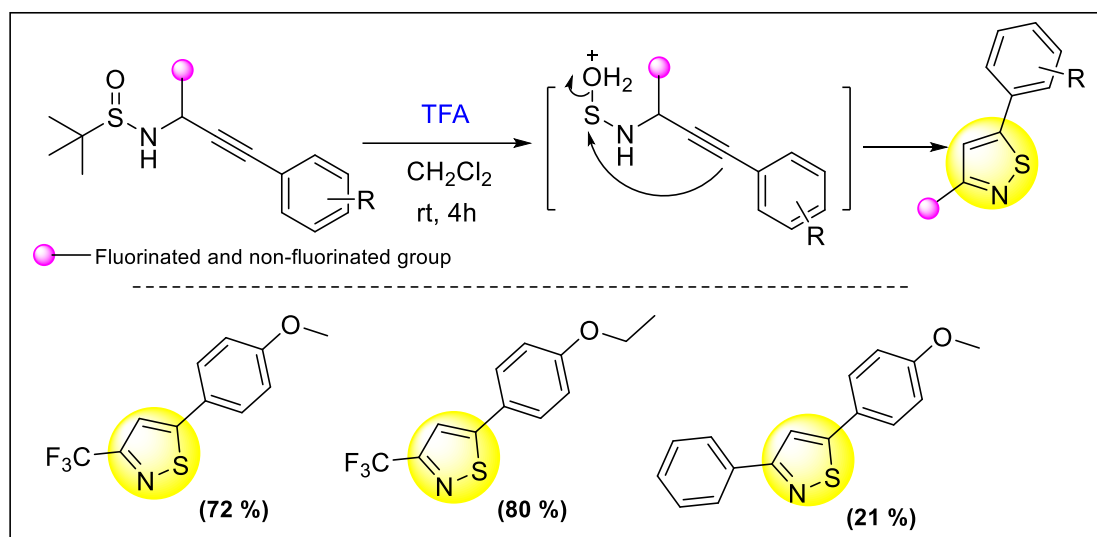
P. H. Lee and his research group¹⁴ described rhodium-catalyzed protocol for obtaining isothiazole moieties. This protocol described 1,2,3-thiadiazoles underwent transannulation with nitriles in presence of Rh-catalyst by the formation of α -thiavinyl Rh-carbenoid intermediate (**Scheme 4.3**).



Scheme 4.3. Rhodium-catalyzed a convenient procedure for preparing isothiazole derivatives.

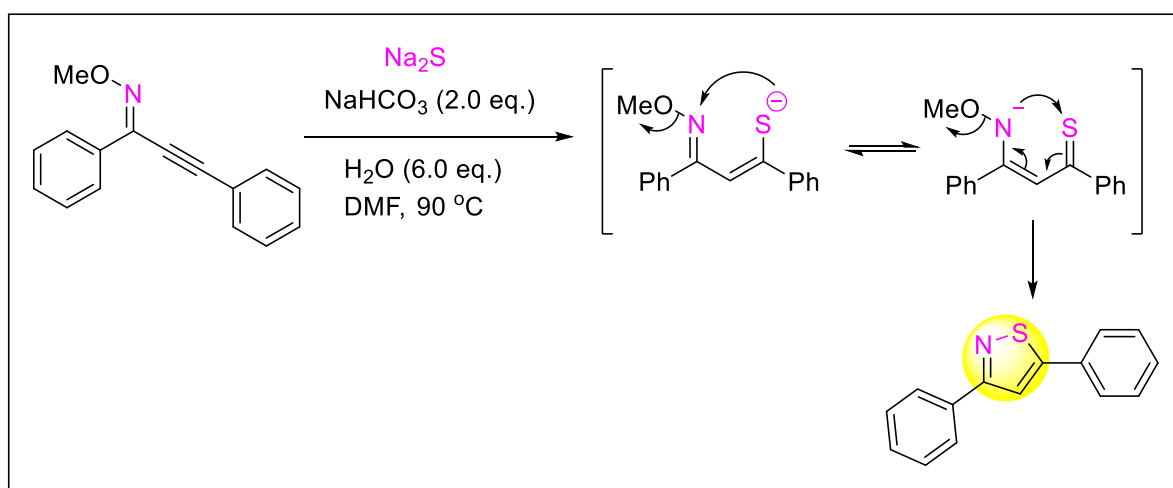
(ii) Metal-free synthetic approaches:

J. Han and his research group¹⁵ discovered a new synthetic route for the formation of isothiazole derivatives using *N*-propargylsulfanyl amide. The group reported a TFA-promoted reaction where *tert*-butanesulfinyl group is involved in intramolecular cyclization of amide and provides rapid synthesis of polyfunctionalized isothiazoles. This protocol represents a new kind of reactivity looks of *tert*-butanesulfinamide and provides valuable isothiazoles (**Scheme 4.4**).



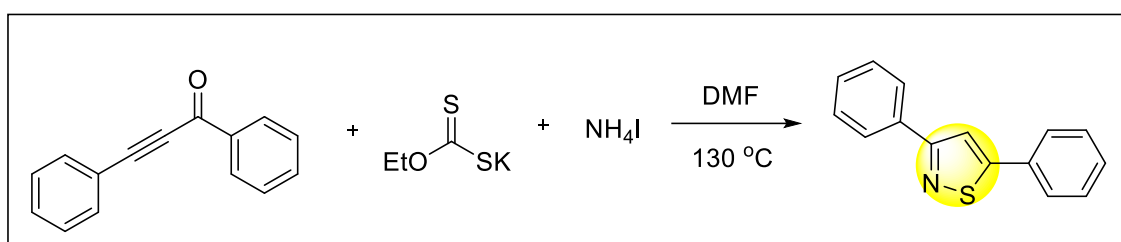
Scheme 4.4. Synthesis of isothiazoles using *N*-propargylsulfanyl amide.

X. G. Zhang and his co-worker¹⁶ have been developed an easy, facile method for the synthetic purpose of isothiazoles. This method describes a demethoxylyative cycloaddition reaction of alkynyl oxime ethers promoted by sodium hydrogen carbonate in presence of Na_2S as sulphur source. Usage of stable and cheap Na_2S and NaHCO_3 are the major advantages of this methodology. This efficient protocol involved formation of multi bond ($N-S$, and $C-S$ bond) in one-pot, wide substrate scope with moderate to excellent yields (**Scheme 4.5**).



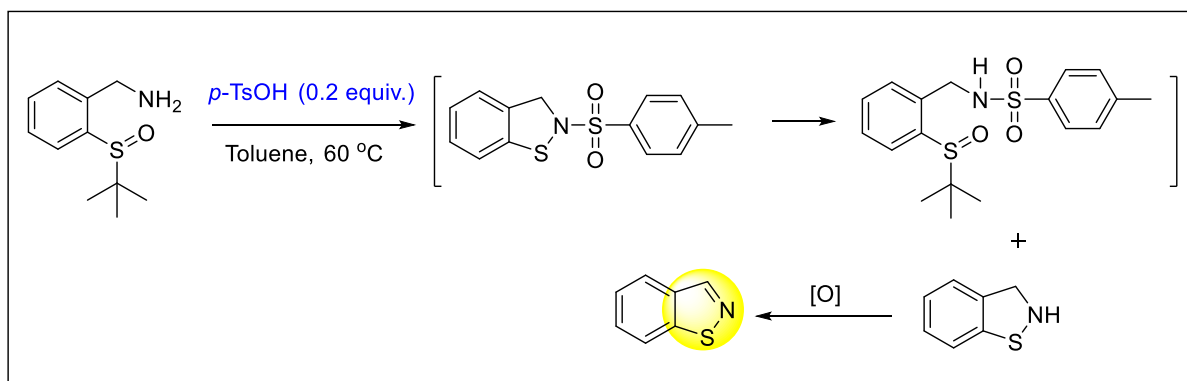
Scheme 4.5. Synthesis of isothiazoles *via* cycloaddition of alkynyl oxime ethers.

Y. Li and his group¹⁷ depicted a transition metal-free synthetic approach of various functionalized isothiazole derivatives. Herein, an efficient, one-pot synthetic protocol has been described through the combination of alkynones, NH_4I , and EtOCS_2K three-component annulation. In this protocol $C-N$, $N-S$, and $C-S$ bonds are consecutively formed and delivered a series of functionalized isothiazoles with excellent yields (**Scheme 4.6**).



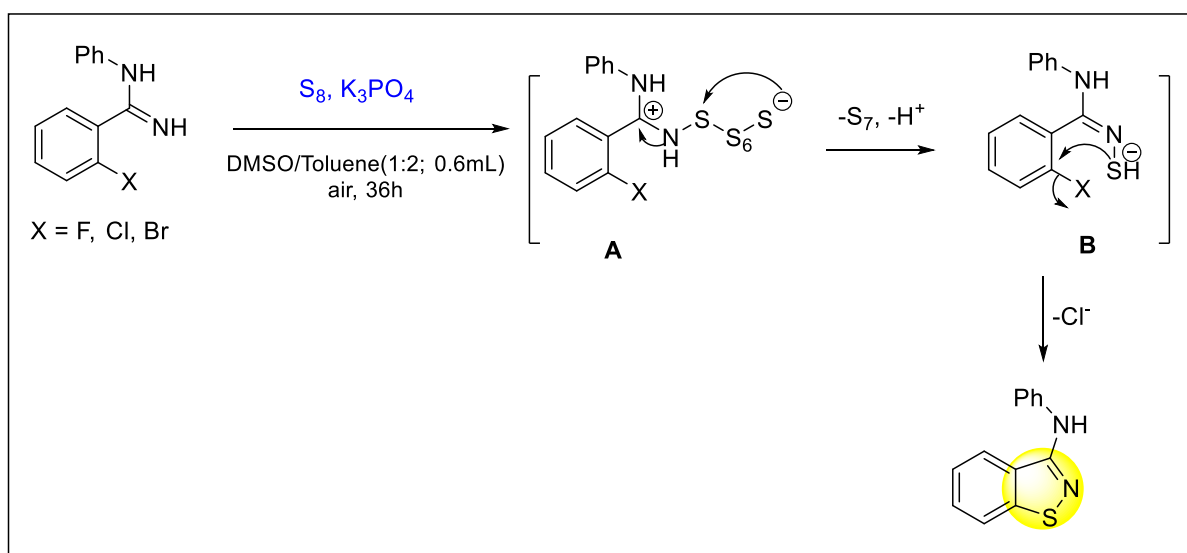
Scheme 4.6. Transition metal-free synthetic route of isothiazoles *via* three-component reaction.

Z. Sun and his co-worker¹⁸ brought to light a thermal reaction for the synthesis of 3-substituted aryl[4,5]isothiazoles by simply heating the starting ingredients in toluene with a catalytic quantity of *p*-toluenesulfonic acid (**Scheme 4.7**).



Scheme 4.7. Synthesis of 3-substituted aryl[4,5]isothiazoles *via* thermal reaction.

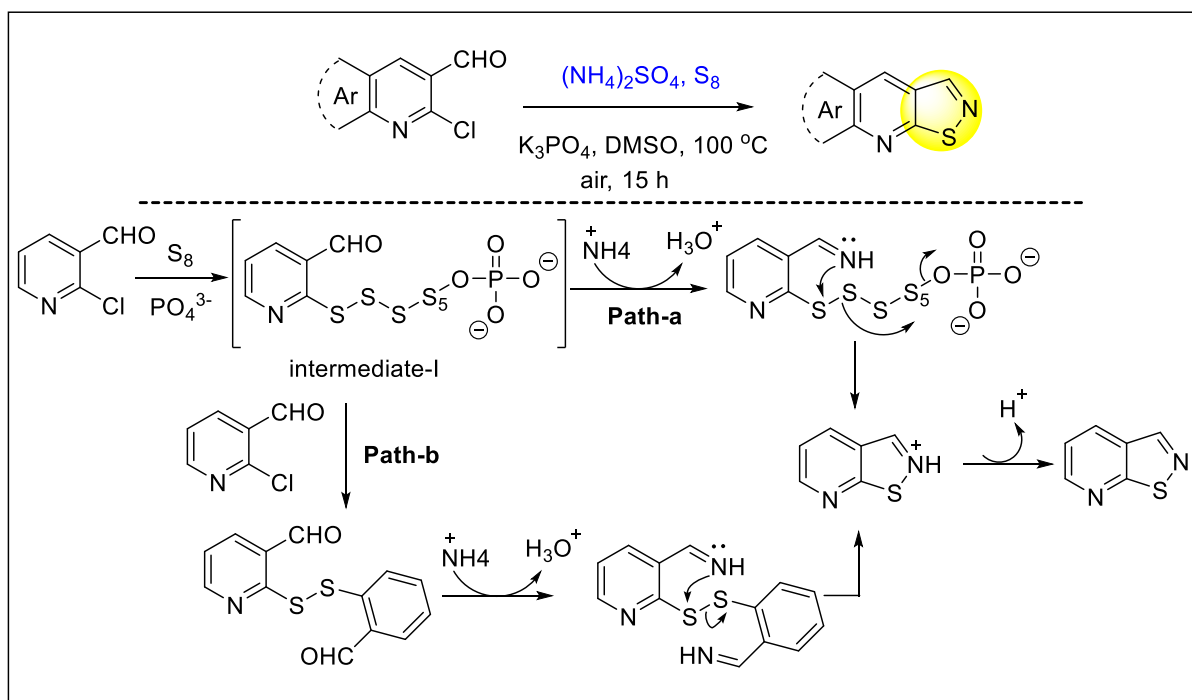
G. J. Deng and his research group¹⁹ developed a novel transition metal-free synthetic approach of 1,2-benzisothiazole derivatives by using amidines and easily available elemental sulphur. This reaction involved formation of *S-N/C-S* bond between elemental sulphur and 2-halo amidines with cheap reagent K_3PO_4 . Initially, *S-N* bond was governed in intermediate A, by the nucleophilic attack of imine with elemental sulphur. Then intermediate B was formed by eliminating S_7 and deprotonation of intermediate A. Finally, intramolecular nucleophilic substitution took place, *C-S* bond was formed and we obtained the desired products with good to excellent yields (**Scheme 4.8**).



Scheme 4.8. Transition metal-free approach of 1,2-benzisothiazole.

M. Wang *et al.*^{8a} developed a synthetic strategy for benzisothiazoles *via* three-component reaction by using ammonium, and elemental sulfur under metal-free conditions. Quinoline or pyridine based *ortho*-functionalized aldehydes are preferably chosen as substrate for this protocol and gets excellent yields. At first, of *o*-halogenated aromatic aldehyde undergoes

phosphate assisted nucleophilic substitution by S_8 produces the intermediate I. **Path-a** explains, amine and aldehyde readily form imine. Then intramolecular substitution reaction followed by deprotonation takes place to obtain the desired product. Alternatively, **Path-b** explains, first the halogenated nucleophilic substitution attack occurs to form the diaryldisulfide, then it follows the same protocols with **path-a** to construct the desired product. This strategy is also applicable for gram-scale reaction with satisfactory yield (**Scheme 4.9**).

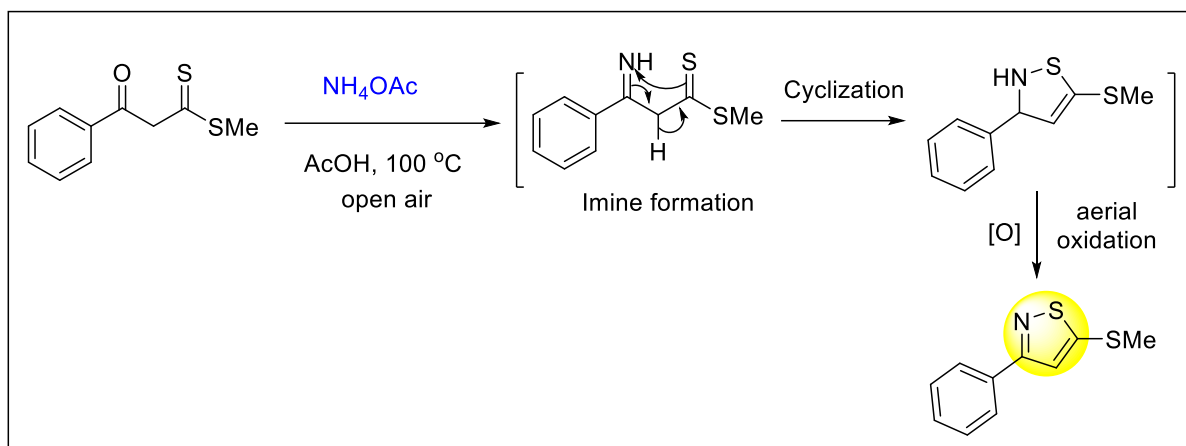


Scheme 4.9. Synthesis of benzisothiazoles *via* metal-free, three-component reaction.

[B] Green synthetic approaches:

(i) Metal- and catalyst-free synthetic approach:

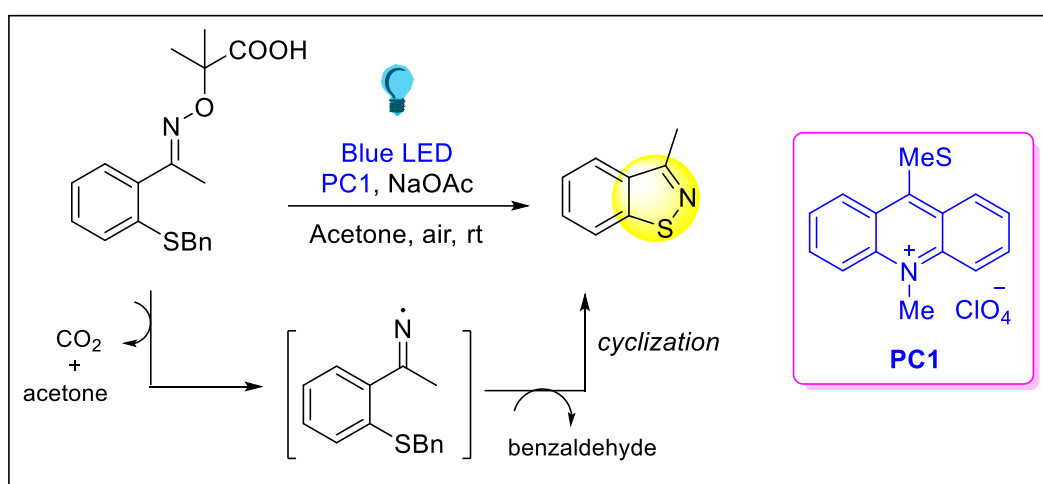
G. Shukla *et al.*²⁰ established an easy operationally simple, user-friendly approach for the synthesis of 3,5-disubstituted isothiazole derivatives *via* [4 + 1] annulation of β -ketodithioesters with NH_4OAc under catalyst- and metal-free condition. Here, ammonium acetate plays a crucial role as the source of both ammonium and base. The formation of substituted-isothiazole involved first imine formation, then cyclization, followed by aerial oxidation, which took place in a sequential manner to form consecutive $C-N$ and $S-N$ bonds in a single pot (**Scheme 4.10**).



Scheme 4.10. A user-friendly protocol for the preparation of 3,5-disubstituted isothiazoles via [4 + 1] annulation.

(ii) Photoinduced synthetic approach:

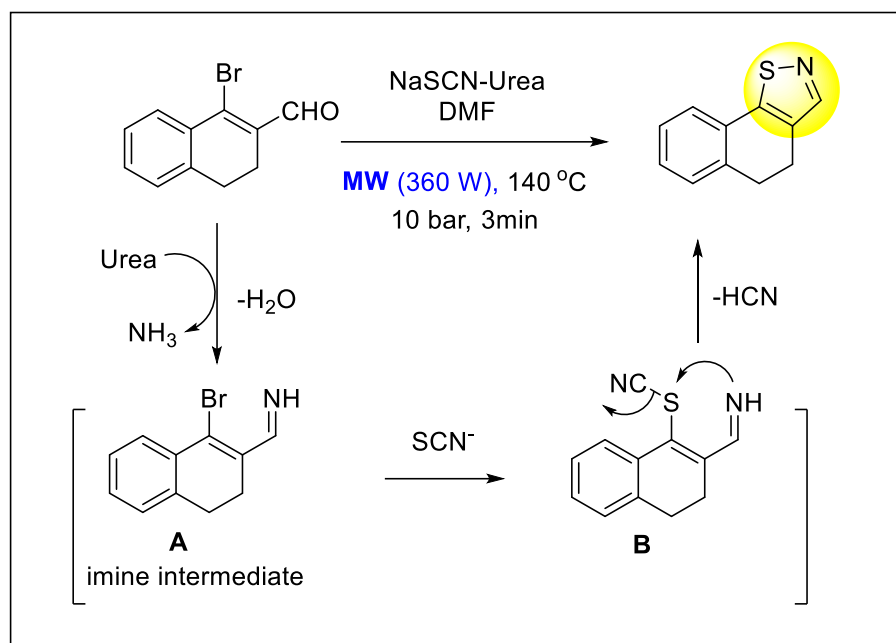
M. J. Cabrera *et al.*²¹ discovered a visible light-assisted synthetic protocol to produce isothiazole derivatives using an α -amino-oxy acid. This method entails the formation of an iminyl radical through a photo redox reaction with a single electron transfer, followed by cyclization, to produce the *N-S* bond. This easy-to-use approach offers metal-free, mild conditions, a wide application, and extensive functional group tolerance, and it represents a novel environmentally acceptable method for producing these extremely valuable isothiazole derivatives (**Scheme 4.11**).



Scheme 4.11. Visible light-promoted synthetic route to produce isothiazoles.

(iii) Microwave assisted synthetic approach:

P. Bezbaruah *et al.*²² depicted a novel, one-pot microwave-assisted synthetic strategy of fused isothiazole derivatives starting from β -bromo vinyl aldehydes with sodium thiocyanate and urea. Under microwave heating ammonia was released from urea, which can easily undergo the reaction with β -bromo vinyl aldehydes and formed imine intermediate **A**. This imine intermediate facilitated to the formation of intermediate **B** by the nucleophilic addition of 'SCN'. Finally, nucleophilic substitution takes place at the S-atom by the elimination of cyanide and desired steroidal, non-steroidal isothiazoles obtained (**Scheme 4.12**).



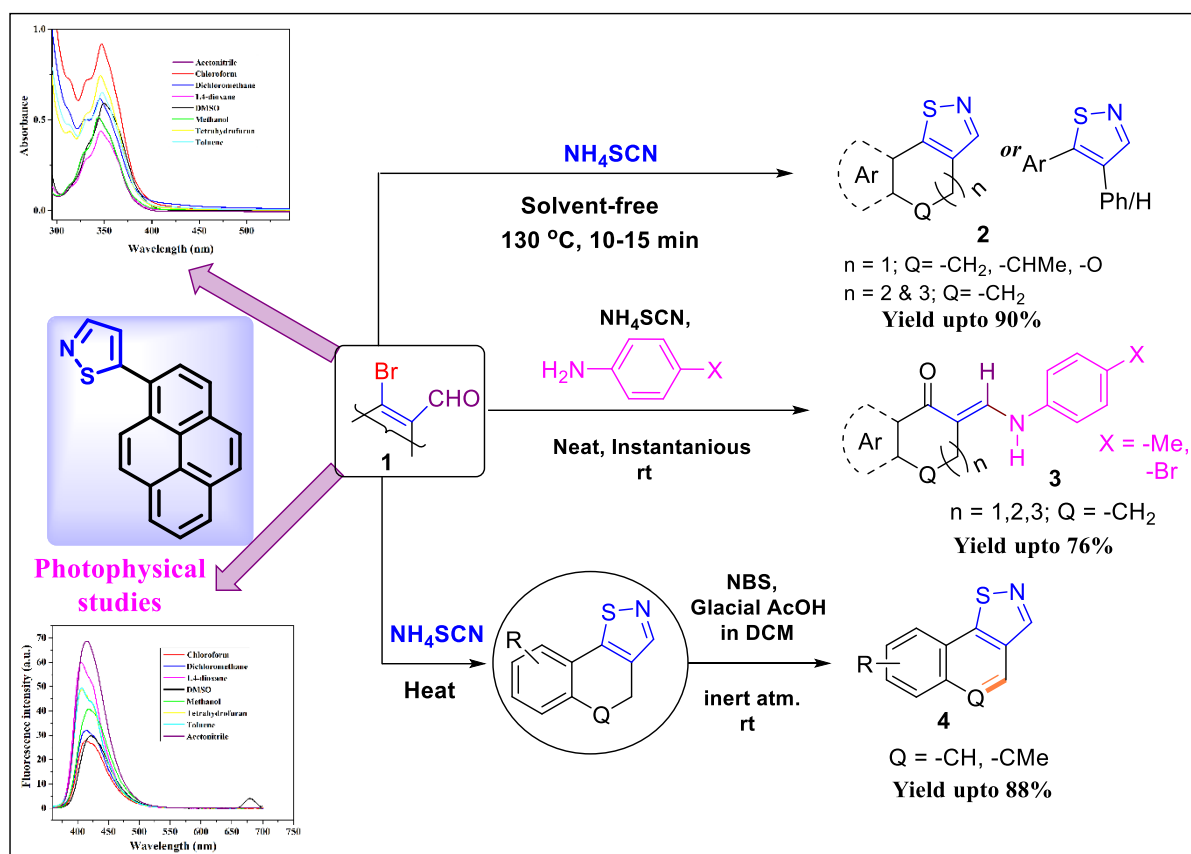
Scheme 4.12. Microwave-assisted synthesis of fused isothiazoles.

According to the literature review, numerous groups have developed distinct processes for synthesising isothiazole derivatives employing various solvents, metals, and catalysts. As far as we are aware, there hasn't been any progress in solvent-free isothiazole synthesis. Therefore, it has been really hard to develop a practical and effective solvent-free synthetic approach using readily available raw ingredients. After a protracted period of research, we succeeded in developing this kind of procedure, which is covered below.

4.3. Present Work:

- ❖ Herein, we report for the first time, Ammonium thiocyanate promoted simple, rapid and eco-friendly neat synthesis of isothiazoles has been developed for the first time. (**Scheme 4.13**).

- ❖ It is noteworthy that an instantaneous valuable synthetic route of β -enaminones has also been documented during the mechanistic investigation of isothiazole formation. Detail mechanistic explanation of isothiazole formation reaction is clearly explained by the control experiments.
- ❖ We were also successful to prepare corresponding aromatized polycyclic isothiazoles **4** from the newly synthesized isothiazole derivatives, **2** by mild oxidative procedure using NBS (*N*-bromo succinimide) (**Scheme 4.13**).
- ❖ A new fluorescence active pyrene substituted isothiazole has been synthesized and its detailed photophysical properties have been documented in the latter section (**Scheme 4.13**) of this article.

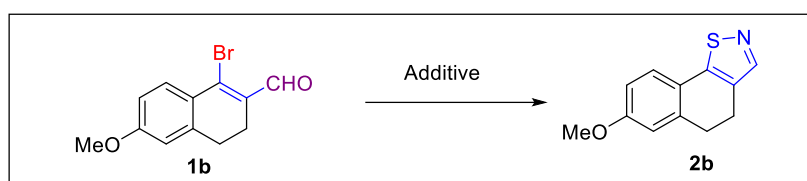


Scheme 4.13. An outlook of our overall observation.

4.4. Results & discussion:

The mission was started with β -bromo vinyl aldehyde which has been used to prepare many useful molecules by our group.²³ β -Bromo vinyl aldehyde has two important functionalities that can participate in metal or metal-free transformations. The replacement of vinyl bromide is very difficult but it becomes easier when electron-withdrawing formyl group is present at

the β -position. Thiocyanate is a good nucleophile which can replace vinyl bromide *via* addition elimination reaction. Therefore, we have used ammonium thiocyanate which may act as the source of both nitrogen and sulfur and reacts with aldehyde as well as vinyl bromide part of **1**. This protocol furnished good yields of isothiazoles **2b** (78%) when 3 mmol of ammonium thiocyanate is used in aqueous methanolic medium (**entry 1, Table 4.1**). The reaction was also found to proceed successfully with $\text{NH}_4\text{Cl}/\text{KSCN}$, $\text{Na}_2\text{S}/\text{NH}_4\text{Cl}$ and $\text{Na}_2\text{S}_2\text{O}_3/\text{NH}_4\text{Cl}$ in aqueous methanolic medium but the yield was poor and requires long time (**entries 2, 3 & 4, Table 4.1**). In order to develop an environmentally benign approach for the synthesis of heterocyclic compound we have used aqueous medium in our current transformation but the reaction did not proceed at all (**entry 5, Table 4.1**). Then we tried the reaction in neat condition and the reaction was found to complete within 5 hours to produce the desired product in 90% yield (**entry 8, Table 4.1**). Surprisingly, it has been found that with increasing the amount of ammonium thiocyanate and temperature, the reaction time period is reduced significantly. The desired product was obtained within 10 minutes at 130 °C under neat conditions in the presence of 10 mmol NH_4SCN (**entry 13, Table 4.1**). Thus, this condition makes a greater impact from the environmental point of view. Neat condition was also tested in presence of $\text{Na}_2\text{S}_2\text{O}_3/\text{NH}_4\text{Cl}$ but the yield of **2b** was only 55% (**entry 14, Table 4.1**).

Table 4.1: Optimization of reaction condition for the synthesis of *d*-fused isothiazole^a

Entry	Additive	Medium	Time (h)	Yield (%)
1	NH ₄ SCN (3 mmol)	MeOH-H ₂ O (1:1)	5	78
2	NH ₄ Cl (1 mmol) KSCN (2 mmol)	MeOH-H ₂ O (1:1)	12	70
3	NH ₄ Cl (1 mmol) Na ₂ S (2 mmol)	MeOH-H ₂ O (1:1)	12	72
4	NH ₄ Cl (1mmol) Na ₂ S ₂ O ₃ (2 mmol)	MeOH-H ₂ O (1:1)	10	70
5	NH ₄ SCN (3 mmol)	Water	10	NR
6	NH ₄ SCN (1 mmol)	Neat	10	NR ^b
7	NH ₄ SCN (2 mmol)	Neat	5	20 ^b
8	NH ₄ SCN (3 mmol)	Neat	5	80 ^b
9	NH ₄ SCN (4 mmol)	Neat	4	84 ^b
10	NH ₄ SCN (5 mmol)	Neat	2.5	86 ^b
11	NH ₄ SCN (6 mmol)	Neat	2	87 ^b
12	NH ₄ SCN (10 mmol)	Neat	1	90 ^b
13	NH₄SCN (10 mmol)	Neat	0.17	90^c
14	NH ₄ Cl (1 mmol) Na ₂ S ₂ O ₃ (2 mmol)	Neat	12	55 ^b

^a **Reaction Conditions:** β -bromo vinyl aldehyde **1b** (1 mmol), solvent (3 mL), NH₄SCN (3 mmol), temperature 70 °C; ^b Reaction performed without solvent at 70 °C; ^c Reaction performed without solvent at 130 °C with 10 mmol of NH₄SCN.

To understand the dependance of yield of reaction on the amount of NH₄SCN used, we have plotted the yields of isothiazole **2b** obtained under neat condition within 1 hour of time period at 70 °C with the different amounts (in mmol) of ammonium thiocyanate used in the reactions

(**Figure 4.7(a)**). It has been observed that the yield of reaction does not increase beyond 10 mmol of NH_4SCN at 70 °C. Next, we have studied another plot at constant amount of NH_4SCN (10 mmol) at different temperature with time periods of the reactions to get the maximum yield of isothiazole (**Figure 4.7(b)**). The time reduced to 10 minutes at 130 °C for completion of the reaction.

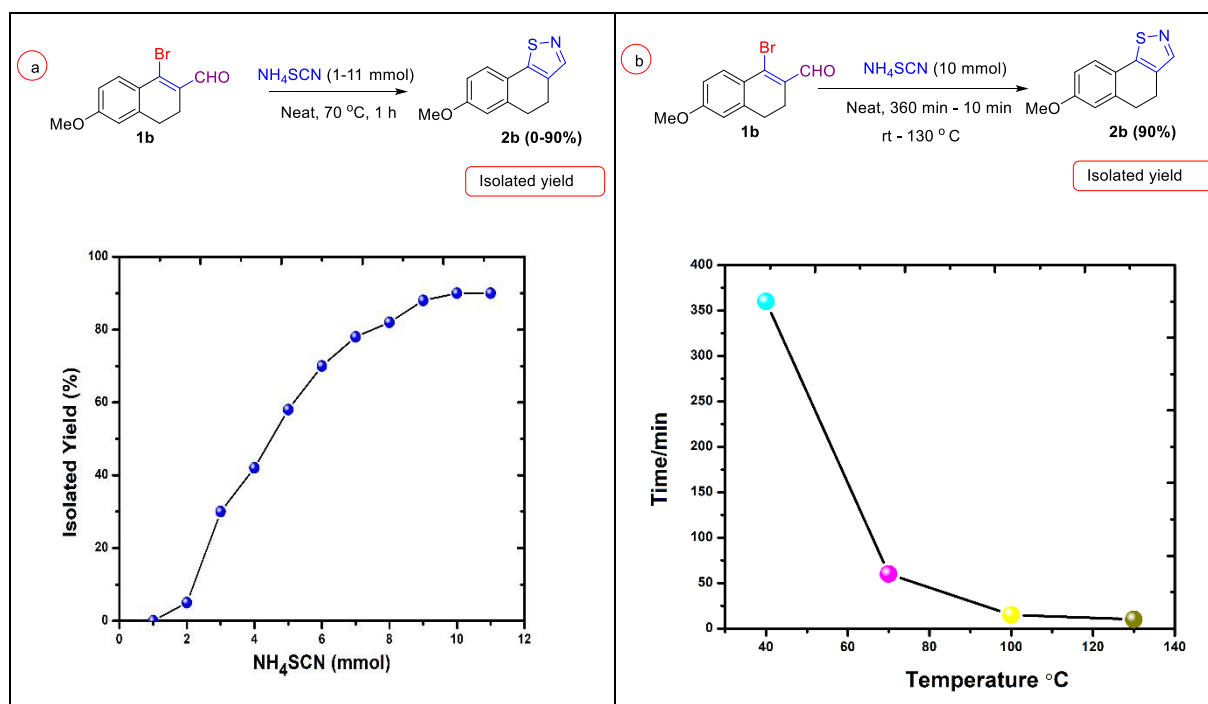
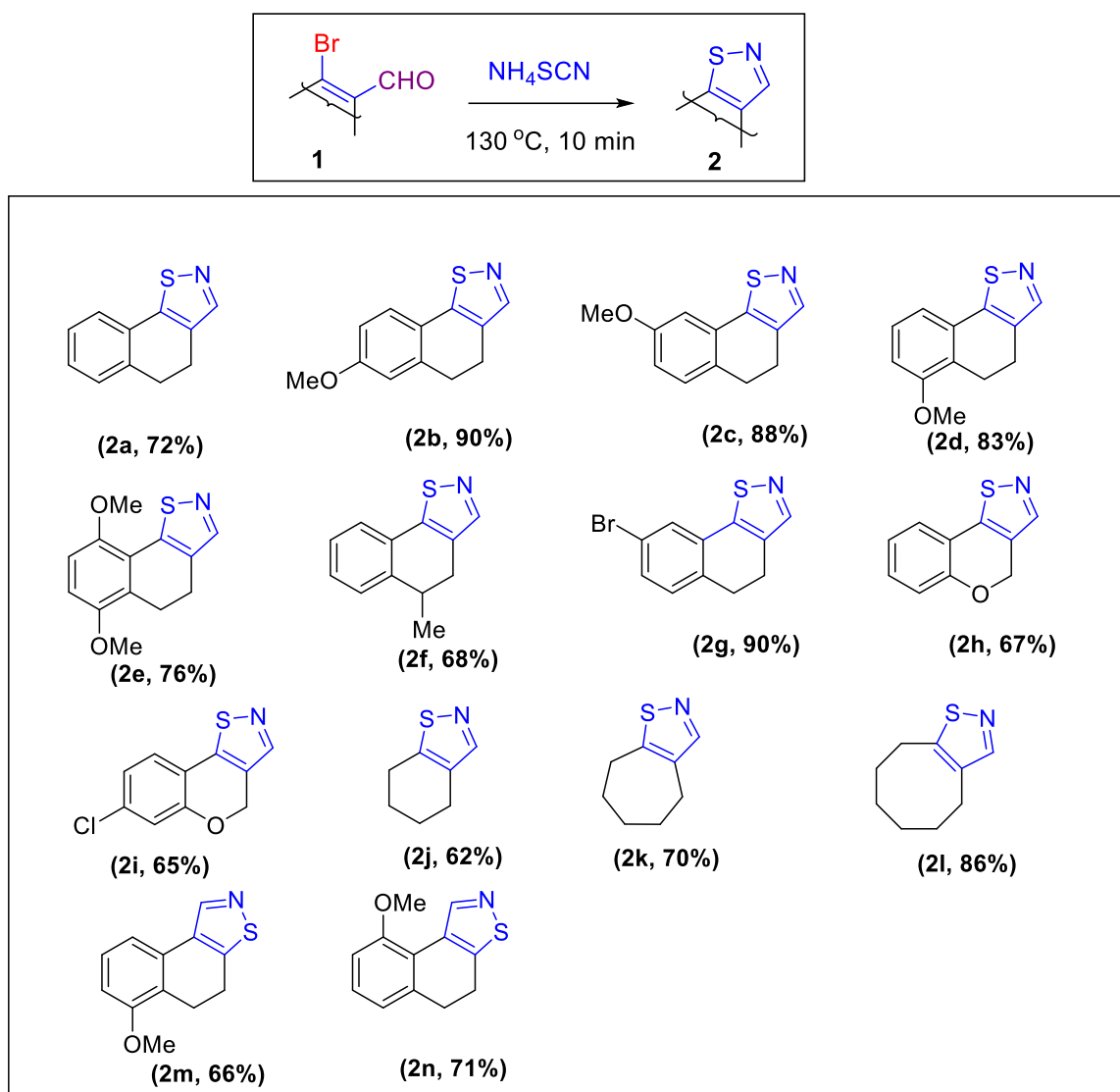


Figure 4.7. Schematic representation of the ammonium thiocyanate promoted neat reaction to produce *d*-fused isothiazole derivatives. (a) Reagent-dependent conversion efficiency of the neat reaction with different mmol of ammonium thiocyanate at constant temperature and time. (b) Temperature and time dependent plot to get maximum yield at constant equivalent of reagent. Yields were determined by isolation of the product *via* column chromatography.

From the **Table 4.1** and **Figure 4.7**, we have found that isothiazole formation becomes very fast at 130 °C in presence of 10 mmol of NH_4SCN under neat condition. With this optimum condition in hand (**Table 4.1, entry 13**), we extended our studies using different substituted β -bromo vinyl aldehydes (**Table 4.2**). Electron donating and withdrawing groups substituted aryl rings furnished the corresponding tricyclic *d*-fused isothiazole products appreciably (**2b-2e & 2g, 76-90%**) under neat conditions in presence of ammonium thiocyanate. Since, both the nucleophilic and electrophilic additions are involved in process of isothiazole ring formation, the reaction is favored by the groups of both types of electronic natures. In case of unsubstituted

aryl ring **1a** and the cycloalkyl substituent **1j-1l** without any electronic sense the yield of isothiazoles got reduced. With increasing ring size in the cycloalkyl ring (**2j-2l**) afforded bicyclic isothiazoles with ascending order (**62-86%**) and it became highest in 8-membered fused isothiazoles **2l** under neat condition. This may be due to the tolerance of temperature of higher molecular weight of cycloalkyl ring under neat conditions. This methodology also provided isomeric isothiazole **2m** and **2n** by taking 2-bromo vinyl aldehyde instead of 1-bromo vinyl aldehyde with effective yield **66%** and **71%** respectively.

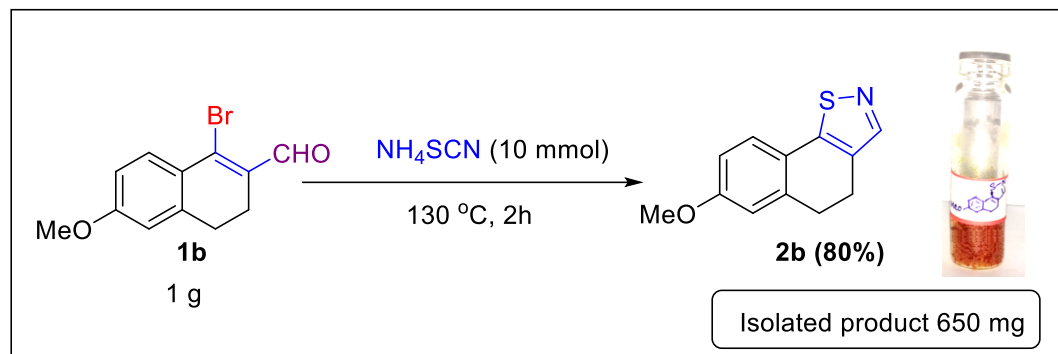
Table 4.2: Neat synthetic approach of isothiazoles



Reaction Conditions: β -bromo vinyl aldehyde **1** (1 mmol), NH_4SCN (10 mmol), $130\text{ }^\circ\text{C}$, 10 minutes.

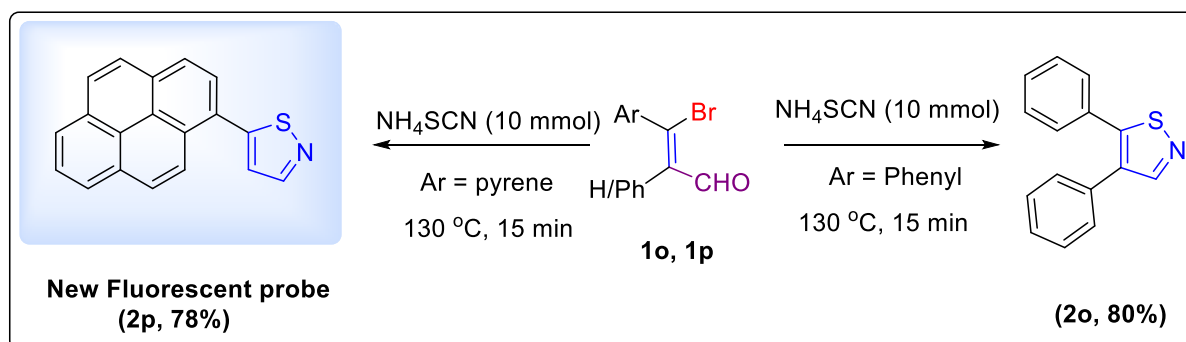
The protocol was also applicable with respect to practical aspect. From a practical standpoint, the reaction was performed in gm scale and found good yield of isothiazole derivative **2b** under

neat conditions. We have got 650 mg of product **2b** from 1 g of **1b** and hence 80 % yield of the desired isothiazoles was obtained at 130 °C after 2 h of heating. The time required in gram scale neat reaction was greater compared to the mg scale reaction (**Scheme 4.14**).



Scheme 4.14. Synthesis of isothiazole **2b** in gram scale.

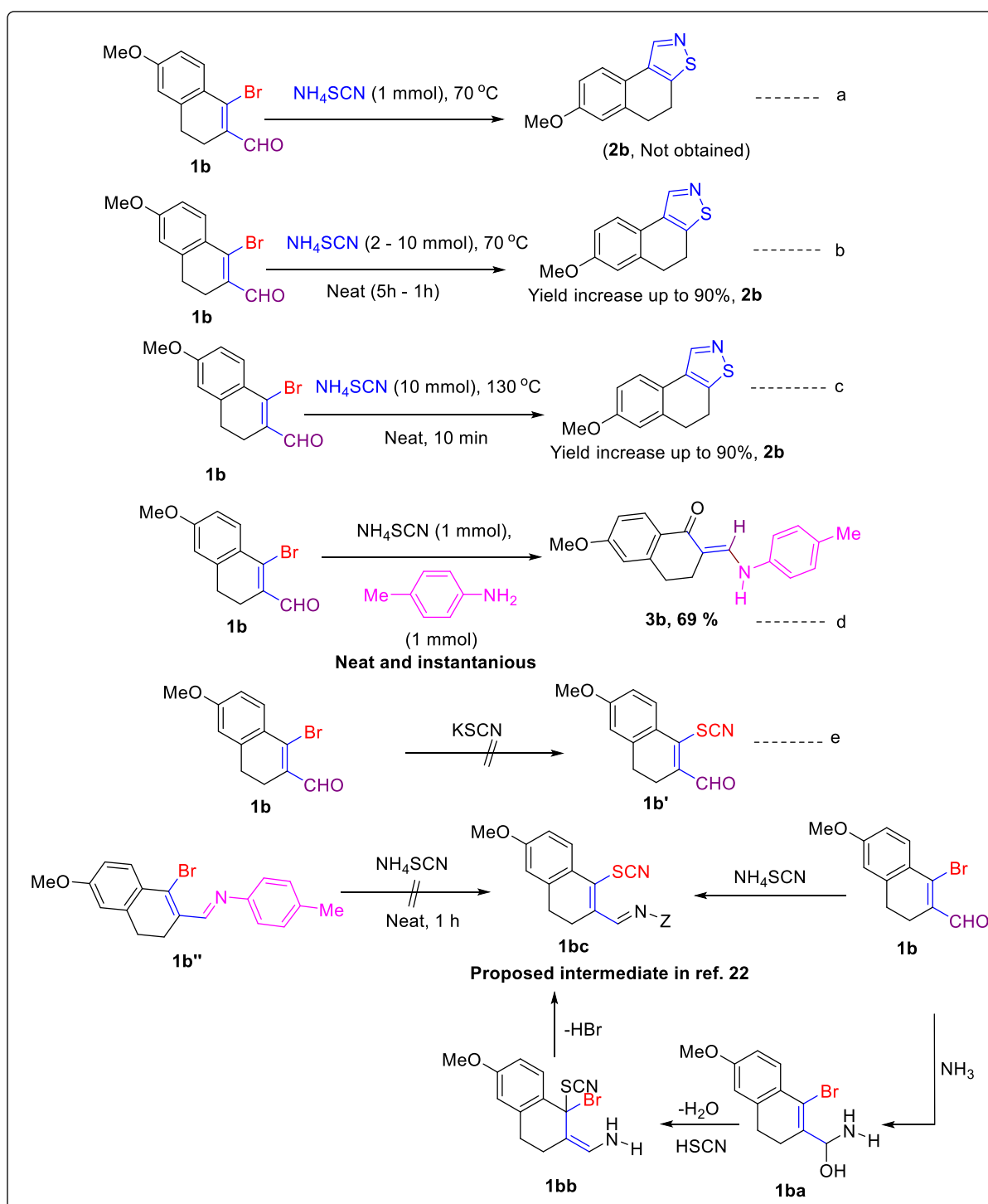
To study the general applicability of our reaction to the acyclic system, we have started our reaction with (*Z*)-3-bromo-2,3-diphenylacrylaldehyde **1o** for the construction of 4,5 diphenyl substituted isothiazole derivatives **2o** under optimum conditions (neat) and found the isothiazole derivatives in good yields within 15 minutes. An engaging result was observed for the substrate (*Z*)-3-bromo-3-(pyren-1-yl)acrylaldehyde **1p** which gave pyrene substituted new blue fluorescent probe **2p** with 78% yield (**Scheme 4.15**). This result enforces us to further study the photophysical behavior and it has been discussed in the next section.



Scheme 4.15. Synthesis of isothiazole from acyclic precursors.

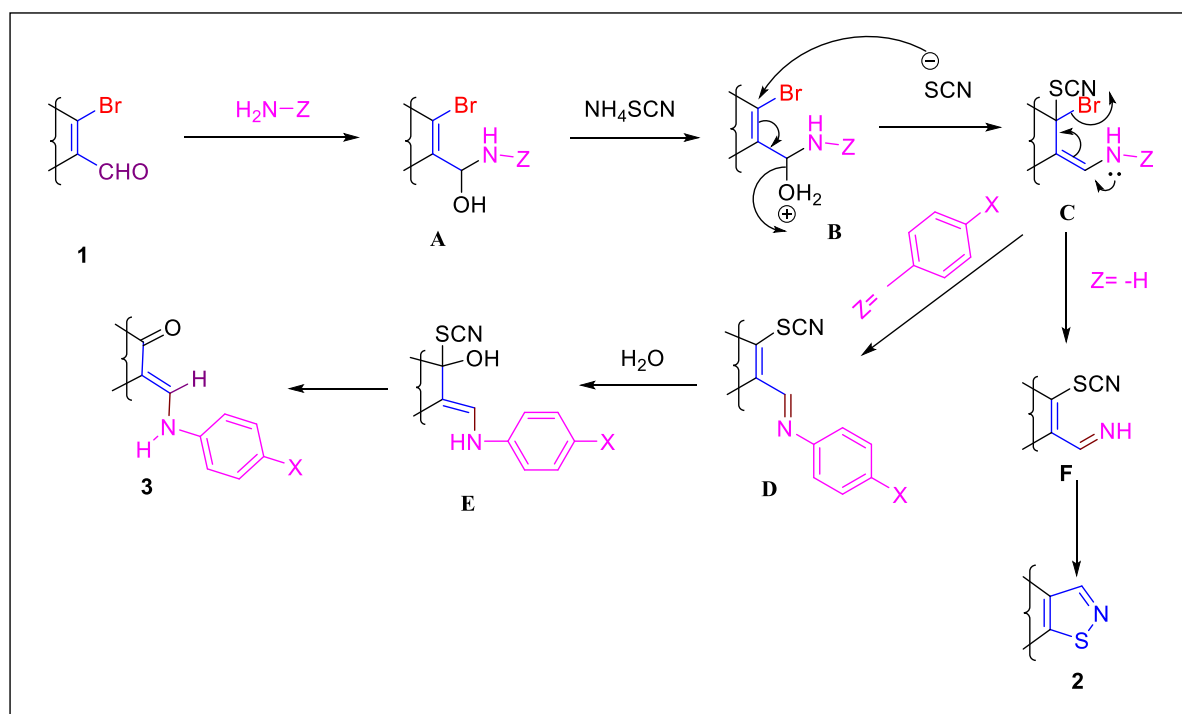
To investigate the mechanism of isothiazole formation under neat condition, we have done some control experiments in presence of ammonium thiocyanate as single reagent (**Scheme 4.16**). The reaction did not take place with 1 mmol NH_4SCN at $70\text{ }^\circ\text{C}$ (**Scheme 4.16a**). The reaction produced 20% yield of **2b** in presence of 2 mmol NH_4SCN at $70\text{ }^\circ\text{C}$ and a dramatic

change was observed after adding 10 mmol of NH_4SCN (**Scheme 4.16c**). After changing the reaction condition by the addition of 1 mmol *p*-toluidine with 1 mmol NH_4SCN , a different product i.e., β -enaminone **3b** was formed with 69% yield (**Scheme 4.16d**). Further, vinyl bromide is not replaced by the addition of KSCN with **1b** (**Scheme 4.16e**). Again *p*-tolyl imine derivative of **1b** did not furnish desired product **3b** or **1bc**. From the literature observation, it was shown that β -thiocyano vinyl imine **1bc** must be formed in the reaction medium during isothiazole formation.²² Again, from our experiment, it has been showed that vinyl bromide is not replaced in the presence of formyl or imine derivative. We can anticipate that thiocyanate replaced vinyl bromide from unstable hemiaminal intermediate **1ba**. This has been facilitated if the reaction medium has sufficient acidity. Consequently, the rate of vinyl bromide displacement is directly proportional to the increase of acidity of NH_4SCN and it has been enhanced with excess addition of NH_4SCN . Therefore, with 10 mmol of NH_4SCN , **2b** was formed exclusively within 10 minutes.



Scheme 4.16. Series of control experiments for isothiazole/ β -enaminone formation.

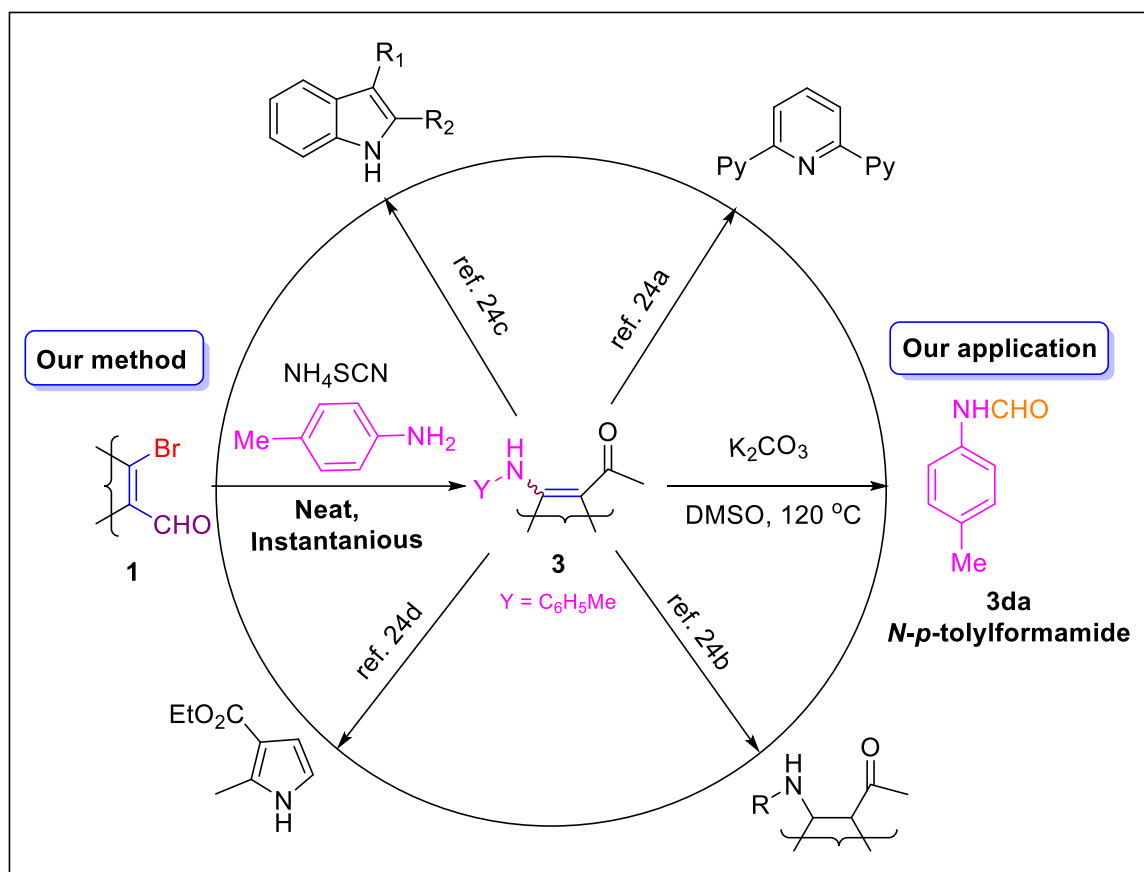
From these observations we have proposed a detailed mechanism of reaction which was not discussed in the earlier report (R. C. Boruah *et al.*).²² At first, substrate **1** reacts with amine source to produce hemiaminal intermediate **A**, then thiocyanate replaces vinyl bromide *via* the elimination of water molecule. The driving force for water elimination is the strength of acidity and then the intermediate **D** or **F** is formed *via* the addition elimination mechanism. The **F** intermediate underwent intramolecular cyclisation to produce desired isothiazole **2**. However, in presence of *p*-toluidine it generates *trans*- β -thiocyano imine **D** which cannot undergo intramolecular cyclisation as it is locked in *trans* form and hence readily hydrolysed to give β -enaminones **3** with good yield. Thus, it has been concluded that a specific stereochemistry is needed for intramolecular aza-cyclisation to get isothiazole derivatives **2** (Scheme 4.17).



Scheme 4.17. Mechanistic explanation of ammonium thiocyanate promoted neat reaction.

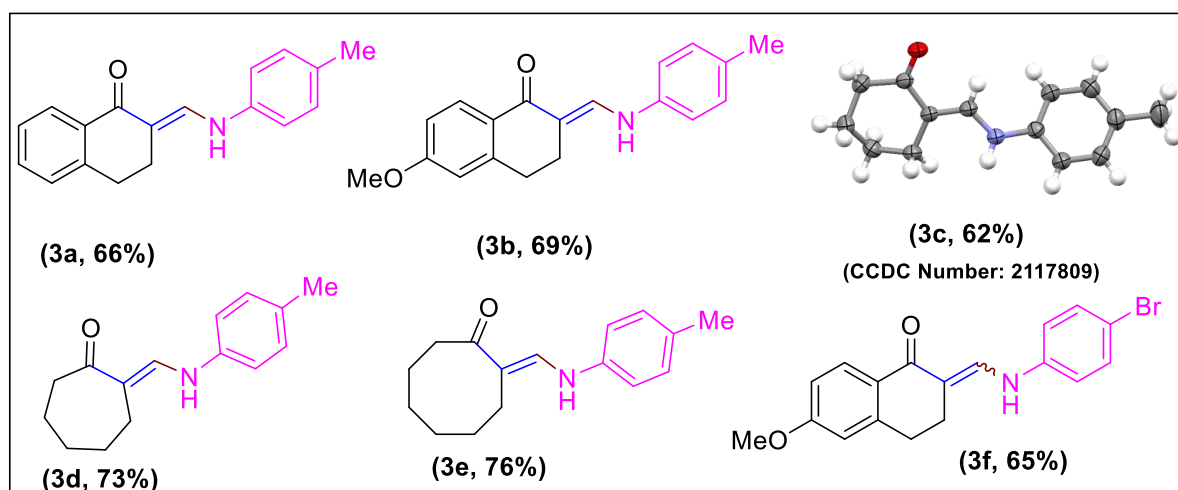
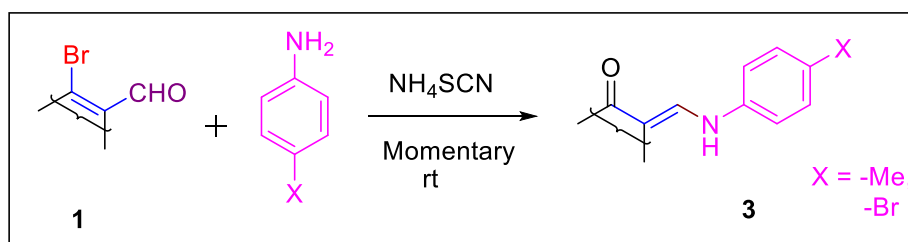
β -Enaminones are important building blocks for the construction of a variety of pharmaceutical compounds, including anti-inflammatory agents, anti-convulsant, anti-cancer agents, and antibacterial.²⁴ In addition, substituted β -enaminones are commonly used as intermediates in the synthesis of heterocycles, such as pyridines, indoles, pyrroles and pyrazole derivatives (Scheme 4.18).²⁵ Due to the wide application of β -enaminones in organic synthesis and drug

development, much attention has been paid to develop a facile, green, and practical method for the preparation of β -enaminones. In addition to isothiazole synthesis, we have also developed a synthetic route of β -enaminones from β -bromo vinyl aldehyde and aryl amine. This valuable intermediate will help to prepare various heterocycles in due time and will be useful to the synthetic organic chemists.



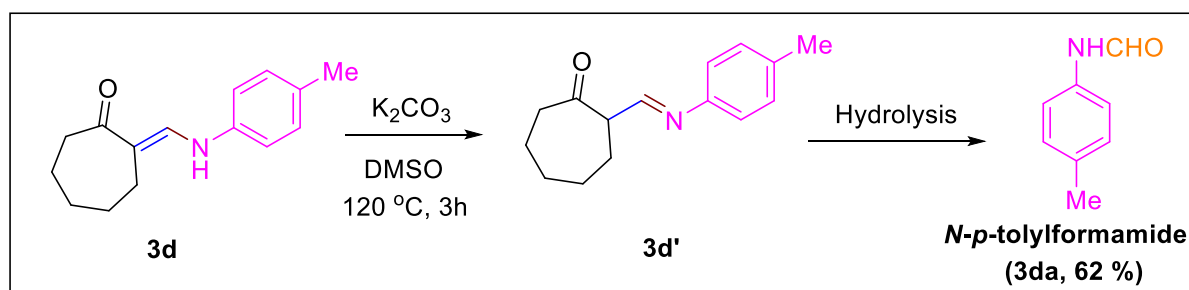
Scheme 4.18. Synthetic use of β -enaminone derivatives.

Considering above findings, we have synthesized different β -enaminones **3a-3f** via momentary change (2-3 minutes) under solvent-free condition (**Table 4.3**) and the structure of one of them **3c** was unambiguously confirmed by X-ray analysis which established the best evidence of the formation of **3**. *N*-aryl- β -enaminones of cyclohexanone, cycloheptanone, cyclooctanone and tetralone derivatives were synthesized with good yields **3a-3f** (62-76%). However, diastereomeric mixture of **3f** (*E*:*Z* = 3:1) was obtained with moderate yield when *p*-bromoaniline was taken as the coupling partner with **1**.

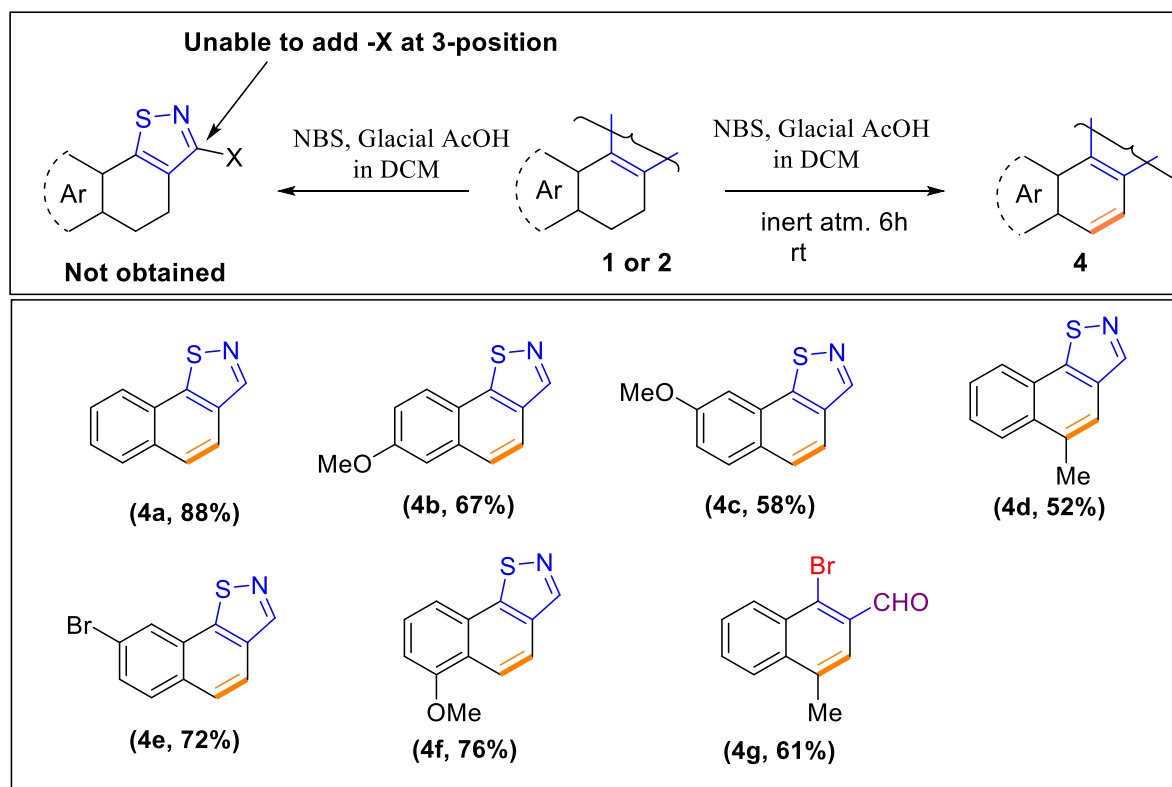
Table 4.3: Momentary synthetic route of *N*-aryl β -enaminones

Reaction Conditions: β -bromo vinyl aldehyde **1** (1 mmol), NH_4SCN (1 mmol), ArNH_2 (1 mmol), room temperature, 2-3 min.

After synthesis of β -enaminones *via* momentary transformation, we wish to utilize the valuable intermediate in organic synthesis. Herein, we have achieved *N*-*p*-tolylformamide **3da** in the presence of potassium carbonate DMSO at 120 °C with the substrate **3d**. The formation of the product can be explained by the base mediated isomerization followed by hydrolysis to afford the desired formyl substituted *p*-tolyl derivative with 62% yield (**Scheme 4.19**).

**Scheme 4.19.** Synthetic application of β -enaminone intermediate.

Next, we concentrated on halogen functionalisation of isothiazole derivatives by considering the utility of chemical properties. Halogen-substituted isothiazoles are highly reactive synthetic building blocks, allowing the ability to obtain polyfunctional isothiazoles with a wide variety of substituents. Hence, we wish to synthesize such halogen-substituted isothiazole ring as our newly tricyclic *d*-fused isothiazole derivatives **2** and we anticipated that 3-position is more susceptible for halogen-substitution as another position is blocked by ring substitution. Hence, we have used NBS for the said transformation. However, the reaction did not produce halogen-substituted isothiazole derivatives and surprisingly afforded complete aromatic compound **4** *via* the two-step mild oxidative reaction (**Table 4.4**). At first, halogenation occurred with NBS/AcOH in dichloromethane at room temperature at benzylic- sp^3 carbon atom and then elimination afforded highly aromatic tri-cyclic fused compounds with good yield within 6 h. To extend the scope for aromatization reactions, we have tested the reaction with a 4-methyl substituted β -bromo vinyl aldehyde derivative and found the formation of aromatized compound **4g** with a 61% yield. Previously, similar aromatic derivatives were obtained by refluxing the reaction mixture at high temperature for 16 hours in toluene medium in presence of stoichiometric amount of DDQ²⁶ but we have achieved the synthesis of aromatic compounds efficiently by NBS promoted clean room temperature protocol.

Table 4.4: NBS-promoted aromatization

Reaction Conditions: Substrate **1** or **2** (1 mmol), NBS (1 mmol), AcOH (1 drop), CH₂Cl₂ (3 mL), room temperature.

4.4.1. Photophysical study:

Pyrene substituted fluorophore has been great attention in material science, organic light-emitting diodes (OLEDs), light-emitting electrochemical materials, etc. due to their having different emissive properties in the functionalized form.²⁷ Although a number of articles have been published regarding fluorescent properties of pyrene with different functionalities mainly at 1/3/6 or 8-position are known but isothiazole substituted pyrene fluorophore is still not reported.²⁸ In continuation application in the fluorescence properties of newly synthesized compounds,^{29, 23} we have designed a new fluorophore which has not been synthesized as a pyrene substituent at 1-position. To establish the photophysical properties of our synthesized pyrene fluorophore, we have determined absorption peak in polar aprotic, polar protic, and nonpolar solvents (**Figure 4.8a and Table 4.5**). It was found that absorption maxima (λ_{max}) fall in the range 344-349 nm in different solvents. Considering the absorption peak in UV-Vis spectra, we have also recorded the emission spectra excited at 344 nm in the same solvents and emission maxima vary from 408-424 nm (**Figure 4.8b and Table 4.5**). Our study also revealed

that the highest emission maxima along with the additional maxima will appear in the 424 nm, 680 nm in DMSO and greater stock shift (77 nm) exhibited in the polar protic MeOH. The higher bathochromic shift in the emission spectra in the polar protic solvent (421 nm) compare to the nonpolar solvent toluene (409 nm) which may be due to the specific interactions such as hydrogen bonding or molecular aggregations.³⁰ In the viscose polar aprotic DMSO solvent the higher bathochromic shift and lower emission intensity can be explained by the rigid rotation of isothiazole unit in pyrene group in the viscose solvent leads to the twisted conformation in the excited state and hence dipole moment has been changed in the excited state.³⁰ Hence, these initial observations in different solvents argued that our newly designed compound may be used for the detection of proton/metal/molecular sensing in due time.

Table 4.5: UV-Vis absorption and fluorescence data of **2p** in different solvents

Solvents	ϵ^a (25 °C)	λ_{max}^b (nm)	λ_{em}^c (nm)	ϵ_{max}^d ($10^5 \text{ M}^{-1}\text{cm}^{-1}$)	Stokes shift e (nm)
1,4-dioxane	2.25	346	408	2.07	62
Toluene	2.38	348	409	3.25	61
Chloroform	4.81	347	414	4.57	67
THF	7.58	346	409	3.71	63
DCM	8.93	346	415	3.09	69
MeOH	32.70	344	421	2.58	77
Acetonitrile	37.50	345	416	2.68	71
DMSO	46.68	349	424, 680	2.91	75

^aDielectric constant at 25 °C. ^bMaximum absorption wavelength. ^cMaximum emission wavelength. ^dMolar absorption coefficient at maximum absorption wavelength. ^eDifference between absorption maximum and emission maximum.

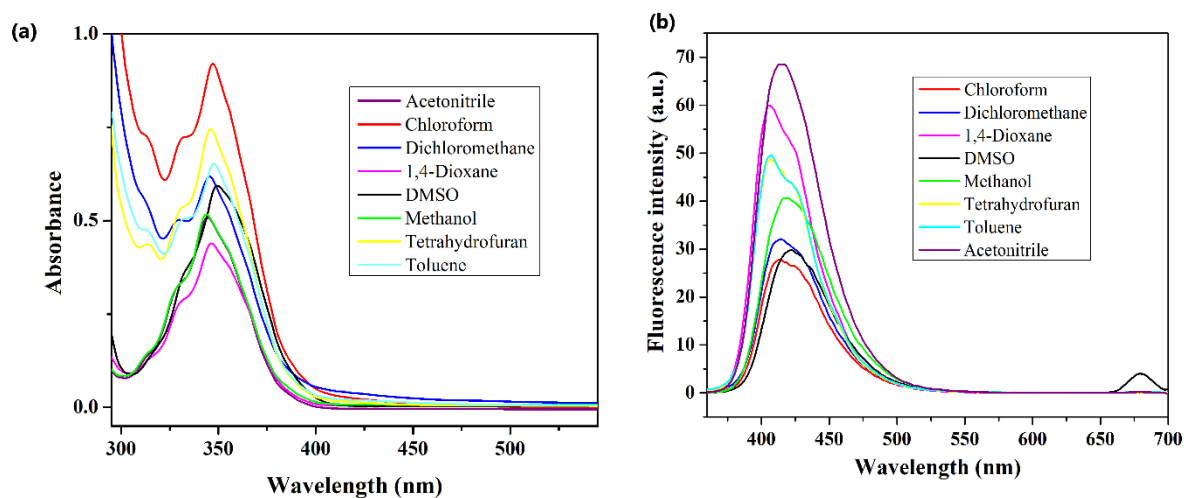


Figure 4.8. Photophysical properties of **2p**, (a) Absorption and (b) fluorescence spectra of **2p** recorded at concentration 2.0×10^{-5} M in different solvents.

4.5. Conclusion:

In conclusion, we have developed ammonium thiocyanate promoted first neat synthetic approach of isothiazole to both cyclic/acyclic precursors and the fate of reaction with different equivalent of ammonium thiocyanate *vs* temperature/time/yield was observed. The availability of various β -bromo vinyl aldehydes and the simplicity of the developed method can provide broad synthetic options for the synthesis of isothiazole derivatives. An instantaneous synthetic transformation to β -enaminones by the addition of aryl amine with ammonium thiocyanate in β -bromo vinyl aldehydes derivatives was also included during the mechanistic consideration of isothiazole formation. Further functionalization in fused isothiazoles *via* NBS promoted aromatization is another application of our developed methodology. We have also successfully investigated emission properties of newly synthesized isothiazole substituted pyrene-based fluorophore and other photophysical properties progress in our laboratory.

4.6. Experimental section:

General information:

^1H NMR spectra of all the synthesized compounds were recorded on a 400 MHz and 500 MHz spectrometers in CDCl_3 solvent using TMS as the internal standard. ^{13}C NMR was recorded in the same MHz instruments. 60-120 or 100-200 mesh silica gels (SRL) were used for column chromatographic purification. Progress of the reaction was monitored by using precoated silica gel 60 F254 TLC sheets (Merck). Petroleum ether (boiling range 60-80 °C) or *n*-hexane and ethyl acetate (b.p. 77.1 °C) were used as the eluent for column chromatographic separation. Solvents were distilled, dried and stored over molecular sieves (4 Å). The UV-Vis absorption spectra were recorded on UV-Vis spectrophotometer (Labtronics Model LT-291) and the fluorescence emission spectra were recorded on PerkinElmer Fluorescence Spectrometer (Model LS 45).

General Procedure for the preparation of 1a – 1o:

At first distilled chloroform (2 mL), DMF (3 mmol) were taken in a dry in a two-neck round-bottom flask and this round-bottom flask was placed in an ice-bath. Then PBr_3 (2.7 mmol) was added dropwise into the round-bottom flask and the resulting mixture was allowed to stir until a white complex formed. After that substrate was dissolved in distilled chloroform and slowly added to the resulting reaction. Finally, the reaction mixture was allowed for stirring 8 h at room temperature. The crude residue was purified by silica-gel (60-120 mesh) in column chromatography using petroleum ether and ethyl acetate (30:1) as an eluent to get the desired product **1**.

General Procedure for the preparation of 2a – 2o:

β -Bromovinyl aldehyde **1** (1mmol) and NH_4SCN (10 mmol) were taken in a one-neck round-bottom flask and it was placed in a heating oil bath. The reaction was heated for 10 minutes at 130 °C under neat conditions The progress of the reaction was monitored by TLC. The crude residue was purified by silica-gel (100-200 mesh) in column chromatography using petroleum ether and ethyl acetate (20:1) as an eluent to get the desired product **2**.

General Procedure for the preparation of 3a – 3e:

β -Bromovinyl aldehyde **1** (1mmol), NH₄SCN (1 mmol) and *p*-toluidine (1 mmol) were taken in a one-neck round-bottom flask. An instantaneous change will occur by the change of colour within 2-3 minutes at room temperature under the neat condition. The crude residue was purified by silica-gel (100-200 mesh) in column chromatography using petroleum ether and ethyl acetate (30:1) as an eluent to get the desired product **3**.

General Procedure for the preparation of *N-p-tolylformamide 3da*:

Substrate **3da** (1mmol) was taken in a one-neck round-bottom flask and dissolved in DMSO (3 mL). Then K₂CO₃ (1 mmol) was added to this reaction mixture and allowed for stirring 3h at 120 °C. The progress of the reaction was monitored by TLC. The crude residue was purified by silica-gel (100-200 mesh) in column chromatography using petroleum ether and ethyl acetate (5:1) as an eluent to get the desired product.

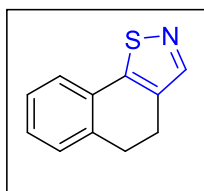
General Procedure for the preparation of 4a – 4g:

Substrate **1** or **2** (1 mmol) was taken in a two-neck round-bottom flask. Then NBS (1 mmol) was dissolved in CH₂Cl₂ (3 mL) and added into this reaction mixture. After that AcOH (1 drop) was dissolved in CH₂Cl₂ and added to it. Finally, the reaction mixture was allowed for stirring under inert conditions at room temperature. The progress of the reaction was monitored by TLC. The crude residue was purified by silica-gel (100-200 mesh) in column chromatography using petroleum ether and ethyl acetate (50:1) as an eluent to get the desired product **4**.

4.6.1. Characterization of NMR data:

4,5-Dihydronaphtho[2,1-d]isothiazole: (2a)

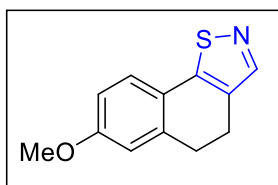
Brown liquid (134.6 mg, 72%). ^1H NMR (500 MHz, CDCl_3) δ 8.31 (s, 1H), 7.42 – 7.41 (m,



1H), 7.29 – 7.23 (m, 3H), 2.99 – 2.96 (m, 2H), 2.92 – 2.89 (m, 2H). ^{13}C NMR (126 MHz, CDCl_3) δ 158.4, 156.8, 135.4, 134.0, 129.2, 128.6, 128.5, 127.3, 125.2, 29.0, 21.3. HRMS calcd. for $\text{C}_{11}\text{H}_{10}\text{NS}$: $(\text{M}+\text{H})^+$ 188.0536, found : 188.0534.

7-Methoxy-4,5-dihydronaphtho[2,1-d]isothiazole: (2b)

Brown solid (195.3 mg, 90%), mp. 59 °C. ^1H NMR (500 MHz, CDCl_3) δ 8.20 (s, 1H), 7.28 (d,

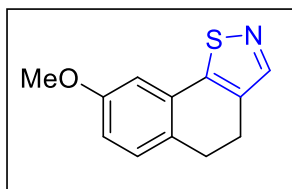


$J = 8.5$ Hz, 1H), 6.76 (d, $J = 2.5$ Hz, 1H), 6.70 (dd, $J = 8.5, 2.5$ Hz, 1H), 3.77 (s, 3H), 2.90 – 2.87 (m, 2H), 2.82 – 2.80 (m, 2H). ^{13}C NMR (126 MHz, CDCl_3) δ 160.3, 158.4, 156.6, 137.4, 132.6, 126.5, 121.8, 114.2, 112.3, 55.4, 29.5, 21.3. HRMS calcd. for $\text{C}_{12}\text{H}_{12}\text{NOS}$: $(\text{M}+\text{H})^+$

218.0641, found : 218.0644.

8-Methoxy-4,5-dihydronaphtho[2,1-d]isothiazole: (2c)

Brown solid (191.0 mg, 88%), mp. 64 °C. ^1H NMR (400 MHz, CDCl_3) δ 8.31 (s, 1H), 7.19 (d,

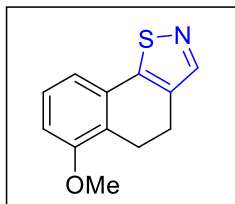


$J = 8.4$ Hz, 1H), 6.95 (d, $J = 2.6$ Hz, 1H), 6.82 (dd, $J = 8.3, 2.6$ Hz, 1H), 3.82 (s, 3H), 2.89 – 2.88 (m, 4H). ^{13}C NMR (101 MHz, CDCl_3) δ 158.8, 158.5, 157.0, 134.5, 131.0, 129.4, 127.7, 114.8, 110.5, 55.6, 28.3, 21.8. HRMS calcd. for $\text{C}_{12}\text{H}_{12}\text{NOS}$: $(\text{M}+\text{H})^+$ 218.0641, found :

218.0638.

6-Methoxy-4,5-dihydronaphtho[2,1-d]isothiazole: (2d)

Yellow solid (180.1 mg, 83%), mp. 82 °C. ^1H NMR (400 MHz, CDCl_3) δ 8.35 (s, 1H), 8.17 –

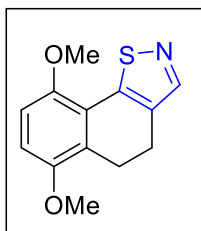


8.07 (m, 1H), 7.49 (d, $J = 8.8$ Hz, 1H), 6.76 (d, $J = 8.8$ Hz, 1H), 3.86 (s, 3H), 3.01 (t, $J = 7.6$ Hz, 2H), 2.89 – 2.85 (m, 2H). ^{13}C NMR (101 MHz, CDCl_3) δ 156.1, 154.9, 153.9, 134.9, 131.9, 127.2, 122.9, 121.2, 112.4, 56.1, 22.4, 21.0. HRMS calcd. for $\text{C}_{12}\text{H}_{12}\text{NOS}$: $(\text{M}+\text{H})^+$ 218.0641, found

: 218.0643.

6,9-Dimethoxy-4,5-dihydronaphtho[2,1-d]isothiazole: (2e)

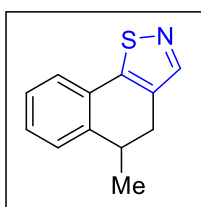
Yellow solid (187.7 mg, 76%), mp. 101 °C. ¹H NMR (500 MHz, CDCl₃) δ 8.28 (s, 1H), 6.84



(d, *J* = 9.0 Hz, 1H), 6.79 (d, *J* = 9.0 Hz, 1H), 3.95 (s, 3H), 3.83 (s, 3H), 3.00 (d, *J* = 8.0 Hz, 2H), 2.92 (d, *J* = 8.0 Hz, 2H). ¹³C NMR (126 MHz, CDCl₃) δ 154.5, 153.0, 151.0, 149.4, 132.7, 124.9, 119.8, 111.7, 108.8, 56.2, 56.0, 21.6, 20.8. HRMS calcd. for C₁₃H₁₄NO₂S: (M+H)⁺ 248.0747, found : 248.0744.

5-Methyl-4,5-dihydronaphtho[2,1-d]isothiazole: (2f)

Brown liquid (136.7 mg, 68%). ¹H NMR (500 MHz, CDCl₃) δ 8.31 (s, 1H), 7.43 (d, *J* = 7.5

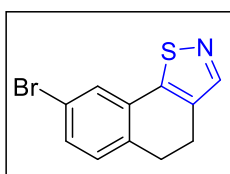


Hz, 1H), 7.32 – 7.28 (m, 2H), 7.26 – 7.23 (m, 1H), 3.14 (q, *J* = 6.8 Hz, 1H), 3.02 (dd, *J* = 15.5, 6.5 Hz, 1H), 2.73 (dd, *J* = 15.5, 6.0 Hz, 1H), 1.23 (d, *J* = 7.0 Hz, 3H). ¹³C NMR (126 MHz, CDCl₃) δ 157.7, 157.3, 140.4, 132.7, 129.5, 127.7, 127.3, 127.1, 125.4, 33.5, 29.0, 20.5. HRMS calcd. for

C₁₂H₁₂NS: (M+H)⁺ 202.0692, found : 202.0690.

8-Bromo-4,5-dihydronaphtho[2,1-d]isothiazole: (2g)

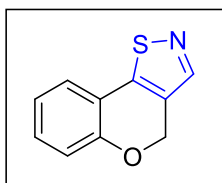
White solid (238.4 mg, 90%), mp. 70 °C. ¹H NMR (500 MHz, CDCl₃) δ 8.34 (s, 1H), 7.57 (d,



J = 1.7 Hz, 1H), 7.40 (dd, *J* = 8.1, 1.7 Hz, 1H), 7.18 (d, *J* = 8.1 Hz, 1H), 2.96 – 2.94 (m, 4H). ¹³C NMR (126 MHz, CDCl₃) δ 156.9, 156.8, 134.5, 134.2, 131.8, 130.4, 130.0, 127.8, 120.6, 28.6, 21.2. HRMS calcd. for C₁₁H₉BrNS: (M+H)⁺ 265.9641, found : 265.9642.

4H-chromenof[3,4-d]isothiazole: (2h)

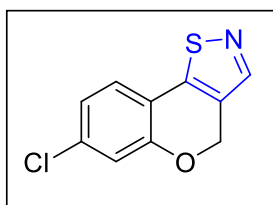
Red liquid (126.6 mg, 67%). ¹H NMR (500 MHz, CDCl₃) δ 8.23 (s, 1H), 7.35 (dd, *J* = 7.7, 1.2



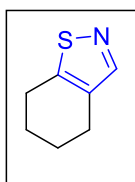
Hz, 1H), 7.25 – 7.23 (m, 1H), 6.99 – 6.96 (m, 2H), 5.34 (s, 2H). ¹³C NMR (126 MHz, CDCl₃) δ 154.8, 153.3, 152.2, 131.4, 128.5, 125.3, 122.3, 117.5, 117.2, 64.7. HRMS calcd. for C₁₀H₈NOS: (M+H)⁺ 190.0328, found : 190.0327.

7-Chloro-4H-chromeno[3,4-d]isothiazole: (2i)

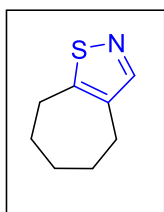
Yellow solid (144.9 mg, 65%), mp. 105 °C. ^1H NMR (500 MHz, CDCl_3) δ 8.29 (s, 1H), 7.38



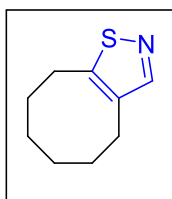
(s, 1H), 7.24 – 7.21 (m, 1H), 6.96 (dd, $J = 8.7, 1.2$ Hz, 1H), 5.41 (s, 2H). ^{13}C NMR (126 MHz, CDCl_3) δ 153.6, 153.1, 150.6, 136.5, 130.9, 127.2, 124.8, 118.7, 118.6, 64.8. HRMS calcd. for $\text{C}_{10}\text{H}_7\text{ClNOS}$: $(\text{M}+\text{H})^+$ 223.9939, found : 223.9936.

4,5,6,7-Tetrahydrobenzo[d]isothiazole: (2j)

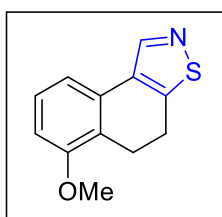
Yellow oil (86.2 mg, 62%). ^1H NMR (400 MHz, CDCl_3) δ 8.19 (s, 1H), 2.86 (t, $J = 6.1$ Hz, 2H), 2.68 (t, $J = 6.1$ Hz, 2H), 1.88 – 1.76 (m, 4H). ^{13}C NMR (101 MHz, CDCl_3) δ 157.6, 131.0, 128.9, 23.4, 23.1, 22.9, 22.4. HRMS calcd. for $\text{C}_7\text{H}_{10}\text{NS}$: $(\text{M}+\text{H})^+$ 140.0536, found : 140.0533.

5,6,7,8-Tetrahydro-4H-cyclohepta[d]isothiazole: (2k)

Yellow oil (107.1 mg, 70%). ^1H NMR (400 MHz, CDCl_3) δ 8.10 (s, 1H), 2.92 – 2.88 (m, 2H), 2.77 – 2.73 (m, 2H), 1.89 – 1.85 (m, 2H), 1.72 – 1.67 (m, 2H), 1.64 – 1.60 (m, 2H). ^{13}C NMR (101 MHz, CDCl_3) δ 159.4, 138.8, 131.7, 32.2 (2C), 27.8, 27.8, 27.7. HRMS calcd. for $\text{C}_8\text{H}_{12}\text{NS}$: $(\text{M}+\text{H})^+$ 154.0692, found : 154.0688.

4,5,6,7,8,9-Hexahydrocycloocta[d]isothiazole: (2l)

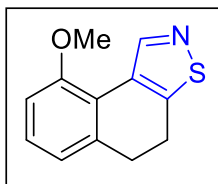
Yellow oil (143.6 mg, 86%). ^1H NMR (400 MHz, CDCl_3) δ 8.17 (s, 1H), 2.97 – 2.94 (m, 2H), 2.74 – 2.71 (m, 2H), 1.65 – 1.64 (m, 4H), 1.41 – 1.40 (m, 4H). ^{13}C NMR (101 MHz, CDCl_3) δ 158.7, 145.6, 131.5, 31.4, 30.8, 25.6, 25.3, 24.7, 24.4. HRMS calcd. for $\text{C}_9\text{H}_{14}\text{NS}$: $(\text{M}+\text{H})^+$ 168.0849, found : 168.0848.

6-Methoxy-4,5-dihydronaphtho[1,2-d]isothiazole: (2m)

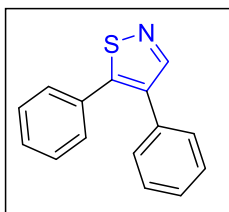
Yellow solid (143.2 mg, 66%), mp. 86 °C. ^1H NMR (500 MHz, CDCl_3) δ 10.21 (s, 1H), 7.31 – 7.28 (m, 1H), 7.20 (t, $J = 7.5$ Hz, 1H), 6.91 (d, $J = 8.0$ Hz, 1H), 3.91 (s, 3H), 3.07 – 2.98 (m, 4H). ^{13}C NMR (126 MHz, CDCl_3) δ 189.1, 156.3, 144.4, 132.1, 130.0, 127.8, 122.6, 114.4, 110.8, 55.5, 31.7, 20.4. HRMS calcd. for $\text{C}_{12}\text{H}_{12}\text{NOS}$: $(\text{M}+\text{H})^+$ 218.0641, found : 218.0638.

9-Methoxy-4,5-dihydronaphtho[1,2-d]isothiazole: (2n)

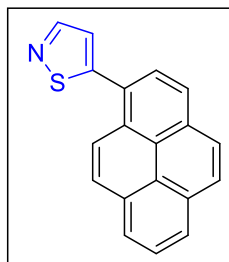
Yellow solid (154.1 mg, 71%), mp. 97 °C. ^1H NMR (400 MHz, CDCl_3) δ 10.04 (s, 1H), 7.28 (t, $J = 7.9$ Hz, 1H), 6.91 – 6.87 (m, 2H), 3.86 (s, 3H), 3.00 – 2.88 (m, 4H).



^{13}C NMR (101 MHz, CDCl_3) δ 171.2, 168.1, 136.9, 131.7, 128.4, 126.9, 124.1, 115.0, 111.6, 61.6, 31.1, 21.1. HRMS calcd. for $\text{C}_{12}\text{H}_{12}\text{NOS}$: $(\text{M}+\text{H})^+$ 218.0641, found : 218.0644.

4,5-Diphenylisothiazole: (2o)

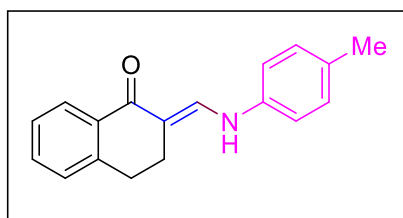
Yellow solid (189.6 mg, 80%), mp. 86 °C. ^1H NMR (300 MHz, CDCl_3) δ 8.52 (s, 1H), 7.34 – 7.32 (m, 10H). ^{13}C NMR (76 MHz, CDCl_3) δ 161.7, 159.3, 135.7, 133.0, 130.6, 129.2, 129.1 (2C), 129.0 (2C), 128.9 (2C), 128.8 (2C), 127.8. HRMS calcd. for $\text{C}_{15}\text{H}_{12}\text{NS}$: $(\text{M}+\text{H})^+$ 238.0692, found : 238.0690.

5-(Pyren-1-yl)isothiazole: (2p)

Brown solid (222.3 mg, 78%), mp. 108 °C. ^1H NMR (400 MHz, CDCl_3) δ 8.66 (s, 1H), 8.30 (d, $J = 9.2$ Hz, 1H), 8.22 – 8.15 (m, 3H), 8.12 – 8.01 (m, 5H), 7.53 (s, 1H). ^{13}C NMR (101 MHz, CDCl_3) δ 166.1, 157.7, 132.0, 131.4, 130.8, 128.8, 128.6, 128.5, 127.8, 127.3, 126.5, 126.0, 125.6, 125.5, 125.0, 124.7, 124.6, 124.5, 124.1. HRMS calcd. for $\text{C}_{19}\text{H}_{12}\text{NS}$: $(\text{M}+\text{H})^+$ 286.0692, found : 286.0688.

(E)-2-((p-tolylamino)methylene)-3,4-dihydronaphthalen-1(2H)-one: (3a)

Brown solid (173.6 mg, 66%), mp. 116 °C. ^1H NMR (300 MHz, CDCl_3) δ 11.89 (d, $J = 12.0$

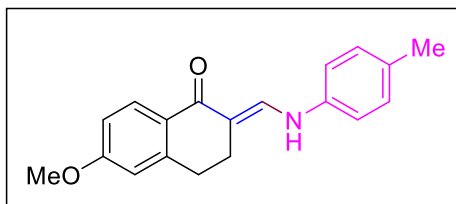


Hz, 1H), 7.95 (dd, $J = 7.5, 1.5$ Hz, 1H), 7.35 – 7.23 (m, 3H), 7.19 – 7.12 (m, 1H), 7.04 (d, $J = 8.4$ Hz, 2H), 6.90 (d, $J = 8.4$ Hz, 2H), 2.88 – 2.81 (m, 2H), 2.61 – 2.57 (m, 2H), 2.23 (s, 3H). ^{13}C NMR (76 MHz, CDCl_3) δ 187.5, 142.3, 142.1, 138.3, 135.3, 132.7, 131.9, 130.3(2C), 128.0, 126.9, 126.6,

116.1 (2C), 104.8, 29.9, 27.8, 20.8. HRMS calcd. for $\text{C}_{18}\text{H}_{18}\text{NO}$: $(\text{M}+\text{H})^+$ 264.1390, found : 264.1386.

(E)-6-methoxy-2-((p-tolylamino)methylene)-3,4-dihydronaphthalen-1(2H)-one: (3b)

Brown solid (202.2 mg, 69%), mp. 122 °C. ¹H NMR (300 MHz, CDCl₃) δ 11.87 (d, *J* = 11.8

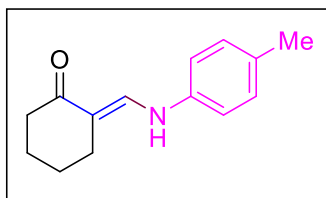


Hz, 1H), 8.02 (d, *J* = 8.6 Hz, 1H), 7.35-7.31 (m, 1H), 7.14 (d, *J* = 8.2 Hz, 2H), 6.99 (d, *J* = 8.5 Hz, 2H), 6.89 (dd, *J* = 8.6, 2.5 Hz, 1H), 6.73 (d, *J* = 2.4 Hz, 1H), 3.88 (s, 3H), 2.93 – 2.89 (m, 2H), 2.71 – 2.66 (m, 2H), 2.33

(s, 3H). ¹³C NMR (76 MHz, CDCl₃) δ 187.1, 162.6, 144.4, 141.5, 138.5, 132.4, 130.3 (2C), 128.9, 128.7, 121.4, 115.9 (2C), 112.7, 104.6, 55.5, 30.4, 28.1, 20.8. HRMS calcd. for C₁₉H₂₀NO₂: (M+H)⁺ 294.1496, found : 294.1494.

(E)-2-((p-tolylamino)methylene)cyclohexan-1-one: (3c)

Yellow solid (133.3 mg, 62%), mp. 85 °C. ¹H NMR (300 MHz, CDCl₃) δ 11.87 (d, *J* = 12.1

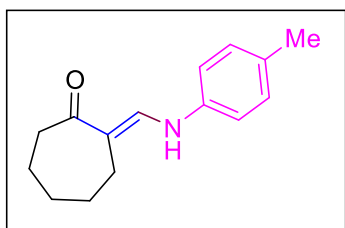


Hz, 1H), 7.14 – 7.08 (m, 3H), 6.92 (d, *J* = 8.4 Hz, 2H), 2.46 – 2.35 (m, 4H), 2.29 (s, 3H), 1.82 – 1.70 (m, 4H). ¹³C NMR (76 MHz, CDCl₃) δ 204.5, 142.2, 138.5, 132.2, 130.1 (2C), 115.8 (2C), 109.9, 44.7, 32.9, 31.8, 31.1, 25.2. HRMS calcd. for C₁₄H₁₈NO: (M+H)⁺

216.1390, found : 216.1393.

(E)-2-((p-tolylamino)methylene)cycloheptan-1-one: (3d)

Yellow solid (167.2 mg, 73%), mp. 91 °C. ¹H NMR (400 MHz, CDCl₃) δ 11.49 (d, *J* = 11.0

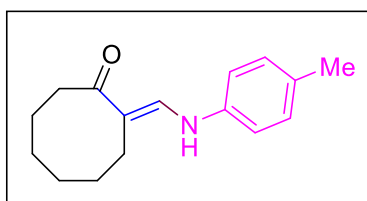


Hz, 1H), 7.15 (d, *J* = 12.0 Hz, 1H), 7.08 (d, *J* = 8.2 Hz, 2H), 6.89 (d, *J* = 8.3 Hz, 2H), 2.57 – 2.54 (m, 2H), 2.38 – 2.35 (m, 2H), 2.28 (s, 3H), 1.74 – 1.64 (m, 6H). ¹³C NMR (101 MHz, CDCl₃) δ 204.5, 142.2, 138.6, 132.2, 130.2 (2C), 115.8 (2C), 110.0, 44.8, 38.2, 33.0, 32.0, 29.8, 22.8. HRMS calcd. for C₁₅H₂₀NO: (M+H)⁺

230.1547, found : 230.1545.

(E)-2-((p-tolylamino)methylene)cyclooctan-1-one: (3e)

Yellow solid (184.8 mg, 76%), mp. 75 °C. ¹H NMR (400 MHz, CDCl₃) δ 11.87 (d, *J* = 11.7 Hz, 1H), 7.13 – 7.06 (m, 3H), 6.90

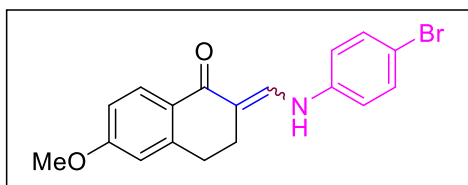


(d, *J* = 8.5 Hz, 2H), 2.57 – 2.53 (m, 2H), 2.44 – 2.40 (m, 2H), 2.27 (s, 3H), 1.77 – 1.71 (m, 2H), 1.59 – 1.50 (m, 6H). ¹³C NMR

(101 MHz, CDCl₃) δ 204.2, 142.7, 138.4, 132.4, 130.2(2C), 116.0(2C), 108.8, 39.7, 33.7, 30.5, 29.0, 26.3, 26.0, 20.8. HRMS calcd. for C₁₆H₂₂NO: (M+H)⁺ 244.1703, found : 244.1701.

2-(((4-bromophenyl)amino)methylene)-6-methoxy-3,4-dihydronaphthalen-1(2H)-one: (3f)

Brown solid (232.0 mg, 65%, Diastereomeric mixture). mp. 92-94 °C. ¹H NMR (300 MHz,

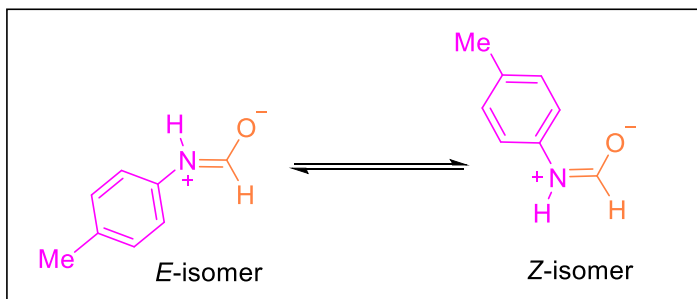


CDCl₃) Z (major) δ 11.73 (d, J = 11.7 Hz, 1H), 7.90 (d, J = 8.6 Hz, 1H), 7.33 – 7.29 (m, 2H), 7.17 – 7.16 (m, 2H), 6.84 – 6.80 (m, 2H), 6.79 – 6.75 (m, 1H), 3.76 (s, 3H), 2.81 – 2.77 (m, 2H), 2.59 – 2.54 (m, 2H); ¹H NMR

(300 MHz, CDCl₃) E (minor) δ 7.21 – 7.18 (m, 2H), 7.03 – 6.97 (m, 1H), 6.89 – 6.86 (m, 1H), 6.69 – 6.62 (m, 2H), 6.47 – 6.45 (m, 2H), 3.71 (s, 3H), 2.74 – 2.69 (m, 2H), 2.48 – 2.39 (m, 2H). ¹³C NMR (76 MHz, CDCl₃) δ 189.9, 187.6, 162.8, 144.6, 144.2, 143.0, 140.1, 140.0, 132.6, 132.3, 132.1, 132.0, 131.9, 130.6, 129.7, 129.1, 128.4, 124.3, 122.2, 121.4, 117.2, 116.8, 116.6, 115.5, 114.9, 113.6, 112.8, 112.7, 111.4, 111.2, 110.7, 109.9, 105.8, 55.5, 55.4, 30.4, 30.2, 28.1, 26.9, 23.5. HRMS calcd. for C₁₈H₁₇BrNO₂: (M+H)⁺ 358.0444, found : 358.0448.

N-p-tolylformamide: (3da)

Brown liquid (87.7 mg, 65%, Diastereomeric mixture). ¹H NMR (500 MHz, CDCl₃) (*E*-isomer)

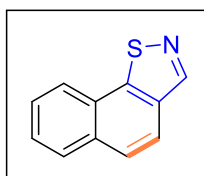


δ 8.64 (d, J = 11.5 Hz, 1H), 7.44 (d, J = 8.4 Hz, 2H), 7.17 (d, J = 8.3 Hz, 2H), 2.36 (s, 3H). (*Z*-isomer) 8.37 (m, 1H), 7.15 (d, 2H, J = 8.5 Hz), 7.01 (d, J = 8.3 Hz, 2H), 2.34 (s, 3H). ¹³C NMR (126 MHz, CDCl₃) (*E*-isomer)

δ 162.5, 135.1, 134.4, 130.2 (2C), 129.8, 129.5 (2C), 20.8. (*Z*-isomer) 158.8, 134.2, 133.9, 121.1, 119.9 (2C), 119.2 (2C), 20.7 HRMS calcd. for C₈H₁₀NO: (M+H)⁺ 136.0764, found : 136.0761.

Naphtho[2,1-d]isothiazole: (4a)

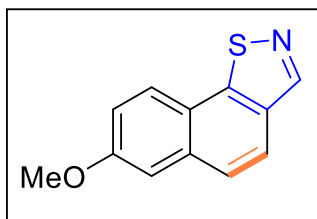
Yellow solid (162.8 mg, 88%), mp. 126 °C. ¹H NMR (400 MHz, CDCl₃) δ 8.97 (s, 1H), 8.12



– 8.10 (m, 1H), 7.98 – 7.96 (m, 1H), 7.92 (d, J = 8.7 Hz, 1H), 7.74 (d, J = 8.6 Hz, 1H), 7.64 – 7.62 (m, 2H). ¹³C NMR (101 MHz, CDCl₃) δ 155.6, 154.6 153.2, 132.1, 129.0, 128.1, 127.4, 126.7, 126.3, 125.4, 120.6. HRMS calcd. for C₁₁H₈NS: (M+H)⁺ 186.0379, found : 186.0377.

7-Methoxynaphtho[2,1-d]isothiazole: (4b)

Off white solid (144.0 mg, 67%), mp. 142 °C. ¹H NMR (400 MHz, CDCl₃) δ 8.93 (s, 1H), 8.18

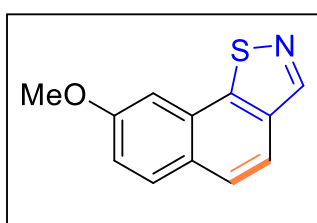


(d, *J* = 9.1 Hz, 1H), 8.06 (d, *J* = 8.9 Hz, 1H), 7.97 (d, *J* = 9.1 Hz, 1H), 7.33 (d, *J* = 9.0 Hz, 1H), 7.28 (m, 1H), 4.06 (s, 3H). ¹³C NMR (101 MHz, CDCl₃) δ 157.5, 155.5, 153.4, 132.4, 131.0, 128.9, 126.1, 125.3, 122.3, 121.9, 113.6, 57.1. HRMS calcd. for

C₁₂H₁₀NOS: (M+H)⁺ 216.0485, found : 216.0484.

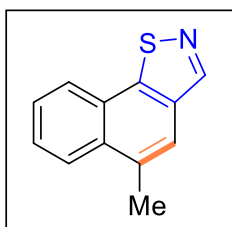
8-Methoxynaphtho[2,1-d]isothiazole: (4c)

Off white solid (124.7 mg, 58%), mp. 155 °C. ¹H NMR (400 MHz, CDCl₃) δ 8.94 (s, 1H), 8.16



(s, 1H), 7.82 (d, *J* = 8.8 Hz, 1H), 7.58 (d, *J* = 8.6 Hz, 1H), 7.46 (s, 1H), 7.30 (s, 1H), 4.06 (s, 3H). ¹³C NMR (101 MHz, CDCl₃) δ 157.0, 155.8, 154.7, 133.3, 127.4, 126.3, 125.3, 119.3, 114.7, 108.4, 104.8, 56.6. HRMS calcd. for C₁₂H₁₀NOS: (M+H)⁺

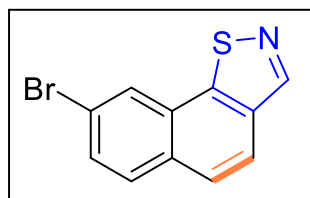
216.0485, found : 216.0488.

5-Methylnaphtho[2,1-d]isothiazole: (4d)

Yellow liquid (103.5 mg, 52%). ¹H NMR (400 MHz, CDCl₃) δ 9.01 (s, 1H), 8.06 (d, *J* = 8.4 Hz, 1H), 8.00 (d, *J* = 7.7 Hz, 1H), 7.76 – 7.58 (m, 3H), 2.79 (s, 3H). ¹³C NMR (101 MHz, CDCl₃) δ 156.7, 155.3, 152.4, 134.2, 131.8, 128.7, 127.2, 125.8, 125.7, 120.4, 116.3, 18.6. HRMS calcd. for C₁₂H₁₀NS: (M+H)⁺ 200.0536, found : 200.0539.

8-Bromonaphtho[2,1-d]isothiazole: (4e)

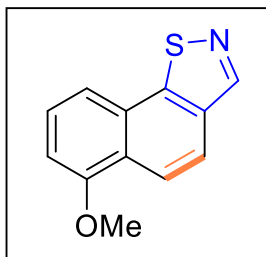
White solid (189.3 mg, 72%), mp. 122 °C. ¹H NMR (500 MHz, CDCl₃) δ 8.99 (s, 1H), 8.27 (s,



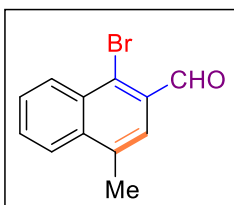
1H), 7.97 (d, *J* = 8.7 Hz, 1H), 7.85 (d, *J* = 8.6 Hz, 1H), 7.73 (d, *J* = 8.6 Hz, 2H). ¹³C NMR (126 MHz, CDCl₃) δ 155.5 (2C), 151.8, 134.4, 131.2, 130.4, 127.6, 127.3, 126.2, 121.2, 121.0. HRMS calcd. for C₁₁H₇BrNS: (M+H)⁺ 263.9484, found : 263.9481.

6-Methoxynaphtho[2,1-d]isothiazole: (4f)

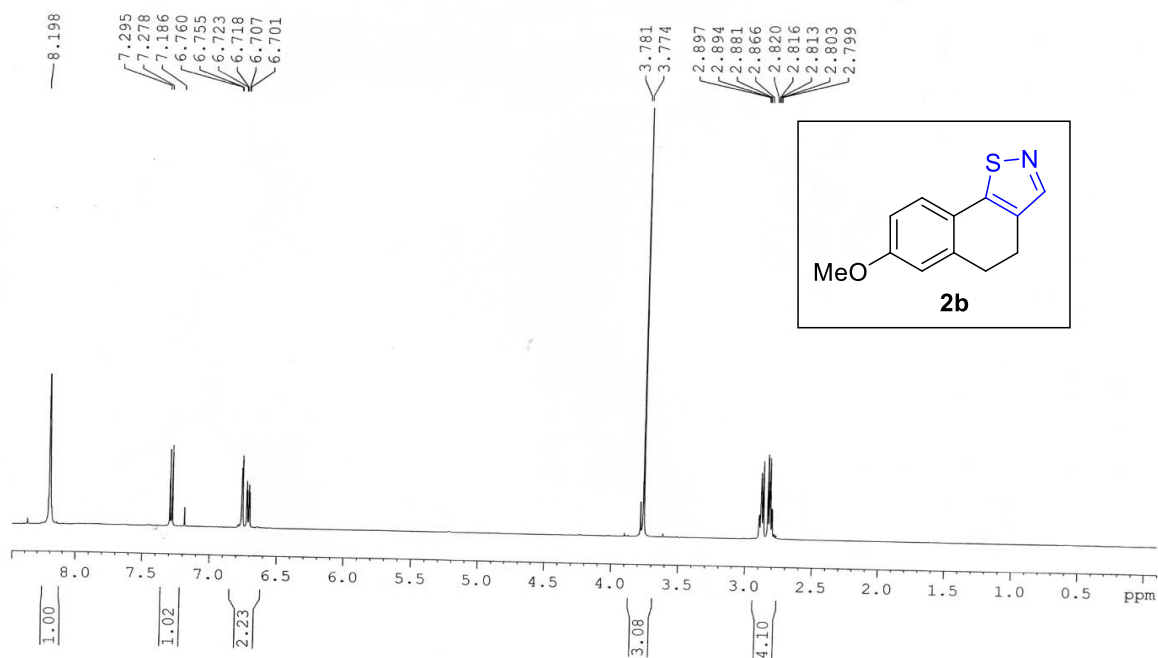
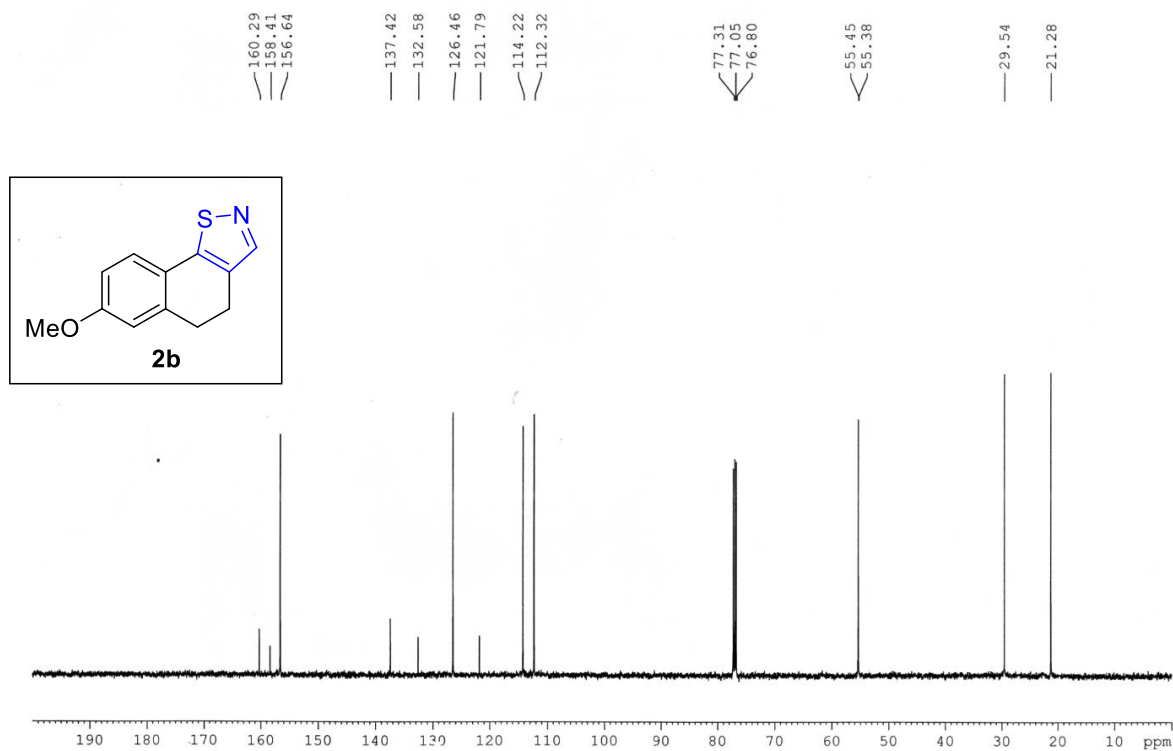
Off white solid (163.4 mg, 76%), mp. 91 °C. ^1H NMR (300 MHz, CDCl_3) δ 9.05 (s, 1H), 8.37 – 8.31 (m, 2H), 8.02 (d, $J = 8.9$ Hz, 1H), 7.88 (d, $J = 8.5$ Hz, 1H), 6.93 (d, $J = 8.5$ Hz, 1H), 4.06 (s, 3H). ^{13}C NMR (76 MHz, CDCl_3) δ 155.6, 153.9, 152.0, 135.8, 131.5, 128.3, 127.2, 125.8, 121.1, 112.3, 107.3, 56.2. HRMS calcd. for $\text{C}_{12}\text{H}_{10}\text{NOS}$: $(\text{M}+\text{H})^+$ 216.0485, found : 216.0480.

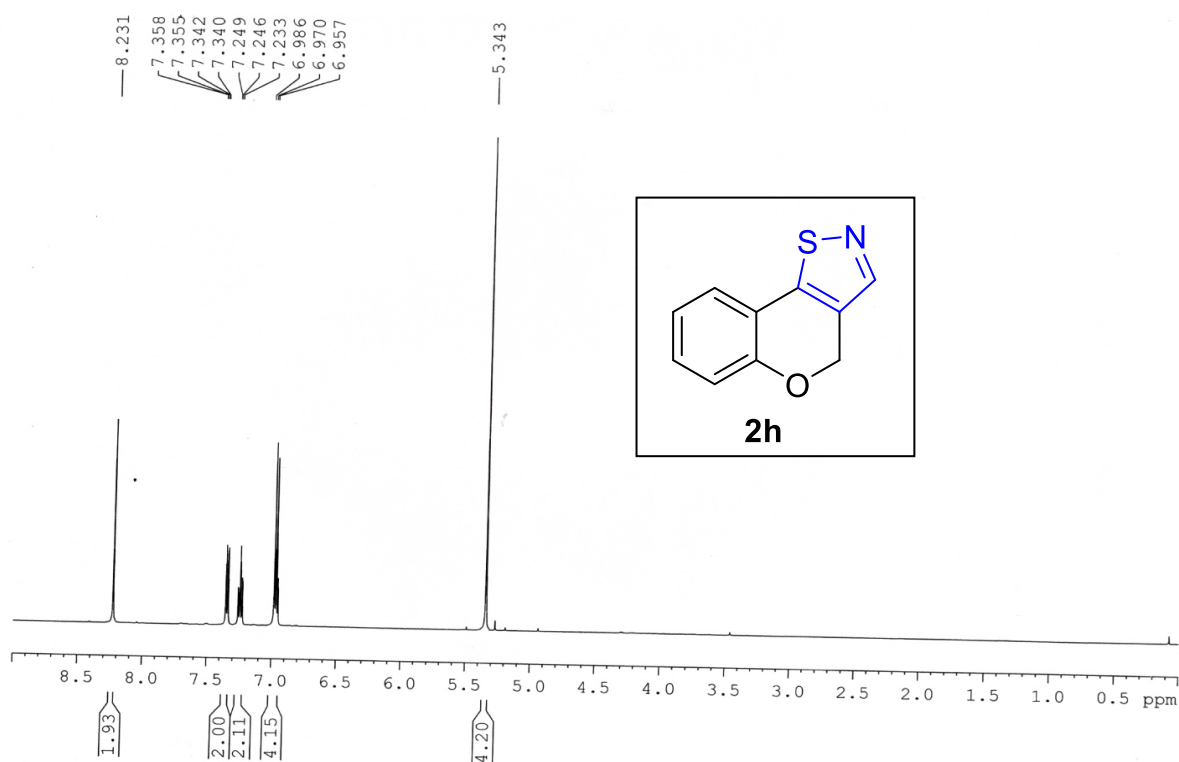
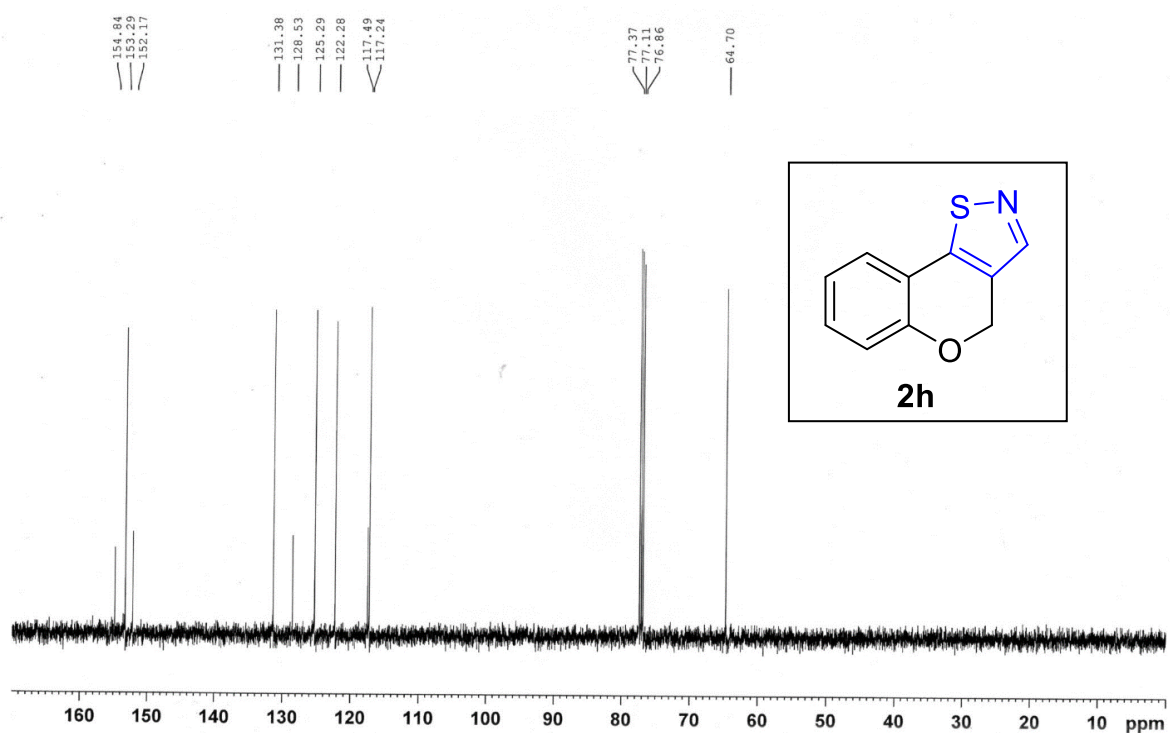
**1-Bromo-4-methyl-2-naphthaldehyde: (4g)**

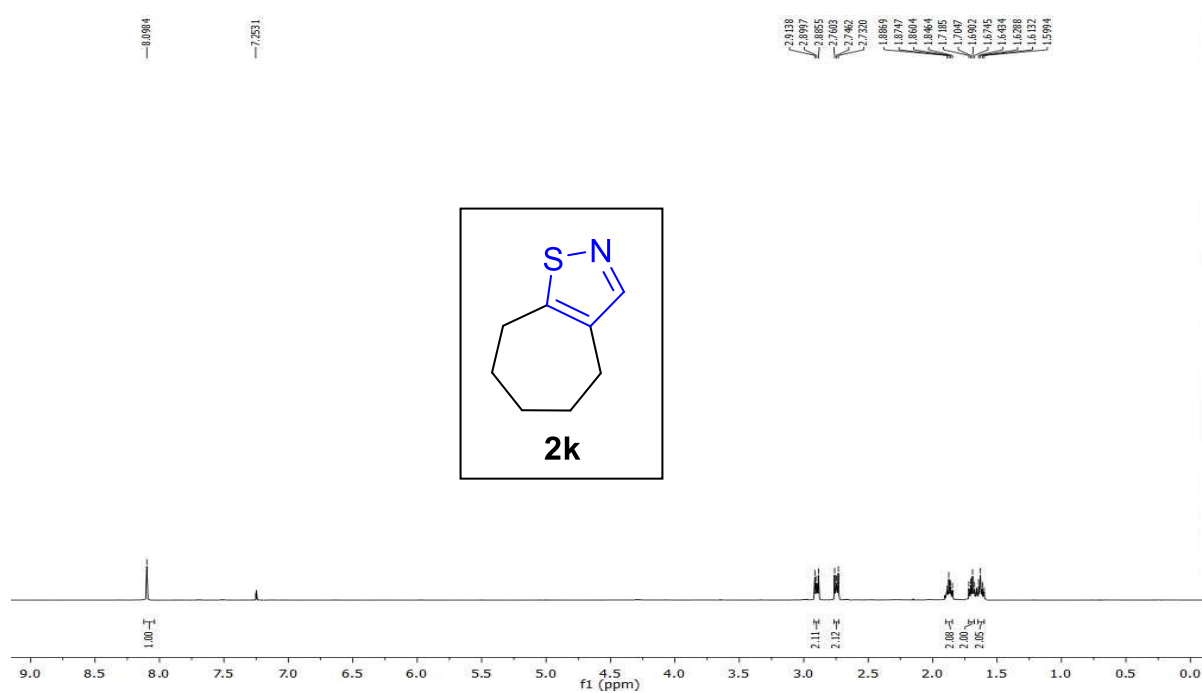
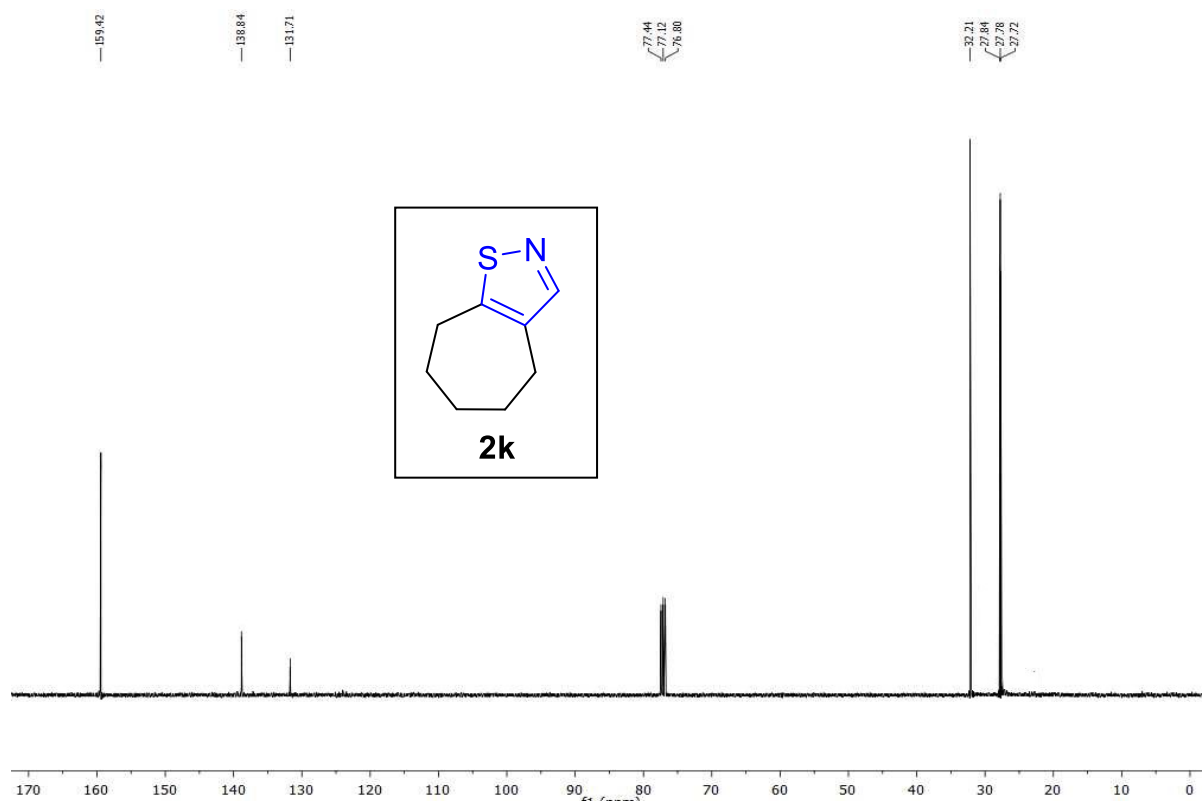
Off white solid (151.2 mg, 61 %), mp. 86 °C. ^1H NMR (300 MHz, CDCl_3) δ 10.51 (s, 1H), 8.42 – 8.39 (m, 1H), 7.89 – 7.87 (m, 1H), 7.64 – 7.54 (m, 3H), 2.56 (s, 3H). ^{13}C NMR (76 MHz, CDCl_3) δ 193.0, 136.7, 135.0, 132.0, 130.8, 129.7, 129.4, 128.7, 127.7, 124.9, 124.4, 19.3. HRMS calcd. for $\text{C}_{12}\text{H}_{10}\text{BrO}$: $(\text{M}+\text{H})^+$ 248.9917, found : 248.9915.

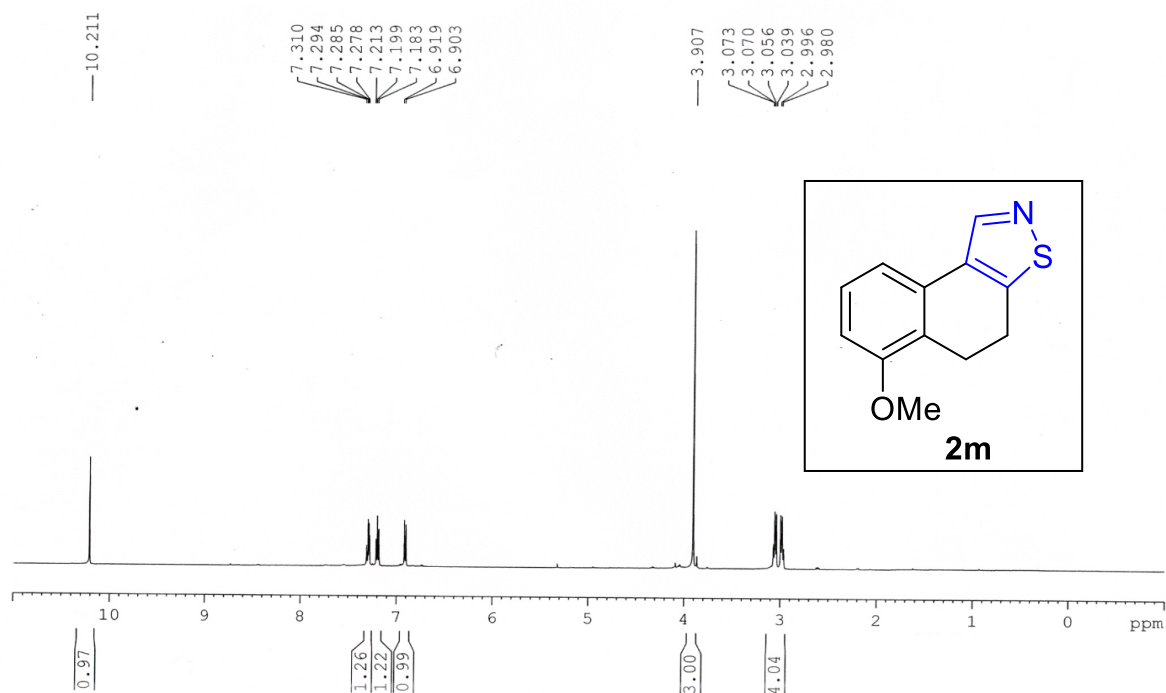
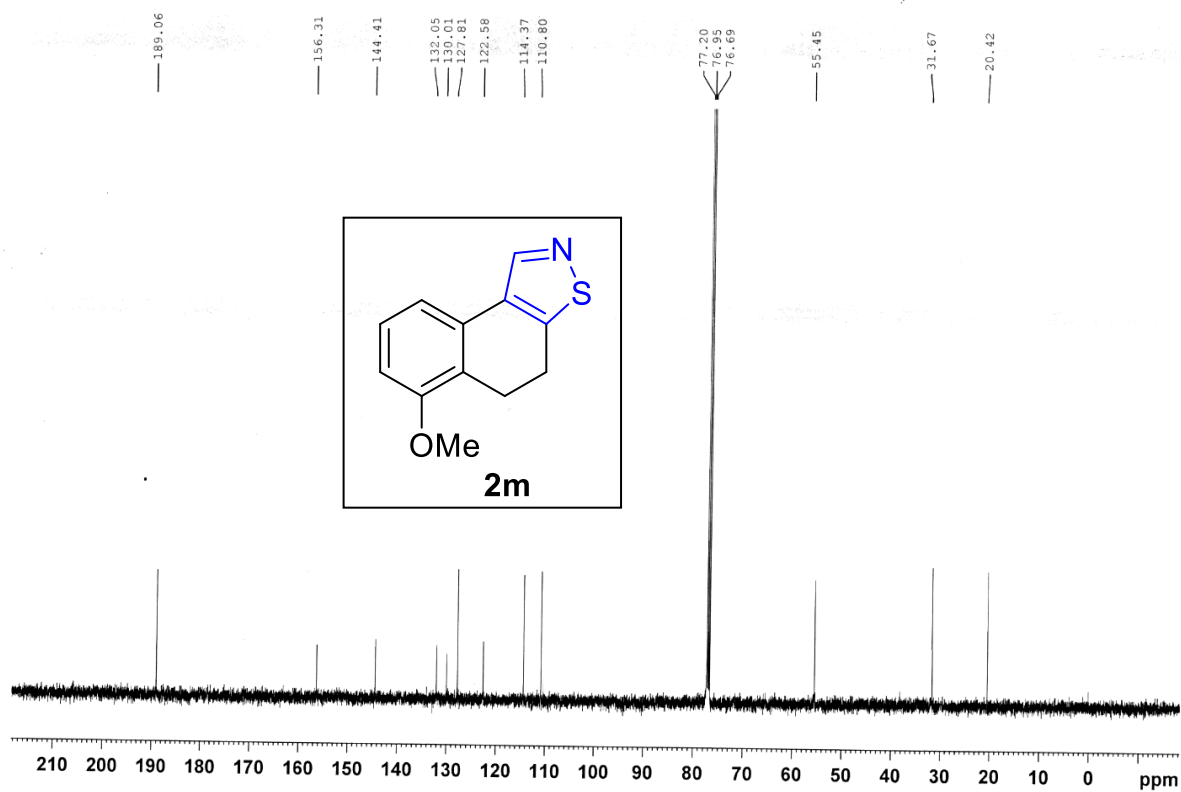


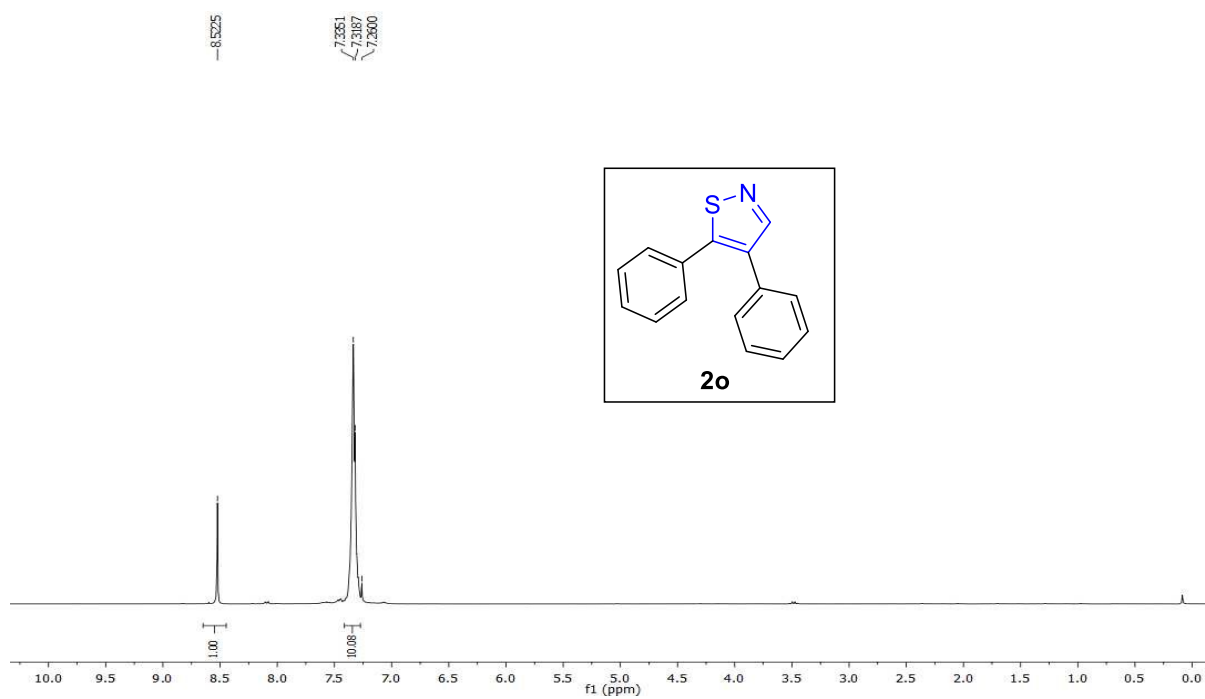
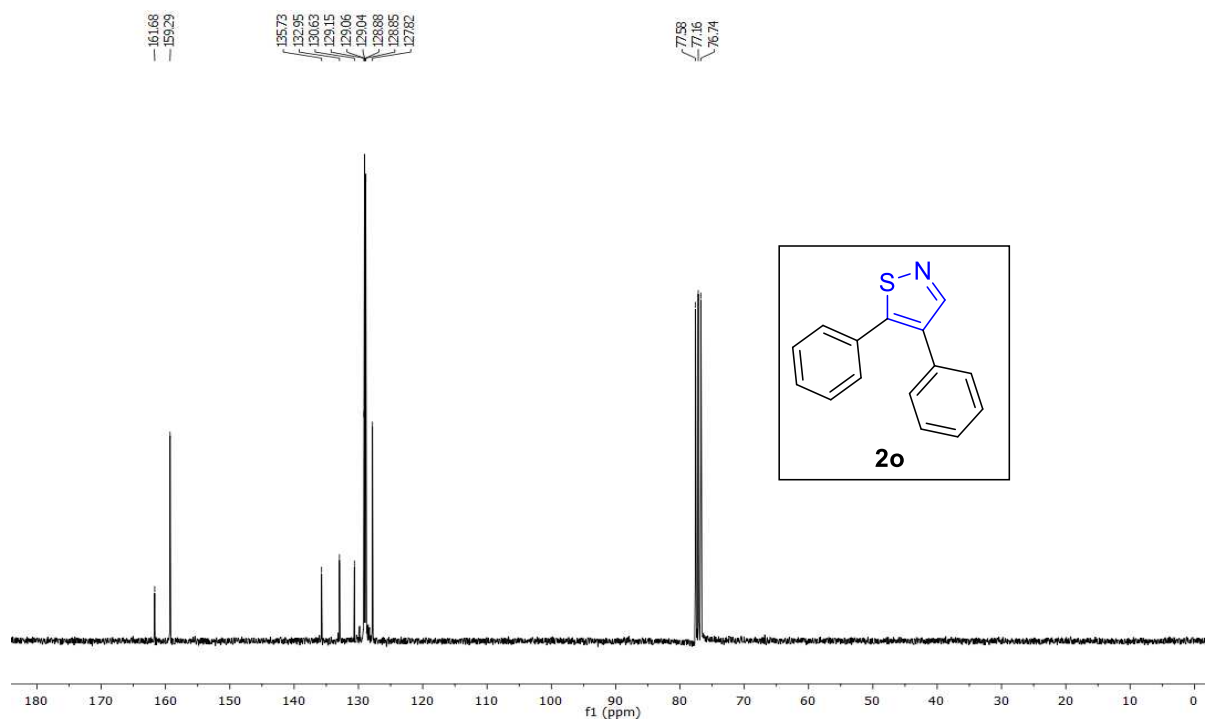
4.6.2. Representative NMR Spectra:

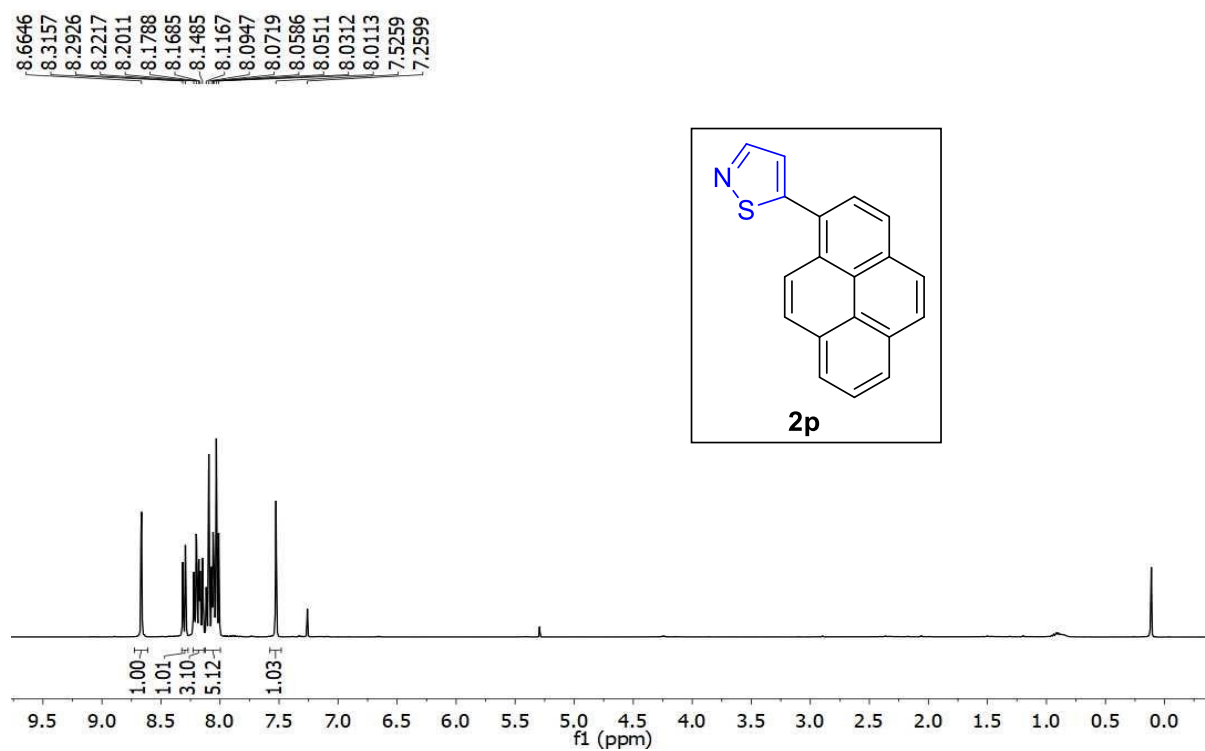
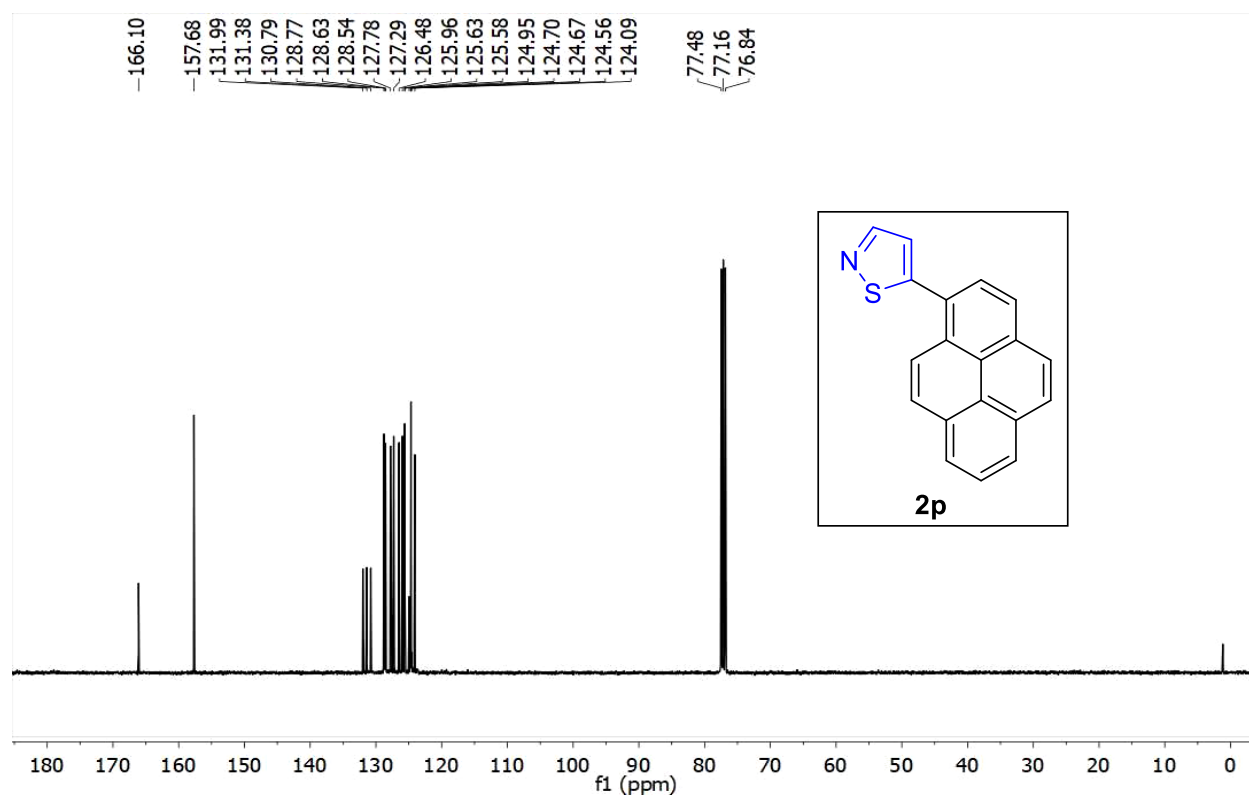
 ^1H NMR of **2b** (500 MHz, CDCl_3): ^{13}C NMR of **2b** (126 MHz, CDCl_3):

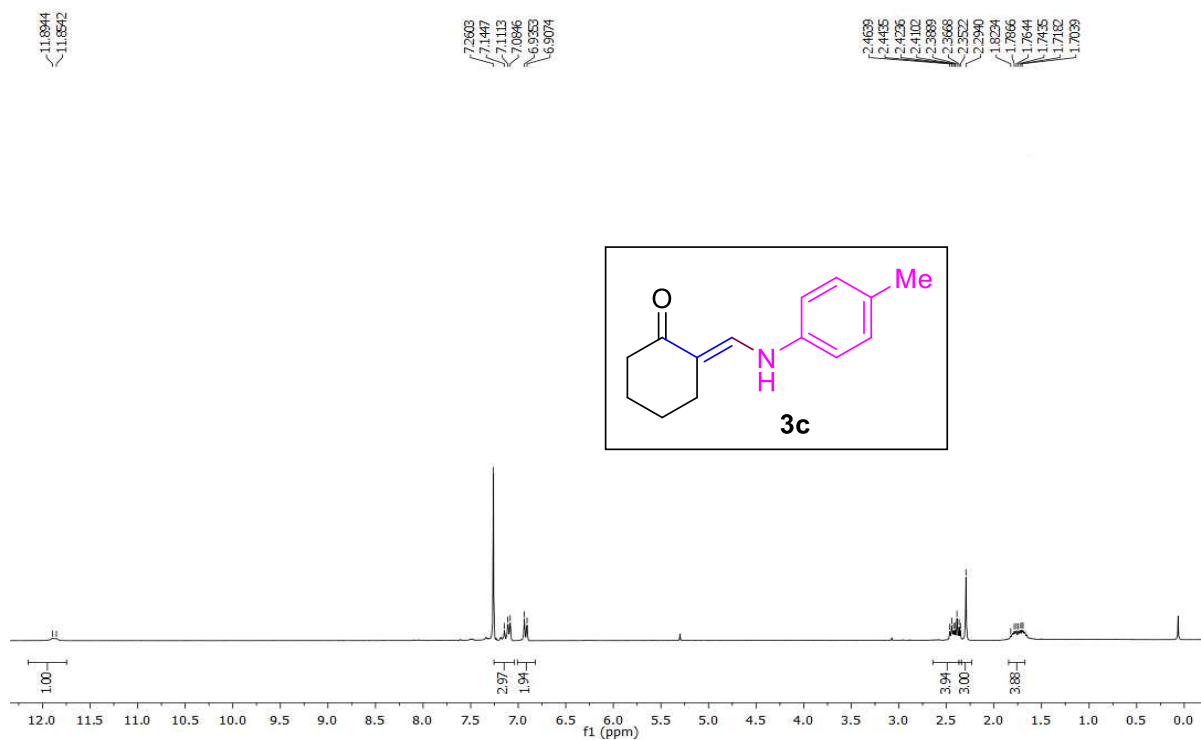
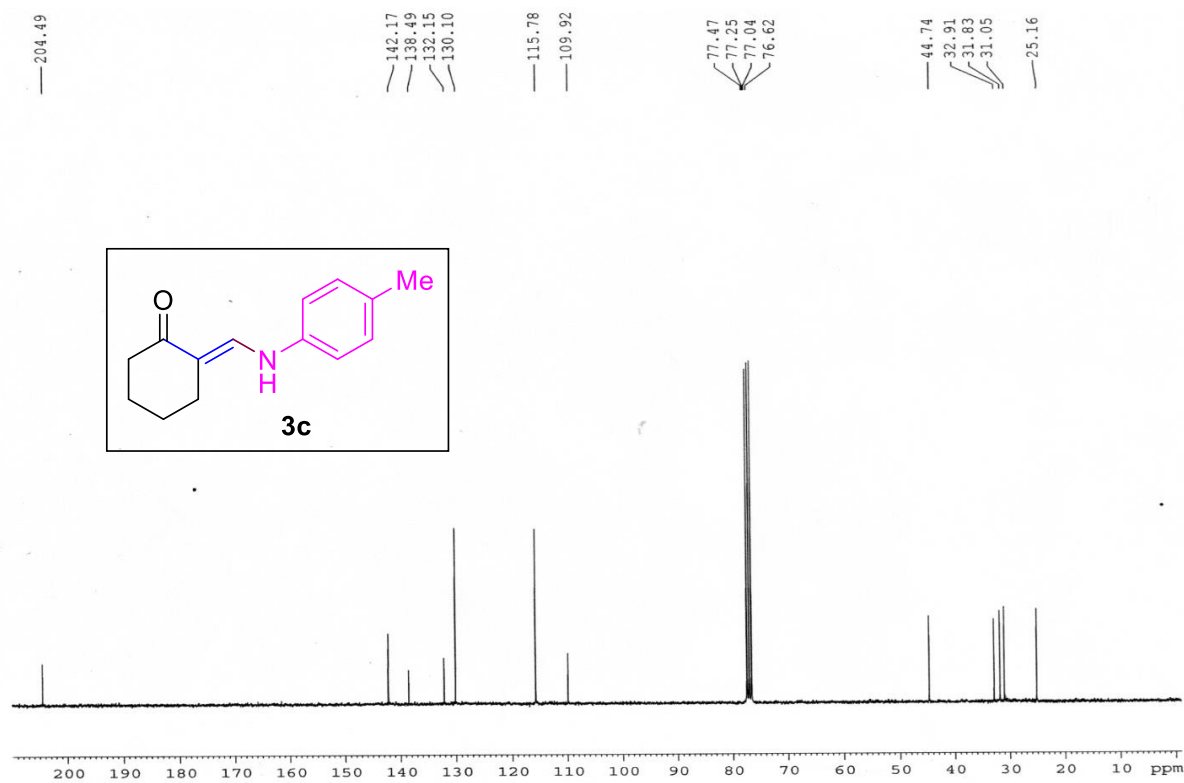
^1H NMR of 2h (500 MHz, CDCl_3): **^{13}C NMR of 2h (126 MHz, CDCl_3):**

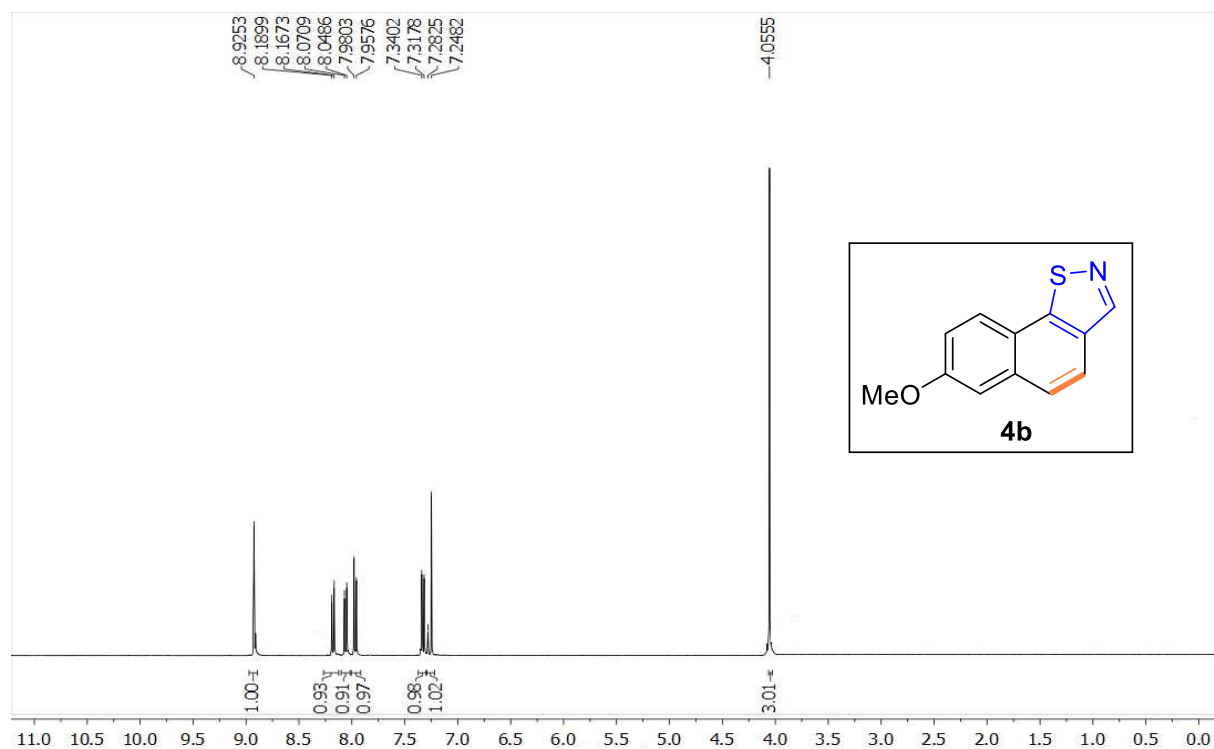
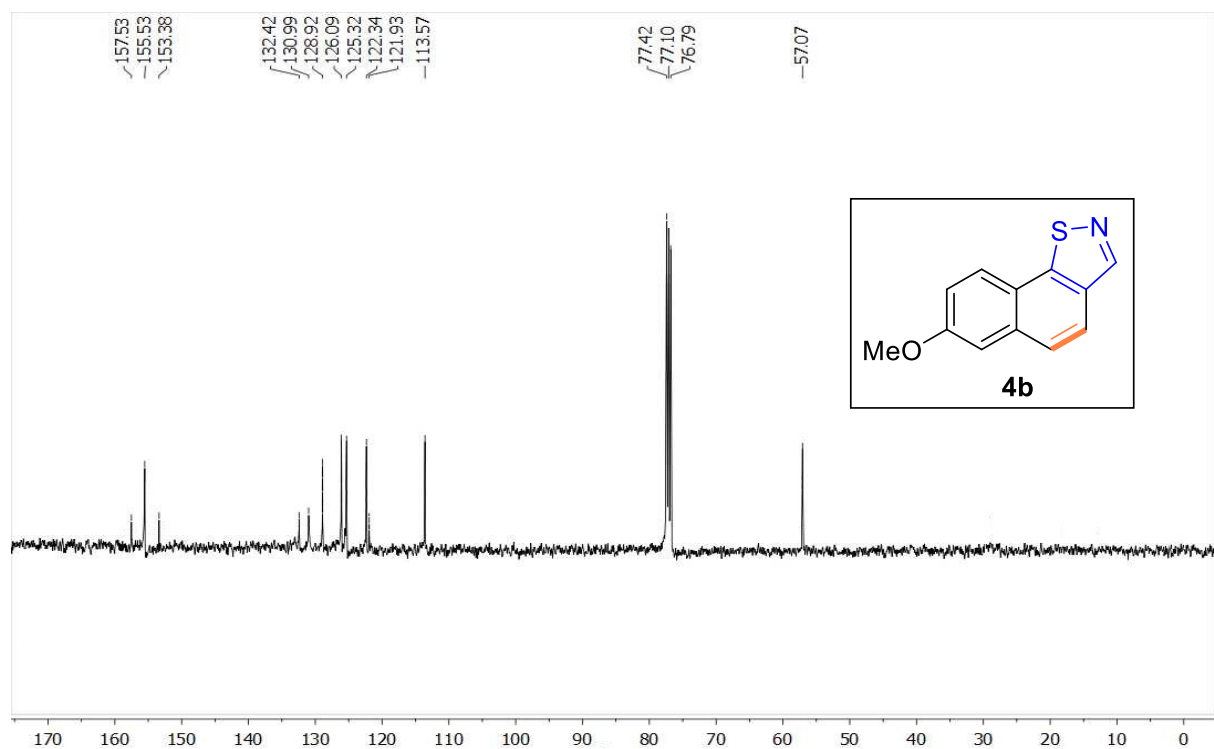
^1H NMR of 2k (400 MHz, CDCl_3): **^{13}C NMR of 2k (101 MHz, CDCl_3):**

^1H NMR of 2m (500 MHz, CDCl_3): **^{13}C NMR of 2m (126 MHz, CDCl_3):**

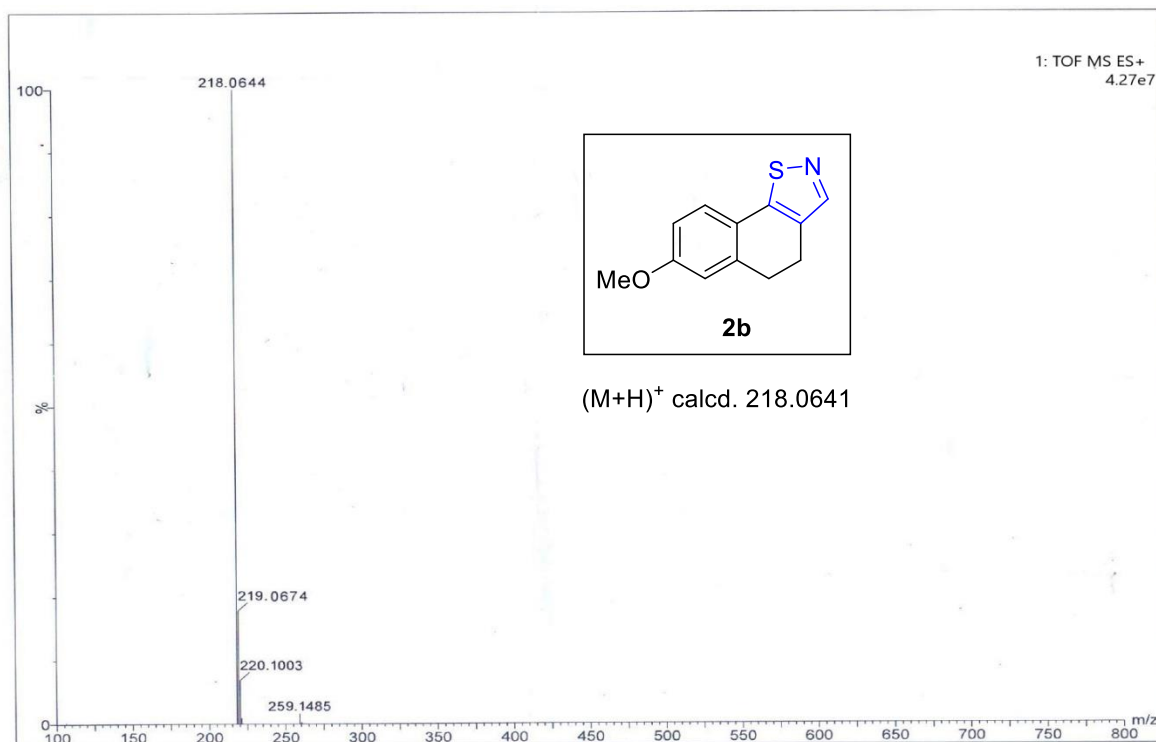
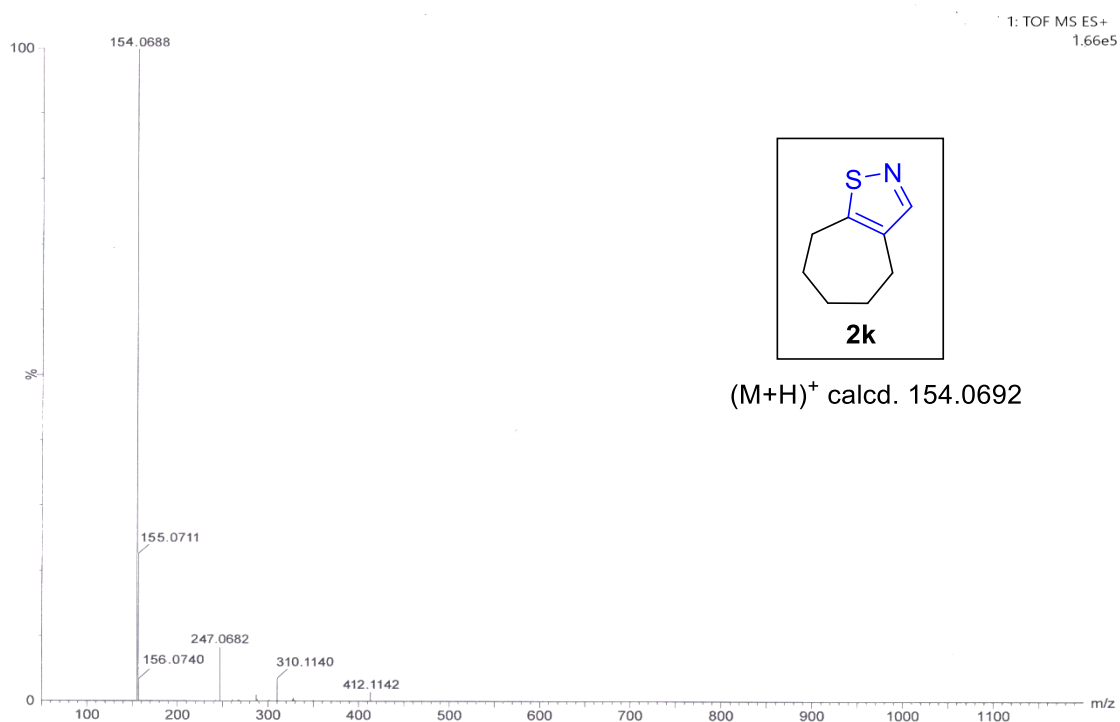
^1H NMR of 2o (300 MHz, CDCl_3): **^{13}C NMR of 2o (76 MHz, CDCl_3):**

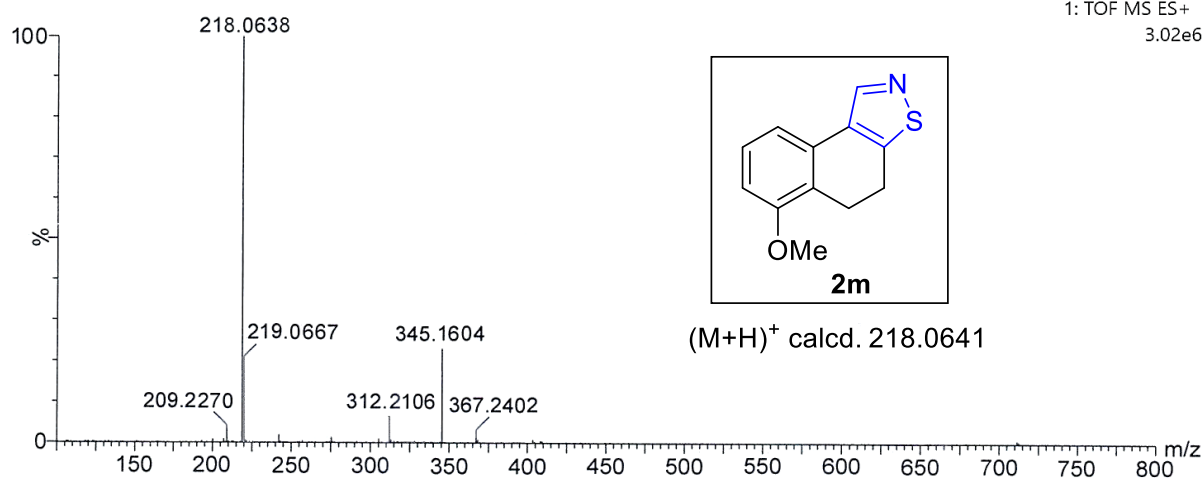
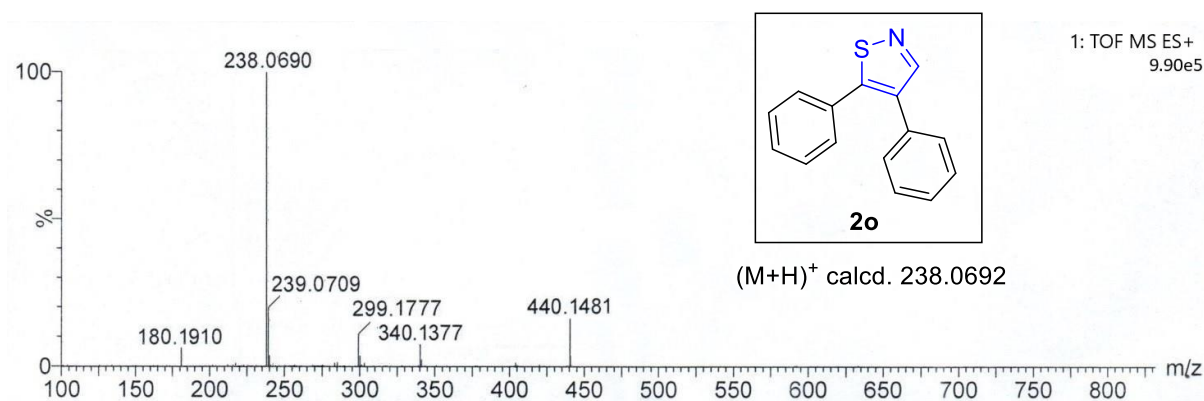
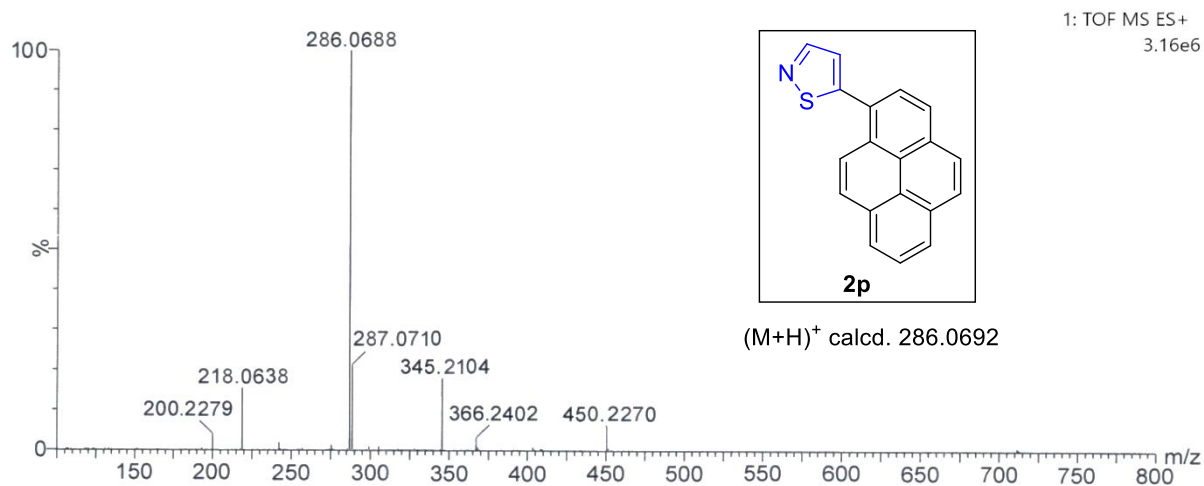
^1H NMR of 2p (400 MHz, CDCl_3): **^{13}C NMR of 2p (101 MHz, CDCl_3):**

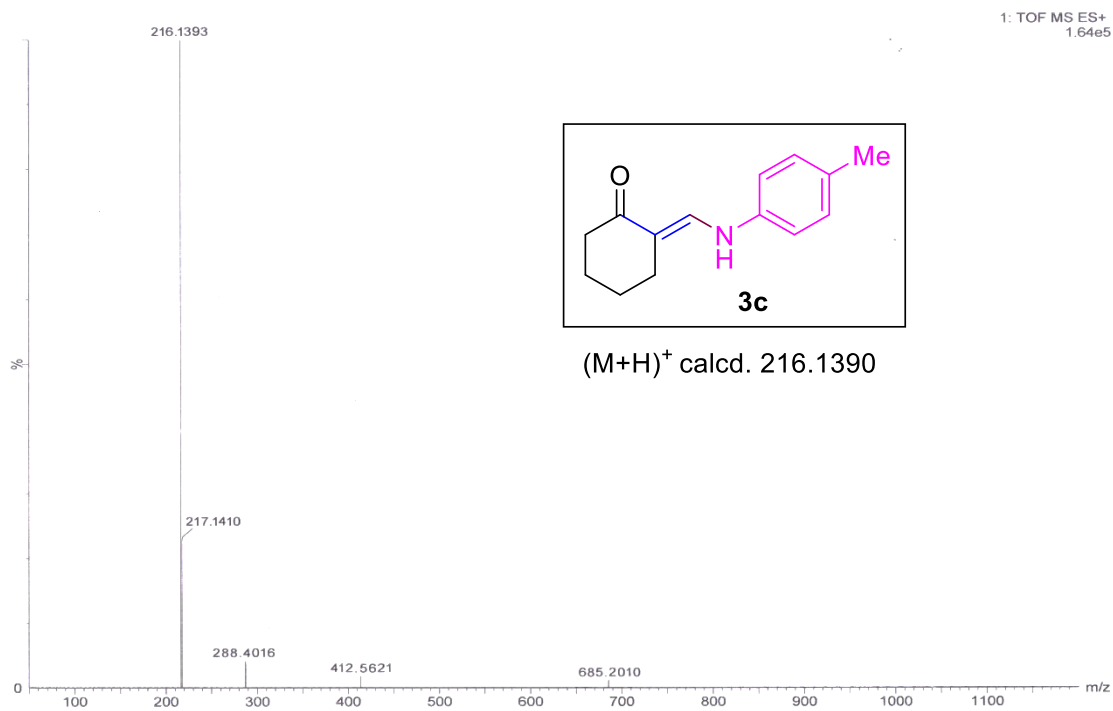
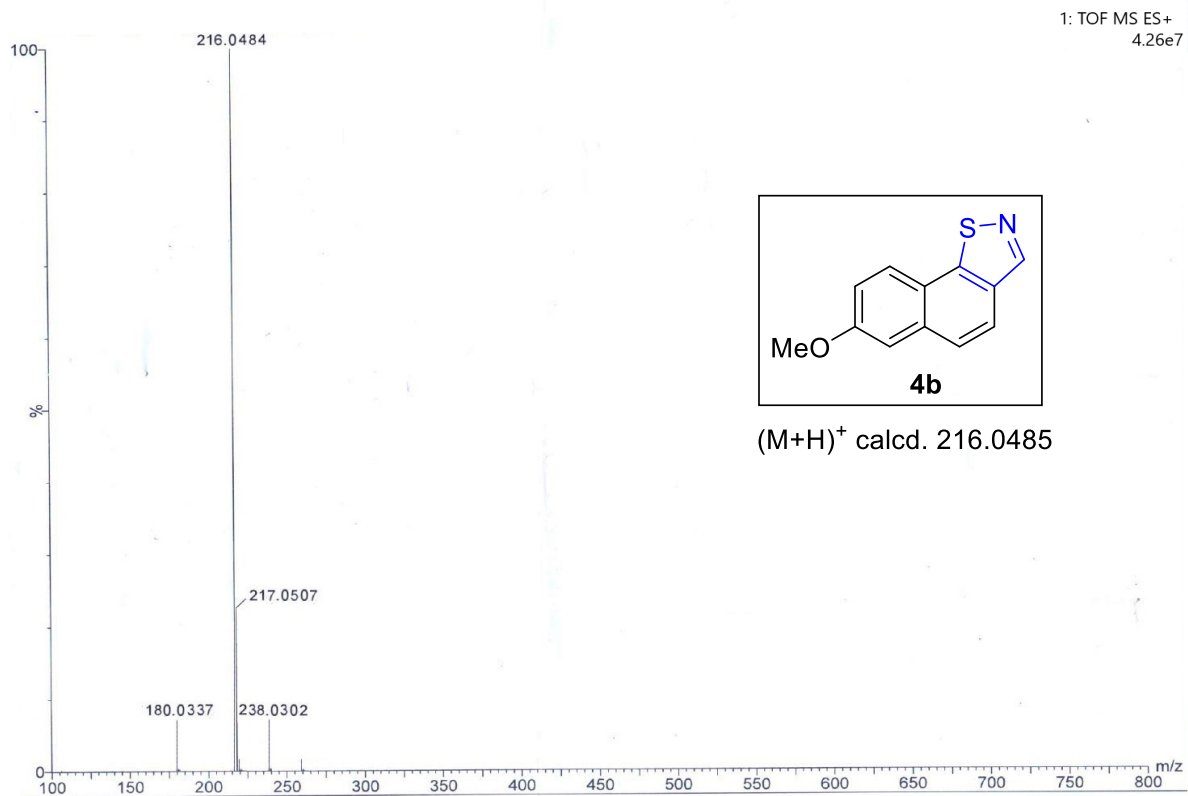
^1H NMR of 3c (300 MHz, CDCl_3): **^{13}C NMR of 3c (76 MHz, CDCl_3):**

^1H NMR of 4b (400 MHz, CDCl_3): **^{13}C NMR of 4b (101 MHz, CDCl_3):**

4.6.3. Representative HRMS spectra:

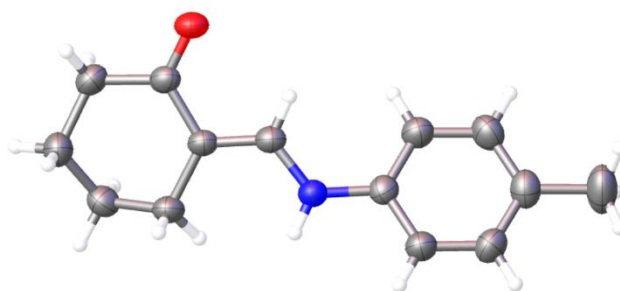
*7-Methoxy-4,5-dihydro*naphtho[2,1-*d*]isothiazole: (**2b**)*5,6,7,8-Tetrahydro-4H-cyclohepta*[*d*]isothiazole: (**2k**)

6-Methoxy-4,5-dihydrophtho[1,2-d]isothiazole: (2m)**4,5-Diphenylisothiazole: (2o)****5-(Pyren-1-yl)isothiazole: (2p)**

(E)-2-((p-tolylamino)methylene)cyclohexan-1-one: (3c)**7-Methoxynaphtho[2,1-d]isothiazole: (4b)**

4.6.4. Crystallographic information:

Identification code	d2nj01962k2
Empirical formula	C ₁₄ H ₁₇ NO
Formula weight	215.28
Temperature/K	273.15
Crystal system	monoclinic
Space group	P2 ₁ /c
a/Å	13.2601(17)
b/Å	6.3866(8)
c/Å	15.0670(18)
α/°	90
β/°	110.852(4)
γ/°	90
Volume/Å ³	1192.4(3)
Z	4
ρ _{calc} /cm ³	1.199
μ/mm ⁻¹	0.075
F(000)	464.0
Crystal size/mm ³	0.2 × 0.16 × 0.1
Radiation	MoKα (λ = 0.71073)
2θ range for data collection/°	5.546 to 56.608
Index ranges	-17 ≤ h ≤ 17, -8 ≤ k ≤ 8, -20 ≤ l ≤ 20
Reflections collected	24583
Independent reflections	2949 [R _{int} = 0.0408, R _{sigma} = 0.0213]
Data/restraints/parameters	2949/0/146
Goodness-of-fit on F ²	1.041
Final R indexes [I ≥ 2σ (I)]	R ₁ = 0.0495, wR ₂ = 0.1339
Final R indexes [all data]	R ₁ = 0.0573, wR ₂ = 0.1407
Largest diff. peak/hole / e Å ⁻³	0.29/-0.15



Molecular structure of **3c** determined by SCXRD analysis. Thermal ellipsoids are shown in 50% probability level. (CCDC Number: 2117809)

Atom color code: Grey = Carbon atom, Blue = Nitrogen atom, Red = Oxygen atom, and White = Hydrogen atom.

4.7. References:

1. (a) F. Hua and M. Szostaka, *Adv. Synth. Catal.*, 2015, **357**, 2583-2614; (b) A. D. O. Silva, J. McQuade and M. Szostak, *Adv. Synth. Catal.*, 2019, **361**, 3050-3067.
2. (a) M. S. C. Pedras and M. Suchy, *Org. Biomol. Chem.*, 2005, **3**, 2002-2007; (b) C. E. Blunt, C. Torcuk, Y. Liu, W. Lewis, D. Siegel, D. Ross and C. J. Moody, *Angew. Chem. Int. Ed.*, 2015, **54**, 8740-8745.
3. K. Stratmann, J. Belli, C. M. Jensen, R. E. Moore and G. M. L. Patterson, *J. Org. Chem.*, 1994, **59**, 6279-6281.
4. K. Nakae, H. Adachi, R. Sawa, N. Hosokawa, M. Hatano, M. Igarashi, Y. Nishimura, Y. Akamatsu and A. Nomoto, *J. Nat. Prod.*, 2013, **76**, 510-515.
5. A. Bera, P. Patra, A. Azad, Sk A. Ali, S. K. Manna, A. Saha and S. Samanta, *New J. Chem.*, 2022, **46**, 11685-11694.
6. M. Matsushita, N. Egashira, S. Harada, R. Okuno, K. Mishima, K. Iwasaki, R. Nishimura and M. Fujiwara, *J Pharmacol Sci*, 2005, **99**, 154-159.
7. Md. A. Alam¹, K. Shimada, Md. W. Khan and Md. D. Hossain, *Med & Analy Chem Int J*, 2019, **3**, 000137.
8. (a) M. Wang, X. Meng, C. Cai, L. Wang and H. Gong, *Green Synthesis and Catalysis*, 2022, **3**, 168-174; (b) L. M. T. Frija, A. J. L. Pombeiro and M. N. Kopylovich, *Coord. Chem. Rev.*, 2016, **308**, 32-55.
9. V. Silva, C. Silva, P. Soares, E. M. Garrido, F. Borges and J. Garrido, *Molecules*, 2020, **25**, 991.
10. Y-G. Wang, Y-H. Wang, T. Tao, H-F. Qian and W. Huang, *J. Mol. Struct.*, 2015, **1095**, 42-50.
11. A. R. Rovira, A. Fin and Y. Tor, *Chem. Sci.*, 2017, **8**, 2983-2993.
12. X. Ma, X. Yu, H. Huang, Y. Zhou and Q. Song, *Org. Lett.*, 2020, **22**, 5284-5288.
13. K. S. Etsè, B. Dassonneville, G. Zaragoza and A. Demonceau, *Tetrahedron Lett.*, 2017, **58**, 789-793.
14. B. Seo, Y. G. Kim and P. H. Lee, *Org. Lett.*, 2016, **18**, 5050-5053.
15. Z. Li, N. Wang, J. Liu, H. Mei, V. A. Soloshonok and J. Han, *Org. Lett.*, 2021, **23**, 6941-6945.
16. Z-Z. Zhang, R. Chen, X-H. Zhang and X-G. Zhang, *J. Org. Chem.*, 2021, **86**, 632-642.
17. J. Li, J. Li, X. Ji, Q. Liu, L. Chen, Y. Huang and Y. Li, *Adv. Synth. Catal.*, 2020, **363**, 1059-1068.

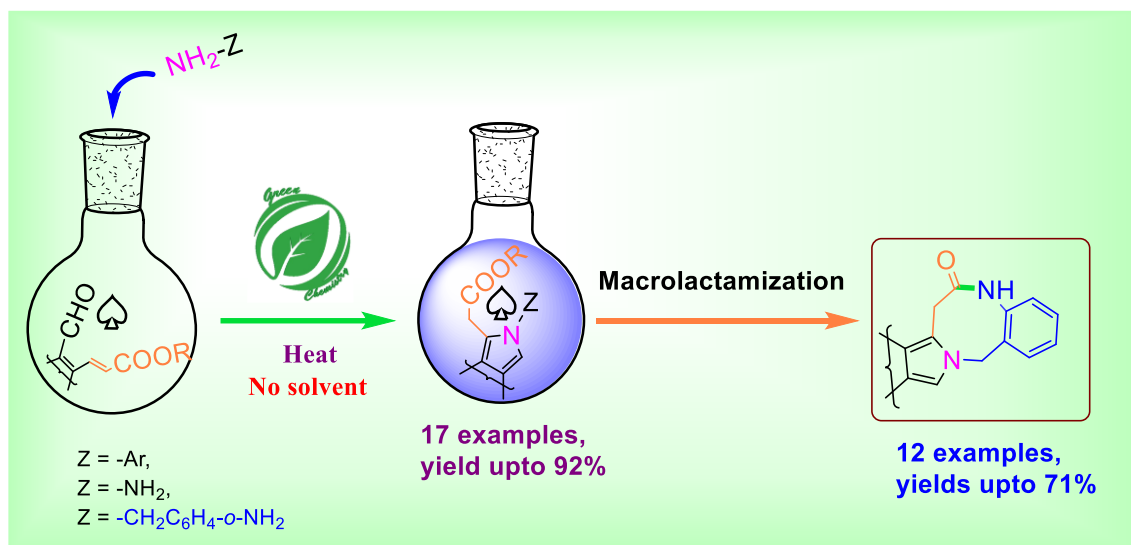
18. H. Yuan and Z. Sun, *Synlett*, 2019, **30**, 1904-1908.
19. H. Xie, G. Li, F. Zhang, F. Xiao and G. J. Denga, *Green Chem.*, 2018, **20**, 827-831.
20. G. Shukla, A. Srivastava and M. S. Singh, *Org. Lett.*, 2016, **18**, 2451-2454.
21. M. J. Cabrera, S. Cembellín, A. H. Salem, M. Berton, L. Marzo, A. Miloudi, M. C. Maestro and J. Alemán, *Green Chem.*, 2020, **22**, 6792-6797.
22. P. Bezbaruah, J. Gogoi, K. S. Rao, P. Gogoi, R. C. Boruah, *Tetrahedron Lett.*, 2012, **53**, 4389-4392.
23. (a) S. K. Manna, A. Mandal, S. K. Mondal, A. K. Adak, A. Jana, S. Das, S. Chattopadhyay, S. Roy, S. K. Ghorai, S. Samanta, M. Hossain and M. Baidya, *Org. Biomol. Chem.*, 2015, **13**, 8037-8047; (b) S. K. Manna, S. K. Mondal, A. Ahmed, A. Mandal, A. Jana, M. Iqbal, S. Samanta and J. K. Ray, *RSC Adv.*, 2014, **4**, 2474-2481; (c) S. K. Mondal, S. K. Manna, A. Mandal, S. Samanta and J. K. Ray, *Tetrahedron Lett.*, 2014, **55**, 6411-6415; (d) A. Jana, S. K. Manna, S. K. Mondal, A. Mandal, A. Jana, B. K. Senapati, M. Jana and S. Samanta, *Tetrahedron Lett.*, 2016, **57**, 3722-3726; (e) S. K. Mondal, A. Mandal, S. K. Manna, S. K. Ali, M. Hossain, V. Venugopal, A. Jana and S. Samanta, *Org. Biomol. Chem.*, 2017, **15**, 2411-2421; (f) S. K. Mondal, S. K. Ali, S. K. Manna, A. Mandal, B. K. Senapati, M. Hossain and S. Samanta, *ChemSelect.*, 2017, **2**, 9312-9318.
24. B. Govindh, B. S. Diwakar and Y. L. N. Murthy, *Org. Commun.*, 2012, **5**, 105-119.
25. (a) M. H. Elnagdi, M. S. Moustafa, S. M. Al-Mousawi, R. A. Mekheimer and K. U. Sadek, *Mol Divers.*, 2015, **19**, 625-651; (b) A. Livoreil, J. P. Sauvage, N. Armarolli, V. Balzani, L. Flamigni and B. Ventura, *J. Am. Chem. Soc.*, 1997, **119**, 12114-12124; (c) C. Caubere, P. Caubere, S. Ianelli, M. Nardelli and B. J. Gregoire, *Tetrahedron*, 1994, **50**, 11903-11920; (d) G. P. Bean and R. A. Jones, *Academic Press: London* 1977, 209-225.
26. F. Rammal, A. C. Gaumont and S. Lakhdar, *Eur. J. Org. Chem.*, 2020, 1482-1485.
27. (a) S. Tao, Z. Peng, X. Zhang, P. Wang, C. S. Lee and S.T. Lee, *Adv. Func. Mater.*, 2005, **15**, 1716-1721; (b) J. Jayabharathi, P. Jeeva, V. Thanikachalam and S. Panimozhi, *J. Photochem. Photobio. A Chem.*, 2017, **346**, 296-310; (c) M. T. Figueira-Duarte and K. Muillen, *Chem. Rev.* 2011, **111**, 7260-7310.
28. M. M. Islam, Z. Hu, Q. Wang, C. Redshaw and X. Feng, *Mater. Chem. Front.*, 2019, **3**, 762-781.

29. S. A. Ali, S. Bhaumik, A. Jana, S. K. Manna, M. Iqbal, A. Mandal, A. Bera, A. Jana, and S. Samanta, *ChemSelect.*, 2018, **3**, 11950-11956.
30. (a) V. Kachwal, P. Alam, H. R. Yadav, S. S. Pasha, A. Roy Choudhury and I. R. Laska *New J. Chem.*, 2018, **42**, 1133-1140; (b) A. Kathiravan, K. Sundaravel, M. Jaccob, G. Dhinakaran, A. Rameshkumar, D. A. Ananth and T. Sivasudha, *J. Phys. Chem. B*, 2014, **118**, 13573-13581; (c) D. Kumar and K. R. J. Thomas, *J. Photochem. Photobiol. A: Chem.*, 2011, **218**, 162-163; (d) J-Y. Hu, H. Hiyoshi, J-H. Do, T. Yamato, *J. Chem. Res.*, 2010, **34**, 278-282.

Chapter 5

Neat synthesis of c-fused pyrroles and its application to macrolactamization

Neat synthesis of *c*-fused pyrroles and its application to macrolactamization



(Contents of this chapter have been published in *Synth. Commun.*, 2021, **51**, 2377-2386)

5.1. Introduction:

The chemistry of nitrogen-fused heterocycles has been widely studied in diverse fields. Pyrrole, one of the most celebrated heterocycles, is extensively found in several bioactive natural alkaloids, drug molecules, and living organisms such as cytochrome, heme protein, etc.¹ Herein, we describe several bioactive natural alkaloids of pyrroles with their natural sources (**Figure 5.1**).

5.1.1. Pyrrole based natural alkaloids:

Fusarine was first discovered in 2012 and is derived from *Aegiceras corniculatum*, a marine mangrove fruit. It was found to have modest antiproliferative and cytotoxic effects on the human cell lines HeLa, HUVEC, and K-562.^{2a, b} Pseudocerolide A, a new bromotyrosine-derived alkaloid, was isolated from a marine sponge, *Pseudoceratina sp.*, found in the South China Sea.^{2a, c} Methyl marinamide, another marine alkaloid, was identified from *Ircinia variabilis*, a marine sponge. It displayed cytotoxic activity against both HepG2 and 95-D cell lines, and besides this, it showed insecticidal activity towards *Aphis gossypii*.^{2a, d-e} Oroidin, a novel bromopyrrole alkaloid obtained from *Stylissa sp.*, possesses bioactivities in a broad spectrum, like antimicrobial, antihistaminic, and antitubercular.^{2f-g}

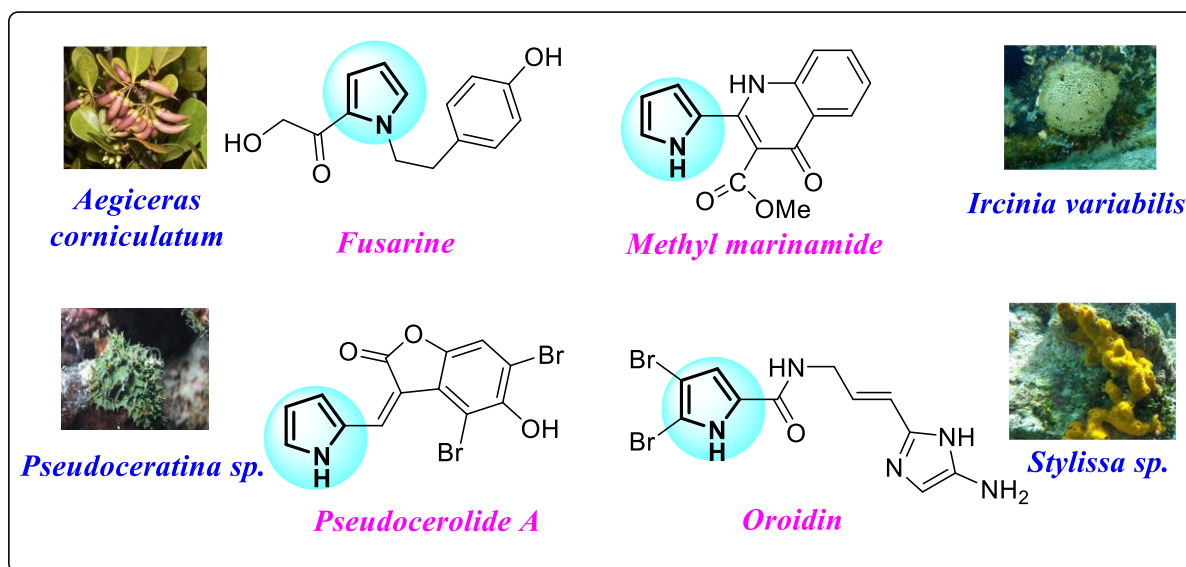


Figure 5.1. Several pyrroles containing natural alkaloids.

5.1.2. Marine alkaloids containing *c*-fused pyrrole:

Pyrroles fused in the *c*-position attract deep attention for their versatile applications. Numerous alkaloids, derived from sources like marine organisms, fungi, insects, and microbes, contain natural compounds with *c*-fused pyrrole rings with variable biological activities.³ **Figure 5.2** shows some examples of *c*-fused pyrrole containing marine alkaloids with their natural sources. Albumycin and Nitricquinomycins A-C exhibited weak antibacterial activity^{2a, 4a} and potent cytotoxic activity towards the human ovarian cancer cell line^{2a, 4b} respectively. Another pyrrole-fused alkaloid, Biscogniauxone, and spirocyclic Spiroindimicins B–D were showed glycogen synthase kinase inhibitor^{2a, 4c} and antitumor activities against several cancer cell lines^{2a, 4d} respectively.

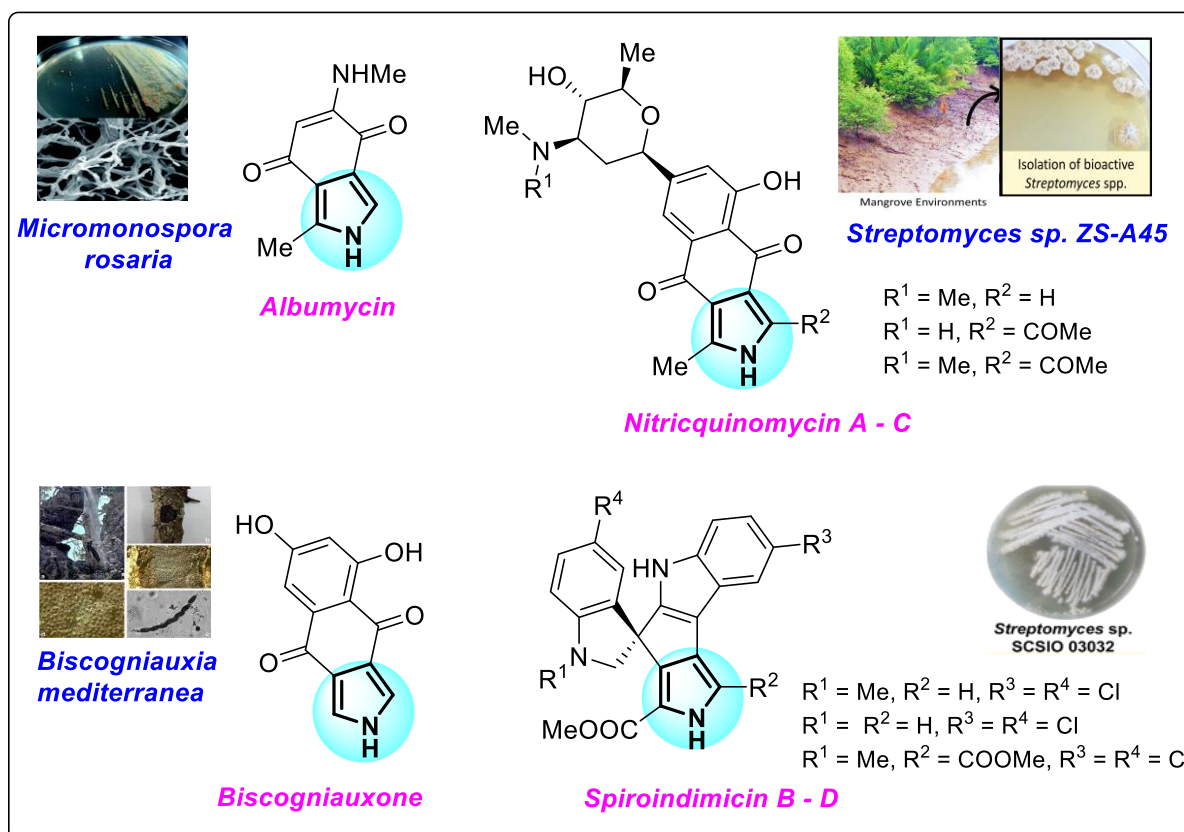


Figure 5.2. Some marine alkaloids based on *c*-fused pyrroles.

5.1.3. Drug molecules:

Many drug molecules are reported in the literature with *c*-fused pyrrole as the key unit in their structure. The medical community has access to a wide variety of drug molecules that incorporate *c*-fused saturated pyrroles. Such types of several drug molecules are listed here (**Figure 5.3**). Telaprevir is an antiviral drug used to treat the Hepatitis C virus infection. It

was also used to inhibit the SARS-CoV-2 3CL and NS3/4A.¹ An antipsychotic drug called lurasidone is used to treat bipolar disorder and schizophrenia. Additionally, it exhibited anti-inflammatory properties.^{5a} Lorpirazole exhibits anxiolytic activity.^{5b} Pomalidomide and Lenalidomide are two drug compounds with 3,4-pyrroledicarboximides that are used as anti-inflammatory medications.^{5a} Another therapeutic molecule that contains saturated pyrrole is asenapine. It is a sublingual pill used as an antipsychotic to treat people with schizophrenia and bipolar I disorder.¹

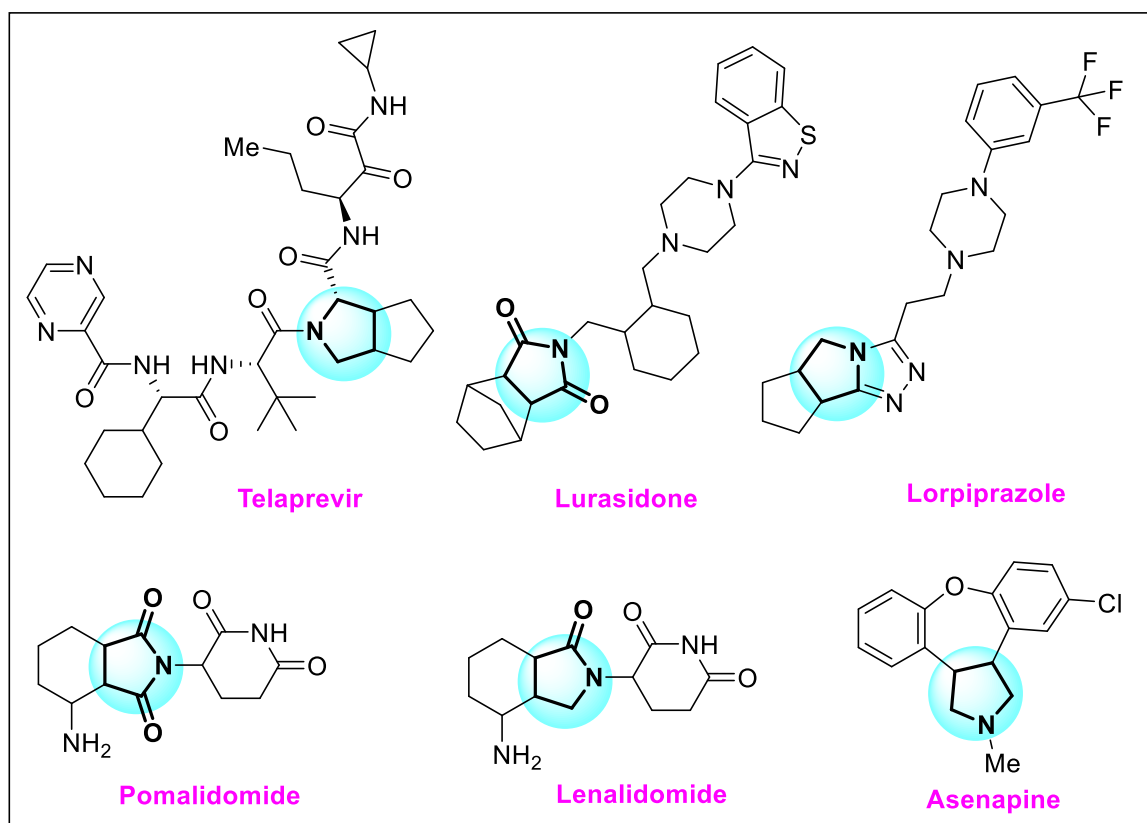


Figure 5.3. Several *c*-fused pyrroles-based drug molecules.

5.1.4. Utilities of small sized lactam rings:

In addition to *c*-fused pyrroles, multi-fused pyrroles are widely employed in a variety of natural product, pharmaceutical, and agrochemical sectors. We are primarily interested in *a,c*-fused pyrrole systems where the lactam ring is one of the valuable scaffolds, along with other categories of heterocycles (**Figure 5.4**). The most well-known broad-spectrum antibiotics are Penicillins which have been used for the treatment of serious infections, and it has been postulated that their bactericidal killing mechanism involves a 4-membered lactam ring.^{6a} SHR2415, a five-membered lactam, has proven to be a very effective ERK1/2 inhibitor.^{6b} Hanishin, a six-membered lactam, has effective cytotoxicity against NSCLCN6, a human

lungs carcinoma.^{6c} Seven-membered lactams, Latonduine A and B, are used as cytotoxic agents, and their regioisomers, paullones, act as cyclin-dependent kinase inhibitors.^{6d}

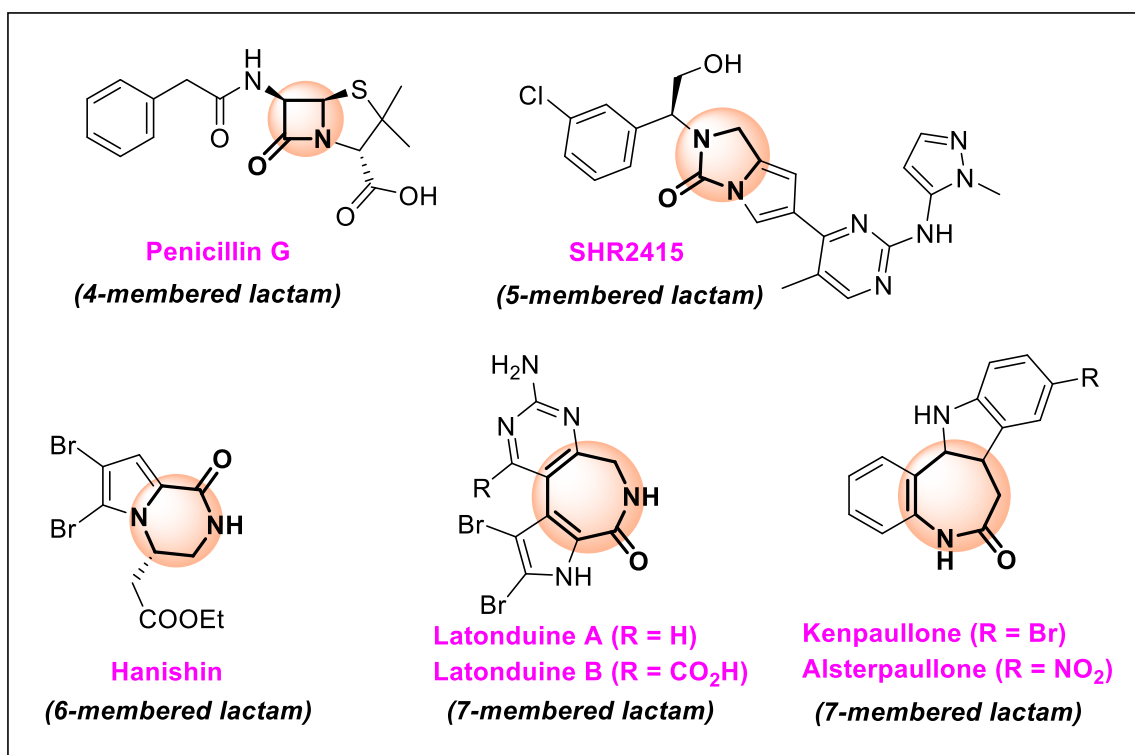


Figure 5.4. Several 4-7 membered lactam rings.

Higher-membered ring lactams are more popular in the medicinal field and appear more often in the natural products, compared to the 5-7-membered lactam. However, their synthetic methods are less studied in the literature. Hence, we are mainly focused on the synthetic and biological activities of medium-sized fused lactams (8-9 members).

5.1.5. Pyrrole fused medium sized lactam ring:

Pyrrole-fused azocines are constantly in demand because of their well-known therapeutic potential and the great abundance of bioactive natural products. Functionalized 8,5-fused bicyclic lactam is used as an antagonist of the X-linked inhibitor of apoptosis protein (XIAP), whose deregulation can result in "cancer and neurodegenerative disorders".^{7a-b} Benzo[*d*]azocinone exhibits antiproliferative activity.^{7c} Indolactam V, the 9-membered lactam ring, possesses tumour-protecting teleocidins^{7d} (**Figure 5.5**).

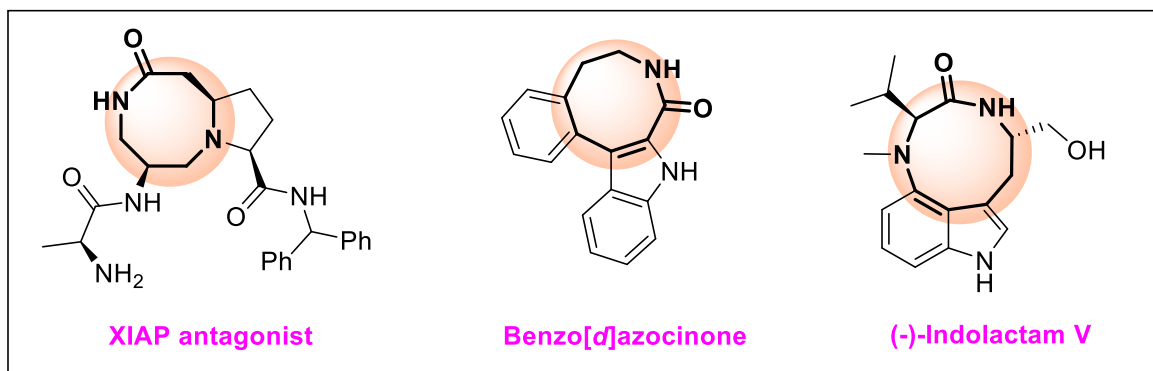


Figure 5.5. Various medium sized (8-9 members) pyrrole fused lactam ring.

5.1.6. Applications in material science:

Pyrrole-fused fluorophores might be useful as light-emitting fluorophores, sensors, and electroluminescence materials for OLEDs, etc. Pyrrolo[3,4-*c*]coumarin is a blue light emitter that can be evaluated for its capacity to transport electrons.^{8a} Indolizino[3,4,5-*ab*]isoindole derivatives **A** and **B** might make promising candidates for monolayer OLEDs that emit blue-light while also being able to transport holes and electrons (**Figure 5.6**).^{8b}

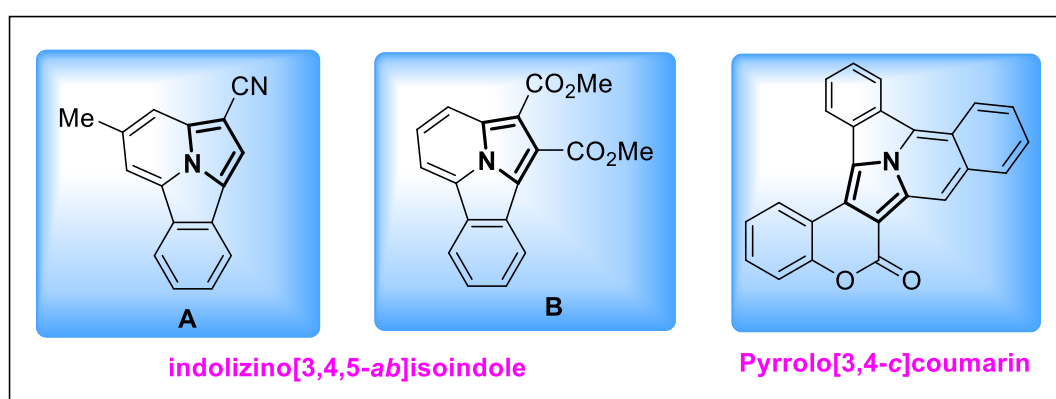


Figure 5.6. Pyrrole based OLEDs and light-emitting fluorophores.

Organic semiconductors are one of the most promising materials for biomedical uses due to their fabulous mechanical attributes in terms of flexibility, functionality, solution processability, and inexpensive processes. The organic polymer semiconductors are also used to detect biological analytes from a human body. Diketopyrrolopyrrol (DPP) is the main building block of DPP-DTT, *p*-type polymer-based semiconductors. A hole serves as a significant charge carrier in *p*-type semiconductors. The source electrode injects a hole that travels through the highest occupied molecular orbital (HOMO) energy level, permitting current to flow into the electronic aspect (**Figure 5.7**).⁹

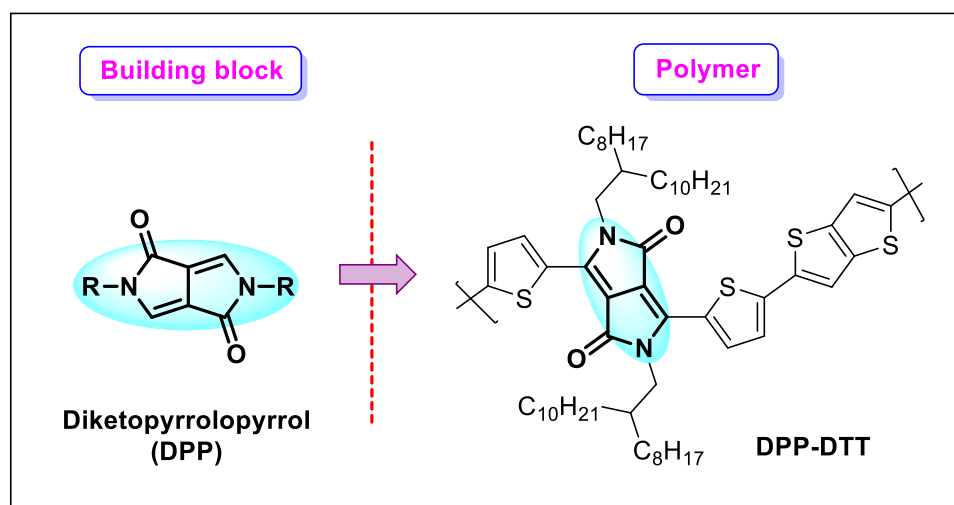


Figure 5.7. Pyrrole fused semiconductor.

5.1.7. Application in dye industry:

BOPYPYs are a brand-new class of 5,6,5,6-tetracyclic fused-pyrroles used as fluorescent dyes, with substantial Stokes shifts and strong fluorescence and molar extinction values. Another dye with extended conjugation was created by combining 4-dimethylaminobenzaldehyde with BOPYPYs, which also functions as a *pH*-detective fluorescence sensor (Figure 5.8).¹⁰

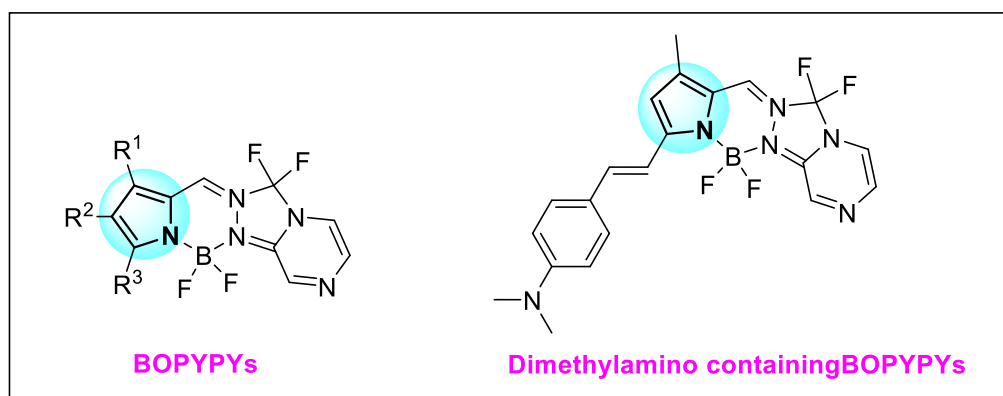


Figure 5.8. Pyrrole fused fluorescence dye.

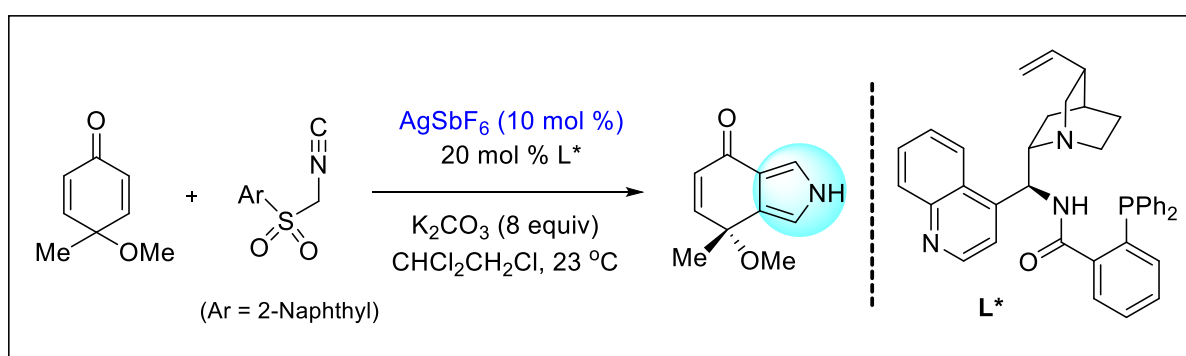
After brief study on the application of different fused pyrroles and their fused lactams, we are now engrossed on the different recent synthetic methodologies of pyrrole/*c*-fused pyrrole/pyrrole fused lactam which have synthesized by green and conventional pathways.

5.2. Literature survey:

(A) Conventional pathways:

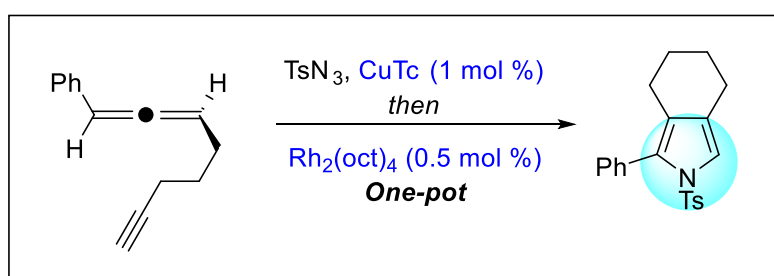
(i) Metal-catalyzed approaches:

K. Oh *et al.*¹¹ described a silver-catalyzed synthetic protocol for pyrrole through Van Leusen pyrrole synthesis by asymmetric desymmetrization of cyclohexadienone. In an environment of Ag (I) catalyst and the chiral phosphino-carboamide ligand, the enantioselective Van Leusen pyrrole synthesis was carried out using NasMIC as an isocyanomethyl sulfone mimic (**Scheme 5.1**).



Scheme 5.1. Silver catalyzed synthetic route of *c*-fused pyrrole.

R. Sarpong *et al.*¹² reported a Rh-catalyzed protocol for the formation of 3,4-fused pyrroles using allenylalkyne substrates. In this one-pot transformation, both CuTc and Rh₂(oct)₄ have been applied (**Scheme 5.2**).

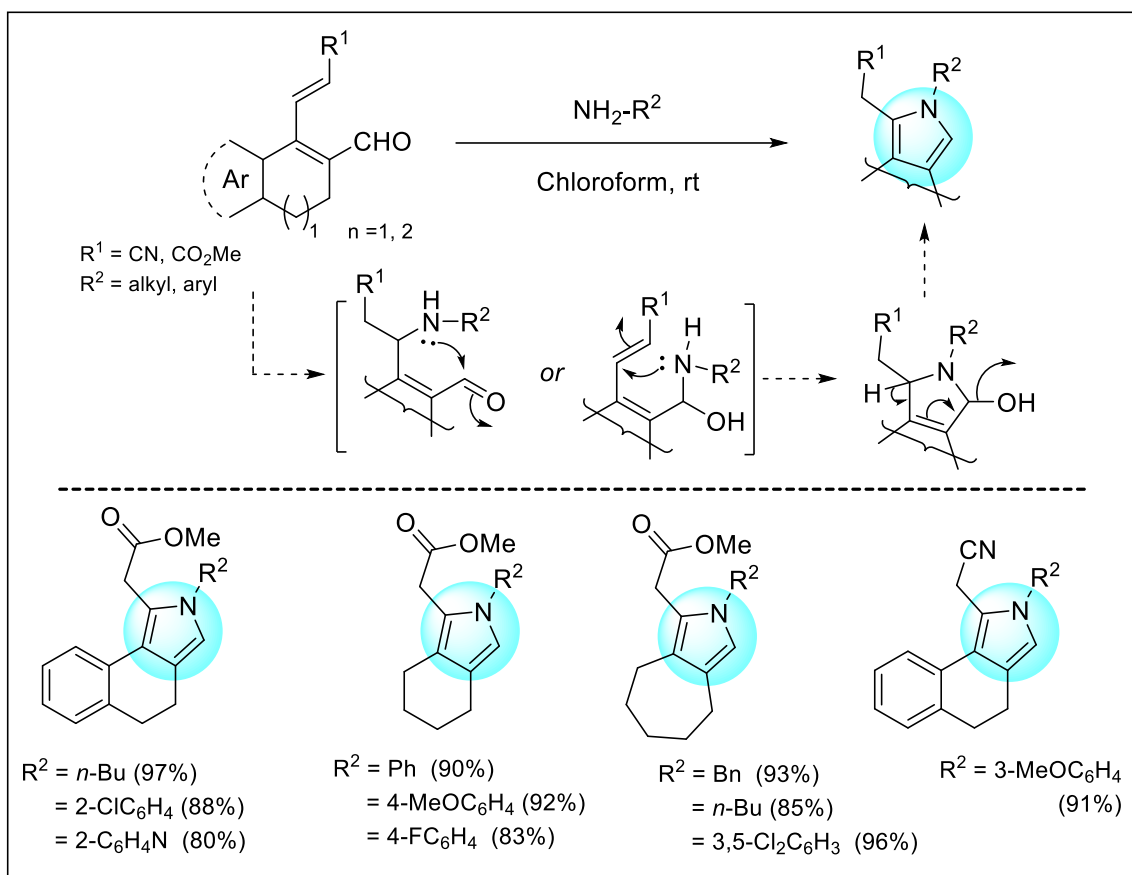


Scheme 5.2. Rh-catalyzed protocol for the 3,4-fused pyrroles.

(ii) Metal-free approaches:

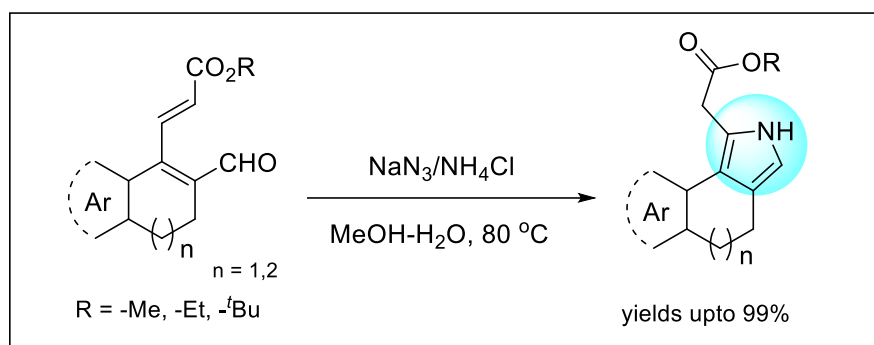
N. Yasmin and J. K. Ray¹³ developed an efficient synthetic protocol for the formation of *c*-fused pyrroles starting from 3-(2-formyl-cycloalkenyl) acrylic esters or 3-(2-formyl-cycloalkenyl) acrylonitriles with various amine partners in chloroform under ambient temperature. Herein, the formation of pyrrole derivatives is described by two possibilities.

One of them, amine, first attacks in an aza-Michael fashion, then intramolecular cyclization takes place, and the elimination of a water molecule helps to facilitate the formation of pyrrole derivatives. Another possibility is that amine first reacts with an aldehyde group, followed by intramolecular cyclization. They proved that latter pathway is more comfortable than the former one (**Scheme 5.3**).



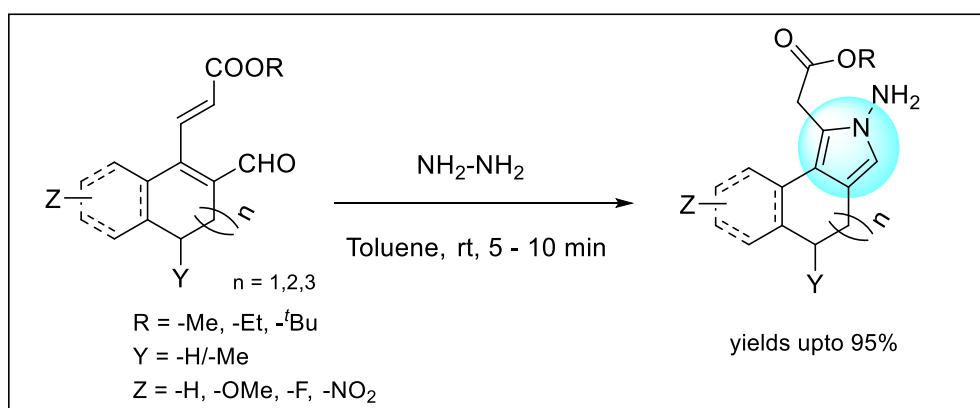
Scheme 5.3. Metal-free synthetic approach of *c*-fused pyrrole.

A. Jana *et al.*¹⁴ described a productive method for synthesising pyrroles by NaN₃/NH₄Cl, promoting intramolecular aza-annulation of the formyl group with the right alkenes at the adjacent position, and describing it in terms of high yield and regioselectivity. In order to synthesise bicyclic or tricyclic pyrroles with excellent yields, a wide range of applications, and high functional group tolerance, the metal-free *exo-trig* aza-cyclization approach has been expanded. As a consequence, this entire process offers mild reaction conditions, air stability, and metal-free synthesis, offering a healthier option for the environment (**Scheme 5.4**).



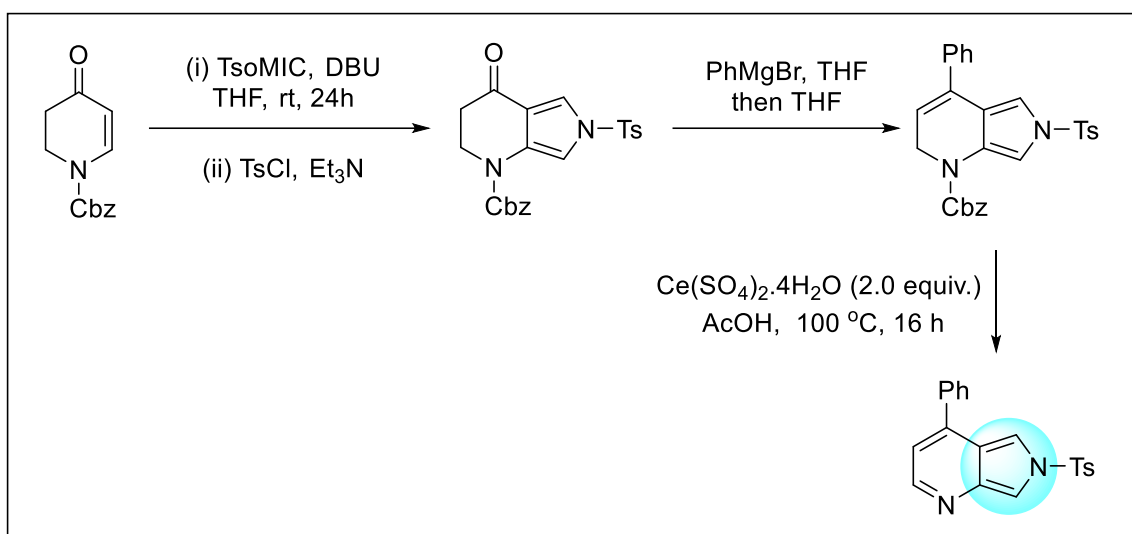
Scheme 5.4. Metal-free $\text{NaN}_3/\text{NH}_4\text{Cl}$ promoting synthetic protocol of *c*-fused pyrrole.

S. Mondal and his co-workers¹⁵ established a convenient, metal- and catalyst-free protocol for the formation of *c*-fused pyrrole *via* a two-component coupling reaction. They have reported the coupling reaction between 3-(2-formylcycloalkenyl)-acrylic ester and hydrazine in toluene solvent under room temperature with good to excellent yields up to 95% (**Scheme 5.5**).



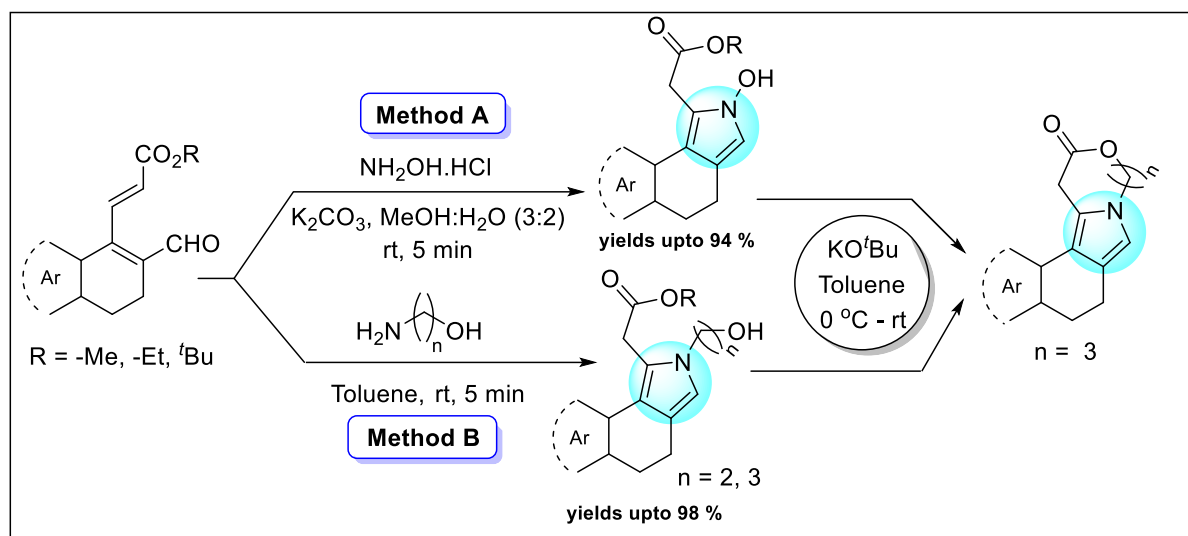
Scheme 5.5. Metal-, catalyst-free two component coupling protocol of *c*-fused pyrrole.

S. Kiren and his group¹⁶ developed a novel, efficient synthetic route for pyrrolo[3,4-*b*]pyridines starting from dihydropyridones. The pyrrole unit was obtained from dihydropyridone *via* three steps by using the toluenesulfonylmethyl isocyanide (TosMIC) reagent. Tosyl chloride is used to protect the pyrrole moieties from oxidation and polymerization. After tosylation, Grignard reagent was applied, and oxidative aromatization was followed to produce substituted pyrrolo[3,4-*b*]pyridines (**Scheme 5.6**).



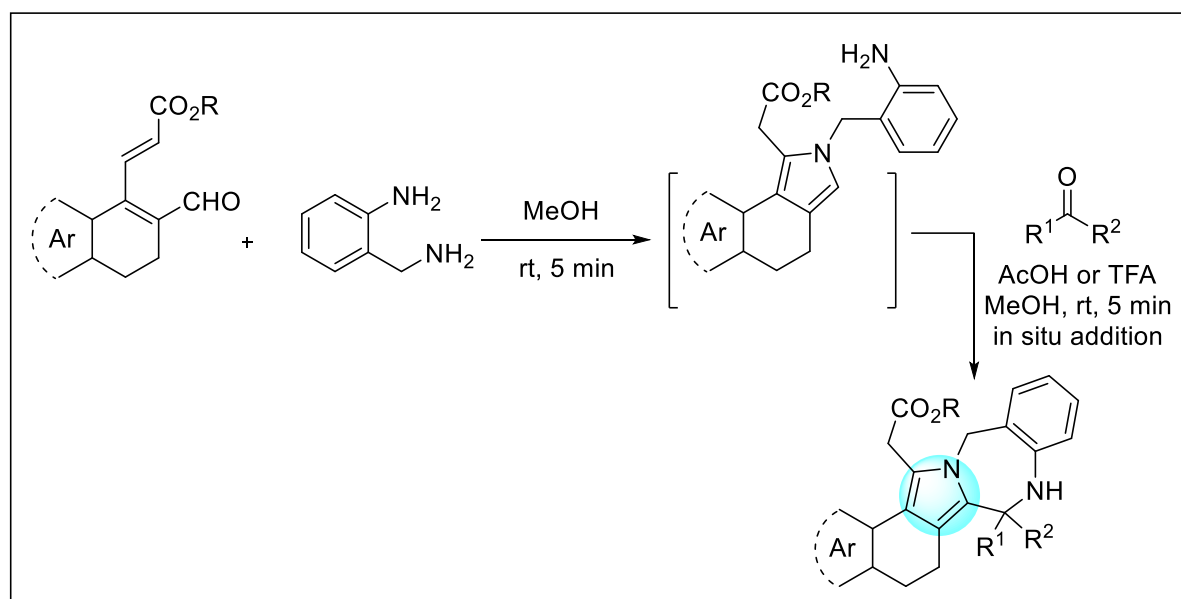
Scheme 5.6. Synthetic route for pyrrolo[3,4-*b*]pyridines.

S. K. Mondal and his group¹⁷ constructed various functionalized *c*-fused pyrroles and their application to intramolecular macrolactonization in their laboratory. For this synthesis purpose, they described a convenient two-component coupling reaction followed by base mediated intramolecular cyclization. In presence of K_2CO_3 , the easily available 3-(2-formylcycloalkenyl)-acrylic ester derivatives and hydroxylamine hydrochloride underwent *aza-exo-trig* cyclization in aqueous methanol solvent under ambient temperature and within 5 minutes the pyrrole derivatives were formed with up to 98 % yields. Interestingly, when they used 2-amino ethanol and 3-amino propanol instead of hydroxylamine hydrochloride, the reactions gave highest yield in toluene solvent. After that, the formation of substituted pyrrole derivatives it underwent intramolecular lactonization in presence of potassium tertiary butoxide ($tBuOK$) and toluene at 0 °C to room temperature with moderate yields (**Scheme 5.7**).



Scheme 5.7. Various approaches of *c*-fused pyrroles and its application to lactonization.

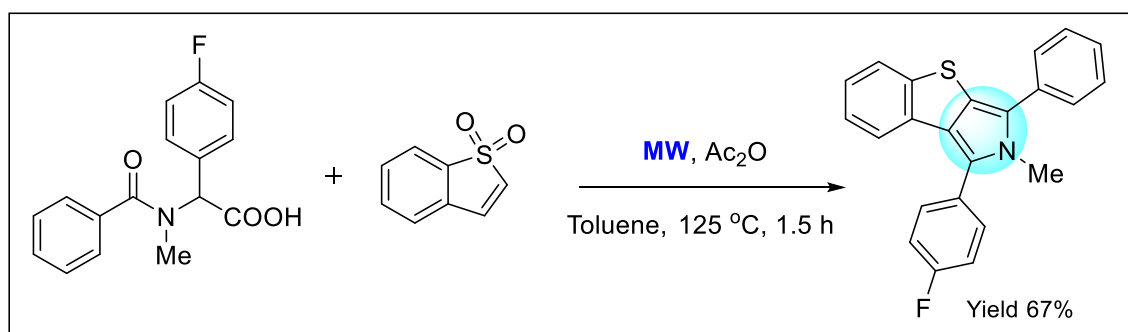
In 2019, our research group¹⁸ has documented another one-pot a modified Pictet–Spengler type tandem cyclization for pyrrolo[1,2-*a*][1,4]-benzodiazepines synthesis *via* formation of *c*-fused pyrrole intermediates under mild reaction condition. For this synthesis purpose, we have used 3-(2-formylcycloalkenyl)-acrylic ester derivatives and amino benzyl amine as a coupling partner in methanol, under room temperature within few minute pyrrole derivatives were obtained. The Pictet–Spengler precursor react with various aldehyde and acetic acid or trifluoroacetic acid, the cyclized pyrrolo[1,2-*a*][1,4]-benzodiazepines were formed (**Scheme 5.8**).



Scheme 5.8. One-pot Pictet–Spengler type tandem protocol of pyrrole-fused benzodiazepines.

(B) Green pathways:**(i) Microwave assisted synthetic approach:**

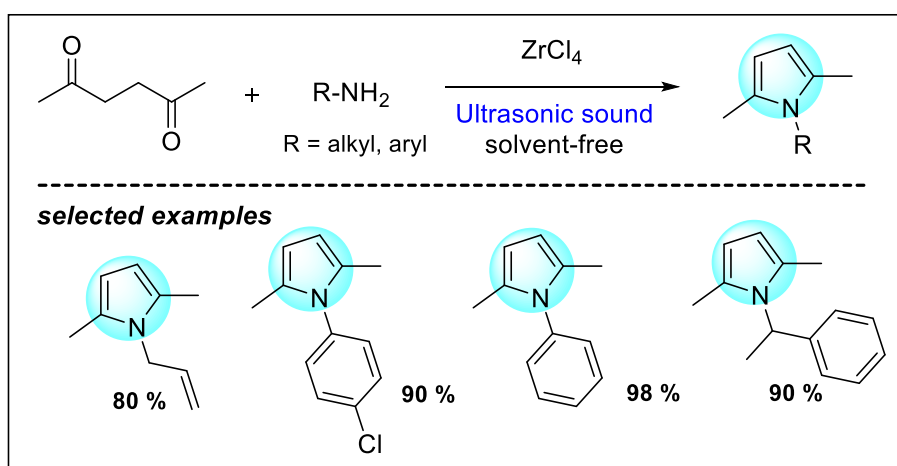
H. Karakus and Y. Dürüst¹⁹ communicated a metal-free cycloaddition reaction between two reacting partner C-(4-substituted-phenyl)-*N*-(benzoyl)-*N*-methylglycines and benzo[*b*]thiophene 1,1-dioxide in the presence of toluene under microwave irradiation to synthesis the *c*-fused pyrroles. Here, acetic anhydride is used as dehydrating agent. This protocol involves sulfone deoxygenation and gives the single regio isomeric product (**Scheme 5.9**).



Scheme 5.9. Microwave assisted synthetic route to *c*-fused pyrrole.

(ii) Ultrasound assisted synthetic approach:

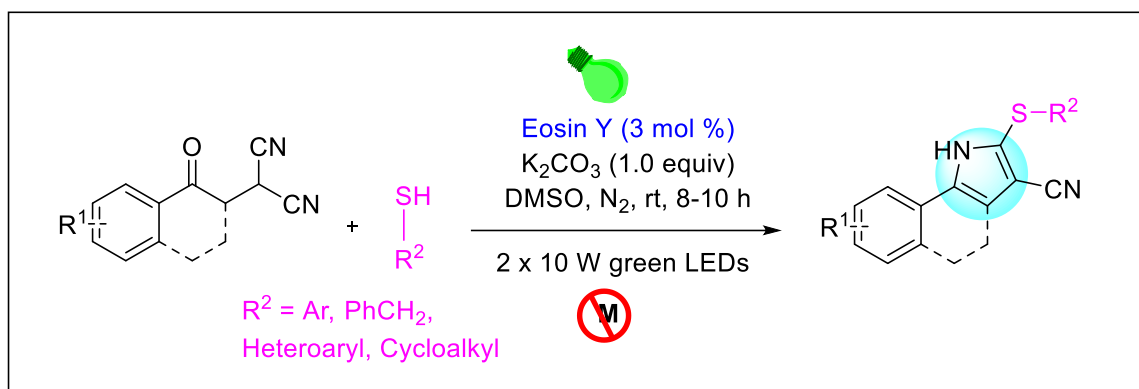
T. S. Li *et al.*²⁰ accomplished an ultrasound-assisted zirconium chloride catalyzed modified Paal-Knorr synthesis to produce the substituted pyrrole derivatives under neat conditions with good to excellent yields. Under ultrasound irradiation, organic reactions offer greater yields, reduce the reaction time, and have mild reaction conditions. Zirconium compounds are comparatively non-toxic, easy to access, inexpensive, and have high catalytic activity, so they can be used as catalysts (**Scheme 5.10**).



Scheme 5.10. Ultrasound assisted zirconium chloride catalyzed, solvent-free procedure of substituted pyrroles.

(iii) Photoinduced synthetic approach:

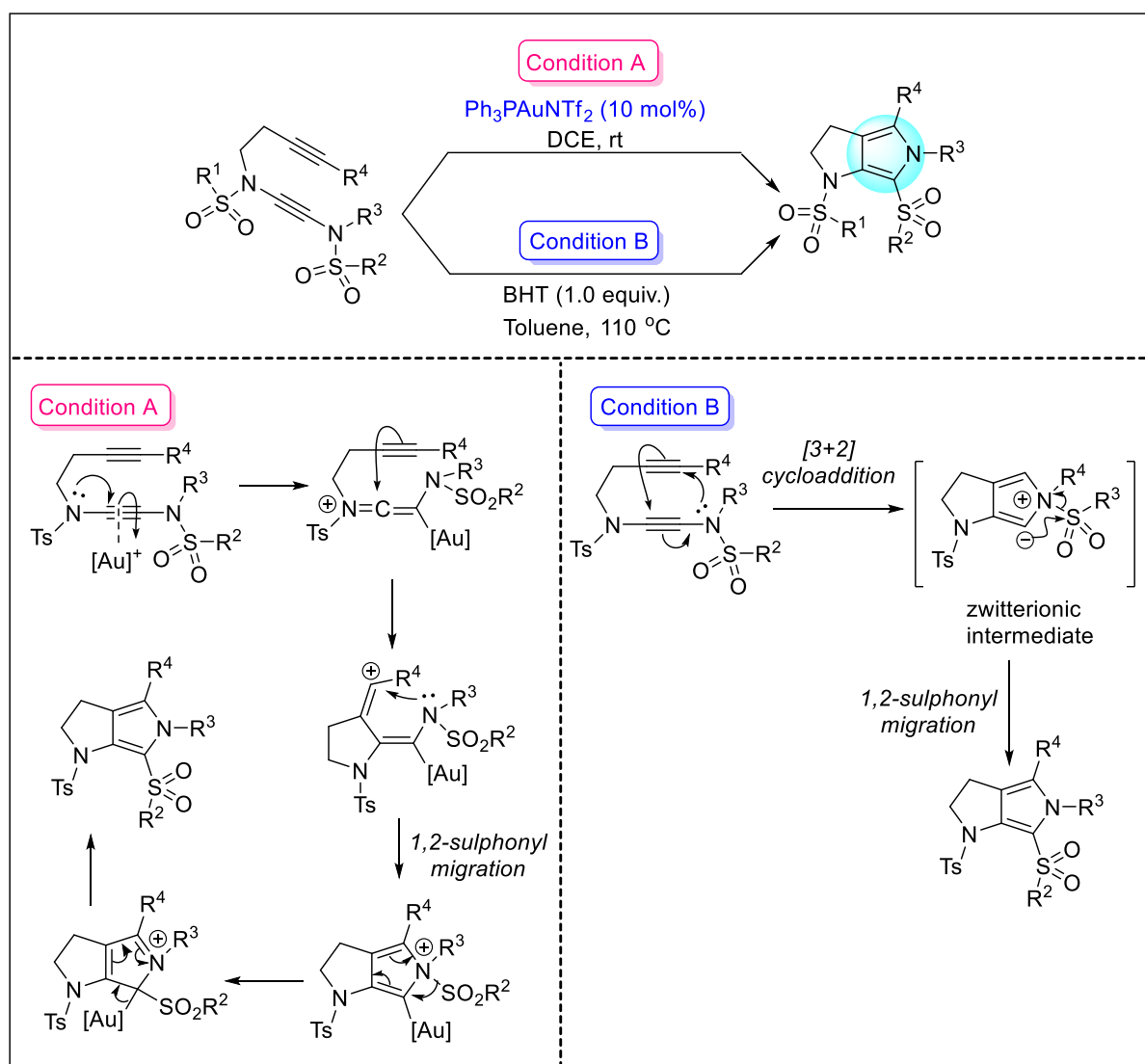
A. K. Sahoo *et al.*²¹ accomplished a green-light-mediated synthetic route of thio-functionalized pyrroles by employing β -ketodinitriles and thiophenols in the presence of a photocatalyst, eosin Y. The detailed mechanistic study describes that the photoinduced thiyl radical attacks the nitrile groups of β -ketodinitriles, then consequently a nucleophilic attack and followed by aromatization take place to give the desired pyrroles (**Scheme 5.11**).



Scheme 5.11. Green-light-mediated synthesis of pyrrole.

(C) Miscellaneous approach:

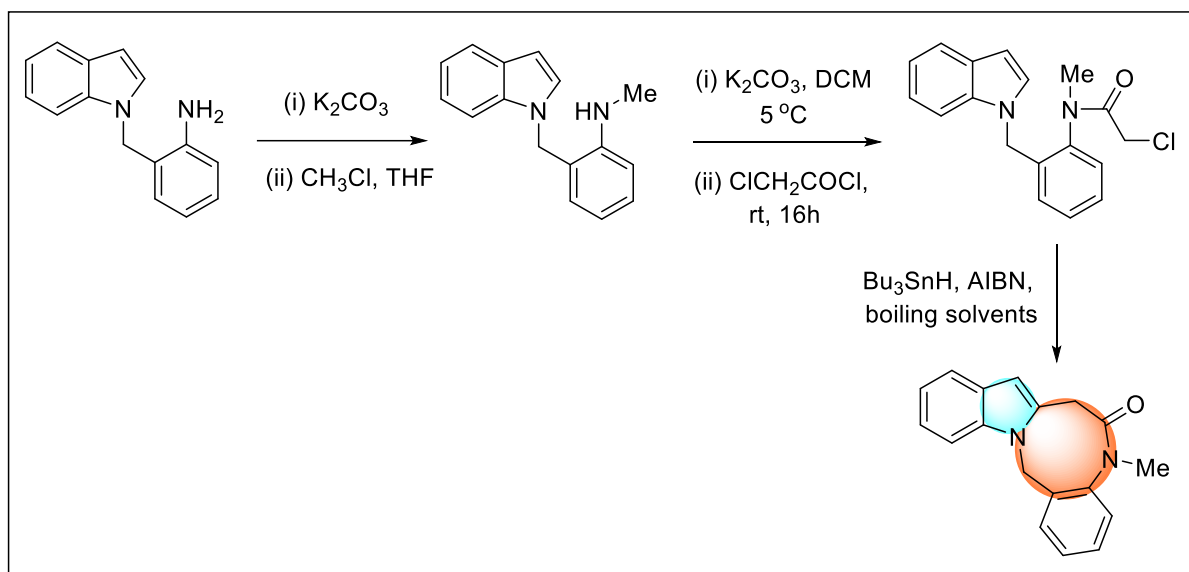
E. A. Anderson and his research group²² established a cycloisomerization to produce polysubstituted pyrrolopyrroles, assisted by gold-catalyzed synthesis from a valuable precursor, yndiamides. Herein, they documented their successful observations for this transformation *via* two optimized conditions at ambient temperature (Condition A) and a thermal cycloisomerization (Condition B). For a gold-catalyzed reaction at ambient temperature, the triple bond of yndiamides is activated towards attacking the alkyne to give the keteniminium ion. This keteniminium ion undergoes nucleophilic attack to produce a vinyl cation. This vinyl cation is trapped by the terminal nitrogen of yndiamides, and another ring is formed. Finally, 1,2-migration of the sulphonyl group followed by aromatization occurs to form the desired product. Under thermal conditions, yndiamides undergo a [3+2] cycloaddition reaction that produces the zwitterionic intermediate, followed by 1,2-migration of the sulphonyl group to give the desired product (**Scheme 5.12**).



Scheme 5.12. Gold-catalyzed and metal-free approaches of fused pyrrole.

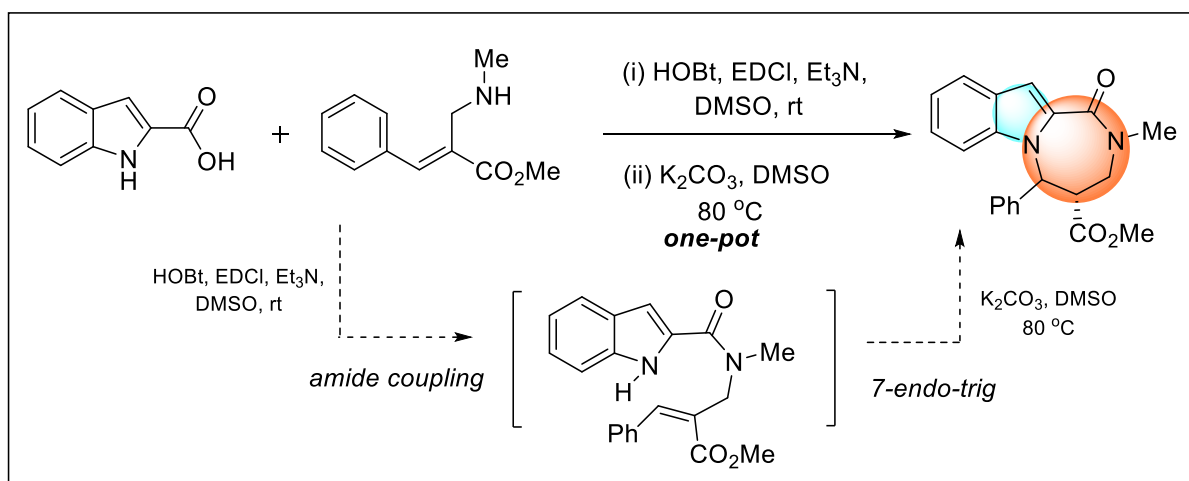
(D) Metal-free synthetic approaches of pyrrole fused lactam:

J. B. Bremner and W. Sengpracha²³ have established a novel, free radical cyclization protocol for the synthesis of indolo[2,1-*d*][1,5]benzodiazocine derivatives starting from 1-substituted indole. The effects of thermal radical 8-*exo-trig* cyclizations of precursor 1-indolyl haloacetamides, using tributyltin hydride, was investigated in an attempt to create a workable regioselective pathway to indolo-benzodiazocinone derivatives (**Scheme 5.13**).



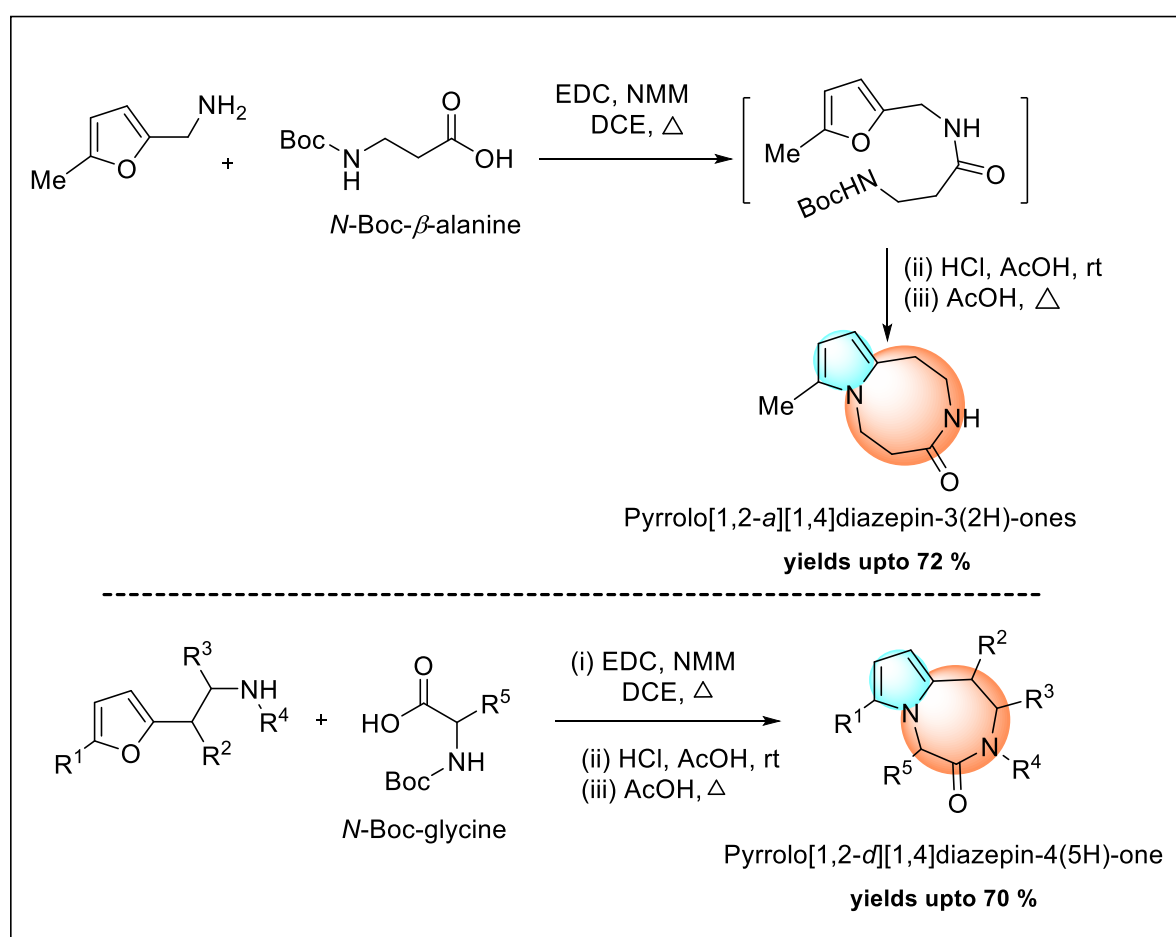
Scheme 5.13. Synthesis of pyrrole fused lactam *via* free radical cyclization.

J. Xiang and his co-workers²⁴ reported an easy one-pot protocol for the development of pyrrole-fused 1,4-diazepanones. This procedure entails the sequential amide coupling reaction/intramolecular aza-Michael addition of pyrrole-2-carboxylic acids with allylamines derived by Morita-Baylis-Hillman. This method is useful for creating highly substituted fused 1,4-diazepanone moieties due to the easily accessible starting ingredients, good stereoselectivity, and ability to be produced on a gram-scale (**Scheme 5.14**).



Scheme 5.14. Synthetic protocol for the development of pyrrole-fused 1,4-diazepanones.

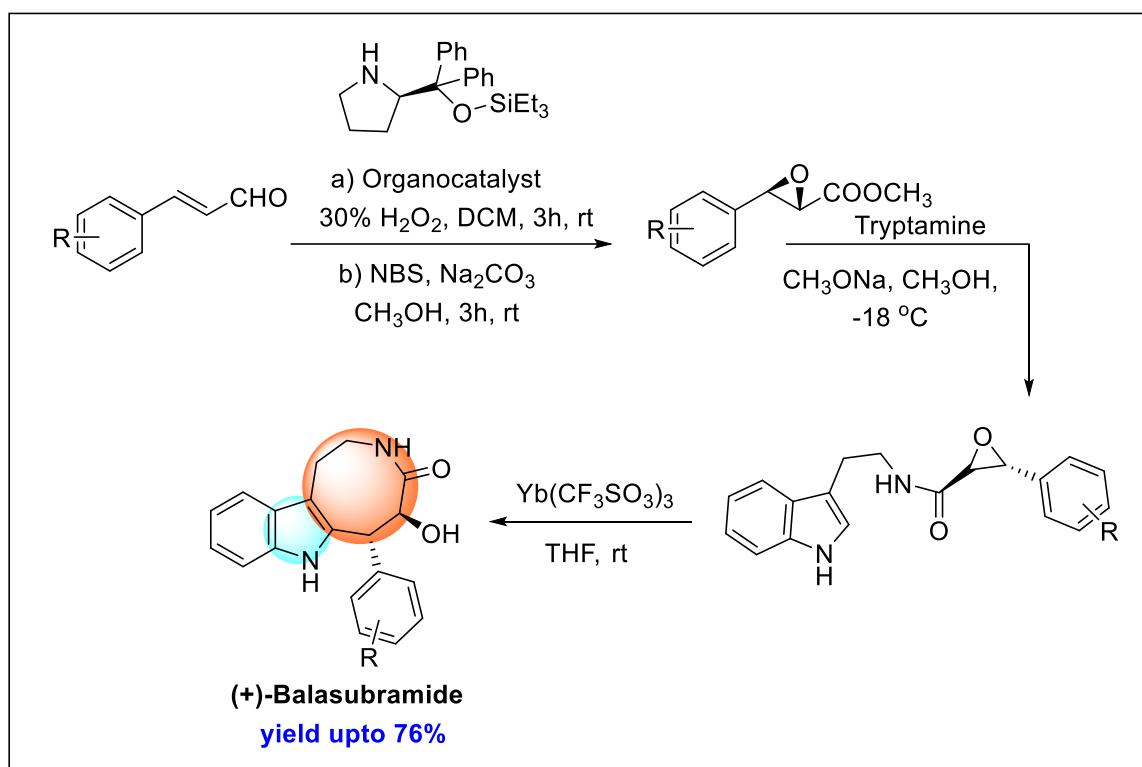
M. G. Uchuskin and his research group²⁵ depicted a one-pot procedure to construct the isomeric pyrrolo[1,2-*x*][1,4]diazepinones. The entire method involves a condensation reaction between easily accessible furan containing aminoalkyl derivatives and amino acids, then deprotection followed by ring opening of furan and Paal-Knorr cyclization takes place. Utilizing this strategy isomeric pyrrolo[1,4]diazepin-3(2*H*)-one derivatives were synthesized. In presence of *N*-methylmorpholine (NMM) the acylation of 5-methylfurfurylamine takes place with *N*-Boc- β -alanine and 1-ethyl-3-[3-(dimethylamino)propyl]carbodiimide (EDC) lead to the formation of corresponding pyrrolo[1,2-*a*][1,4]diazepin-3(2*H*)-ones with good to excellent yield. Similarly, the combination of *N*-Boc-glycine and 2-(5-methylfuran-2-yl)ethylamine governed the pyrrolo[1,2-*d*][1,4]diazepin-4(5*H*)-one with moderate yield (**Scheme 5.15**).



Scheme 5.15. Synthesis of pyrrole-fused 1,4-diazepanones from *N*-Boc- β -alanine and *N*-Boc-glycine.

(E) Total synthesis of (+)-Balasubramide:

(+)-Balasubramide, an eight-membered lactam ring, was isolated from the leaves of *Clausena indica*. J. Li *et al.*²⁶ revealed the total synthesis of (+)-Balasubramide, starting with cinnamaldehyde and utilising an organocatalyst, diphenyl prolinol TES ether. This protocol involved the amine-ester interchange with *N*-methyltryptamine, followed by intramolecular cyclization using ytterbium (III) triflate [$\text{Yb}(\text{CF}_3\text{SO}_3)_3$] as the catalyst (**Scheme 5.16**).



Scheme 5.16. Organocatalysed asymmetric synthesis of (+)-Balasubramide.

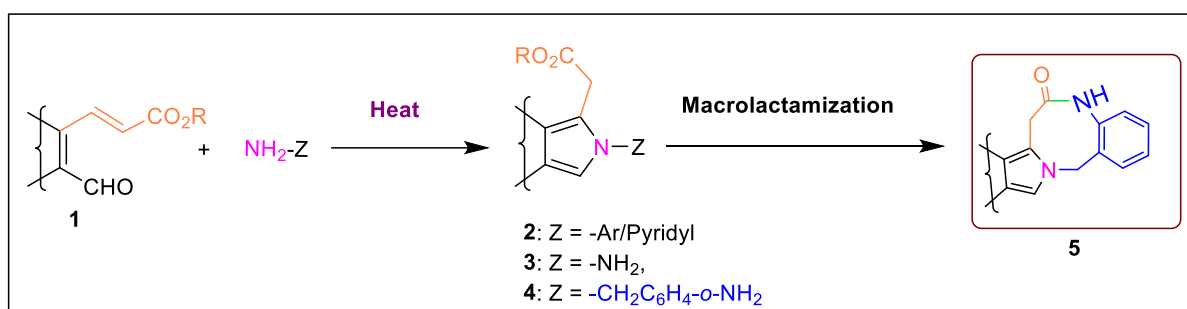
According to the literature study, several groups have created unique approaches for synthesising *c*-fused pyrroles and pyrrole-fused lactams employing various solvents, metals, and catalysts. As far as we know, no advancement has been made in solvent-free protocols. Therefore, we were inspired to develop a solvent-free protocol for synthesising *c*-fused pyrroles using conventional heating with readily available raw ingredients and also applied them in macrolactamization reactions, which are discussed below.

5.3. Present work:

- ❖ The current study describes an efficient environmental benign synthetic route of *N*-aryl substituted *c*-fused pyrrole derivatives *via* neat approach.
- ❖ We also documented the base-mediated intramolecular macrolactamization using amine ester amidation reaction, which led to fused diazocin-6(5*H*)-one with effective yields.

5.4. Results and discussion:

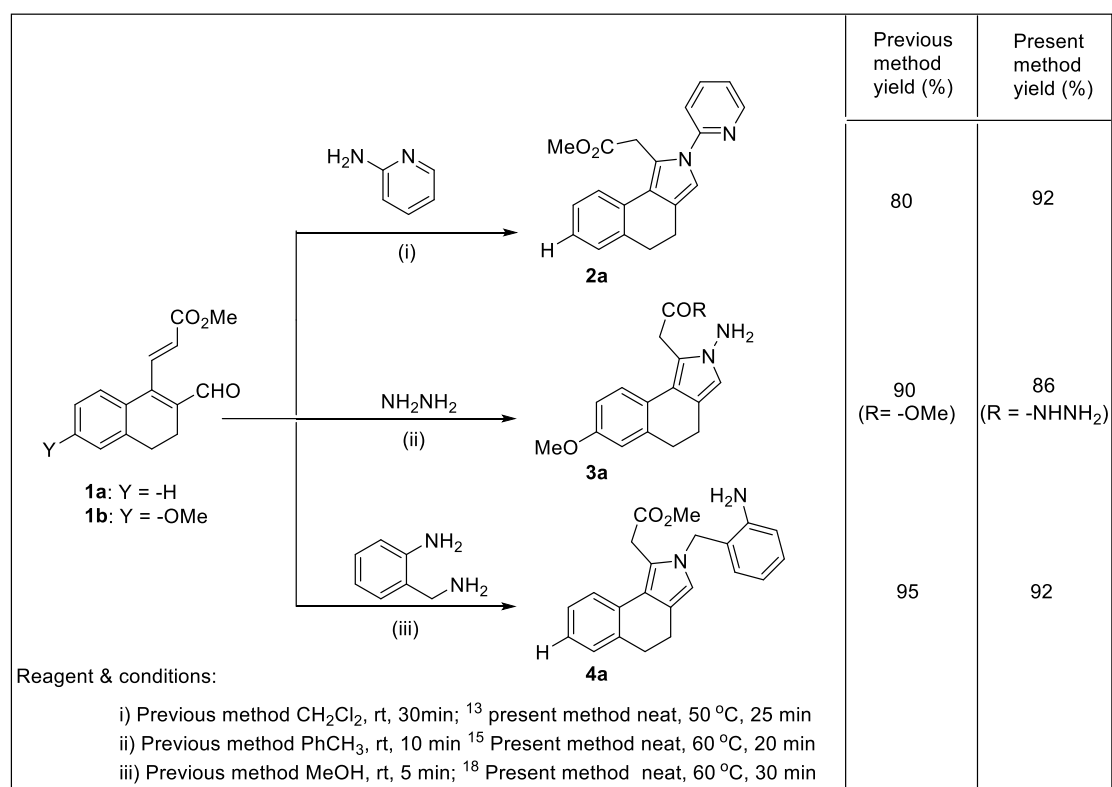
The cyclizations strategies for the synthesis of 5-5, 5-6, 5-7 fused bicyclic ring systems are very common²⁷ in the literature, but the formation of 5-8 fused ring heterocycles is very rare due to enthalpic factors, entropic factors and transannular interactions.²⁸ In this context, we have developed neat synthetic approach for *N*-aryl/benzyl/amino fused pyrrole derivatives (**2-4**) from 3-(3-formyl cycloalkenyl)-acrylic ester derivatives **1** and then macrolactamization was performed using the properly functionalized pyrrole system (**Scheme 5.17**).



Scheme 5.17. Synthesis and macrolactamization of *c*-fused pyrroles.

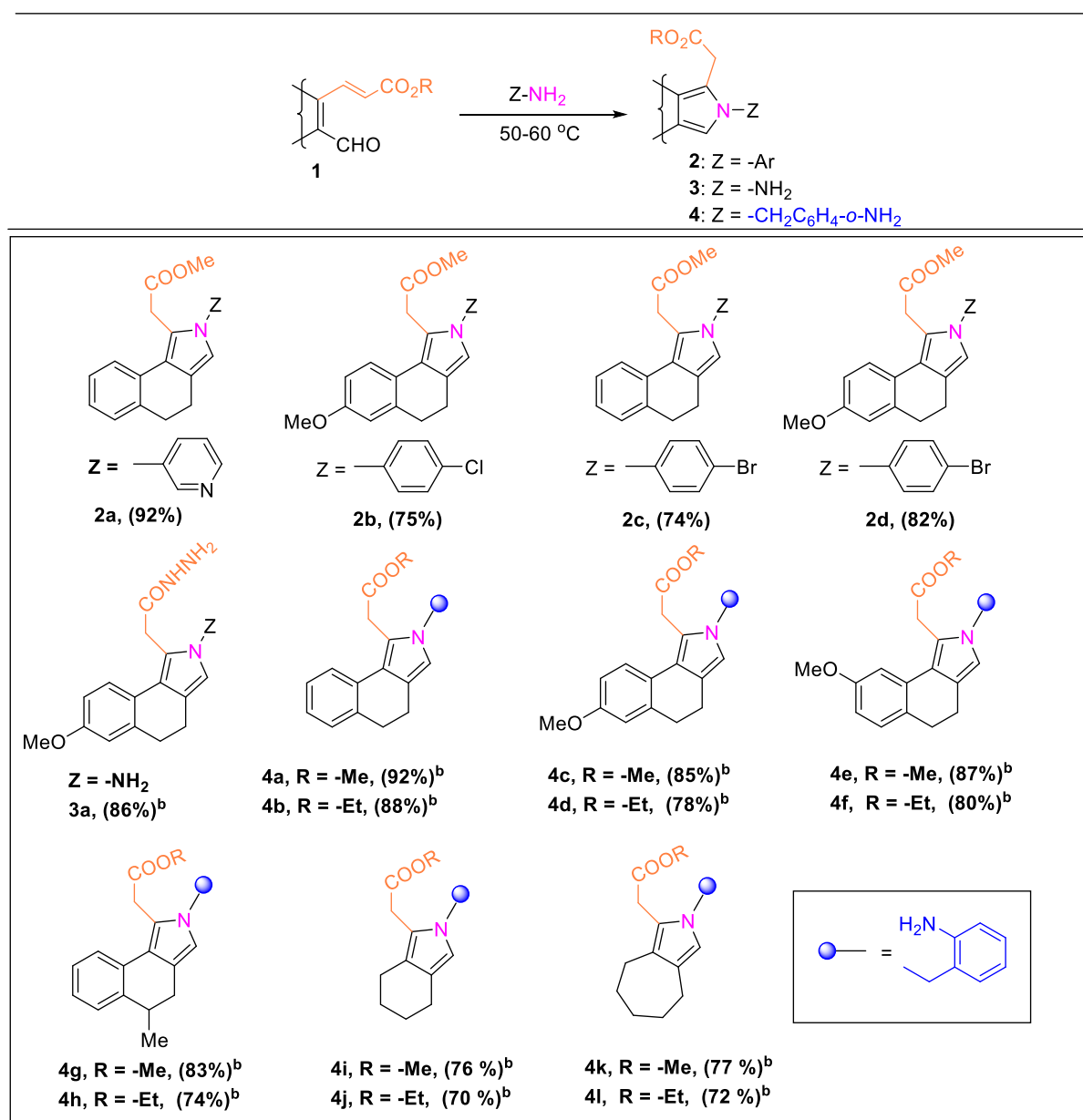
In our recent reported method, we have synthesized a series of pyrrole derivatives from the substrate **1** in solution phase. Previously, couplings of **1** with the aromatic amine, hydrazine and 2-aminobenzylamine were performed using the organic solvents, like dichloromethane, toluene and methanol respectively.^{13, 15, 17-19, 29} As, most of the organic solvents are toxic to the environment and health, we prompted to synthesize various isoindole derivatives under the neat reaction conditions. In our first attempt, the substrate **1a** was allowed to react with amine coupling partners, 2-aminopyridine and 2-aminobenzylamine to produce the similar isoindole derivatives (**2a** and **4a**, **Scheme 5.18**) in comparable yields within 30 minutes at 50-60 °C and **1b** was subjected to react with hydrazine which generates amide substituted isoindole derivative in 86% yield (**3a**, **Scheme 5.18**). Although the solvent added reaction requires less time compare to the solvent-free reaction, but solvent-free conditions is more

environmentally benign and less hazardous. It reduces use of hazardous chlorinated solvents and avoids the work-up process which is essential step for any solvent added reaction.



Scheme 5.18. A comparative study between solvent-medium and solvent-free reaction.

Our environmental benign neat protocol was applied in the reactions of different substituted acrylic ester derivatives with variety of amines. Thus, we have developed a general method for efficient synthesis of a series of polysubstituted fused pyrroles as shown in **Table 5.1**. From **Table 5.1**, we can see those anilines bearing electron withdrawing and electron donating substituents afforded tricyclic *c*-fused pyrroles in excellent yields (74-92%) within 20-30 minutes at 50 °C under solvent-free open flask conditions **2a-2d**. It is worth to point out that in case of the reaction with hydrazine corresponding *N*-substituted amine containing an amide functionality (**3a**) was obtained in 86% yield under neat condition at 60 °C. This compound has two fruitful functional groups for intramolecular nucleophilic addition which may further produce pyrrole fused heterocycles in due time. To explore the neat reaction condition, we have examined our reaction with 2-aminobenzylamine as coupling partner with the substrate **1**. It was observed that different acrylic ester furnished *c*-fused pyrrole derivative **4a-4l** with excellent yields (70-92%) within 30 minutes at 60 °C.

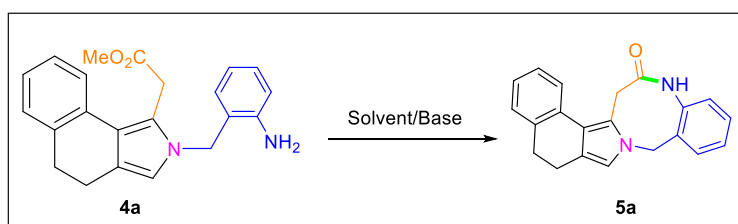
Table 5.1: Solvent-free synthesis of bicyclic & tricyclic *c*-fused pyrroles^{ab}

^{ab}**Reagent & conditions:** Substrate **1** (1 mmol), substituted amine (2 mmol), 50 °C, 20-30 min; ^btemperature needed 60 °C.

We were pleased to find that our substrate **4** has two important functionalities (-NH₂ & -CO₂R) in proper location for intramolecular reaction. The efficiency of the intramolecular amide formation reaction was tested using different bases and solvents. From this screening experiment (**Table 5.2**), we found that the weak base K₂CO₃ (**entry 1**) is not suitable for lactamization. Aza-cyclization was started in presence of strong potassium tertiary butoxide as base in DMSO at room temperature (**entry 2**). Upon lowering the temperature to 0 °C, the yield of intramolecular amide formation increased significantly (80% yield) within 15 minutes of time period in presence of the same base (**entry 3**). In presence of sodium hydride,

the yield of the reaction decreases compared to the KO^tBu (**entry 4**). Exothermic nature of NaH/DMSO mixture³⁰ reduces the yield of intramolecular amidation reaction. No conversion was observed using triethylamine as base (**entry 5**). In acetonitrile reaction medium the desired product was obtained with much lower yield (**entry 6**). Toluene, dioxane and chlorinated solvents did not furnish any cyclization product (**entry 7-10**).

Table 5.2: Optimization studies for the intramolecular lactamization^a



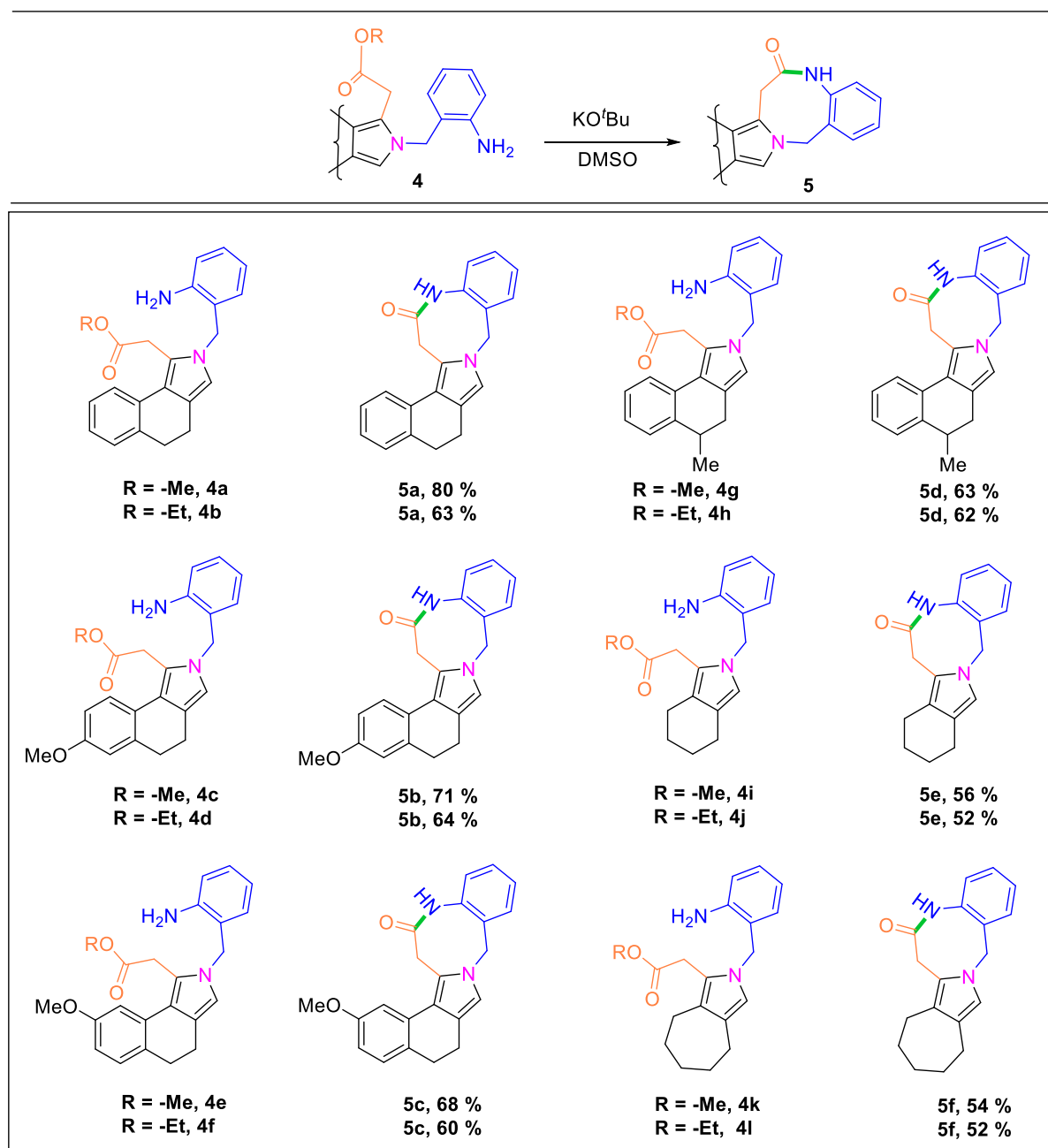
Entry	Solvent	Base	Temperature (°C)	Yield (%)
1.	DMSO	K ₂ CO ₃	0	NR
2.	DMSO	KO ^t Bu	RT	20
3.	DMSO	KO^tBu	0	80
4.	DMSO	NaH	0	73
5.	DMSO	Et ₃ N	0	NR
6.	CH ₃ CN	KO ^t Bu	0	71
7.	Toluene	KO ^t Bu	0	NR
8.	Dioxane	KO ^t Bu	0	NR
9.	CHCl ₃	KO ^t Bu	0	NR
10.	CH ₂ Cl ₂	KO ^t Bu	0	NR

^a**Reagent & conditions:** Substrate **4a** (1 mmol), base (2 mmol), solvent 4 mL, 15 min; NR: No reaction.

A variety of compounds containing pentacyclic and tetracyclic fused 8-membered lactam rings **5a-5f** were prepared by using the optimized reaction conditions in acceptable yields (**Table 5.3**). Intramolecular lactamization proceeded smoothly using methyl & ethyl substituted ester derivatives. But the yields of pentacyclic fused pyrrolo 8-membered lactam derivatives **5a-5d** are higher compared to the tetracyclic lactam **5e** and **5f**. It was noteworthy

that ethyl esters of **4** furnished poor yields of **5** compare to methyl ester due to the lower leaving aptitude of $-OEt$ group. The lower yield of macrocyclic rings (**5e** and **5f**) can be explained by the conformational strained of tetracyclic system. All the synthesized compounds were well characterized by spectral data (NMR & HRMS).

Table 5.3: Base-promoted intramolecular lactamization reaction^a



^a**Reagent & conditions:** Substrate **4a-4l** (1 mmol), KO^tBu (2 mmol), DMSO (4 mL), 0 °C, 15-20 min.

5.5. Conclusion:

In conclusion, we have developed environmental benign synthetic route of different substituted fused pyrrole derivatives using neat approach. The suitably functionalised pyrrole derivatives undergo intramolecular macrolactamization to furnish a broad array of rare 8-5 fused oxacinones with good yields.

5.6. Experimental section:

General information for synthetic compounds:

^1H and ^{13}C NMR spectra of all the synthesized compounds were recorded in 400 MHz and 500 MHz spectrometer in CDCl_3 and $\text{DMSO-}d^6$ solvent using TMS as the internal standard. HRMS was measured by using a TOF analyzer. Precoated silica gel 60 F254 TLC sheets (Merck) was used for monitoring the reaction. For purification in column chromatography 60-120 or 100-200 mesh silica gels (SRL) were used. *n*-Hexane (Merck) or petroleum ether (boiling range 60-80 °C) and ethyl acetate (b.p. 77.1 °C) eluent were used in column chromatographic separation. All solvents were dried, distilled and stored over molecular sieves (4 Å).

General Procedure for preparation of 2, 3, 4:

Substrate **1** (1 mmol) and aryl amine/hydrazine (1mmol) were taken in a one-neck round-bottom flask. The reaction mixture was heated for 20-30 min at 50-60 °C under neat condition. The reaction was monitored by TLC. After completion the reaction, the crude residue was purified in column chromatography by using silica-gel (60-120 mesh) and petroleum ether - ethyl acetate (5:1) eluent to obtain the desired product **2**.

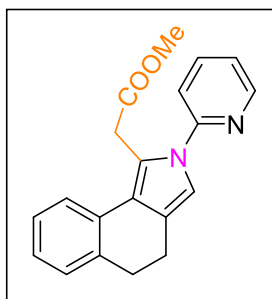
General Procedure for preparation of (5a – 5f):

At first KO^tBu (2 mmol) and DMSO (4 mL) were taken in a two-neck round-bottom flask. This two-necked round-bottom flask was placed in an ice-bath and allowed to stirring 10-15 min. Then the substrate **4** (1 mmol) was dissolved in minimum amount of DMSO and added drop wise to the reaction mixture. The reaction was allowed for stirring 15-20 minutes at inert atmosphere. The reaction was monitored by TLC. After completion the reaction, the crude residue was purified in column chromatography by using basic alumina and ethyl acetate - dichloromethane (1:1) eluent to obtain the desired product **5**.

5.6.1. Characterization of data:

Methyl 2-(2-(pyridin-2-yl)-4,5-dihydro-2H-benzo[e]isoindol-1-yl)acetate: (2a) (See the reference 31)

Yellow solid (292.6 mg, 92%), m.p. 92-95 °C. ¹H NMR (400 MHz, CDCl₃): δ 8.41 (ddd, *J* =

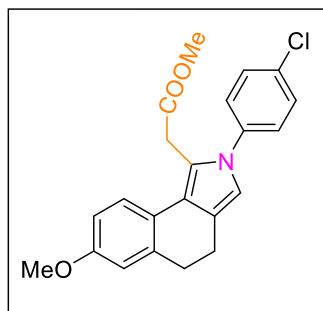


2.8, 2.0, 0.8 Hz, 1H), 7.77 – 7.73 (m, 1H), 7.47 (d, *J* = 8.4 Hz, 1H), 7.33- 3.31 (m, 1H), 7.25 – 7.22 (m, 2H), 7.15 – 7.10 (m, 2H), 6.90 (s, 1H), 4.16 (s, 2H), 3.70 (s, 3H), 2.88 – 2.85 (m, 2H), 2.73 – 2.69 (m, 2H). ¹³C NMR (101 MHz, CDCl₃): δ 171.9, 152.7, 148.3, 138.6, 137.4, 132.1, 128.6, 126.8, 125.6, 123.8, 123.0, 122.7, 120.9, 120.6, 115.9, 115.3, 52.1, 33.9, 31.4, 21.1. HRMS calcd. for C₂₀H₁₉N₂O₂:

(M+H)⁺: 319.1448, found: 319.1450.

Methyl 2-(2-(4-chlorophenyl)-7-methoxy-4,5-dihydro-2H-benzo[e]isoindol-1-yl)acetate: (2b)

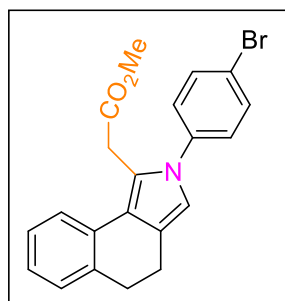
Yellow liquid (285.8 mg, 75%). ¹H NMR (500 MHz, CDCl₃): δ 7.43 (d, *J* = 8.6 Hz, 2H), 7.32



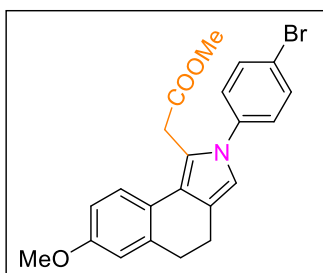
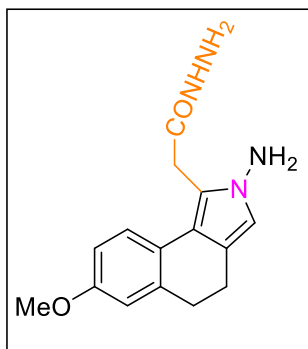
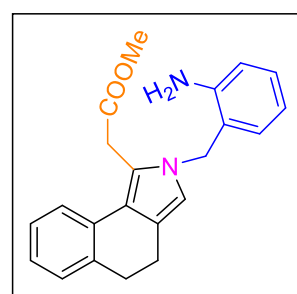
(d, *J* = 8.7 Hz, 3H), 6.85 – 6.80 (m, 2H), 6.61 (s, 1H), 3.84 (s, 3H), 3.78 (s, 2H), 3.72 (s, 3H), 2.90 – 2.88 (m, 2H), 2.75 – 2.72 (m, 2H). ¹³C NMR (126 MHz, CDCl₃): δ 171.4, 157.4, 138.5, 133.2, 129.4 (2C), 127.8 (2C), 125.1, 124.0, 121.2, 120.6, 119.3, 117.5, 116.2, 114.7, 111.7, 55.2, 52.3, 32.2, 31.6, 20.9. HRMS calcd. for C₂₂H₂₁ClNO₃: (M+H)⁺ 382.1212, found : 382.1214.

2-(4-Bromophenyl)-1-(2-(methylperoxy)-2H-ethyl)-4,5-dihydro-2H-benzo[e]isoindole: (2c)

Yellow liquid (292.3 mg, 74%). ¹H NMR (500 MHz, CDCl₃): δ 7.60 (d, *J* = 8.6 Hz, 2H), 7.38

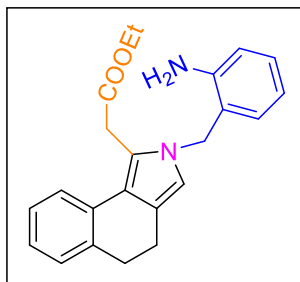


(d, *J* = 7.9 Hz, 2H), 7.28 – 7.27 (m, 4H), 6.63 (s, 1H), 3.81 (s, 2H), 3.73 (s, 3H), 2.93 – 2.91 (m, 2H), 2.77 – 2.74 (m, 2H). ¹³C NMR (126 MHz, CDCl₃): δ 171.3, 138.9, 136.8, 132.4 (2C), 128.7, 128.1 (2C), 126.7, 125.3, 123.1, 121.8, 121.3, 120.8, 120.3, 117.6, 115.4, 52.3, 32.2, 31.2, 20.9. HRMS calcd. for C₂₁H₁₉BrNO₂: (M+H)⁺ 396.0601, found : 396.0602.

Methyl 2-(2-(4-bromophenyl)-7-methoxy-4,5-dihydro-2H-benzo[e]isoindol-1-yl)acetate:**(2d)**Yellow liquid (348.5 mg, 82%). ^1H NMR (500 MHz, CDCl_3): δ 7.59 (d, $J = 8.6$ Hz, 2H), 7.32– 7.26 (m, 3H), 6.86 – 6.80 (m, 2H), 6.62 (s, 1H), 3.84 (s, 3H), 3.78 (s, 2H), 3.73 (s, 3H), 2.91 – 2.88 (m, 2H), 2.75 – 2.72 (m, 2H). ^{13}C NMR (126 MHz, CDCl_3): δ 171.4, 157.4, 139.0, 138.5, 132.4 (2C), 128.1 (2C), 125.1, 124.0, 121.3, 120.7, 119.2, 117.5, 116.7, 114.7, 111.7, 55.3, 52.3, 32.2, 31.6, 20.9. HRMS calcd. for $\text{C}_{22}\text{H}_{21}\text{BrNO}_3$: $(\text{M}+\text{H})^+$ 426.0707, found : 426.0708.**2-(2-Amino-7-methoxy-4,5-dihydro-2H-benzo[e]isoindol-1-yl)acetohydrazide: (3a)**Yellow solid (246.0 mg, 86%), m.p. 154 °C. ^1H NMR (400 MHz, $\text{DMSO}-d_6$): δ 9.14 (s, 1H),7.35 (d, $J = 8.4$ Hz, 1H), 6.78 (s, 1H), 6.72 (d, $J = 8.2$ Hz, 1H), 6.49 (s, 1H), 5.72 (s, 2H), 4.26 (m, 2H), 3.72 (s, 3H), 3.67 (s, 2H), 2.73 – 2.67 (m, 2H). ^1H NMR (400 MHz, D_2O exchange): δ 7.32 (d, $J = 8.4$ Hz, 1H), 6.77 (s, 1H), 6.72 – 6.70 (m, 1H), 6.49 (s, 1H), 3.75 – 3.66 (m, 5H), 2.65 (m, 2H), 2.45 (m, 2H). ^{13}C NMR (126 MHz, CDCl_3): δ 171.5, 161.1, 149.0, 142.9, 139.8, 134.6, 126.2, 124.1, 118.6, 113.9, 112.9, 55.4, 52.8, 28.4, 25.5. HRMS calcd. for $\text{C}_{15}\text{H}_{19}\text{N}_4\text{O}_2$: $(\text{M}+\text{H})^+$ 287.1510, found : 287.1511.**Methyl 2-(2-(2-aminobenzyl)-4,5-dihydro-2H-benzo[e]isoindol-1-yl)acetate: (4a)**Yellow solid (318.4 mg, 92%), m.p. 117 °C. ^1H NMR (400 MHz, CDCl_3): δ 7.48 (d, $J = 7.6$ Hz, 1H), 7.23 (d, $J = 7.6$ Hz, 2H), 7.17 – 7.08 (m, 2H), 6.90 (d, $J = 7.2$ Hz, 1H), 6.75 (t, $J = 7.6$ Hz, 1H), 6.69 (d, $J = 7.9$ Hz, 1H), 6.34 (s, 1H), 4.99 (s, 2H), 3.93 (s, 2H), 3.73 (s, 3H), 2.83 (t, $J = 6.9$ Hz, 2H), 2.62 (t, $J = 6.9$ Hz, 2H). ^{13}C NMR (126 MHz, CDCl_3): δ 171.4, 145.1, 136.7, 132.5, 129.8, 129.2, 128.6, 126.7, 124.9, 123.1, 120.7, 120.5, 119.9, 119.8, 118.5, 116.1, 116.0, 52.4, 48.1, 31.7, 31.4,21.0. HRMS calcd. for $\text{C}_{22}\text{H}_{23}\text{N}_2\text{O}_2$: $(\text{M}+\text{H})^+$ 347.1761, found : 347.1762.

Ethyl 2-(2-(2-aminobenzyl)-4,5-dihydro-2H-benzo[e]isoindol-1-yl)acetate: (4b)

Yellow solid (316.9 mg, 88%), m.p. 114 °C. ¹H NMR (400 MHz, CDCl₃): δ 7.53 (d, *J* = 7.6



Hz, 1H), 7.25 (d, *J* = 7.5 Hz, 2H), 7.19 – 7.15 (m, 1H), 7.11 (t, *J* = 7.2 Hz, 1H), 6.93 (d, *J* = 7.3 Hz, 1H), 6.76 (t, *J* = 7.3 Hz, 1H), 6.70 (d, *J* = 7.9 Hz, 1H), 6.33 (s, 1H), 5.01 (s, 2H), 4.22 (q, *J* = 7.2 Hz, 2H), 3.93 (s, 2H), 3.88 (s, 2H), 2.85 (t, *J* = 6.8 Hz, 2H), 2.63 (t, *J* = 6.8 Hz, 2H), 1.32 (t, *J* = 7.1 Hz, 3H). ¹³C NMR (101 MHz, CDCl₃): δ 171.1, 145.3, 136.8, 132.7, 130.1, 129.3, 128.7, 126.7, 125.0,

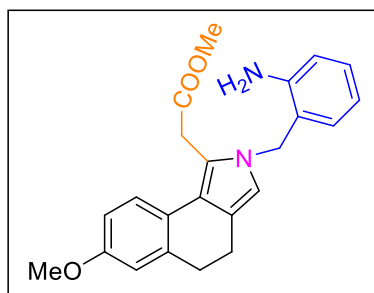
123.3, 120.7, 120.6, 120.1, 120.0, 118.5, 116.1, 116.0, 61.5, 48.2, 32.0, 31.5, 21.2, 14.4.

HRMS calcd. for C₂₃H₂₅N₂O₂: (M+H)⁺ 361.1918, found : 361.1917.

Methyl 2-(2-(2-aminobenzyl)-7-methoxy-4,5-dihydro-2H-benzo[e]isoindol-1-yl)acetate: (4c)

(4c)

Off white solid (319.7 mg, 85%), m.p. 115 °C. ¹H NMR (400 MHz, CDCl₃): δ 7.42 (d, *J* =



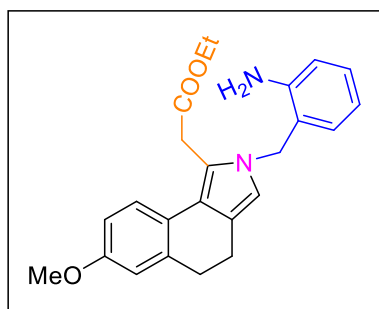
8.4 Hz, 1H), 7.16 (td, *J* = 7.6, 1.2 Hz, 1H), 6.91 (d, *J* = 6.4 Hz, 1H), 6.82 – 6.75 (m, 2H), 6.75 – 6.73 (m, 1H), 6.69 (d, *J* = 8.0 Hz, 1H), 6.32 (s, 1H), 4.99 (s, 2H), 3.90 (s, 2H), 3.82 (s, 3H), 3.73 (s, 3H), 2.83 – 2.79 (m, 2H), 2.63 – 2.59 (m, 2H). ¹³C NMR (101 MHz, CDCl₃): δ 171.5, 157.3, 145.2, 138.5, 130.0, 129.3, 125.6, 124.2, 121.0, 120.1, 119.9, 119.0,

118.6, 116.2, 116.0, 114.7, 111.8, 55.4, 52.5, 48.2, 31.9, 31.8, 21.2. HRMS calcd. for

C₂₃H₂₅N₂O₃: (M+H)⁺ 377.1867, found : 377.1865.

Ethyl 2-(2-(2-aminobenzyl)-7-methoxy-4,5-dihydro-2H-benzo[e]isoindol-1-yl)acetate: (4d)

Off white solid (242.7 mg, 78%), m.p. 112 °C. ¹H NMR (400 MHz, CDCl₃): δ 7.46 (d, *J* =

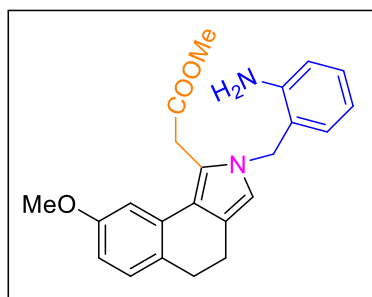
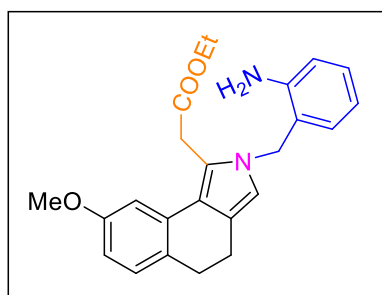
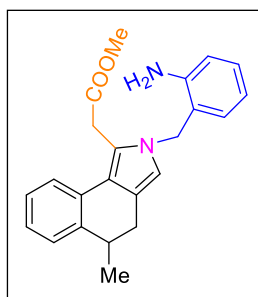


8.0 Hz, 1H), 7.16 (t, *J* = 8.0 Hz, 1H), 6.92 (d, *J* = 6.8 Hz, 1H), 6.82 – 6.68 (m, 4H), 6.31 (s, 1H), 4.99 (s, 2H), 4.20 (q, *J* = 7.2 Hz, 2H), 3.89 (s, 2H), 3.82 (s, 3H), 2.83 – 2.78 (m, 2H), 2.63 – 2.59 (m, 2H), 1.31 (t, *J* = 7.2 Hz, 3H). ¹³C NMR (101 MHz, CDCl₃): δ 171.2, 157.2, 145.3, 138.5, 130.1, 129.3, 125.7, 124.3, 120.9, 120.1, 119.8, 119.1, 118.5, 116.1, 115.9,

114.7, 111.8, 61.4, 55.4, 48.2, 32.1, 31.9, 21.2, 14.3. HRMS calcd. for C₂₄H₂₇N₂O₃: (M+H)⁺ 391.2023, found : 391.2024.

Methyl 2-(2-(2-aminobenzyl)-8-methoxy-4,5-dihydro-2H-benzo[e]isoindol-1-yl)acetate: (4e)

(4e)

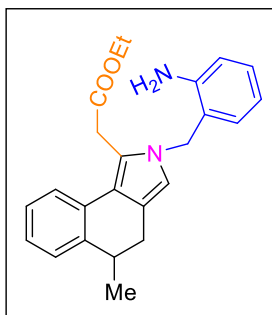
Off white solid (327.2 mg, 87%), m.p. 84 °C. ¹H NMR (400 MHz, CDCl₃): δ 7.17 – 7.12 (m,3H), 6.89 (d, *J* = 7.4 Hz, 1H), 6.74 (td, *J* = 7.2, 0.8 Hz, 1H), 6.70 – 6.65 (m, 2H), 6.33 (s, 1H), 5.01 (s, 2H), 3.92 (s, 2H), 3.84 (s, 3H), 3.72 (s, 3H), 2.77 – 2.74 (m, 2H), 2.60 – 2.56 (m, 2H). ¹³C NMR (101 MHz, CDCl₃): δ 171.2, 158.5, 145.0, 133.3, 129.8, 129.2, 129.1, 129.0, 120.7, 120.6, 120.0, 119.9, 118.5, 116.1, 116.0, 110.4, 109.0, 55.2, 52.4, 48.0, 31.7, 30.4,21.3. HRMS calcd. for C₂₃H₂₅N₂O₃: (M+H)⁺ 377.1867, found : 377.1866.**Ethyl 2-(2-(2-aminobenzyl)-8-methoxy-4,5-dihydro-2H-benzo[e]isoindol-1-yl)acetate: (4f)**Off white solid (312.1 mg, 80%), m.p. 82 °C. ¹H NMR (400 MHz, CDCl₃): δ 7.17 – 7.11 (m,3H), 6.90 (d, *J* = 7.4 Hz, 1H), 6.74 (td, *J* = 7.4, 0.9 Hz, 1H), 6.70 – 6.64 (m, 2H), 6.31 (s, 1H), 5.01 (s, 2H), 4.19 (q, *J* = 7.2 Hz, 2H), 3.90 (s, 2H), 3.83 (s, 3H), 2.76 – 2.73 (m, 2H), 2.59 – 2.55 (m, 2H), 1.28 (t, *J* = 7.2 Hz, 3H). ¹³C NMR (101 MHz, CDCl₃): δ 171.0, 158.6, 145.2, 133.5, 130.0, 129.6, 129.3, 129.2, 129.1, 120.7, 120.1, 120.0, 118.5, 116.1, 116.0,110.4, 109.1, 61.6, 55.4, 48.2, 32.0, 30.5, 21.4, 14.3. HRMS calcd. for C₂₄H₂₇N₂O₃: (M+H)⁺ 391.2023, found : 391.2022.**Methyl 2-(2-(2-aminobenzyl)-5-methyl-4,5-dihydro-2H-benzo[e]isoindol-1-yl)acetate: (4g)**White solid (298.9 mg, 83%), m.p. 116 °C. ¹H NMR (500 MHz, CDCl₃): δ 7.39 (d, *J* = 7.6Hz, 1H), 7.18 – 7.13 (m, 2H), 7.07 – 7.02 (m, 2H), 6.77 (d, *J* = 7.4 Hz, 1H), 6.65 (t, *J* = 7.5 Hz, 1H), 6.61 (d, *J* = 8.0 Hz, 1H), 6.26 (s, 1H), 4.91 (s, 2H), 3.84 (d, *J* = 16.5 Hz, 1H), 3.79 (d, *J* = 16.5 Hz, 1H), 3.62 (s, 3H), 2.90 – 2.87 (m, 1H), 2.67 (dd, *J* = 14.5, 5.1 Hz, 1H), 2.33 (dd, *J* = 14.5, 5.9 Hz, 1H), 1.11 (d, *J* = 6.9 Hz, 3H). ¹³C NMR (126 MHz, CDCl₃): δ 171.5, 144.8, 141.5, 131.8, 129.7, 129.2, 127.3, 126.7,

125.3, 123.4, 121.3, 119.8, 119.5, 119.1, 118.8, 117.0, 116.3, 52.5, 48.2, 35.1, 31.9, 28.7,

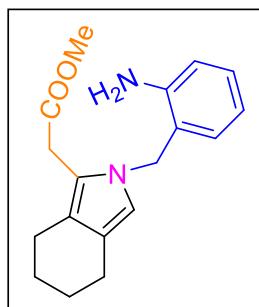
20.4. HRMS calcd. for C₂₃H₂₅N₂O₂: (M+H)⁺ 361.1918, found : 361.1917.

Ethyl 2-(2-(2-aminobenzyl)-5-methyl-4,5-dihydro-2H-benzo[e]isoindol-1-yl)acetate: (4h)

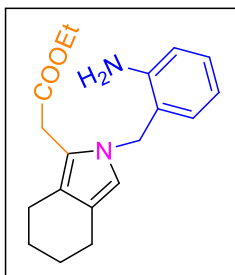
White solid (276.9 mg, 74%), m.p. 117 °C. ¹H NMR (500 MHz, CDCl₃): δ 7.50 (d, *J* = 7.6 Hz, 1H), 7.28 – 7.20 (m, 2H), 7.12 (q, *J* = 8.2, 7.6 Hz, 2H), 6.88 (d, *J* = 7.4 Hz, 1H), 6.72 (t, *J* = 7.4 Hz, 1H), 6.67 (d, *J* = 7.9 Hz, 1H), 6.32 (s, 1H), 4.99 (s, 2H), 4.18 (qd, *J* = 7.1, 1.8 Hz, 2H), 4.00 – 3.71 (m, 4H), 2.98 – 2.95 (m, 1H), 2.75 (dd, *J* = 14.5, 5.1 Hz, 1H), 2.40 (dd, *J* = 14.5, 6.0 Hz, 1H), 1.27 (t, *J* = 7.1 Hz, 3H), 1.19 (d, *J* = 7.0 Hz, 3H). ¹³C NMR (176 MHz, CDCl₃): δ 171.0, 145.1, 141.4, 131.8, 129.8, 129.2, 127.2, 126.5, 125.1, 123.4, 120.9, 119.9, 119.3, 118.9, 118.5, 116.8, 116.0, 61.4, 48.1, 35.0, 32.0, 28.6, 20.3, 14.3. HRMS calcd. for C₂₄H₂₇N₂O₂: (M+H)⁺ 375.2074, found : 375.2075.

**Methyl 2-(2-(2-aminobenzyl)-4,5,6,7-tetrahydro-2H-isoindol-1-yl)acetate: (4i)**

Yellow solid (226.6 mg, 76%), m.p. 71 °C. ¹H NMR (500 MHz, CDCl₃): δ 7.04 (t, *J* = 7.6 Hz, 1H), 6.83 (d, *J* = 7.1 Hz, 1H), 6.65 (t, *J* = 7.4 Hz, 1H), 6.57 (d, *J* = 7.8 Hz, 1H), 6.11 (s, 1H), 4.80 (s, 2H), 3.56 (s, 3H), 3.47 (s, 2H), 2.41 – 2.39 (m, 4H), 1.68 – 1.60 (m, 4H). ¹³C NMR (126 MHz, CDCl₃): δ 171.5, 145.2, 130.1, 129.1, 121.1, 119.2, 119.1, 119.0, 118.4, 116.1, 116.0, 52.1, 48.2, 30.3, 24.0, 23.9, 22.0, 21.5. HRMS calcd. for C₁₈H₂₃N₂O₂: (M+H)⁺ 299.1761, found : 299.1762.

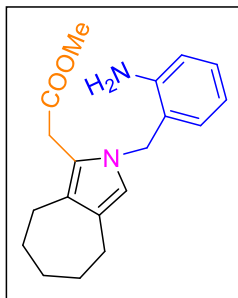
**Ethyl 2-(2-(2-aminobenzyl)-4,5,6,7-tetrahydro-2H-isoindol-1-yl)acetate: (4j)**

Yellow solid (218.5 mg, 70%), m.p. 69 °C. ¹H NMR (500 MHz, CDCl₃): δ 7.16 (td, *J* = 7.8, 1.4 Hz, 1H), 6.97 (d, *J* = 7.0 Hz, 1H), 6.78 – 6.74 (m, 1H), 6.69 (d, *J* = 7.9 Hz, 1H), 6.21 (s, 1H), 4.92 (s, 2H), 4.13 (q, *J* = 7.1 Hz, 2H), 3.57 (s, 2H), 2.52 – 2.50 (m, 4H), 1.76 – 1.71 (m, 4H), 1.28 (t, *J* = 7.1 Hz, 3H). ¹³C NMR (126 MHz, CDCl₃): δ 171.2, 145.3, 130.3, 129.1, 121.0, 119.4, 119.1, 119.0, 118.3, 116.0, 115.9, 61.0, 48.2, 30.5, 24.0, 23.9, 22.0, 21.5, 14.2. HRMS calcd. for C₁₉H₂₅N₂O₂: (M+H)⁺ 313.1918, found : 313.1917.



Methyl 2-(2-(2-aminobenzyl)-2,4,5,6,7,8-hexahydrocyclohepta[c]pyrrol-1-yl)acetate: (4k)

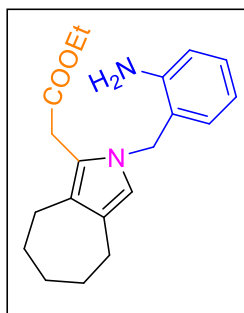
Yellow solid (240.3 mg, 77%), m.p. 78 °C. ¹H NMR (500 MHz, CDCl₃): δ 7.16 (td, *J* = 7.8,



1.4 Hz, 1H), 6.92 (d, *J* = 7.4 Hz, 1H), 6.76 (td, *J* = 7.4, 0.9 Hz, 1H), 6.69 (d, *J* = 7.9 Hz, 1H), 6.23 (s, 1H), 4.88 (s, 2H), 3.66 (s, 3H), 3.62 (s, 2H), 2.55 – 2.49 (m, 4H), 1.82 – 1.81 (m, 2H), 1.65 – 1.60 (m, 4H). ¹³C NMR (126 MHz, CDCl₃): δ 171.7, 145.2, 130.0, 129.0, 125.0, 124.6, 121.2, 120.4, 118.4, 117.3, 116.0, 52.1, 48.1, 33.2, 30.2, 30.1, 29.9, 28.2, 27.0. HRMS calcd. for C₁₉H₂₅N₂O₂: (M+H)⁺ 313.1918, found : 313.1919.

Ethyl 2-(2-(2-aminobenzyl)-2,4,5,6,7,8-hexahydrocyclohepta[c]pyrrol-1-yl)acetate: (4l)

Yellow solid (234.8 mg, 72%), m.p. 75 °C. ¹H NMR (500 MHz, CDCl₃): δ 7.17 (t, *J* = 7.6

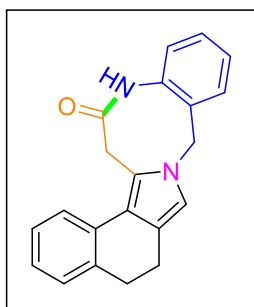


Hz, 1H), 6.96 – 6.94 (m, 1H), 6.76 (t, *J* = 7.7 Hz, 1H), 6.70 (d, *J* = 7.9 Hz, 1H), 6.22 (s, 1H), 4.90 (s, 2H), 4.13 (q, *J* = 7.1 Hz, 2H), 3.61 (s, 2H), 2.56 – 2.49 (m, 4H), 1.83 – 1.80 (m, 2H), 1.66 – 1.60 (m, 4H), 1.27 (t, *J* = 7.1 Hz, 3H). ¹³C NMR (126 MHz, CDCl₃): δ 171.3, 145.3, 130.1, 129.0, 124.9, 124.6, 121.1, 120.6, 118.3, 117.2, 116.0, 61.0, 48.1, 33.2, 30.4, 30.3, 30.0, 28.2, 27.0, 14.2. HRMS calcd. for

C₂₀H₂₇N₂O₂: (M+H)⁺ 327.2074, found : 327.2072.

5,12,13,16-Tetrahydrobenzo[g]benzo[6,7][1,5]diazocino[2,1-a]isoindol-6(7H)-one: (5a)

Off white liquid (251.3 mg for **4a** 80%; 197.9 mg for **4b** 63%). ¹H NMR (400 MHz, CDCl₃):

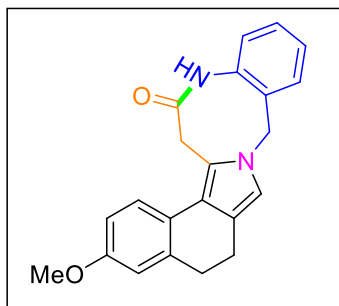


δ 8.25 (s, 1H), 7.52 (dd, *J* = 7.4, 1.6 Hz, 1H), 7.45 – 7.34 (m, 3H), 7.28 – 7.26 (m, 1H), 7.19 – 7.14 (m, 2H), 7.04 (td, *J* = 9.2, 1.2 Hz, 1H), 6.53 (s, 1H), 4.95 (s, 2H), 3.72 (s, 2H), 2.79 – 2.76 (m, 2H), 2.62 – 2.58 (m, 2H). ¹³C NMR (101 MHz, CDCl₃): δ 171.6, 137.9, 137.1, 132.6, 132.1, 131.4, 130.2, 128.6, 128.5, 126.7, 125.4, 125.0, 123.5, 120.6, 120.3, 119.2, 117.8, 50.3, 33.0, 31.5, 21.1. HRMS calcd. for

C₂₁H₁₉N₂O: (M+H)⁺ 315.1499, found : 315.1498.

10-Methoxy-5,12,13,16-tetrahydrobenzo[g]benzo[6,7][1,5]diazocino[2,1-a]isoindol-6(7H)-one: (5b)

Yellow oil (244.3 mg for **4c** 71%; 220.2 mg for **4d** 64%). ¹H NMR (500 MHz, DMSO-*d*₆): δ

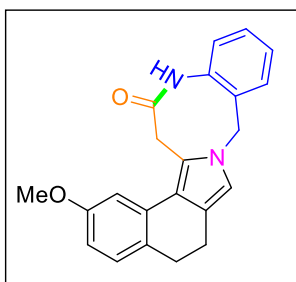


10.05 (s, 1H), 7.72 – 7.58 (m, 4H), 7.47 – 7.36 (m, 1H), 7.26 (dd, *J* = 12.9, 8.2 Hz, 1H), 6.89 – 6.82 (m, 1H), 6.75 – 6.71 (m, 1H), 4.92 (s, 2H), 4.03 – 4.00 (m, 2H), 3.72 (s, 3H), 2.99 (s, 1H), 2.89 (s, 1H), 2.73 – 2.67 (m, 2H). ¹³C NMR (101 MHz, CDCl₃): δ 171.8, 158.4, 138.2, 133.5, 131.9, 131.2, 130.1, 129.5, 129.0, 128.4, 125.4, 120.7, 120.2, 119.4, 117.8, 109.9, 109.7, 55.3,

50.2, 33.1, 30.6, 21.4. HRMS calcd. for C₂₂H₂₁N₂O₂: (M+H)⁺ 345.1605, found : 345.1606.

9-Methoxy-5,12,13,16-tetrahydrobenzo[g]benzo[6,7][1,5]diazocino[2,1-a]isoindol-6(7H)-one: (5c)

Yellow oil (234.0 mg for **4e** 68%; 206.4 mg for **4f** 60%). ¹H NMR (400 MHz, CDCl₃): δ 8.04

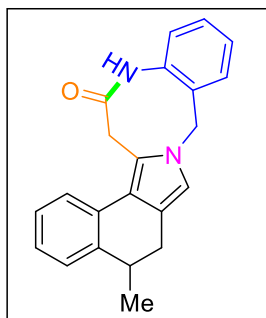


(d, *J* = 5.2 Hz, 1H), 7.52 (dd, *J* = 7.4, 1.6 Hz, 1H), 7.43 – 7.36 (m, 2H), 7.27 (s, 1H), 7.14 – 7.12 (m, 2H), 6.69 (dd, *J* = 6.3, 2.9 Hz, 1H), 6.52 (s, 1H), 4.94 (s, 2H), 3.82 (s, 3H), 3.71 (s, 2H), 2.82 – 2.78 (m, 2H), 2.57 – 2.54 (m, 2H). ¹³C NMR (101 MHz, CDCl₃): δ 171.5, 156.9, 137.9, 133.7, 132.1, 131.5, 130.1, 128.6, 126.7, 125.4,

125.1, 120.7, 120.4, 119.4, 117.6, 116.6, 107.7, 55.6, 50.2, 32.9, 22.6, 20.4. HRMS calcd. for C₂₂H₂₁N₂O₂: (M+H)⁺ 345.1605, found : 345.1604.

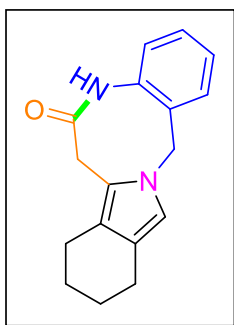
12-Methyl-5,12,13,16-tetrahydrobenzo[g]benzo[6,7][1,5]diazocino[2,1-a]isoindol-6(7H)-one: (5d)

Yellow oil (206.7 mg, for **4g** 63%; 203.4 mg for **4h** 62%). ¹H NMR (500 MHz, DMSO-*d*₆): δ

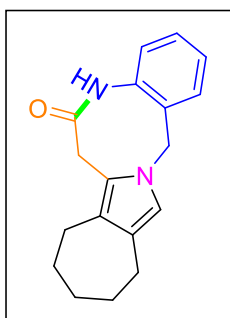


10.09 (s, 1H), 7.72 – 7.66 (m, 1H), 7.60 (d, *J* = 7.3 Hz, 1H), 7.47 (t, *J* = 8.1 Hz, 1H), 7.38 (t, *J* = 7.7 Hz, 1H), 7.24 (dd, *J* = 16.4, 7.6 Hz, 2H), 7.15 (t, *J* = 7.3 Hz, 1H), 7.06 (t, *J* = 7.3 Hz, 1H), 6.76 (s, 1H), 4.95 (s, 2H), 3.54 – 3.46 (m, 2H), 2.90 – 2.86 (m, 1H), 2.66 – 2.62 (m, 2H), 1.13 (d, *J* = 6.9 Hz, 3H). ¹³C NMR (101 MHz, CDCl₃): δ 172.1, 141.6, 138.2, 131.9, 131.8, 131.3, 130.1, 128.4, 127.0, 126.5, 125.4,

125.1, 123.7, 119.6, 119.2, 119.0, 118.5, 50.3, 35.1, 33.2, 28.7, 20.1. HRMS calcd. for C₂₂H₂₁N₂O: (M+H)⁺ 329.1656, found : 329.1657.

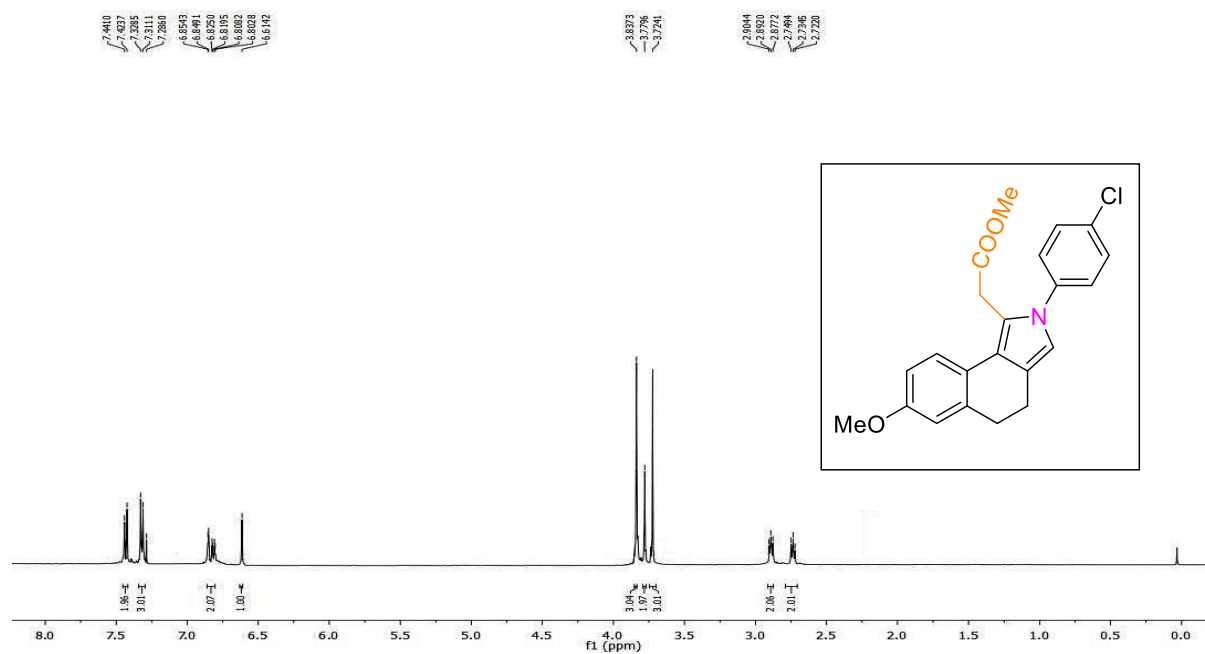
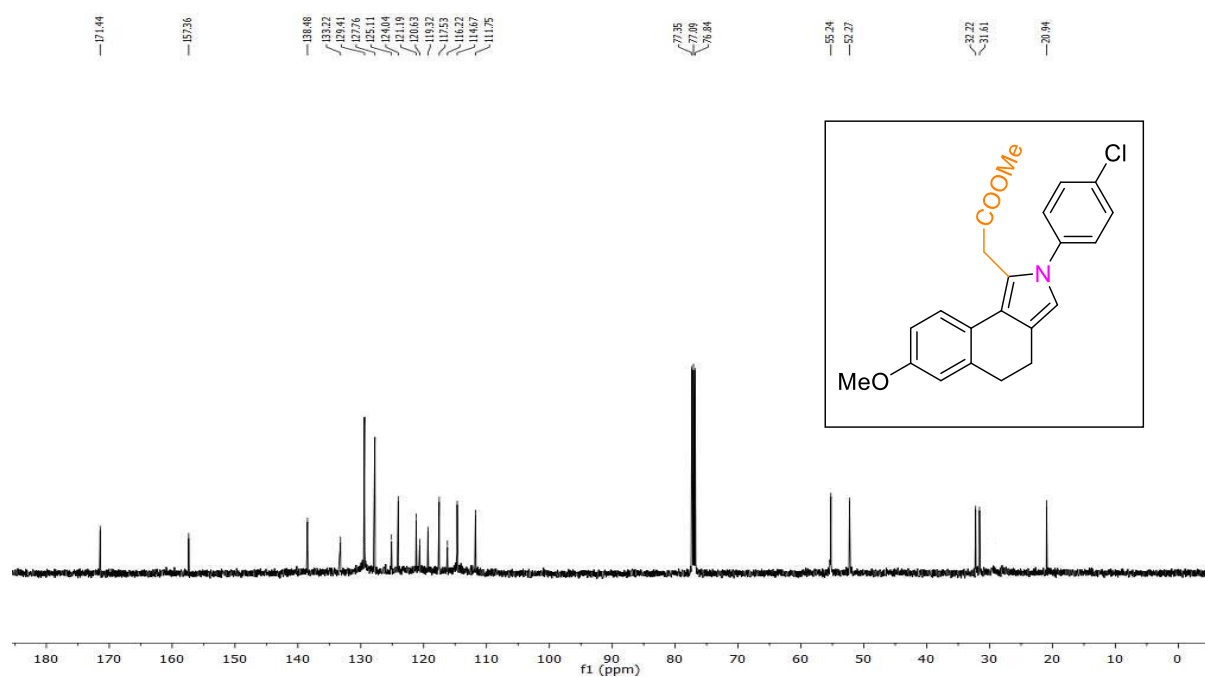
5,8,9,10,11,14-Hexahydrobenzo[6,7][1,5]diazocino[2,1-a]isoindol-6(7H)-one: (5e)

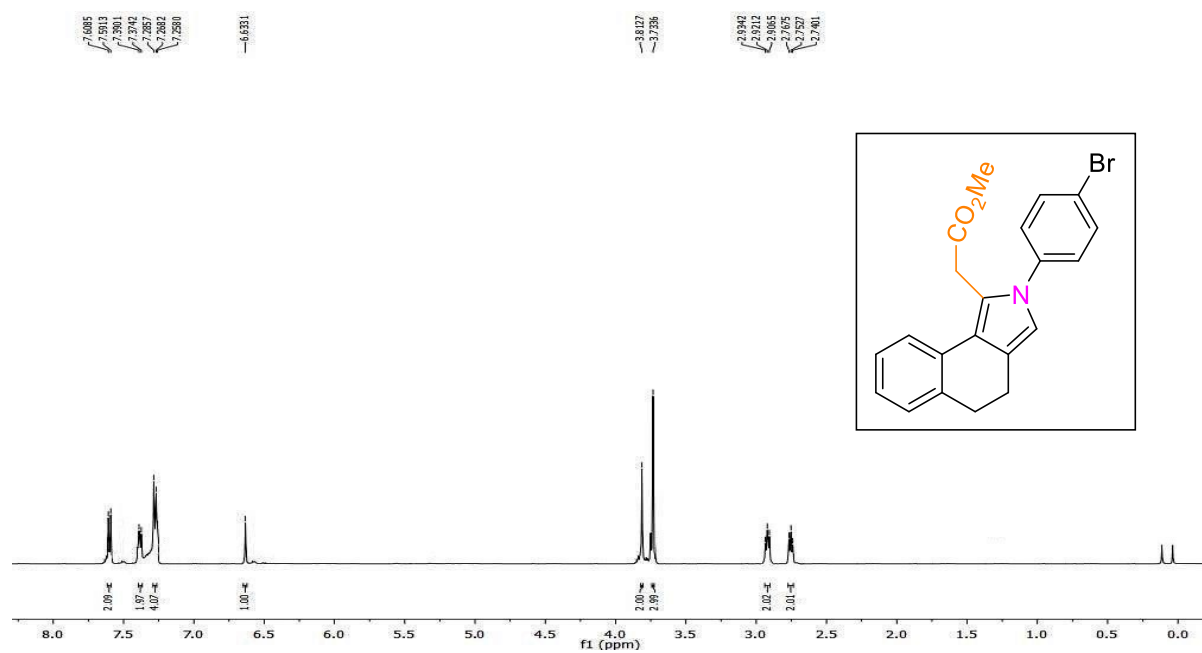
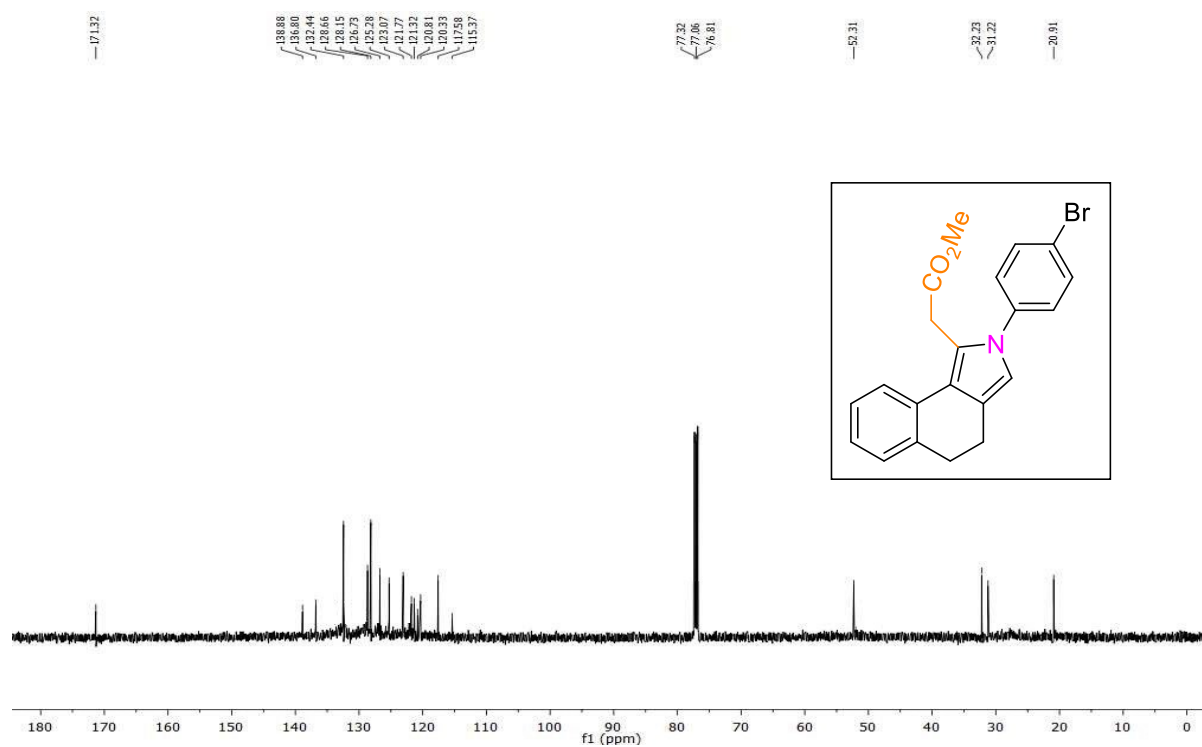
Off white liquid (149.0 mg, for **4i** 56%; 138.3 mg for **4j** 52%). ^1H NMR (400 MHz, CDCl_3): δ 7.12 (d, $J = 7.4$ Hz, 1H), 7.06 (t, $J = 7.3$ Hz, 1H), 6.66 – 6.61 (m, 3H), 4.67 (s, 2H), 2.60 (s, 2H), 2.32 – 2.28 (m, 4H), 1.62 – 1.49 (m, 4H). ^{13}C NMR (101 MHz, CDCl_3): δ 171.8, 137.8, 132.0, 131.9, 129.9, 128.6, 125.6, 119.2, 119.0, 118.5, 117.9, 50.0, 31.9, 24.0, 23.9, 21.9, 21.4. HRMS calcd. for $\text{C}_{17}\text{H}_{19}\text{N}_2\text{O}$: $(\text{M}+\text{H})^+$ 267.1499, found : 267.1498.

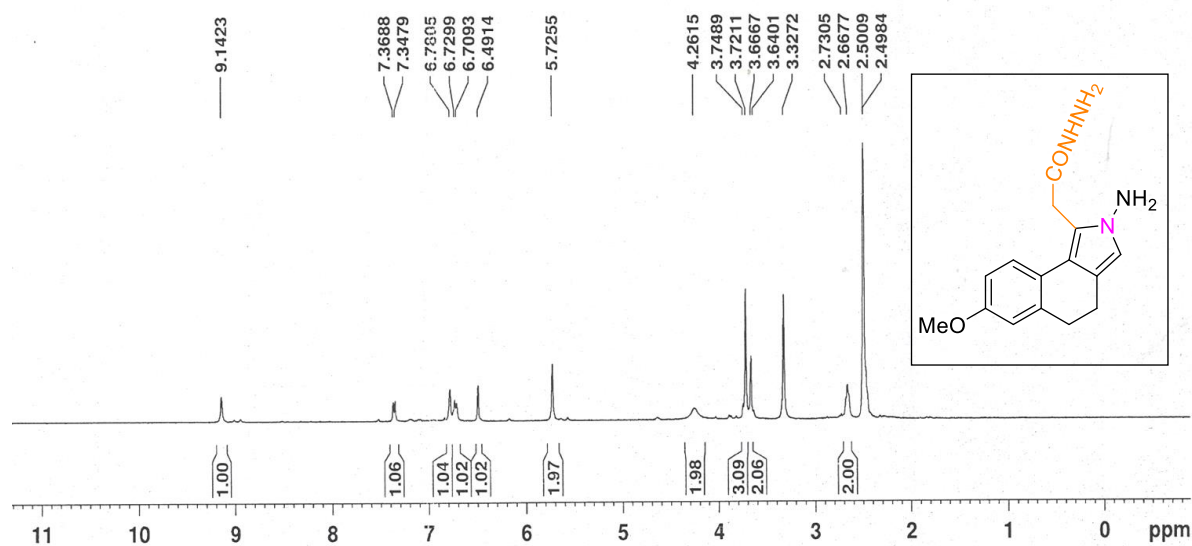
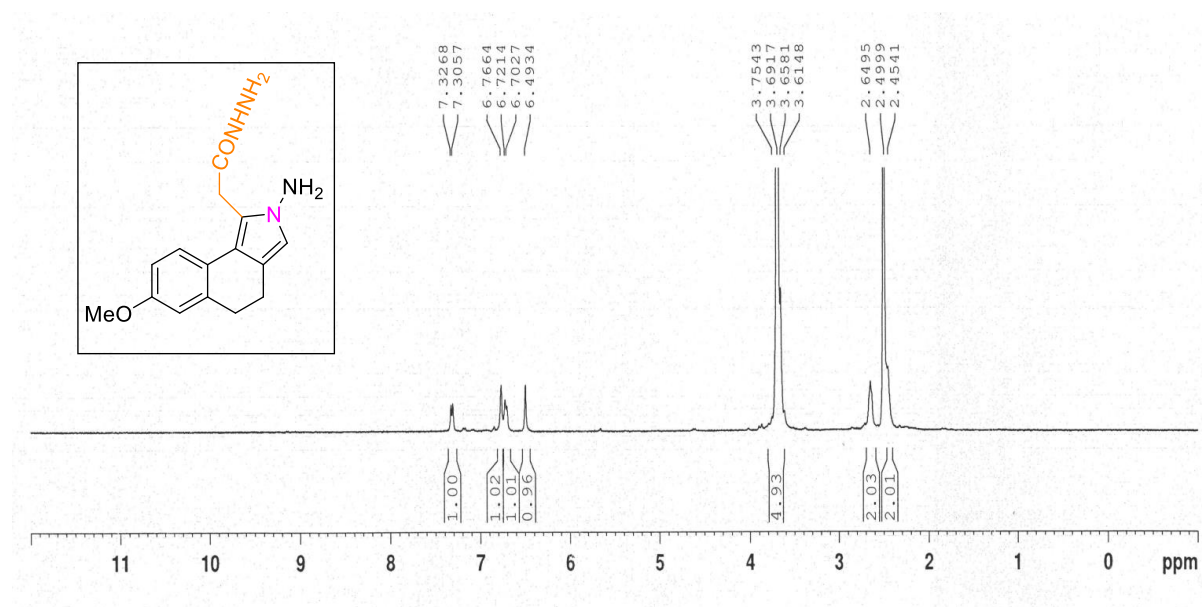
5,7,8,9,10,11,12,15-Octahydro-6H-benzo[f]cyclohepta[3,4]pyrrolo[1,2-a][1,5]diazocin-6-one: (5f)

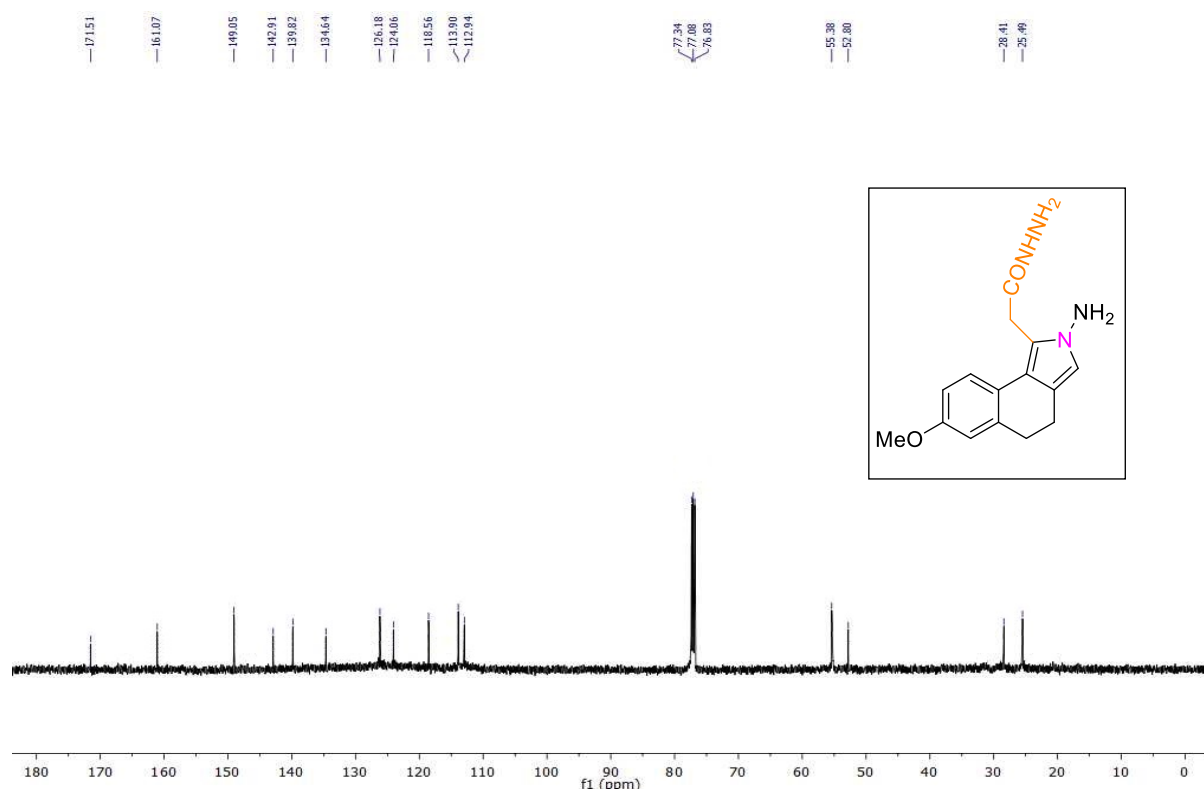
Off white liquid (151.2 mg for **4k** 54%; 145.6 mg for **4l** 52%). ^1H NMR (400 MHz, CDCl_3): δ 8.37 (s, 1H), 7.48 (dd, $J = 7.4, 1.6$ Hz, 1H), 7.40 – 7.31 (m, 2H), 7.23 (d, $J = 7.2$ Hz, 1H), 6.41 (s, 1H), 4.83 (s, 2H), 3.26 (s, 2H), 2.51 – 2.43 (m, 4H), 1.76 – 1.72 (m, 3H), 1.59 – 1.56 (m, 3H). ^{13}C NMR (101 MHz, CDCl_3): δ 172.2, 138.0, 132.1, 131.9, 129.9, 128.4, 125.4, 124.8, 124.7, 119.6, 119.1, 49.9, 33.2, 31.7, 30.1, 29.9, 28.1, 26.7. HRMS calcd. for $\text{C}_{18}\text{H}_{21}\text{N}_2\text{O}$: $(\text{M}+\text{H})^+$ 281.1656, found : 281.1657.

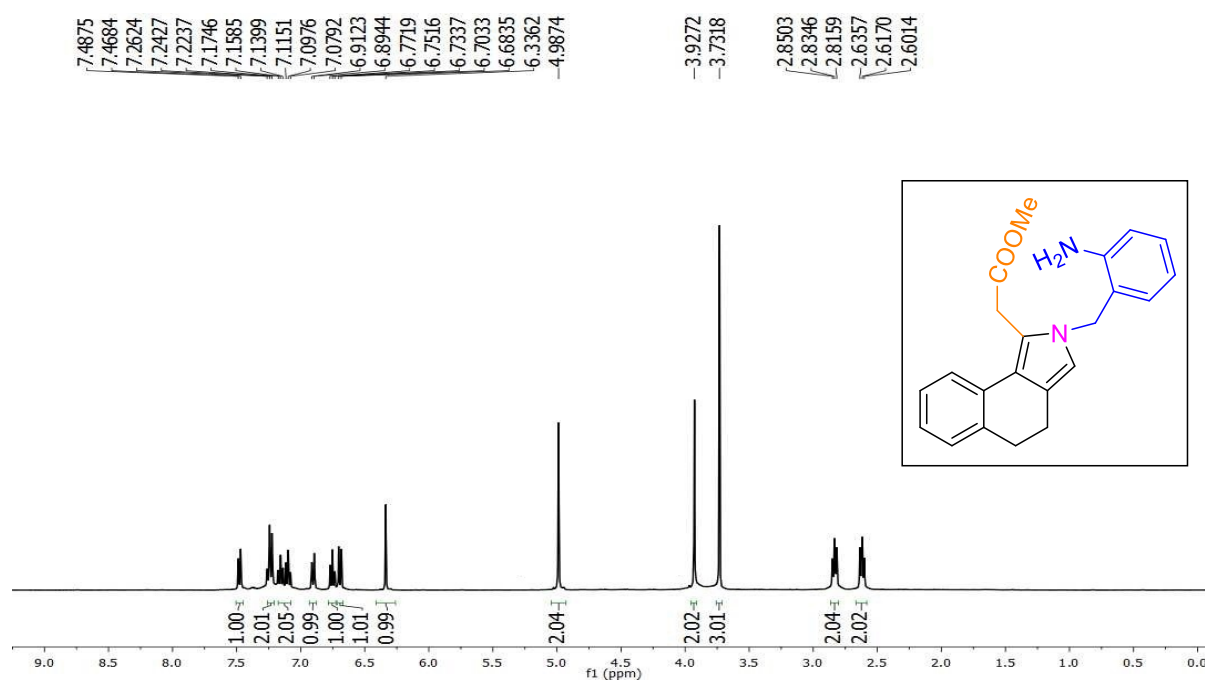
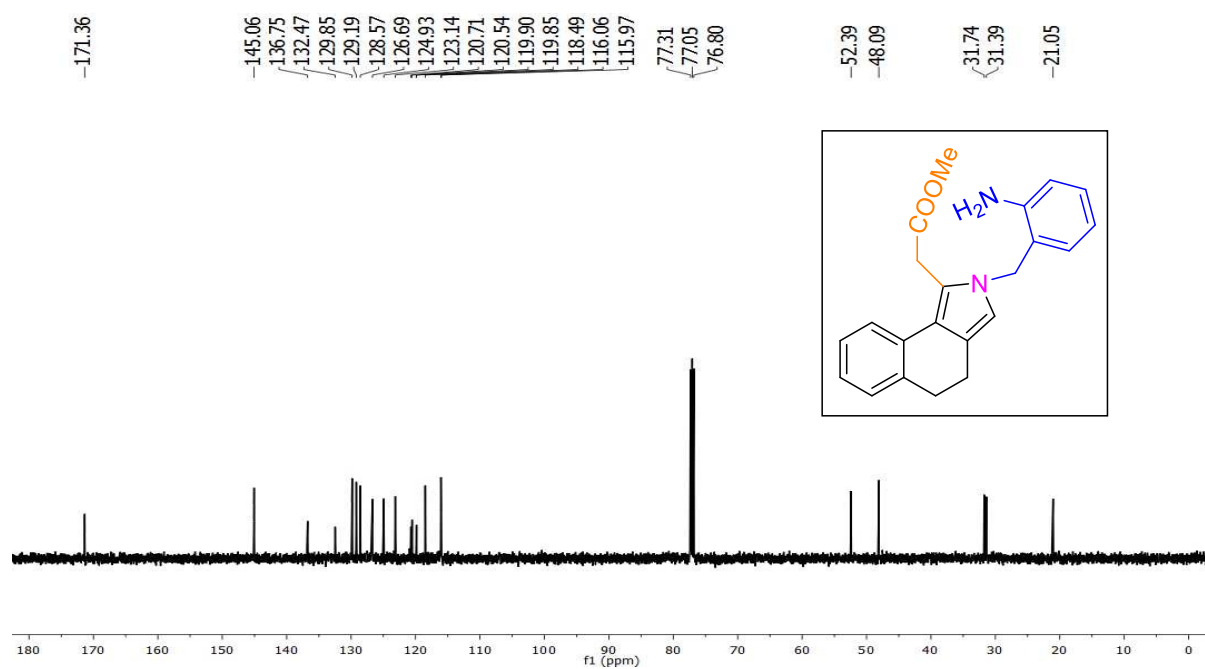
5.6.2. Representative NMR spectra:

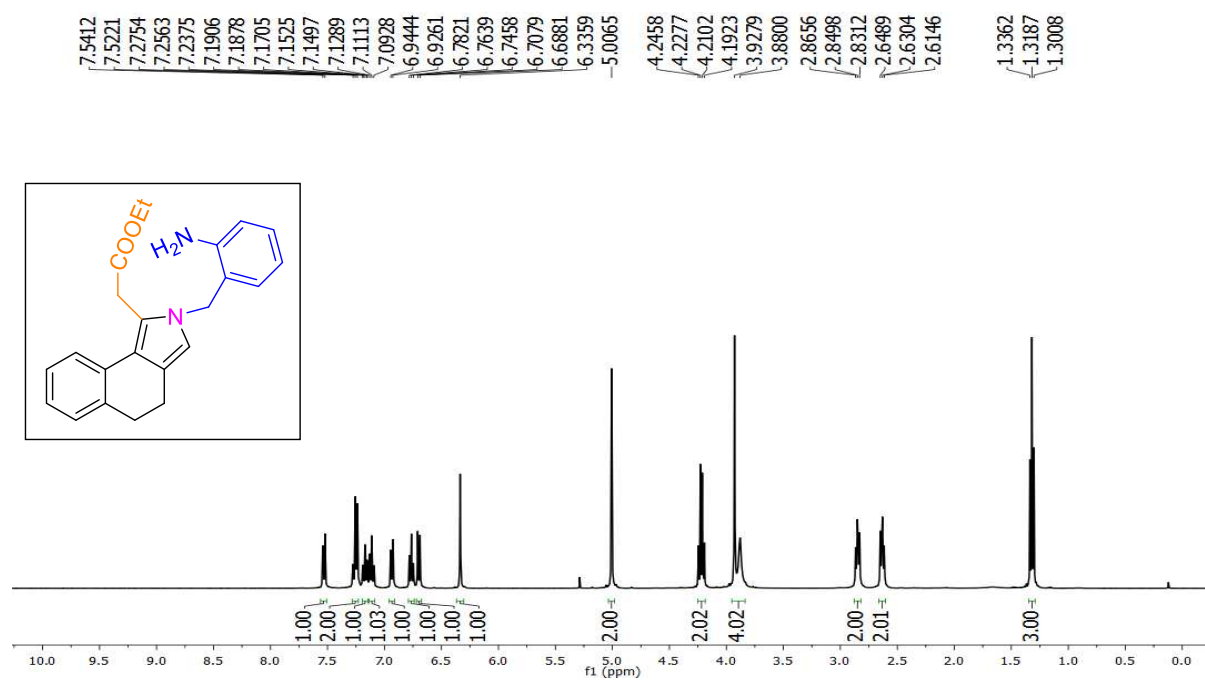
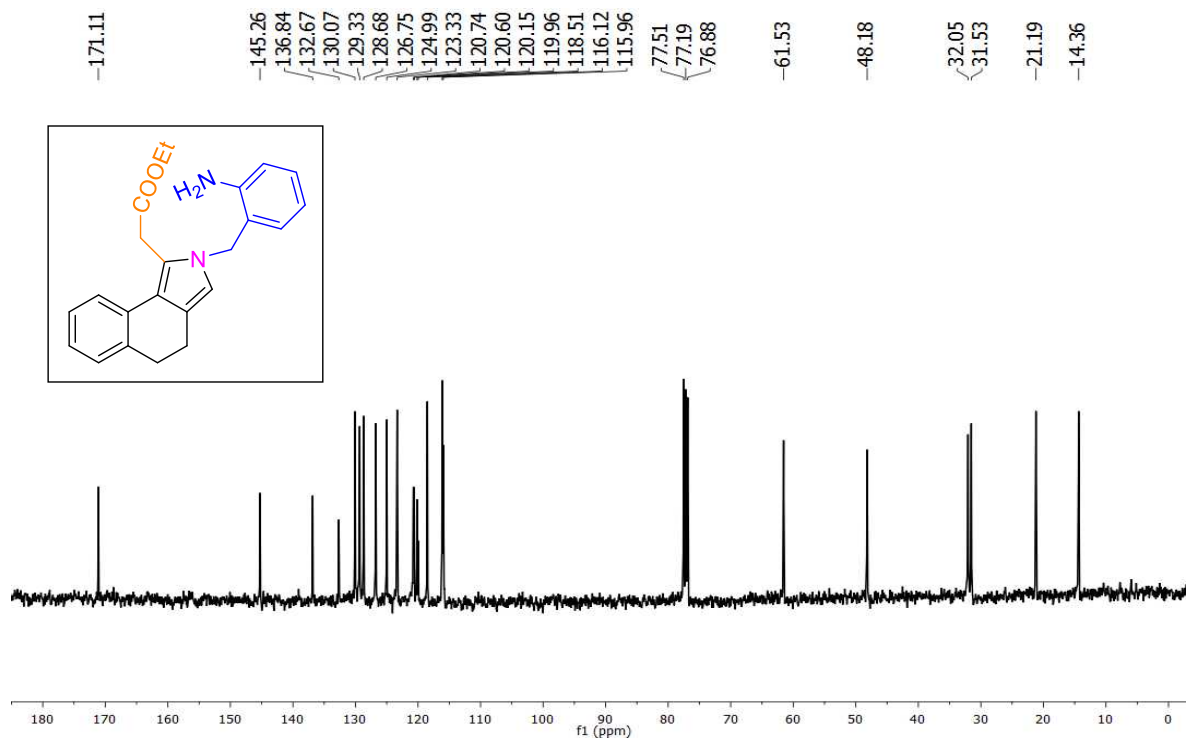
 ^1H NMR spectra of 2b (500 MHz, CDCl_3): ^{13}C NMR spectra of 2b (126 MHz, CDCl_3):

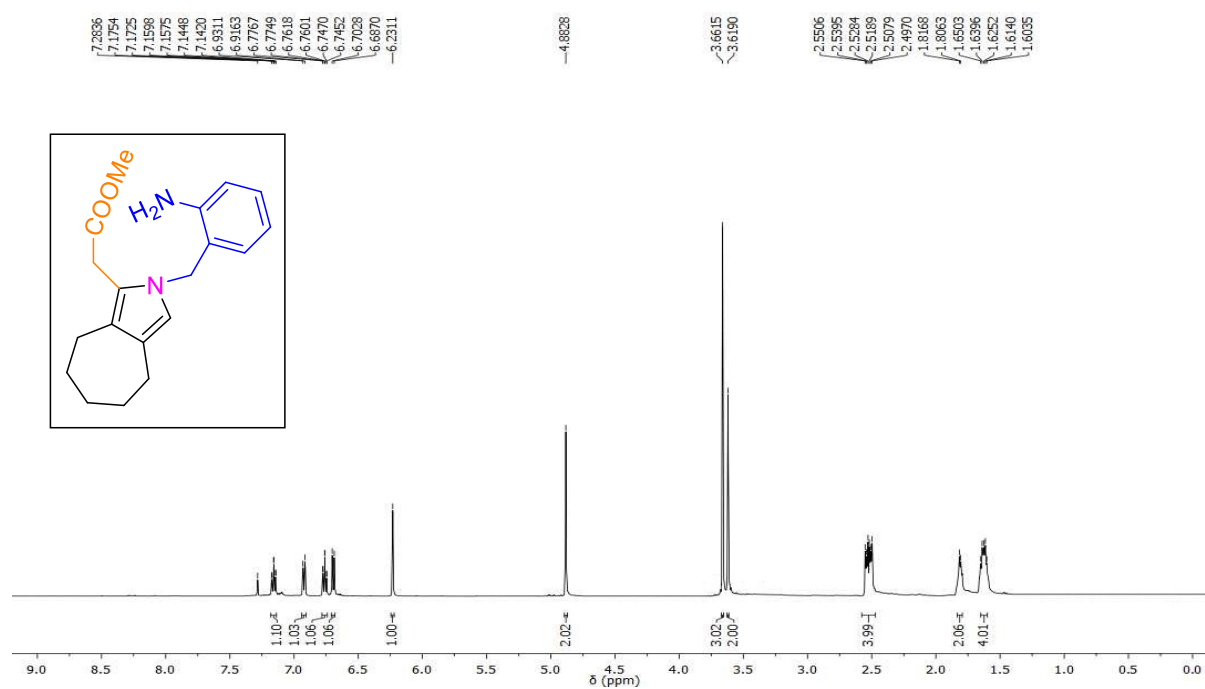
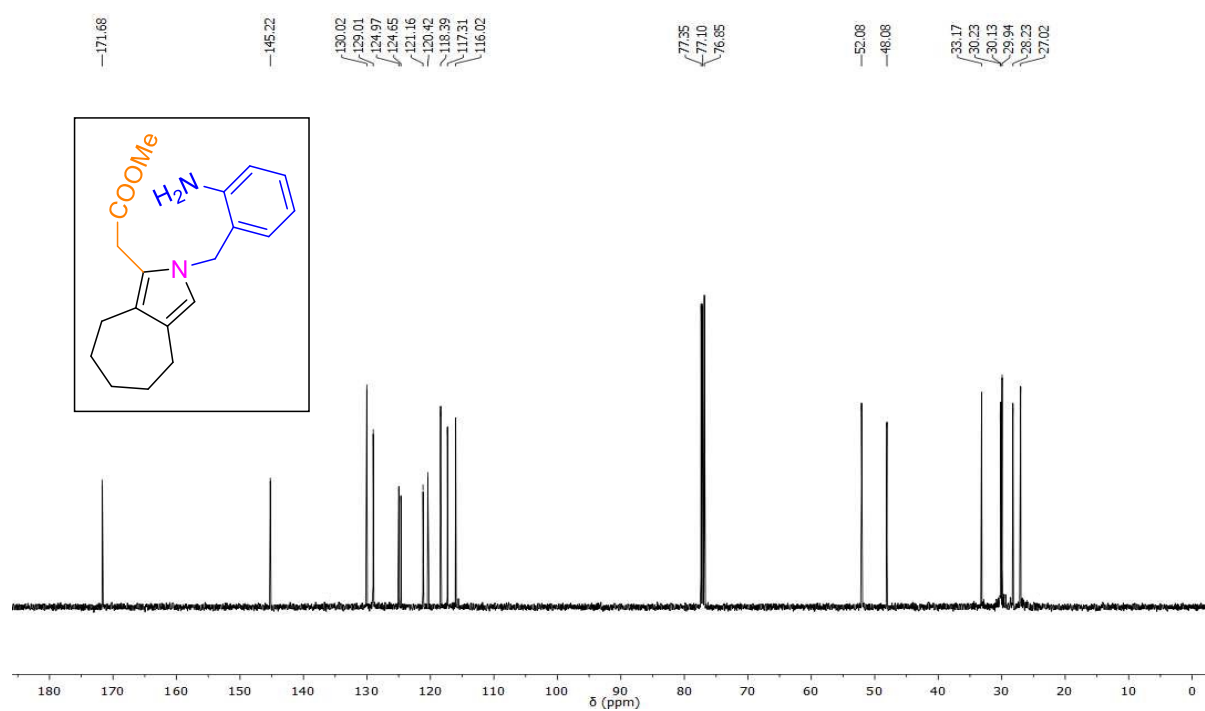
^1H NMR spectra of 2c (500 MHz, CDCl_3): **^{13}C NMR spectra of 2c (126 MHz, CDCl_3):**

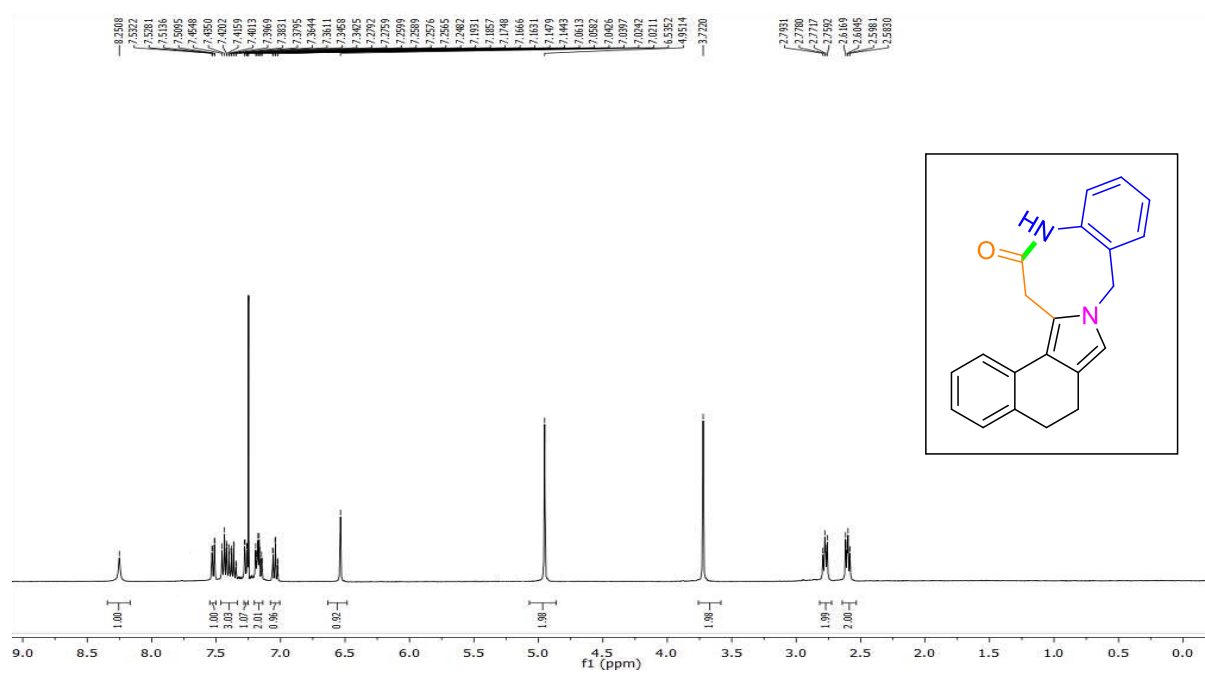
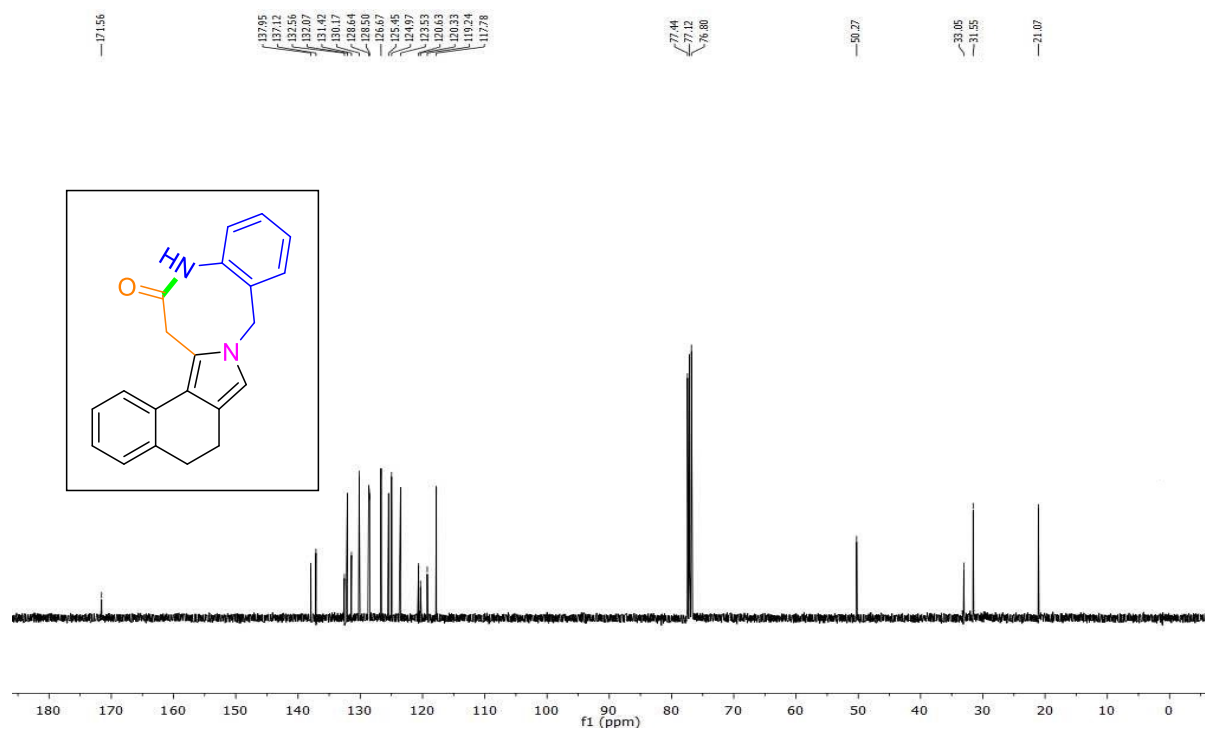
^1H NMR spectra of 3a (400 MHz, DMSO- d_6): **^1H NMR spectra of 3a (400 MHz, D $_2$ O exchange):**

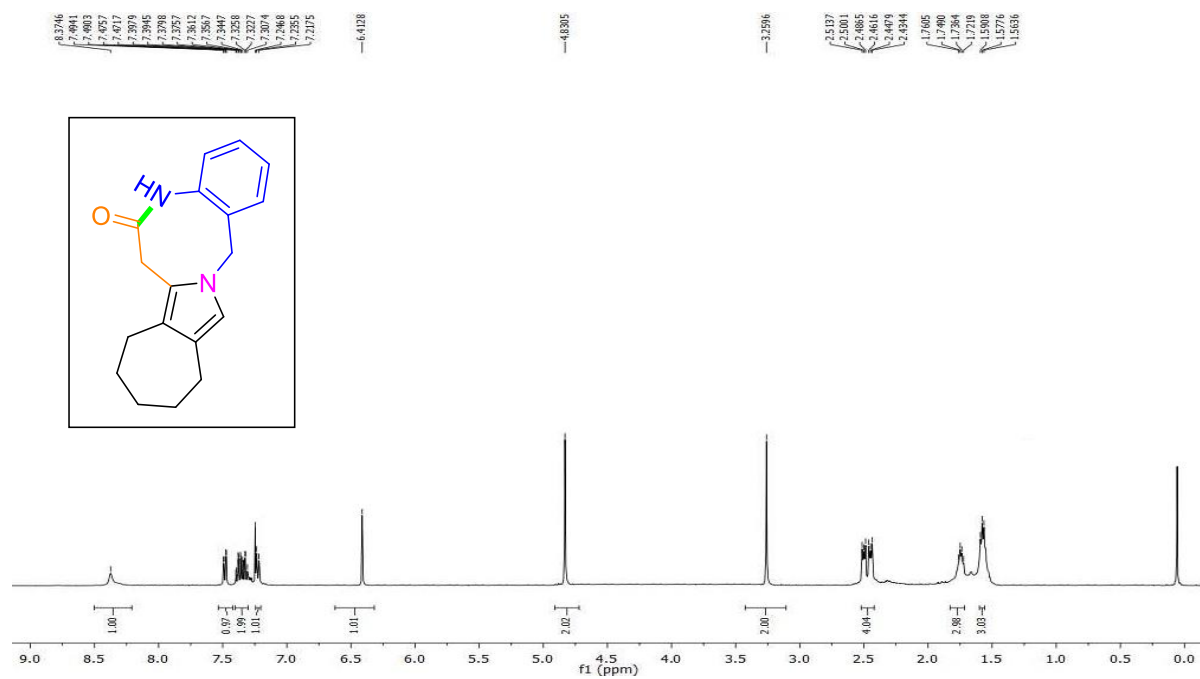
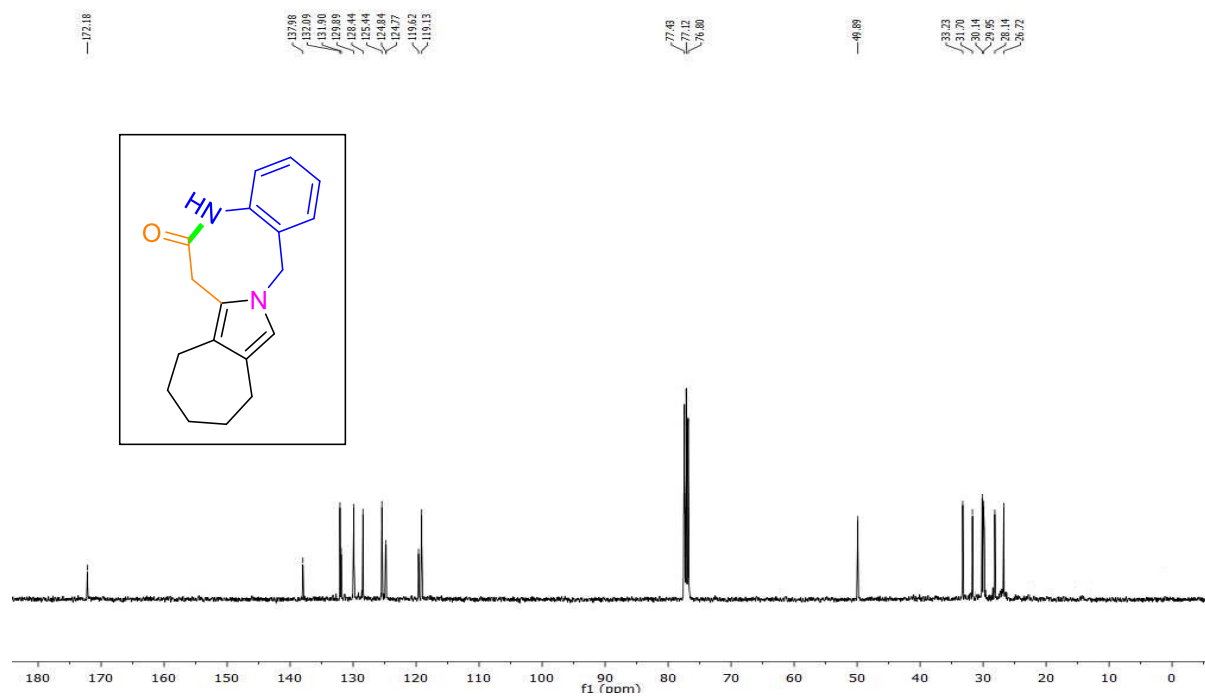
^{13}C NMR spectra of 3a (126 MHz, CDCl_3):

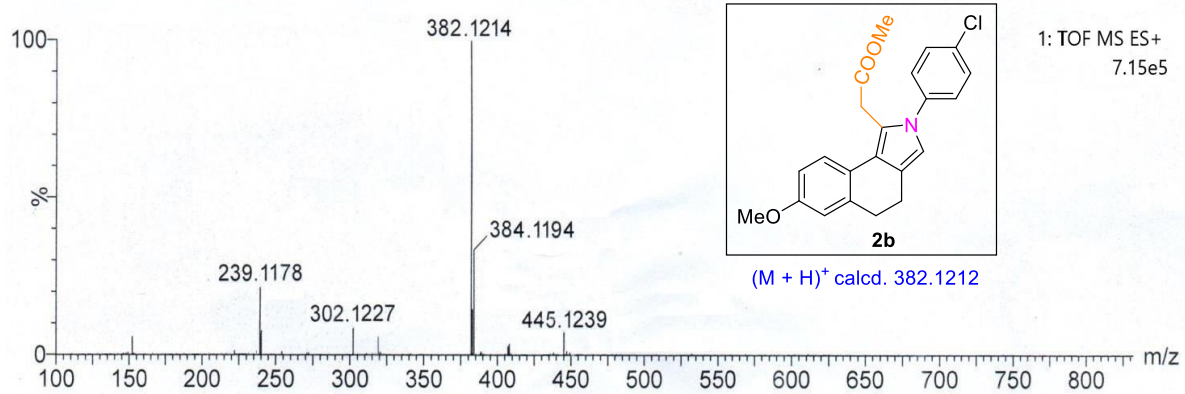
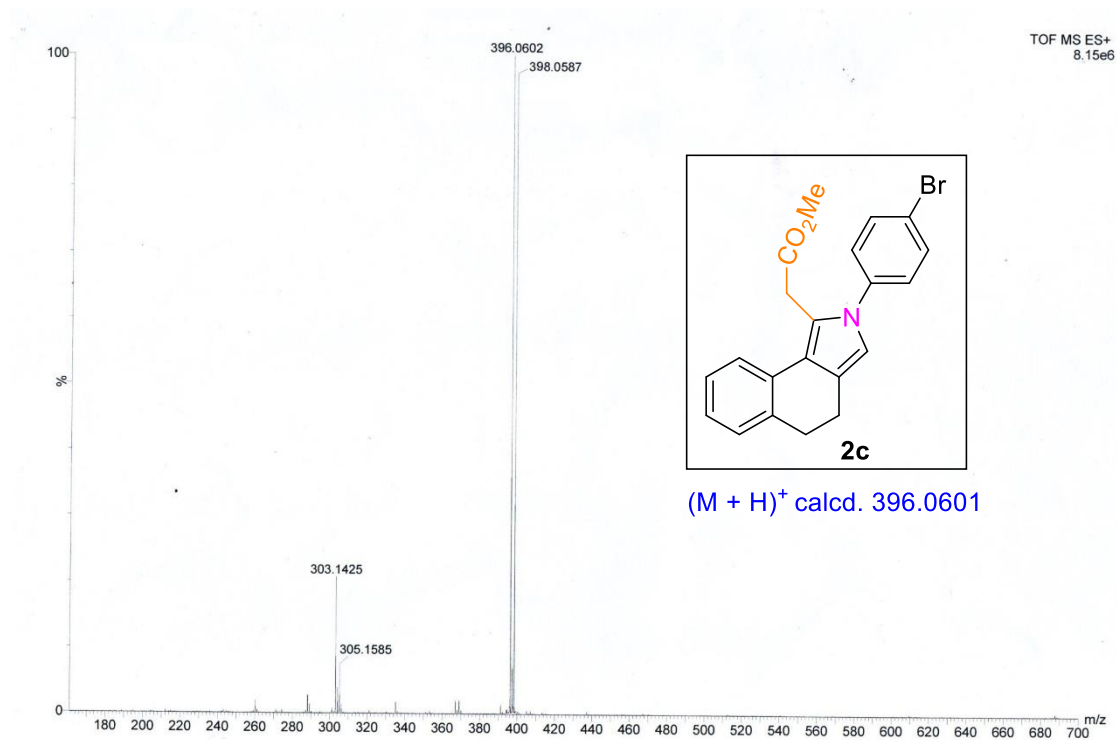
^1H NMR spectra of 4a (400 MHz, CDCl_3): **^{13}C NMR spectra of 4a (126 MHz, CDCl_3):**

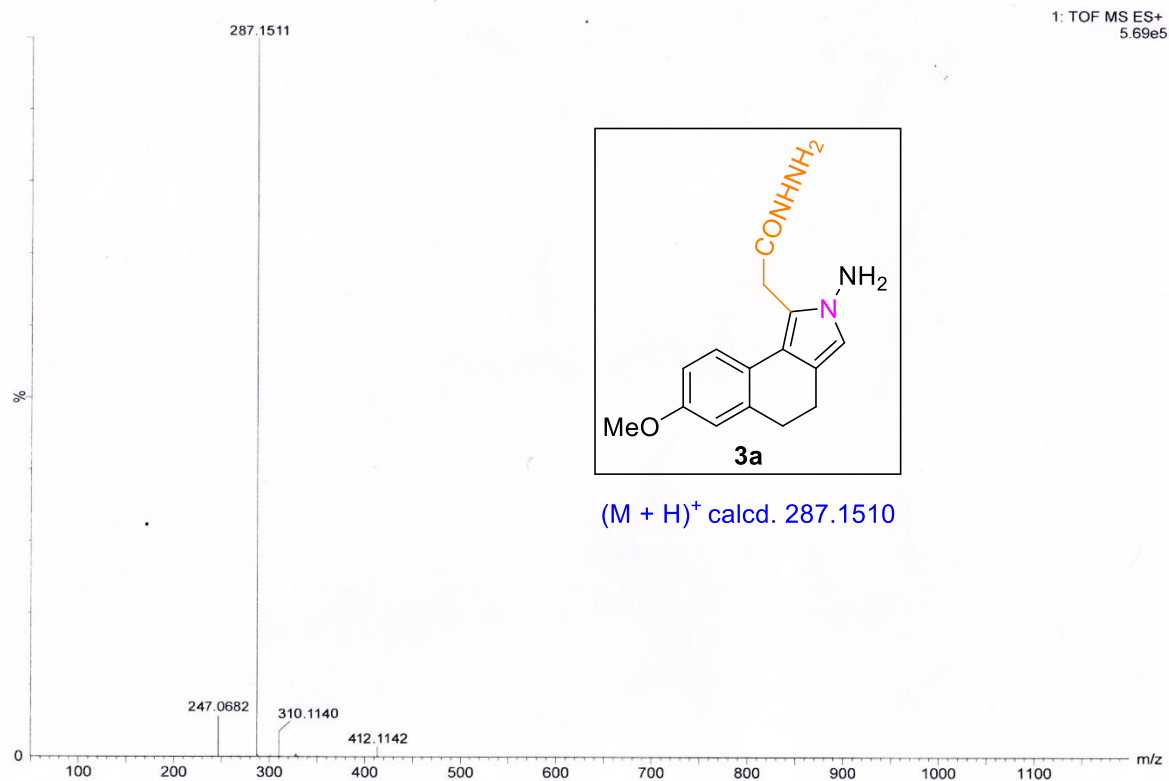
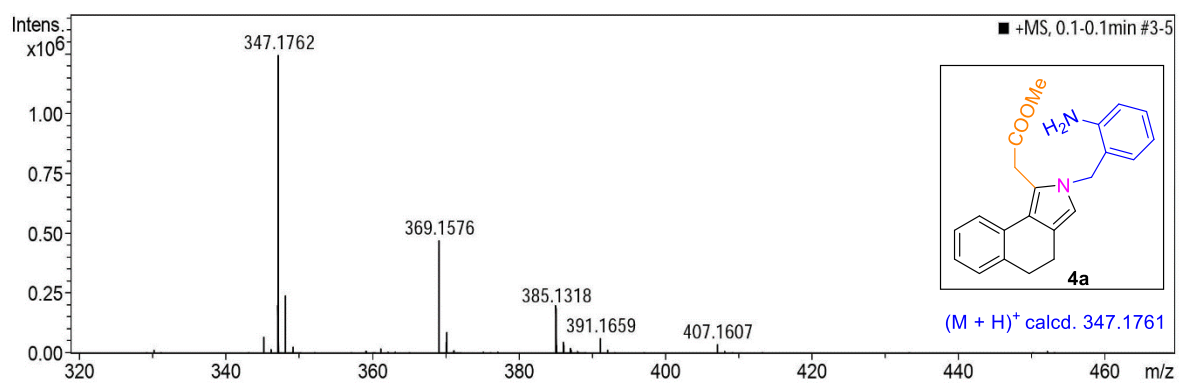
^1H NMR spectra of 4b (400 MHz, CDCl_3): **^{13}C NMR spectra of 4b (101 MHz, CDCl_3):**

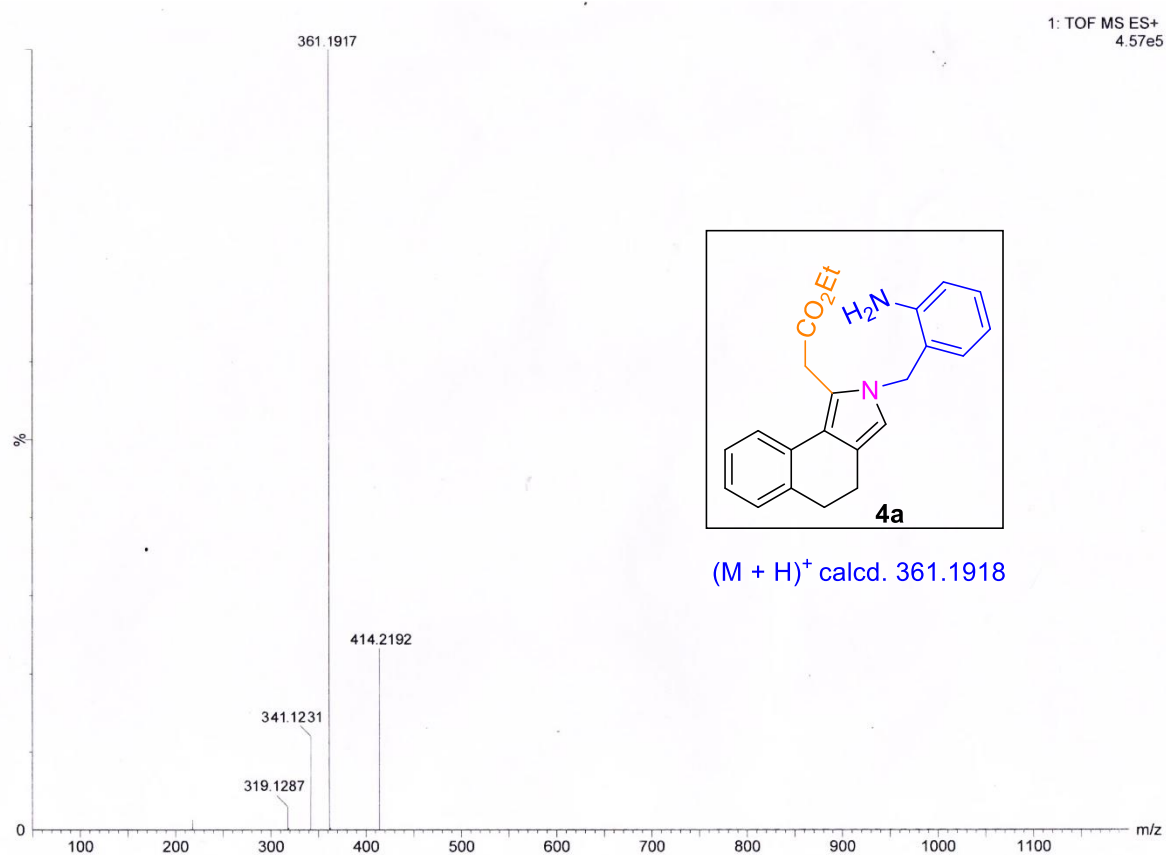
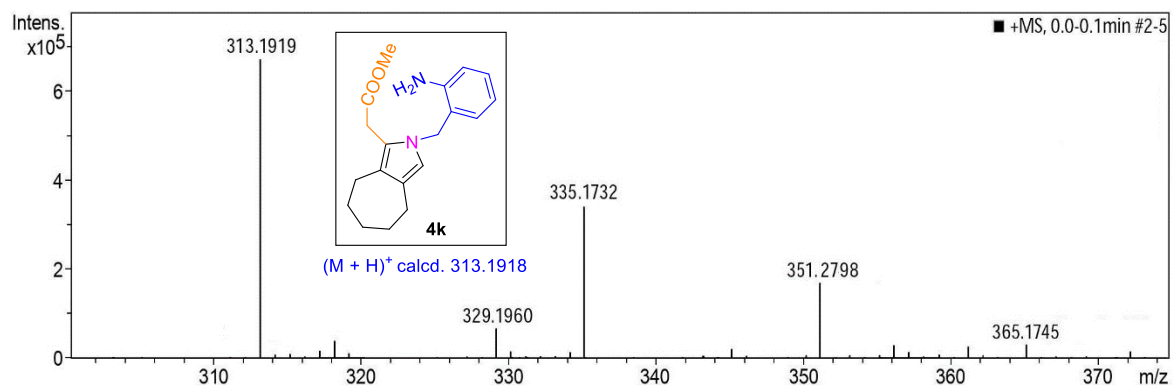
^1H NMR spectra of 4k (500 MHz, CDCl_3): **^{13}C NMR spectra of 4k (126 MHz, CDCl_3):**

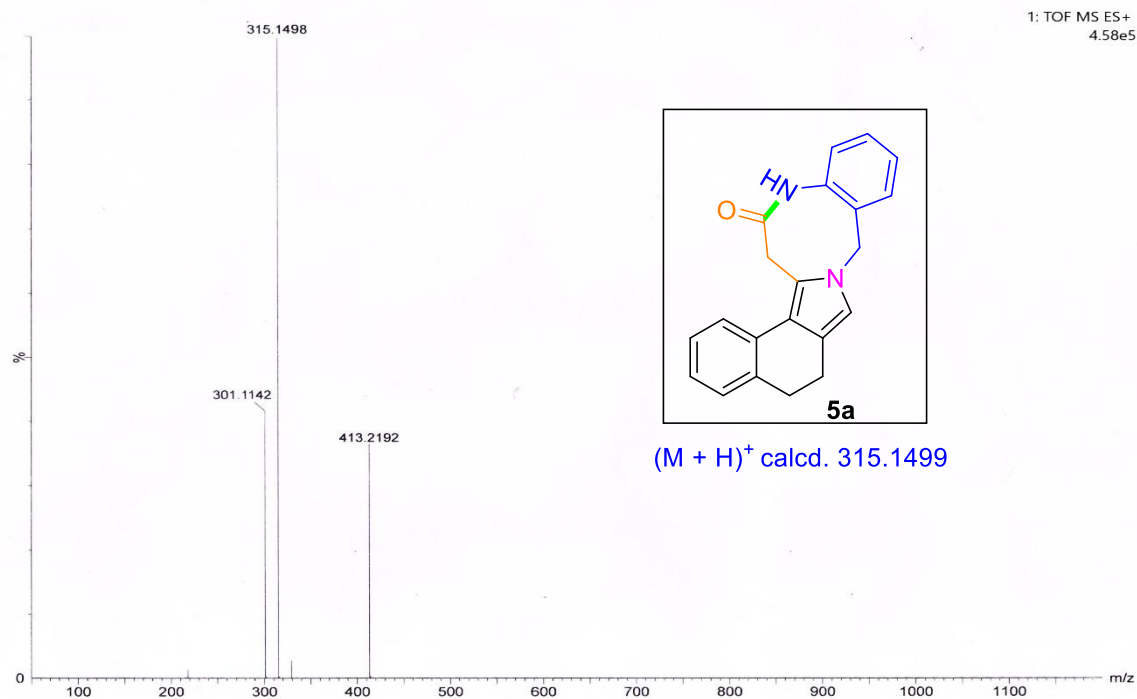
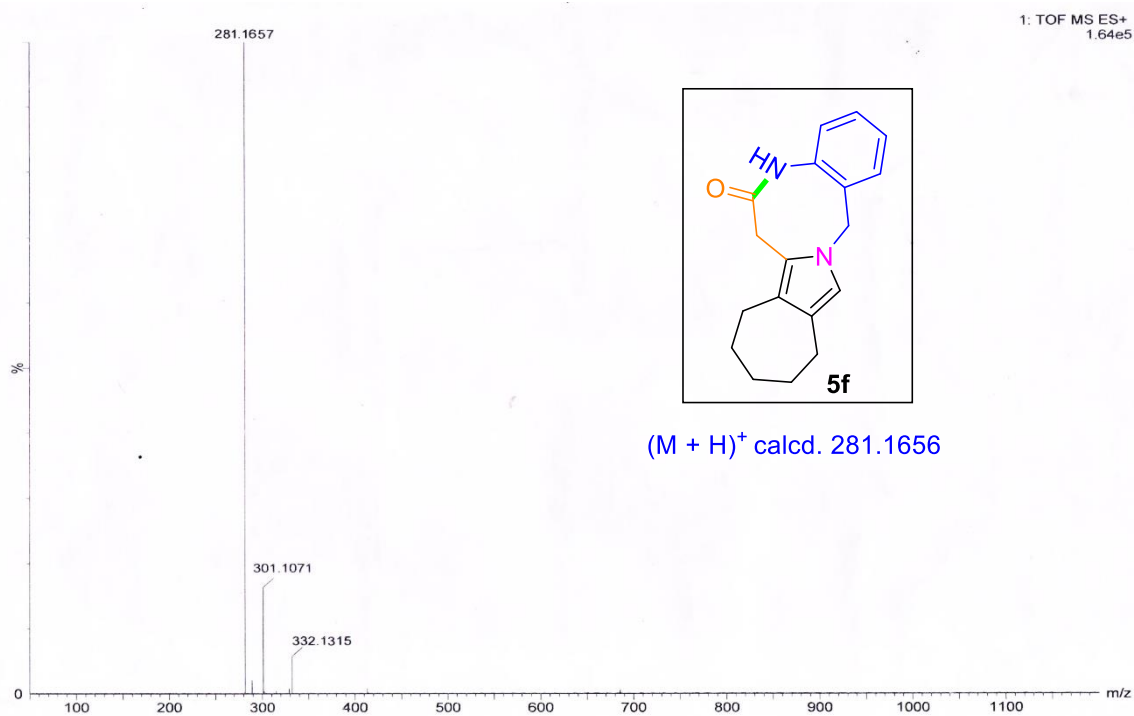
^1H NMR spectra of 5a (400 MHz, CDCl_3): **^{13}C NMR spectra of 5a (101 MHz, CDCl_3):**

^1H NMR spectra of 5f (400 MHz, CDCl_3): **^{13}C NMR spectra of 5f (101 MHz, CDCl_3):**

5.6.3. Representative High-resolution mass spectra:**Methyl 2-(2-(4-chlorophenyl)-7-methoxy-4,5-dihydro-2H-benzo[e]isoindol-1-yl)acetate:****(2b)****2-(4-bromophenyl)-1-(2-(methylperoxy)-2l-ethyl)-4,5-dihydro-2H-benzo[e]isoindole: (2c)**

2-(2-Amino-7-methoxy-4,5-dihydro-2H-benzo[e]isoindol-1-yl)acetohydrazide: (3a)**Methyl 2-(2-(2-aminobenzyl)-4,5-dihydro-2H-benzo[e]isoindol-1-yl)acetate: (4a)**

Ethyl 2-(2-(2-aminobenzyl)-4,5-dihydro-2H-benzo[e]isoindol-1-yl)acetate: (4b)**Methyl 2-(2-(2-aminobenzyl)-2,4,5,6,7,8-hexahydrocyclohepta[c]pyrrol-1-yl)acetate: (4k)**

5,12,13,16-Tetrahydrobenzo[g]benzo[6,7][1,5]diazocino[2,1-a]isoindol-6(7H)-one: (5a)**5,7,8,9,10,11,12,15-Octahydro-6H-benzo[f]cyclohepta[3,4]pyrrolo[1,2-a][1,5]diazocin-6-one: (5f)**

5.7. References:

1. N. J. Basha, S. M. Basavarajaiah and K. Shyamsunder, *Mol. Divers.*, 2022, **26**, 2915-2937.
2. (a) K. Seipp, L. Geske and T. Opatz, *Mar. Drugs*, 2021, **19**, 514; (b) L. Ding, H-M. Dahse and C. Hertweck, *J. Nat. Prod.*, 2012, **75**, 617-621; (c) M. Chen, Y. Yan, H. Ge, W-H. Jiao, Z. Zhang and H-W Lin, *Eur. J. Org. Chem.*, 2020, **2020**, 2583-2591; (d) F. Zhuab, G. Y. Chena, J. Wub and J. Pan, *Nat. Prod. Res.*, 2013, **27**, 1960-1964; (e) C-L Shao, C-Y Wang, Y-C. Gu, M-Y Wei, J-H. Pan, D-S. Deng, Z-G. She and Y-C. Lin, *Bioorg. Med. Chem.*, 2010, **20**, 3284-3286; (f) A. Domagala, T. Jarosz and M. Lapkowski, *Eur. J. Med. Chem.*, 2015, **100**, 176-187; (g) H. Hoffmann and T. Lindel, *Synthesis*, 2003, **12**, 1753-1783.
3. M. A-Abbasinejada, F. N-Shshrokhhabadi and M. Mohammad, *Mol. Divers.*, 2020, **24**, 1205-1222.
4. (a) C. Huang, C. Yang, W. Zhang, Y. Zhu, L. Ma, Z. Fang and C. Zhang, *J Antibiot*, 2019, **72**, 311-315; (b) B. Zhou, Y. Huang, H-J. Zhang, J-Q. Li and W-j. Ding, *Tetrahedron*, 2019, **75**, 3958-3961; (c) B. Wu, J. Wiese, R. Schmaljohann and J. F. Imhoff, *Mar. Drugs*, 2016, **14**, 204; (d) W. Zhang, Z. Liu, S. Li, T. Yang, Q. Zhang, L. Ma, X. Tian, H. Zhang, C. Huang, S. Zhang, J. Ju, Y. Shen and C. Zhang, *Org. Lett.*, 2102, **14**, 3364-3367.
5. (a) A. Redzicka, Z. Czyznikowska, B. Wiatrak, K. Gebczak and A. Kochel, *Int. J. Mol. Sci.*, 2021, **22**, 1410; (b) D. Tzankova, S. Vladimirova, L. Peikova and M. Georgieva, *J. Chem. Technol. Metall.*, 2018, **53**, 451-464.
6. (a) R. Ferraz, D. Silva, A. R. Dias, V. Dias, M. M. Santos, L. Pinheiro, C. Prudêncio, J. P. Noronha, Ž. Petrovski and L. C. Branco, *Pharmaceutics*, 2020, **12**, 221; (b) X. Li, P. Dong, T. Zhang, G. Cai, Y. Chen, H. Dong, F. Yang, L. Zhang, Y. Mao, J. Feng, C. Bai, F. He and W. Tao, *ACS Med. Chem. Lett.*, 2022, **13**, 701-706; (c) C-X. Zhuo, X. Zhang and S-L. You, *ACS Catal.*, 2016, **6**, 5307-5310; (d) S. Boonya-udtayan, M. Eno, S. Ruchirawat, C. Mahidol and N. Thasana, *Tetrahedron*, 2012, **68**, 10293-10301.
7. (a) A. Bera, Sk A. Ali, A. Saha and S. Samanta, *Synth. Commun.*, 2021, **51**, 2377-2386; (b) Z. J. Sheng, Y. M. Shi, X. Xu, S. Bellyneck, K. Zhang, Z. Y. Du, X. Xu, F. Maurel and C-Z. Dong, *ChemistryOpen*, 2019, **8**, 34-40; (c) B. Zhou, Y-Q. Zhang, K. Zhang, M-Y. Yang, Y-B. Chen, Y. Li, Q. Peng, S-F. Zhu, Q-L. Zhou and L-W. Ye,

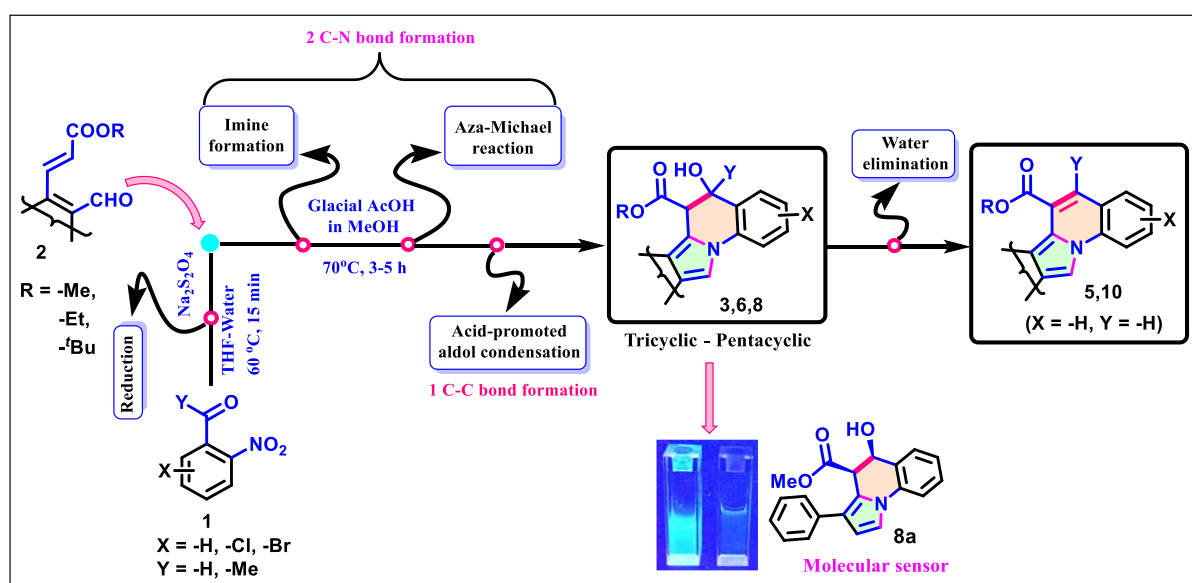
- Nat. Commun.*, 2019, **10**, 3234; (d) P. A. N. V. Harita, P. S. Kumar, S. K. R. Guduru, P. Ravula, J N N. S. Chandra, *EXCLI J.*, 2017, **16**, 1090-1098.
8. (a) I. A. Kochnev, A. Y. Barkov, N. S. Zimnitskiy, V. Y. Korotaev and V. Y. Sosnovskikh, *Molecules*, 2022, **27**, 8456; (b) Y-M. Shen, G. Grampp, N. Leesakul, H-W. Hu and J-H. Xu, *Eur. J. Org. Chem.*, 2007, **2007**, 3718-3726.
9. K. Kim, H. Yoo and E. K. Lee, *Polymers*, 2022, **14**, 2960.
10. X. Jiang, S. Yue, K. Chen, Z. Shao, C. Li, Y. Su and J. Zhao, *Chin Chem Lett*, 2019, **30**, 2271-2273.
11. M. A. Abozeid, H.Y. Kim and K. Oh, *Org. Lett.*, 2022, **24**, 1812-1816.
12. E. E. Schultz and R. Sarpong, *J. Am. Chem. Soc.*, 2013, **135**, 4696-4699.
13. N. Yasmin and J. K. Ray, *Synlett*, 2010, **6**, 924-930.
14. A. Jana, S. K. Manna, S. K. Mondal, A. Mandal, S. K. Manna, A. Jana, B. K. Senapati, M. Jana and S. Samanta, *Tetrahedron Lett.*, 2016, **57**, 3722-3726.
15. S. K. Mondal, S. K. Manna, A. Mandal, S. Samanta and J. K. Ray, *Tetrahedron Lett.* 2014, **55**, 6411-6415.
16. S. Kiren, F. Grimes, H. Mohammed and D. Alazawi, *Tetrahedron*, 2021, **78**, 131807.
17. S. K. Mondal, A. Mandal, S. K. Manna, Sk A. Ali, M. Hossain, V. Venugopal, Avijit Jana and S. Samanta, *Org. Biomol. Chem.*, 2017, **15**, 2411-2421.
18. Sk. A. Ali, S. K. Mondal, T. Das, S. K. Manna, A. Bera, D. Dafadar, S. Nasakar, M. R. Molla and S. Samanta, *Org. Biomol. Chem.*, 2019, **17**, 4652-4662.
19. (a) G. Meera, K. R. Rohit, S. Saranyaa and G. Anilkumar, *RSC Adv.*, 2020, **10**, 36031-36041; (b) H. Karakus and Y. Dürüst, *Mol. Divers.*, 2017, **21**, 53-60.
20. Z-H. Zhang, J-J. Li and T-S. Li, *Ultrason. Sonochem.*, 2008, **15**, 673-676.
21. A. K. Sahoo, A. Rakshit, A. Dahiya, A. Pan and B. K. Patel, *Org. Lett.*, 2022, **24**, 1918-1923.
22. P. J. Smith, Y. Jiang, Z. Tong, H. D. Pickford, K. E. Christensen, J. Nugent and E. A. Anderson, *Org. Lett.*, 2021, **23**, 6547-6552.
23. J. B. Bremner and W. Sengpracha, *Tetrahedron*, 2005, **61**, 941-953.
24. (a) C. Pramanik, P. Barik, Sk A. Ali, D. S. Nayak, M. Iqbal, A. Mandal, R. Jana, S. Giri and S. Samanta, *New J. Chem.*, 2023, **47**, 6476-6527; (b) S. Wang, S. Wang, S. Song, Q. Gao, C. Wen, Z. Zhang, L. Zheng and J. Xiang, *J. Org. Chem.*, 2021, **86**, 6458-6466.
25. E. Y. Zelina, T. A. Nevolina, Ludmila N. Sorotskaja, D. A. Skvortsov, I. V. Trushkov and M. G. Uchuskin, *J. Org. Chem.*, 2018, **83**, 11747-11757.

-
26. J. Li, J. Li, Y. Xu, Y. Wang, L. Zhang, L. Ding, Y. Xuan, T. Pang and H. Lin, *Nat. Prod. Res.*, 2016, **30**, 800-805.
27. (a) R. E. Khidre, B. F. Abdel-Wahab, O. Y. Alothman, *J. Chem.*, 2014, *Article ID 217596*, 1-15; (b) M. Vlasselaer and W. Dehaen, *Molecules*, 2016, **21**, 785; (c) T. Hoshi, E. Ota, Y. Inokuma and J. Yamaguchi, *Org. Lett.*, 2019, **21**, 10081-10084.
28. (a) H. Pessoa-Mahana, K. G. M. Ara'nguiz, R. Araya-Maturana and C. D. Pessoa-Mahana, *Synth. Commun.*, 2005, **35**, 1493-1500; (b) X. Che, L. Zheng, Q. Dang and X. Bai, *J. Org. Chem.*, 2008, **73**, 1147-1149; (c) K. C. Majumdar, *RSC Adv.*, 2011, **1**, 1152-1170; (d) J. B. Bremner, H. F. Russell, B. W. Skelton and A. H. White, *Heterocycles*, 2000, **53**, 277-290; (e) J. B. Bremner and W. Sengpracha, *Tetrahedron*, 2005, **61**, 941-953.
29. (a) S. K. Manna, A. Mandal, S. K. Mondal, A. K. Adak, A. Jana, S. Das, S. Chattopadhyay, S. Roy, S. K. Ghorai, S. Samanta, M. Hossain and M. Baidya, *Org. Biomol. Chem.*, 2015, **13**, 8037-8047; (b) S. K. Manna, S. K. Mondal, A. Ahmed, A. Mandal, A. Jana, M. Iqbal, S. Samanta and J. K. Ray, *RSC Adv.*, 2014, **4**, 2474-2481; (c) S. K. Mondal, Sk. A. Ali, S. K. Manna, A. Mandal, B. K. Senapati, M. Hossain and S. Samanta, *ChemSelect.*, 2017, **2**, 9312-9318.
30. Q. Yang, M. Sheng, J. J. Henkelis, S. Tu, E. Wiensch, H. Zhang, Y. Zhang, C. Tucker and D. E. Ejeh, *Org. Process Res. Dev.*, 2019, **23**, 2210-2217.
31. Sk. A. Ali, A. Bera, S. K. Manna, S. Santra, M. R. Molla and S. Samanta, *Eur. J. Org. Chem.*, 2020, **18**, 2754-2760.

Chapter 6

Synthesis of multi-fused pyrrolo[1,2-a]quinoline systems by tandem aza-Michael-aldol reactions and their application to molecular sensing studies

Synthesis of multi-fused pyrrolo[1,2-*a*]quinoline systems by tandem aza-Michael-aldol reactions and their application to molecular sensing studies



(Contents of this chapter have been published in *J.Org. Chem.*, 2023, **88**, 5622-5638)

6.1. Introduction:

Multi-fused pyrroles expand the fused pyrrole family and generate a new class pyrrolo[1,2-*a*]quinoline. Pyrrolo[1,2-*a*]quinoline systems are one the most important scaffold of fused pyrrole family. Tricyclic to pentacyclic pyrrolo[1,2-*a*]quinolines are extensively found in numerous number of natural products with their biological activities such as anti-cancer, antiviral, antibacterial, antioxidant, antihypoxia, multidrug-resistance reversing, and HIV-1 integrase inhibitory activities as depicted in **Figure 6.1**.¹

6.1.1. Pyrroloquinoline based natural alkaloids:

An ancient Chinese folk remedy, Crispine A, was identified from *Carduus crispus* and was used to alleviate stomachaches, colds, and rheumatism.^{1a} KC 11404, another tricyclic natural product, is used as an anti-asthmatic agent.^{1b} Jantinine and Hirsutine, isoquinoline alkaloids, are isolated from *Cocculus hirsutus*, and it is highly reputed for its medicinal properties.^{1c-e} Goniomitine was obtained from the root bark of *Gonioma Malagasy*,^{1f, g} and Leucomidine B was identified from the bark of *Leuconotis griffithii*.^{1f, h} Both substances are used as 5-HT₆ antagonists.^{1f} CRR-271, a novel alkaloid, can inhibit the poly (ADP-ribose) polymerase-1 and protect cells from oxidative DNA damage.^{1c, i} Tronocarpine is a pentacyclic alkaloid that is used as an anticancer agent.^{1b} Lamellarins D, pentacyclic pyrroloquinoline-based alkaloids, were isolated from the marine prosobranch mollusk *Lamellaria sp.* in 1985. The anti-cancer activity of Lamellarin helps the development of new drugs. Lamellarin D has the effective potential to inhibit topoisomerase I. Recently, it has been used as the only topoisomerase I inhibitor in clinic instead of camptothecin-based medicine.^{1j-1}

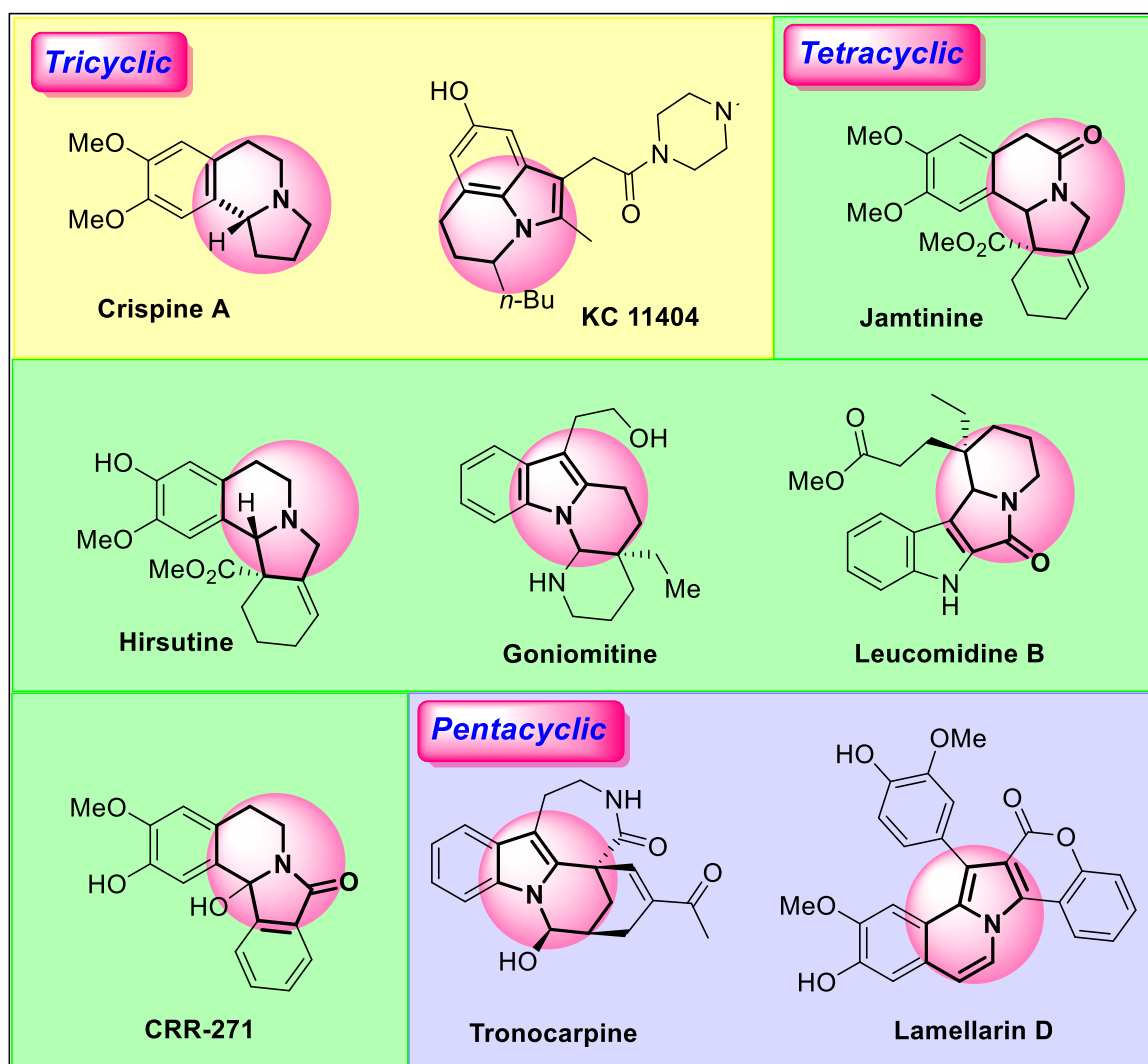


Figure 6.1. Tricyclic-Pentacyclic pyrrolo[1,2-*a*]quinoline based natural products.

6.1.2. Pyrroloquinoline based drug molecules:

Besides the availability of a large number of bio-active natural products pyrroloquinoline pharmacophores have tremendous benefits in medicinal chemistry. The medicinal potential of this scaffold opened a new window to the medicinal chemists for the development of drug synthesis. Topotecan and Camptothecin are two valuable pyrroloquinoline based marketed drug used as anti-cancer medicine (**Figure 6.2**).²

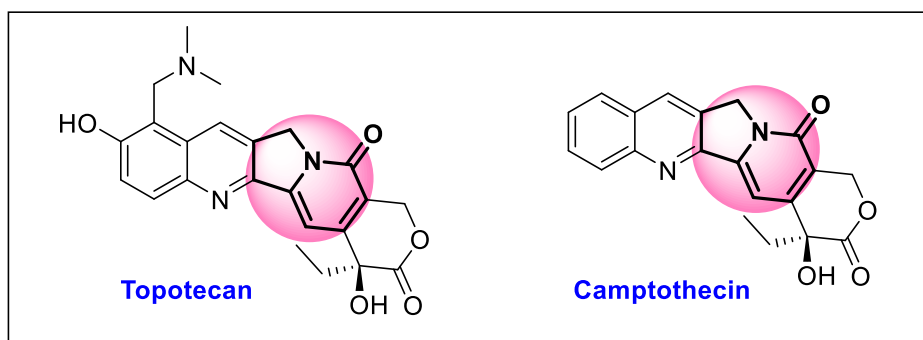
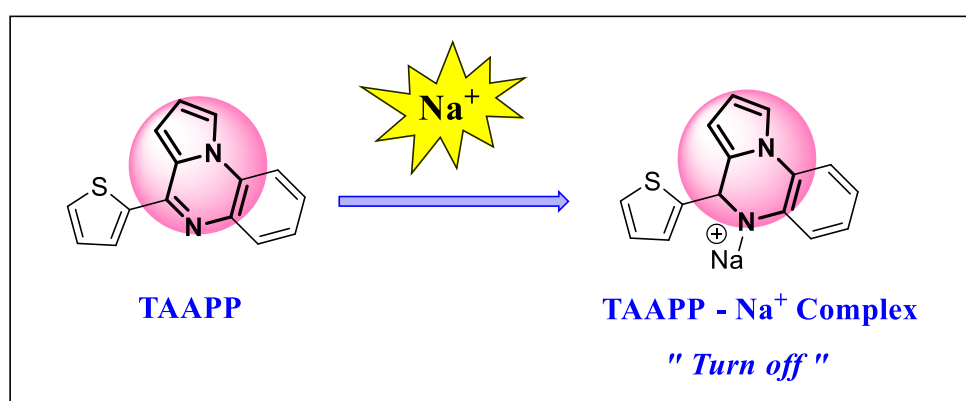


Figure 6.2. Pyrroloquinoline based marketed drug.

6.1.3. Pyrroloquinoline based fluorescent probe:

In addition, the pyrrolo[1,2-*a*]quinoline derivatives have equal importance as a fluorescence probe. A novel thiophene-embedded pyrrolo[1,2-*a*]quinoxaline, TAAPP, was developed as a fluorescent sensor for the detection of selective nanomolar sodium ions. The emission spectra show that the ligand selectively recognised the Na^+ ions *via* a “turn-off” mechanism. The emission intensity of TAAPP was significantly changed by the quenching effect with the addition of Na^+ ions (**Scheme 6.1**).³



Scheme 6.1. Detection of sodium ions of a pyrrolo[1,2-*a*]quinoxaline based fluorescent sensor.

The organic emission-tunable fluorescent probe Seoul-Fluor and its analogous compound named Kaleidolizine (KIz) have aggregation-induced emission (AIE) properties, and C3-Indo-Fluoro, a full-color-tunable fluorophore, was developed (**Figure 6.3**).⁴

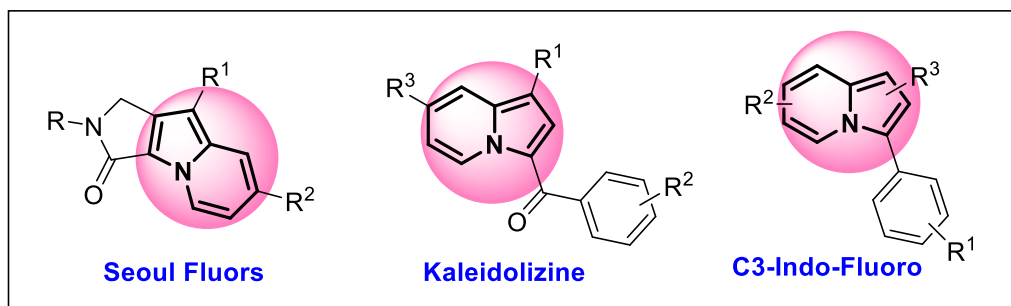
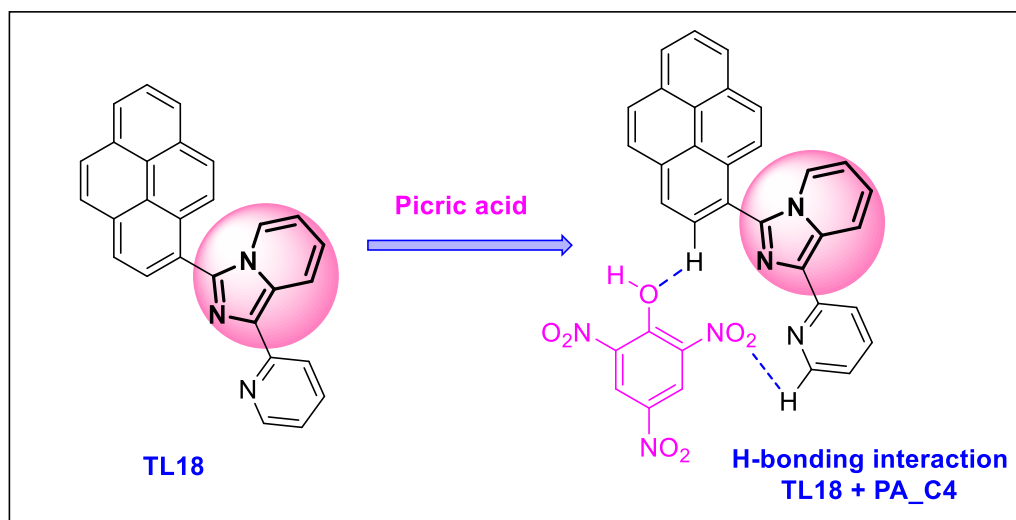


Figure 6.3. Pyrroloquinoline based organic fluorophore.

6.1.4. Molecular sensing properties:

Besides these versatile applications, pyrroloquinoline moieties show good molecular sensing properties. In this context, a new pyrene tethered 1-(pyridin-2-yl)imidazo[1,5-*a*]pyridine-based fluorescent probe, TL18, has been developed and has shown high selectivity and sensitivity towards picric acid compared to other explosives and organic/inorganic acids (**Scheme 6.2**). This probe successfully attained a detection limit of 63 nM, according to the quantitative analysis of fluorescence titration TL18 with picric acid.⁵



Scheme 6.2. Molecular sensing properties of pyrroloquinoline based fluorophore.

6.1.5. Pyrroloquinolines in material science:

In the world of lighting technology, organic light-emitting diodes (OLEDs) have gathered an enormous amount of attention, and they emit light by utilising their electroluminescence behaviour. Different researcher designed the substrates *via* the balancing the holes and electrons in the emitting layer, bipolar host materials have typically been employed in phosphorescent organic light-emitting diodes (PhOLEDs). Herein, three bipolar materials

such as 4-(9-phenyl-9*H*-carbazol-3-yl)pyrrolo[1,2-*a*]quinoxaline (3CBZ-PQ), 4-(4-(9*H*-carbazol-9-yl)phenyl)pyrrolo[1,2-*a*]quinoxaline (4CBZ-PQ), and *N,N*-diphenyl-4-(pyrrolo[1,2-*a*]quinoxalin-4-yl)aniline (TPA-PQ) have been employed as highly efficient red PhOLEDs (**Figure 6.4**).⁶

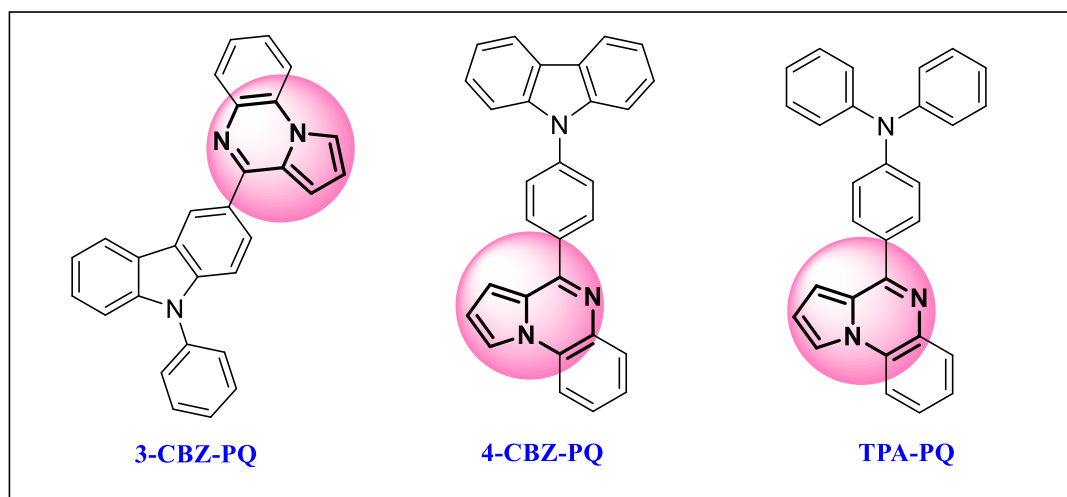


Figure 6.4. Pyrrolo[1,2-*a*]quinoxaline based organic light emitting diodes.

Besides the sensing or AIE properties, it has been used in the electroluminescence material when dicyanomethylene-4*H*-pyran chromophores (DCM) are attached with pyrroloquinoline derivatives, i.e., DCQTB. Chemists have shown a great deal of interest in dicyanomethylene-4*H*-pyran chromophores (DCM), one type of electroluminescent diode (OLED) emitter, due to their superior photophysical characteristics. DCM chromophores have a donor- π -acceptor structure with a wide absorption band resulting from the internal charge transfer (ICT) process. DCQTB displays blue-shifted absorbance, improved electroluminescence (EL) efficiency, and red-shifted fluorescence (**Figure 6.5**).⁷

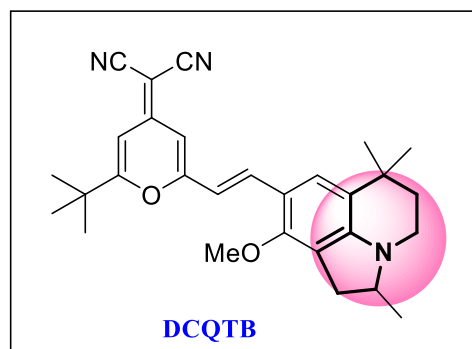


Figure 6.5. Pyrrolo[1,2-*a*]quinoline containing chromophore.

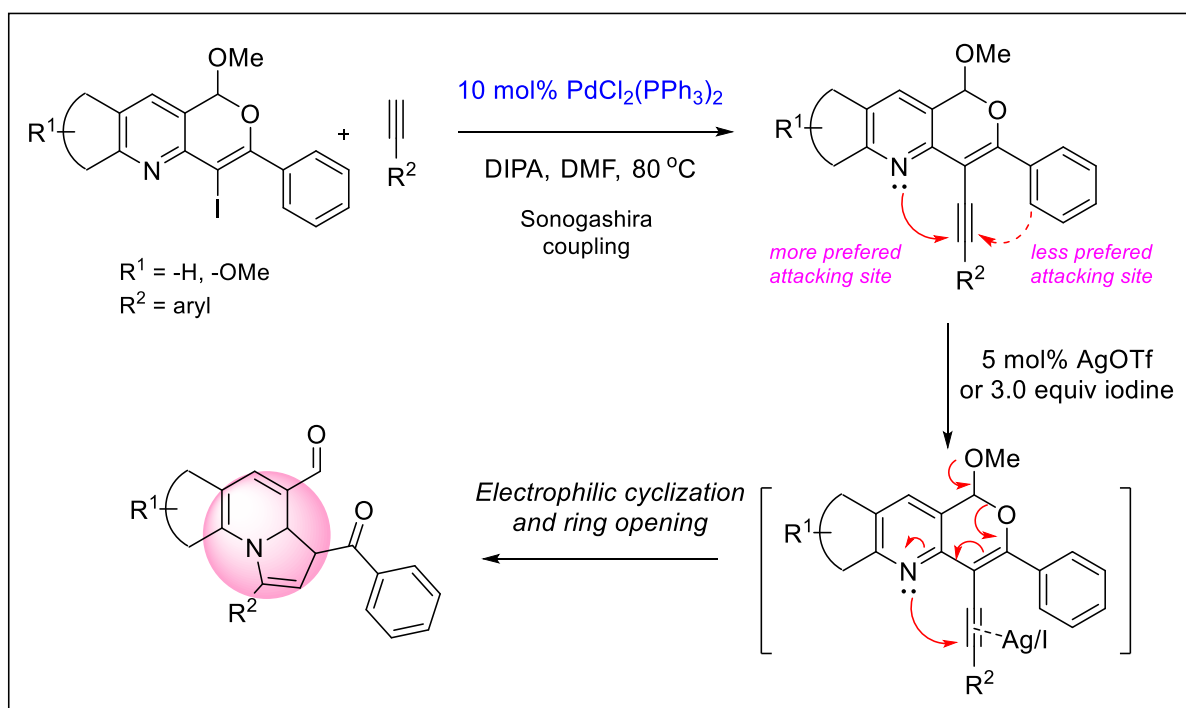
After a brief study on the numerous numbers of bioactive alkaloids and the diverse uses of pyrroloquinolines, we are now engrossed on the various synthetic methodologies of pyrroloquinolines that have been synthesized by conventional and green pathways with a pyridine ring, a pyrrole ring, or without a pyridine and pyrrole ring at all.

6.2. Literature survey:

6.2.1. Synthesis of pyrroloquinoline in the presence of pyridine ring:

(a) Metal-catalyzed synthetic approaches:

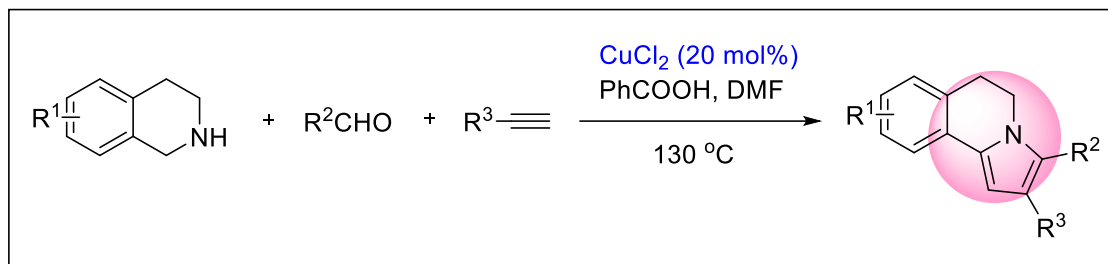
A. K. Verma *et al.*⁸ developed an efficient synthetic strategy for the pyrrolo[1,2-*a*]quinoline derivatives through a site-selective cyclization, and consequently, in the presence of a silver catalyst or inexpensive iodine, a ring opening of pyran takes place under mild conditions (**Scheme 6.3**). In this site-selective approach, the attack by the pyridyl nitrogen predominates over the attack by the aryl ring and leads to the *5-endo-dig* cyclization. The preferential attacking site was also demonstrated by Density Functional Theory.



Scheme 6.3. Silver catalyzed site selective synthetic route to pyrrolo[1,2-*a*]quinolines.

H-L. Cui and X-H. Chen⁹ established a copper-catalyzed synthetic methodology for pyrrolo[2,1-*a*]isoquinoline derivatives using tetrahydroisoquinolines, aldehydes, and terminal

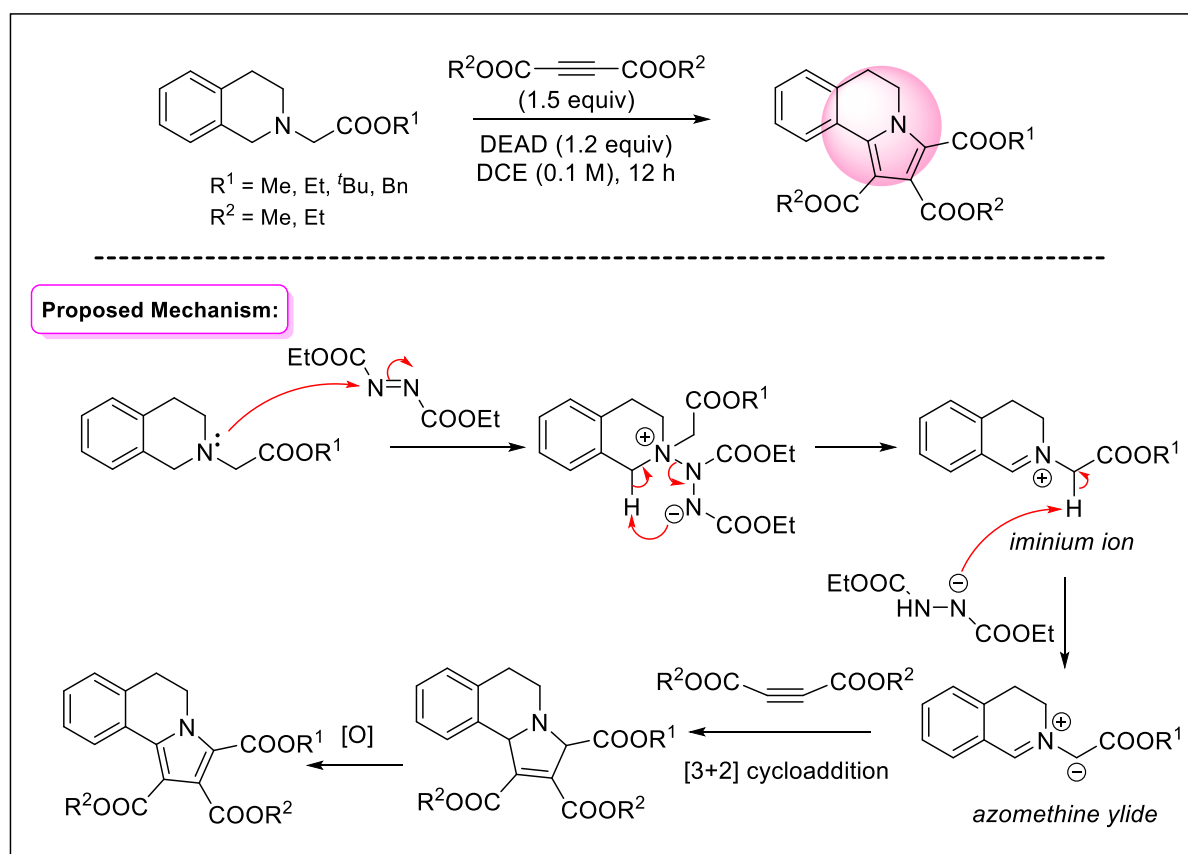
alkynes *via* a cascade sequence of condensation, addition, oxidation, and cyclization (**Scheme 6.4**).



Scheme 6.4. Copper-catalyzed synthetic methodology for pyrrolo[2,1-*a*]isoquinolines.

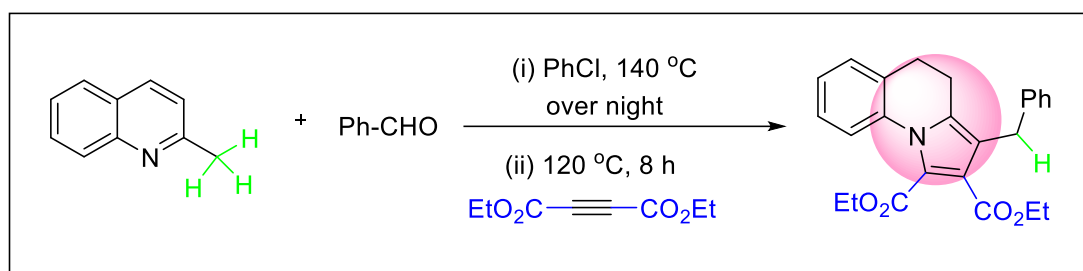
(b) Metal-free synthetic approaches:

L. Zhen and his research group¹⁰ developed a novel diethyl azodicarboxylate (DEAD)-promoted metal-free methodology for the formation of pyrrolo[2,1-*a*]isoquinolines *via* an oxidative tandem [3+2] cycloaddition reaction (**Scheme 6.5**). DEAD is a versatile oxidant that helps the transformation from tertiary amines to azomethine ylides smoothly through iminium ion formation by oxidation-deprotonation steps. The entire protocol offers a simple oxidation step with wide substrate scope and good to excellent yields.



Scheme 6.5. DEAD promoted metal-free synthetic route of pyrrolo[1,2-*a*]quinolines.

X. L. Ma and his co-workers¹¹ established an easy operational catalyst-free synthesis for the pyrrolo[1,2-*a*]quinolines *via* a [3+2] cycloaddition reaction starting from 2-methylquinolines, alkynoates, and aldehydes (**Scheme 6.6**). A one-pot reaction has two steps, beginning with readily available materials and the air-tolerant reaction condition, all of which simplify the process. Only water molecules are eliminated here as a by-product, thus the protocol offers an environmentally friendly process with a broad application in organic chemistry.

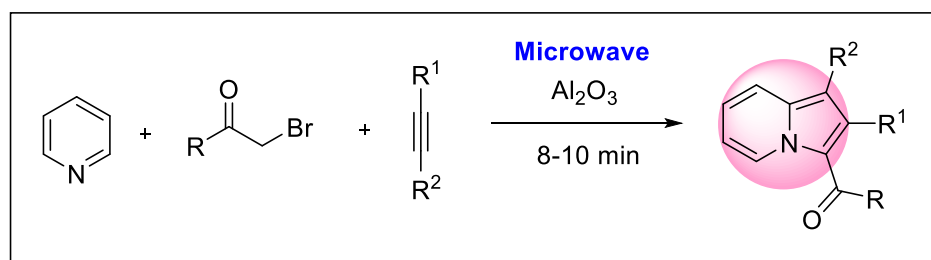


Scheme 6.6. Synthesis of pyrrolo[1,2-*a*]quinolines *via* [3+2] cycloaddition reaction.

(c) Green approaches:

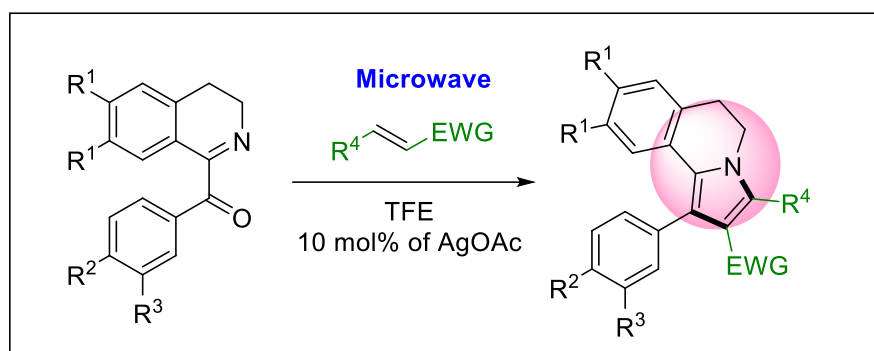
(i) Microwave assisted synthetic approaches:

R. C. Boruah *et al.*¹² reported a microwave-assisted three-component indolizine synthesis process using pyridine, acyl bromide, and acetylene in the presence of basic alumina in a one-pot strategy (**Scheme 6.7**).



Scheme 6.7. Microwave promoted three-component synthesis procedure of indolizine.

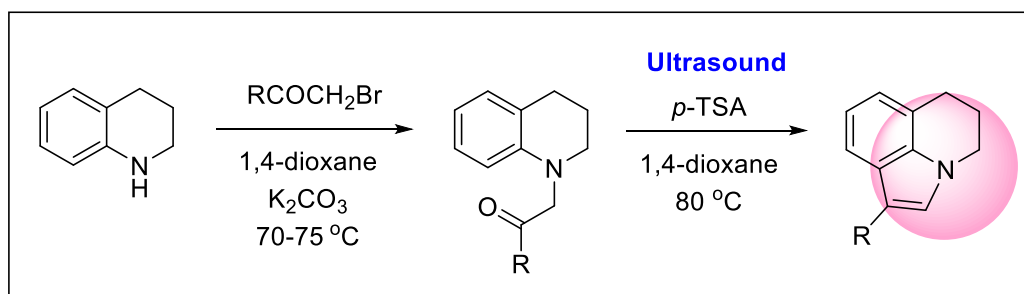
G. S. Astakhov *et al.*¹³ found a convenient synthetic protocol for the formation of 5,6-dihydropyrrolo[2,1-*a*]isoquinolines bearing different electron-withdrawing groups at the C-2 position, involving a two-component domino-type reaction in between 1-aryl-3,4-dihydroisoquinolines and conjugated alkenes (**Scheme 6.8**).



Scheme 6.8. Microwave assisted two-component domino-type synthetic protocol of 5,6-dihydropyrrolo[2,1-*a*]isoquinolines.

(ii) Ultrasound assisted synthetic approach:

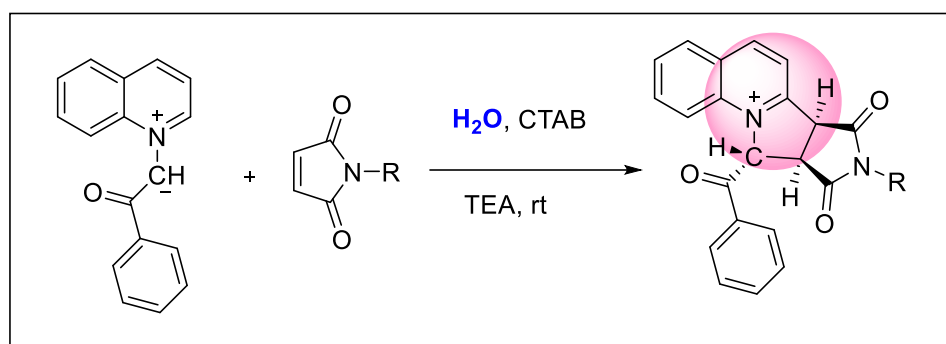
M. Pal *et al.*¹⁴ designed an ultrasound-mediated Bischler-type synthetic protocol of 6-substituted 2,3-dihydro-1*H*-pyrrolo[3,2,1-*ij*]quinolines. In this process, 2-(3,4-dihydroquinolin-1(2*H*)-yl)-1-alkyl/aryl ethanones had been cyclodehydrated while being exposed to ultrasound and *p*-TSA (**Scheme 6.9**). By using this protocol, they synthesized a series of derivatives with good yields.



Scheme 6.9. Ultrasound assisted synthetic protocol of 2,3-dihydro-1*H*-pyrrolo[3,2,1-*ij*]quinolines.

(iii) Synthetic approach using green solvent:

S. Kumar *et al.*¹⁵ described a water-mediated, simple, clean, and green protocol for tetracyclic pyrrolo[1,2-*a*]quinoline derivatives from *N*-ylide and *N*-aryl maleimides involving the [3 + 2] cycloaddition reaction at room temperature (**Scheme 6.10**). The easy operational cycloaddition reaction, benign solvent use, shorter reaction time, and high yielding procedure are the major advantages of this protocol.

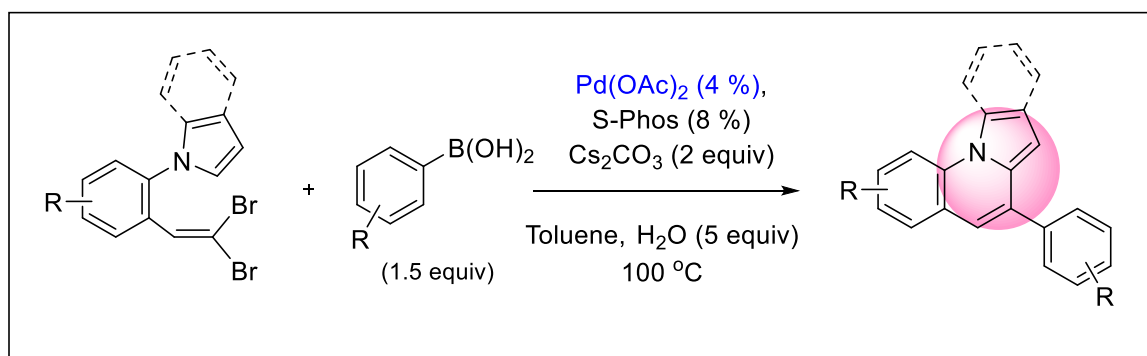


Scheme 6.10. Water mediated synthetic protocol of tetracyclic pyrrolo[1,2-*a*]quinoline derivatives.

6.2.2. Synthesis of pyrroloquinoline in the presence of pyrrole ring:

(a) Metal-catalyzed approaches:

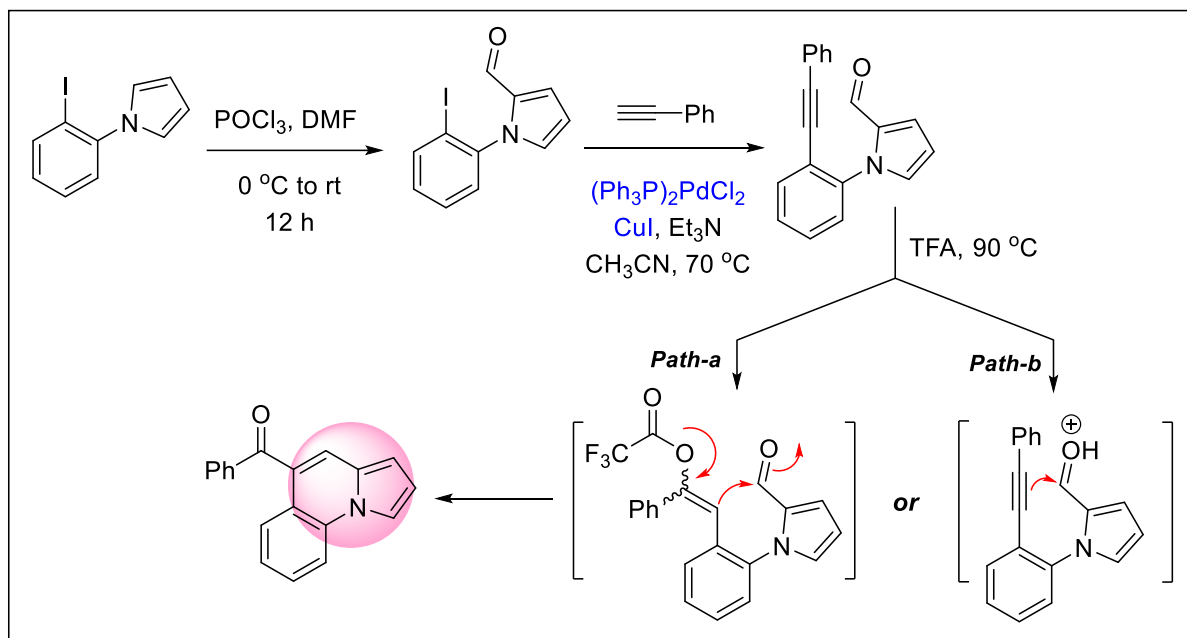
D. I. Chai and M. Lautens¹⁶ have reported a water-accelerated palladium-catalyzed tandem reaction between *gem*-dibromoolefins and boronic acid *via* Suzuki-Miyaura coupling to construct the pyrrolo[1,2-*a*]quinolines (**Scheme 6.11**). This methodology is compatible with various functionalized phenyl rings of *gem*-dibromovinyl and with a wide variation of alkenyl, alkyl, and aryl boronic acids. In addition, mechanistic study indicates that water has a crucial role in accelerating the Suzuki-Miyaura coupling reaction. Water also helps to reduce the by-products.



Scheme 6.11. Palladium-catalyzed tandem approach of pyrrolo[1,2-*a*]quinolines.

M. Nayak and I. Kim¹⁷ accomplished a synthetic way for the novel pyrrolo[1,2-*a*]quinoline moieties employing a sequential Sonogashira coupling reaction/intramolecular alkyne-carbonyl metathesis process (**Scheme 6.12**). At first, 1-(2-haloaryl)-1H-pyrrole-2-carbaldehydes were prepared by the Paal-Knorr synthesis of the pyrrole ring and

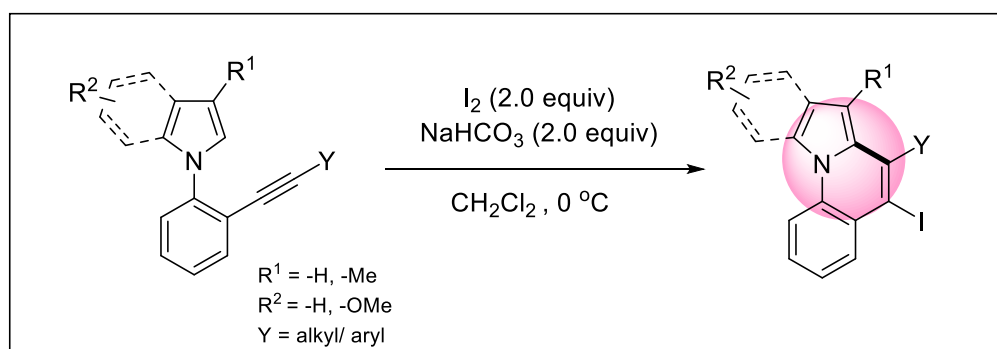
consequently the Vilsmeier-Haack formylation of 2-haloanilines. Then 1-(2-haloaryl)-1H-pyrrole-2-carbaldehydes underwent the Sonogashira coupling reaction by using Pd catalyst, CuI, and Et₃N in acetonitrile solvent, followed by intramolecular alkyne-aldehyde metathesis occurs in the presence of TFA to give the cyclized pyrrolo[1,2-*a*]quinoline derivatives.



Scheme 6.12. Metal catalyzed synthetic approach of pyrrolo[1,2-*a*]quinolines.

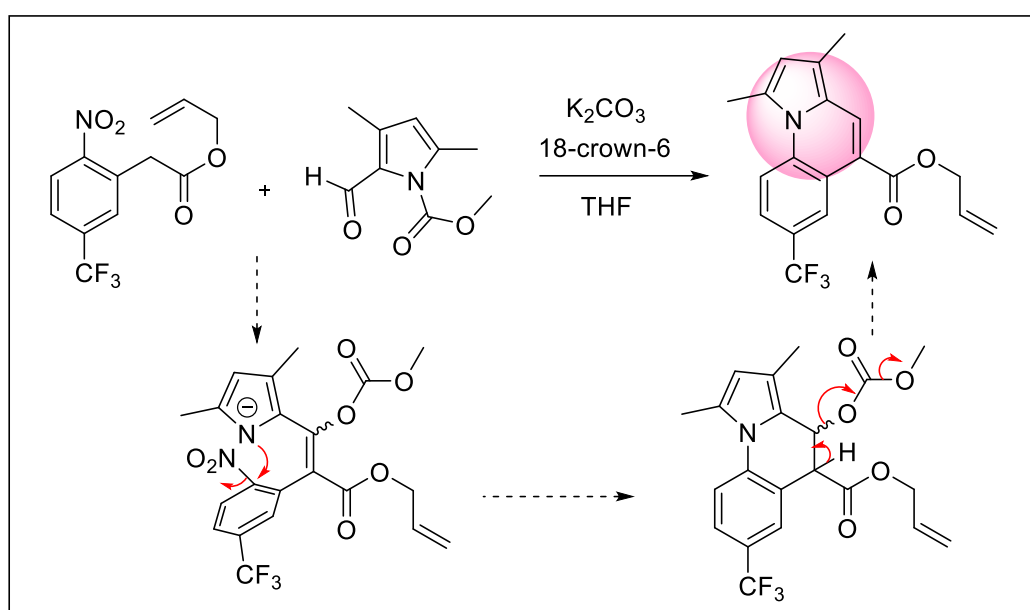
(b) Metal-free approaches:

A. K. Verma and his co-workers¹⁸ reported an iodine-mediated electrophilic ring closure reaction for the construction of 5-iodopyrrolo[1,2-*a*]quinolines with excellent yields. This procedure involves the C-C bond formation *via* regioselective and electrophilic 6-*endo-dig* cyclization (**Scheme 6.13**). Here, employing iodine media is safer for handling and more cost-effective. The iodo derivatives of pyrroloquinolines offer diversifying functionalities on quinoline moieties, which is extremely helpful for assessing morphological and biological activities.

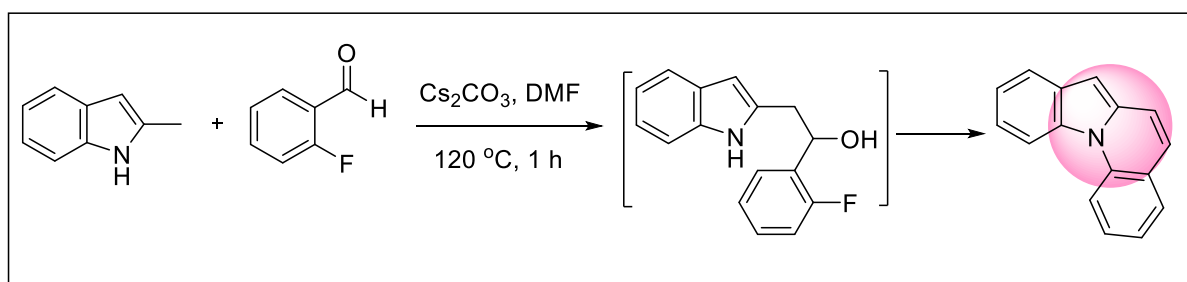


Scheme 6.13. Iodine-mediated ring closure reaction of 5-iodopyrrolo[1,2-*a*]quinolines.

C. Richardson and his research group¹⁹ discovered a new synthetic route of pyrrolo[1,2-*a*]quinoline derivatives carrying carboxylate functionalities in the 5-position. This protocol is totally temperature-dependent and requires a low temperature. The intramolecular S_NAr -elimination takes place at low temperature, leading to the construction of pyrroloquinoline. The pyrrolide anion intermediate, depending on the temperature of the reaction and the electron deficiency of the nitroaryl ring, accelerated the intramolecular S_NAr reaction, which is responsible for the pyrroloquinoline formation. This method avoids using solvents with high boiling points and permits collaboration with thermosensitive substrates (**Scheme 6.14**).

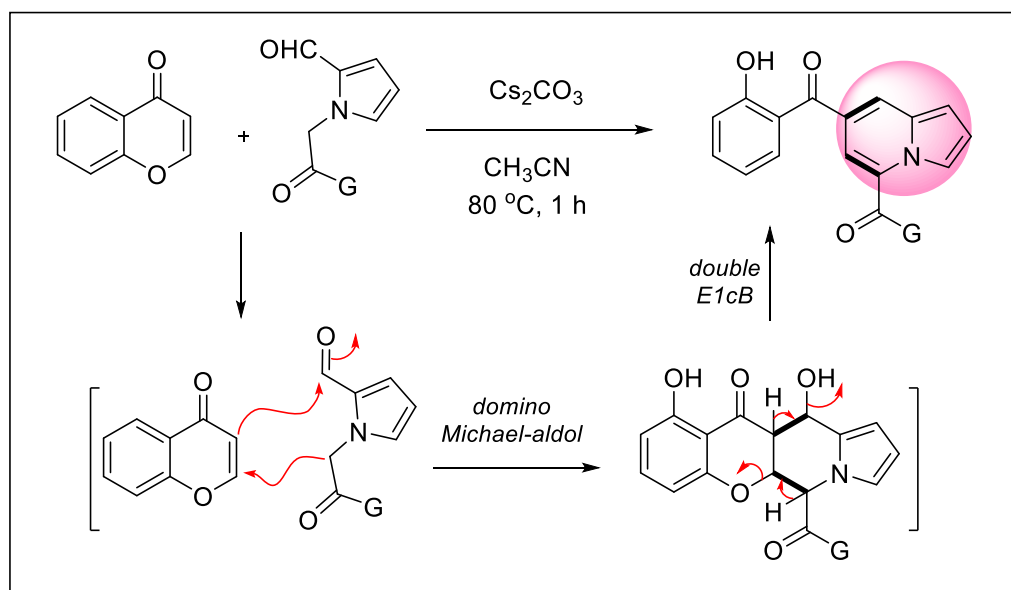
**Scheme 6.14.** Metal-free synthetic approach of pyrrolo[1,2-*a*]quinolines.

P. Ngermmeesri and his group²⁰ found a novel synthetic, transition-metal-free pathway for indolo[1,2-*a*]quinolines. This procedure uses 2-fluorobenzaldehyde and 2-methylindoles in combination with Cs_2CO_3 , DMF, and 120 °C to perform an aromatic substitution reaction sequentially followed by Knoevenagel condensation to get the desired product (**Scheme 6.15**).



Scheme 6.15. Transition-metal-free synthetic pathway for indolo[1,2-*a*]quinolines.

According to D. R. Joshi and I. Kim,²¹ a base-promoted Michael-aldol double elimination synthesis process makes it simple to access novel indolizines having two acyl groups at C5 and C7 positions, where chromone is used as a two-carbon unit for the first-time synthesis of a pyridine moiety. Under metal-free and environmentally friendly circumstances, several equivalents might be easily accessible in good quantities (**Scheme 6.16**).

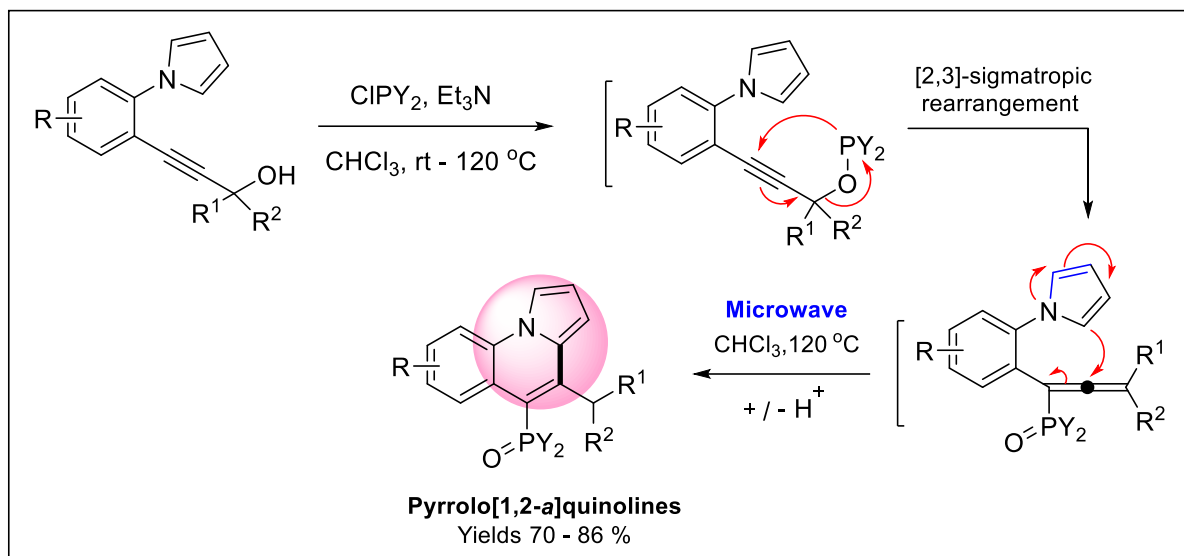


Scheme 6.16. Metal-free base promoted synthetic route of indolizines.

(c) Green approaches:

(i) Microwave assisted synthetic approach:

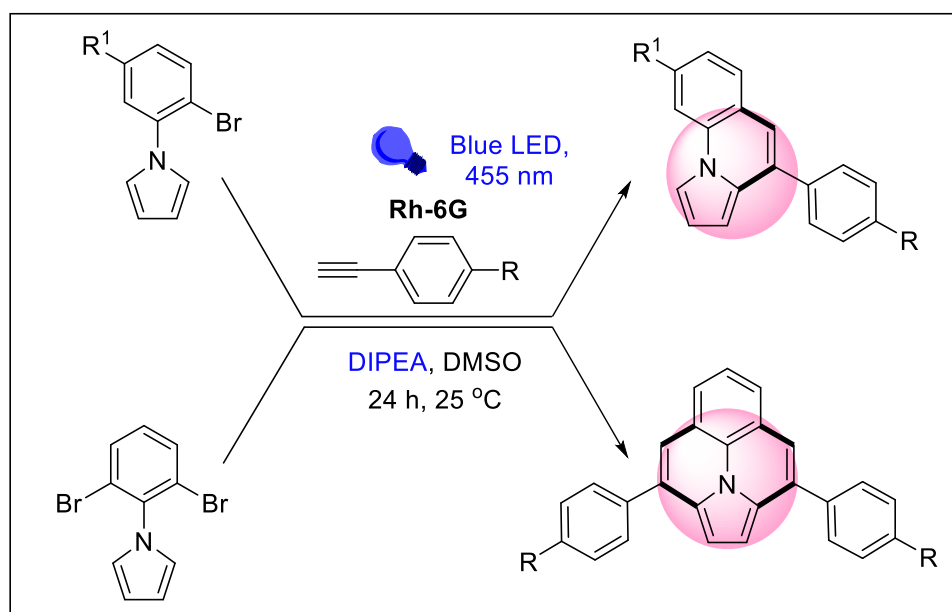
M. Baumann and I. R. Baxendale²² prepared a series of tricyclic pyrrolo[1,2-*a*]quinolines containing phosphine oxide or phosphonate by an efficient cascade reaction. This novel cascade sequence makes use of the *in-situ* conversion of propargylic alcohols into transitory allenes employing an ingenious [2,3]-sigmatropic rearrangement, followed by the trapping of the subsequent allenes by an adjoining pyrrole ring. Additionally, the first small-scale batch technique was successfully converted into a continuous flow process, enabling the effective fabrication of particular pyrrolo[1,2-*a*]quinolines on a multigram scale (**Scheme 6.17**).



Scheme 6.17. Microwave assisted synthetic protocol for tricyclic pyrrolo[1,2-*a*]quinolines.

(ii) Photoinduced synthetic approach:

B. König *et al.*²³ first reported a photocatalytic synthetic route for pyrrolo[1,2-*a*]quinolines starting from *N*-aryl halides and aryl alkynes. 1-(2,6-dibromophenyl)-1*H*-pyrrole and 1-(2-Bromophenyl)-1*H*-pyrrole react with aromatic alkynes in the presence of rhodamine 6G in catalytic amount and *N,N*-diisopropylethylamine (DIPEA) under the influence of blue light irradiation to produce the corresponding intramolecular cyclized product. This approach offers a single step, a mild reaction environment, and avoids transition metals (**Scheme 6.18**).

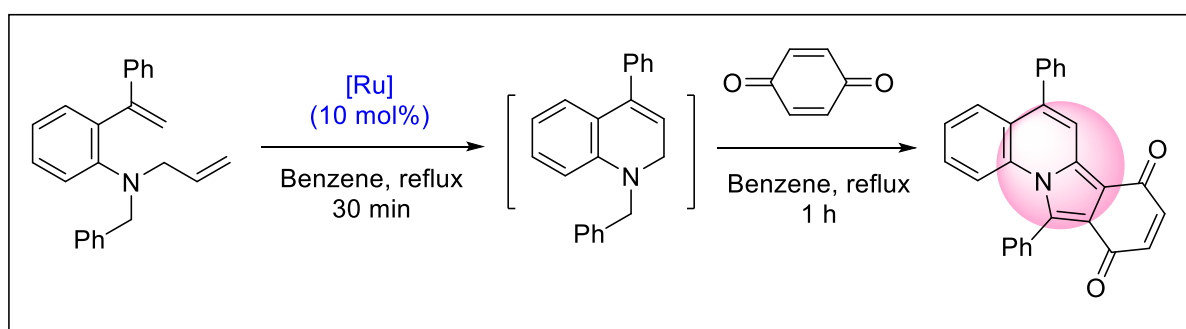


Scheme 6.18. Photoinduced synthetic route for pyrrolo[1,2-*a*]quinolines.

6.2.3. Synthesis of pyrroloquinoline in the absence of pyridine/pyrrole ring:

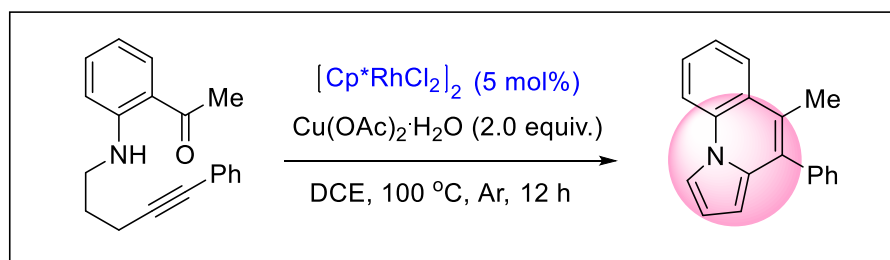
(a) Metal-catalyzed approaches:

M. Arisawa *et al.*²⁴ invented a one-pot ruthenium-catalysed ring-closing metathesis/oxidation protocol to construct several isoindolo[2,1-*a*]quinolines starting from *N*-allyl-*N*-benzyl-2-vinylaniline derivatives (**Scheme 6.19**). This tandem approach illustrated that 1,2-dihydroquinolines were produced by first treating *N*-allyl-*N*-benzyl-2-vinylaniline with a ruthenium catalyst (10 mol%) in benzene solvent under reflux conditions for 30 minutes. After that, without any purification, these 1,2-dihydroquinolines facilitate 1,3-dipolar cycloaddition with 1,3-dipolarophiles to give the desired products in good quantities.



Scheme 6.19. Ruthenium-catalysed one-pot synthetic protocol of isoindolo[2,1-*a*]quinolines.

W. Zhou *et al.*²⁵ described a rhodium (III)-catalyzed synthetic protocol for the pyrrolo[1,2-*a*]quinolines *via* intramolecular annulation and successive aromatization of *o*-alkynyl amino aromatic ketones. This procedure governs the pyrrole and quinoline rings of pyrrolo[1,2-*a*]quinolines in one-pot (**Scheme 6.20**).

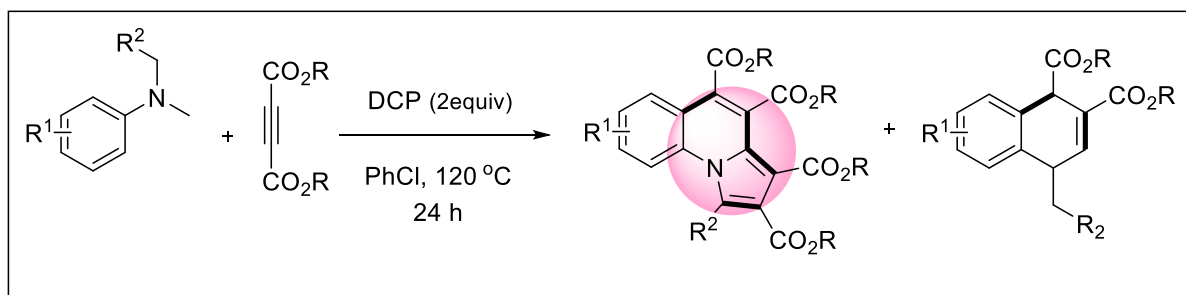


Scheme 6.20. Rhodium (III)-catalyzed synthetic protocol for the pyrrolo[1,2-*a*]quinolines.

(b) Metal-free approaches:

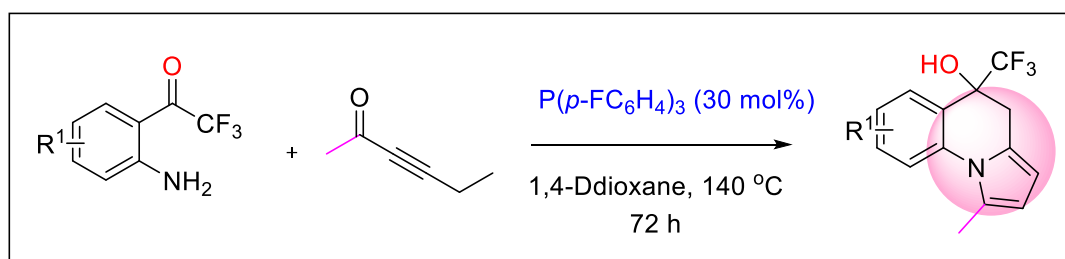
In a one-pot procedure, Z. Luo *et al.*²⁶ have invented a catalyst-free, highly effective, and useful approach for the synthesis of physiologically intriguing pyrrolo[1,2-*a*]quinolines and 1,4-dihydroquinolines by employing *N*-methylanilines and alkynoates. According to this

approach, a sp^3 C-H bond can be directly functionalized *via* a pathway including a α -amino alkyl radical to produce C-C bonds. In detail, the mechanism study states that the intermolecular [4+2] reaction then undergoes a [3+2] radical cyclization step (**Scheme 6.21**).



Scheme 6.21. Metal-free synthetic route for pyrrolo[1,2-*a*]quinolines.

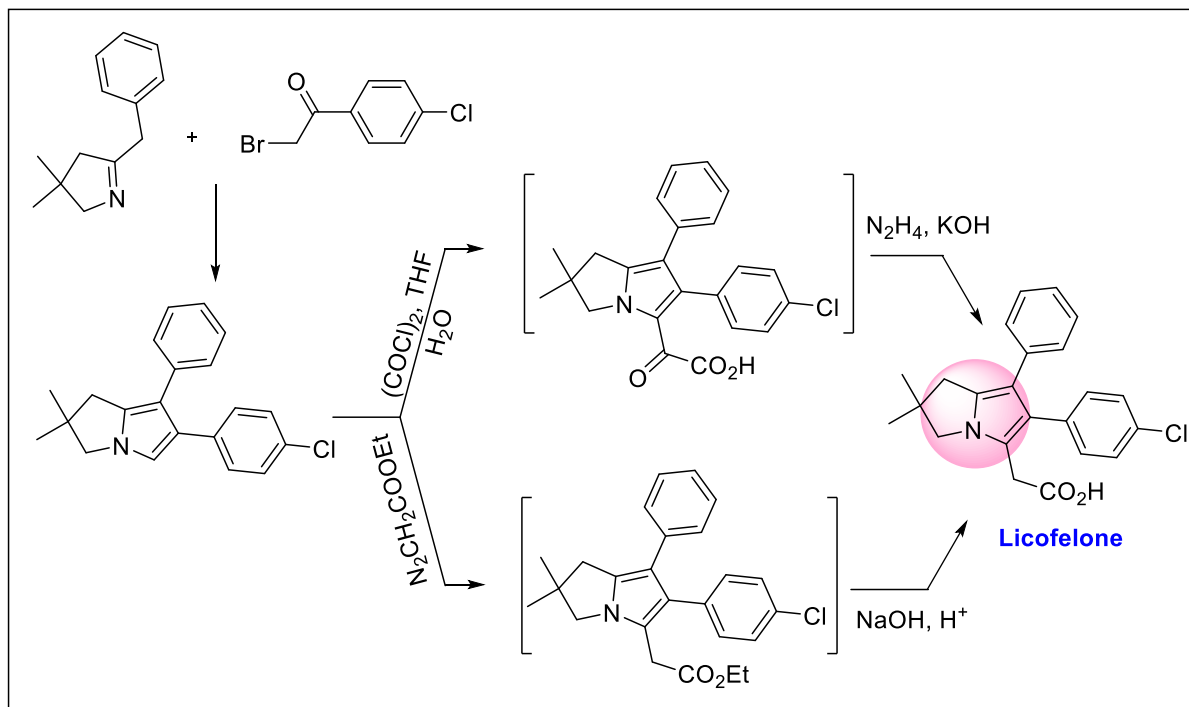
M. Shi and his associates²⁷ depicted a switchable intermolecular annulation between substituted ortho-aminoacetophenones and alkynones by employing phosphine-catalyzed reactions to produce the benzo-fused indolizine derivatives. This cyclized product was selectively formed with good yields by the *in-situ* generation of a zwitterionic intermediate. To produce the equivalent pyrrolo[1,2-*a*]quinolines, the zwitterionic intermediate could proceed through a cascade of intermolecular nucleophilic assault, cycloaddition, and intramolecular condensation with a broad substrate scope (**Scheme 6.22**).



Scheme 6.22. Phosphine-catalyzed intermolecular annulation reaction of benzo-fused indolizines.

6.2.4. Total synthesis of Licofelone drug molecule:

Licofelone, a nonsteroidal anti-inflammatory pill, is presently being studied in phase-III clinical trials to treat osteoarthritis. In order to build Licofelone, S. Rádl *et al.*²⁸ used Fenton's reagent to catalyse a successful radical alkylation between 2,3-dihydro-1*H*-pyrrolizine and iodoacetonitrile or iodoacetates (**Scheme 6.23**).



Scheme 6.23. Total synthesis of Licofelone.

From the aforementioned literature review, it is clear that numerous techniques have been established by various groups in order to synthesise pyrroloquinoline derivatives with a pyridine ring, a pyrrole ring, or without a pyridine and pyrrole ring. However, there are still certain limitations on pyrroloquinoline synthesis in green pathways that start without a pyridine or pyrrole ring. Therefore, discovering a green synthesis route to produce pyrrolo[1,2-*a*]quinolines has been a difficult task. After a protracted inquiry, we have successfully developed a green approach employing methanol solvent, which is discussed below.

6.3. Present work:

- ❖ We have presented a weak acid promoted tandem aza-Michael-aldol strategy for the synthesis of diversely fused pyrrolo[1,2-*a*]quinoline (tricyclic to pentacyclic scaffolds) by the construction of both pyrrole as well as quinoline ring in one-pot.
- ❖ Ketorolac drug analogue has been synthesized following the current protocol.
- ❖ One of the synthesized tricyclic pyrrolo[1,2-*a*]quinoline fluorophore has been used to detect the highly toxic picric acid *via* fluorescent quenching effect.

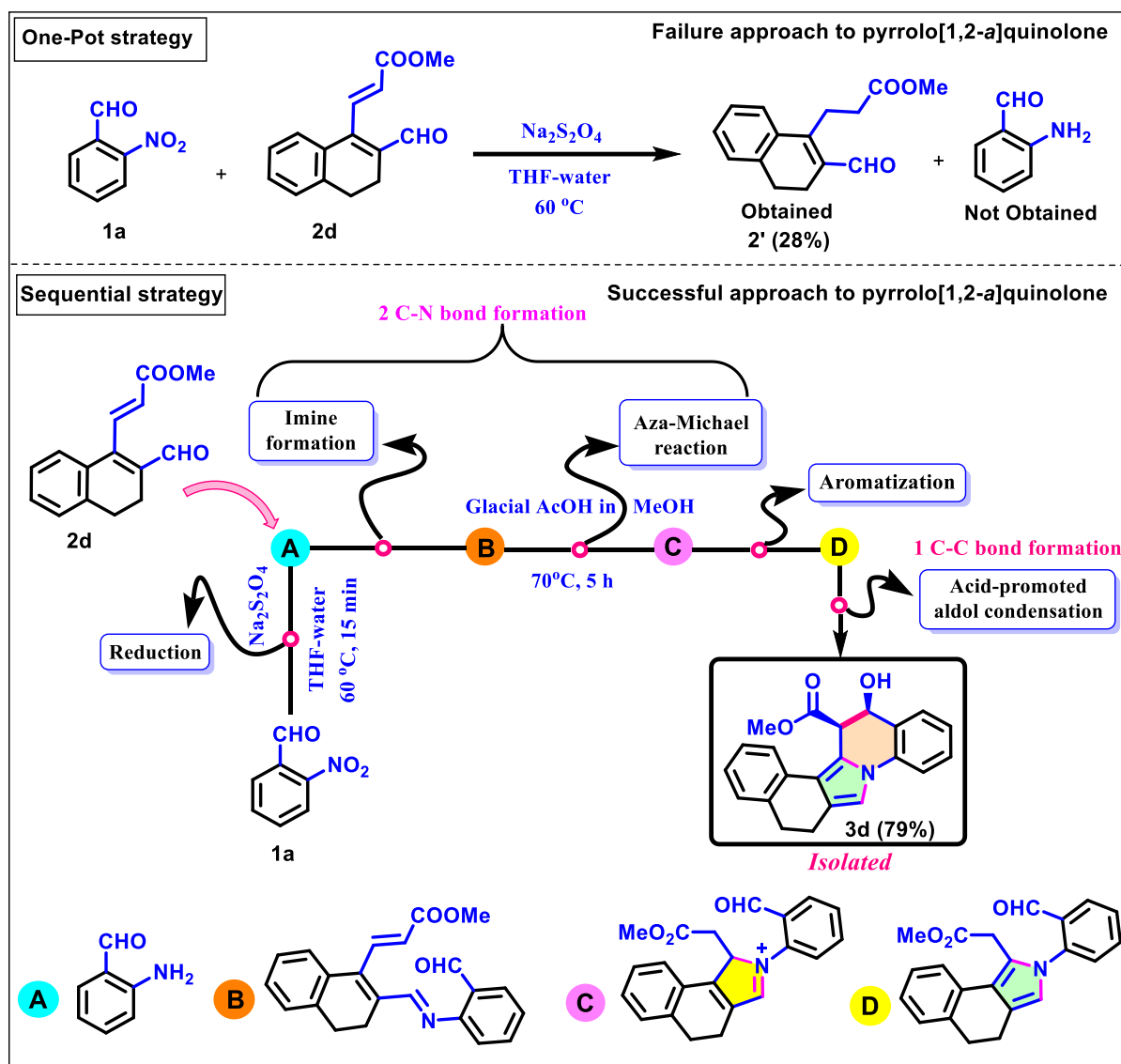
Herein, we have designed a protocol for the synthesis of pyrrolo[1,2-*a*]quinoline (tricyclic to pentacyclic) in a single-pot Michael-aldol reaction within a short reaction time under green condition. The coupling reactions were performed with two substrates 2-nitrobenzaldehyde **1a** and 3-(2-formylcycloalkenyl)-acrylic ester derivatives **2** in the presence of weak organic acid catalyst AcOH in MeOH. The generation of nontoxic by-products is another attraction of this protocol.

3-(2-Formylcycloalkenyl)-acrylic ester derivatives with two reactive functional groups (α,β -unsaturated ester and aldehyde) have been explored for the synthesis of heterocyclic compounds by our research group.²⁹ In these consequences, we have taken two partners which underwent reduction/aza-Michael addition/aldol condensation smoothly to form multiple C-C and C-N bonds in a sequential reaction.

6.4. Results and Discussion:

From the retrosynthetic analysis, we have planned to synthesize the fused bicyclic ring structure of pyrroloquinoline by the reaction of easily available precursor 3-(2-Formylcycloalkenyl)-acrylic ester derivative and 2-aminobenzaldehyde. However, 2-aminobenzaldehyde has a tendency for dimerization. So, we anticipated that 2-nitrobenzaldehyde could be taken as a good alternative to aminoaldehyde and it can readily take part in the reductive cyclization.³⁰ Sodium dithionite is one of the popular transition-metal-free chemoselective reducing agents and it has been successfully used in the direct preparation of 2-aminoaldehyde from 2-nitrobenzaldehyde. Hence, we have first started our mission with the reductive cyclization *via* tandem protocol in the presence of 2-nitrobenzaldehyde with substrate **2d** for the construction of two rings in one reaction vessel. The attempt failed to get the desired aminoaldehyde for aza-addition with the substrate **2d**, instead, we have found the chemo-selective reduction of π -bond in the presence of sodium dithionite in the boiling THF-H₂O to get **2'** (Scheme 6.24, one-pot strategy). This result further proves that sodium dithionite has a greater tendency for reduction of polar π -bond compared to the nitro group reduction. Next, we have planned an alternative pathway by two-pot sequential reactions where 2-nitrobenzaldehyde was first reduced to the aminoaldehyde with sodium dithionite and after aqueous work-up it was added to the solution of the substrate **2d** in methanol (Scheme 6.24, sequential strategy). Substrate **2d** could not add to the reductive part of **1a** even after 24 h of reflux in methanol. However, reduction/aza-Michael/aldol reactions have successfully happened with **1a** and **2d** in presence of AcOH in

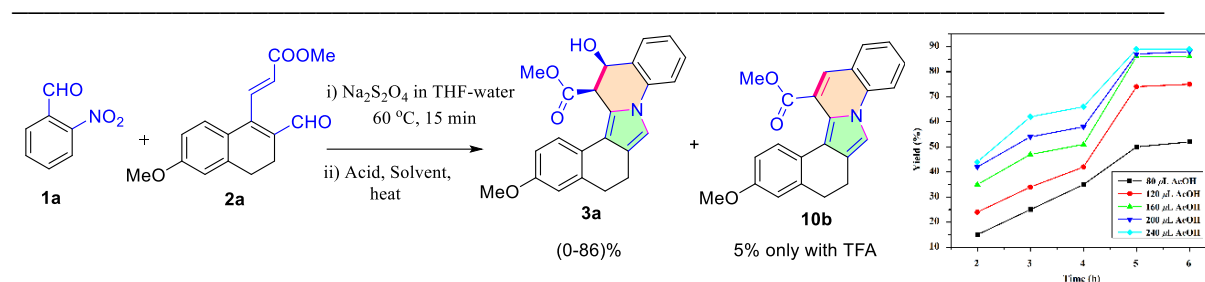
methanol under refluxing conditions. Hence, we have envisaged that direct construction of the pyrrole/isoindole ring along with isoquinoline ring was carried out in a consecutive manner involving four steps (A-B-C-D) without need of isolation and purification technique and formed desired pyrrolo/isoindolo[1,2-*a*]quinoline with excellent yield.



Scheme 6.24. Schematic representation for stepwise formation of our target compound.

According to our hypothesis, initially, we planned to establish the tandem protocol by selecting the model substrates methyl (*E*)-3-(2-formyl-6-methoxy-3,4-dihydronaphthalen-1-yl)acrylate **2a** and 2-nitrobenzaldehyde as coupling partners. Coupling reaction was started with the addition of 40 μL of acetic acid at 40 $^\circ\text{C}$ or 70 $^\circ\text{C}$ in MeOH but did not achieve desired product **3a** (entry 1 & 2, Table 6.1). Interestingly, pentacyclic angular multi-substituted isoindoloquinoline scaffold was formed with 86% yield by the addition 160 μL of

AcOH (**entry 4, Table 6.1**). However, the yield of **3a** did not improve significantly even after the addition of 240 μL of AcOH (**entry 5, Table 6.1**). This has been confirmed by the study of the kinetics of the developed protocol with respect to the amount of AcOH (μL) used at a constant temperature (70 $^{\circ}\text{C}$) and found that the yield of the cyclized product was gradually increased up to 6 h (**Table 6.1**, graphical plot of yield vs time). With respect to the environmental concern, we wanted to perform a reaction under solvent-free conditions by the addition of 60 μL AcOH but only 60% yield of **3a** (**entry 6, Table 6.1**) was obtained. The comfortability of the developed protocol was also checked with protic, aprotic and non-polar solvents (e.g., Water, THF, 1,4-dioxane, and toluene) in the presence of 160 μL of AcOH and found that the desired scaffolds were formed with 25-55% yield except DMF (**entry 7-11, Table 6.1**). In the presence of TFA (20 μL) and *p*-TsOH (0.5 equiv) (**entry 12-13, Table 6.1**) the desired product was formed with 40 and 65% yield respectively. However, in the case of TFA small amount of water elimination product was obtained along with **3a**. The efficiency of the cyclization reaction was also checked with the transition metal catalyst $\text{Cu}(\text{OTf})_2$ in methanol to produce the product with 54% yield after 6 h (**entry 14, Table 6.1**).

Table 6.1. Optimization of reaction condition for the synthesis of pyrrolo[1,2-*a*]quinoline


Sl. No.	Reaction conditions	Temperature (°C)	Time (h)	Yield (%)
1.	AcOH (40 μL) in MeOH	40	8	NR
2.	AcOH (40 μL) in MeOH	70	8	NR
3.	AcOH (120 μL) in MeOH	70	6	75
4.	AcOH (160 μL) in MeOH	70	5	86
5.	AcOH (240 μL) in MeOH	70	5	87
6.	AcOH (60 μL) in Neat	75	8	60
7.	AcOH (160 μL) in Water	75	8	50
8.	AcOH (160 μL) in THF	70	10	45
9.	AcOH (160 μL) in 1,4-Dioxane	70	7	25
10.	AcOH (160 μL) in DMF	70	12	NR
11.	AcOH (160 μL) in Toluene	70	6	55
12.	TFA (20 μL) in MeOH	70	4	40
13.	<i>p</i> -TsOH (0.5 equiv) in MeOH	70	6	65
14.	Cu-Triflet (0.5 equiv) in MeOH	70	6	54

Reaction and conditions: Substrate (i) 2-nitrobenzaldehyde **1a** (1 mmol, 1 equiv), Na₂S₂O₄ (6 mmol, 6 equiv), THF-Water, 60 °C, 15 min.; (ii) (*E*)-3-(2-formyl-6-methoxy-3,4-dihydronaphthalen-1-yl)acrylate **2a** (1 mmol, 1 equiv.), Solvent (4 mL), Glacial AcOH (40 - 240 μL).

After the successful optimization studies, we have examined the scope of reaction using the reaction condition (**entry 4, Table 6.1**) which was supported by the corresponding kinetics study. The reactions were investigated in presence of different substituents in the naphthyl ring of **2** using different Michael acceptors at position-1 (**Table 6.2**). The Michael and aldol addition both were unfavorable in presence of -O^tBu group but it become favorable with -OMe, -OEt in ester. The 5-OMe/7-OMe groups in **2** have no resonance effect with the C-1 substituent in the naphthyl ring but it has electron withdrawing inductive effect and hence it shows a similar effect with 7-Br/7-Cl substituents. They gave moderate yields of products **3f**, **3i**, **3k** and **3l** (64-75%). This may be due to the lower rate of enolization during aldol addition in the presence of electron-withdrawing groups. The product **3** has two stereocentres which have been formed after aldol addition. Hence, there is a possibility to form the diastereoselective products during the aldol addition. Our protocol furnishes exclusively only one diastereomer (see experimental section, **Figure 6.12**) except **3g**, **3h** and **3j**. In case of **3g** and **3h**, two diastereomeric mixture have been observed with the ratio 56:44 and 62:38 respectively and it has been confirmed by NMR/HPLC analysis (see experimental section, **Figure 6.13**). This may be due to the presence of another chiral center at C-4 position. Diastereomeric ratio (74:26) of **3j** has been obtained due to presence of -COMe group instead of -CHO group in the substrate **1**. All the synthesized products are characterized by NMR and HRMS analysis. The structure of product **3a** was unambiguously confirmed by X-ray crystallographic study (**Figure 6.6**), which reveals that two rings are formed *via* tandem aza-Michael-aldol reactions. From the X-ray analysis it has been shown that **3a** compound was produced diastereoselectively. It has been further proved by HPLC analysis, (see experimental section, **Figure 6.12**). The *cis* orientation of two stereogenic centers was further supported by the series of 2D NMR (NOESY, HSQC, HMBC and COSY; see experimental section) experiments. For example, NOESY spectrum exhibited strong correlation between H-16 and H-17 hence H-16/H-17 are *cis* oriented. Spatial correlation was observed between H-7 and H-17 in NOESY; HMBC experiment showed strong correlation H-17/C-16 and H-16/C-17.

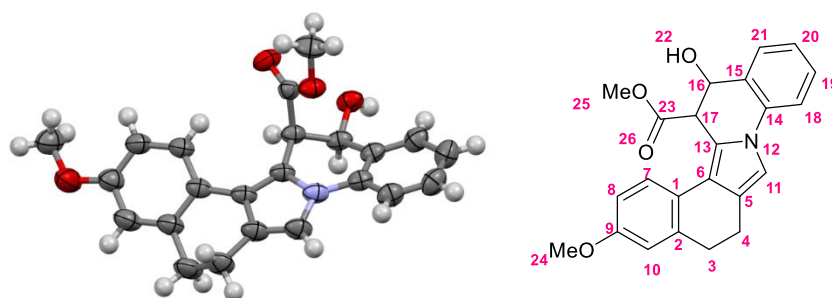
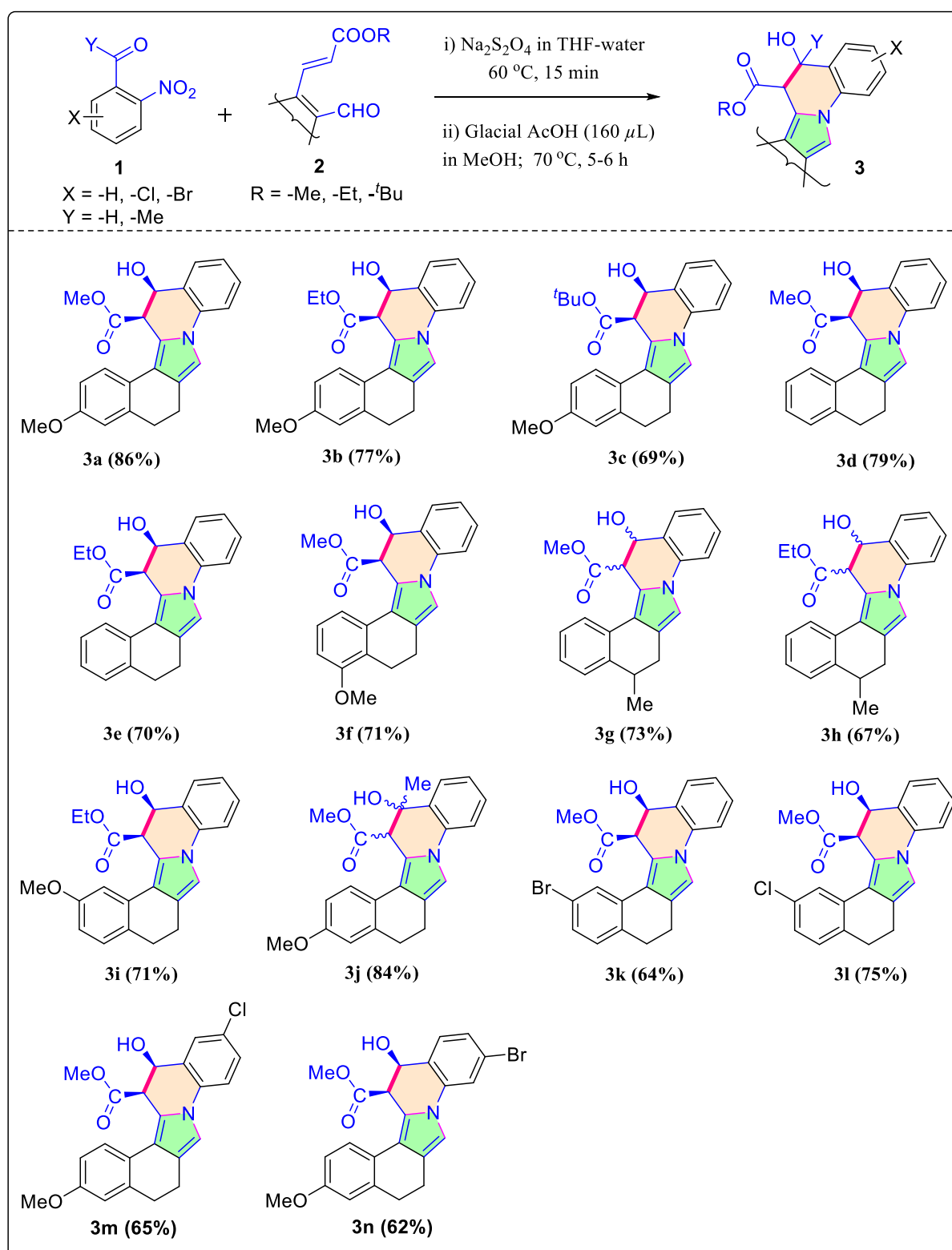
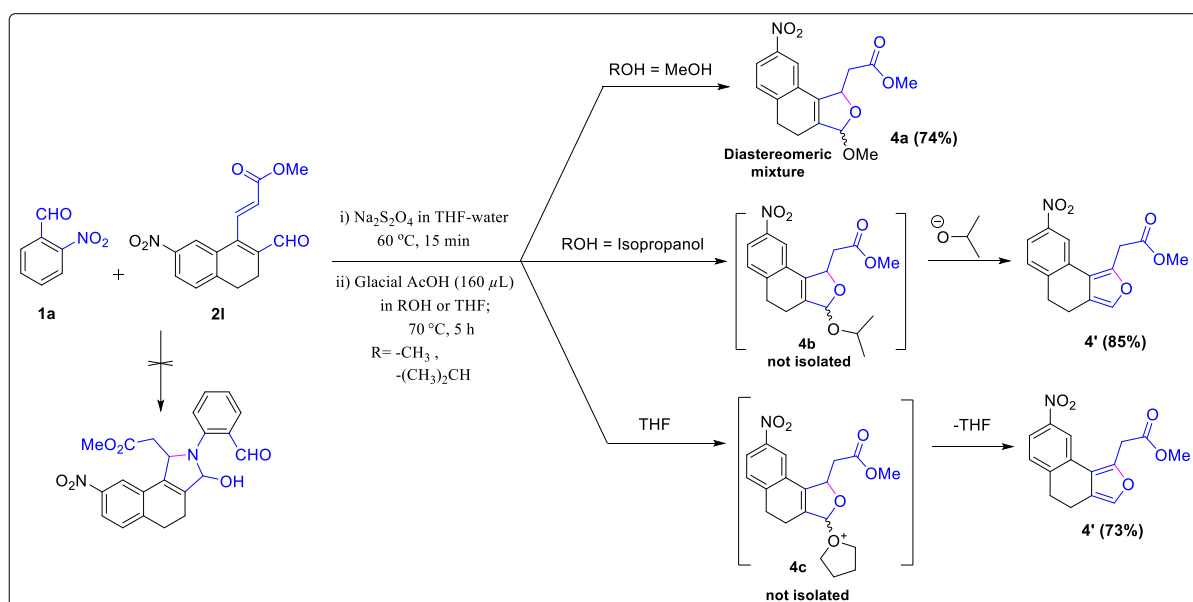


Figure 6.6. X-ray structure of **3a** and it numbers-assigned structure.

Table 6.2. Substrate scope of pyrrolo[1,2-*a*]quinoline synthesis

Reaction Conditions: (i) Substituted 2-nitrobenzaldehyde **1** (1 mmol, 1 equiv), $\text{Na}_2\text{S}_2\text{O}_4$ (6 mmol, 6 equiv), THF-Water, 60 °C, 15 min.; (ii) 3-(2-formylcycloalkenyl)-acrylic ester derivatives **2** (1 mmol, 1equiv), MeOH (4-5 mL), Glacial AcOH (160 μL), 70 °C, 5-6 h.

To check the tolerance of our developed protocol with stronger electron withdrawing group, we took $-\text{NO}_2$ group in the aryl ring in **2** under identical condition but it did not couple with **1a** rather it underwent intramolecular oxa-Michael addition by methanol molecules and furnished diastereomeric mixture (55:45) of dihydrofuran derivatives **4a** (Scheme 6.25). Similar diastereomeric mixture **4b**, **4c** was also formed (not isolated) with the change of the solvent molecule from methanol to isopropanol or THF in the presence of AcOH which readily eliminate the added solvent molecule to form *c*-fused furan derivative **4'** 85% & 73% respectively. Hence, we think that electronic effect is more prominent for inhibit the formation desired product pyrrolo[1,2-*a*]quinoline where highly electrophilic carbonyl group of **2i** readily attack by the alcohol molecules compare to the less nucleophilic **1a** substrate.

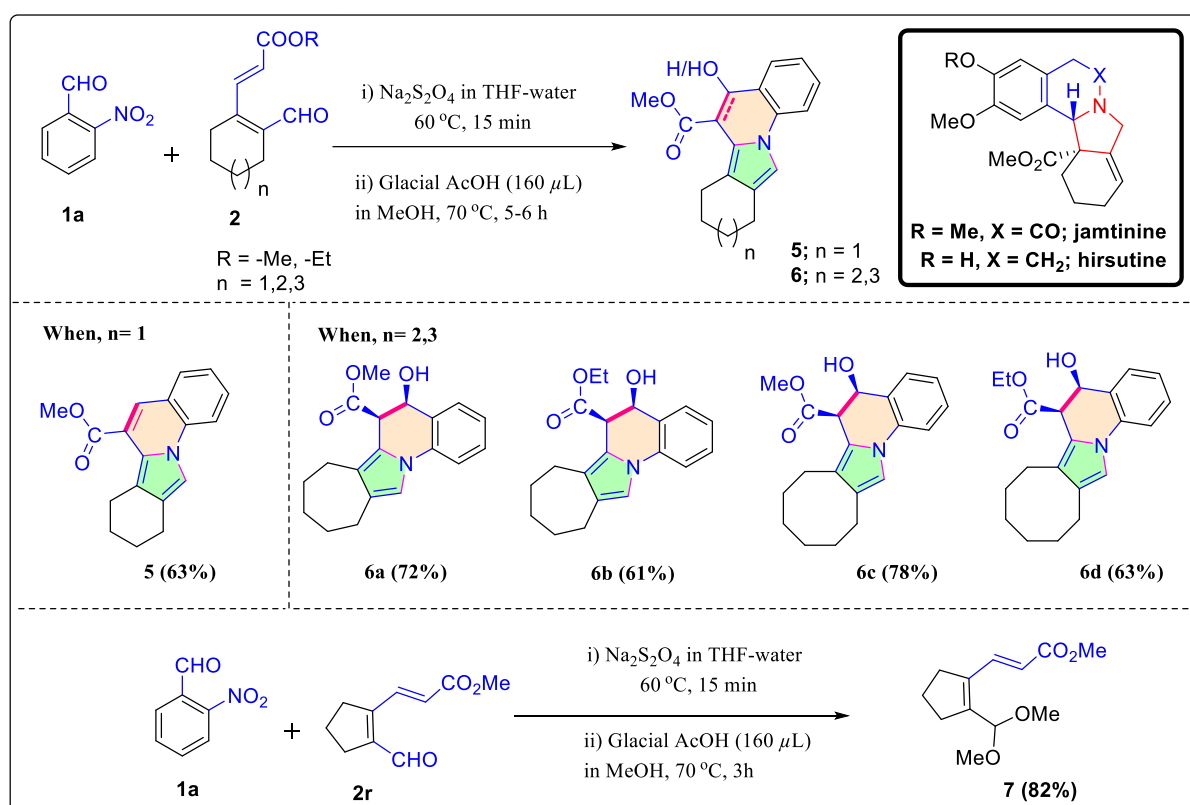


Scheme 6.25. Study of the reaction with stronger electron withdrawing substituent.

To further explore the utility of our method, we wanted to examine the reaction in the cycloalkenyl system to get the tetracyclic fused pyrrolo[1,2-*a*]quinoline which has been found in biologically active natural alkaloids such as jamicotine and hirsutine.³¹ These natural product analogs were successfully synthesized using reductive/aza-Michael/aldol reaction under the optimized reaction condition as described in **Table 6.3**. The yield of the cyclized products depends on the ring size as well as alkoxy substituents. Similar effect of ester functionality ($-\text{OMe}$ to $-\text{OEt}$) for the formation of **3** and **6** has been observed under optimized condition (e.g., 72 to 61% for **6a-6b** & 78 to 63% for **6c-6d**) (**Table 6.3**). The cyclooctyl ring furnished better yields compared to the cycloheptyl rings but the cyclohexyl ring deliberately eliminate the water molecules after sequential cyclization and furnished **5** with 63% yields.

From the series of results, it has been argued that lowering the ring size is uncomfortable for the aldol product formation and hence cyclohexyl leads to dissimilar results by the formation of stable geometry product **5** after extrusion of water. The formation of pyrrolo[1,2-*a*]quinoline became completely stopped in the case cyclopentenyl system and it underwent acetal formation **7** in the presence of methanol and AcOH. Here, the unstabilization factor in the small ring proves to inhibit aza-Michael reaction with the aryl amine partner.

Table 6.3. Substrate scope for the synthesis of tetracyclic fused pyrrolo[1,2-*a*]quinoline systems

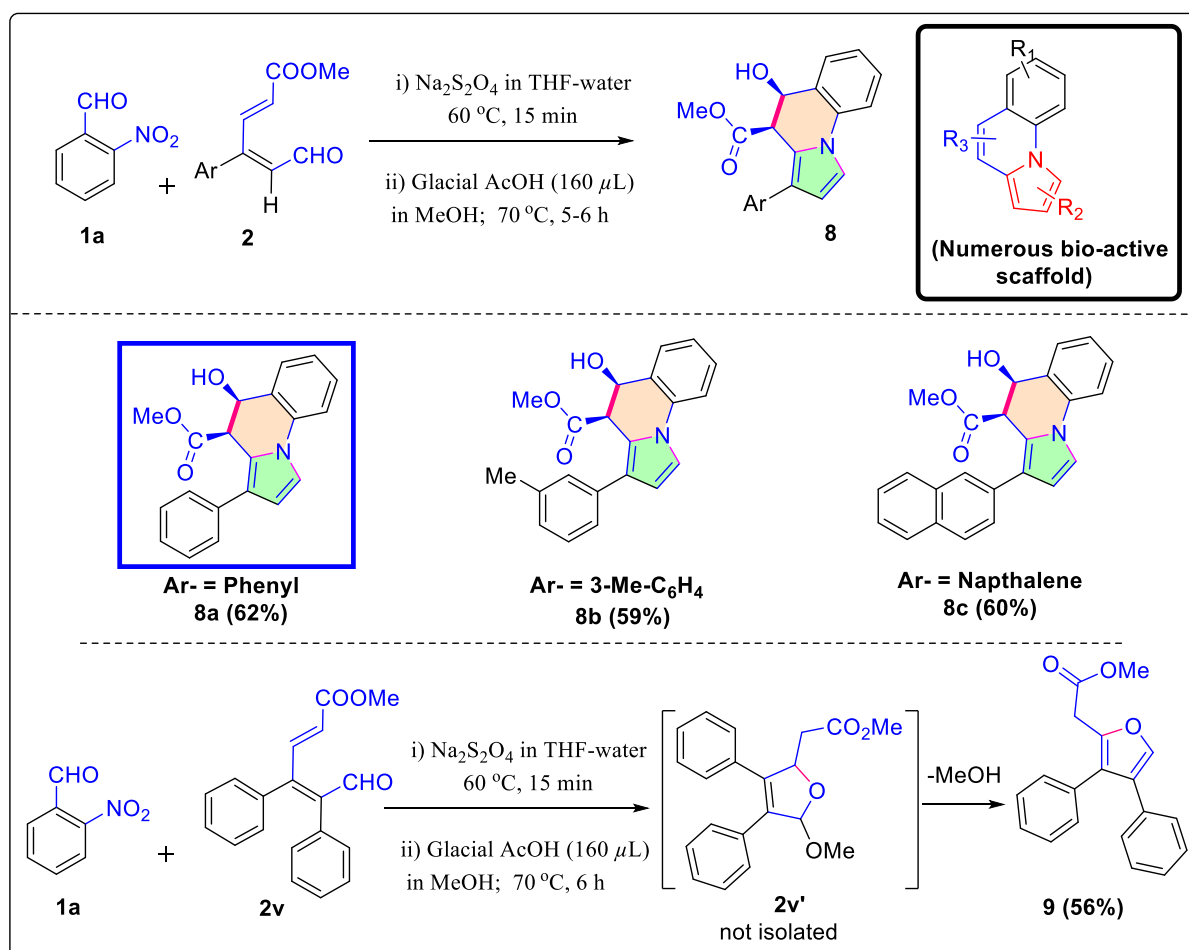


Reaction Conditions: (i) 2-nitrobenzaldehyde **1a** (1 mmol, 1 equiv), $\text{Na}_2\text{S}_2\text{O}_4$ (6 mmol, 6 equiv), THF-Water, 60 °C, 15 min.; (ii) 3-(2-formylcycloalkenyl)-acrylic ester derivatives **2** (1 mmol, 1 equiv), MeOH (4-5 mL), Glacial AcOH (160 μL), 70 °C, 5-6 h.

Besides the tetracyclic and pentacyclic scaffolds, we have further elaborated our methodology to the synthesis of tricyclic scaffolds of pyrrolo[1,2-*a*]quinolines which exist in different natural products and have been isolated from various sources and show diverse biological activities in the folk medicines of tropical and subtropical regions.³² These moieties have been synthesized from methyl (2*E*,4*E*)-4-aryl-6-oxohexa-2,4-dienoate **2** under identical optimized conditions with the 2-nitrobenzaldehyde **1a** as coupling partners (Table

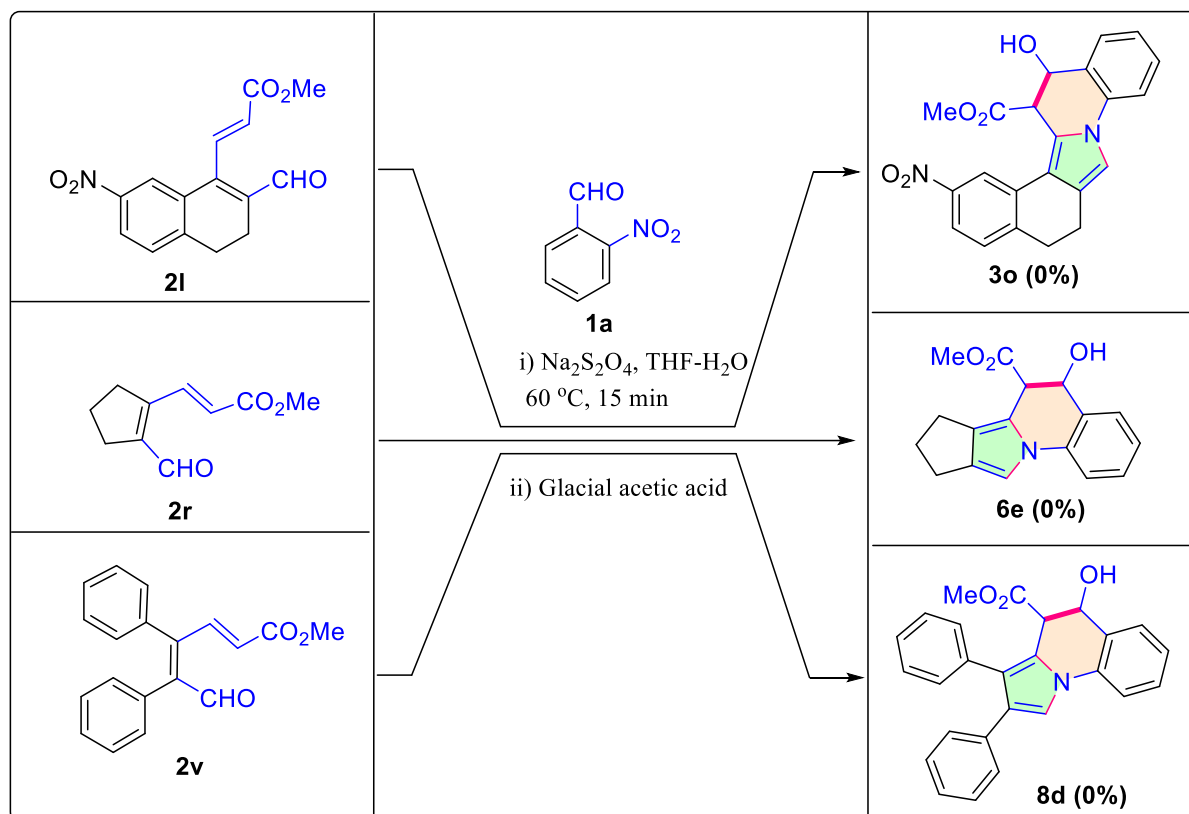
6.4). Yields of the tandem cyclized products were comparatively lowered than the tetracyclic or pentacyclic pyrrolo[1,2-*a*]quinoline analogs. Substrates containing Ar = Ph, 3-Me-C₆H₄, 2-naphthyl furnished moderate yields of tricyclic derivatives (62-59%). Among them an interesting blue fluorescent was observed for the compound **8a**. Hence, detailed photophysical study was carried out for the further utilization of our product **8a** and it is discussed in the latter section. In case of the substrate **2v** (4- and 5-positions are substituted with -Ph groups), oxa-Michael addition is preferable over the aza-Michael reaction and it gave 3,4-diphenyl substituted furan **9** (56%) instead of pyrroloquinoline derivative.

Table 6.4. Substrate scope of pyrrolo[1,2-*a*]quinoline synthesis from acyclic precursors



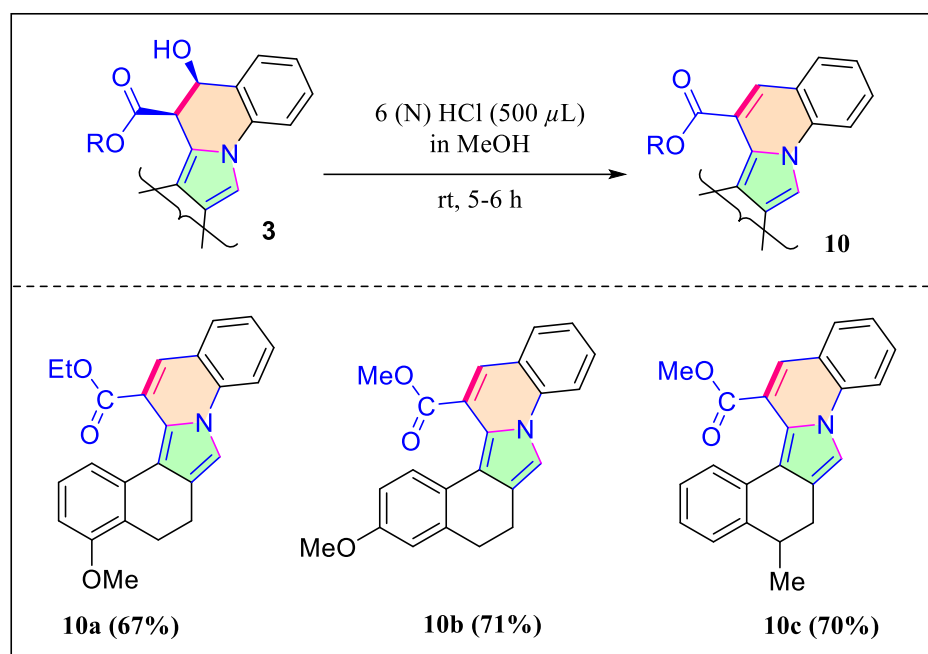
Reaction Conditions: (i) 2-nitrobenzaldehyde **1a** (1 mmol, 1 equiv), Na₂S₂O₄ (6 mmol, 6 equiv), THF-Water, 60 °C, 15 min.; (ii) 3-(2-formylcycloalkenyl)-acrylic ester derivatives **2** (1 mmol, 1 equiv), MeOH (4-5 mL), Glacial AcOH (160 μ L), 70 °C, 5-6 h.

From the systematic substrate scope analysis it has been found that the substrates **2l**, **2r**, **2v** fail to produce desired pyrrolo[1,2-*a*]quinolines under the optimized conditions (Table 6.1, entry 4). In all cases MeOH takes part in the side reaction to form dihydrofuran/acetal/furan **4**, **7**, **9** derivatives. Consequently, we anticipated that in the absence of MeOH may reach to our goal. Hence we have applied neat conditions (Table 6.1, entry 6) but unfortunately we did not get any pyrrolo[1,2-*a*]quinolines (Scheme 6.26).



Scheme 6.26. Unsuccessful results for the synthesis pentacyclic to tricyclic pyrrolo[1,2-*a*]quinoline under neat conditions.

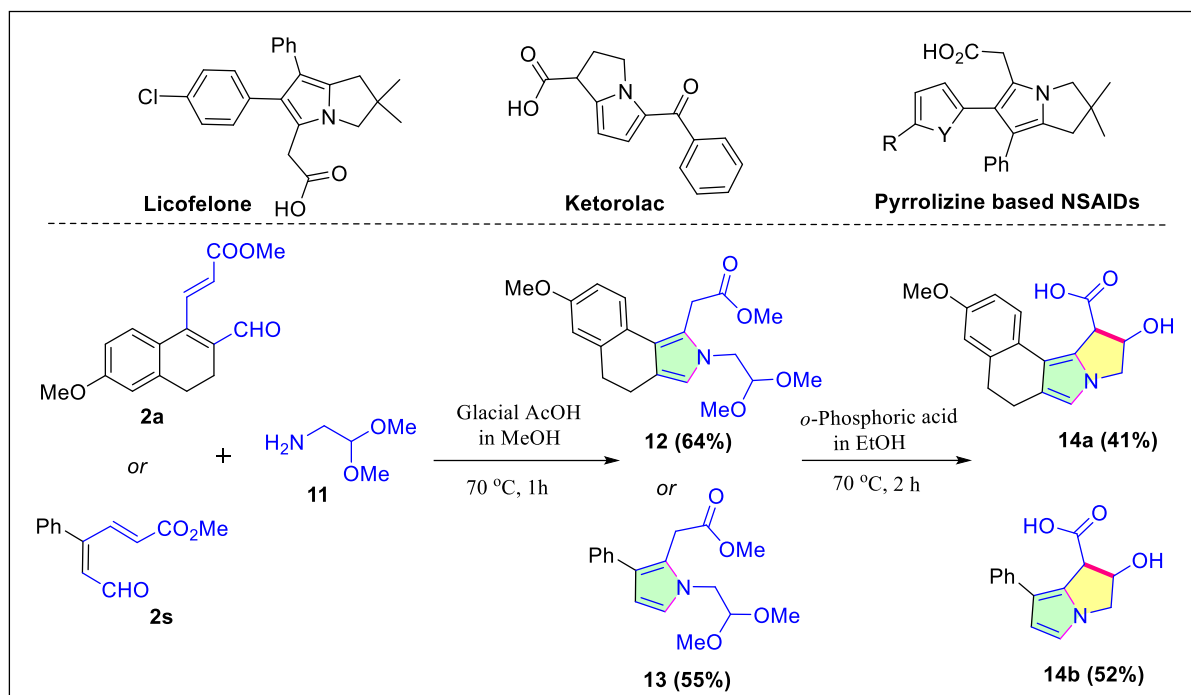
After successful synthesis of pentacyclic to tricyclic embedded pyrrolo[1,2-*a*]quinoline ring, we tried to eliminate water molecules from the hydroxyl substituted pyrroloquinoline derivatives under the standardized conditions using an increased amount of AcOH. The $-\text{OH}$ group remains intact even after adding $600\ \mu\text{L}$ AcOH. This result reveals that the acidity of AcOH is not sufficient to remove the water molecule. In order to obtain the dehydrated products, the hydroxyl substituted pyrrolo[1,2-*a*]quinoline derivatives **3** were stirred at room temperature in presence of 6 (N) HCl ($500\ \mu\text{L}$) in MeOH. It has been found that the unsaturated desired compounds **10** were obtained in 67-71% yields (Table 6.5).

Table 6.5. Synthetic approach of water eliminated products of pyrrolo[1,2-*a*]quinoline

Reaction Conditions: Substrate **3** (1 mmol, 1 equiv), MeOH (4-5 mL), 6 (N) HCl (500 μ L), rt, 5 - 6 h.

We have added another useful feather to our developed protocol by synthesizing the Ketorolac analog. Ketorolac is the non-steroidal anti-inflammatory drug (NSAIDs) that helps to reduce the prostaglandins production by the cells of the immune system that causes fever and pain due to inflammation and hence it is enormously used as pain reliever.³³ However, these molecules have some adverse effects, consequently, there have been ongoing efforts to develop more effective and less toxic compounds. In this connection, we wish to synthesize such analog applying our developed protocol where aminoacetaldehyde dimethyl acetal was used instead of 2-nitrobenzaldehyde as the partner to react with the substrate **2a**. Ketorolac is a pyrrolizine which contains one pyrrole ring attached at C1-C2 position with another saturated analog of pyrrole ring. Hence, our target is to synthesize pyrrolizine ring by aza-Michael reaction followed by aldol reaction using the aldehyde-protected amine partner **11** and substrate **2a** or **2s** in presence of AcOH in MeOH at 70 °C. But in the said conditions, we only got *c*-fused pyrrole **12** or **13** where *N*-alkyl contains aldehyde in the protected form (Table 6.6). The remaining aldol reaction was succeeded in the presence of *o*-phosphoric acid in EtOH at 70 °C with moderate yields.

Table 6.6. Synthetic approach of analogous compounds of various bio-active natural products

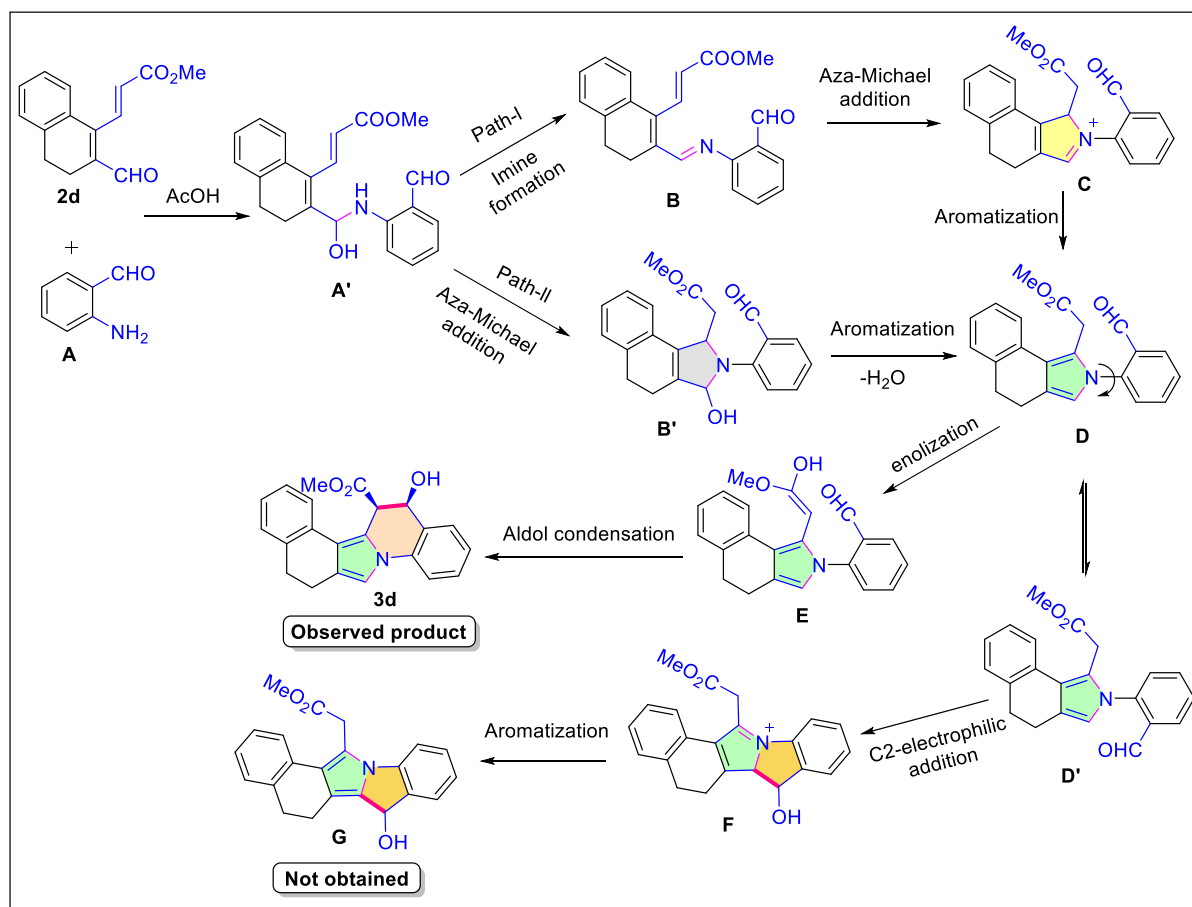


Reaction Conditions: (i) Substrate **2a** or **2s** (1 mmol, 1 equiv), amino acetaldehyde dimethyl acetal **11** (1 mmol, 1 equiv), MeOH (4-5 mL), Glacial AcOH (120 μ L), 70 °C, 1h (ii) Substrate **12** (229.8 mg) or **13** (166.7 mg), *o*-Phosphoric acid (4 mL) in EtOH (4 mL), 70 °C, 2h.

6.4.1. Theoretical study for mechanism:

Amine group of 2-aminobenzaldehyde attack to the aldehyde group of **2d** instead of at the β -position of α,β -unsaturated ester could produce the intermediate hemiaminal compound **A'**. Now, the compound **A'** could convert into the compound **D** in two pathways. In the first path, water elimination of **A'** gives the imine **B** which can be converted to the **D** through the aromatization of **C** (2H-pyrrol-1-ium compound) obtained from intra-molecular aza-Michael of imine **B**. However, in the second path, it can be predicted that the intra-molecular aza-Michael of **A'** can produce 2,5-dihydro-1H-pyrrole compound **B'** which could form pyrrole derivative **D** through aromatization by water elimination reaction. It is interesting to note that the compound **D** could exist in two diastereoisomeric forms (**D** and **D'**) in an equilibrium by the rotation of C-N bond. Aromatic electrophilic attack on aldehyde group of **D'** by C2 of pyrrole produce **F** which could give expected product **G** (not obtained). However, the

obtained product **3d** could be formed through the intramolecular aldol reaction of enol **E** which was produced from **D**. The plausible mechanism is shown in the **Scheme 6.27**.



Scheme 6.27. The plausible reaction mechanism for the formation of compound **3d**.

A computational study on the production of unexpected product **3d** from compounds 2-aminobenzaldehyde and **2d** have been performed here with the help of DFT method. The reaction prefers only one reaction path and produce compound **3d** as the only product. The DFT calculation may help to understand the preference of the path. The formation of intermediate **A'** from 2-aminobenzaldehyde and **2d** is low energy process and ΔG (change of free energy) involved in this process is -15.82 kcal/mol (**Figure 6.7**). From **A'**, either water elimination to give **B** ($\Delta G = 19.05$ kcal/mol) or the formation of **B'** ($\Delta G = 12.04$ kcal/mol) by intramolecular cyclization through the nucleophilic attack of amine at β -position of α,β -unsaturated ester are endothermic reaction. Now conversion of **B** to **C** ($\Delta G = -18.55$ kcal/mol) through the imine *N*-nucleophilic attack at β -position of α,β -unsaturated ester is favorable. Aromatization the ionic intermediate **C** to form **D** ($\Delta G = 0.105$ kcal/mol) make aldehyde and ester groups closer to each other. However, the same process (aromatization) of

B' (where aldehyde and ester groups are already in close proximity) to give **D** is a favored process. Now, rotation of N-C (phenyl) bond of **D** can produce **D'** ($\Delta G = -3.21$ kcal/mol) where the said groups are far apart from each other. Enol **E** ($\Delta G = -1.58$ kcal/mol) formation from **D** is favored due to formation of hydrogen bond between enol hydrogen and aldehyde oxygen. Such hydrogen bond in **E** make susceptible the aldol type intramolecular attack by enol to the aldehyde which give the product **3d** ($\Delta G = -28.02$ kcal/mol). However, the stable conformer **D'** of **D** do not have stabilization by hydrogen bond formation after enolization. Therefore, it can produce stable (with respect to **D'**) compound **F** ($\Delta G = -11.35$ kcal/mol) by intramolecular aromatic electrophilic substitution reaction at the C2 of pyrrole ring of **D**. The formation of **G** ($\Delta G = -0.165$ kcal/mol) from **F** is not favored which may be due to the strain of the molecule having reactive *1H*-pyrrolizine ring.

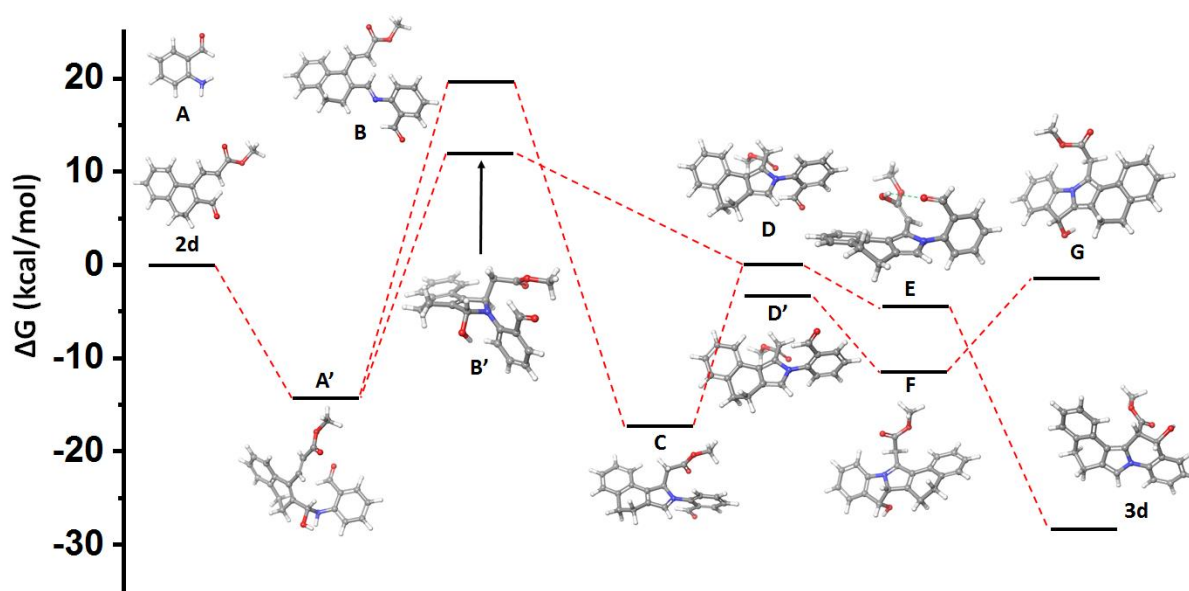


Figure 6.7. Energy profile diagram of the formation of **3d**.

6.4.2. Photophysical studies:

After successful synthesis of pyrrolo[1,2-*a*]quinoline derivatives in different class *via* environmentally benign protocol, we wanted to investigate photophysical properties of newly synthesized and highly functionalized fluorescent molecule in correlation with the prevention of environmental pollution. The explosive nature of the nitroaromatic compounds is enormously used in chemical laboratories, mining units, chemical industries, and military training and hence it is highly exposed to the nature.³⁴ Extensive consumptions of toxic

nitrophenol compounds in industries regularly contaminate the waste waters and eventually causes detrimental effects to the living organisms even at their trace amounts. Hence, the specific recognition of such toxic material has been developed using various methodologies based on several small molecule sensors, nanoparticles, nano-fibers, gels polymers and metal-organic frameworks (MOFs) etc.³⁵ Though the different techniques have been listed in literature for the detection of nitro-aromatic compounds in micromolar level but fluorescence sensors have high demanding techniques due to their high sensitivity, cost efficiency, simple instrumentation, easy sample preparation and quick response. Herein, we have synthesized a pyrrolo[1,2-*a*]quinoline based a sensor containing Phenyl, hydroxyl and ester functionalities which exhibited good fluorescent properties for the detection of picric acid *via* quenching effect. Notably, most of the literature reports on picric acid/4-NP sensors *via* fluorescence quenching effect. To the best of our knowledge, there are no literature reports found where the fluorescent intensity of the fluorophore enhances with all analytes except picric acid which showed quenching effect. To establish this effect, we first measured the UV-Vis absorption spectra of the solution (2×10^{-5} M for **8a**; **Figure 6.8**) in different solvents and found the λ_{max} around 276-293 nm which are displayed in **Table 6.7**. Furthermore, we have measured the emission wavelength in the different solvents from the less polar to higher polar solvents including polar protic MeOH solvent (**Table 6.7**). We observed that the emission spectra are controlled by the viscosity of the solvents instead of the solvent polarity. Our synthesized fluorophore **8a** has ability to show atropisomerism *via* C-C bond rotation (see experimental section, **Figure 6.14**) and hence the emission intensity of the molecule was governed by the viscosity of solvents through fluorescence emission and non-radiative de-excitation.³⁶ Restricted rotation of the C-C bond is inhibited with increasing viscosity of the solvents. The **Figure 6.9** showed the higher emission intensity of **8a** in DMSO ($\eta_{20^\circ\text{C}} = 1.99$ cP) and dioxane solvents ($\eta_{20^\circ\text{C}} = 1.17$ cP) and it exhibited similar observation in lower viscose solvents (CHCl₃ for $\eta_{20^\circ\text{C}} = 0.51$ cP, CH₂Cl₂ for $\eta_{20^\circ\text{C}} = 0.44$ cP, MeOH for $\eta_{20^\circ\text{C}} = 0.54$ cP, CH₃CN for $\eta_{20^\circ\text{C}} = 0.38$ cP).

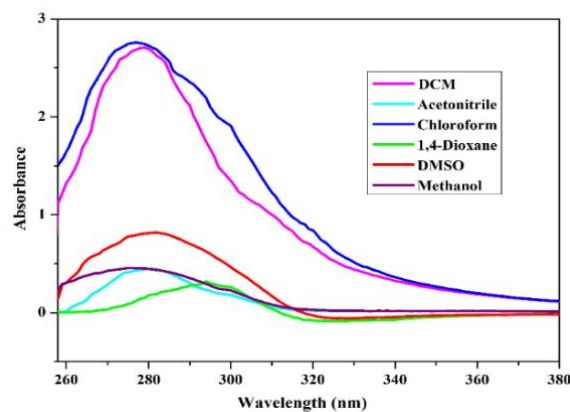


Figure 6.8. Absorption spectra of **8a** recorded at concentration 2.0×10^{-5} M in different solvents.

Table 6.7. UV-Vis absorption and emission data of **8a** in different solvents

Solvent	ϵ^a (25 °C)	Viscosity ^b (cP)	λ_{max}^c (nm)	λ_{emi}^d (nm)	ϵ_{max}^e ($10^5 \text{ M}^{-1} \text{ cm}^{-1}$)	Stokes Shift ^f (nm)
1,4-dioxane	2.25	1.17	293	334	0.15	41
Chloroform	4.81	0.51	277	353	1.82	76
DCM	8.93	0.44	279	337	1.67	58
MeOH	32.70	0.54	276	334	0.23	58
Acetonitrile	37.5	0.38	281	333	0.16	52
DMSO	46.68	1.99	282	337	0.41	55

^aDielectric constant at 25 °C. ^bViscosity of different solvents at 20 °C. ^cMaximum absorption wavelength. ^dMaximum emission wavelength. ^eMolar absorption co-efficient at maximum absorption wavelength. ^fDifference between emission maxima and absorption maxima.

Since the attached phenyl ring in the pyrrolo[1,2-*a*]quinoline can freely rotate in non-viscous solvent, in DMSO solvent the rotation becomes restricted and results in enhanced emission. With the addition of non-viscous toluene in DMSO solution of **8a** (2×10^{-5} M), emission intensity was gradually decreased (**Figure 6.9. (b)**). This is attributed to the free rotation of the phenyl ring of the pyrrolo[1,2-*a*]quinoline derivative and resulting non-radiative decay of the excited state energy.

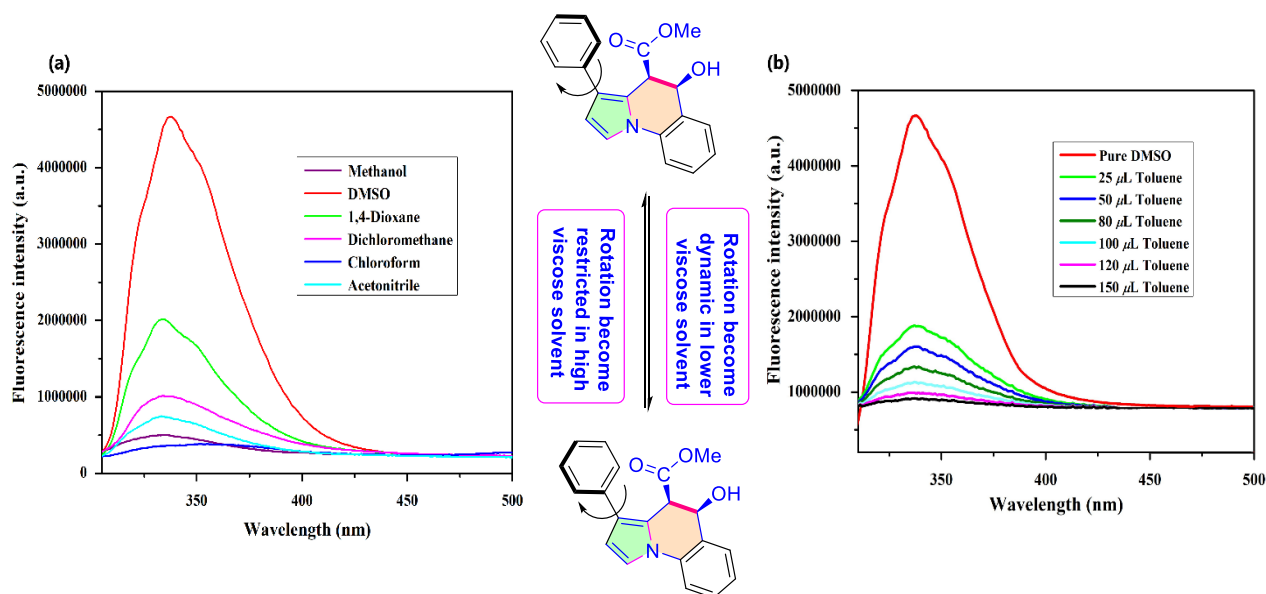


Figure 6.9. (a) Fluorescence spectra of **8a** recorded at concentration 2.0×10^{-5} M in different solvents. (b) Fluorescence quenching of **8a** by stepwise addition of Toluene (μL) in DMSO-Toluene mixture.

Our synthesized fluorophore has different functionality for acid-base reaction and $-\text{OH}$ group has greater tendency to eliminate the water molecule to form more stabilized α,β -unsaturated ester and hence we choose some organic aromatic nitro phenol compounds that create environmental pollution in huge extent along with the aromatic carboxyl derivative for the acid-base interaction. To get an insight into the interaction of compounds with electron-deficient nitroaromatics and carboxylic acids, emission studies were carried out (**Figure 6.10**). The emission of **8a** displayed a significant change upon the addition of picric acid thus making it as an interesting sensor for the detection of toxic material (see experimental section, **Figure 6.15**). The emission intensity of compound **8a** was significantly enhanced by the addition of 0.2 mL of 20 μM different nitro phenols, aromatic carboxylic acids and trifluoroacetic acid (TFA) into a 2 mL solution of compound **8a** in CH_3CN (20 μM) except picric acid which quenches the fluorescence intensity. The disappearance of bluish green emission of compound **8a** was observed more effectively with picric acid which could be visualized under UV light of long wavelength (lamp excitation-365 nm) (**Scheme 6.28**).

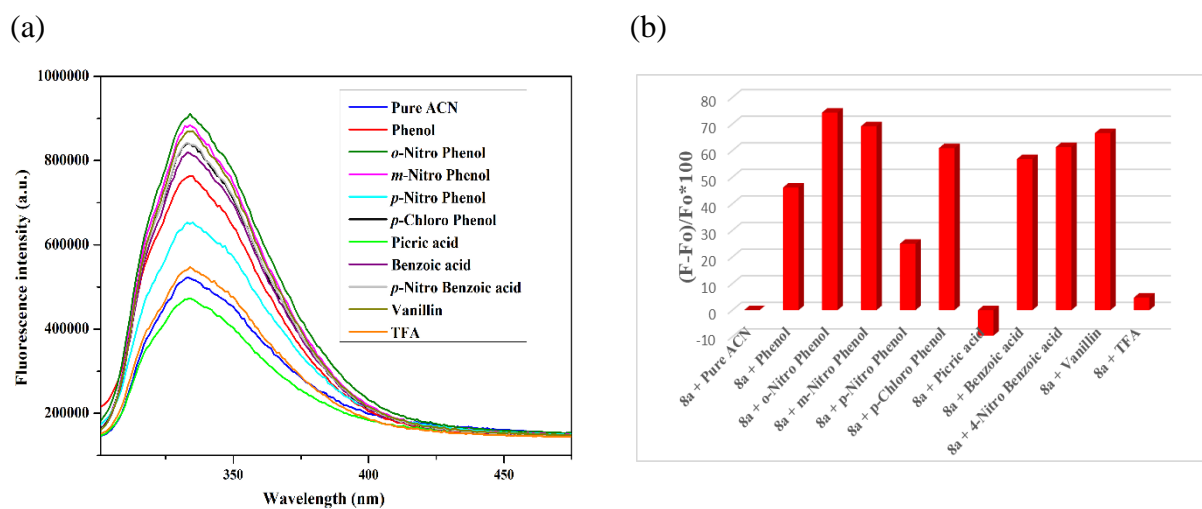
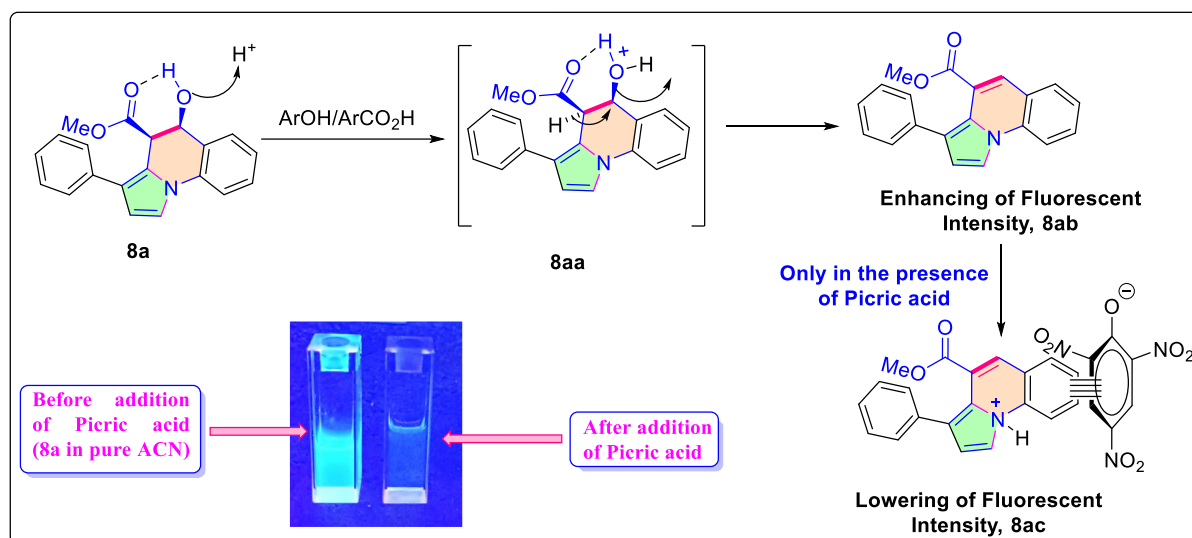


Figure 6.10. (a) Emission spectra of compound **8a** with different organic compounds [$\lambda_{ext} = 285$ nm] (Concentration: 2×10^{-5} M solution in CH_3CN). (b) Changes in fluorescence intensity of the fluorophores **8a** [plotted as $(F-F_0)/F_0 \times 100$] observed upon the addition of various analytes.

This unusual phenomenon can be explained by the greater capability of picric acid to protonate $-\text{OH}$ group as well as the N -atom of fluorophore **8a**, due to the lower pKa (0.3) value compared to the other examined analytes. The eliminating tendency of $-\text{OH}$ group in the fluorophore make it more planar form which can strongly interact with the most electron deficient aromatic compound *via* π - π interactions.³⁷ Furthermore, the higher acidity of picric acid also protonates the N -atom of **8a**, forming charge complexes. This also results in the excited state energy transfer from **8a** to the picrate anion and accordingly radiation less deactivation of the excited state to observe the fluorescence quenching.^{29b} The acidic properties of other analytes are sufficient to interact with $-\text{OH}$ group but not sufficient to protonate the N -atom of **8a**. Consequently, in the presence of other nitroaromatics/nitrocarboxylic acids, **8a** can form **8ab** which enhances the fluorescence intensity due to the planar and conjugated structure but cannot form **8ac** which quenches the fluorescence intensity. However, pKa of TFA (0.5) is very close to picric acid, so the enhancement of fluorescent intensity is not so much as like of other acidic analytes. This can be attributed as the picric acid has lower pKa value than TFA, hence it has stronger capability to protonate the N -atom of pyrrole ring of **8ab** and picrate ion has extra π -electron in the aromatic ring which further interacts with the planar **8ab** leads to the quenching effect. These observations indicated that our synthetic fluorophore **8a** has the good capacity to detect

the picric acid in the presence different nitro phenols, aromatic carboxylic acids and trifluoroacetic acid (TFA).



Scheme 6.28. Chemical interaction of fluorophore with analytes.

6.5. Conclusion:

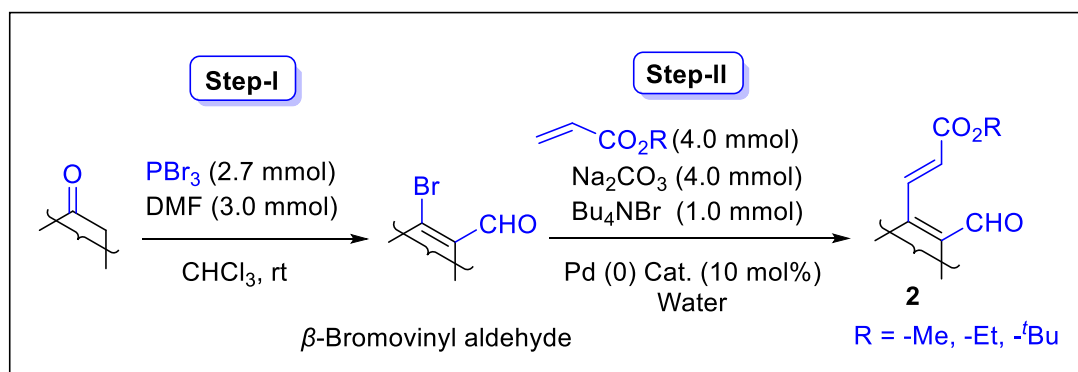
In summary, we have disclosed a tandem cyclization using Michael-aldol reaction between reductive partners of 2-nitrobenzaldehyde with 3-(2-formylcycloalkenyl)-acrylic ester derivatives with being the formation of C–N and C–C bonds in one step by the elimination of water molecule as the only by-product. This process chronologically furnished highly substituted tri/tetra/pentacyclic pyrrolo[1,2-*a*]quinoline embedded scaffolds with moderate to good yields. In addition, the target-oriented synthetic route of pyrrole fused drugs analog, Toradol/Ketorol has also been documented with the help of modified reacting aliphatic amine partners instead of 2-nitrobenzaldehyde. We have also included a detailed mechanistic observation *via* DFT study with the comparison reactivity to the addition of –CHO by the C-2 position and C-5 substituents (–CH₂CO₂R) of the pyrrole ring. Furthermore, the photophysical application of new synthetic fluorophores and preliminary sensing properties add a new era to our developed protocol. The broad substrate scope and the significant application of the cyclized products (drugs analog and photophysical study) revealed the potential value of this novel synthetic protocol.

6.6. Experimental Section:

General information:

^1H NMR spectra of all the synthesized compounds were recorded on a 300 MHz, 400 MHz and 500 MHz spectrometers in CDCl_3 and d^6 -DMSO solvents using TMS as the internal standard. ^{13}C NMR spectra were recorded in the same MHz instruments. Structural assignments were made with additional information from gCOSY, gHSQC, and gHMBC experiments. Mass spectra were recorded in High-resolution (ESI-TOF) mass spectrometer. Silica gels 60-120 or 100-200 mesh (SRL) were used for column chromatographic purification. Progress of the reaction was monitored by using precoated silica gel 60 F254 TLC sheets (Merck). Petroleum ether (boiling range 60-80 °C) or n-hexane and ethyl acetate (b.p. 77.1 °C) were used as the eluent for column chromatographic separation. Solvents were distilled, dried and stored over molecular sieves (4 Å). The UV-Vis absorption spectra were recorded on UV-Vis spectrophotometer (Shimadzu UV spectrophotometer UV-1800) and the fluorescence emission spectra were recorded on Jobin Yvon Fluoromax spectrofluorometer. All the reaction temperatures mentioned above 25 °C refer to oil bath temperature.

General Procedure for the preparation of 2:



Step-I: Preparation of β -Bromovinyl aldehyde.¹

Step-II: Preparation of acrylic ester derivatives **2**.²

General Procedure for the preparation of 3–9:

Reaction was conducted in consecutive two-step procedures:

Step I: At first 2-nitrobenzaldehyde **1** (1 mmol, 1 equiv.) was reduced to the 2-aminobenzaldehyde with sodium dithionite (6 mmol, 6 equiv.) in THF- H_2O (1:1) at 60 °C within 15-20 minutes. The progress of the reaction was monitored by TLC. After completion

the reduction, the reaction mixture was diluted with EtOAc (20.0 mL) and washed with brine water (3 × 20.0 mL). The organic layer was dried (anhydrous Na₂SO₄), filtered, and concentrated under reduced pressure.

Step II: The crude reduced product from **step I**, i.e., 2-aminobenzaldehyde was added to the substrate **2** (1 mmol, 1 equiv.) in methanol (4-5 mL). Then glacial AcOH (160 μL) was added into this reaction mixture. After that, the reaction mixture was allowed for stirring up to 5-6 h at 70 °C. The progress of the reaction was monitored by TLC. After the completion of the reaction, the crude mixture was neutralized with NaHCO₃ solution (500 mg in 10 mL water). Then it was extracted with EtOAc (20.0 mL) followed by washing with brine water (2 × 10.0 mL) and then solvent was removed under reduced pressure. The crude residue was purified by column chromatography (100-200 mesh of silica gel) using ethyl acetate and petroleum ether (1:5) as an eluent to get the desired product **3-9**.

General Procedure for the preparation of 10:

Compound **3** (1 mmol, 1 equiv.) was taken in methanol (4-5 mL) and 500 μL of 6 (N) HCl was added into this reaction mixture. The reaction was allowed for stirring up to 5-6 h at room temperature. The progress of the reaction was monitored by TLC. After formation of desired product, the crude mixture was obtained by dilution with EtOAc (20.0 mL) followed by wash with brine water (2 × 10.0 mL). Then it was concentrated under reduced pressure, The crude residue was purified by column chromatography (100-200 mesh of silica-gel) using ethyl acetate and petroleum ether (1:10) as an eluent to get the desired product **10**.

General Procedure for the preparation of 14:

This reaction has been carried out in two steps procedures:

Setp I: Substrates **2a** or **2s** (1 mmol, 1 equiv.) and amino acetaldehyde dimethyl acetal **11** (1 mmol, 1 equiv.) in presence of glacial AcOH (120 μL) in MeOH (4-5 mL) were taken in a reaction vessel. This reaction mixture was allowed for stirring 1 h at 70 °C. The reaction mixture was extracted EtOAc (20 mL) followed by wash with brine water (2 × 10.0 mL). Then the solvent was evaporated under reduced pressure. After that, the pure *c*-fused pyrrole **12** (229.8 mg) or **13** (166.7 mg) respectively were obtained by column chromatography (100-200 mesh of silica-gel) using ethyl acetate and petroleum ether (1:5) eluent.

Step II: Then this *c*-fused pyrrole **12** (229.8 mg) or **13** (166.7 mg) was taken in ethanol (4 mL) and *o*-phosphoric acid (4 mL) was added into the reaction mixture. The reaction mixture

was allowed for stirring up to 2 h at 70 °C. The progress of the reaction was monitored by TLC. Then the resulting mixture was neutralized with NaHCO₃ solution (500 mg in 10 ml water) and it was extracted with EtOAc (20.0 mL) followed by washing with brine water (2 × 10.0 mL). After that, solvent was removed under reduced pressure. The crude residue was purified by column chromatography (100-200 mesh of silica-gel) using ethyl acetate and petroleum ether (1:1) as an eluent to get the desired product **14**.

Preparation of single crystal *via* diffusion method:

30.0 mg solid compound of **3a** was dissolved with 1-2 mL acetonitrile solvent in a crystal tube (inner vessel). Then this crystal tube was placed carefully in a Borosil glass tube (outer vessel) which contain diethyl ether (2-3 mL). Finally, it kept at room temperature upon a sand tray. After several days by slow evaporation of solvent single crystal of **3a** was observed (Figure 6.11).

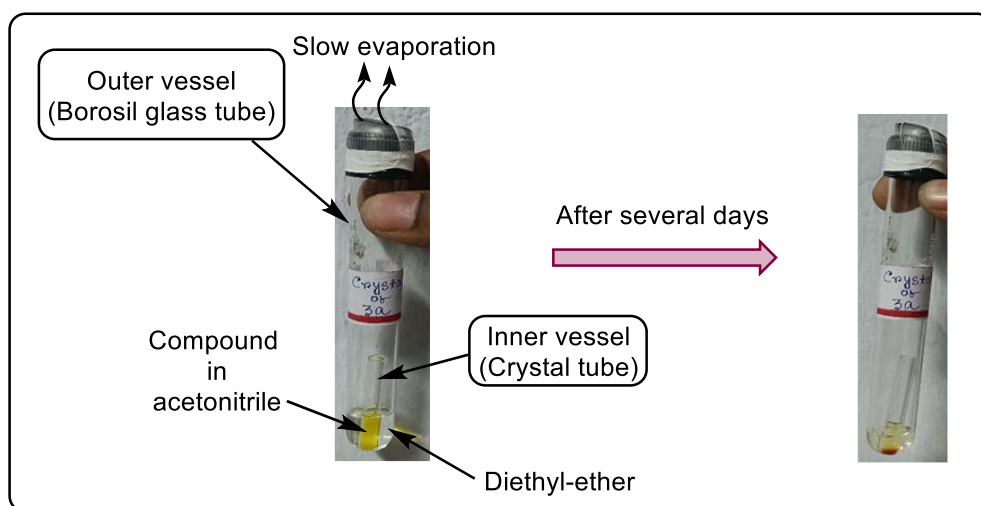
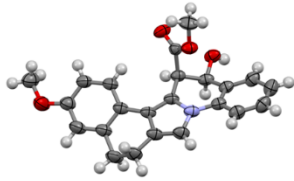


Figure 6.11: Crystal growth technique (diffusion method).

6.6.1. Crystallographic information of compound **3a**:

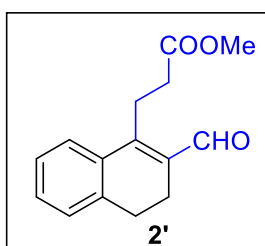
For the determination of X-ray crystal structures, a single crystal of **3a** was selected and mounted with paratone oil on a glass fiber using gum. The crystallographic data was recorded on a CMOS based Bruker D8 Venture PHOTON 100 diffractometer at 298K equipped with a INCOATEC micro-focus source with graphite monochromatic Mo K α radiation ($\lambda = 0.71073$ Å) operation at 50 kV and 30 mA. The CCDC 2114554 of **3a** has been obtained after the deposition at Cambridge Crystallographic Data Centre.

Empirical formula	C ₂₃ H ₂₁ NO ₄	 <p>X-ray crystal structure of 3a with 50% probability ellipsoids (CCDC 2114554).</p> <p>Atom color code: grey = carbon atom, sky blue = nitrogen atom, red = oxygen atom, and white = hydrogen atom.</p>
Formula weight	375.41	
Temperature/K	273.15	
Crystal system	triclinic	
Space group	P-1	
<i>a</i> /Å	9.3667(8)	
<i>b</i> /Å	10.4746(11)	
<i>c</i> /Å	19.6039(19)	
α /°	90.087(3)	
β /°	91.203(3)	
γ /°	93.931(3)	
Volume/Å ³	1918.4(3)	
<i>Z</i>	4	
ρ_{calc} /cm ³	1.300	
μ /mm ⁻¹	0.089	
<i>F</i> (000)	792.0	
Crystal size/mm ³	0.28 × 0.24 × 0.18	
Radiation	MoK α (λ = 0.71073)	
2 θ range for data collection/°	4.412 to 56.604	
Index ranges	-12 ≤ <i>h</i> ≤ 11, -13 ≤ <i>k</i> ≤ 13, -25 ≤ <i>l</i> ≤ 26	
Reflections collected	63916	
Independent reflections	9285 [<i>R</i> _{int} = 0.0433, <i>R</i> _{sigma} = 0.0285]	
Data/restraints/parameters	9285/0/511	
Goodness-of-fit on <i>F</i> ²	1.092	
Final <i>R</i> indexes [<i>I</i> ≥ 2 σ (<i>I</i>)]	<i>R</i> ₁ = 0.0570, <i>wR</i> ₂ = 0.1242	
Final <i>R</i> indexes [all data]	<i>R</i> ₁ = 0.0756, <i>wR</i> ₂ = 0.1385	
Largest diff. peak/hole / e Å ⁻³	0.20/-0.15	

6.6.2. Characterization of spectral data:

Methyl 3-(2-formyl-3,4-dihydronaphthalen-1-yl)propanoate: (**2'**)

Purified by silica gel column chromatography (eluent: petroleum ether/ethyl acetate = 20:1 to

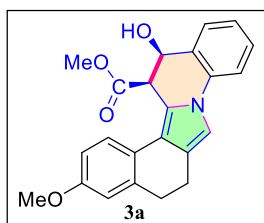


8:1); yellow liquid, 28% yield, 68.3 mg. ¹H NMR (300 MHz, CDCl₃) δ 10.35 (s, 1H), 7.53 – 7.50 (m, 1H), 7.31 – 7.28 (m, 2H), 7.24 – 7.21 (m, 1H), 3.68 (s, 3H), 3.43 – 3.37 (m, 2H), 2.75 – 2.70 (m, 2H), 2.61 – 2.48 (m, 4H). ¹³C{¹H} NMR (76 MHz, CDCl₃) δ 190.5, 172.7, 150.5, 139.6, 134.8, 133.3, 130.3, 128.5, 127.1, 124.7, 52.0, 34.7, 27.8, 21.5,

20.2. HRMS (ESI) *m/z*: [M + H]⁺ Calcd for C₁₅H₁₇O₃ 245.1179; Found 245.1181.

Methyl (13R,14R)-13-hydroxy-3-methoxy-5,6,13,14-tetrahydrobenzo[6,7]isoindolo[2,1-a]quinoline-14-carboxylate: (3a)

Purified by silica gel column chromatography (eluent: petroleum ether/ethyl acetate = 20:1 to 5:1); yellow solid, 86% yield, 322.6 mg; mp 54-55 °C. ^1H NMR (300 MHz, CDCl_3) δ 7.58

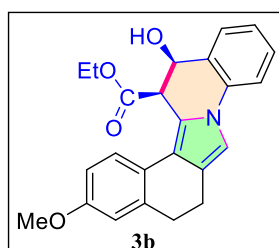


(d, $J = 7.6$ Hz, 1H), 7.44 (d, $J = 8.1$ Hz, 1H), 7.23 – 7.19 (m, 2H), 7.13 – 7.08 (m, 1H), 6.91 (s, 1H), 6.74 (s, 1H), 6.73 (m, 1H), 5.02 (d, $J = 6.0$ Hz, 1H), 4.51 (d, $J = 5.7$ Hz, 1H), 3.72 (s, 3H), 3.50 (s, 3H), 2.82 – 2.71 (m, 2H), 2.69 – 2.54 (m, 2H). $^{13}\text{C}\{^1\text{H}\}$ NMR (76 MHz, CDCl_3) δ 171.9, 157.8, 138.6, 134.9, 129.4, 128.4, 125.4, 124.9, 124.6, 124.4,

122.7, 120.1, 117.6, 114.9, 114.7, 112.1, 111.6, 68.0, 55.4, 52.7, 45.0, 31.5, 21.1. HRMS (ESI) m/z : $[\text{M} + \text{H}]^+$ Calcd for $\text{C}_{23}\text{H}_{22}\text{NO}_4$ 376.1551; Found 376.1548.

Ethyl (13R,14R)-13-hydroxy-3-methoxy-5,6,13,14-tetrahydrobenzo[6,7]isoindolo[2,1-a]quinoline-14-carboxylate: (3b)

Purified by silica gel column chromatography (eluent: petroleum ether/ethyl acetate = 20:1 to 5:1); yellow solid, 77% yield, 299.6 mg; mp 52-54 °C. ^1H NMR (300 MHz, CDCl_3) δ 7.69 (d,

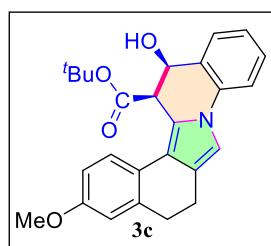


$J = 7.5$ Hz, 1H), 7.61 (d, $J = 8.1$ Hz, 1H), 7.34 – 7.27 (m, 3H), 7.03 (s, 1H), 6.88 – 6.84 (m, 2H), 5.14 – 5.10 (m, 1H), 4.59 (d, $J = 5.9$ Hz, 1H), 4.06 (qd, $J = 7.1, 1.4$ Hz, 2H), 3.86 (s, 3H), 2.91 – 2.88 (m, 2H), 2.84 – 2.68 (m, 2H), 1.04 (t, $J = 7.1$ Hz, 3H). $^{13}\text{C}\{^1\text{H}\}$ NMR (76 MHz, CDCl_3) δ 171.2, 157.7, 138.5, 135.1, 129.3, 128.3, 125.3, 125.1,

124.6, 124.2, 122.6, 119.9, 117.7, 114.8, 114.6, 111.9, 111.5, 67.9, 61.5, 55.4, 45.4, 31.4, 21.1, 13.9. HRMS (ESI) m/z : $[\text{M} + \text{H}]^+$ Calcd for $\text{C}_{24}\text{H}_{24}\text{NO}_4$ 390.1707; Found 390.1703.

Tert-butyl (13R,14R)-13-hydroxy-3-methoxy-5,6,13,14-tetrahydrobenzo[6,7]isoindolo[2,1-a]quinoline-14-carboxylate: (3c)

Purified by silica gel column chromatography (eluent: petroleum ether/ethyl acetate = 15:1 to

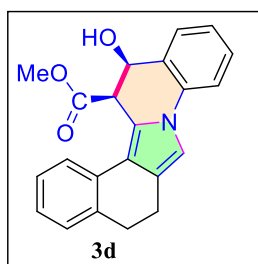


5:1); yellow solid, 69% yield, 287.8 mg; mp 54-55 °C. ^1H NMR (500 MHz, CDCl_3) δ 7.66 (d, $J = 7.6$ Hz, 1H), 7.58 (d, $J = 8.2$ Hz, 1H), 7.33 – 7.28 (m, 2H), 7.18 (td, $J = 7.4, 1.4$ Hz, 1H), 7.00 (s, 1H), 6.84 – 6.82 (m, 2H), 5.10 – 5.07 (m, 1H), 4.47 (d, $J = 6.0$ Hz, 1H), 3.84 (s, 3H), 2.89 – 2.67 (m, 4H), 1.20 (s, 9H). $^{13}\text{C}\{^1\text{H}\}$ NMR (126 MHz,

CDCl_3) δ 170.3, 157.7, 138.5, 135.2, 129.6, 128.2, 125.3, 125.2, 124.8, 124.1, 122.7, 119.8, 118.4, 114.7, 114.6, 111.9, 111.2, 82.8, 68.0, 55.4, 46.4, 31.5, 27.9 (3C), 21.2. HRMS (ESI) m/z : $[\text{M} + \text{H}]^+$ Calcd for $\text{C}_{26}\text{H}_{28}\text{NO}_4$ 418.2020; Found 418.2024.

Methyl (13R,14R)-13-hydroxy-5,6,13,14-tetrahydrobenzo[6,7]isoindolo[2,1-a]quinoline-14-carboxylate: (3d)

Purified by silica gel column chromatography (eluent: petroleum ether/ethyl acetate = 15:1 to 5:1); yellow solid, 79% yield, 272.6 mg; mp 68-69 °C. ^1H NMR (500 MHz, CDCl_3) δ 7.70 (d,

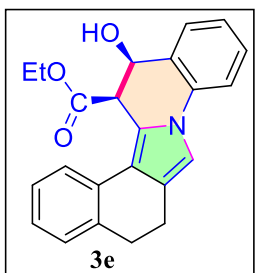


$J = 7.7$ Hz, 1H), 7.61 (d, $J = 7.6$ Hz, 1H), 7.36 – 7.17 (m, 6H), 7.04 (s, 1H), 5.13 – 5.09 (m, 1H), 4.66 (d, $J = 5.9$ Hz, 1H), 3.88 (s, 1H), 3.60 (s, 3H), 2.93 – 2.84 (m, 3H), 2.75 – 2.69 (m, 1H). $^{13}\text{C}\{^1\text{H}\}$ NMR (126 MHz, CDCl_3) δ 171.9, 136.9, 134.9, 131.6, 129.5, 128.8, 128.5, 126.9, 125.8, 125.4, 124.6, 123.9, 123.2, 120.2, 118.7, 115.0, 111.7, 68.0,

52.7, 44.9, 31.1, 21.1. HRMS (ESI) m/z : $[\text{M} + \text{H}]^+$ Calcd for $\text{C}_{22}\text{H}_{20}\text{NO}_3$ 346.1445; Found 346.1442.

Ethyl (13R,14R)-13-hydroxy-5,6,13,14-tetrahydrobenzo[6,7]isoindolo[2,1-a]quinoline-14-carboxylate: (3e)

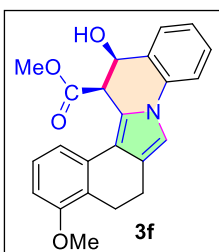
Purified by silica gel column chromatography (eluent: petroleum ether/ethyl acetate = 20:1 to 5:1); yellow solid, 70% yield, 251.4 mg; mp 66-68 °C. ^1H NMR (400 MHz, CDCl_3) δ 7.67



(d, $J = 7.6$ Hz, 1H), 7.63 (d, $J = 8.0$ Hz, 1H), 7.34 – 7.27 (m, 4H), 7.18 (dt, $J = 15.3, 7.4$ Hz, 2H), 7.02 (s, 1H), 5.12 (s, 1H), 4.61 (d, $J = 5.9$ Hz, 1H), 4.05 (dtt, $J = 10.7, 7.1, 3.6$ Hz, 2H), 3.79 (s, 1H), 2.92 – 2.66 (m, 4H), 1.02 (t, $J = 7.1$ Hz, 3H). $^{13}\text{C}\{^1\text{H}\}$ NMR (76 MHz, CDCl_3) δ 171.3, 136.9, 135.0, 131.7, 129.8, 129.4, 128.8, 128.4, 126.9, 125.7,

125.4, 124.5, 124.1, 123.2, 118.9, 114.9, 111.6, 68.0, 61.7, 45.2, 31.1, 21.1, 13.9. HRMS (ESI) m/z : $[\text{M} + \text{H}]^+$ Calcd for $\text{C}_{23}\text{H}_{22}\text{NO}_3$ 360.1601; Found 360.1605.

Methyl (13R,14R)-13-hydroxy-4-methoxy-5,6,13,14-tetrahydrobenzo[6,7]isoindolo[2,1-a]quinoline-14-carboxylate: (3f)

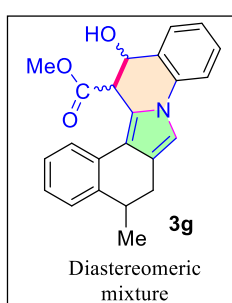


Purified by silica gel column chromatography (eluent: petroleum ether/ethyl acetate = 20:1 to 5:1); yellow solid, 71% yield, 266.3 mg; mp 73-75 °C. ^1H NMR (500 MHz, CDCl_3) δ 7.69 (d, $J = 7.6$ Hz, 1H), 7.36 – 7.31 (m, 2H), 7.29 – 7.27 (m, 2H), 7.24 – 7.21 (m, 1H), 7.04 (s, 1H), 6.83

– 6.81 (m, 1H), 5.12 – 5.09 (m, 1H), 4.66 (d, $J = 5.9$ Hz, 1H), 3.90 (s, 3H), 3.60 (s, 3H), 3.33 – 3.29 (m, 1H), 2.87 – 2.83 (m, 1H), 2.66 – 2.55 (m, 2H). $^{13}\text{C}\{^1\text{H}\}$ NMR (126 MHz, CDCl_3) δ 171.9, 157.1, 134.9, 132.8, 129.5, 128.5, 127.1, 125.4, 124.5, 123.2, 120.2, 118.9, 117.6, 116.8, 115.1, 111.6, 108.4, 68.1, 55.7, 52.7, 45.0, 22.3, 20.4. HRMS (ESI) m/z : $[\text{M} + \text{H}]^+$ Calcd for $\text{C}_{23}\text{H}_{22}\text{NO}_4$ 376.1551; Found 376.1549.

Methyl (14R)-13-hydroxy-5-methyl-5,6,13,14-tetrahydrobenzo[6,7]isoindolo[2,1-a]quinoline-14-carboxylate: (3g)

Purified by silica gel column chromatography (eluent: petroleum ether/ethyl acetate = 18:1 to 5:1); yellow solid, 73% yield, 262.1 mg; mp 59-61 °C. ^1H NMR (300 MHz, CDCl_3) δ Major:

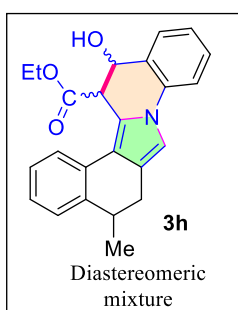


7.64 (d, $J = 7.7$ Hz, 2H), 7.34 – 7.21 (m, 6H), 6.99 (s, 1H), 5.10 – 5.07 (m, 1H), 4.59 (d, $J = 5.9$ Hz, 1H), 3.55 (s, 3H), 3.12 – 3.08 (m, 1H), 2.92 – 2.90 (m, 1H), 2.60 (dd, $J = 14.8, 2.6$ Hz, 1H), 1.36 (d, $J = 7.1$ Hz, 3H), Minor: 7.56 – 7.54 (m, 2H), 7.18 – 7.11 (m, 6H), 6.98 (s, 1H), 5.05 – 5.02 (m, 1H), 4.63 (d, $J = 5.9$ Hz, 1H), 3.51 (s, 3H), 2.87 – 2.86 (m, 1H), 2.79 (dd, $J = 14.5, 5.0$ Hz, 1H), 2.42 (dd, $J = 14.7, 10.9$ Hz, 1H), 1.08

(d, $J = 7.1$ Hz, 3H). $^{13}\text{C}\{^1\text{H}\}$ NMR (76 MHz, CDCl_3) δ 171.9 (2C), 142.0, 141.2, 134.9 (2C), 131.3, 130.3, 129.4, 129.3 (2C), 128.5, 128.4, 128.3, 126.9, 126.7, 126.3, 126.1, 126.0, 125.5, 125.4, 124.5 (2C), 124.2, 123.9, 122.7, 121.1, 120.1, 119.4, 118.6, 118.5, 114.9, 113.0, 111.8, 67.9 (2C), 52.7 (2C), 45.1, 45.0, 35.3, 34.4, 29.5, 27.9, 21.5, 19.5. HRMS (ESI) m/z : $[\text{M} + \text{H}]^+$ Calcd for $\text{C}_{23}\text{H}_{22}\text{NO}_3$ 360.1601; Found 360.1599.

Ethyl (14R)-13-hydroxy-5-methyl-5,6,13,14-tetrahydrobenzo[6,7]isoindolo[2,1-a]quinoline-14-carboxylate: (3h)

Purified by silica gel column chromatography (eluent: petroleum ether/ethyl acetate = 15:1 to 5:1); yellow solid, 67% yield, 250.0 mg; mp 50-52 °C. ^1H NMR (300 MHz, CDCl_3) δ Major:



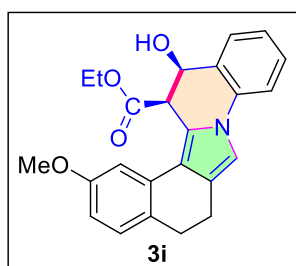
7.64 (d, $J = 7.7$ Hz, 2H), 7.28 – 7.15 (m, 6H), 7.03 (s, 1H), 5.12 – 5.07 (m, 1H), 4.61 (d, $J = 5.9$ Hz, 1H), 4.02 – 3.94 (m, 2H), 2.84 (dd, $J = 14.5, 5.0$ Hz, 1H), 2.65 (dd, $J = 4.9, 2.6$ Hz, 1H), 2.48 (dd, $J = 14.0, 10.2$ Hz, 1H), 1.13 (d, $J = 7.1$ Hz, 3H), 1.04 (t, $J = 7.1$ Hz, 3H). Minor: 7.68 (d, $J = 7.1$ Hz, 2H), 7.37 – 7.30 (m, 6H), 7.04 (s, 1H), 5.16 – 5.14 (m, 1H), 4.67 (d, $J = 5.8$ Hz, 1H), 4.09 – 4.04 (m, 2H), 3.16 – 3.12 (m,

1H), 2.93 (dd, $J = 14.2, 5.2$ Hz, 2H), 1.38 (d, $J = 6.8$ Hz, 3H), 0.97 (t, $J = 7.1$ Hz, 3H). $^{13}\text{C}\{^1\text{H}\}$ NMR (76 MHz, CDCl_3) δ 171.3 (2C), 141.9, 141.3, 135.1, 135.0, 131.4, 130.4, 129.5, 129.4, 128.4 (2C), 128.3, 126.8, 126.6, 126.4, 126.0, 125.9, 125.4 (2C), 124.5, 124.4

(2C), 124.0, 122.6, 121.0, 120.0, 119.4, 118.8, 118.7, 114.9 (2C), 112.9, 111.7, 68.1, 68.0, 61.7, 61.6, 45.3, 45.2, 35.3, 34.5, 29.4, 27.9, 21.6, 19.6, 14.0, 13.9. HRMS (ESI) m/z : $[M + H]^+$ Calcd for $C_{24}H_{24}NO_3$ 374.1758; Found 374.1756.

Ethyl (13R,14R)-13-hydroxy-2-methoxy-5,6,13,14-tetrahydrobenzo[6,7]isoindolo[2,1-a]quinoline-14-carboxylate: (3i)

Purified by silica gel column chromatography (eluent: petroleum ether/ethyl acetate = 20:1 to 5:1); yellow solid, 71% yield, 276.3 mg; mp 55-57 °C. 1H NMR (300 MHz, $CDCl_3$) δ 7.63

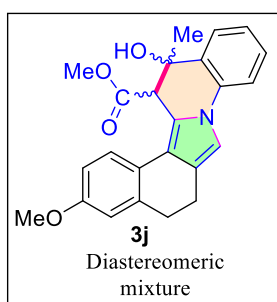


(d, $J = 7.5$ Hz, 1H), 7.29 – 7.14 (m, 5H), 6.99 (s, 1H), 6.70 (dd, $J = 8.3, 2.6$ Hz, 1H), 5.08 – 5.04 (m, 1H), 4.58 (d, $J = 6.0$ Hz, 1H), 4.02 (q, $J = 4.8$ Hz, 2H), 3.82 (s, 3H), 2.81 – 2.65 (m, 4H), 1.00 (t, $J = 7.1$ Hz, 3H). $^{13}C\{^1H\}$ NMR (76 MHz, $CDCl_3$) δ 170.9, 158.7, 134.9, 132.5, 129.8, 129.4, 129.3, 129.1, 128.3, 125.3, 124.4, 123.2, 118.8,

114.9, 111.7, 110.9, 110.1, 67.8, 61.6, 55.5, 45.4, 30.1, 21.3, 13.9. HRMS (ESI) m/z : $[M + H]^+$ Calcd for $C_{24}H_{24}NO_4$ 390.1707; Found 390.1705.

Methyl (13S,14R)-13-hydroxy-3-methoxy-13-methyl-5,6,13,14-tetrahydrobenzo[6,7]isoindolo[2,1-a]quinoline-14-carboxylate: (3j)

Purified by silica gel column chromatography (eluent: petroleum ether/ethyl acetate = 15:1 to 5:1); yellow solid, 84% yield, 326.8 mg; mp 44-46 °C. 1H NMR (500 MHz, $CDCl_3$) δ Major:

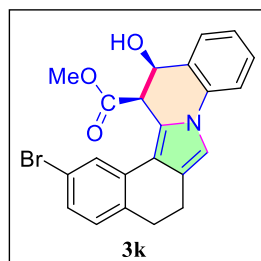


7.55 (d, $J = 8.5$ Hz, 1H), 7.49 (d, $J = 7.8$ Hz, 1H), 7.38 (m, 2H), 7.14 – 7.12 (m, 1H), 7.05 (s, 1H), 6.86 (m, 2H), 4.43 (s, 1H), 3.83 (s, 3H), 3.56 (s, 3H), 2.87 – 2.80 (m, 4H), 1.83 (s, 3H). Minor: 7.69 (d, $J = 8.0$ Hz, 1H), 7.62 (d, $J = 8.4$ Hz, 1H), 7.30 – 7.28 (m, 2H), 7.20 – 7.18 (m, 1H), 6.99 (s, 1H), 6.83 (s, 2H), 4.34 (s, 1H), 3.84 (s, 3H), 3.59 (s, 3H), 2.71 – 2.61 (m, 4H), 1.32 (s, 3H). $^{13}C\{^1H\}$ NMR (126 MHz, $CDCl_3$) δ 172.3, 170.4, 157.8, 138.6, 138.5, 135.4, 134.4, 133.9, 129.6, 129.5, 128.3, 125.5,

125.4, 125.0, 124.8, 124.7, 124.6, 124.5, 124.1, 122.9, 122.7, 121.6, 120.5, 118.1, 117.3, 116.9, 115.6, 115.0, 114.7 (2C), 114.1, 112.1, 111.5 (2C), 71.9, 69.7, 55.4 (2C), 52.9 (2C), 52.7, 52.4, 52.3, 50.8, 31.5, 31.4, 24.3, 21.1. HRMS (ESI) m/z : $[M + H]^+$ Calcd for $C_{24}H_{24}NO_4$ 390.1707; Found 390.1705.

Methyl (13R,14R)-2-bromo-13-hydroxy-5,6,13,14-tetrahydrobenzo[6,7]isoindolo[2,1-a]quinoline-14-carboxylate: (3k)

Purified by silica gel column chromatography (eluent: petroleum ether/ethyl acetate = 20:1 to 10:1); yellow solid, 64% yield, 270.7 mg; mp 114-116 °C. ¹H NMR (300 MHz, CDCl₃) δ

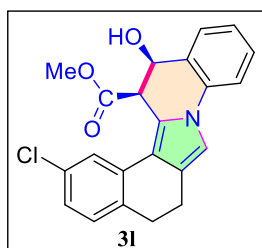


7.78 (d, *J* = 2.1 Hz, 1H), 7.70 (d, *J* = 7.5 Hz, 1H), 7.35 – 7.24 (m, 4H), 7.13 (d, *J* = 8.1 Hz, 1H), 7.03 (s, 1H), 5.13 (dd, *J* = 10.4, 5.7 Hz, 1H), 4.61 (d, *J* = 5.8 Hz, 1H), 3.81 (d, *J* = 10.5 Hz, 1H), 3.64 (s, 3H), 2.88 – 2.65 (m, 4H). ¹³C{¹H} NMR (76 MHz, CDCl₃) δ 171.5, 135.6,

134.6, 133.7, 130.2, 129.6, 128.5, 128.4, 126.8, 125.5, 124.9, 122.9, 120.5, 119.2, 119.1, 115.1, 111.9, 67.9, 52.8, 44.8, 30.6, 20.8. HRMS (ESI) *m/z*: [M + H]⁺ Calcd for C₂₂H₁₉BrNO₃ 424.0550; Found 424.0550.

Methyl (13R,14R)-2-chloro-13-hydroxy-5,6,13,14-tetrahydrobenzo[6,7]isoindolo[2,1-a]quinoline-14-carboxylate: (3l)

Purified by silica gel column chromatography (eluent: petroleum ether/ethyl acetate = 20:1 to 8:1); yellow solid, 75% yield, 284.3 mg; mp 119-121 °C. ¹H NMR (300 MHz, CDCl₃) δ 7.72

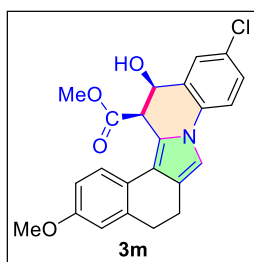


(d, *J* = 7.7 Hz, 1H), 7.64 (d, *J* = 2.1 Hz, 1H), 7.37 – 7.21 (m, 4H), 7.15 (dd, *J* = 8.1, 2.1 Hz, 1H), 7.06 (s, 1H), 5.15 (dd, *J* = 10.0, 5.9 Hz, 1H), 4.64 (d, *J* = 5.9 Hz, 1H), 3.87 (d, *J* = 10.7 Hz, 1H), 3.66 (s, 3H), 2.89 – 2.81 (m, 3H), 2.73 – 2.68 (m, 1H). ¹³C{¹H} NMR (76 MHz, CDCl₃) δ 171.5, 135.1, 134.7, 133.2, 132.4, 129.9, 129.5, 128.5, 125.5 (2C),

124.9, 123.9, 122.9, 119.3, 119.1, 115.1, 111.9, 67.9, 52.7, 44.8, 30.5, 20.9. HRMS (ESI) *m/z*: [M + H]⁺ Calcd for C₂₂H₁₉ClNO₃ 380.1055; Found 380.1053.

Methyl (13R,14R)-11-chloro-13-hydroxy-3-methoxy-5,6,13,14-tetrahydrobenzo[6,7]isoindolo[2,1-a]quinoline-14-carboxylate: (3m)

Purified by silica gel column chromatography (eluent: petroleum ether/ethyl acetate = 20:1 to 6:1); off white solid, 65% yield, 265.9 mg; mp 172-173 °C. ¹H NMR (300 MHz, CDCl₃) δ

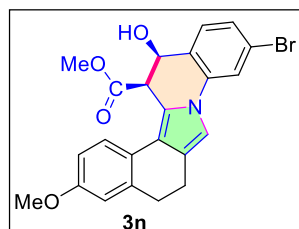


7.66 (s, 1H), 7.52 (d, *J* = 7.5 Hz, 1H), 7.29 – 7.18 (m, 2H), 6.96 (s, 1H), 6.85 – 6.82 (m, 2H), 5.09 – 5.04 (m, 1H), 4.59 (d, *J* = 5.9 Hz, 1H), 3.84 (s, 3H), 3.80 (s, 1H), 3.61 (s, 3H), 2.90 – 2.64 (m, 4H). ¹³C{¹H} NMR (76 MHz, CDCl₃) δ 171.7, 157.9, 138.7, 133.6, 131.2,

129.9, 128.4, 125.9, 125.0, 124.3, 123.1, 120.4, 117.3, 116.2, 114.7, 112.1, 111.7, 67.7, 55.4, 52.8, 44.8, 31.4, 21.1. HRMS (ESI) *m/z*: [M + H]⁺ Calcd for C₂₃H₂₁ClNO₄ 410.1161; Found 410.1158.

Methyl (13R,14R)-10-bromo-13-hydroxy-3-methoxy-5,6,13,14-tetrahydrobenzo[6,7]isoindolo[2,1-a]quinoline-14-carboxylate: (3n)

Purified by silica gel column chromatography (eluent: petroleum ether/ethyl acetate = 20:1 to 5:1); yellow solid, 62% yield, 280.8 mg; mp 153-155 °C. ¹H NMR (300 MHz, CDCl₃) δ 7.53

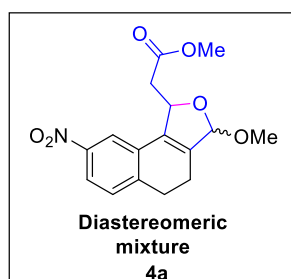


(t, *J* = 7.2 Hz, 2H), 7.42 (s, 1H), 7.30 (d, *J* = 8.2 Hz, 1H), 6.96 (s, 1H), 6.85 – 6.82 (s, 2H), 5.06 – 5.01 (m, 1H), 4.58 (d, *J* = 5.9 Hz, 1H), 3.84 (s, 3H), 3.77 (d, *J* = 10.3 Hz, 1H), 3.61 (s, 3H), 2.88 – 2.64 (m, 4H). ¹³C{¹H} NMR (76 MHz, CDCl₃) δ 171.8, 158.0,

138.7, 136.1, 128.4, 127.2 (2C), 125.1, 124.2, 123.4, 121.9, 120.6, 118.1, 117.6, 114.7, 112.2, 111.7, 67.8, 55.4, 52.8, 44.8, 31.3, 21.0. HRMS (ESI) *m/z*: [M + H]⁺ Calcd for C₂₃H₂₁BrNO₄ 454.0656; Found 454.0652.

Methyl 2-(3-methoxy-8-nitro-2,3,4,5-tetrahydro-1H-cyclopenta[*a*]naphthalen-1-yl)acetate: (4a)

Purified by silica gel column chromatography (eluent: petroleum ether/ethyl acetate = 10:1 to 3:1); brown liquid, 74% yield, 236.1 mg. ¹H NMR (300 MHz, DMSO-*d*⁶) δ Major: 8.08 (d, *J*

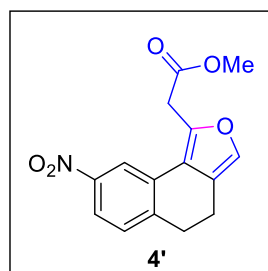


= 1.9 Hz, 1H), 7.81 (d, *J* = 2.4 Hz, 1H), 7.54 – 7.53 (m, 1H), 5.83 (d, *J* = 4.0 Hz, 1H), 5.63 (s, 1H), 3.61 (s, 3H), 3.20 (s, 3H), 3.06 – 2.98 (m, 3H), 2.49 – 2.44 (m, 3H). Minor: 8.05 (d, *J* = 2.1 Hz, 1H), 7.79 (d, *J* = 2.3 Hz, 1H), 7.52 – 7.51 (m, 1H), 5.68 – 5.65 (m, 1H), 5.51 – 5.47 (m, 1H), 3.64 (s, 3H), 3.31 (s, 3H), 2.95 – 2.90 (m, 3H), 2.42 –

2.40 (m, 3H). ¹³C{¹H} NMR (76 MHz, DMSO-*d*⁶) δ 170.6 (2C), 146.6, 144.2, 137.5 (2C), 135.9, 135.8, 130.2, 130.1, 129.2 (2C), 122.9, 122.8, 117.3, 117.2, 108.4, 108.2, 80.4, 79.7, 78.8, 75.3, 53.7, 52.6, 51.6 (2C), 40.9, 39.9, 27.9, 27.8, 19.4, 19.0. HRMS (ESI) *m/z*: [M + Na]⁺ Calcd for C₁₆H₁₇NO₆Na 342.0954; Found 342.0956.

Methyl 2-(8-nitro-4,5-dihydronaphtho[1,2-*c*]furan-1-yl)acetate: (4')

Purified by silica gel column chromatography (eluent: petroleum ether/ethyl acetate = 30:1 to 10:1); yellow liquid, 85% yield, 244.0 mg and 73% yield, 209.5 mg for 2-propanol and THF

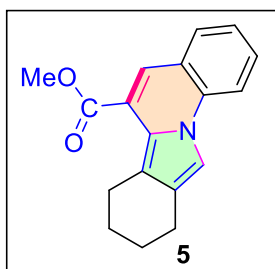


respectively. ¹H NMR (300 MHz, CDCl₃) δ 8.39 (d, *J* = 2.5 Hz, 1H), 8.04 (dd, *J* = 8.3, 2.5 Hz, 1H), 7.41 (d, *J* = 8.3 Hz, 1H), 7.27 (s, 1H), 3.99 (s, 2H), 3.81 (s, 3H), 2.99 - 2.95 (m, 2H), 2.76 - 2.72 (m, 2H). ¹³C{¹H} NMR (76 MHz, CDCl₃) δ 169.4, 147.4, 144.3, 143.4, 136.2, 131.1, 129.6, 122.3, 121.5, 119.1, 118.6, 52.8, 34.3, 30.8, 18.8. HRMS

(ESI) *m/z*: [M + H]⁺ Calcd for C₁₅H₁₄NO₅ 288.0874; Found 288.0874.

Methyl 7,8,9,10-tetrahydroisindolo[2,1-a]quinoline-6-carboxylate: (5)

Purified by silica gel column chromatography (eluent: petroleum ether/ethyl acetate = 30:1 to 20:1); yellow solid, 63% yield, 175.8 mg; mp 84-86 °C. ¹H NMR (300 MHz, CDCl₃) δ 7.76

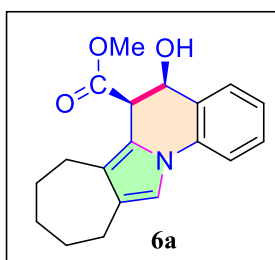


(d, *J* = 8.4 Hz, 1H), 7.67 – 7.61 (m, 2H), 7.53 (ddd, *J* = 8.5, 7.2, 1.5 Hz, 1H), 7.37 (s, 1H), 7.28 – 7.23 (m, 1H), 3.97 (s, 3H), 2.84 – 2.82 (m, 4H), 1.85 – 1.81 (m, 4H). ¹³C{¹H} NMR (76 MHz, CDCl₃) δ 167.6, 134.1, 129.6 (2C), 125.8, 123.4, 123.3, 122.7, 121.9, 121.5, 114.6, 113.9, 109.3, 52.3, 24.2, 23.9, 23.5, 22.9. HRMS (ESI) *m/z*:

[*M* + *H*]⁺ Calcd for C₁₈H₁₈NO₂ 280.1339; Found 280.1337.

Methyl (5*R*,6*R*)-5-hydroxy-6,7,8,9,10,11-hexahydro-5*H*-cyclohepta[3,4]pyrrolo[1,2-*a*]quinoline-6-carboxylate: (6a)

Purified by silica gel column chromatography (eluent: petroleum ether/ethyl acetate = 25:1 to 10:1); yellow solid, 72% yield, 224.0 mg; mp 110-112 °C. ¹H NMR (300 MHz, CDCl₃) δ

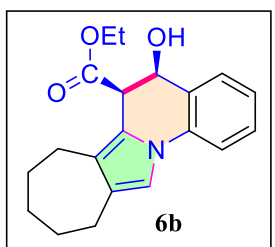


7.67 (d, *J* = 7.6 Hz, 1H), 7.31 - 7.28 (m, 1H), 7.22 – 7.12 (m, 2H), 6.91 (s, 1H), 5.12 – 5.06 (m, 1H), 4.26 (d, *J* = 5.9 Hz, 1H), 3.82 – 3.76 (m, 1H), 3.58 (s, 3H), 2.63 – 2.59 (m, 4H), 1.89 – 1.82 (m, 3H), 1.69 – 1.68 (m, 3H). ¹³C{¹H} NMR (76 MHz, CDCl₃) δ 172.1, 134.9, 128.9, 128.3, 128.2, 125.6, 125.4, 123.9, 119.4, 114.4, 112.4, 67.8,

52.4, 43.5, 33.1, 30.1, 29.6, 28.4, 26.7. HRMS (ESI) *m/z*: [*M* + *H*]⁺ Calcd for C₁₉H₂₂NO₃ 312.1601; Found 312.1599.

Ethyl (5*R*,6*R*)-5-hydroxy-6,7,8,9,10,11-hexahydro-5*H*-cyclohepta[3,4]pyrrolo[1,2-*a*]quinoline-6-carboxylate: (6b)

Purified by silica gel column chromatography (eluent: petroleum ether/ethyl acetate = 25:1 to 10:1); yellow solid, 61% yield, 198.3 mg; mp 116-118 °C. ¹H NMR (500 MHz, CDCl₃) δ

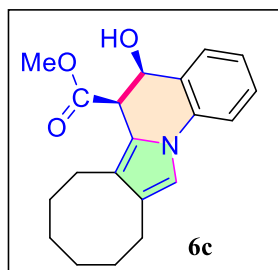


7.66 (d, *J* = 7.7 Hz, 1H), 7.29 – 7.27 (m, 1H), 7.20 (d, *J* = 7.9 Hz, 1H), 7.14 (t, *J* = 7.5 Hz, 1H), 6.90 (s, 1H), 5.08 (dd, *J* = 10.1, 5.7 Hz, 1H), 4.24 (d, *J* = 6.0 Hz, 1H), 4.10 – 3.94 (m, 2H), 3.74 (d, *J* = 11.1 Hz, 1H), 2.62 – 2.61 (m, 5H), 1.86 – 1.84 (m, 2H), 1.70 – 1.64 (m, 3H), 1.12 (t, *J* = 7.1 Hz, 3H). ¹³C{¹H} NMR (126 MHz, CDCl₃) δ 171.6,

134.9, 129.0, 128.3, 128.2, 125.6, 125.4, 123.8, 119.6, 114.3, 112.3, 67.8, 61.3, 43.7, 33.2, 30.1, 29.7, 28.4, 26.7, 14.0. HRMS (ESI) *m/z*: [*M* + *H*]⁺ Calcd for C₂₀H₂₄NO₃ 326.1758; Found 326.1760.

Methyl (5*R*,6*R*)-5-hydroxy-5,6,7,8,9,10,11,12-octahydrocycloocta[3,4]pyrrolo[1,2-*a*]quinoline-6-carboxylate: (6c)

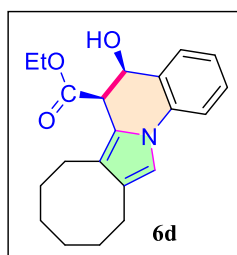
Purified by silica gel column chromatography (eluent: petroleum ether/ethyl acetate = 20:1 to 5:1); yellow solid, 78% yield, 253.6 mg; mp. 108-109 °C. ¹H NMR (500 MHz, CDCl₃) δ 7.64



(d, *J* = 7.5 Hz, 1H), 7.29 – 7.28 (m, 1H), 7.22 (d, *J* = 8.1 Hz, 1H), 7.14 (t, *J* = 7.5 Hz, 1H), 6.90 (s, 1H), 5.05 (s, 1H), 4.22 (d, *J* = 5.8 Hz, 1H), 3.82 (m, 1H), 3.55 (s, 3H), 2.65 – 2.56 (m, 4H), 1.65 – 1.58 (m, 4H), 1.47 (s, 4H). ¹³C{¹H} NMR (126 MHz, CDCl₃) δ 172.2, 135.0, 128.9, 128.3, 126.4, 125.5, 123.9, 123.4, 119.5, 114.4, 112.5, 67.9, 52.3 (2C), 43.7, 32.3, 30.5, 25.9, 24.3, 22.6. HRMS (ESI) *m/z*: [M + H]⁺ Calcd for C₂₀H₂₄NO₃ 326.1758; Found 326.1755.

Ethyl (5*R*,6*R*)-5-hydroxy-5,6,7,8,9,10,11,12-octahydrocycloocta[3,4]pyrrolo[1,2-*a*]quinoline-6-carboxylate: (6d)

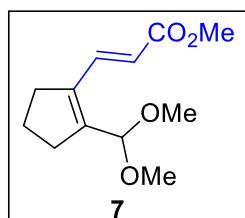
Purified by silica gel column chromatography (eluent: petroleum ether/ethyl acetate = 30:1 to 20:1); pale yellow liquid, 63% yield, 213.6 mg. ¹H NMR (300 MHz, CDCl₃) δ 7.64 (d, *J* =



7.6 Hz, 1H), 7.28 – 7.20 (m, 2H), 7.13 (td, *J* = 7.5, 1.4 Hz, 1H), 6.89 (s, 1H), 5.04 (dd, *J* = 10.8, 5.7 Hz, 1H), 4.18 (d, *J* = 5.7 Hz, 1H), 4.08 – 3.92 (m, 2H), 3.81 (d, *J* = 10.8 Hz, 1H), 2.63 – 2.54 (m, 4H), 1.62 (s, 4H), 1.47 – 1.46 (m, 4H), 1.07 (t, *J* = 7.1 Hz, 3H). ¹³C{¹H} NMR (76 MHz, CDCl₃) δ 171.8, 135.1, 129.2, 128.3, 126.4, 125.5, 123.8, 123.2, 119.7, 114.4, 112.4, 68.1, 61.4, 43.8, 32.4, 30.5, 25.9 (2C), 24.4, 22.6, 14.0. HRMS (ESI) *m/z*: [M + H]⁺ Calcd for C₂₁H₂₆NO₃ 340.1914; Found 340.1910.

Methyl (*E*)-3-(2-(dimethoxymethyl)cyclopent-1-en-1-yl)acrylate: (7)

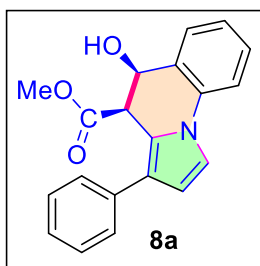
Purified by silica gel column chromatography (eluent: petroleum ether/ethyl acetate = 30:1 to



20:1); pale yellow liquid, 82% yield, 185.4 mg. ¹H NMR (300 MHz, CDCl₃) δ 7.75 (d, *J* = 15.6 Hz, 1H), 5.79 (d, *J* = 15.6 Hz, 1H), 5.14 (s, 1H), 3.72 (s, 3H), 3.31 (s, 6H), 2.55 – 2.54 (m, 4H), 1.92 – 1.81 (m, 2H). ¹³C{¹H} NMR (76 MHz, CDCl₃) δ 167.8, 146.7, 137.6, 137.5, 119.4, 100.6, 53.9 (2C), 51.6, 33.7, 33.1, 21.5. HRMS (ESI) *m/z*: [M + Na]⁺ Calcd for C₁₂H₁₈O₄Na 249.1102; Found 249.1104.

Methyl (4*R*,5*R*)-5-hydroxy-3-phenyl-4,5-dihydropyrrolo[1,2-*a*]quinoline-4-carboxylate:**(8a)**

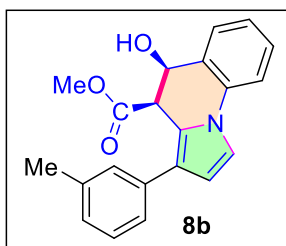
Purified by silica gel column chromatography (eluent: petroleum ether/ethyl acetate = 15:1 to



5:1); yellow solid, 62% yield, 197.8 mg; mp 41-43 °C. ¹H NMR (300 MHz, CDCl₃) δ 7.70 (dd, *J* = 7.6, 1.0 Hz, 1H), 7.51 – 7.27 (m, 9H), 6.53 (d, *J* = 3.1 Hz, 1H), 5.09 – 5.07 (m, 1H), 4.44 (d, *J* = 5.6 Hz, 1H), 3.58 (s, 3H). ¹³C{¹H} NMR (76 MHz, CDCl₃) δ 172.2, 135.4, 135.0, 129.8, 128.8 (2C), 128.6, 127.8 (2C), 126.5, 125.8, 125.0, 124.9, 120.5, 116.6, 115.2, 110.7, 68.4, 52.7, 44.3. HRMS (ESI) *m/z*: [M + H]⁺ Calcd for C₂₀H₁₈NO₃ 320.1288; Found 320.1282.

Methyl (4*R*,5*R*)-5-hydroxy-3-(*m*-tolyl)-4,5-dihydropyrrolo[1,2-*a*]quinoline-4-carboxylate:**(8b)**

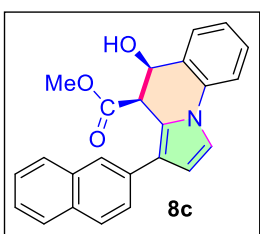
Purified by silica gel column chromatography (eluent: petroleum ether/ethyl acetate = 15:1 to



5:1); yellow liquid, 59% yield, 196.5 mg. ¹H NMR (300 MHz, CDCl₃) δ 7.70 (d, *J* = 8.3 Hz, 1H), 7.38 – 7.37 (m, 2H), 7.33 – 7.31 (m, 3H), 7.27 – 7.25 (m, 3H), 6.53 (d, *J* = 3.0 Hz, 1H), 5.09 (s, 1H), 4.45 (d, *J* = 5.6 Hz, 1H), 3.58 (s, 3H), 2.43 (s, 3H). ¹³C{¹H} NMR (76 MHz, CDCl₃) δ 172.2, 138.3, 135.3, 134.9, 129.8, 129.3, 128.7, 128.6, 127.2, 125.7, 124.9 (2C), 120.4, 120.2, 116.6, 115.2, 110.8, 68.3, 52.7, 44.3, 21.7. HRMS (ESI) *m/z*: [M + H]⁺ Calcd for C₂₁H₂₀NO₃ 334.1445; Found 334.1444.

Methyl (*R*)-5-hydroxy-3-(naphthalen-2-yl)-4,5-dihydropyrrolo[1,2-*a*]quinoline-4-carboxylate: (8c)

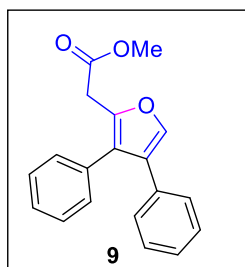
Purified by silica gel column chromatography (eluent: petroleum ether/ethyl acetate = 15:1 to



7:1); yellow liquid, 60% yield, 221.4 mg. ¹H NMR (300 MHz, CDCl₃) δ 7.95 (d, *J* = 5.4 Hz, 1H), 7.91 – 7.88 (m, 2H), 7.74 – 7.66 (m, 2H), 7.56 – 7.50 (m, 2H), 7.42 – 7.40 (m, 1H), 7.33 (d, *J* = 3.1 Hz, 1H), 7.30 – 7.27 (m, 3H), 6.66 (d, *J* = 3.0 Hz, 1H), 5.11 (s, 1H), 4.55 (d, *J* = 5.6 Hz, 1H), 3.61 (s, 3H). ¹³C{¹H} NMR (76 MHz, CDCl₃) δ 172.1, 134.9, 133.8, 129.8, 129.3 (2C), 128.9, 128.7, 128.2, 127.8, 127.2, 126.3, 125.9, 125.1, 124.5, 124.4, 124.2, 120.2, 117.6, 115.3, 110.9, 68.3, 52.7, 44.5. HRMS (ESI) *m/z*: [M + H]⁺ Calcd for C₂₄H₂₀NO₃ 370.1445; Found 370.1444.

Methyl 2-(3,4-diphenylfuran-2-yl)acetate: (9)

Purified by silica gel column chromatography (eluent: petroleum ether/ethyl acetate = 15:1 to

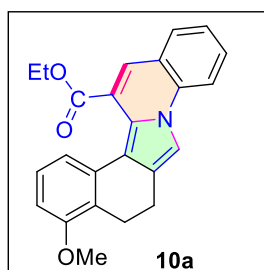


5:1); yellow solid, 56% yield, 163.5 mg; mp 45-47 °C. ^1H NMR (300 MHz, CDCl_3) δ 7.60 (s, 1H), 7.38 – 7.35 (m, 3H), 7.30 – 7.23 (m, 5H), 7.18 (dd, J = 7.2, 2.6 Hz, 2H), 3.79 (s, 3H), 3.75 (s, 2H). $^{13}\text{C}\{^1\text{H}\}$ NMR (76 MHz, CDCl_3) δ 170.2, 145.4, 139.0, 132.3, 132.1, 129.9 (2C), 128.5 (2C), 128.4 (2C), 128.3 (2C), 127.3, 127.1, 126.9, 123.6, 52.5, 32.8.

HRMS (ESI) m/z : $[\text{M} + \text{H}]^+$ Calcd for $\text{C}_{19}\text{H}_{17}\text{O}_3$ 293.1179; Found 293.1175.

Ethyl 4-methoxy-5,6-dihydrobenzo[6,7]isoindolo[2,1-a]quinoline-14-carboxylate: (10a)

Purified by silica gel column chromatography (eluent: petroleum ether/ethyl acetate = 40:1 to 20:1); brown liquid, 67% yield, 248.6 mg. ^1H NMR (500 MHz, CDCl_3) δ 7.82 (d, J = 8.4 Hz,

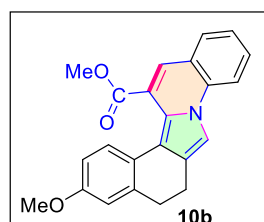


1H), 7.77 (s, 1H), 7.70 (d, J = 7.9 Hz, 1H), 7.58 – 7.54 (m, 2H), 7.31 (t, J = 7.5 Hz, 1H), 7.17 (t, J = 8.0 Hz, 1H), 6.82 (d, J = 7.7 Hz, 1H), 6.76 (d, J = 8.1 Hz, 1H), 4.10 (q, J = 7.1 Hz, 2H), 3.89 (s, 3H), 3.00 – 2.98 (m, 2H), 2.84 – 2.81 (m, 2H), 0.85 (t, J = 7.1 Hz, 3H). $^{13}\text{C}\{^1\text{H}\}$ NMR (126 MHz, CDCl_3) δ 168.1, 156.5, 134.3, 134.1, 130.2, 129.9,

127.8, 125.9, 124.8, 124.3, 124.2, 123.7, 122.3, 122.2, 118.8, 116.2, 114.1, 108.7, 107.9, 61.8, 55.8, 21.9, 21.4, 13.4. HRMS (ESI) m/z : $[\text{M} + \text{H}]^+$ Calcd for $\text{C}_{24}\text{H}_{22}\text{NO}_3$ 372.1601; Found 372.1602.

Methyl 3-methoxy-5,6-dihydrobenzo[6,7]isoindolo[2,1-a]quinoline-14-carboxylate: (10b)

Purified by silica gel column chromatography (eluent: petroleum ether/ethyl acetate = 25:1 to 10:1); orange solid, 71% yield, 253.5 mg; mp. 151-152 °C. ^1H NMR (300 MHz, CDCl_3) δ

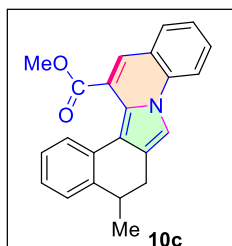


7.82 – 7.76 (m, 2H), 7.69 (d, J = 7.9 Hz, 1H), 7.58 – 7.50 (m, 2H), 7.32 – 7.27 (m, 1H), 7.03 (d, J = 8.4 Hz, 1H), 6.87 – 6.77 (m, 2H), 3.84 (s, 3H), 3.68 (s, 3H), 2.94 – 2.91 (m, 2H), 2.88 – 2.85 (m, 2H). $^{13}\text{C}\{^1\text{H}\}$ NMR (76 MHz, CDCl_3) δ 168.5, 157.4, 138.4, 134.4, 130.2,

129.8, 127.1, 126.4, 125.7, 124.1, 123.9, 123.6, 122.2, 121.3, 115.9, 114.0, 113.8, 111.3, 108.8, 55.4, 52.5, 31.4, 21.9. HRMS (ESI) m/z : $[\text{M} + \text{H}]^+$ Calcd for $\text{C}_{23}\text{H}_{20}\text{NO}_3$ 358.1445; Found 358.1448.

Methyl 5-methyl-5,6-dihydrobenzo[6,7]isoindolo[2,1-a]quinoline-14-carboxylate: (10c)

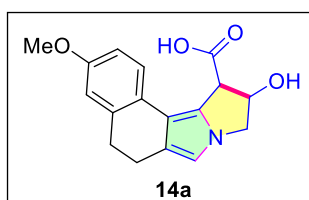
Purified by silica gel column chromatography (eluent: petroleum ether/ethyl acetate = 25:1 to 10:1); yellow liquid, 70% yield, 238.7 mg. ^1H NMR (300 MHz, CDCl_3) δ 7.84 – 7.78 (m,



2H), 7.72 – 7.69 (m, 2H), 7.60 – 7.54 (m, 2H), 7.34 – 7.29 (m, 2H), 7.22 – 7.11 (m, 2H), 3.62 (s, 3H), 3.14 – 3.07 (m, 1H), 2.98 (dd, $J = 14.9, 5.0$ Hz, 1H), 2.68 – 2.61 (m, 1H), 1.00 – 0.96 (m, 3H). $^{13}\text{C}\{^1\text{H}\}$ NMR (76 MHz, CDCl_3) δ 168.5, 141.1, 134.3, 132.0, 131.1, 130.2, 129.9, 128.9, 126.4, 126.2, 125.8, 125.6, 125.5, 124.2, 124.1, 123.7, 122.2, 114.1, 109.4, 52.3, 34.5, 29.6, 19.5. HRMS (ESI) m/z : $[\text{M} + \text{H}]^+$ Calcd for $\text{C}_{23}\text{H}_{20}\text{NO}_2$ 342.1496; Found 342.1497.

(10R,11R)-10-Hydroxy-3-methoxy-5,9,10,11-tetrahydro-6H-benzo[g]pyrrolo[2,1-*a*]isoindole-11-carboxylic acid: (14a)

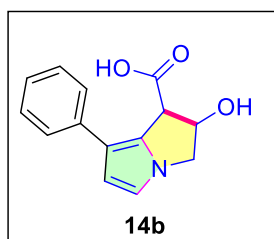
Purified by silica gel column chromatography (eluent: petroleum ether/ethyl acetate = 10:1 to 2:1); yellow liquid, 41% yield, 78.4 mg. ^1H NMR (300 MHz, CDCl_3) δ 7.99 (d, $J = 8.6$ Hz,



1H), 6.84 – 6.80 (m, 2H), 6.68 – 6.67 (m, 1H), 4.17 – 4.07 (m, 2H), 3.85 (s, 3H), 3.82 – 3.80 (m, 2H), 3.67 (bs, 1H), 2.99 – 2.95 (m, 2H), 2.50 – 2.45 (m, 2H). $^{13}\text{C}\{^1\text{H}\}$ NMR (76 MHz, CDCl_3) δ 167.8, 157.5, 151.0, 138.5, 131.0 (2C), 128.9 (2C), 124.4, 114.8, 112.0, 65.7, 55.4, 53.6, 38.9, 32.1, 22.8. HRMS (ESI) m/z : $[\text{M}]^+$ Calcd for $\text{C}_{17}\text{H}_{17}\text{NO}_4$ 299.1158; Found 299.1155.

(1R,2R)-2-Hydroxy-7-phenyl-2,3-dihydro-1H-pyrrolizine-1-carboxylic acid: (14b)

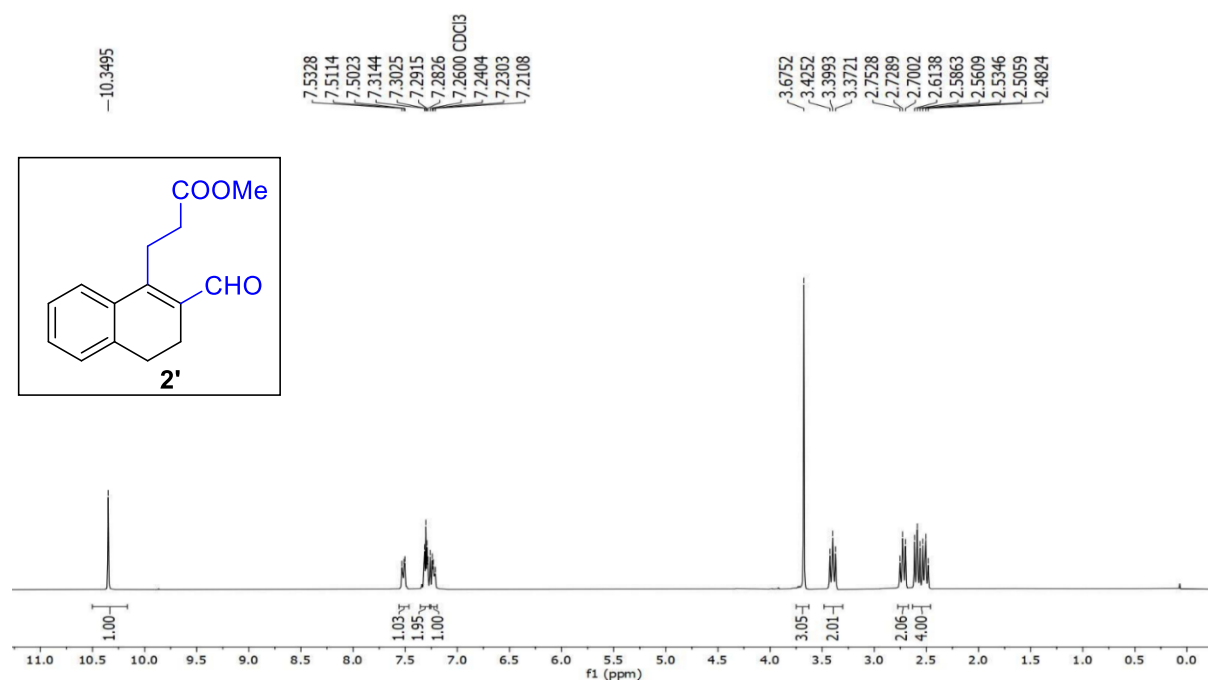
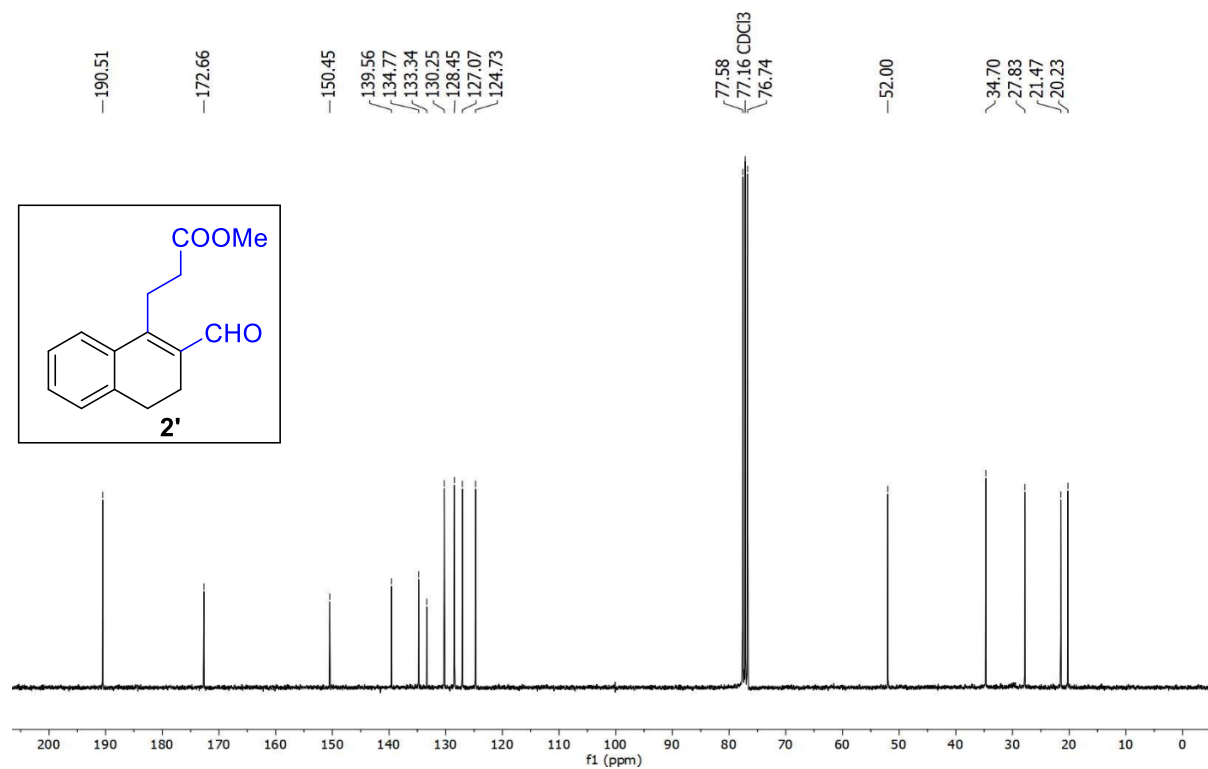
Purified by silica gel column chromatography (eluent: petroleum ether/ethyl acetate = 10:1 to

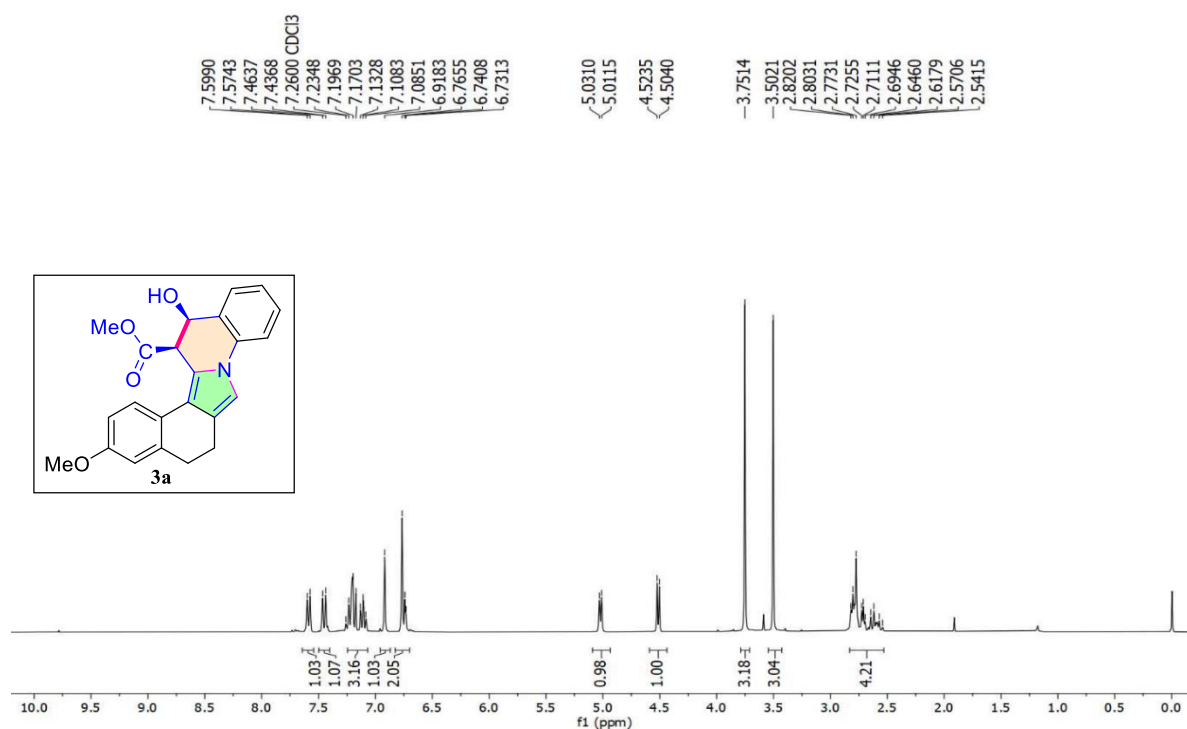
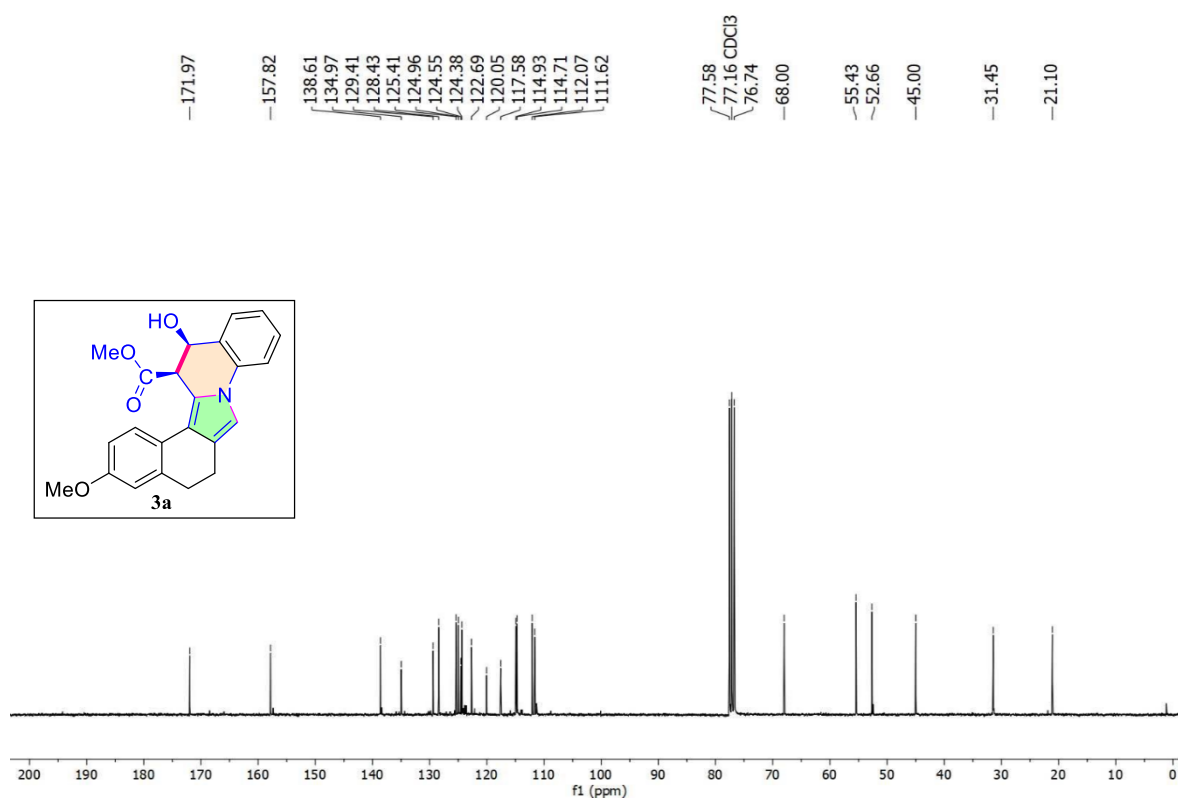


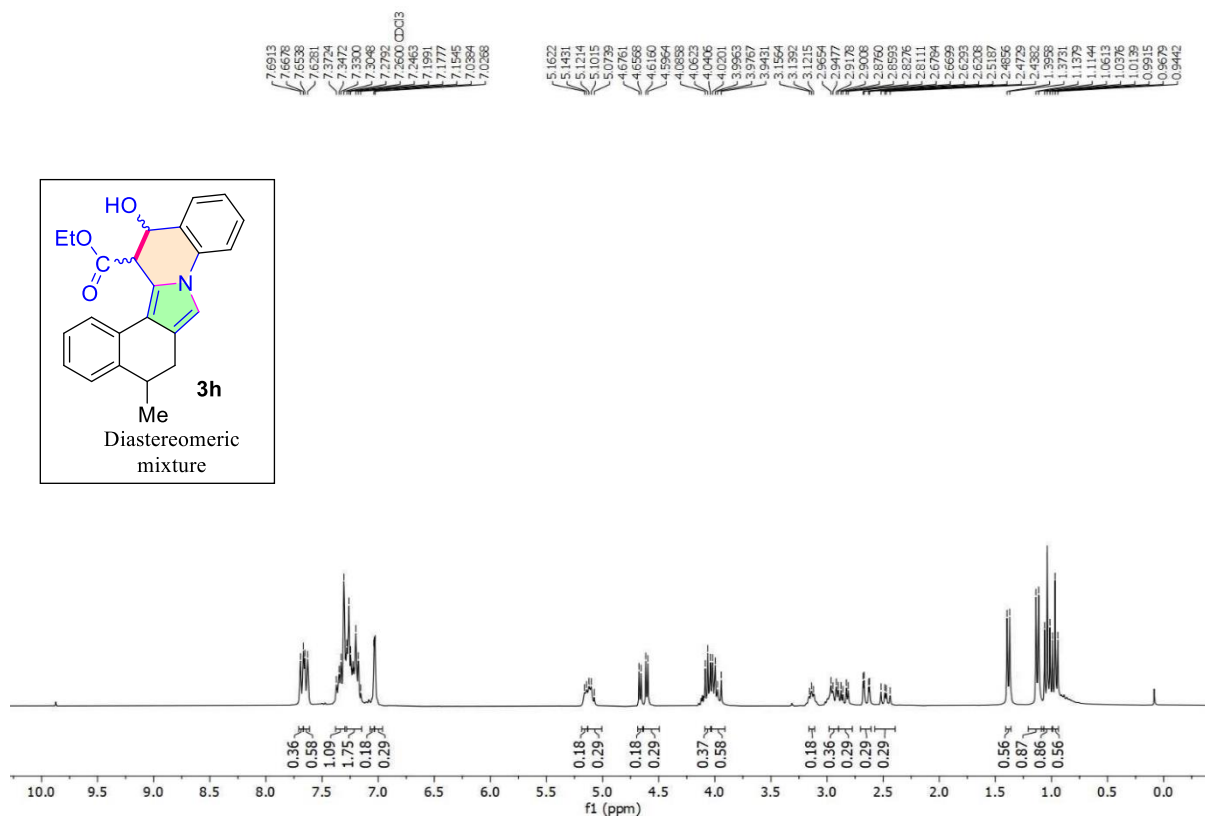
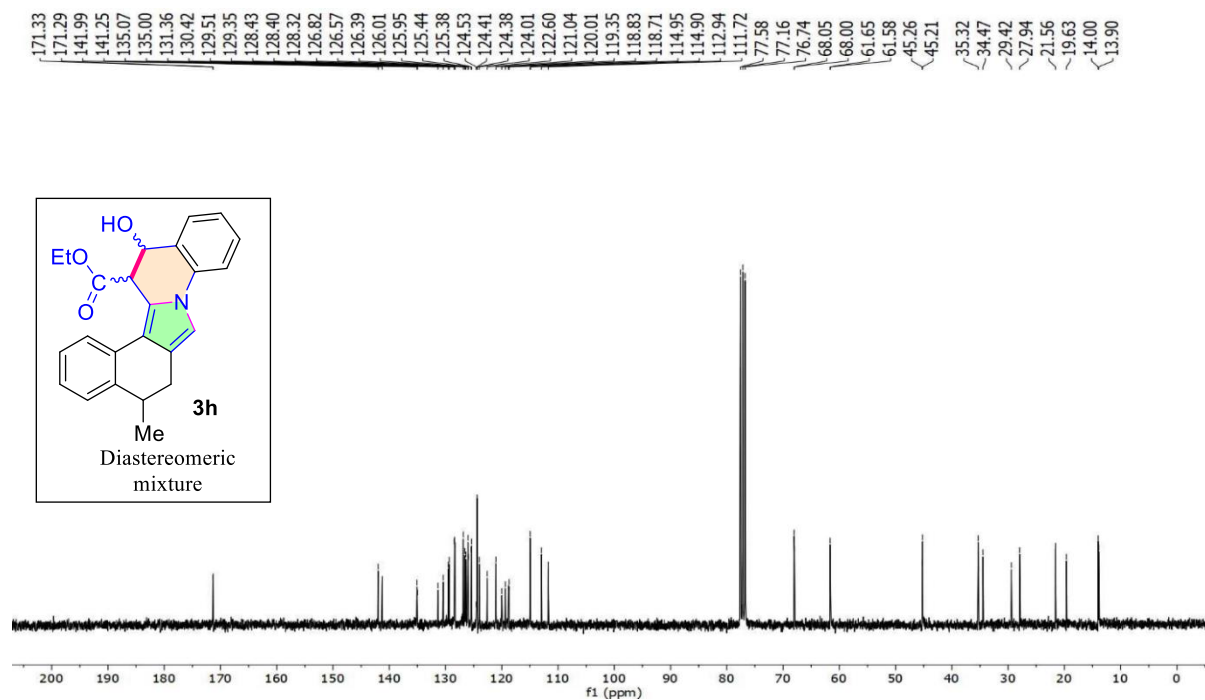
2:1); brown liquid, 52% yield, 69.5 mg. ^1H NMR (400 MHz, CDCl_3) δ 7.40 – 7.34 (m, 5H), 6.70 (d, $J = 3.0$ Hz, 1H), 6.39 (d, $J = 3.0$ Hz, 1H), 4.31 (t, $J = 6.7$ Hz, 2H), 4.09 (d, $J = 6.8$ Hz, 1H), 3.73 – 3.72 (m, 1H), 3.68 (bs, 1H). $^{13}\text{C}\{^1\text{H}\}$ NMR (101 MHz, CDCl_3) δ 167.9, 131.0, 128.9, 128.6 (2C), 128.5 (2C), 128.3, 126.2, 122.1, 109.8, 65.7, 56.7,

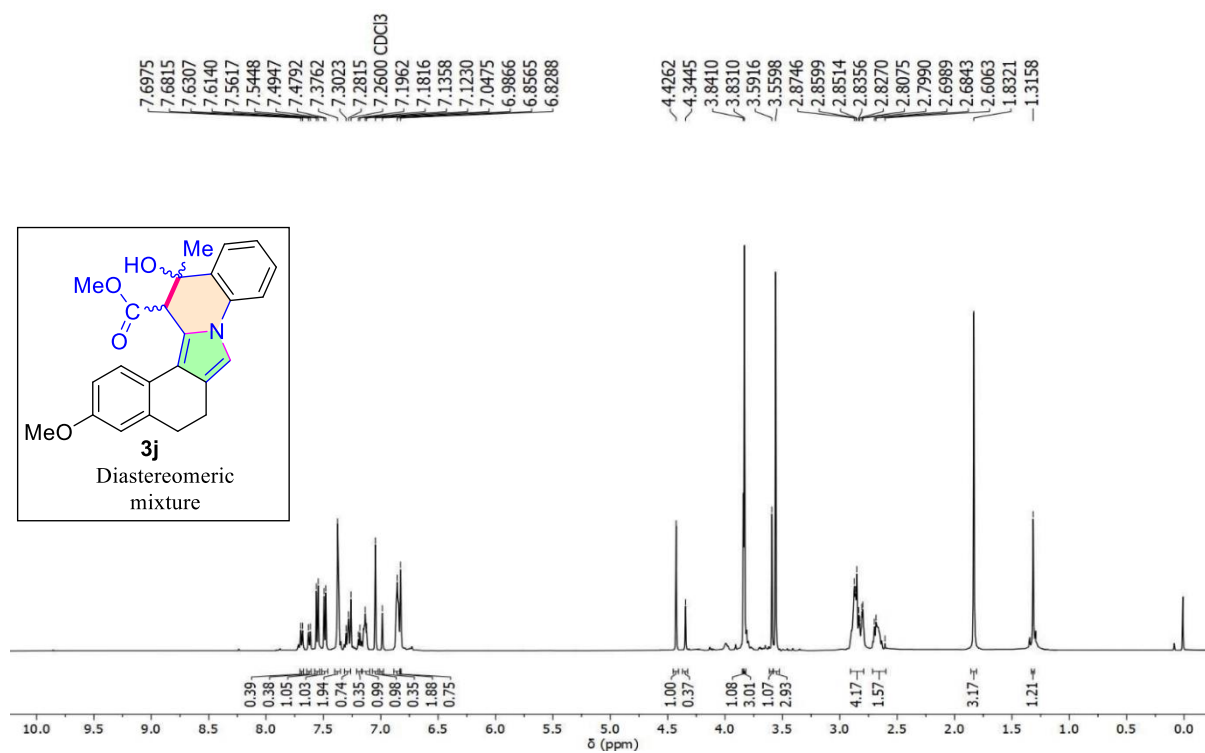
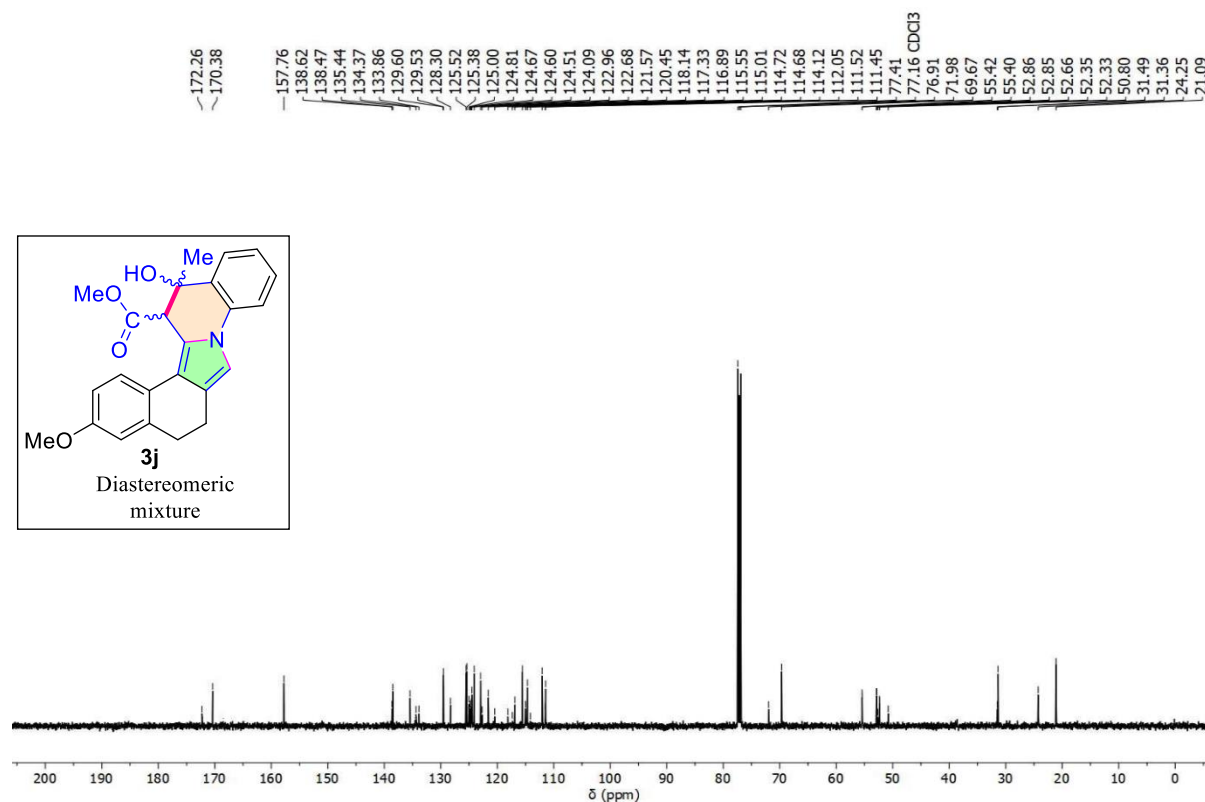
32.1. HRMS (ESI) m/z : $[\text{M} + \text{H}]^+$ Calcd for $\text{C}_{14}\text{H}_{14}\text{NO}_3$ 244.0975; Found 244.0975.

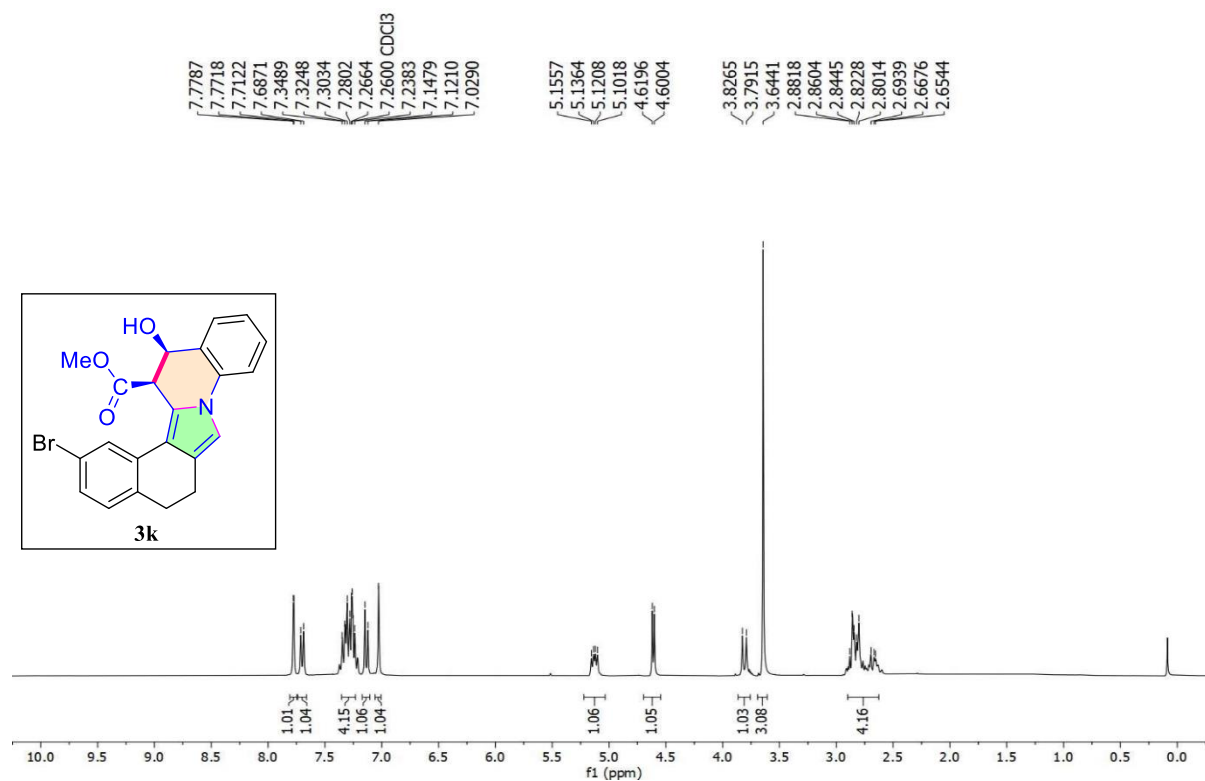
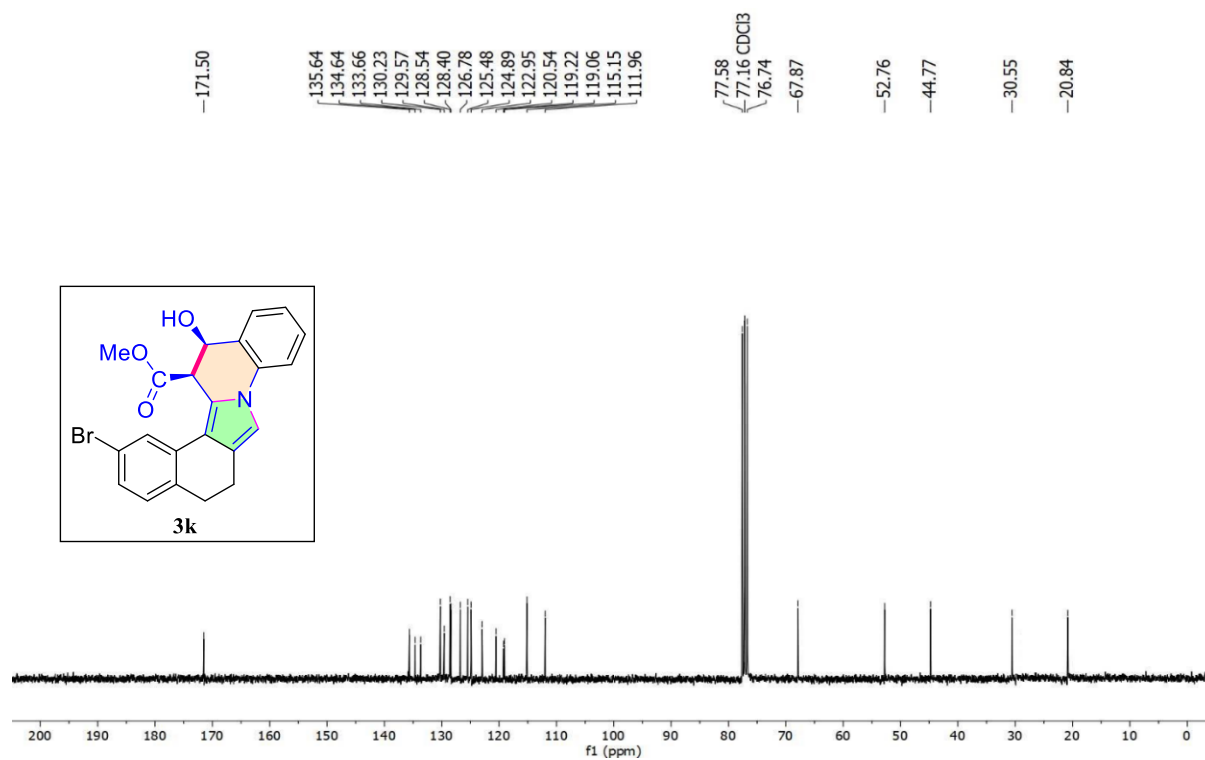
6.6.3. Representative NMR spectra:

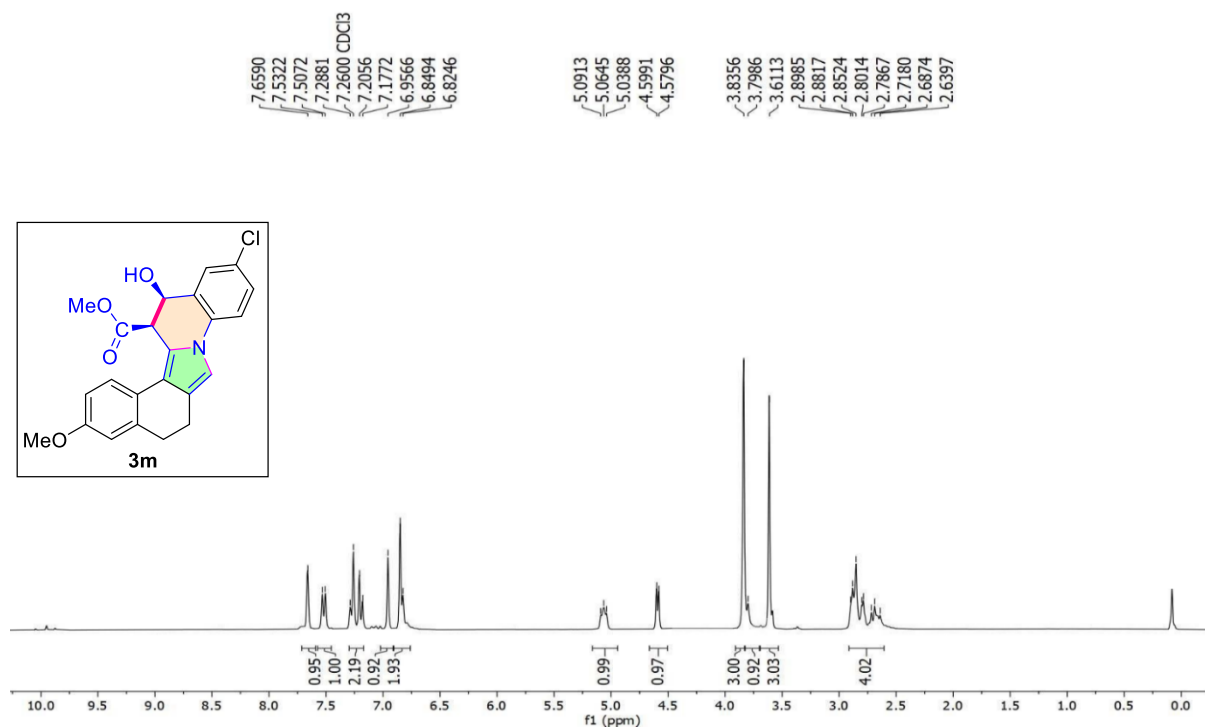
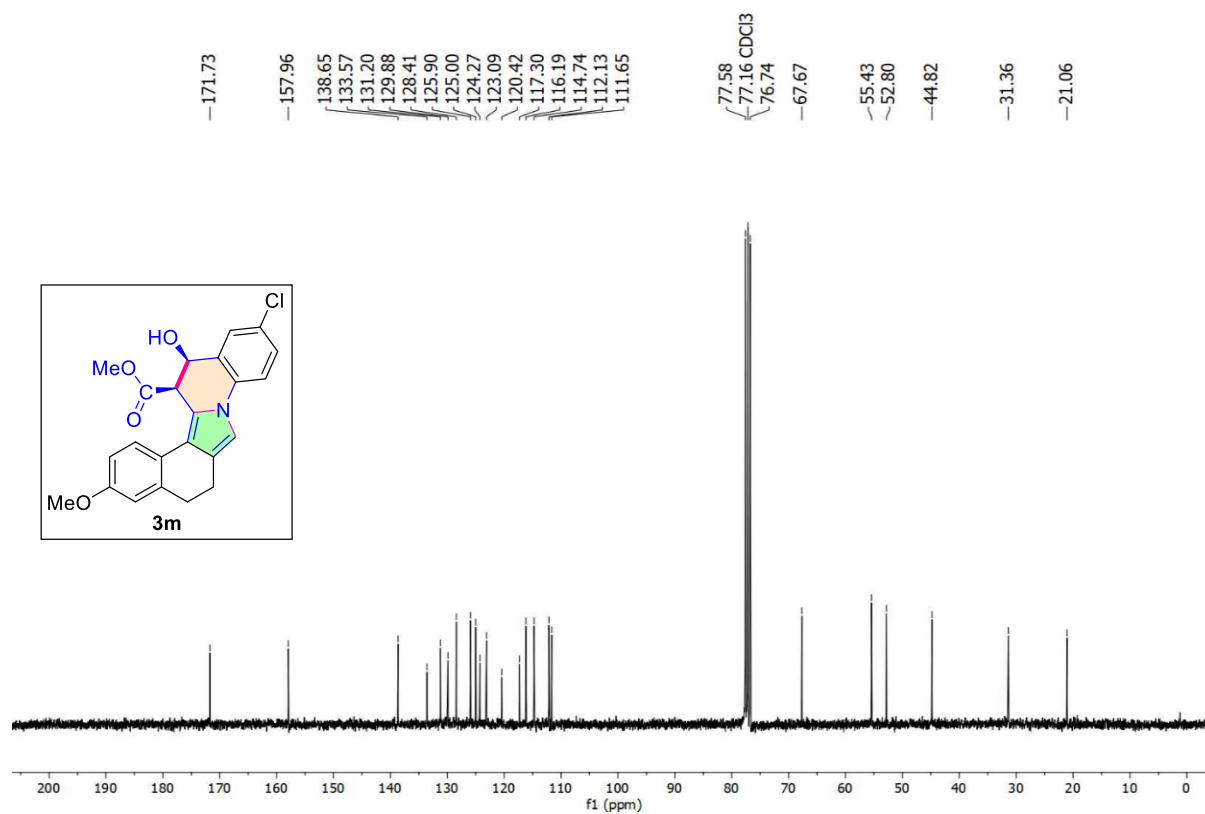
 ^1H NMR of 2' (300 MHz, CDCl_3): $^{13}\text{C}\{^1\text{H}\}$ NMR of 2' (76 MHz, CDCl_3):

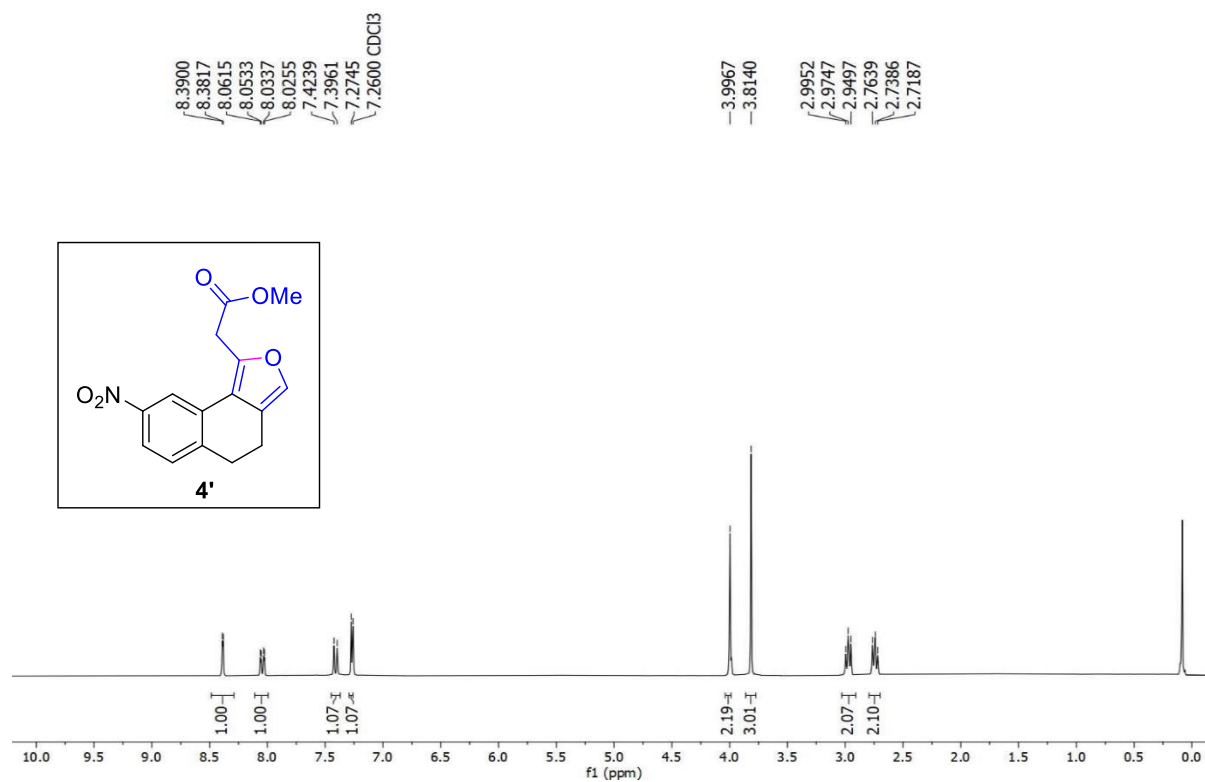
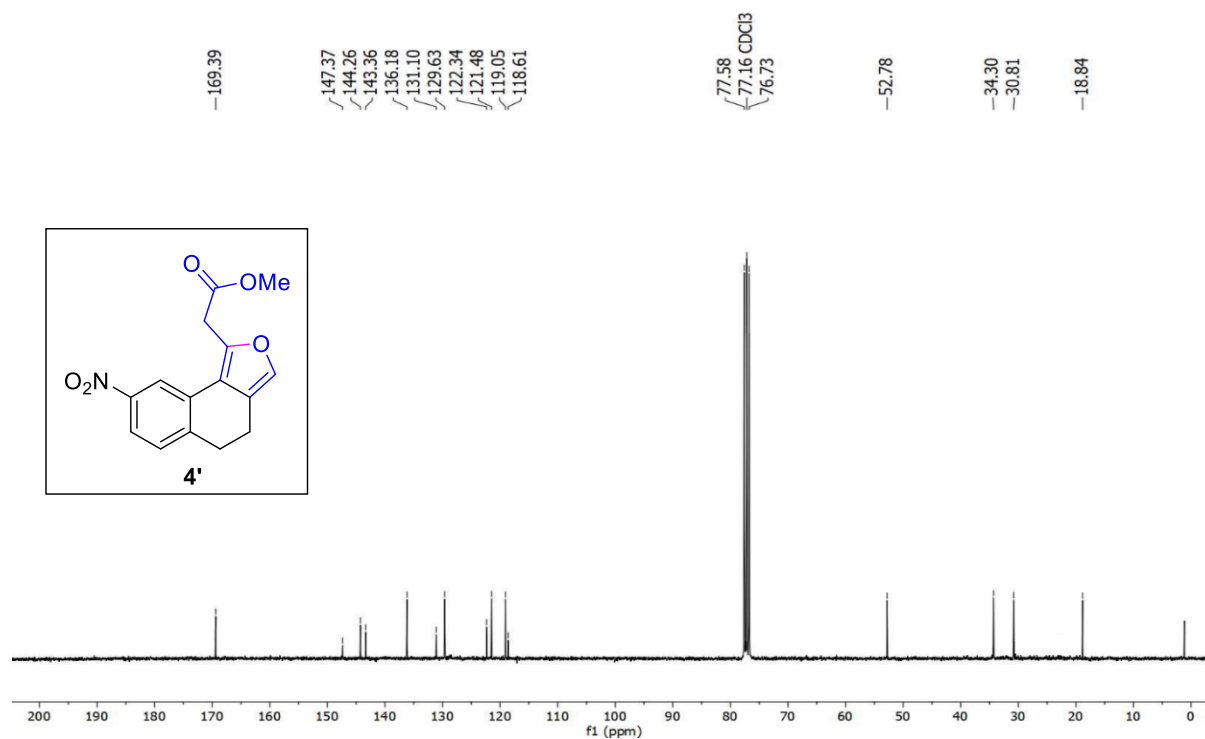
^1H NMR of 3a (300 MHz, CDCl_3): **$^{13}\text{C}\{^1\text{H}\}$ NMR of 3a (76 MHz, CDCl_3):**

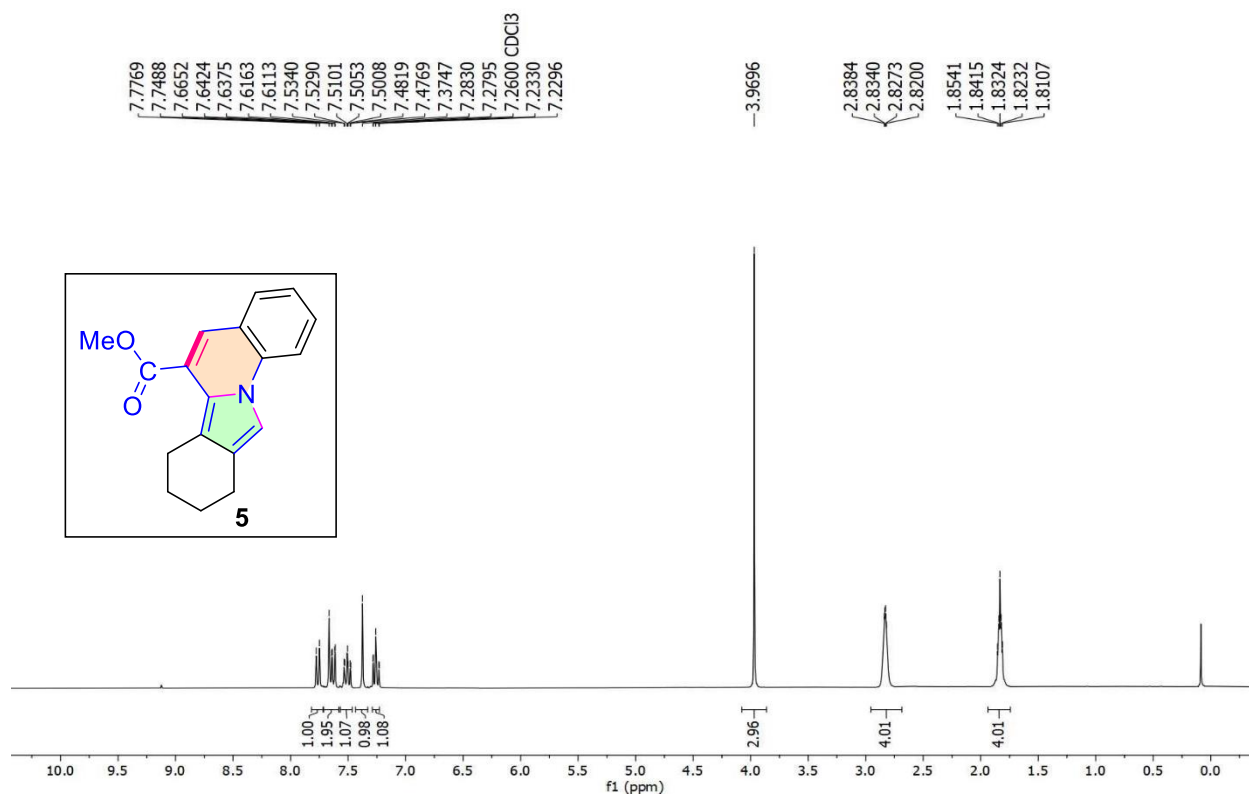
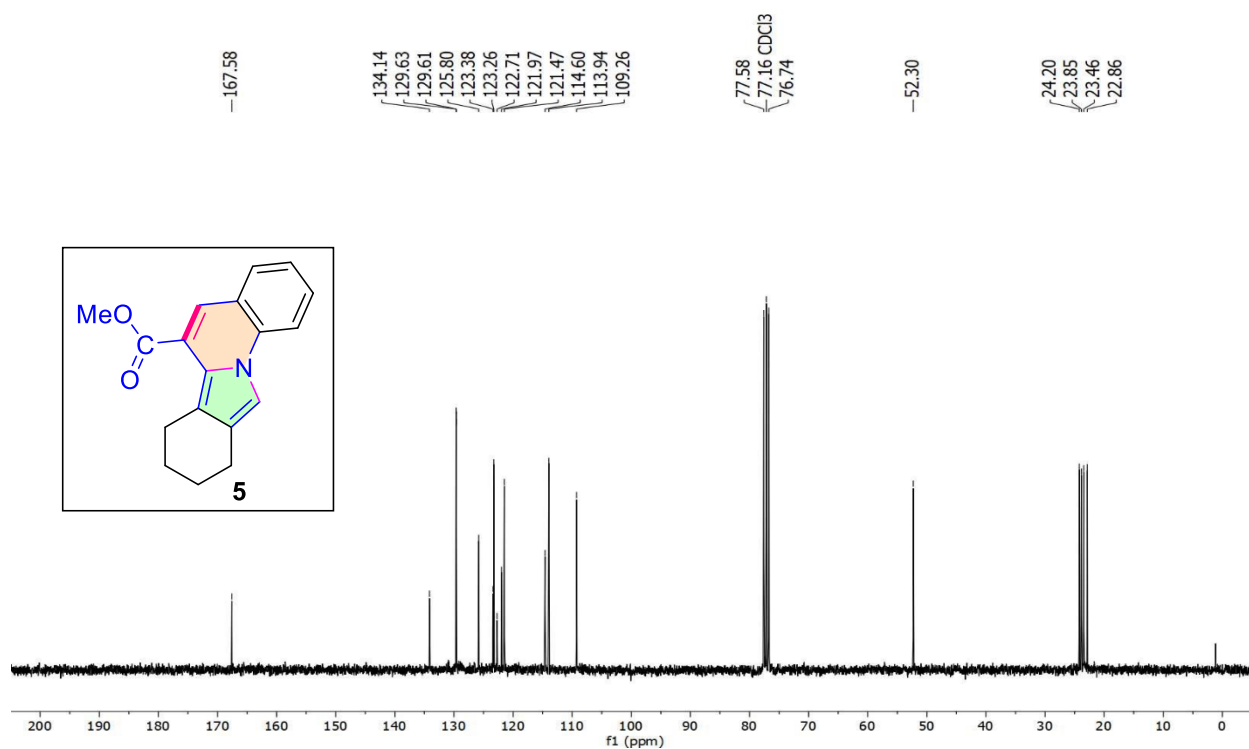
^1H NMR of 3h (300 MHz, CDCl_3): **$^{13}\text{C}\{^1\text{H}\}$ NMR of 3h (76 MHz, CDCl_3):**

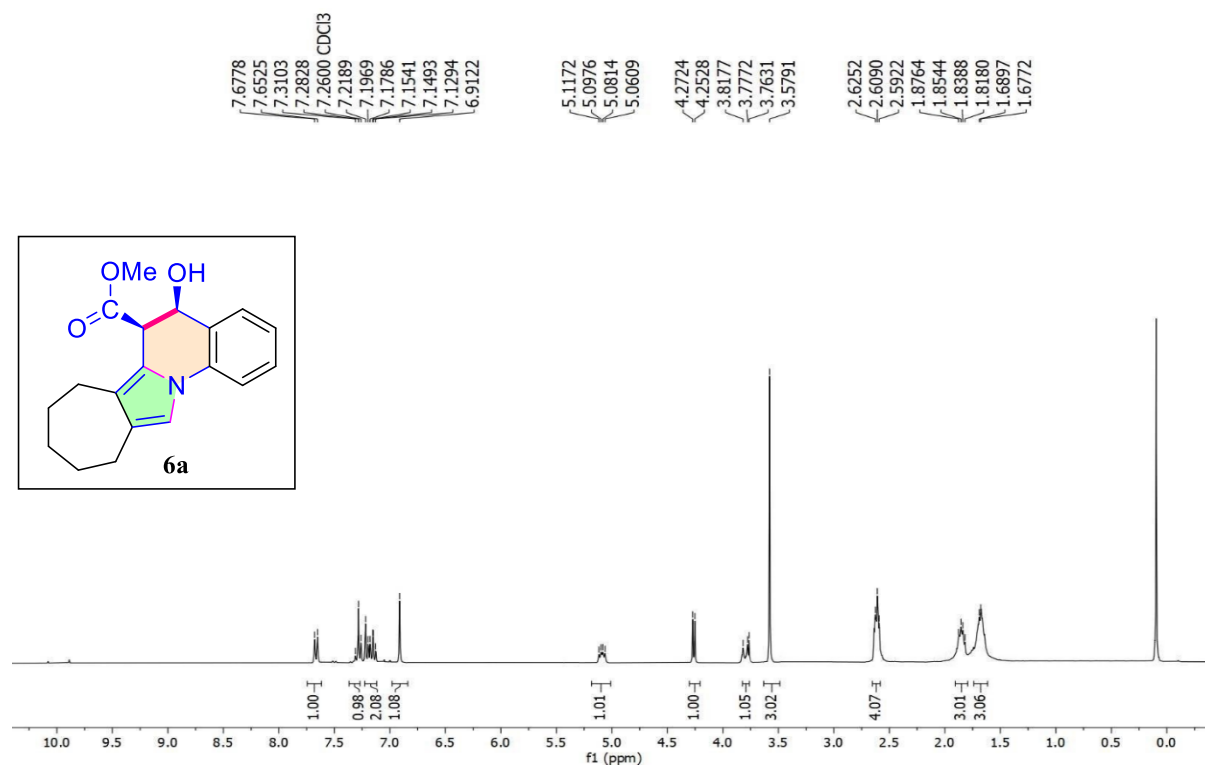
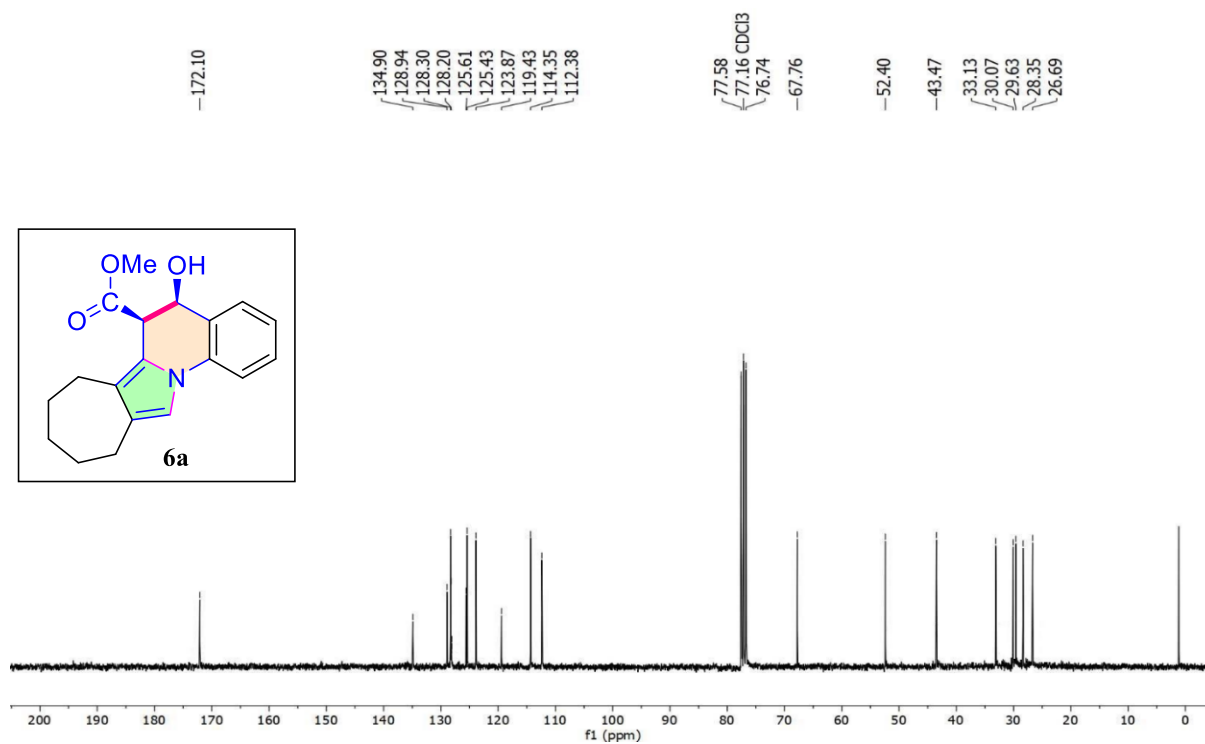
^1H NMR of **3j (500 MHz, CDCl_3):** **$^{13}\text{C}\{^1\text{H}\}$ NMR of **3j** (126 MHz, CDCl_3):**

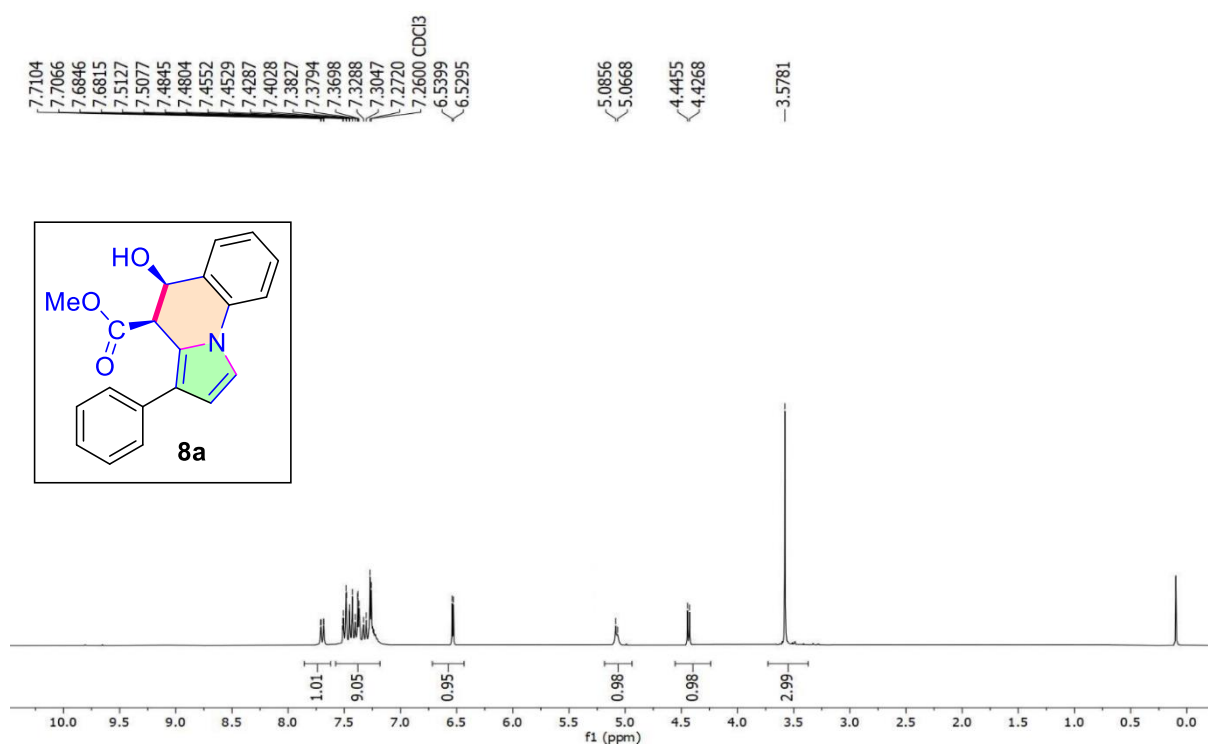
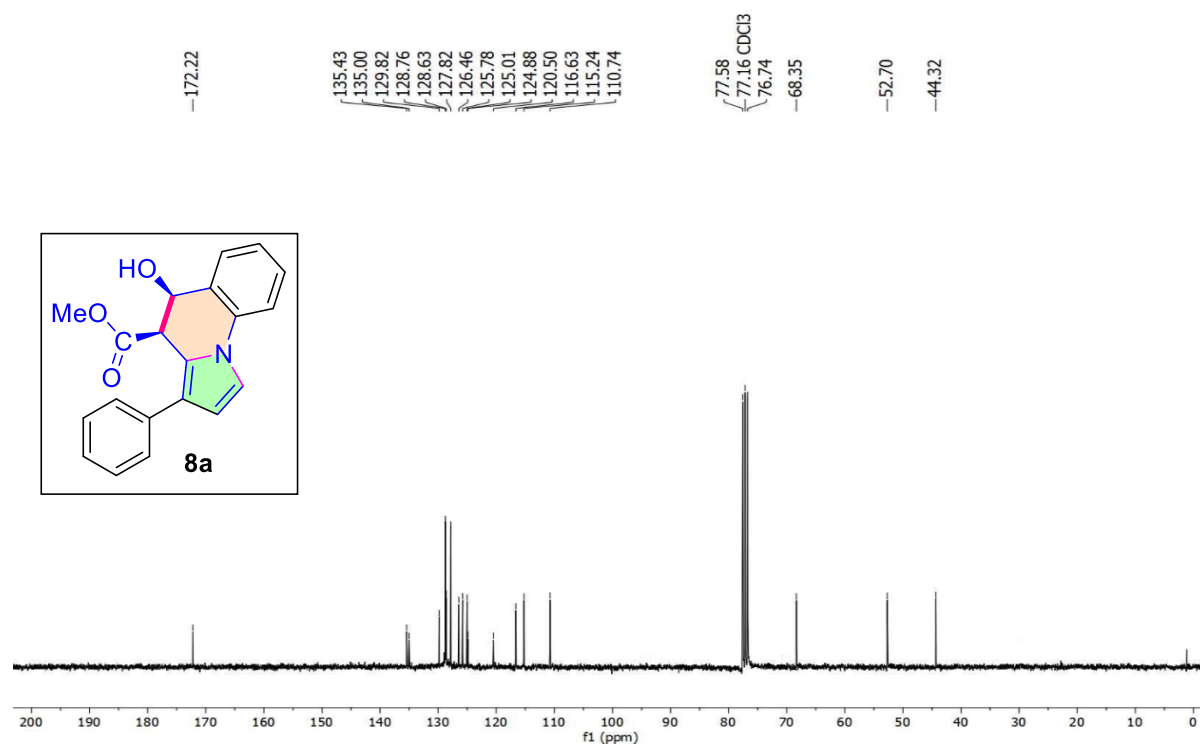
^1H NMR of 3k (300 MHz, CDCl_3): $^{13}\text{C}\{^1\text{H}\}$ NMR of 3k (76 MHz, CDCl_3):

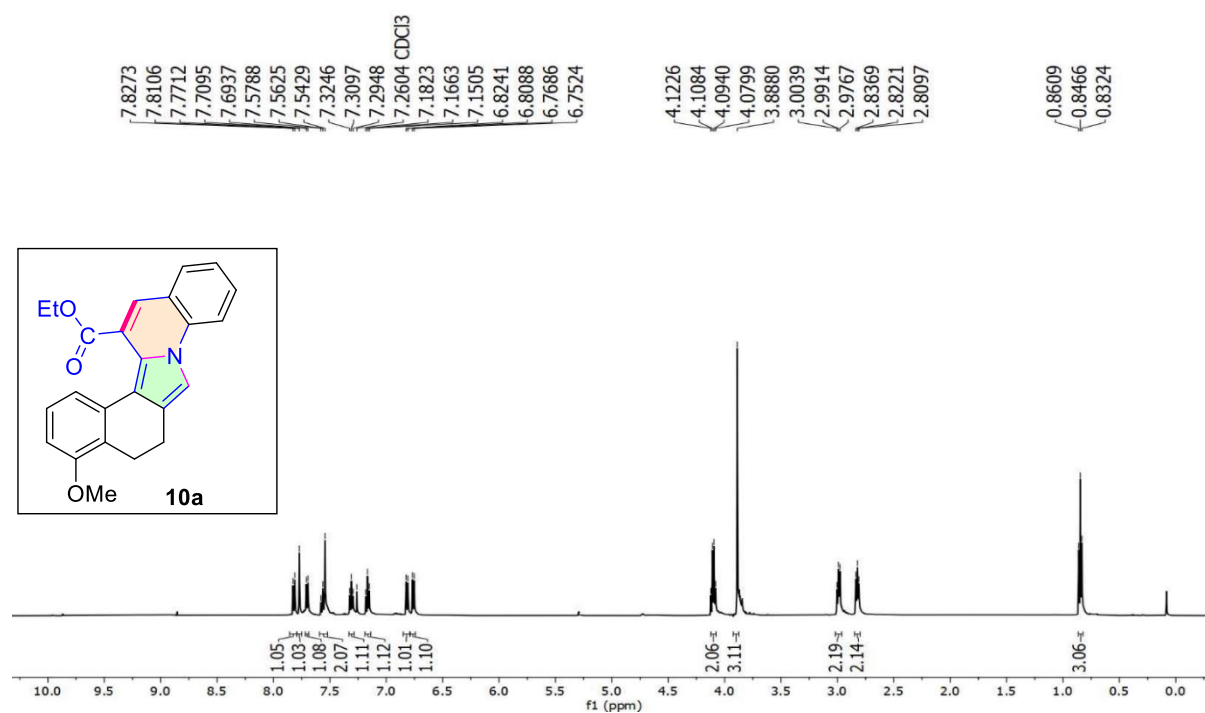
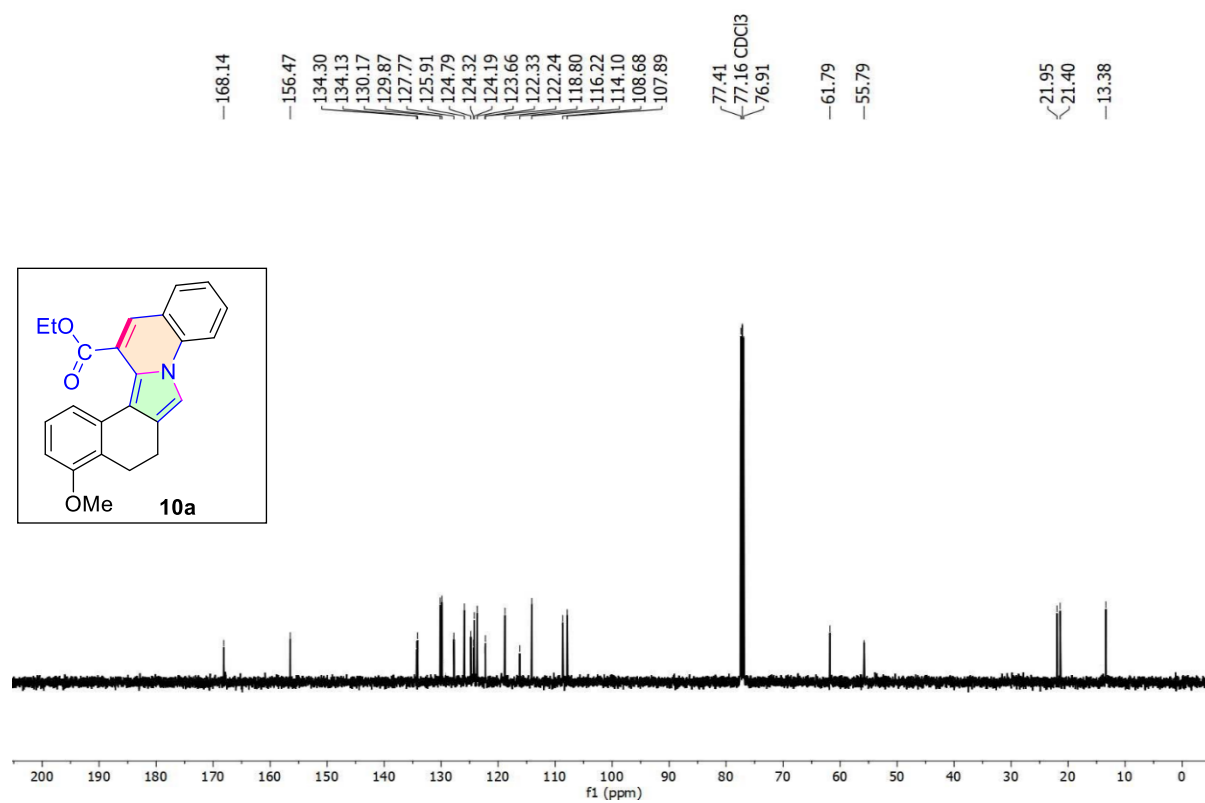
^1H NMR of 3m (300 MHz, CDCl_3): $^{13}\text{C}\{^1\text{H}\}$ NMR of 3m (76 MHz, CDCl_3):

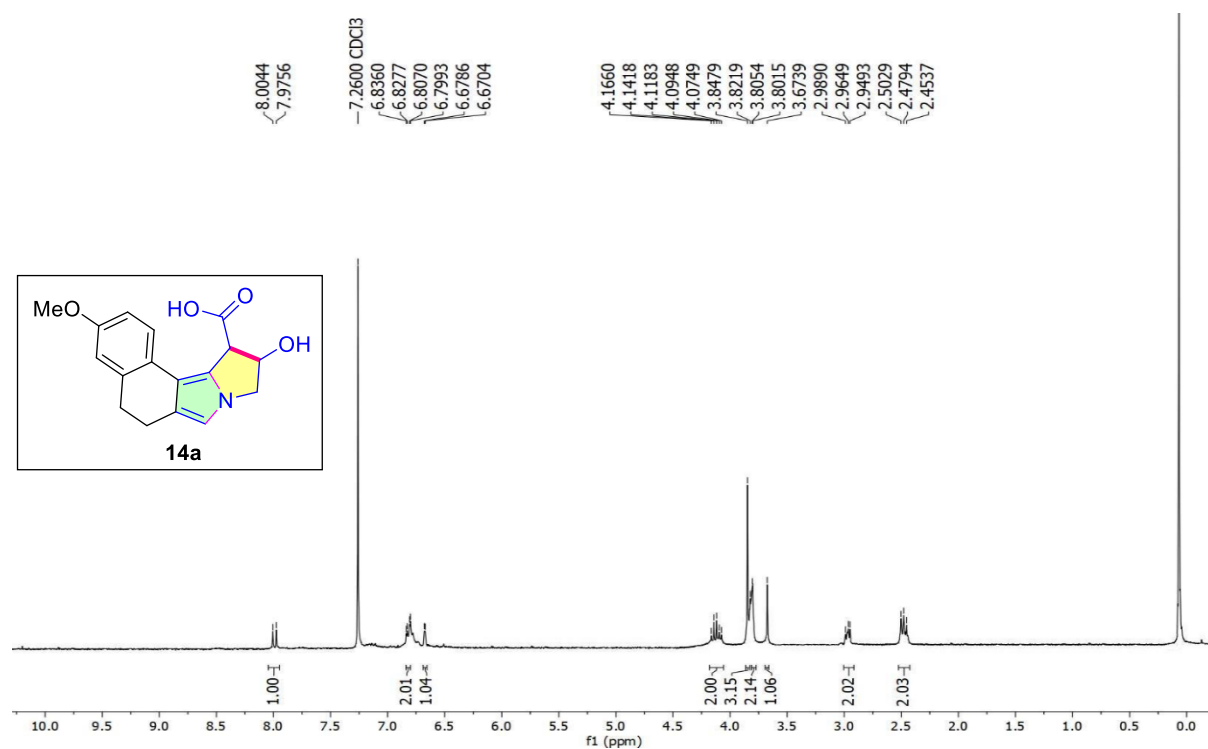
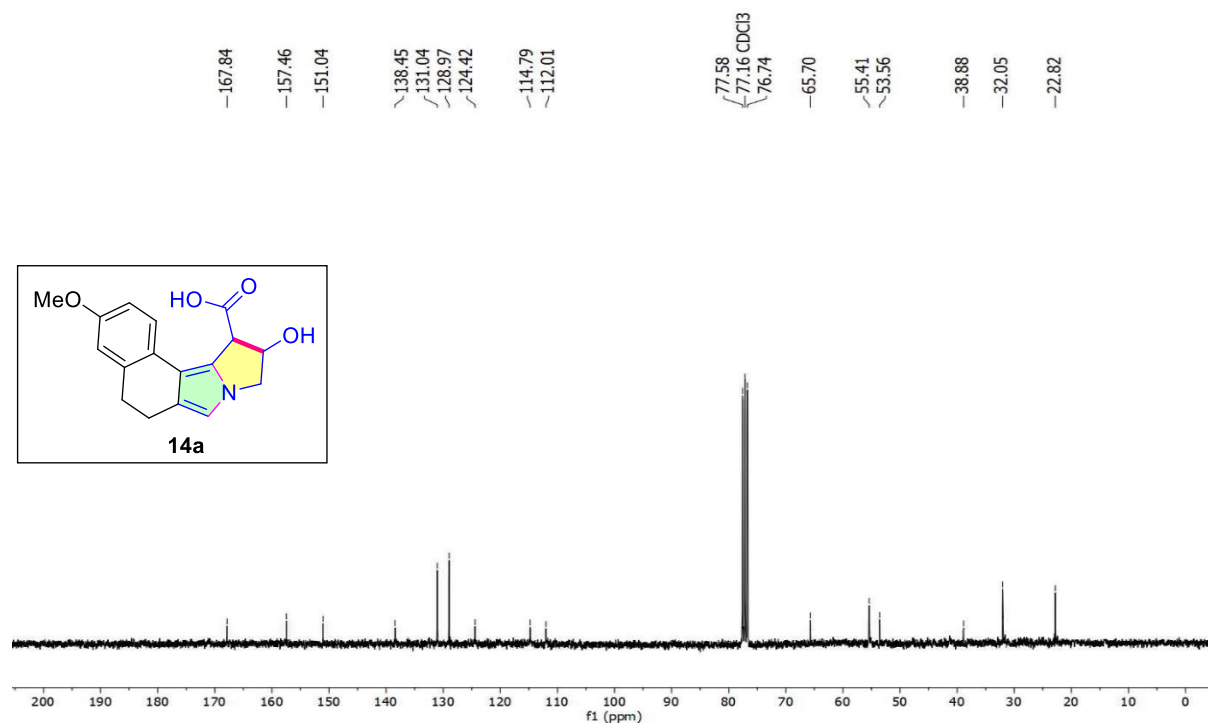
^1H NMR of 4' (300 MHz, CDCl_3): **$^{13}\text{C}\{^1\text{H}\}$ NMR of 4' (76 MHz, CDCl_3):**

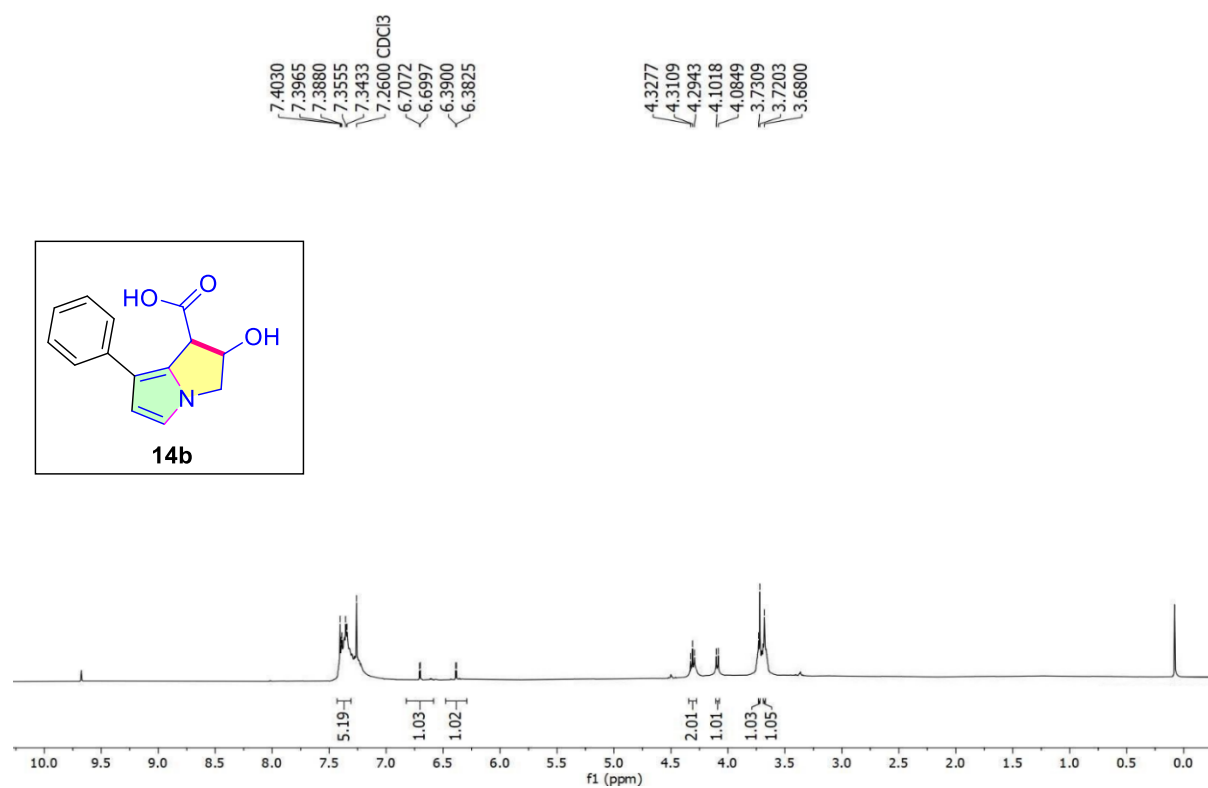
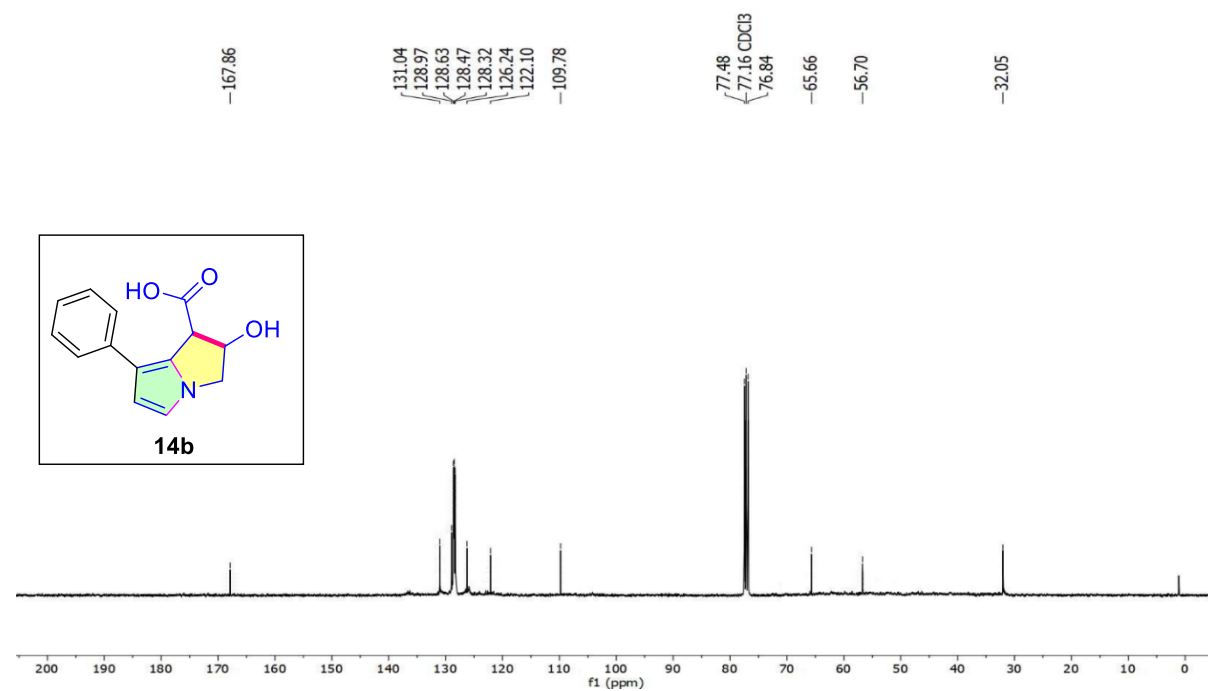
^1H NMR of 5 (300 MHz, CDCl_3): **$^{13}\text{C}\{^1\text{H}\}$ NMR of 5 (76 MHz, CDCl_3):**

^1H NMR of 6a (300 MHz, CDCl_3): **$^{13}\text{C}\{^1\text{H}\}$ NMR of 6a (76 MHz, CDCl_3):**

^1H NMR of 8a (300 MHz, CDCl_3): $^{13}\text{C}\{^1\text{H}\}$ NMR of 8a (76 MHz, CDCl_3):

^1H NMR of 10a (500 MHz, CDCl_3): **$^{13}\text{C}\{^1\text{H}\}$ NMR of 10a (126 MHz, CDCl_3):**

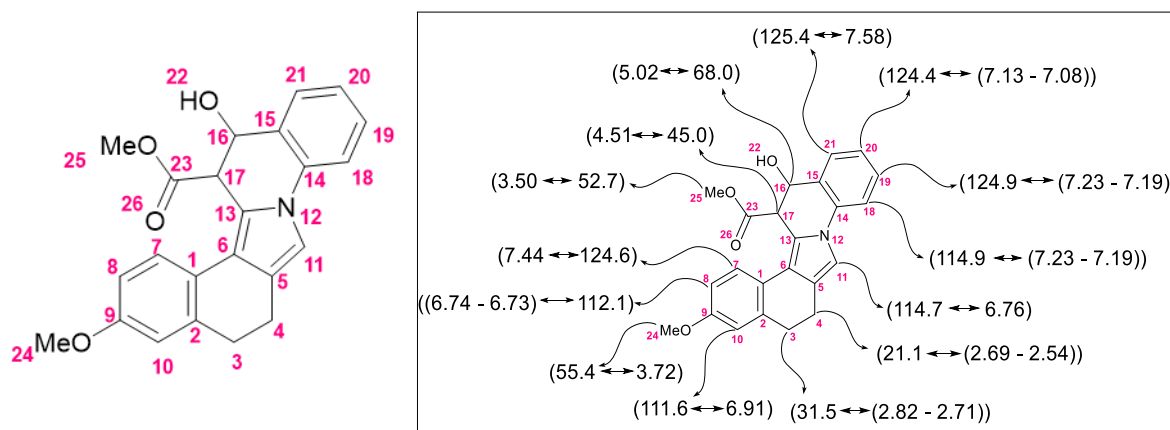
^1H NMR of 14a (300 MHz, CDCl_3): $^{13}\text{C}\{^1\text{H}\}$ NMR of 14a (76 MHz, CDCl_3):

^1H NMR of 14b (400 MHz, CDCl_3): **$^{13}\text{C}\{^1\text{H}\}$ NMR of 14b (101 MHz, CDCl_3):**

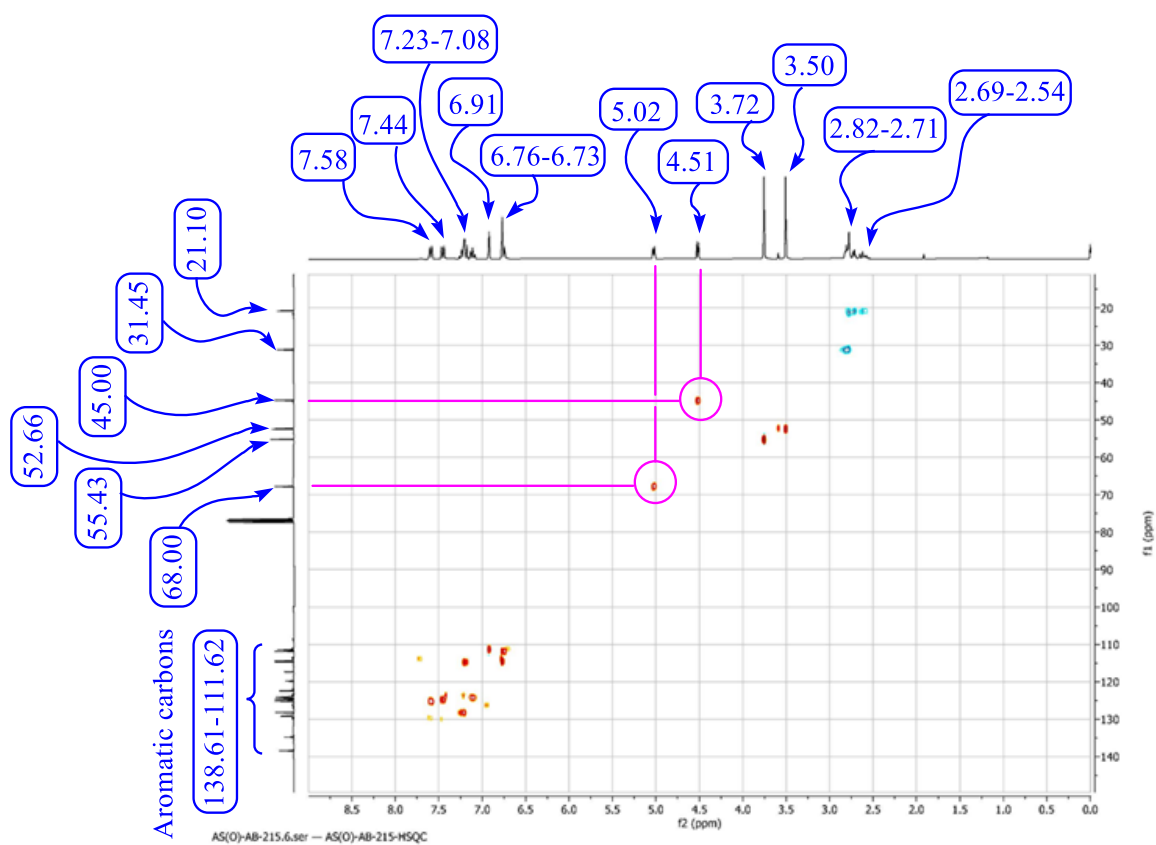
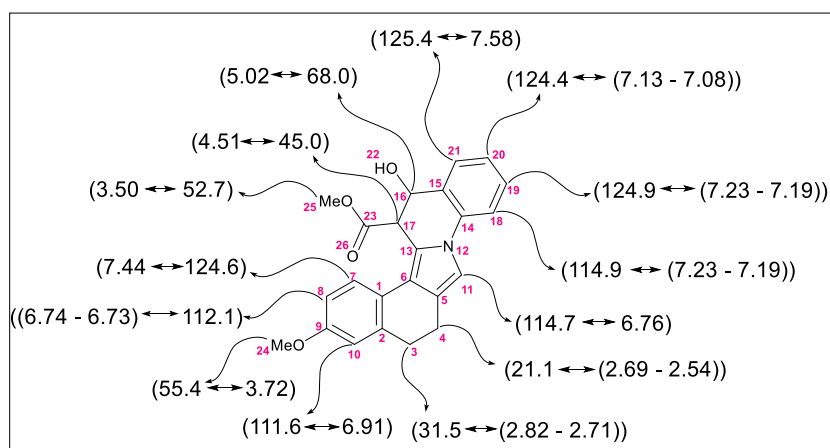
6.6.4. 2D NMR Spectra of 3a:

At first, we have designated the particular resonance value of different protons and carbons of **3a** using HSQC and HMBC experiment and the ^1H - ^{13}C correlation has summarized in the tables.

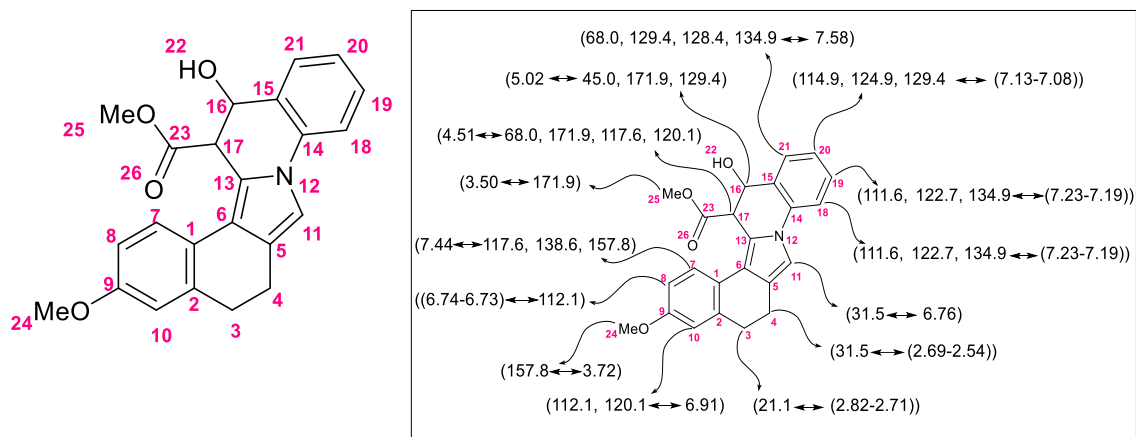
HSQC experiment:



^1H NMR	$^{13}\text{C}\{^1\text{H}\}$ NMR
2.69-2.54 (H4)	21.1 (C4)
2.82-2.71 (H3)	31.5 (C3)
3.50 (s, 3H) (H25)	52.7 (C25)
3.72 (s, 3H), (H24)	55.4 (C24)
4.51 (d, 1H, $J = 5.7$ Hz) (H17)	45.0 (C17)
5.02 (d, 1H, $J = 6.0$ Hz) (H16)	68.0 (C16)
6.74-6.73 (m, 1H) (H8)	112.1 (C8)
6.76 (s, 1H) (H11)	114.7 (C11)
6.91 (s, 1H) (H10)	111.6 (C10)
7.13-7.08 (m, 1H) (H20)	124.4 (H20)
7.23-7.19 (m, 2H) (H18, H19)	124.9 (H19), 114.9 (H18)
7.44 (d, 1H, $J = 8.1$ Hz) (H7)	124.6 (C7)
7.58 (d, 1H, $J = 7.6$ Hz) (H21)	125.4 (C21)

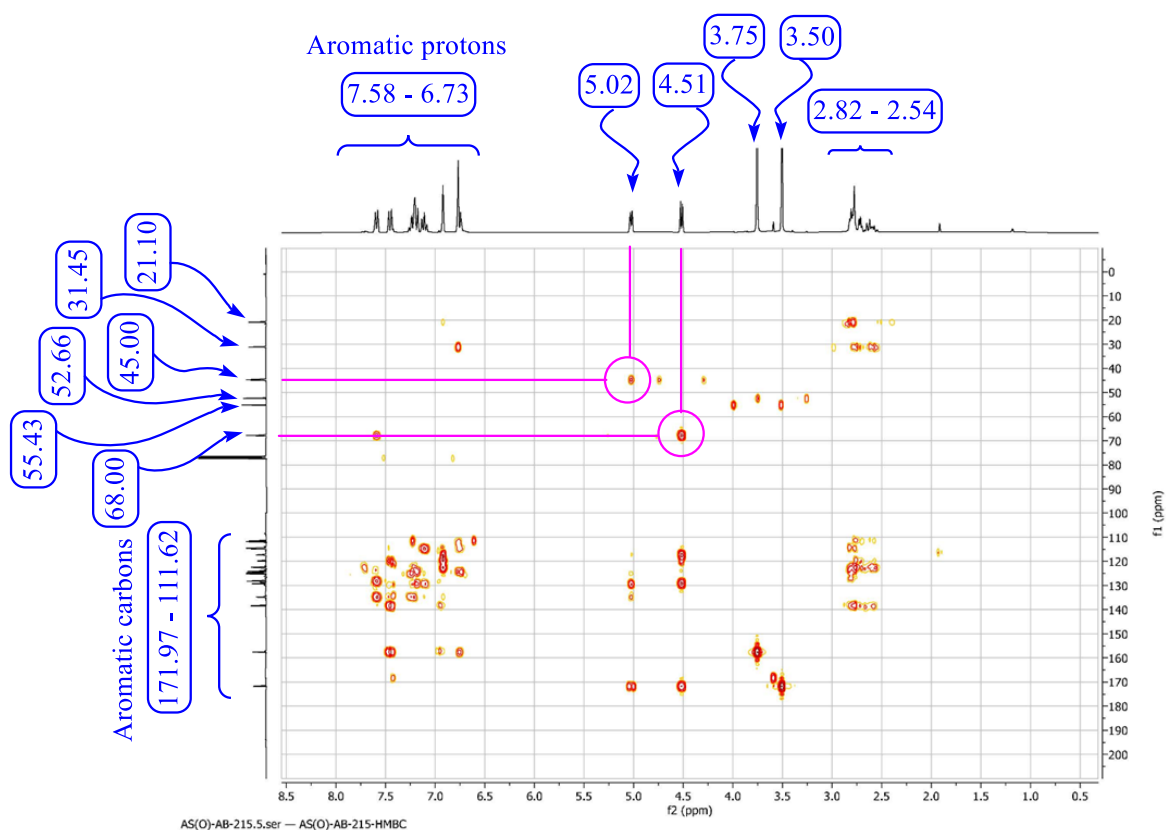
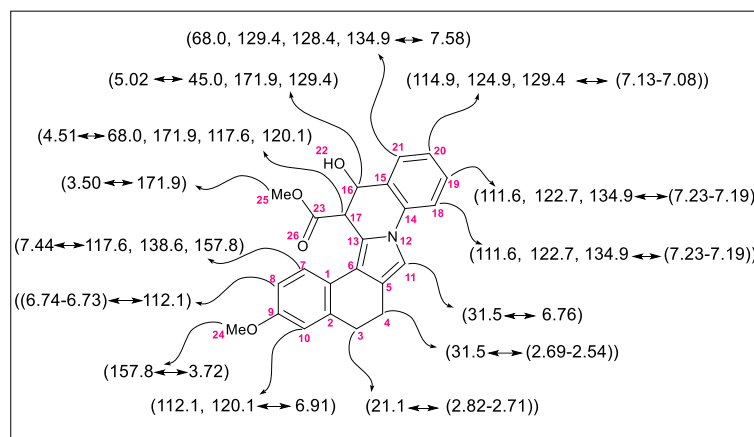


HMBC experiment:



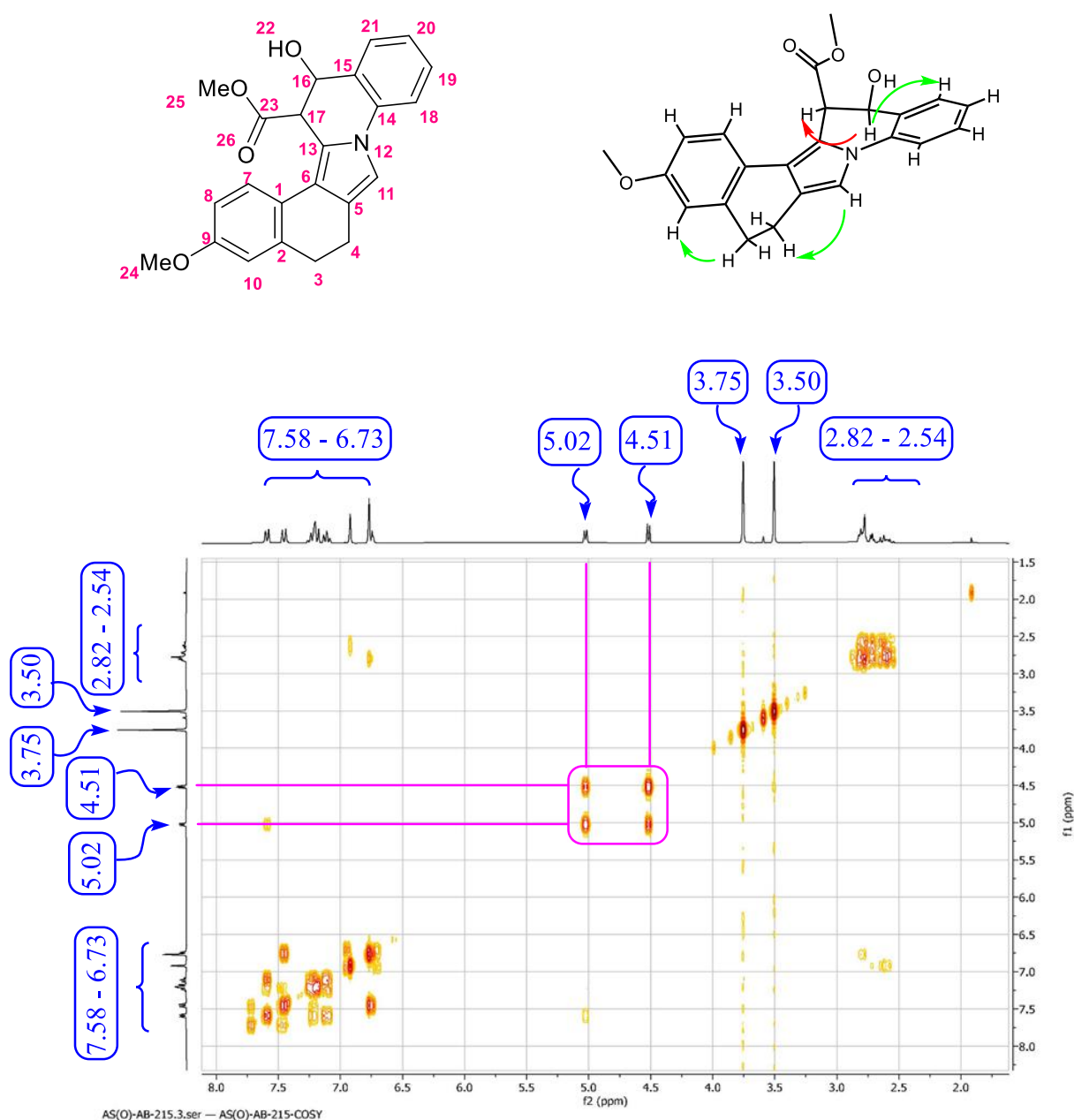
^1H NMR	$^{13}\text{C}\{^1\text{H}\}$ NMR
2.69-2.54 (H4)	31.5
2.82-2.71 (H3)	21.1
3.50 (s, 3H) (H25)	171.9
3.72 (s, 3H), (H24)	157.8
4.51 (d, 1H, $J = 5.7$ Hz) (H17)	68.0, 171.9, 117.6, 120.1
5.02 (d, 1H, $J = 6.0$ Hz) (H16)	45.0, 171.9, 129.4
6.74-6.73 (m, 1H) (H8)	112.1
6.76 (s, 1H) (H11)	31.5
6.91 (s, 1H) (H10)	112.1, 120.1
7.13-7.08 (m, 1H) (H20)	114.9, 124.9, 129.4
7.23-7.19 (m, 2H) (H18, H19)	111.6, 122.7, 134.9
7.44 (d, 1H, $J = 8.1$ Hz) (H7)	117.6, 138.6, 157.8
7.58 (d, 1H, $J = 7.6$ Hz) (H21)	68.0, 129.4, 128.4, 134.9

From these tables it has clearly showed that the stereogenic protons are resonate at $\delta 4.51$ (H-17) and $\delta 5.02$ (H-16) and the corresponding ^{13}C $\delta 45.0$ (C-17), $\delta 68.0$ (C-16) respectively. Nearest protons resonate at $\delta 7.44$ (H-7), $\delta 7.58$ (H-21) with corresponding ^{13}C $\delta 124.6$ (C-7), $\delta 125.4$ (C-21). H-25 resonate at $\delta 3.50$ for $^1\text{H-NMR}$ $\delta 52.7$ for ^{13}C NMR. H-22, -OH proton is not observed due to it exchangeable nature.



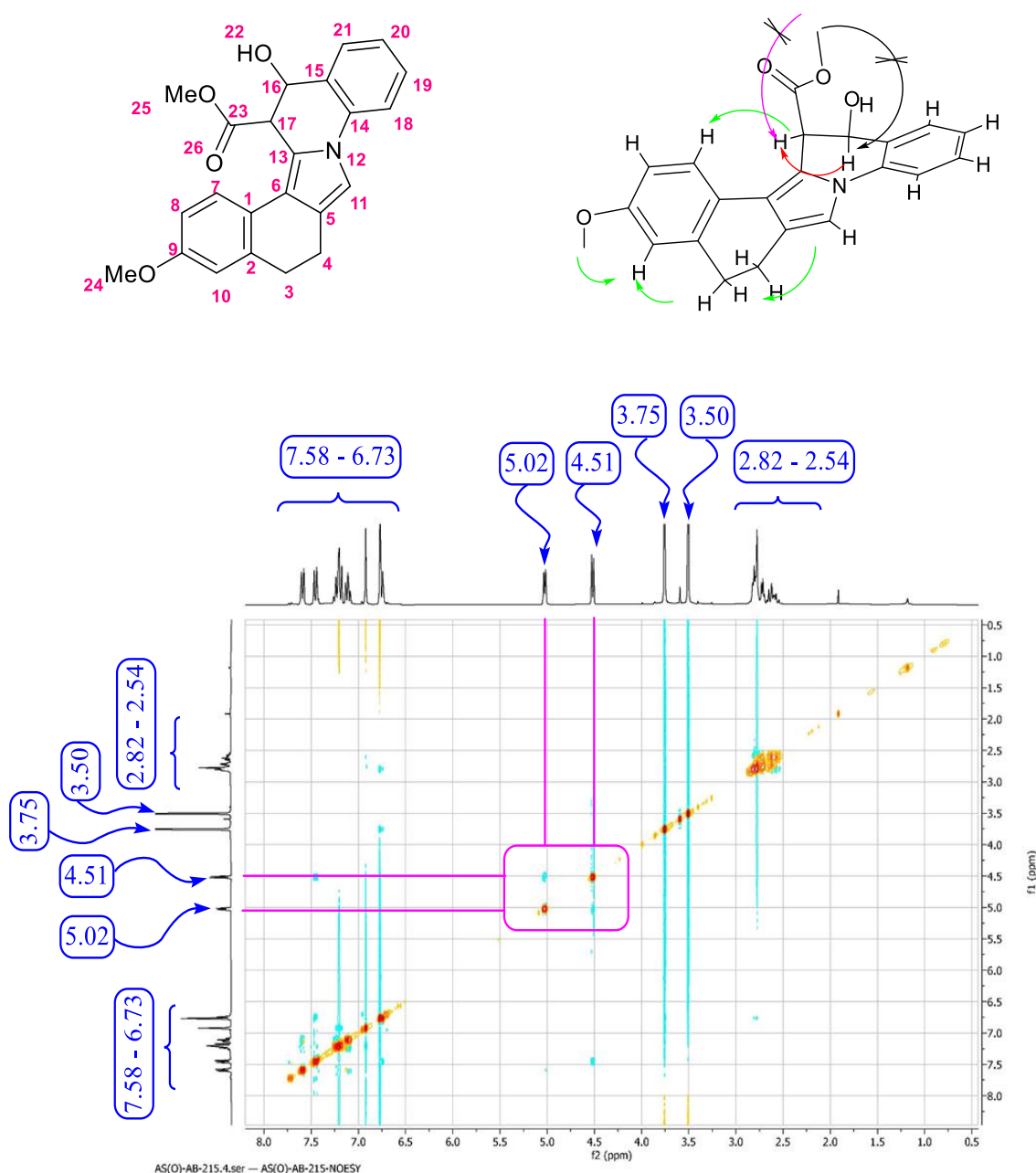
COSY experiment:

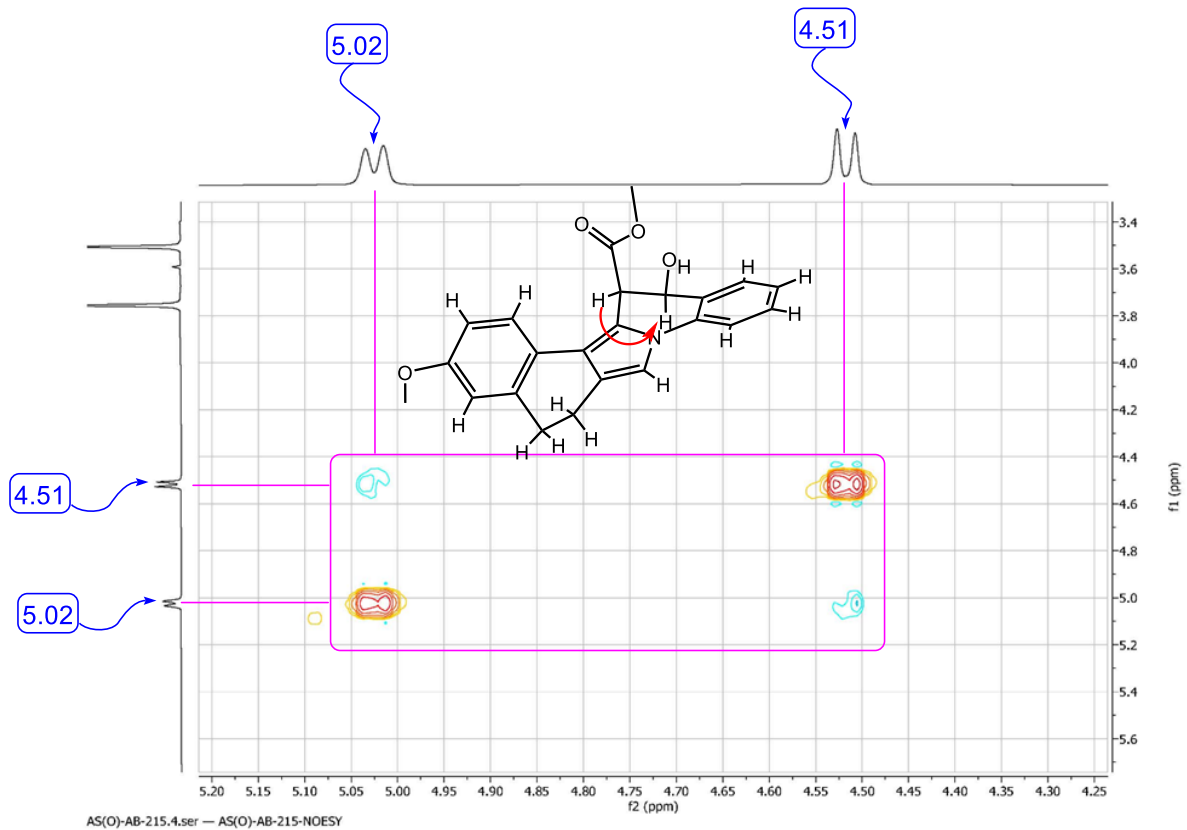
After designation of particular value of proton/carbon correlation, we have carried out 2D COSY experiment for find out primary correlation between coupling protons. The characteristics peak at $\delta 4.51$ (H-16) and $\delta 5.02$ (H-17) are strongly coupled to each other (designate as red arrow) and weak coupling occurred with H-16/H-21, H-11/H-4, and H-3/H-10. From the literature study it has been argued that strong correlation occurred between cis oriented protons compared to the trans oriented protons. Hence the new stereogenic centers are cis with respect to two H-atoms.



NOESY experiment:

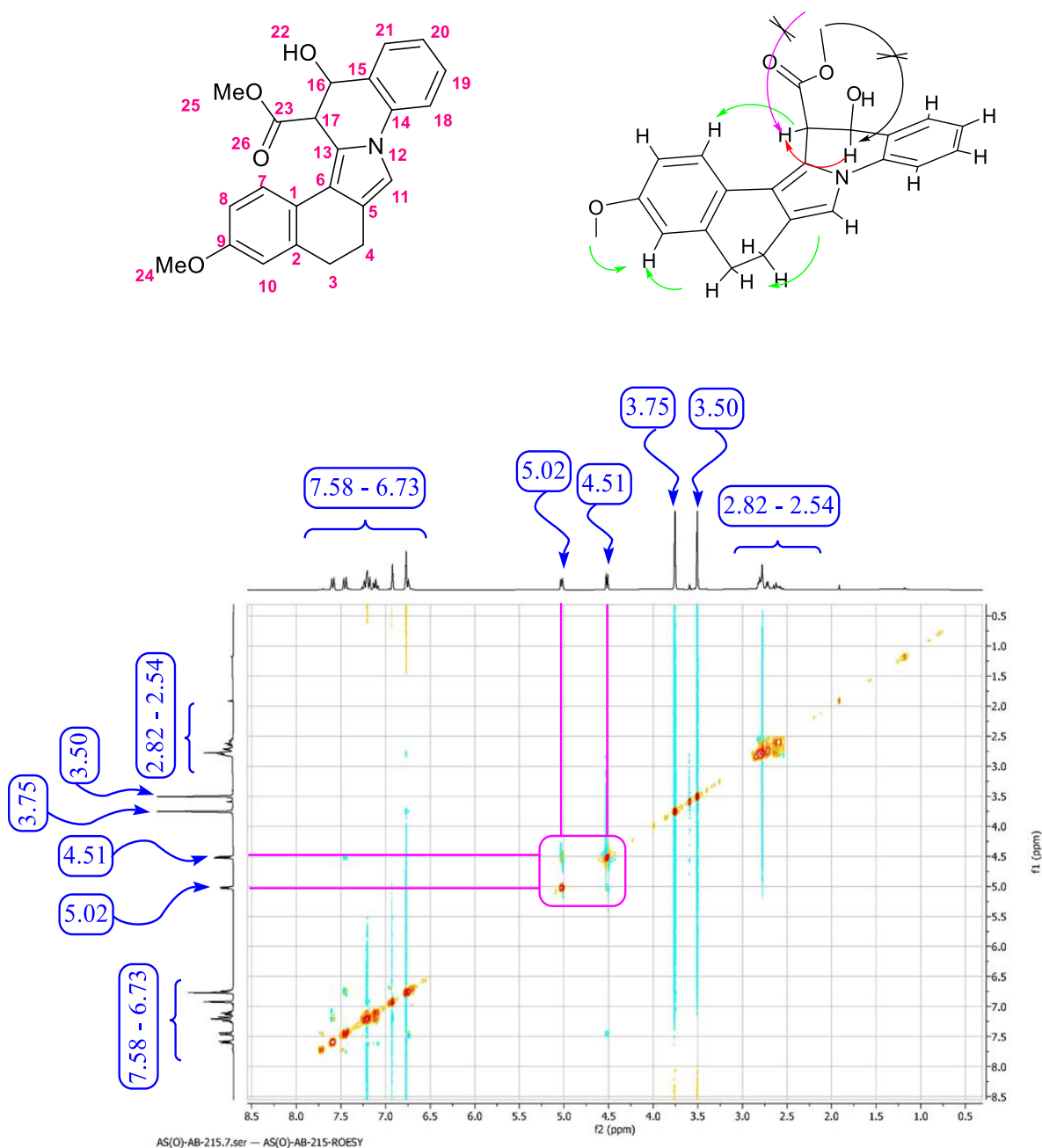
NOESY has also support the space correlation between H-16/H-17 (red arrow in the below structure) which are present in proximity and it is possible if they are cis-oriented. Additional space correlation also found between H-17/H-7. There is no correlation with H-25/H-16 or H-25/H-17. Hence $-\text{CO}_2\text{Me}/\text{H}16$ are present in the trans orientation. If H-16/H17 oriented in trans relationship then we should not get correlation in NOESY spectrum but in practical we get a strong correlation and hence it is further proof that H-16/H-17 are cis oriented.





ROESY experiment:

We have got similar cross peak pattern in the ROESY as that of the NOESY. Same space correlation observed between two stereogenic centers H-16/H-17 and H-17/H-7. This observation indicated that the peak obtained NOESY is not due to the diffusion correlation it is the actual space correlation for the cis-orientation of H-16/H-17.



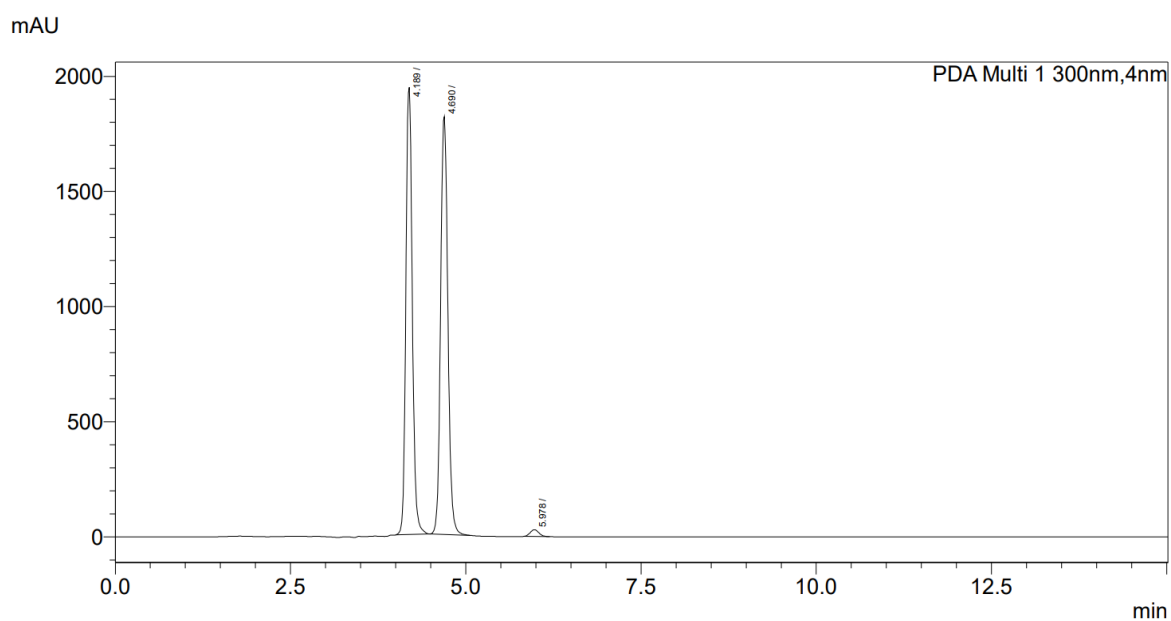
From this series of experiment, it has been concluded that our synthetic compound **3a** is diastereomerically pure and racemic and H-16/H-17 are cis oriented.

6.6.5. HPLC analysis report:

Report of the chiralpak column of 3a:

COLUMN :CHIRALPAK IG (250X4.6)mm,5 μ
M.P.- Hexane/DCM/EtOH/IPAmine - 50/25/25/0.1
Flow Rate - 1.0 ml/min

<Chromatogram>



<Batch Table>

PDA Ch1 300nm

Peak#	Ret. Time	Area	Area%
1	4.189	12409116	48.257
2	4.690	13049547	50.747
3	5.978	256202	0.996
Total		25714865	100.000

Peak Table

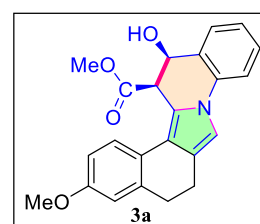
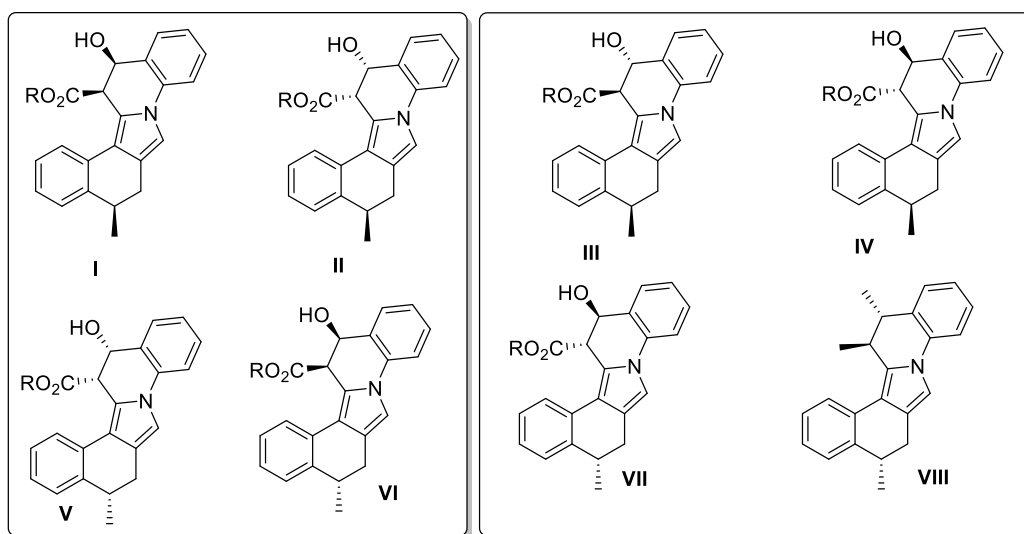


Figure 6.12. HPLC analysis report of compound 3a.

Explanation for the diastereomeric mixture of 3g and 3h:

The tandem aza-Michael-aldol strategy for the formation of fused diastereomeric mixture **3g** and **3h** can be explained in the presence of extra stereogenic center at the substrates **2g** and **2h**. Here 4 diastereomeric pairs are possible according to the stereochemical terminology of the substrate **3g** and **3h**, but two pairs are easily omitted as our protocol produce cis-aldol product (I/II/V/VI) and trans aldol product III/IV/VII/VIII are not formed. Here –Me group at 4-position distinguish the two diastereomeric pairs (I/V and II/VI). This is the indirect evidence for the formation of cis aldol product; if trans-aldol product was obtained then we get actually 4-set of peaks for –Me group. But in practice, we get two set of –Me group. So, we got the mixture of two diastereomeric pairs for the substrate **3g** and **3h**. This can be further proved by HPLC experiment of **3h** where two diastereomers I & II are present in the appreciable amount.



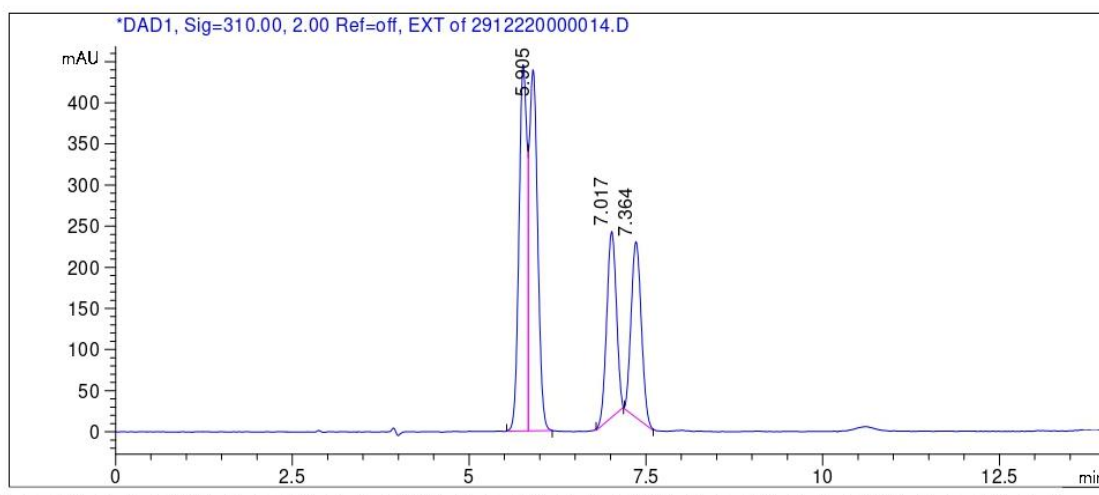
Obtained product I/V : II/VI = 56:44 or 62:38

Not obtained

Report of the chiralpak column of 3h:

Column Name : Chiralpak IG (4.6 x 250 mm), 5 μ
 ARD/K/
 Mobile Phase : Hexane/EtOH/IPAmine : 80/20/0.1
 Flow Rate : 1.0 ml/min
 Solubility : MeOH

->



Signal 1: DAD1, Sig=310.00, 2.00 Ref=off, EXT

Peak #	RT [min]	Area	Area %
1	5.77	3589.58	31.34
2	5.91	3564.72	31.12
3	7.02	2150.73	18.78
4	7.36	2149.02	18.76

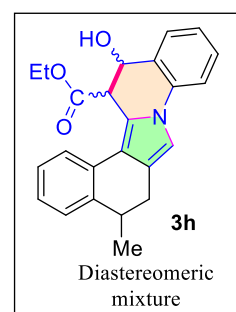
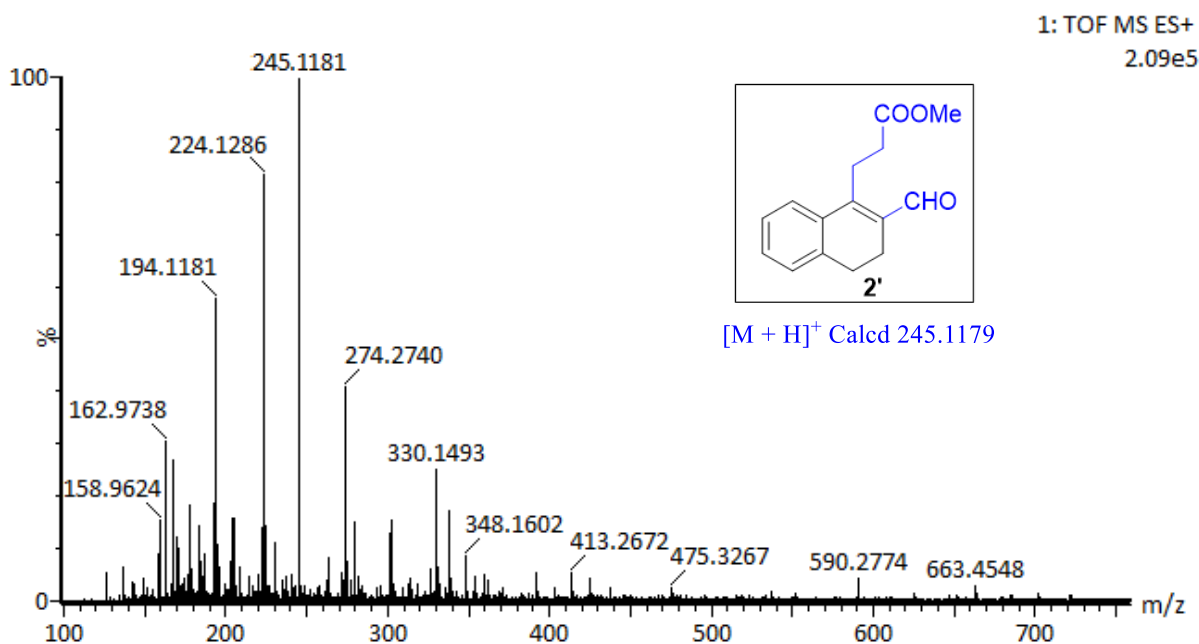
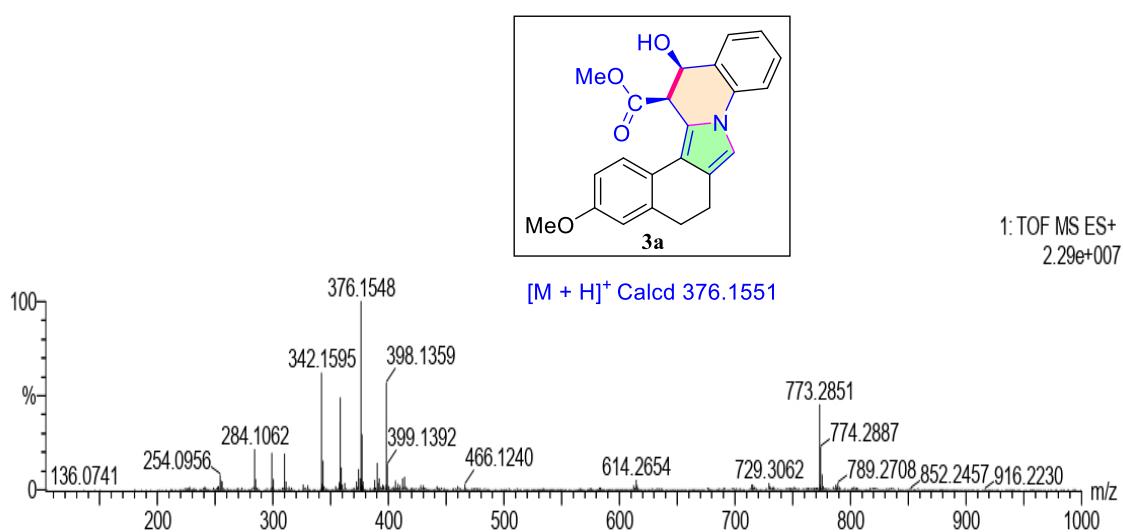
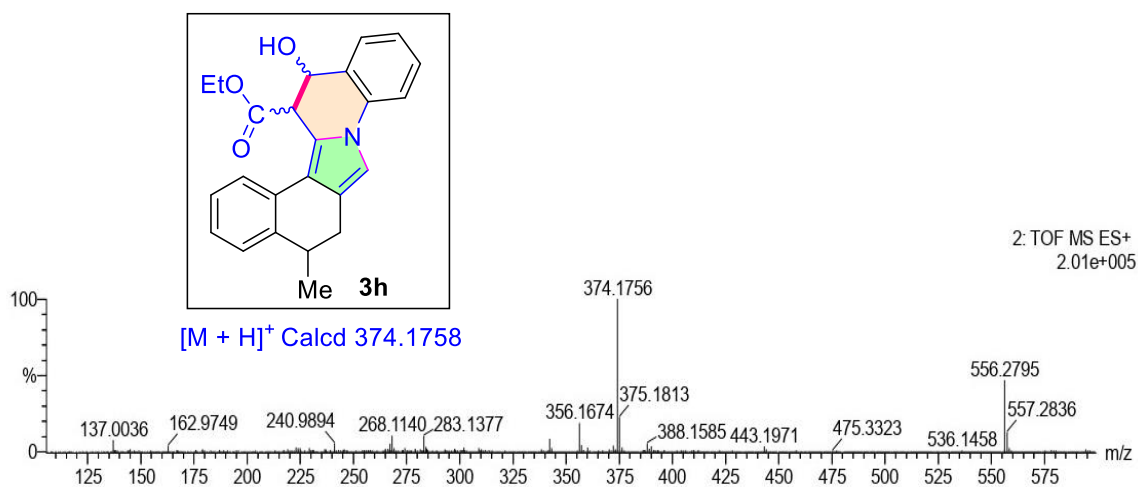


Figure 6.13. HPLC analysis report of compound 3h.

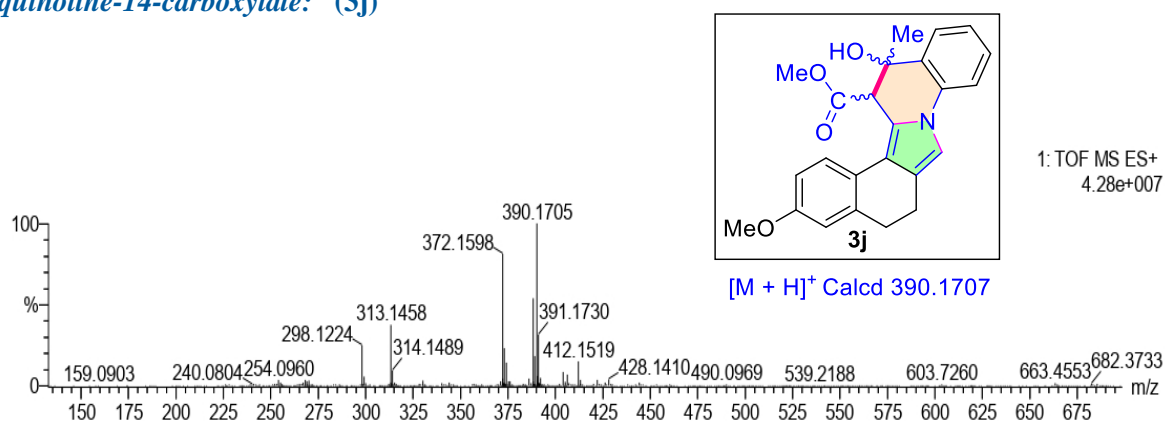
6.6.6. Representative HRMS spectra:

Methyl 3-(2-formyl-3,4-dihydronaphthalen-1-yl)propanoate: (2')*Methyl (13R,14R)-13-hydroxy-3-methoxy-5,6,13,14-tetrahydrobenzo[6,7]isoindolo[2,1-a]quinoline-14-carboxylate: (3a)*

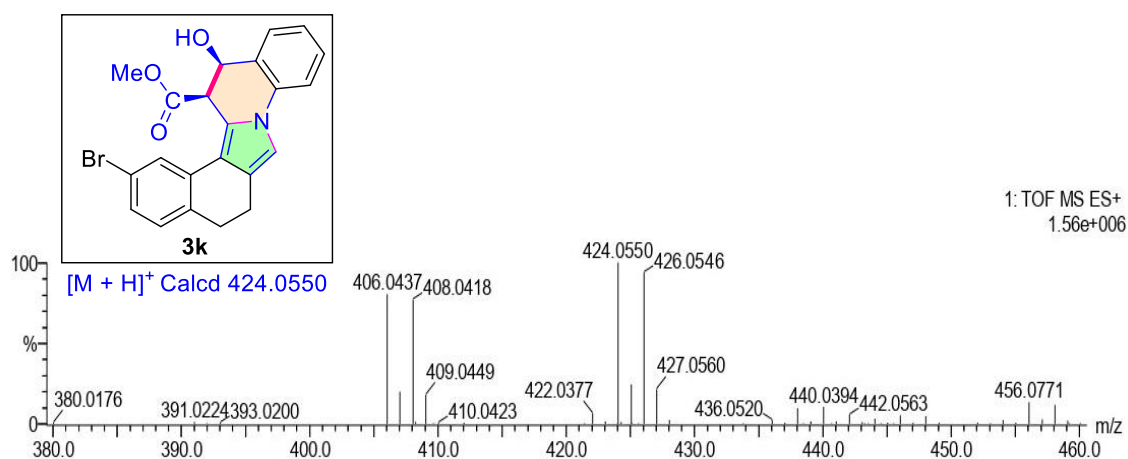
Ethyl (14R)-13-hydroxy-5-methyl-5,6,13,14-tetrahydrobenzo[6,7]isoindolo[2,1-a]quinoline-14-carboxylate: (3h)



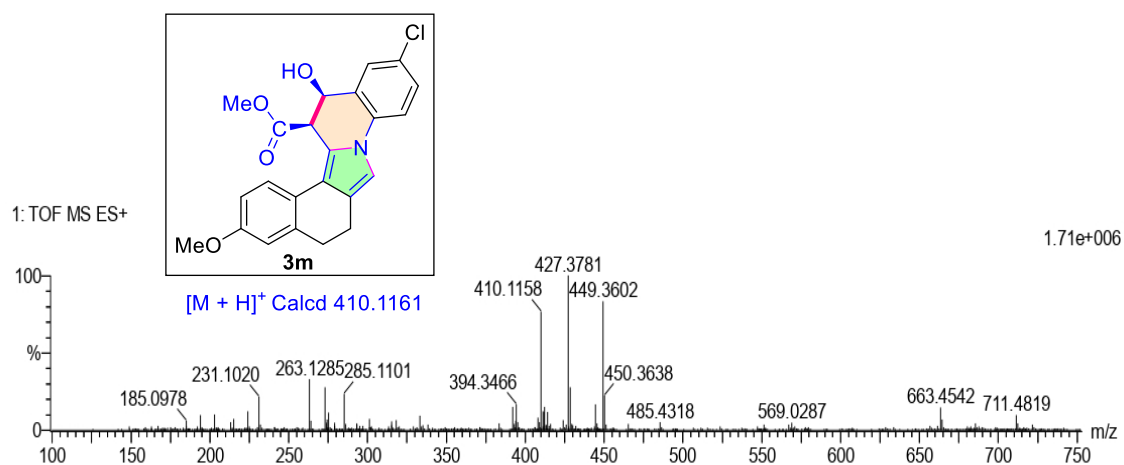
Methyl (13S,14R)-13-hydroxy-3-methoxy-13-methyl-5,6,13,14-tetrahydrobenzo[6,7]isoindolo[2,1-a]quinoline-14-carboxylate: (3j)



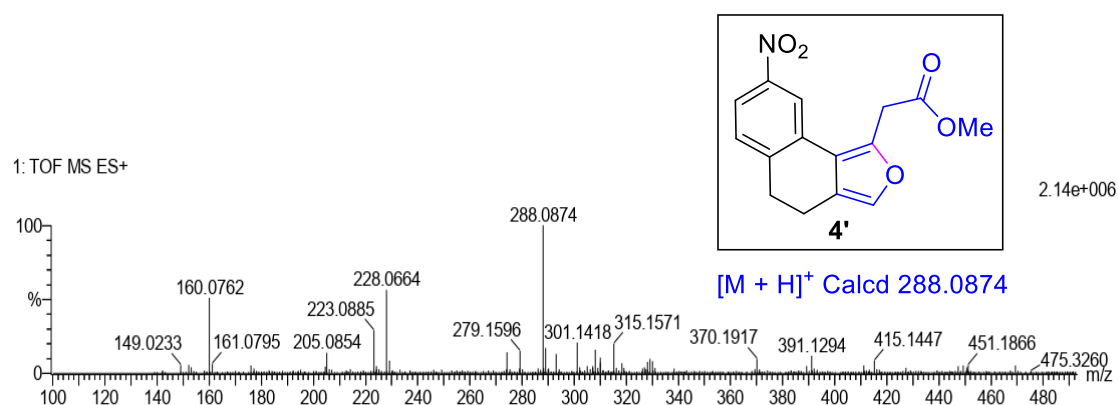
Methyl (13R,14R)-2-bromo-13-hydroxy-5,6,13,14-tetrahydrobenzo[6,7]isoindolo[2,1-a]quinoline-14-carboxylate: (3k)



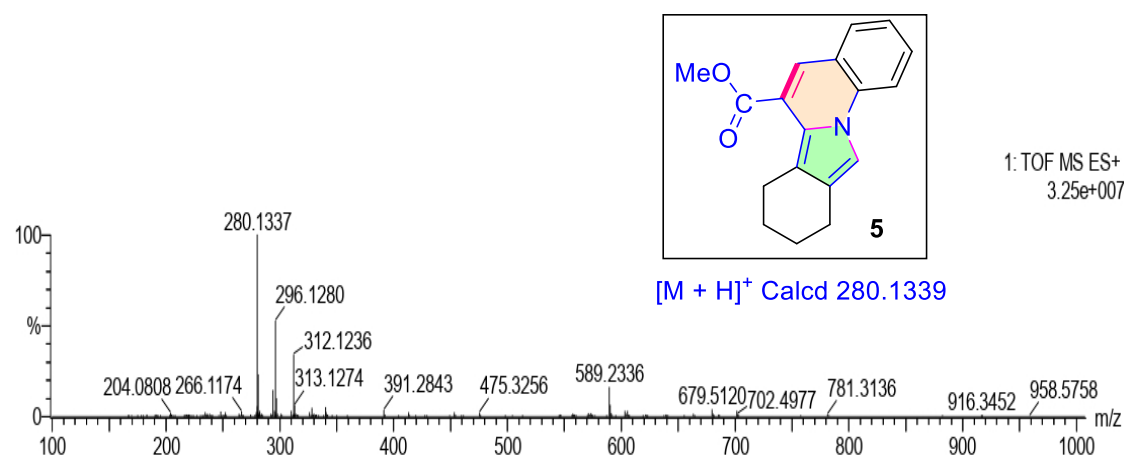
Methyl (13R,14R)-11-chloro-13-hydroxy-3-methoxy-5,6,13,14-tetrahydrobenzo[6,7]isoindolo[2,1-a]quinoline-14-carboxylate: (3m)



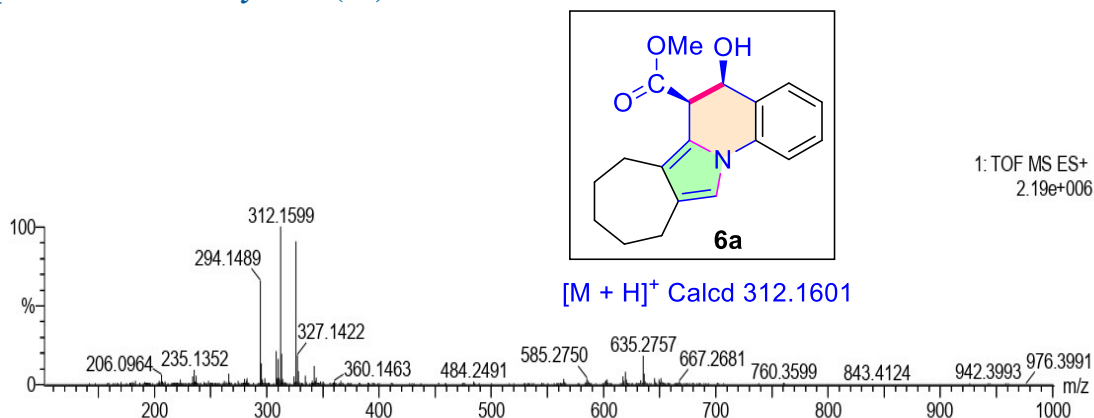
Methyl 2-(8-nitro-4,5-dihydronaphtho[1,2-c]furan-1-yl)acetate: (4')



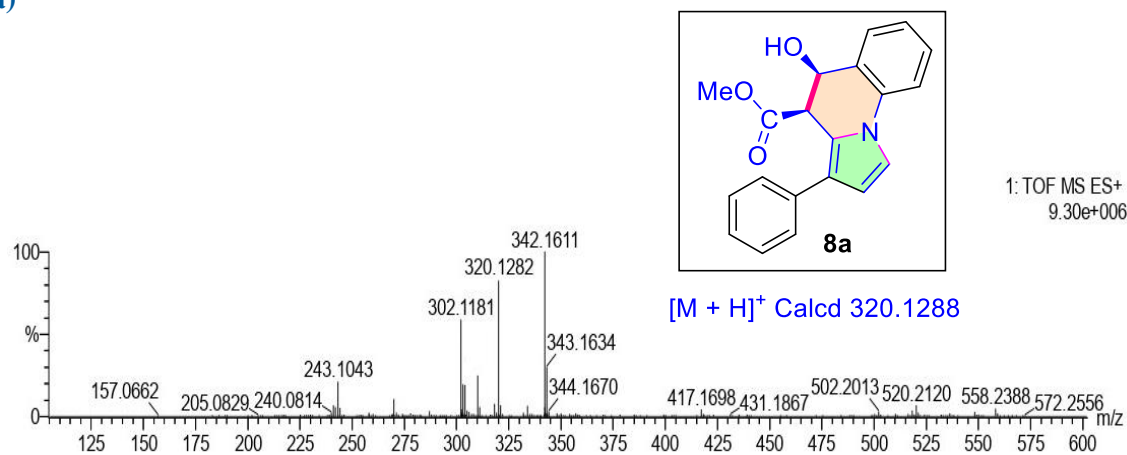
Methyl 7,8,9,10-tetrahydroisoindolo[2,1-a]quinoline-6-carboxylate: (5)



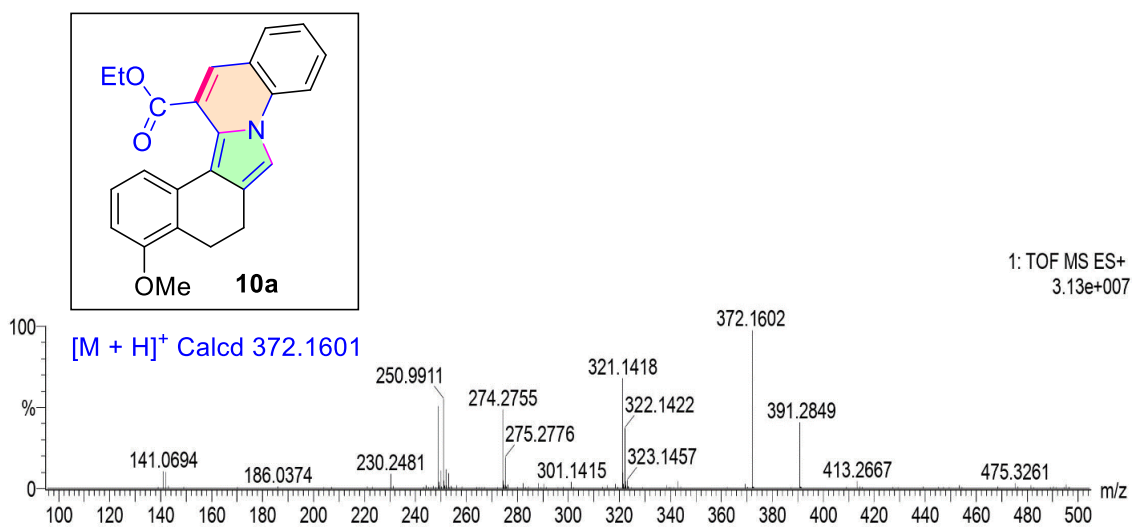
Methyl (5R,6R)-5-hydroxy-6,7,8,9,10,11-hexahydro-5H-cyclohepta[3,4]pyrrolo[1,2-a]quinoline-6-carboxylate: (6a)



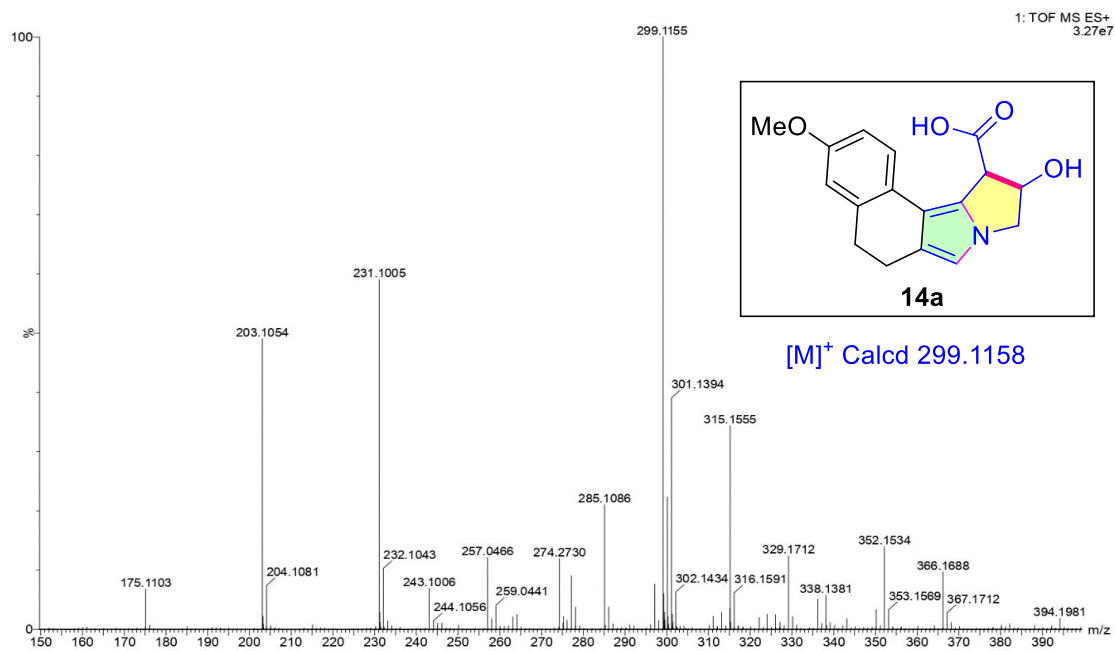
Methyl (4R,5R)-5-hydroxy-3-phenyl-4,5-dihydropyrrolo[1,2-a]quinoline-4-carboxylate: (8a)



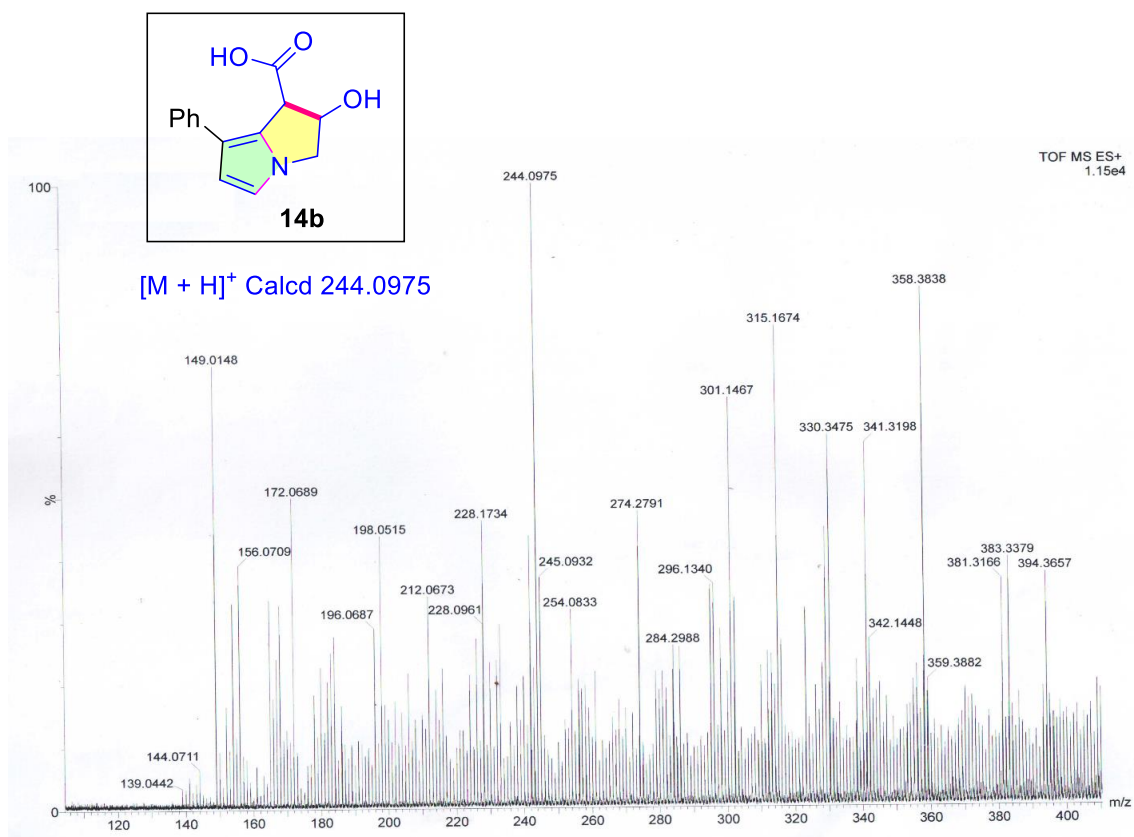
Ethyl 4-methoxy-5,6-dihydrobenzo[6,7]isoindolo[2,1-a]quinoline-14-carboxylate: (10a)



(10R,11R)-10-Hydroxy-3-methoxy-5,9,10,11-tetrahydro-6H-benzo[g]pyrrolo[2,1-*a*]isoindole-11-carboxylic acid: (14a)



(1R,2R)-2-Hydroxy-7-phenyl-2,3-dihydro-1H-pyrrolizine-1-carboxylic acid: (14b)



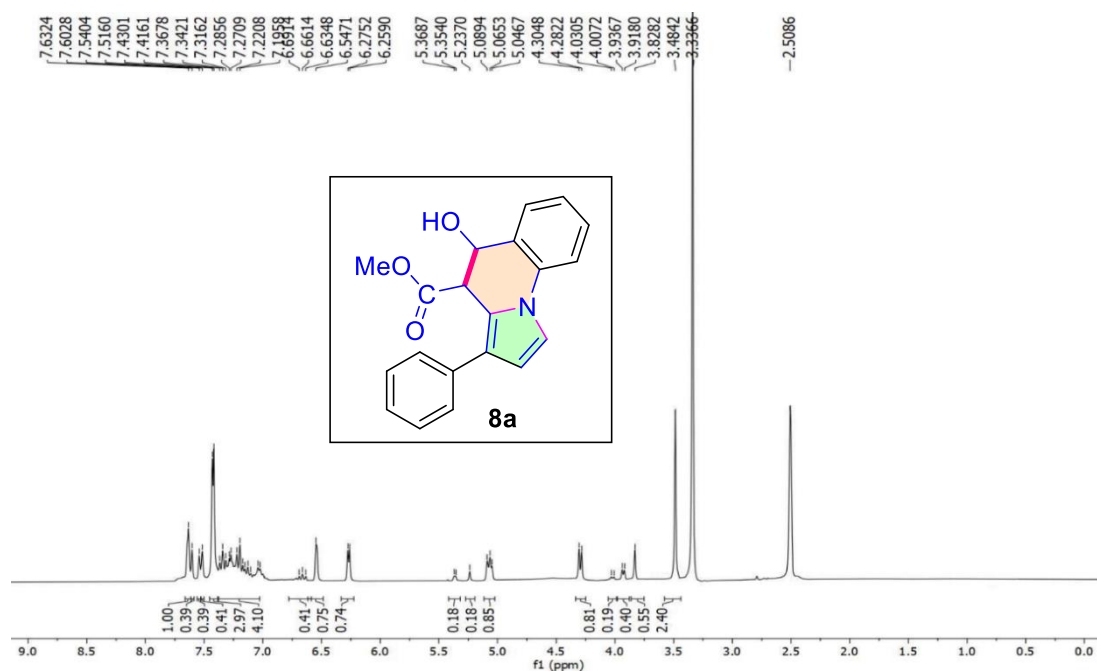
❖ ^1H NMR of **8a** in the highly viscous DMSO solvent:

Figure 6.14. ^1H NMR of **8a** in the highly viscous DMSO solvent.

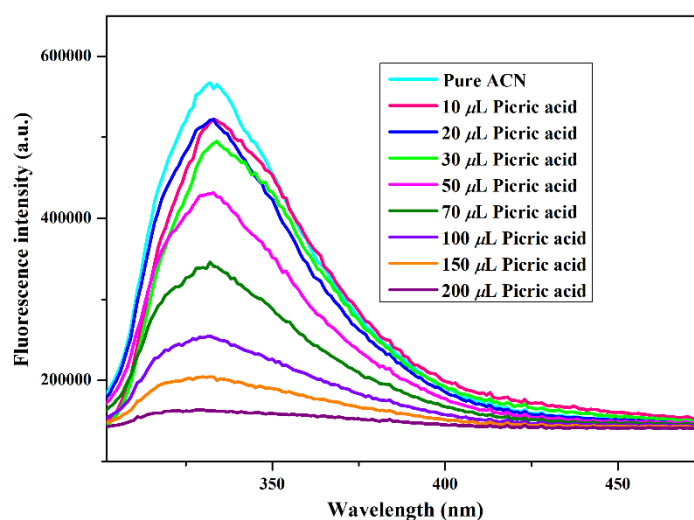
❖ Picric acid sensing fluorescence quenching plot of **8a**:

Figure 6.15. Fluorescence quenching of **8a** (2×10^{-5} M solution in ACN) by stepwise addition of picric acid (2×10^{-3} M solution in ACN).

6.7. References:

1. (a) C. Mohan, R. B. Krishna, S. T. Sivanandan, and I. Ibnu Saud, *Eur. J. Org. Chem.*, 2021, **2021**, 4911-4926; (b) A. J. Das, R. Chouhan, and S. K. Das, *J. Org. Chem.*, 2021, **86**, 8274-8285; (c) Z. Huang, Y. Meng, Y. Wu, C. Song, and J. Chang, *Tetrahedron*, 2021, **93**, 132280; (d) V. U. Ahmad, A.-u. Rahaman, T. Rasheed, and H.-u. Rahaman, 1987, *Heterocycles*, **26**, 1251-1255; (e) T. Rasheed, M. N. I. Khan, S. S. A. Zhadi, and S. Durrani, *J. Nat. Prod.*, 1991, **54**, 582-584; (f) Y. Gao, J. Li, S. Bai, D. Tu, C. Yang, Z. Ye, B. Hu, X. Qi, and C. Jiang, *Org. Chem. Front.*, 2020, **7**, 1149-1157; (g) L. Randriambola, J. C. Quirion, C. Kan-Fan, and H. P. Husson, *Tetrahedron Lett.*, 1987, **28**, 2123-2126; (h) M. Motegi, A. E. Nugroho, Y. Hirasawa, T. Arai, A. H. A. Hadi, and H. Morita, *Tetrahedron Lett.*, 2012, **53**, 1227-1230; (i) A. Suyavaran, C. Ramamurthy, R. Mareeswaran, Y. V. Shanthi, J. Selvakumar, S. Mangalaraj, M. S. Kumar, C. R. Ramanathan, and C. Thirunavukkarasu, *Bioorg. Med. Chem.*, 2015, **23**, 488-498; (j) P. Ploypradith, T. Petchmanee, P. Sahakitpichan, N. D. Litvinas, and S. Ruchirawat, *J. Org. Chem.*, 2006, **71**, 9440-9448; (k) C. Bailly, *Mar. Drugs*, 2015, **13**, 1105-1123; (l) R. Mishra, A. Jana, A. K. Panday, and L. H. Choudhury, *Org. Biomol. Chem.*, 2018, **16**, 3289-3302.
2. O. O. Ajani, K. T. Iyaye, and O. T. Ademosun, *RSC Adv.*, 2022, **12**, 18594-18614.
3. K. M. Divya, D. P. Savitha, G. Anjali Krishna, T. M. Dhanya, and P. V. Mohanan, *J. Photochem. Photobiol. A*, 2022, **431**, 114046.
4. T. Kim and J. Kim, *Molecules*, 2022, **27**, 1-15.
5. A. Kathiravan, A. Gowri, T. Khamrang, M. D. Kumar, N. Dhenadhayalan, K.-C. Lin, M. Velusamy, and M. Jaccob, *Anal. Chem.*, 2019, **91**, 13244-13250.
6. B. N. Patil, J. J. Lade, K. S. Vadagaonkar, P. Chetti, and A. C. Chaskar, *Chem. Select*, 2018, **3**, 10010-10018.
7. Z. Guo, W. Zhu, and H. Tian, *ChemComm*, 2012, **48**, 6073-6084.
8. T. Aggarwal, S. Kumar, D. K. Dhaked, R. K. Tiwari, P. V. Bharatam, and A. K. Verma, *J. Org. Chem.*, 2012, **77**, 8562-8573.
9. H-L. Cui, and X-H. Chen, *J. Org. Chem.*, 2022, **87**, 15435-15447.
10. Y-W. Xu, J. Wang, G. Wang, and L. Zhen, *J. Org. Chem.*, 2021, **86**, 91-102.
11. F-s. Wu, H-y. Zhao, Y-l. Xu, K. Hu, Y-m. Pan, and X-l. Ma, *J. Org. Chem.*, 2017, **82**, 4289-4296.
12. U. Bora, A. Saikia, and R. C. Boruah, *Org. Lett.*, 2003, **5**, 435-438.

13. G. S. Astakhov, R. R. Shigaev, T. N. Borisova, A. A. Ershova, A. A. Titov, A. V. Varlamov, L. G. Voskressensky, and M. D. Matveeva, *Mol. Divers.*, 2021, **25**, 2441-2446.
14. M. S. Rao, M. Haritha, N. Chandrasekhar, M. V. Basaveswara Rao, and M. Pal, *Arab. J. Chem.*, 2019, **12**, 2697-2703.
15. M. Kaur, M. Yusuf, and S. Kumar, *Sustain. Chem. Pharm.*, 2023, **31**, 100926.
16. D. I. Chai, and M. Lautens, *J. Org. Chem.*, 2009, **74**, 3054-3061.
17. M. Nayak, and I. Kim, *Org. Biomol. Chem.*, 2015, **13**, 9697-9708.
18. A. K. Verma, S. P. Shukla, J. Singh, and V. Rustagi, *J. Org. Chem.*, 2011, **76**, 5670-5684.
19. G. N. Sansom, J. Semken, M. J. Kelso, and C. Richardson, *Tetrahedron Lett.*, 2022, **98**, 153794.
20. A. Thanetchaiyakup, H. Rattananarat, N. Chuanopparat, and P. Ngermmeesri, *Tetrahedron Lett.*, 2018, **59**, 1014-1018.
21. D. R. Joshi, and I. Kim, *J. Org. Chem.*, 2021, **86**, 10235-10248.
22. M. Baumann, and I. R. Baxendale, *J. Org. Chem.*, 2015, **80**, 10806-10816.
23. A. Das, I. Ghosh, and B. König, *ChemComm*, 2016, **52**, 8695-8698.
24. M. Arisawa, Y. Fujii, H. Kato, H. Fukuda, T. Matsumoto, M. Ito, H. Abe, Y. Ito, and S. Shuto, *Angew. Chem. Int. Ed.*, 2013, **52**, 1003-1007.
25. Y. Hu, Y. Jia, Z. Tuo, and W. Zhou, *Org. Lett.*, 2023, **25**, 1845-1849.
26. Z. Luo, X. Han, C. Liu, Q. Liu, R. Li, P. Liu, and X. Xu, *Synthesis*, 2020, **52**, 1067-1075.
27. Y. Zhang, Y. Sun, Y. Wei, and M. Shi, *Adv. Synth. Catal.*, 2019, **361**, 2129-2135.
28. S. Rádl, J. Černý, O. Klecán, J. Stach, L. Plaček, and Z. Mandelová, *Tetrahedron Lett.*, 2008, **49**, 5316-5318.
29. (a) A. Jana, S. K. Manna, S. K. Mondal, A. Mandal, A. Jana, B. K. Senapati, M. Jana, and S. Samanta, *Tetrahedron Lett.*, 2016, **57**, 3722-3726; (b) S. K. Mondal, A. Mandal, S. K. Manna, Sk. A. Ali, M. Hossain, V. Venugopal, A. Jana, and S. Samanta, *Org. Biomol. Chem.*, 2017, **15**, 2411-2421; (c) J. Ray and N. Yasmin, *Synlett*, 2010, **2010**, 924-930; (d) Sk A. Ali, S. K. Mondal, T. Das, S. K. Manna, A. Bera, D. Dafadar, S. Naskar, M. R. Molla, and S. Samanta, *Org. Biomol. Chem.*, 2019, **17**, 4652-4662; (e) A. Bera, P. Patra, A. Azad, Sk A. Ali, S. K. Manna, A. Saha, and S. Samanta, *New J. Chem.*, 2022, **46**, 11685-11694; (f) S. Samanta, Sk A. Ali, A. Bera, S. Giri, and K. Samanta, *New J. Chem.*, 2022, **46**, 7780-7830; (g) A. Bera, Sk A. Ali, A. Saha, and S. Samanta, *Synth. Commun.*, 2021, **51**, 2377-2386; (h) Sk A. Ali, A. Bera, S. K. Manna, S. Santra, M. R. Molla, and S.

- Samanta, *Eur. J. Org. Chem.*, 2020, **2020**, 2754-2760; (i) A. Bera, Sk A. Ali, S. K. Manna, M. Iqbal, S. Misra, A. Saha, and S. Samanta, *New J. Chem.*, 2020, **44**, 4324-4331.
30. (a) M. A. Fouad, F. Ferretti, D. Formenti, F. Milani, and F. Ragaini, *Eur. J. Org. Chem.*, 2021, **2021**, 4876-4894; (b) H. Naeimi and N. Alishahi, *J. Ind. Eng. Chem.*, 2014, **20**, 2543-2547; (c) F. Ferretti, D. R. Ramadan, and F. Ragaini, *ChemCatChem*, 2019, **11**, 4450-4488.
31. (a) T. Rasheed, M. N. I. Khan, S. S. A. Zhadi, and S. Durrani, *J. Nat. Prod.*, 1991, **54**, 582-584; (b) Z. Huang, Y. Meng, Y. Wu, C. Song, and J. Chang, *Tetrahedron*, 2021, **93**, 132280-132289.
32. (a) L.-L. Wei, R. P. Hsung, H. M. Sklenicka, and A. I. Gerasyuto, *Angew. Chem., Int. Ed.*, 2001, **40**, 1516-1518; (b) M. Santarem, C. Vanucci-Bacqué, and G. Lhommet, *J. Org. Chem.* 2008, **73**, 6466-6469; (c) T. Ikeda, T. Yaegashi, T. Matsuzaki, S. Hashimoto, and S. Sawada, *Bioorg. Med. Chem. Lett.*, 2011, **21**, 342-345; (d) A. Hazra, S. Mondal, A. Maity, S. Naskar, P. Saha, R. Paira, B. K. Sahu, P. Paira, S. Ghosh, C. Sinha, A. Samanta, A. Banerjee, N. S. Mondal, *Eur. J. Med. Chem.*, 2011, **46**, 2132-2140; (e) L. Leontie, I. Druta, R. G. Danac, and I. Rusa, *Synth. Met.*, 2005, **155**, 138-145.
33. D. A. Madrigal, C. H. Escalante, G. A. Gutiérrez-Rebolledo, L. J. Cristobal, O. Gómez-García, R. I. Hernández-Benitez, A. L. Esquivel-Campos, S. Pérez-Gutiérrez, G. A. Chamorro-Cevallos, F. Delgado, and J. Tamariz, *Bioorg. Med. Chem.*, 2019, **27**, 115053.
34. (a) G. V. Perez and A. L. Perez, *J. Chem. Educ.*, 2000, **77**, 910-915; (b) M. Nipper, R. S. Carr, J. M. Biedenbach, R. L. Hooten, and K. Miller, *Mar. Pollut. Bull.*, 2005, **50**, 1205-1217; (c) C. Beyer, U. Bohme, C. Pietzsch, and G. Roewer, *J. Organomet. Chem.*, 2002, **654**, 187-201.
35. (a) J. R. Junqueira, W. R. de Araujo, M. O. Salles, and T. R. Paixao, *Talanta*, 2013, **104**, 162-168; (b) S. Shanmugaraju and P. S. Mukherjee, *Chem.-Eur. J.*, 2015, **21**, 6656-6666; (c) Y. Jiang, H. Zhao, N. Zhu, Y. Lin, P. Yu, and L. Mao, *Angew. Chem., Int. Ed.*, 2008, **47**, 8601-8604; (d) Y. Yang, H. Wang, K. Su, Y. Long, Z. Peng, N. Li, and F. Liu, *J. Mater. Chem.*, 2011, **21**, 11895-11900; (e) V. Bhalla, A. Gupta, M. Kumar, D. S. S. Rao, and S. K. Prasad, *ACS Appl. Mater. Interfaces*, 2013, **5**, 672-679.
36. C. Zheng, W. Zhai, J. Hong, X. Zhang, Z. Zhu, and L. Wang, *Tetrahedron Lett.*, 2017, **58**, 3008-3013.
37. S. Shanmugaraju, S. A. Joshi, and P. S. Mukherjee, *J. Mater. Chem.*, 2011, **21**, 9130.

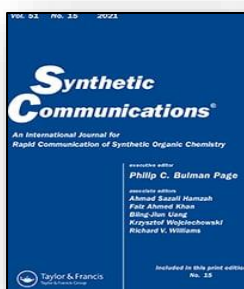
Annexure I

List of Publications

List of Publications as a First Author:



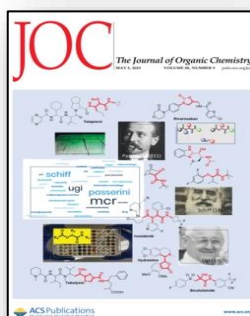
(1) A solvent- and catalyst-free tandem reaction: synthesis, and photophysical and biological applications of isoindoloquinazolinones; **Anirban Bera**, Sk Asraf Ali, Susanta Kumar Manna, Mohammed Iqbal, Sandip Misra, Amit Saha and Shubhankar Samanta; *New J. Chem.*, 2020, **44**, 4324-4331.



(2) Neat synthesis of *c*-fused pyrroles and its application to macrolactamization; **Anirban Bera**, Sk Asraf Ali, Amit Saha and Shubhankar Samanta; *Synth. Commun.*, 2021, **51**, 2377-2386.



(3) Neat synthesis of isothiazole compounds, and studies on their synthetic applications and photophysical properties; **Anirban Bera**, Prasanta Patra, Sk Abul Kalam Azad, Sk Asraf Ali, Susanta Kumar Manna, Amit Saha and Shubhankar Samanta; *New J. Chem.*, 2022, **46**, 11685-11694.



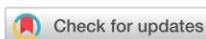
(4) Synthesis of Multifused Pyrrolo[1,2-*a*]quinoline Systems by Tandem Aza-Michael–Aldol Reactions and Their Application to Molecular Sensing Studies; **Anirban Bera**, Sk Abul Kalam Azad, Prasanta Patra, Nayim Sepay, Rathin Jana, Tapas Das, Amit Saha and Shubhankar Samanta; *J. Org. Chem.*, 2023, **88**, 5622-5638.

List of Publications as a Co-Author:

- (1) NaN₃/NH₄Cl-Promoted Aza-Cyclization: A Convenient Route for Bio-Active Diverse Isoindolinone Derivatives; Sk Asraf Ali, Sanjay Bhaumik, Akash Jana, Susanta Kumar Manna, Mohammed Iqbal, Arabinda Mandal, **Anirban Bera**, Avijit Jana and Shubhankar Samanta; *ChemSelect.*, 2018, **3**, 11950-11956.
- (2) One-pot tandem cyclisation to pyrrolo[1,2-*a*][1,4]-benzodiazepines: a modified approach to the Pictet–Spengler reaction; Sk Asraf Ali, Suresh Kumar Mondal, Tapas Das, Susanta Kumar Manna, **Anirban Bera**, Debabrata Dafadar, Sourenjit Naskar, Mijanur Rahaman Molla and Shubhankar Samanta, *Org. Biomol. Chem.*, 2019, **17**, 4652-4662.
- (3) First Example of Copper(I) Catalyzed Decarboalkoxymethylation of Alkyl 2-[1-(Pyridin-2-yl)-1*H*-pyrrol-2-yl]acetates; Sk Asraf Ali, **Anirban Bera**, Susanta Kumar Manna, Subrata Santra, Mijanur Rahaman Molla and Shubhankar Samanta, *Eur. J. Org. Chem.*, 2020, **18**, 2754-2760.
- (4) Amidation and Intramolecular Aza-Michael Reaction: One-Pot Synthetic Strategy of Isoindolinones; Sk Asraf Ali, **Anirban Bera**, Mijanur Rahaman Molla, Shubhankar Samanta; *ChemSelect.*, 2021, **6**, 5603-5609.
- (5) Transition metal-free advanced synthetic approaches for isoindolinones and their fused analogues; Shubhankar Samanta, Sk Asraf Ali, **Anirban Bera**, Soumen Giri and Khokan Samanta; *New J. Chem.*, 2022, **46**, 7780-7830.
- (6) Recent development of solvent-free synthesis of heterocycles; Nilabrata Dey, Arabinda Mandal, Rathin Jana, **Anirban Bera**, Sk Abulkalam Azad, Soumen Giri, Mohammed Iqbal and Shubhankar Samanta; *New J. Chem.*, 2023, Article in press.

Annexure II

Reprint of Published Papers

Cite this: *New J. Chem.*, 2020, 44, 4324Received 21st November 2019,
Accepted 13th February 2020

DOI: 10.1039/c9nj05808g

rsc.li/njc

A solvent- and catalyst-free tandem reaction: synthesis, and photophysical and biological applications of isoindoloquinazolinones†

Anirban Bera,^{ab} Sk Asraf Ali,^{ab} Susanta Kumar Manna,^a Mohammed Ikbal,^c Sandip Misra,^d Amit Saha^{ab} * and Shubhankar Samanta^{ab} *

An easy green synthetic approach for fused isoindoloquinazolinones has been developed under neat reaction (yields up to 91%) conditions. This new one-pot tandem methodology involves condensation of readily available anthranilamide with 3-(2-formylcycloalkenyl)-acrylic ester under solvent- and catalyst-free conditions. This strategy avoids the use of oxidant, and heavy metal catalysts and also is free from work-up and generation of toxic by-products. A dramatic change of photophysical properties of dihydroisoindoloquinazolinones in basic and aqueous media has also been documented in our study. Moreover, our model synthetic compound shows cytotoxic activity towards metastatic HepG2 and PC3 cancer cell lines.

Introduction

In recent years, one-pot tandem chemical transformations under metal- and solvent-free conditions have widely been used for complex organic molecule syntheses with reduced reaction time period and minimum energy requirement. A variety of chemical conversions, like oxidation, reduction, substitution, condensation, *etc.* have been developed using this principle.¹ Hence, heterocyclic ring formation using this green technique has been an active and attractive field in the recent era.²

Among the heterocyclic molecular architectures, *N*-fused heterocycles are ubiquitous in nature and a common structural motif for bioactive molecules and drug candidates. In particular, substituted quinazolinones have a wide range of biological and pharmacological activities, such as diuretic, anti-inflammatory, antidiabetic, anti-hepatitis C, anticonvulsant, antileishmanial, anticancer and so forth.³ Two major types of fused quinazolinones available in nature are carbocycle fused quinazolinones, such as phaitanthrin, tryptanthrin, vasicione *etc.* (Fig. 1)⁴ and heterocycle fused quinazolinones, like luotonin A and wuzhuyurutine A.⁵ Quinazolinone molecular frameworks are also popular as efficient organic fluorescence materials.⁶ Hence, development of a modern

synthetic strategy for fused quinazolinones and their applications in *in vitro* and *in vivo* bio-systems are highly needed.⁷

Different approaches have been reported in the literature to synthesize highly condensed quinazolinone derivatives.⁸ Suzuki coupling followed by Pd/Cu catalysed oxidative C–H amination,⁹ and tandem Sonogashira coupling and hydroamination cyclization¹⁰ are the two independent approaches towards fused quinazolinone, where 2-bromobenzaldehyde and anthranilamide were taken as the starting materials. Another recent report involves ruthenium(II)-catalyzed one-pot oxidative C–H/N–H functionalization of substituted dihydroquinazolinones with alkynes.¹¹ Radical cyclization of *N*-(2-iodobenzyl)-*N*-acylcyanamides is another reported strategy to access fused pyrroloquinazolinone.¹² Li-Jiang Xuan and his group synthesized the same scaffolds *via* ruthenium-catalyzed oxidative coupling of 2-arylquinazolinones followed by an intramolecular aza-Michael reaction.¹³ However, to the best of our knowledge, no attention has been devoted towards the synthesis of fused quinazolinones under metal- and solvent-free conditions. For eco-friendly reaction conditions, the chemical community always searches for green reactions under metal-free and solvent-free conditions. It is always better to perform the reaction in a non-hazardous solvent medium such as water, but it is also far better to run a reaction without any solvent, which reduces the steps in a multistep procedure *e.g.* work up and purification. As a part of our ongoing studies devoted towards the development of new heterocycles,¹⁴ we have disclosed here an operatively simple, catalyst- and solvent-free synthesis of pyrrolo/isoindolo quinazolinone derivatives from 3-(2-formylcycloalkenyl)-acrylic ester derivatives **1** and anthranilamide **2** under heating conditions (120 °C) with moderate to good yields (Scheme 1). In addition, their photophysical properties have been studied, which are limited in the literature.

^a Department of Chemistry, Bidhannagar College, Kolkata 700064, India.

E-mail: chemshubha@gmail.com; Fax: (9133) 2337 4782; Tel: +919775550193

^b Department of Chemistry, Jadavpur University, Kolkata 700032, India.

E-mail: amit.saha@jadavpuruniversity.in

^c Department of Chemistry Berhampore Girls' College, Berhampore 742101, India^d Department of Microbiology, Bidhannagar College, Kolkata 700064, India

† Electronic supplementary information (ESI) available. CCDC 1945935. For ESI and crystallographic data in CIF or other electronic format see DOI: 10.1039/c9nj05808g

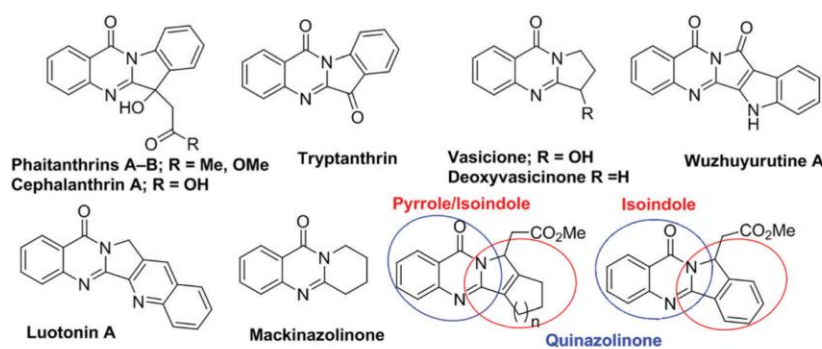
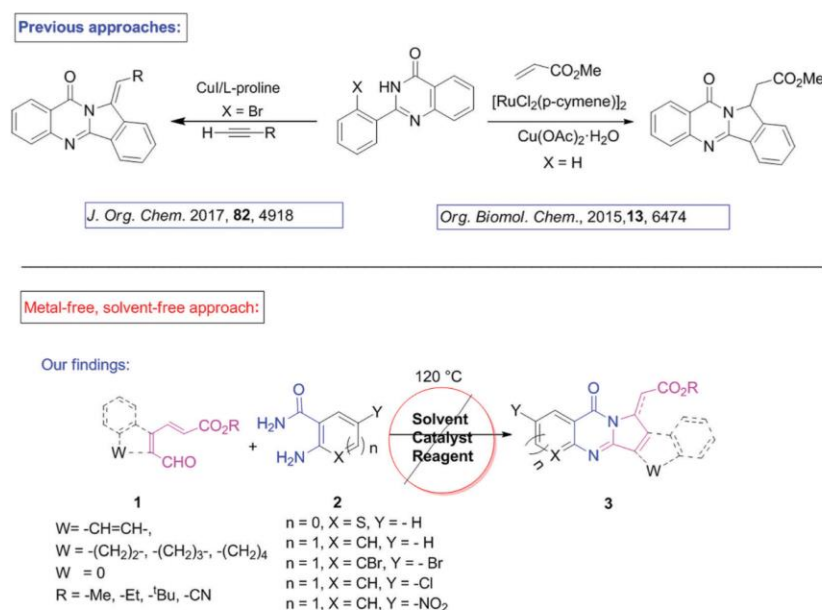


Fig. 1 Naturally occurring bioactive fused quinazolinone scaffolds.



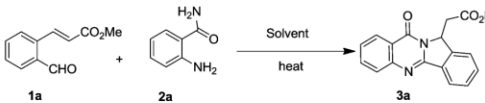
Scheme 1 Previous approaches vs. the present approach towards polycyclic fused quinazolinone.

Results and discussion

At the outset of this investigation to synthesize highly condensed fused quinazolinone derivatives **3**, the reaction was commenced with (*E*)-methyl 3-(2-formylphenyl)acrylate **1a** and anthranilamide **2a** in DMSO at room temperature, but no reaction occurred (Table 1; entry 1). However, the intermolecular condensation reaction followed by intramolecular aza-cyclization in one-pot succeeded by increasing the temperature up to 120 °C in DMSO (entry 4). It was found that cyclization was inefficient below 120 °C (entries 2 and 3). The two component coupling reaction proceeds satisfactorily in toluene and ethanol (entries 5 and 6). However, no fruitful product was isolated in acetonitrile, THF

and dioxane (entries 7–9). In order to increase the efficacy of our developed methodology, studies without any solvent were carried out and the desired fused quinazolinone **3a** was obtained in very good yield (91%), (entry 10).

With the optimal conditions in hand, the scope of the new two-component neat reaction was evaluated with a variety of substrates as shown in Table 2. Methyl/ethyl/tertiary butyl (*E*)-3-(2-formylphenyl)acrylates were smoothly converted to the corresponding isoindoloquinazolines **3a–3c** in moderate to high yields. The cyclised product **3b** was unambiguously confirmed by X-ray crystal structure as shown in Table 2.¹⁵ With this encouraging result in hand, the scope of the neat reaction was examined with different cycloalkenyl derivatives. Formation of

Table 1 Optimization of the reaction conditions towards a highly condensed quinazolinone^a


Entry	Solvent	T (°C)	Time (h)	Yield of 3a (%)
1	DMSO	25	8	0
2	DMSO	60	8	0
3	DMSO	80	8	0
4	DMSO	120	2	82
5	Ethanol	78	2.5	73
6	Toluene	110	3	85
7	Acetonitrile	82	6	0
8	THF	66	6	0
9	Dioxane	101	6	0
10	—	120	2	91 ^b

^a Conditions: (*E*)-methyl 3-(2-formylphenyl)acrylate **1a** (1 mmol), anthranilamide **2a** (1 mmol), and solvent (2 ml). ^b Reaction performed without solvent.

the oxidized and reduced forms of the cyclized product depends on the nature of the ring. Aromatic moieties of ester derivatives were prone to air oxidation and lead to **3a–3f**, whereas the corresponding cycloalkenyl ester derivatives **3i–3p** (7 and 8 membered rings) are reluctant to undergo air oxidation. On the contrary, methyl/ethyl (*E*)-3-(2-formylcyclohexenyl)acrylates **3g** and **3h** smoothly transformed to their corresponding oxidized quinazolinones.

The two component coupling reactions of 2-aminothiophene-3-carboxamide **2d** with (*E*)-3-(2-formylphenyl)acrylates under neat conditions were well tolerated and deliver **3f**, **3m** and **3n**. We further extended the scope of the novel methodology to pentacyclic quinazolinones **3o** but the yield of the desired product was reduced to 55% due to the high steric constancy of the starting material. Notably, chloride and bromide substituted anthranilamides (**2b–2c**) were unable to produce cyclized products **3d** and **3e** at 120 °C under neat conditions and the condensations were performed at 140 °C under solvent-free conditions, which resulted in the formation of the desired products (**3d** and **3e**) in good yields. The neat reaction of **1a** furnished a very low yield of **3r** for an electron withdrawing substituted anthranilamide (–NO₂), but the same reaction gave satisfactory yield of two isomeric quinazolinones **3r** and **3s** in DMSO at 120 °C. Nevertheless, only one isomer **3p** was generated for the cycloheptenyl system under equivalent conditions. Our green protocol was equally adequate compared to another acrylonitrile-substituted aza-Michael acceptor and furnished a good yield of quinazolinone derivative **3q**. Furthermore, we have extended the scope of the reaction to the substrate (*2E,4E*)-methyl 6-oxo-4-phenylhexa-2,4-dienoate, which furnished cyclised product **3t** with a good yield of 72%.

The mechanism of the reaction could be ascertained *via* a four-step sequential process in one-pot (Scheme 2). The step-atom economical mechanistic pathway involves Schiff base (**A**) formation followed by intramolecular aza-cyclisation to produce intermediate **B**, which affords the quinazolinone derivative after air oxidation.¹⁶ The quinazolinone intermediate **C** undergoes intramolecular aza-Michael reaction and provided

fruitful condensed derivatives **3a–3h** and **3q–3r**.¹³ The product formation of **3i–3p** could be elucidated *via* a competitive intramolecular aza-Michael reaction of more nucleophilic amide *N*-atoms.

The formation of **3s** and **3t** could be explained *via* a two-step 1,5-H shift of intermediate **I** (Scheme 3).

Interestingly, it is noticed that the substrate **3j** possesses high fluorescent properties and hence investigation of the photophysical properties has also been discussed. The tolerance of these valuable functional groups would offer an opportunity for further transformations.

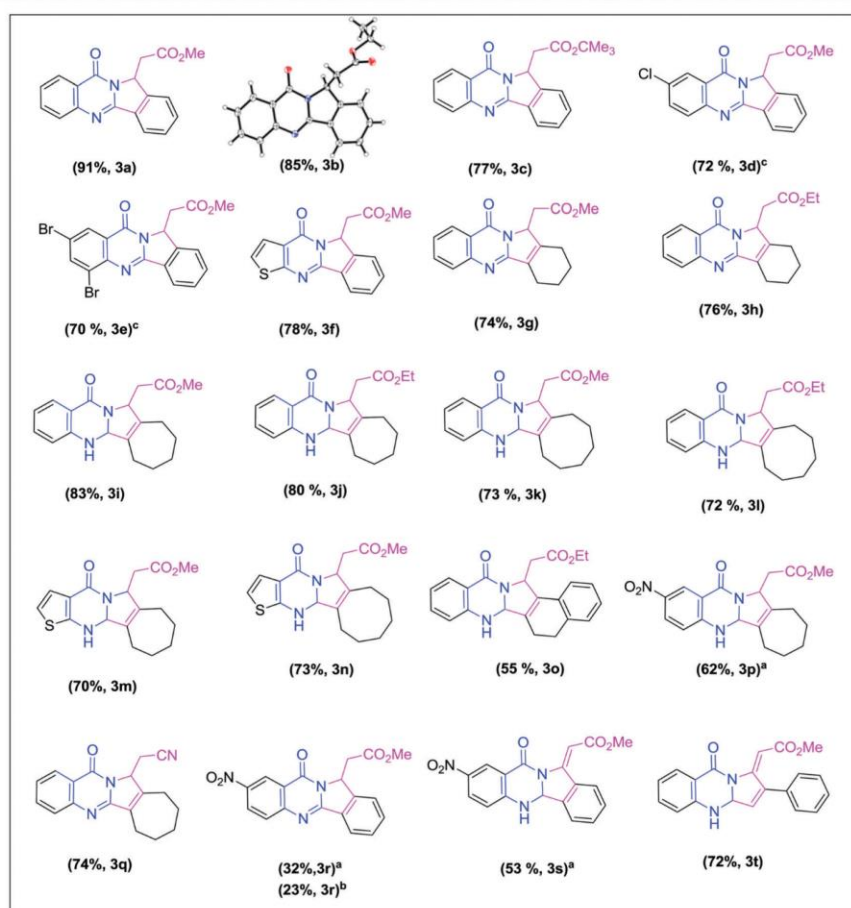
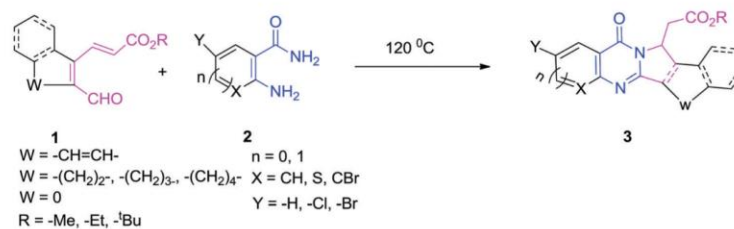
Photophysical studies

After successful synthetic studies, attention was drawn towards photophysical studies of the synthesized dihydroquinazolinone molecule **3j**. The UV/Vis absorption spectra of degassed 2×10^{-6} M solution of **3j** in different solvents have been recorded (ESI;† Fig. S1), and the results are tabulated in Table 3.

Excited state properties of quinazolinone derivative **3j** were investigated by fluorescence emission spectroscopy. Like those of other quinazolinone derivatives, the fluorescence properties of **3j** were also found to be strongly dependent on solvent polarity.¹⁷ The heterocyclic compound **3j** showed negative solvatochromatic emission (Fig. 2) as a function of solvent polarity.¹⁸ As the solvent polarity increases (from non-polar *e.g.* toluene to polar *e.g.* acetonitrile (MeCN)), a hypsochromic shift for **3j** was noticed and the emission maximum was found to shift from 431 to 416 nm. The above solvent effect observed is due to the close lying (¹π–π*) and (¹n–π*) singlet excited states.¹⁹ The higher dissolving ability of a solvent with lower dielectric constant (non-polar solvent) favours the π–π* interaction in the quinazolinone unit and produces greater emission.²⁰ Conversely, in polar protic solvent (*e.g.* MeOH) due to the intermolecular H-bonding effect with the quinazolinone unit, the π–π* transition dominates, which results in shifting of the emission band towards longer wave length.

The fluorescence properties of dihydroquinazolinone derivative **3j** were also investigated in an aqueous binary solvent system to understand the effect of hydrogen bonding interaction. The emission spectra (Fig. 3) of **3j** in MeCN–H₂O binary mixtures were recorded and it was observed that with an increasing amount of water in the MeCN–H₂O mixture, there is a bit of a bathochromic shift with a gradual decrease in fluorescence intensity. The above fact can be attributed to solute–solvent interactions through the formation of hydrogen bonds between the solvent and the heterocyclic part of the quinazolinone moiety (Scheme 4).²¹

As the quinazolinone derivative contains a basic labile proton (NH), it is quite interesting to check the emission spectral behaviour with increase of pH (Fig. 4). The fluorescence maximum of **3j** in neutral MeCN is around 412 nm, which is red shifted to ≈437 nm by the successive addition of different concentrations of NaOH (micromolar). This is because in pure MeCN, protonated **3j** is the predominant species. Thus the fluorescence spectrum in pure MeCN is mainly due to

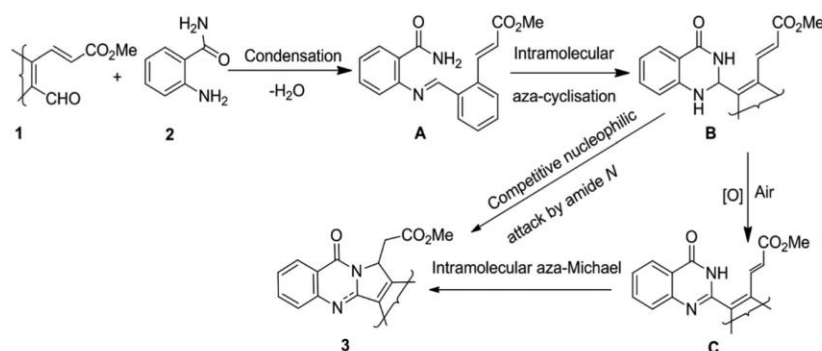
Table 2 Substrate scope for tandem one-pot neat reaction^b

^a Reactions were performed in DMSO. ^b Conditions: (*E*)-methyl 3-(2-formylcycloalkenyl)acrylate **1a** (1 mmol), and anthranilamide **2** (1 mmol). ^c Reactions were performed at 140 °C.

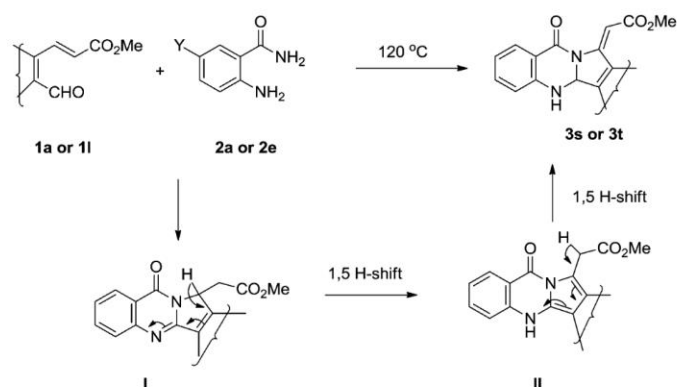
protonated **3j** in the excited state. At higher pH, a bathochromic shift was obtained due to the deprotonation of **3j** followed by extended conjugation and the decrease of fluorescence intensity may be explained by the lower solubility of the molecule in an alkaline solution (Scheme 5).

Biological study

After successful investigation of the photophysical properties, our research turned towards biological application of our model compound **3j** using two different metastatic cancer cell



Scheme 2 Plausible mechanism for the synthesis of fused quinazolinones.

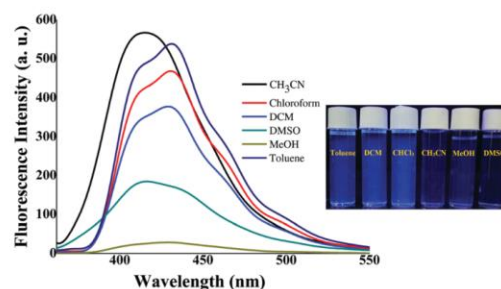


Scheme 3 Synthetic route of isomerised quinazolinone.

Table 3 UV-Vis absorption and fluorescence data of **3j** in different solvents

Solvent	ϵ^a (25 °C)	δH hydrogen bonding ^b	λ_{max}^c (nm)	ϵ_{max}^d	λ_{emi}^e (nm)	Stokes' shift ^f (nm)
Toluene	2.38	2.0	330	132 000	431	101
Chloroform	4.81	7.1	329	159 000	431	101
DCM	9.10	7.1	331	133 000	429	98
MeOH	33.00	19.4	333	120 500	430	97
CAN	37.50	6.1	331	119 000	416	82
DMSO	46.70	7.8	329	87 500	416	87

^a Dielectric constant at 25 °C. ^b Hydrogen bonding capability. ^c Maximum absorption wavelength. ^d Molar absorption coefficient at maximum absorption wavelength. ^e Maximum emission wavelength. ^f Difference between maximum absorption wavelength and maximum emission.

Fig. 2 Fluorescence spectra of quinazolinone derivatives **3j** in different solvents.

lines; hepatocellular carcinoma (HepG2) and prostate cancer (PC3). HepG2 is a human liver cancer cell line, obtained from the liver tissue of a 15-year-old American adolescent boy of European ancestry.²² The human prostate cancer cell line (PC3) is derived from bone metastasis of a grade IV prostatic adenocarcinoma from a 62-year-old male Caucasian, which is used

widely in research and drug development.²³ To examine the anticancer activity of the compound **3j**, HepG2 and PC3 were seeded in 48-well plates at 1×10^4 cells per well in DMEM and RPMI (10% FBS) medium, respectively, and exposed to **3j** at different concentrations for 24 h (Fig. 5). After incubation, the cells were washed twice with PBS and incubated with MTT

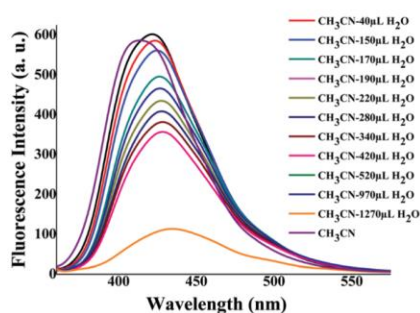


Fig. 3 Fluorescence quenching of **3j** vs. water % in MeCN–H₂O mixtures.

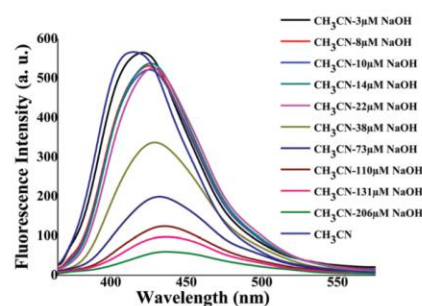
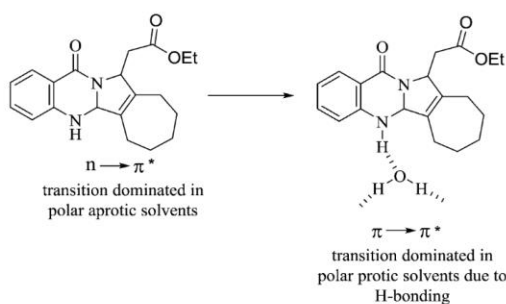


Fig. 4 Fluorescence spectral change of **3j** by stepwise addition of NaOH in MeCN (λ_{max} shifted from 408 nm in pure MeCN to 438 nm in MeCN–206 μM NaOH).



Scheme 4 Solvent–solute H-bonding interactions.

solution ($450 \mu\text{g ml}^{-1}$) for 3 h at 37°C . The resulting formazan crystals were dissolved in an MTT solubilising buffer and the absorbances were measured at 570 nm by using a microplate reader (Biotek, USA). Each point was assessed in triplicate. Untreated cells were considered as 100% viable. We found that this compound has significant anticancer activity against both of the cell lines. The IC-50 values of this compound were found to be $134 \mu\text{g ml}^{-1}$ for HepG2 cells and $112 \mu\text{g ml}^{-1}$ for PC3 cells.

Cells were incubated with increasing concentrations of the compound for 24 h and their percentage of survivability was assessed by the MTT assay. Data represented are means \pm SD of three identical experiments made in three replicates.

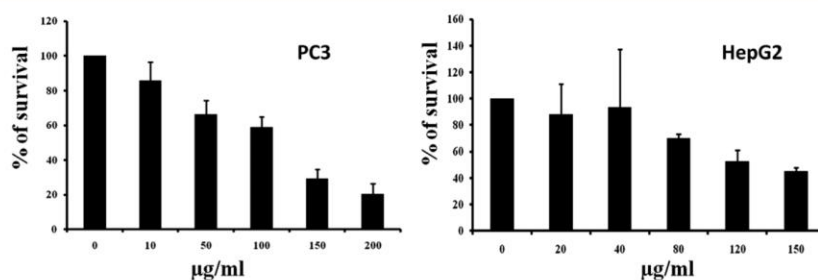
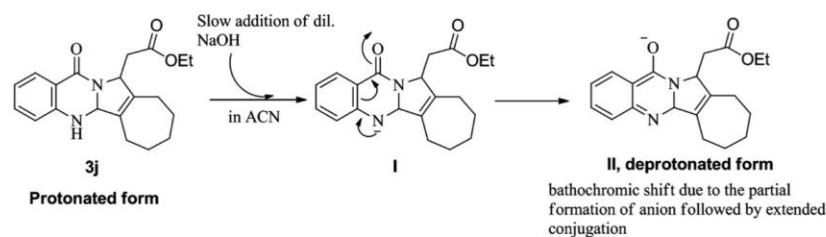


Fig. 5 Cytotoxic effects of the compound **3j** on PC3 and HepG2 cells.



Scheme 5 Solute–alkali interaction in the excited state.

Conclusion

To conclude, an environmentally benign catalyst and solvent-free tandem approach for the synthesis of highly functionalized fused quinazolinones with good to excellent yields has been demonstrated. The designed substrates, 3-(2-formylcycloalkenyl)-acrylic ester derivatives, are effective coupling partners for anthranilamide compounds to synthesize highly fused quinazolinones under neat conditions with wide substrate scope, step-atom economy and minimal work-up procedure. The synthesized compounds show good fluorescence properties and hence photophysical properties in different solvents and solvent-solute interactions in the excited state of the synthesized fluorophore are also documented. Since our study compound chemosensitized HepG2 and PC3 cell lines, we will use this compound in an *in vivo* mouse model for future research.

Conflicts of interest

There are no conflicts to declare.

Acknowledgements

We thank the Department of Science, Technology and Biotechnology under the Government of West Bengal (212 (sanc.)/ST/P/S&T/15G-44/2017) for financial support.

References

- (a) K. Tanaka and F. Toda, *Chem. Rev.*, 2000, **100**, 1025–1074; (b) F. Toda, M. Yagi and K. Kiyoshige, *J. Chem. Soc., Chem. Commun.*, 1988, 958; (c) F. Toda, K. Kiyoshige and M. Yagi, *Angew. Chem., Int. Ed. Engl.*, 1989, **28**, 320; (d) F. Toda, K. Tanaka and K. Hamai, *J. Chem. Soc., Perkin Trans. 1*, 1990, 3207; (e) C. M. Etter, M. G. Frankenbach and J. Bernstein, *Tetrahedron Lett.*, 1989, **30**, 3617; (f) Y. Hayashi, *Chem. Sci.*, 2016, **7**, 866.
- (a) S. A. Ali, S. K. Mondal, T. Das, S. K. Manna, A. Bera, D. Dafadar, S. Nasakar, M. R. Molla and S. Samanta, *Org. Biomol. Chem.*, 2019, **17**, 4652; (b) G. C. Senadi, V. S. Kudale and J.-J. Wang, *Green Chem.*, 2019, **21**, 979; (c) L.-R. Wen, Z.-R. Li, M. Li and H. Cao, *Green Chem.*, 2012, **14**, 707; (d) H. Wei, L. Zhou, Y. Zhou and Q. Zeng, *Toxicol. Environ. Chem.*, 2015, **97**, 2.
- (a) H. Wang and A. Ganesan, *J. Org. Chem.*, 2000, **65**, 1022; (b) P. Molina, A. Tàrraga, A. Gonzalez-Tejero, I. Rioja, A. Ubeda, M. C. Terencio and M. J. Alcaraz, *J. Nat. Prod.*, 2001, **64**, 1297; (c) S. E. deLaszlo, C. S. Quagliato, W. J. Greenlee, A. A. Patchett, R. S. L. Chang, V. J. Lotti, T. B. Chen, S. A. Scheck, K. A. Faust, S. S. Kivlighn, T. S. Schorn, G. J. Zingaro and P. K. S. Siegl, *J. Med. Chem.*, 1993, **36**, 3207; (d) M. Sharma, K. Chauhan, R. Shivahare, P. Vishwakarma, M. K. Suthar, A. Sharma, S. Gupta, J. K. Saxena, J. Lal and P. Chandra, *J. Med. Chem.*, 2013, **56**, 4374.
- (a) U. A. Kshirsagar, *Org. Biomol. Chem.*, 2015, **13**, 9336; (b) A. M. Tucker and P. Grundt, *ARKIVOC*, 2012, 546; (c) X. Liu, P. Qian, Y. Wang and Y. Pan, *Org. Chem. Front.*, 2017, **4**, 2370.
- (a) J. Teng and X. W. Yang, *Heterocycles*, 2006, **68**, 1691; (b) K. Jayapaul, K. P. B. Kavi and R. K. Janardhan, *In Vitro Cell. Dev. Biol.: Plant*, 2005, **41**, 682–685.
- (a) I. Kahn, A. Ibrar, N. Abbas and A. Saeed, *Eur. J. Med. Chem.*, 2014, **76**, 193; (b) I. Kahn, A. Ibrar, N. Abbas and A. Saeed, *Eur. J. Med. Chem.*, 2015, **90**, 124.
- (a) C. Kogawa, A. Fujiwara, R. Sekiguchi, T. Shoji, J. Kawakami, M. Okazaki and S. Ito, *Tetrahedron*, 2018, **74**, 7018; (b) L. Liu, Y. Zhang, J. Zhou, J. Yang, C. Zhong, Y. Zhang, Y. Luo, Y. Fu, J. Huang, Z. Song and Y. Peng, *Dyes Pigm.*, 2019, **165**, 58.
- (a) L. He, H. Li, J. Chen and X.-F. Wu, *RSC Adv.*, 2014, **4**, 12065; (b) R. K. Saunthwal, M. Patel, R. K. Tiwari, K. Parang and A. K. Verma, *Green Chem.*, 2015, **17**, 1434; (c) H. Wang, S. Jiao, K. Chen, X. Zhang, L. Zhao, D. Liu, Y. Zhou and H. Liu, *Beilstein J. Org. Chem.*, 2015, **11**, 416; (d) R. Cheng, L. Tang, T. Guo, D. Zhang-Negrerie, Y. Du and K. Zhao, *RSC Adv.*, 2014, **4**, 26434; (e) N. Y. Kim and C.-H. Cheon, *Tetrahedron Lett.*, 2014, **55**, 2340; (f) H. Lu, Q. Yang, Y. Zhou, Y. Guo, Z. Deng, Q. Ding and Y. Peng, *Org. Biomol. Chem.*, 2014, **12**, 758; (g) H. Baguia, C. Deldaele, E. Romero, B. Michelet and G. Evano, *Synthesis*, 2018, 3022; (h) L. Xie, C. Lu, D. Jing, X. Ou and K. Zheng, *Eur. J. Org. Chem.*, 2019, 3649; (i) G. Bairy, S. Das, H. M. Begam and R. Jana, *Org. Lett.*, 2018, **20**, 7107; (j) S. Chatterjee, R. Srinath, S. Bera, K. Khamaru, A. Rahman and B. Banerji, *Org. Lett.*, 2019, **21**, 9028.
- B. Banerji, S. Bera, S. Chatterjee, S. K. Killi and S. Adhikary, *Chem. – Eur. J.*, 2016, **22**, 3506.
- J.-Q. Liu, Y.-G. Ma, M.-M. Zhang and X.-S. Wang, *J. Org. Chem.*, 2017, **82**, 4918.
- R. Lingayya, M. Vellakkaran, K. Nagaiah and J. B. Nanubolu, *Asian J. Org. Chem.*, 2015, **4**, 462.
- A. Servais, M. Azzouz, D. Lopes, C. Courillon and M. Malacria, *Angew. Chem., Int. Ed.*, 2007, **46**, 576.
- Y. Zheng, W.-B. Song, S.-W. Zhang and L.-J. Xuan, *Org. Biomol. Chem.*, 2015, **13**, 6474.
- (a) S. K. Manna, A. Mandal, S. K. Mondal, A. K. Adak, A. Jana, S. Das, S. Chattopadhyay, S. Roy, S. K. Ghorai, S. Samanta, M. Hossain and M. Baidya, *Org. Biomol. Chem.*, 2015, **13**, 8037; (b) S. K. Manna, S. K. Mondal, A. Ahmed, A. Mandal, A. Jana, M. Iqbal, S. Samanta and J. K. Ray, *RSC Adv.*, 2014, **4**, 2474; (c) S. K. Mondal, S. K. Manna, A. Mandal, S. Samanta and J. K. Ray, *Tetrahedron Lett.*, 2014, **55**, 6411; (d) A. Jana, S. K. Manna, S. K. Mondal, A. Mandal, A. Jana, B. K. Senapati, M. Jana and S. Samanta, *Tetrahedron Lett.*, 2016, **57**, 3722; (e) S. K. Mondal, A. Mandal, S. K. Manna, Sk. A. Ali, M. Hossain, V. Venugopal, A. Jana and S. Samanta, *Org. Biomol. Chem.*, 2017, **15**, 2411; (f) S. K. Mondal, S. A. Ali, S. K. Manna, A. Mandal, B. K. Senapati, M. Hossain and S. Samanta, *ChemistrySelect*, 2017, **2**, 9312.
- CCDC **3b** is 1945935†.
- N. Y. Kim and C.-H. Cheon, *Tetrahedron Lett.*, 2014, **55**, 2340.
- A. Yuan, C. Zheng, Z. Zhang, L. Yang, C. Liu and H. Wang, *J. Fluoresc.*, 2014, **24**, 557.
- A. V. Kulinich, E. K. Mikitenko and A. Ishchenko, *Phys. Chem. Chem. Phys.*, 2016, **18**, 3444.

Paper

NJC

- 19 C. Reichardt, *Chem. Rev.*, 1994, **94**, 8.
- 20 A. S. Klymchenko, *Acc. Chem. Res.*, 2017, **50**, 366.
- 21 P. R. Dongare, A. H. Gore, U. R. Kondekar, G. B. Kolekar and B. D. Ajalkar, *Inorg. Nano-Met. Chem.*, 2018, **48**, 49.
- 22 (a) A. Jemal, R. Siegel, E. Ward, Y. Hao, J. Xu and M. J. Thun, *Ca-Cancer J. Clin.*, 2009, **59**, 225; (b) R. Singh and M. J. Czaja, *Cancer Biol. Ther.*, 2005, **4**, 1419; (c) J. Song, Z. Qu, X. Guo, Q. Zhao, X. Zhao, L. Gao, K. Sun, F. Shen, M. Wu and L. Wei, *Autophagy*, 2009, **5**, 1131–1144.
- 23 (a) S. Singh, D. Chitkara, R. Mehrazin, S. Behrman, R. Wake and R. Mahato, *PLoS One*, 2012, **7**, e40021; (b) J. T. Lee, L. S. Steelman and J. A. McCubrey, *Cancer Res.*, 2004, **64**, 8397.



Synthetic Communications

An International Journal for Rapid Communication of Synthetic Organic Chemistry

ISSN: (Print) (Online) Journal homepage: <https://www.tandfonline.com/loi/lscy20>



Neat synthesis of *c*-fused pyrroles and its application to macrolactamization

Anirban Bera, Sk Asraf Ali, Amit Saha & Shubhankar Samanta

To cite this article: Anirban Bera, Sk Asraf Ali, Amit Saha & Shubhankar Samanta (2021) Neat synthesis of *c*-fused pyrroles and its application to macrolactamization, *Synthetic Communications*, 51:15, 2377-2386, DOI: [10.1080/00397911.2021.1939054](https://doi.org/10.1080/00397911.2021.1939054)

To link to this article: <https://doi.org/10.1080/00397911.2021.1939054>

 View supplementary material [↗](#)

 Published online: 24 Jun 2021.

 Submit your article to this journal [↗](#)

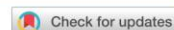
 Article views: 105

 View related articles [↗](#)

 View Crossmark data [↗](#)

 Citing articles: 3 View citing articles [↗](#)

Full Terms & Conditions of access and use can be found at
<https://www.tandfonline.com/action/journalInformation?journalCode=lscy20>



Neat synthesis of *c*-fused pyrroles and its application to macrolactamization

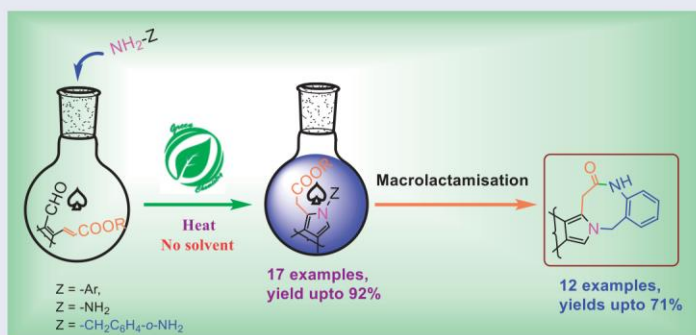
Anirban Bera^{a,b}, Sk Asraf Ali^a, Amit Saha^b, and Shubhankar Samanta^a

^aDepartment of Chemistry, Bidhannagar College, Kolkata, India; ^bDepartment of Chemistry, Jadavpur University, Kolkata, India

ABSTRACT

The current study describes an efficient environmental benign synthetic route of *N*-aryl substituted *c*-fused pyrrole derivatives *via* neat approach. It also provides base-mediated intramolecular macrolactamization using amine ester amidation reaction and leads to fused diazocine-6(5H)-one with effective yields.

GRAPHICAL ABSTRACT



ARTICLE HISTORY

Received 27 February 2021

KEYWORDS

Aza-Michael addition; *c*-fused pyrrole; diazocine-6(5H)-one; macrolactamization; neat reaction

Introduction

In any synthetic transformation, solvent plays a very significant role as the reaction medium and in washing, extraction, purification of the ultimate product. However, most of the pollutants generated from the chemical industry come from solvents.^[1] To avoid traditional solvent-mediated chemical transformation, solvent-free reaction is a well-known green technique for reduction of pollution, and hence scientists have devoted their research in the synthesis of molecules in the absence of solvent. Synthesis of pyrrole using solvent-free conditions does not belong to the exception.^[2] The classical method for the synthesis of pyrrole and derivatives mainly involves Knorr, Hantzsch, and Paal-Knorr condensations.^[3] However, neat approach for the synthesis of pyrroles is limited in the literature.^[2] These molecules possess diverse biological

CONTACT Shubhankar Samanta  chemshubha@gmail.com  Bidhannagar College, Sector-1, Salt Lake, Kolkata-700064, India; Amit Saha  amit.saha@jadavpuruniversity.in  Jadavpur University, Raja Subodh Chandra Mallick Rd, Jadavpur, Kolkata-700032, India.

 Supplemental data for this article can be accessed on the publisher's website.

© 2021 Taylor & Francis Group, LLC

2378 A. BERA ET AL.

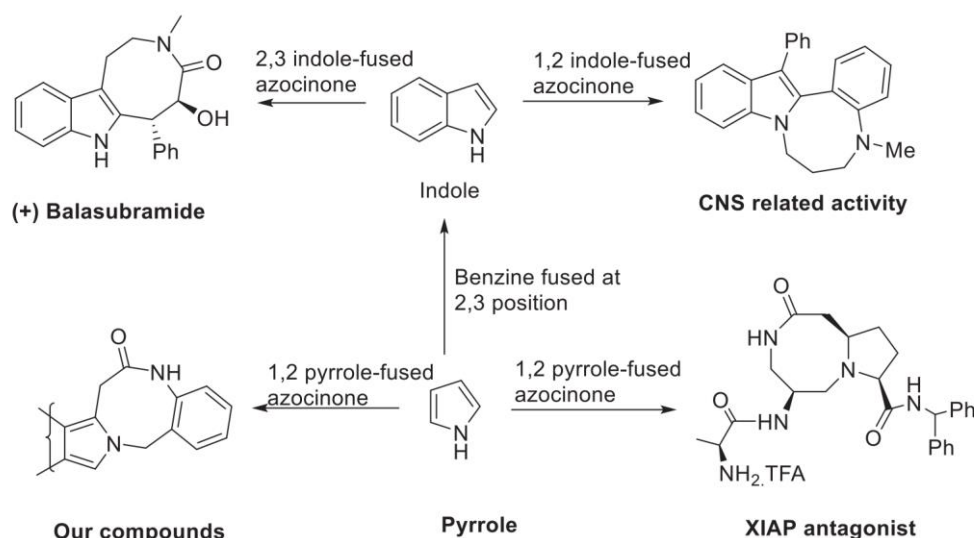
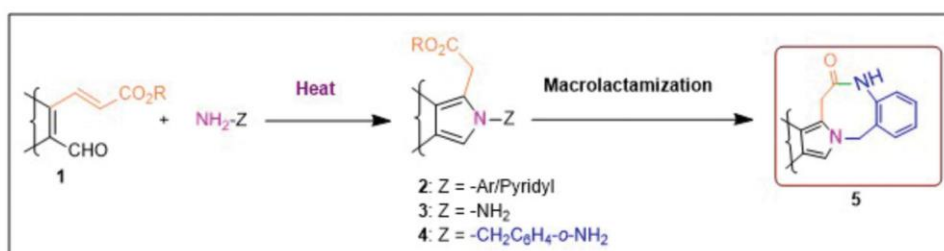


Figure 1. Different pyrrole and indole fused bio-active azocinones.



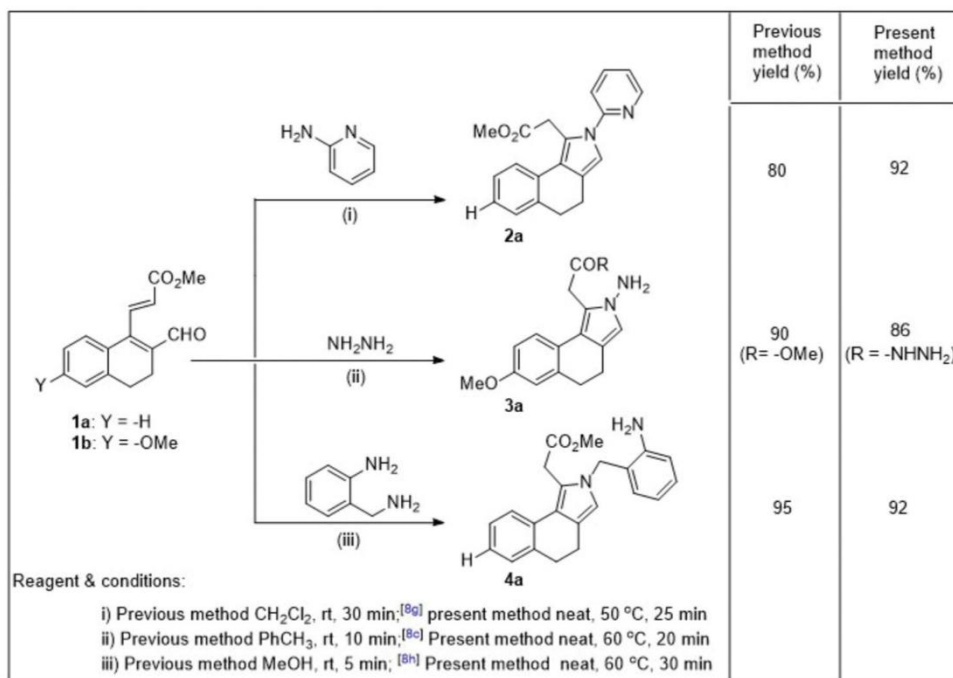
Scheme 1. Synthesis and macrolactamization of c-fused pyrroles.

activities such as antioxidant, antibacterial, anti-inflammatory, antihyperlipidemic, anti-tumor, antifungal, anti-HIV, antiviral, and analgesic effects.^[4]

Pyrrole-fused azocines (eight-membered heterocyclic compounds) are in continuous demand because of their well-known biological properties and pharmaceutical applications (Figure 1). The indole fused azocine alkaloids grandilodines A–C is known to exhibit reverse multidrug resistance in vincristine-resistant KB cells and another natural product (+)Balasubramide possesses neuroprotective, antioxidative, and anti-neuroinflammatory properties.^[5a] Further, proper functionalized 8,5-fused bicyclic lactam used as antagonists of X-linked inhibitor of apoptosis protein (XIAP) which deregulation can result in “cancer, neurodegenerative disorders.”^[5b] Thus, the development of efficient, simple, and economic synthetic protocol for 8,5-fused polycyclic lactam derivatives is highly desirable.

Results and discussion

The cyclization strategies for the synthesis of 5,5-, 5,6-, 5,7-fused bicyclic ring systems are very common^[6] in the literature, but the formation of 5,8-fused ring heterocycles is very rare due to enthalpic factors, entropic factors, and transannular interactions.^[7] In

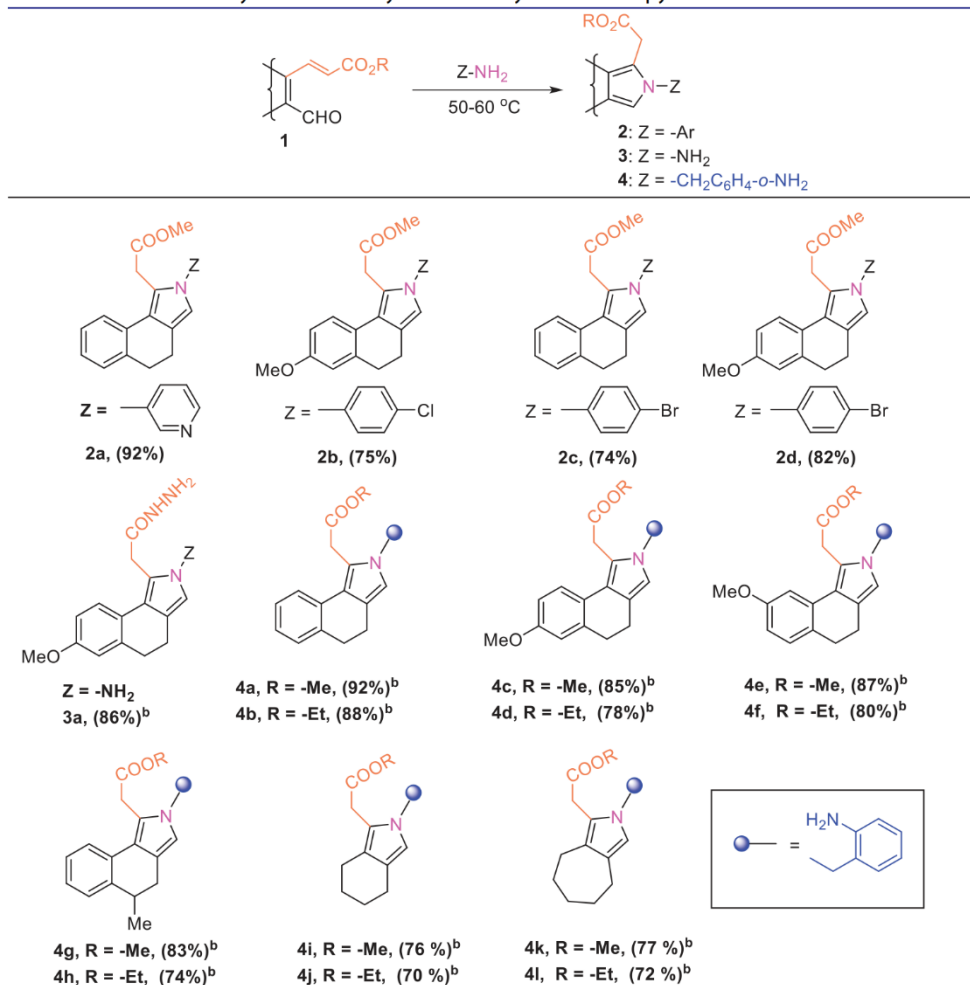


Scheme 2. A comparative study between solvent added and solvent-free reaction.

this context, we have developed neat synthetic approach for *N*-aryl/benzyl/amino fused pyrrole derivatives (2–4) from 3-(3-formyl cycloalkenyl)-acrylic ester derivatives **1** and then macrolactamization was performed using the properly functionalized pyrrole system (Scheme 1).

In our recent reported method, we have synthesized a series of pyrrole derivatives from substrate **1** in solution phase. Previously, couplings of **1** with the aromatic amine, hydrazine, and 2-amino benzylamine were performed using the organic solvents, like dichloromethane, toluene, and methanol respectively.^[8] As most of the organic solvents are toxic to the environment and health, we were prompted to synthesize various isoindole derivatives under the neat reaction conditions. In our first attempt, the substrate **1a** was allowed to react with amine coupling partners, 2-amino pyridine and 2-amino benzylamine to produce the similar isoindole derivatives (**2a** and **4a**, Scheme 2) in comparable yields within 30 min at 50–60 °C and **1b** was subjected to react with hydrazine which generates amide substituted isoindole derivative in 86% yield (**3a**, Scheme 2). Although the solvent added reaction requires less time compared to the solvent-free reaction, solvent-free conditions are more environmentally benign and less hazardous. It reduces the use of hazardous chlorinated solvents and avoids the work-up process which is an essential step for any solvent added reaction.

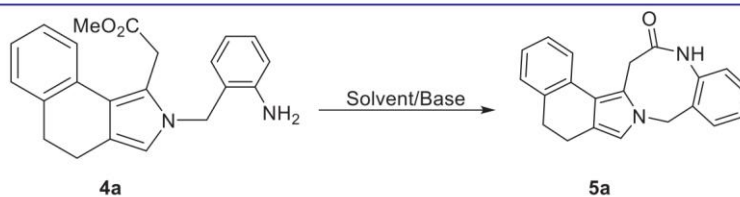
Our environmentally benign neat protocol was applied in the reactions of different substituted acrylic ester derivatives with a variety of amines. Thus, we have developed a general method for efficient synthesis of a series of polysubstituted fused pyrroles as shown in Table 1. From Table 1, we can see that anilines bearing electron-withdrawing and electron-donating substituents afforded tricyclic *c*-fused pyrroles in excellent yields

Table 1. Solvent-free synthesis of bicyclic and tricyclic *c*-fused pyrroles^{a,b}.

^aReagents and conditions: substrate **1** (1 mmol), substituted amine (1 mmol), 50 °C, 20–30 min; ^btemperature needed 60 °C.

(74–92%) within 20–30 min at 50 °C under solvent-free open flask conditions **2a–2d**. It is worth pointing out that in case of the reaction with hydrazine corresponding *N*-substituted amine containing an amide functionality (**3a**) was obtained in 86% yield under the neat condition at 60 °C. This compound has two fruitful functional groups for intramolecular nucleophilic addition which may further produce pyrrole-fused heterocycles in due time. To explore the neat reaction condition, we have examined our reaction with 2-amino benzylamine as coupling partner with substrate **1**. It was observed that different acrylic ester furnished *c*-fused pyrrole derivative **4a–4l** with excellent yields (70–92%) within 30 min at 60 °C.

We were pleased to find that our substrate **4** has two important functionalities (-NH₂ and -CO₂R) in proper location for intramolecular reaction. The efficiency of the intramolecular amide formation reaction was tested using different bases and

Table 2. Optimization studies for the intramolecular lactamization^a.

Entry	Solvent	Base	Temperature (°C)	Yield (%)
1	DMSO	K ₂ CO ₃	0	NR
2	DMSO	KO ^t Bu	RT	20
3	DMSO	KO ^t Bu	0	80
4	DMSO	NaH	0	73
5	DMSO	Et ₃ N	0	NR
6	CH ₃ CN	KO ^t Bu	0	71
7	Toluene	KO ^t Bu	0	NR
8	Dioxane	KO ^t Bu	0	NR
9	CHCl ₃	KO ^t Bu	0	NR
10	CH ₂ Cl ₂	KO ^t Bu	0	NR

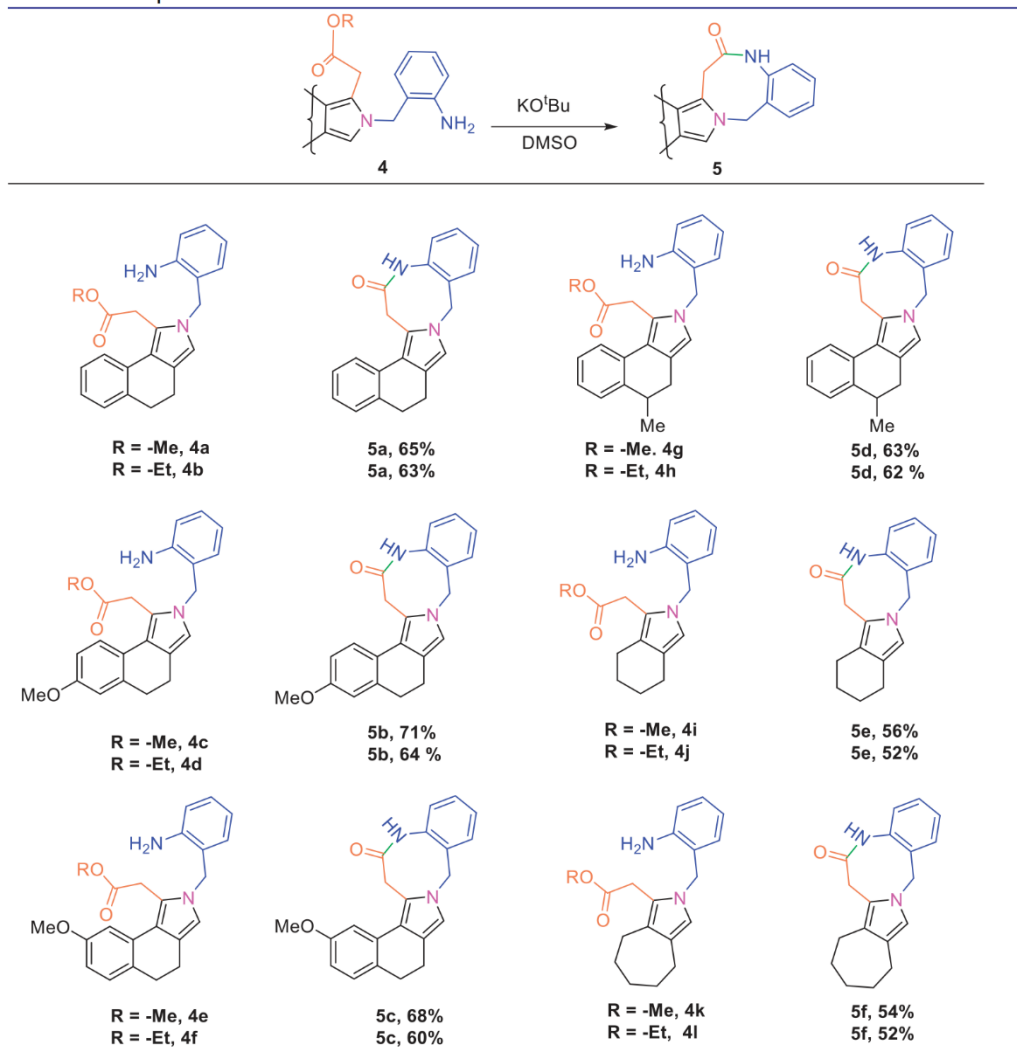
^aReagents and conditions: substrate 4a (1 mmol), base (2 mmol), solvent 4 mL, 15 min; NR: no reaction; RT: room temperature.

solvents. From this screening experiment (Table 2), we found that the weak base K₂CO₃ (entry 1) is not suitable for lactamization. Aza-cyclization was started in the presence of strong potassium tertiary butoxide as base in DMSO at room temperature (entry 2). Upon lowering the temperature to 0 °C, the yield of intramolecular amide formation increased significantly (80% yield) within 15 min of time period in the presence of the same base (entry 3). In the presence of sodium hydride, the yield of the reaction decreases compared to the KO^tBu (entry 4). Exothermic nature of NaH/DMSO mixture^[9] reduces the yield of intramolecular amidation reaction. No conversion was observed using triethylamine as base (entry 5). In acetonitrile reaction medium the desired product was obtained with much lower yield (entry 6). Toluene, dioxane, and chlorinated solvents did not furnish any cyclization product (entry 7–10).

A variety of compounds containing pentacyclic and tetracyclic fused 8-membered lactam rings **5a–5f** were prepared by using the optimized reaction conditions in acceptable yields (Table 3). Intramolecular lactamization proceeded smoothly using methyl and ethyl substituted ester derivatives. But the yields of pentacyclic-fused pyrrolo 8-membered lactam derivatives **5a–5d** are higher compared to the tetracyclic lactam **5e, 5f**. It was noteworthy that ethyl esters of **4** furnished poor yields of **5** compare to methyl ester due to the lower leaving aptitude of –OEt group. The lower yield of macrocyclic rings (**5e** and **5f**) can be explained by the conformational strain of tetracyclic system. All the synthesized compounds were well characterized by spectral data (NMR and HRMS).

Conclusion

In conclusion, we have developed environmental benign synthetic route of different substituted fused pyrrole derivatives using the neat approach. The suitably

Table 3. Base-promoted intramolecular lactamization reaction^a.

^aReagents and conditions: substrate 4a–4l (1 mmol), KO^tBu(2 mmol), DMSO (4 mL), 0 °C, 15–20 min.

functionalized pyrrole derivatives undergo intramolecular macrolactamization to furnish a broad array of rare 8,5-fused oxacinones with good yields.

Experimental section

General information for synthetic compounds

¹H and ¹³C NMR spectra of all the synthesized compounds were recorded in 400 MHz and 500 MHz spectrometer in CDCl₃/DMSO-*d*₆ CDCl₃ solvent using TMS as the internal standard. HRMS was measured by using a TOF analyzer. Precoated silica gel 60 F254 TLC sheets (Merck) was used for monitoring the reaction. For purification in column chromatography, 60–120 or 100–200 mesh silica gels (SRL) were used. n-Hexane

(Merck) or petroleum ether (boiling range 60–80 °C) and ethyl acetate (b.p. 77.1 °C) eluent were used in column chromatographic separation. All solvents were dried, distilled, and stored over molecular sieves (4 Å).

General procedure for preparation of 2, 3, and 4

Substrate **1** (1 mmol) and aryl amine/hydrazine (1 mmol) were taken in a one-neck round-bottom flask. The reaction mixture was heated for 20–30 min at 50–60 °C under neat conditions. The reaction was monitored by TLC. After completion of the reaction, the crude residue was purified in column chromatography by using silica gel (60–120 mesh) and petroleum ether–ethyl acetate (5:1) eluent to obtain the desired product **2**.

Representative NMR data of 2a: Methyl 2-(2-(pyridin-2-yl)-4,5-dihydro-2H-benzo[e]isoindol-1-yl)acetate

Yellow solid (42.6 mg, 92%), mp: 92–95 °C. ¹H NMR (400 MHz, CDCl₃): δ 8.41 (ddd, *J* = 2.8, 2.0, 0.8 Hz, 1H), 7.77–7.73 (m, 1H), 7.47 (d, *J* = 8.4 Hz, 1H), 7.33–3.31 (m, 1H), 7.25–7.22 (m, 2H), 7.15–7.10 (m, 2H), 6.90 (s, 1H), 4.16 (s, 2H), 3.70 (s, 3H), 2.88–2.85 (m, 2H), 2.73–2.69 (m, 2H). ¹³C NMR (101 MHz, CDCl₃): δ 171.9, 152.7, 148.3, 138.6, 137.4, 132.1, 128.6, 126.8, 125.6, 123.8, 123.0, 122.7, 120.9, 120.6, 115.9, 115.3, 52.1, 33.9, 31.4, 21.1. HRMS calcd. for C₂₀H₁₉N₂O₂: (M + H)⁺: 319.1448, found: 319.1450.

Representative NMR data of 3a: 2-(2-Amino-7-methoxy-4,5-dihydro-2H-benzo[e]isoindol-1-yl)acetohydrazide

Yellow solid (24 mg, 86%), mp. 154 °C. ¹H NMR (400 MHz, DMSO-*d*₆): δ 9.14 (s, 1H), 7.35 (d, *J* = 8.4 Hz, 1H), 6.78 (s, 1H), 6.72 (d, *J* = 8.2 Hz, 1H), 6.49 (s, 1H), 5.72 (s, 2H), 4.26 (m, 2H), 3.72 (s, 3H), 3.67 (s, 2H), 2.73–2.67 (m, 2H).

¹H NMR (400 MHz, D₂O exchange): δ 7.32 (d, *J* = 8.4 Hz, 1H), 6.77 (s, 1H), 6.72–6.70 (m, 1H), 6.49 (s, 1H), 3.75–3.66 (m, 5H), 2.65 (m, 2H), 2.45 (m, 2H).

¹³C NMR (126 MHz, CDCl₃): δ 171.5, 161.1, 149.0, 142.9, 139.8, 134.6, 126.2, 124.1, 118.6, 113.9, 112.9, 55.4, 52.8, 28.4, 25.5. HRMS calcd. for C₁₅H₁₉N₄O₂: (M + H)⁺: 287.1510, found: 287.1511.

Representative NMR data of 4a: Methyl 2-(2-(2-aminobenzyl)-4,5-dihydro-2H-benzo[e]isoindol-1-yl)acetate

Yellow solid (44 mg, 92%), mp. 117 °C. ¹H NMR (400 MHz, CDCl₃): δ 7.48 (d, *J* = 7.6 Hz, 1H), 7.23 (d, *J* = 7.6 Hz, 2H), 7.17–7.08 (m, 2H), 6.90 (d, *J* = 7.2 Hz, 1H), 6.75 (t, *J* = 7.6 Hz, 1H), 6.69 (d, *J* = 7.9 Hz, 1H), 6.34 (s, 1H), 4.99 (s, 2H), 3.93 (s, 2H), 3.73 (s, 3H), 2.83 (t, *J* = 6.9 Hz, 2H), 2.62 (t, *J* = 6.9 Hz, 2H). ¹³C NMR (126 MHz, CDCl₃): δ 171.4, 145.1, 136.7, 132.5, 129.8, 129.2, 128.6, 126.7, 124.9, 123.1, 120.7, 120.5, 119.9, 119.8, 118.5, 116.1, 116.0, 52.4, 48.1, 31.7, 31.4, 21.0. HRMS calcd. for C₂₂H₂₃N₂O₂: (M + H)⁺: 347.1761, found: 347.1762.

General procedure for preparation of (5a–5f)

At first KO^tBu (2 mmol) and DMSO (3 ml) were taken in a two-neck round-bottom flask. This two-neck round-bottom flask was placed in an ice bath and allowed to stir for 10–15 min. Then the substrate **4** (1 mmol) was dissolved in minimum amount of DMSO and added dropwise to the reaction mixture. The reaction was allowed for stirring 15–20 min at inert atmosphere. The reaction was monitored by TLC. After completion of the reaction, the crude residue was purified in column chromatography by using basic alumina and ethyl acetate–dichloromethane (1:1) eluent to obtain the desired product **5**.

Representative NMR data of 5a: 5,12,13,16-Tetrahydrobenzo[g]benzo[6,7][1,5]diazocino[2,1-a]isoindol-6(7H)-one

Off white liquid (47 mg for **4a** 65%; 34 mg for **4b** 63%). ¹H NMR (400 MHz, CDCl₃): δ 8.25 (s, 1H), 7.52 (dd, *J*=7.4, 1.6 Hz, 1H), 7.45–7.34 (m, 3H), 7.28–7.26 (m, 1H), 7.19–7.14 (m, 2H), 7.04 (td, *J*=9.2, 1.2 Hz, 1H), 6.53 (s, 1H), 4.95 (s, 2H), 3.72 (s, 2H), 2.79–2.76 (m, 2H), 2.62–2.58 (m, 2H). ¹³C NMR (101 MHz, CDCl₃): δ 171.6, 137.9, 137.1, 132.6, 132.1, 131.4, 130.2, 128.6, 128.5, 126.7, 125.4, 125.0, 123.5, 120.6, 120.3, 119.2, 117.8, 50.3, 33.0, 31.5, 21.1. HRMS calcd. for C₂₁H₁₉N₂O: (M + H)⁺ 315.1499, found: 315.1498.

Acknowledgments

The authors thank the Department of Science & Technology And Biotechnology under the Government of West Bengal [1208 (sanc.)/ST/P/S&T/15G-44/2017] for providing the financial support.

Disclosure statement

No potential conflict of interest was reported by the author(s).

References

- [1] (a) Alfonsi, K.; Colberg, J.; Dunn, P. J.; Fevig, T.; Jennings, S.; Johnson, T. A.; Kleine, H. P.; Knight, C.; Nagy, M. A.; Perry, D. A.; Stefaniak, M. Green Chemistry Tools to Influence a Medicinal Chemistry and Research Chemistry Based Organisation. *Green Chem.* **2008**, *10*, 31–36. DOI: 10.1039/B711717E. (b) Curzons, A. D.; Constable, D. C.; Cunningham, V. L. Solvent Selection Guide: A Guide to the Integration of Environmental, Health and Safety Criteria into the Selection of Solvents. *Clean Prod. Process.* **1999**, *1*, 82–90. DOI: 10.1007/s100980050014. (c) Jimenez-Gonzalez, C.; Curzons, A. D.; Constable, D. J. C.; Cunningham, V. L. Expanding GSK's Solvent Selection Guide? Application of Life Cycle Assessment to Enhance Solvent Selections. *Clean Techn. Environ. Policy* **2004**, *7*, 42–50. DOI: 10.1007/s10098-004-0245-z. (d) Capello, C.; Fischer, U.; Hungerbuhler, K. What is a Green Solvent? A Comprehensive Framework for the Environmental Assessment of Solvents. *Green Chem.* **2007**, *9*, 927–934. DOI: 10.1039/b617536h.
- [2] (a) De, S. K. Simple Synthesis of Pyrroles under Solvent-Free Conditions. *Synth. Commun.* **2008**, *38*, 2768–2774. DOI: 10.1080/00397910701833791. (b) Mukherjee, S.; Sarkar, S.; Pramanik, A. A Sustainable Synthesis of Functionalized Pyrrole Fused Coumarins under

- Solvent-Free Conditions Using Magnetic Nanocatalyst and a New Route to Polyaromatic Indolocoumarins. *ChemSelect* **2018**, 3, 1537–1544. DOI: [10.1002/slct.201703146](https://doi.org/10.1002/slct.201703146).(c) Marvi, O.; Nahzomi, H. T. Grinding Solvent-Free Paal-Knorr Pyrrole Synthesis on Smectites as Recyclable and Green Catalysts. *Bull. Chem. Soc. Ethiop.* **2018**, 32, 139–147. DOI: [10.4314/bcse.v32i1.13](https://doi.org/10.4314/bcse.v32i1.13).(d) Patil, R. N.; Kumar, A. V. Biomimetic Clauson-Kass and Paal-Knorr Pyrrole Synthesis Using β -Cyclodextrin-SO₃H under Aqueous and Neat Conditions – Application to Formal Synthesis of Polygonatine. *ChemistrySelect* **2018**, 3, 9812–9818. DOI: [10.1002/slct.201801559](https://doi.org/10.1002/slct.201801559).(e) Borghs, J. C.; Lebedev, Y.; Rueping, M.; El-Sepelgy, O. Sustainable Manganese-Catalyzed Solvent-Free Synthesis of Pyrroles from 1,4-Diols and Primary Amines. *Org. Lett.* **2019**, 21, 70–74. DOI: [10.1021/acs.orglett.8b03506](https://doi.org/10.1021/acs.orglett.8b03506).
- [3] (a) Balakrishna, A.; Aguiar, A.; Sobral, P. J. M.; Wani, M. Y.; e Silva, J. A.; Sobral, A. J. F. N. Paal-Knorr Synthesis of Pyrroles: From Conventional to Green Synthesis. *Catal. Rev.* **2019**, 61, 84–110. DOI: [10.1080/01614940.2018.1529932](https://doi.org/10.1080/01614940.2018.1529932). (b) Estévez, V.; Villacampa, M.; Menéndez, J. C. Three-Component Access to Pyrroles Promoted by the CAN–Silver Nitrate System under High-Speed Vibration Milling Conditions: A Generalization of the Hantzsch Pyrrole Synthesis. *Chem. Commun.* **2013**, 49, 591–593. DOI: [10.1039/C2CC38099D](https://doi.org/10.1039/C2CC38099D).(c) Minetto, G.; Raveglia, L. F.; Segal, A.; Taddei, M. Microwave-Assisted Paal-Knorr Reaction – Three-Step Regiocontrolled Synthesis of Polysubstituted Furans, Pyrroles and Thiophenes. *Eur. J. Org. Chem.* **2005**, 24, 5277–5288. DOI: [10.1002/ejoc.200500387](https://doi.org/10.1002/ejoc.200500387). (d) Tzankova, D.; Vladimirova, S.; Peikova, L.; Georgieva, M. *J. Chem. Technol. Metall.* **2018**, 53, 451–464.
- [4] (a) Bhardwaj, V.; Gumber, D.; Abbot, V.; Dhiman, S.; Sharma, P. Pyrrole: A Resourceful Small Molecule in Key Medicinal Hetero-Aromatics. *RSC Adv.* **2015**, 5, 15233–15266. DOI: [10.1039/C4RA15710A](https://doi.org/10.1039/C4RA15710A). (b) Wilkerson, W. W.; Copeland, R. A.; Covington, M.; Trzaskos, J. M. Antiinflammatory 4,5-Diarylpyrroles. 2. Activity as a Function of Cyclooxygenase-2 Inhibition. *J. Med. Chem.* **1995**, 38, 3895–3901. DOI: [10.1021/jm00020a002](https://doi.org/10.1021/jm00020a002).(c) Wurz, R. P.; Charette, A. B. Doubly Activated Cyclopropanes as Synthetic Precursors for the Preparation of 4-Nitro- and 4-Cyano-Dihydropyrroles and Pyrroles. *Org. Lett.* **2005**, 7, 2313–2316. DOI: [10.1021/ol050442l](https://doi.org/10.1021/ol050442l).(d) Lee, H.; Lee, J.; Shin, S.; Jung, Y.; Kim, W.; Park, J. H.; Kim, K.; Cho, K.; Ro, H. S.; et al. A Novel Class of Highly Potent, Selective, and Non-Peptidic Inhibitor of Ras Farnesyltransferase (FTase). *Bioorg. Med. Chem. Lett.* **2001**, 11, 3069–3072. DOI: [10.1016/S0960-894X\(01\)00624-2](https://doi.org/10.1016/S0960-894X(01)00624-2).
- [5] (a) Ni, H.; Tang, X.; Zheng, W.; Yao, W.; Ullah, N.; Lu, Y. Enantioselective Phosphine-Catalyzed Formal [4 + 4] Annulation of α,β -Unsaturated Imines and Allene Ketones: Construction of Eight-Membered Rings. *Angew. Chem. Int. Ed.* **2017**, 56, 14222–14226. DOI: [10.1002/anie.201707183](https://doi.org/10.1002/anie.201707183). (b) Sheng, Z. J.; Shi, Y. M.; Xu, X.; Belyncck, S.; Zhang, K.; Du, Z. Y.; Xu, X.; Maurel, F.; Dong, C.-Z. Development of XIAP Antagonists Based on De Novo 8,5-Fused Bicyclic Lactams. *ChemistryOpen* **2019**, 8, 34–40. DOI: [10.1002/open.201800260](https://doi.org/10.1002/open.201800260).
- [6] (a) Khidre, R. E.; Abdel-Wahab, B. F.; Alothman, O. Y. Fused Imidazopyrazoles: Synthetic Strategies and Medicinal Applications. *J. Chem.* **2014**, 2014, 1–15. DOI: [10.1155/2014/217596](https://doi.org/10.1155/2014/217596). (b) Vlasselaer, M.; Dehaen, W. Synthesis of Linearly Fused Benzodipyrrole Based Organic Materials. *Molecules* **2016**, 21, 785. DOI: [10.3390/molecules21060785](https://doi.org/10.3390/molecules21060785).(c) Hoshi, T.; Ota, E.; Inokuma, Y.; Yamaguchi, J. Asymmetric Synthesis of a 5,7-Fused Ring System Enabled by an Intramolecular Buchner Reaction with Chiral Rhodium Catalyst. *Org. Lett.* **2019**, 21, 10081–10084. DOI: [10.1021/acs.orglett.9b04048](https://doi.org/10.1021/acs.orglett.9b04048).
- [7] (a) Pessoa-Mahana, H.; Martínez Aránguiz, K. G.; Araya-Maturana, R. *Synth. Commun.* **2005**, 35, 1493–1500. DOI: [10.1081/SCC-200057990](https://doi.org/10.1081/SCC-200057990). (b) Che, X.; Zheng, L.; Dang, Q.; Bai, X. Synthesis of Novel Pyrimidine Fused 8-Membered Heterocycles via Iminium Ion Cyclization Reactions. *J. Org. Chem.* **2008**, 73, 1147–1149. DOI: [10.1021/jo7020746](https://doi.org/10.1021/jo7020746).(c) Majumdar, K. C. Regioselective Formation of Medium-Ring Heterocycles of Biological Relevance by Intramolecular Cyclization. *RSC Adv.* **2011**, 1, 1152–1170. DOI: [10.1039/c1ra00494h](https://doi.org/10.1039/c1ra00494h).(d) Bremner, J. B.; Russell, H. F.; Skelton, B. W.; White, A. H. *Heterocycles* **2000**, 53, 277–290. DOI: [10.3987/COM-99-8737](https://doi.org/10.3987/COM-99-8737).(e) Bremner, J. B.; Sengpracha, W. A Free

- Radical Cyclization Approach to Indolo-Benzodiazocine Derivatives. *Tetrahedron* **2005**, *61*, 941–953. DOI: [10.1016/j.tet.2004.11.007](https://doi.org/10.1016/j.tet.2004.11.007).
- [8] (a) Manna, S. K.; Mandal, A.; Mondal, S. K.; Adak, A. K.; Jana, A.; Das, S.; Chattopadhyay, S.; Roy, S.; Ghorai, S. K.; Samanta, S.; et al. Pyrido[1,2-*a*]Pyrimidinium Ions – A Novel Bridgehead Nitrogen Heterocycles: Synthesis, Characterisation, and Elucidation of DNA Binding and Cell Imaging Properties. *Org. Biomol. Chem.* **2015**, *13*, 8037–8047. DOI: [10.1039/C5OB01082A](https://doi.org/10.1039/C5OB01082A). (b) Manna, S. K.; Mondal, S. K.; Ahmed, A.; Mandal, A.; Jana, A.; Ikbal, M.; Samanta, S.; Ray, J. K. One-Pot Synthesis of Highly Fluorescent Polycyclic Benzimidazole Derivatives. *RSC Adv.* **2014**, *4*, 2474–2481. DOI: [10.1039/C3RA44521F](https://doi.org/10.1039/C3RA44521F). (c) Mondal, S. K.; Manna, S. K.; Mandal, A.; Samanta, S.; Ray, J. K. A Facile, Catalyst-Free Synthesis of New Polycyclic Pyrrolo[1,2-*b*]Pyrazolone Derivatives. *Tetrahedron Lett.* **2014**, *55*, 6411–6415. DOI: [10.1016/j.tetlet.2014.09.106](https://doi.org/10.1016/j.tetlet.2014.09.106). (d) Jana, A.; Manna, S. K.; Mondal, S. K.; Mandal, A.; Manna, S. K.; Jana, A.; Senapati, B. K.; Jana, M.; Samanta, S. An Efficient Synthesis of Pyrrole and Fluorescent Isoquinoline Derivatives Using $\text{NaN}_3/\text{NH}_4\text{Cl}$ Promoted Intramolecular Aza-Annulation. *Tetrahedron Lett.* **2016**, *57*, 3722–3726. DOI: [10.1016/j.tetlet.2016.07.002](https://doi.org/10.1016/j.tetlet.2016.07.002). (e) Mondal, S. K.; Mandal, A.; Manna, S. K.; Ali, S. A.; Hossain, M.; Venugopal, V.; Jana, A.; Samanta, S. Intramolecular Macrolactonization, Photophysical and Biological Studies of New Class of Polycyclic Pyrrole Derivatives. *Org. Biomol. Chem.* **2017**, *15*, 2411–2421. DOI: [10.1039/C7OB00160F](https://doi.org/10.1039/C7OB00160F). (f) Mondal, S. K.; Ali, S. A.; Manna, S. K.; Mandal, A.; Senapati, B. K.; Hossain, M.; Samanta, S. Palladium-Catalyzed Intramolecular Cyclization: Access to Rare Pentacyclic N-Fused Heterocycles. *ChemSelect* **2017**, *2*, 9312–9318. DOI: [10.1002/slct.201701800](https://doi.org/10.1002/slct.201701800). (g) Yasmin, N.; Ray, J. K. A New Facile Approach to Isoindole and Pyrrole Derivatives. *Synlett.* **2010**, *2010*, 924–930. DOI: [10.1055/s-0029-1219563](https://doi.org/10.1055/s-0029-1219563). (h) Ali, S. A.; Mondal, S. K.; Das, T.; Manna, S. K.; Bera, A.; Dafadar, D.; Naskar, S.; Molla, M. R.; Samanta, S. One-Pot Tandem Cyclisation to Pyrrolo[1,2-*a*][1,4]Benzodiazepines: A Modified Approach to the Pictet–Spengler Reaction. *Org. Biomol. Chem.* **2019**, *17*, 4652–4662. DOI: [10.1039/C9OB00448C](https://doi.org/10.1039/C9OB00448C).
- [9] Yang, Q.; Sheng, M.; Henkelis, J. J.; Tu, S.; Wiensch, E.; Zhang, H.; Zhang, Y.; Tucker, C.; Ejeh, D. E. Explosion Hazards of Sodium Hydride in Dimethyl Sulfoxide, *N,N*-Dimethylformamide, and *N,N*-Dimethylacetamide. *Org. Process Res. Dev.* **2019**, *23*, 2210–2217. DOI: [10.1021/acs.oprd.9b00276](https://doi.org/10.1021/acs.oprd.9b00276).

Cite this: *New J. Chem.*, 2022, 46, 11685

Neat synthesis of isothiazole compounds, and studies on their synthetic applications and photophysical properties†

Anirban Bera,^{a,b} Prasanta Patra,^c Abulkalam Azad,^a Sk Asraf Ali,^a Susanta Kumar Manna,^a Amit Saha^{a,*b} and Shubhankar Samanta^{a*}Received 21st April 2022,
Accepted 12th May 2022

DOI: 10.1039/d2nj01962k

rsc.li/njc

Ammonium thiocyanate-promoted simple, rapid and eco-friendly neat synthesis of isothiazoles is developed for the first time. It is noteworthy that an instantaneous valuable synthetic route of β -enaminones is also documented during the mechanistic investigation of isothiazole formation. A detailed mechanistic explanation of the isothiazole formation reaction is clearly explained by the control experiments. NBS-promoted aromatisation of isothiazole derivatives and photophysical properties of an isothiazole-pyrene hybrid molecule have been investigated.

Introduction

Nitrogen (N) and sulfur (S) are the main constituents of alkaloids and hence five membered heterocyclic compounds containing those heteroatoms, *i.e.* thiazoles, are very common in Nature.¹ Although their isomeric compounds,^{2a} isothiazoles, are rarely found in Nature (*e.g.* brassilexin, sinalexin *etc.*), they are highly important due to their pharmacological interest in biological science (Fig. 1).² Substituted isothiazoles and their fused derivatives are well known in drug discovery due to their significant biological activities, such as analgesic, antipyretic, fungicidal, and herbicidal properties.³ Monocyclic isothiazole skeletons, such as sulfasomizole and denotivir, display antibacterial and antiviral properties, respectively (Fig. 1).⁴ Isothiazolonaphthoquinone, aulosirazole, isolated from blue-green algae exhibited tumor-selective cytotoxicity (Fig. 1).⁵ Another quinone-embedded isothiazole pronquodine A, regulates prostaglandin release from human synovial sarcoma cells (Fig. 1). The antipsychotic drug zipracidone containing a *d*-fused isothiazole (brand name Geodon) is used to treat schizophrenia and bipolar disorder (Fig. 1).⁶ Isothiazole scaffolds have emissive properties when they are attached with ribonucleoside purine mimics or a pyridine nucleus. Highly electron-rich polyfunctional isothiazoles have exceptional importance in the construction of metal complexes of different

types, in particular, valuable organometallic frameworks and functional materials.⁷

The broad spectrum of pharmaceutical use and low natural abundance of the isothiazole moiety have inspired synthetic chemists to prepare such molecules decorated with valuable functionalities.⁸ Modern preparative methods for the isothiazole compounds include *S*-nitrosation of *o*-mercaptoacylphenones followed by intramolecular aza-Wittig reaction,^{9a} transition metal-free oxidative cyclization using amidines and elemental sulfur,^{9b} and cyclization of aryl *tert*-butyl sulfoxides with an *ortho*-sulfinamidomethyl group in the presence of NBS/acid.^{9c} Two independent groups reported the synthesis of 4,5-diaryl isothiazoles and *d*-fused isothiazole from β -halo vinyl aldehyde using ammonium thiocyanate in an acetone medium and NaSCN/urea in the presence of microwave irradiation, respectively.¹⁰ However, these procedures suffer from drawbacks such as longer reaction times, tedious workups, harsh reaction conditions, lower yields, and use of special microwave techniques to synthesize the isothiazole molecules. Therefore, the development of more economic and environmentally benign procedures that can avoid or reduce the use of volatile organic solvents without imposing longer reaction times is not only attractive, but has also become essential to organic synthesis. Although many common heterocyclic compounds have been synthesized following the neat approach, but synthesis of isothiazoles under solvent-free conditions has not been reported to date.

In continuation of our research work involving the neat reaction technology,¹¹ we report here for the first time, a solvent-free rapid synthetic route of isothiazoles 2 *via* ammonium thiocyanate-promoted single reagent transformation from β -halo vinyl aldehyde 1. The current protocol reduces

^a Department of Chemistry, Bidhannagar College, Kolkata, 700064, India.

E-mail: chemshubha@gmail.com; Fax: +9133 2337 4782; Tel: +919775550193

^b Department of Chemistry, Jadavpur University, Kolkata, 700032, India^c Jhargram Raj College, Jhargram, West Bengal, 721507, India† Electronic supplementary information (ESI) available. CCDC 2117809. For ESI and crystallographic data in CIF or other electronic format see DOI: <https://doi.org/10.1039/d2nj01962k>

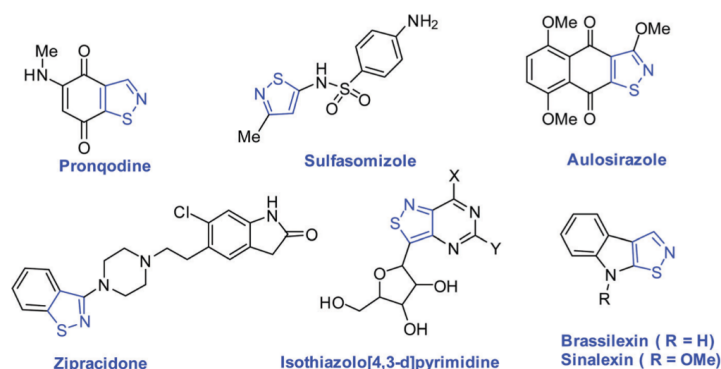
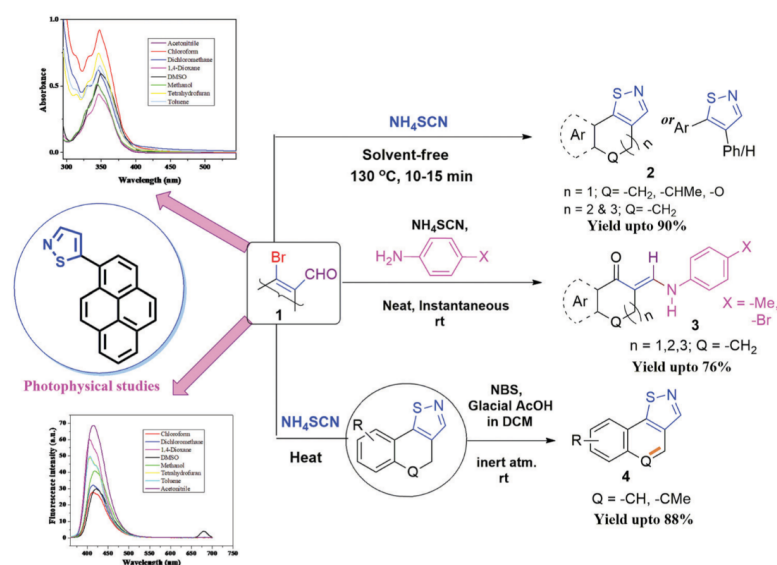


Fig. 1 Bio-active molecules with an isothiazole moiety.

the use of volatile solvents, avoids the conventional work-up process and offers an improved green reaction methodology (Scheme 1). During the mechanistic study, we have further originated valuable intermediate *N*-aryl substituted β -enaminone derivatives, **3**, from the same precursor *via* ammonium thiocyanate-promoted instantaneous transformation in the presence of arylamine (Scheme 1). We were also successful in preparing the corresponding aromatized polycyclic isothiazoles **4** from the newly synthesized isothiazole derivatives, **2**, by a mild oxidative procedure using NBS (*N*-bromo succinimide) (Scheme 1). A new fluorescence active pyrene substituted isothiazole has been synthesized and its detailed photophysical properties have been documented in the latter section (Scheme 1) of this article.

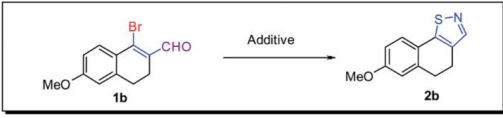
Results and discussion

The mission was started with β -bromo vinyl aldehyde, which has been used to prepare many useful molecules by our group.¹² β -Bromo vinyl aldehyde has two important functionalities that can participate in metal or metal-free transformations. The replacement of vinyl bromide is very difficult but it becomes easier when an electron-withdrawing formyl group is present at the β -position. Thiocyanate is a good nucleophile, which can replace vinyl bromide *via* an addition elimination reaction. Therefore, we have used ammonium thiocyanate, which may act as the source of both nitrogen and sulfur and reacts with the aldehyde and vinyl bromide part of **1**. This protocol furnished good yields of isothiazoles **2b** (78%) when 3 mmol



Scheme 1 An outlook of our overall observation.

Table 1 Optimization of the reaction conditions for the synthesis of *d*-fused isothiazole^a



Entry	Additive	Medium	Time (h)	Yield (%)
1	NH ₄ SCN (3 mmol)	MeOH-H ₂ O (1:1)	5	78
2	NH ₄ Cl (1 mmol)	MeOH-H ₂ O (1:1)	12	70
3	KSCN (2 mmol)	MeOH-H ₂ O (1:1)	12	72
4	NH ₄ Cl (1 mmol)	MeOH-H ₂ O (1:1)	10	70
5	Na ₂ S ₂ O ₃ (2 mmol)	Water	10	NR
6	NH ₄ SCN (3 mmol)	Neat	10	NR ^b
7	NH ₄ SCN (1 mmol)	Neat	5	20 ^b
8	NH ₄ SCN (2 mmol)	Neat	5	80 ^b
9	NH ₄ SCN (4 mmol)	Neat	4	84 ^b
10	NH ₄ SCN (5 mmol)	Neat	2.5	86 ^b
11	NH ₄ SCN (6 mmol)	Neat	2	87 ^b
12	NH ₄ SCN (10 mmol)	Neat	1	90 ^b
13	NH ₄ SCN (10 mmol)	Neat	0.17	90 ^c
14	NH ₄ Cl (1 mmol)	Neat	12	55 ^b

^a Reaction Conditions: β -bromo vinyl aldehyde **1b** (1 mmol), solvent (3 mL), NH₄SCN (3 mmol), and temperature 70 °C. ^b Reaction was performed without solvent at 70 °C. ^c Reaction was performed without solvent at 130 °C with 10 mmol of NH₄SCN.

of ammonium thiocyanate is used in an aqueous methanolic medium (entry 1, Table 1). The reaction was also found to proceed successfully with NH₄Cl/KSCN, Na₂S/NH₄Cl and Na₂S₂O₃/NH₄Cl in an aqueous methanolic medium but the

yield was poor and requires long times (entries 2, 3 and 4, Table 1). In order to develop an environmentally benign approach for the synthesis of heterocyclic compounds, we have used an aqueous medium in our current transformation but the reaction did not proceed at all (entry 5, Table 1). Then we tried the reaction in neat conditions and the reaction was found to complete within 5 hours to produce the desired product in 90% yield (entry 8, Table 1). Surprisingly, it has been found that with increasing the amount of ammonium thiocyanate and temperature, the reaction time period is reduced significantly. The desired product was obtained within 10 minutes at 130 °C under neat conditions in the presence of 10 mmol NH₄SCN (entry 13, Table 1). Thus, this condition has a greater impact from the environmental point of view. Neat conditions were also tested in the presence of Na₂S₂O₃/NH₄Cl but the yield of **2b** was only 55% (entry 14, Table 1).

To understand the dependence of the yield of reaction on the amount of NH₄SCN used, we have plotted the yields of isothiazole **2b** obtained under neat conditions within 1 hour of time period at 70 °C with different amounts (in mmol) of ammonium thiocyanate used in the reactions (Fig. 2(a)). It has been observed that the yield of the reaction does not increase beyond 10 mmol of NH₄SCN at 70 °C. Next, we studied another plot at a constant amount of NH₄SCN (10 mmol) at different temperatures with the time periods of the reactions to get the maximum yield of isothiazole (Fig. 2(b)). The time reduced to 10 minutes at 130 °C for completion of the reaction.

From Table 1 and Fig. 2, we found that isothiazole formation becomes very fast at 130 °C in the presence of 10 mmol of NH₄SCN under neat conditions. With these optimum conditions in hand (Table 1, entry 13), we extended our studies using different substituted β -bromo vinyl aldehydes (Table 2).

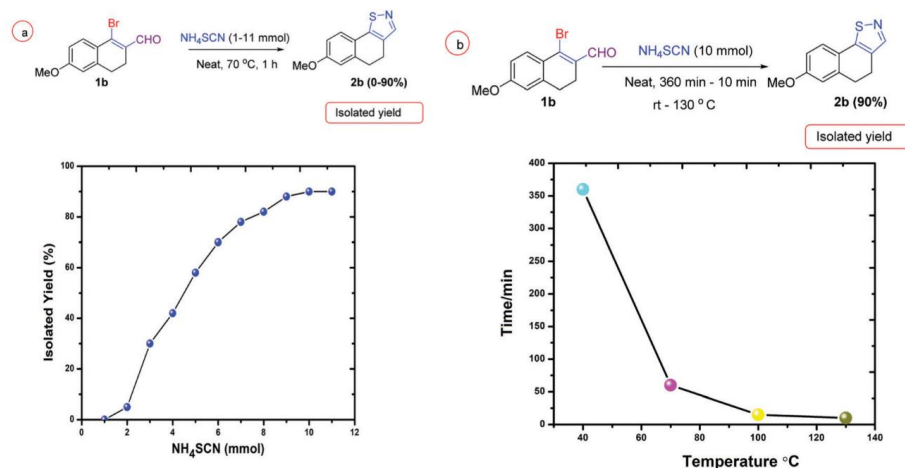
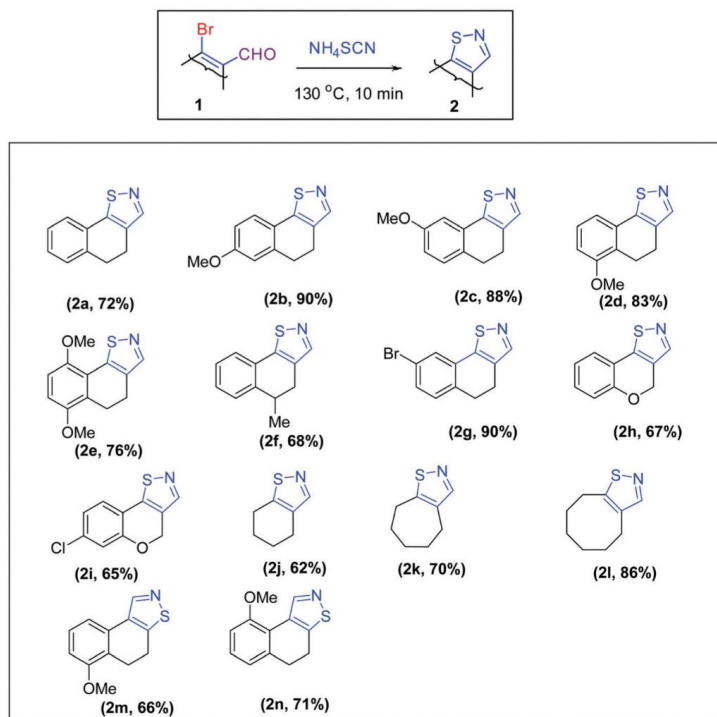


Fig. 2 Schematic representation of the ammonium thiocyanate-promoted neat reaction to produce *d*-fused isothiazole derivatives. (a) Reagent-dependent conversion efficiency of the neat reaction with different mmols of ammonium thiocyanate at constant temperature and time. (b) Temperature- and time-dependent plot to get maximum yield at constant equivalent of the reagent. Yields were determined by isolation of the product *via* column chromatography.

Table 2 Neat synthetic approach of isothiazoles^a

^a Reaction conditions: β -bromo vinyl aldehyde **1** (1 mmol), NH_4SCN (10 mmol), $130\text{ }^\circ\text{C}$, and 10 minutes.

Electron donating and withdrawing group-substituted aryl rings furnished the corresponding tricyclic *d*-fused isothiazole products appreciably (**2b**–**2e** and **2g**, 76–90%) under neat conditions in the presence of ammonium thiocyanate. Since both the nucleophilic and electrophilic additions are involved in the process of isothiazole ring formation, the reaction is favored by the groups of both types of electronic natures. In the case of unsubstituted aryl ring **1a** and the cycloalkyl substituent **1j**–**1l** without any electronic sense, the yield of isothiazoles got reduced. Increasing ring size in the cycloalkyl ring (**2j**–**2l**) afforded bicyclic isothiazoles in ascending order (62–86%) and it became the highest with 8-membered fused isothiazole

2l under neat conditions. This may be due to the tolerance of temperature by the higher molecular weight of the cycloalkyl ring under neat conditions. This methodology also provided isomeric isothiazoles **2m** and **2n** by taking 2-bromo vinyl aldehyde instead of 1-bromo vinyl aldehyde with effective yields (66–71%).

The protocol was also applicable with respect to practical aspects. From a practical standpoint, the reaction was performed in gm scale and found to give a good yield of isothiazole derivative **2b** under neat conditions. We got 650 mg of product **2b** from 1 g of **1b** and hence 79% yield of the desired isothiazoles was obtained at $130\text{ }^\circ\text{C}$ after 2 h of heating.

Scheme 2 Synthesis of isothiazole **2b** in gram scale.

The time required in the gram scale neat reaction was greater compared to the mg scale reaction (Scheme 2).

To study the general applicability of our reaction to the acyclic systems, we started our reaction with (*Z*)-3-bromo-2,3-diphenylacrylaldehyde **1o** for the construction of 4,5 diphenyl substituted isothiazole derivatives **2o** under optimum conditions (neat) and obtained the isothiazole derivatives in good yields within 15 minutes. An engaging result was observed for substrate (*Z*)-3-bromo-3-(pyrene-1-yl)acrylaldehyde **1p**, which gave pyrene-substituted new blue fluorescent probe **2p** with 78% yield (Scheme 3). This result enforces us to further study the photo-physical behavior and it is discussed in the next section.

To investigate the mechanism of isothiazole formation under neat conditions, we have done some control experiments in the presence of ammonium thiocyanate as a single reagent (Scheme 4). The reaction did not take place with 1 mmol of NH₄SCN at 70 °C (Scheme 4a). The reaction produced a 20% yield of **2b** in the presence of 2 mmol of NH₄SCN at 70 °C and a dramatic change was observed after adding 10 mmol of NH₄SCN (Scheme 4c). After changing the reaction conditions by the addition of 1 mmol *p*-toluidine with 1 mmol of NH₄SCN, a different product, *i.e.* β-enaminone **3b**, was formed with a 69% yield (Scheme 4d). Furthermore, vinyl bromide is not replaced by the addition of KSCN with **1b** (Scheme 4e). Again the *p*-tolyl imine derivative of **1b** did not furnish the desired product **3b** or **1bc**. From the literature observation, it was shown that β-thiocyno vinyl imine **1bc** must be formed in the reaction medium during isothiazole formation.^{10a} Again, from our experiment, it is shown that vinyl bromide is not replaced in the presence of formyl or imine derivatives. We can anticipate that thiocyanate replaced vinyl bromide from unstable hemiaminal intermediate **1ba**. This is facilitated if the reaction medium has sufficient acidity. Consequently, the rate of vinyl bromide displacement is directly proportional to the increase of acidity of NH₄SCN and it has been enhanced with excess addition of NH₄SCN. Therefore, with 10 mmol of NH₄SCN, **2b** was formed exclusively within 10 minutes.

From these observations we have proposed a detailed mechanism of reaction, which was not discussed in the earlier report (R. C. Boruah *et al.*).^{10a} At first, substrate **1** reacts with the amine source to produce hemiaminal intermediate **A**, and then thiocyanate replaces vinyl bromide *via* the elimination of a water molecule. The driving force for water elimination is the strength of acidity and then intermediate **D** or **F** is formed *via*

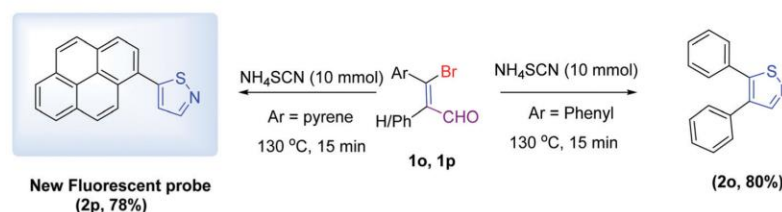
the addition elimination mechanism. Intermediate **F** underwent intramolecular cyclisation to produce the desired isothiazole **2**. However, in the presence of *p*-toluidine it generates *trans*-β-thiocyno imine **D**, which cannot undergo intramolecular cyclisation as it is locked in the *trans* form and hence readily hydrolyzes to give β-enaminone **3** with a good yield. Thus, it has been concluded that a specific stereochemistry is needed for intramolecular aza-cyclization to get isothiazole derivative **2** (Scheme 5).

β-Enaminones are important building blocks for the construction of a variety of pharmaceutical compounds, including anti-inflammatory agents, anti-convulsants, anti-cancer agents, and antibacterials.¹³ In addition, substituted β-enaminones are commonly used as intermediates in the synthesis of heterocycles, such as pyridines, indoles, pyrroles and pyrazole derivatives (Scheme 6).¹⁴ Due to the wide application of β-enaminones in organic synthesis and drug development, much attention has been paid to developing a facile, green, and practical method for the preparation of β-enaminones. In addition to isothiazole synthesis, we have also developed a synthetic route of β-enaminones from β-bromo vinyl aldehydes and aryl amines. This valuable intermediate will help in preparing various heterocycles in due time and will be useful to the synthetic organic chemists.

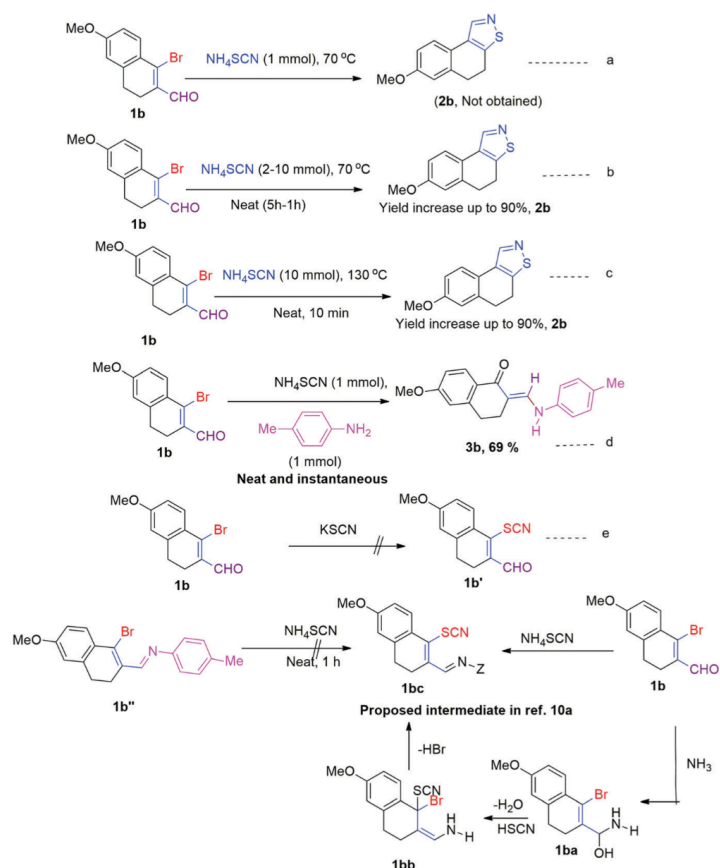
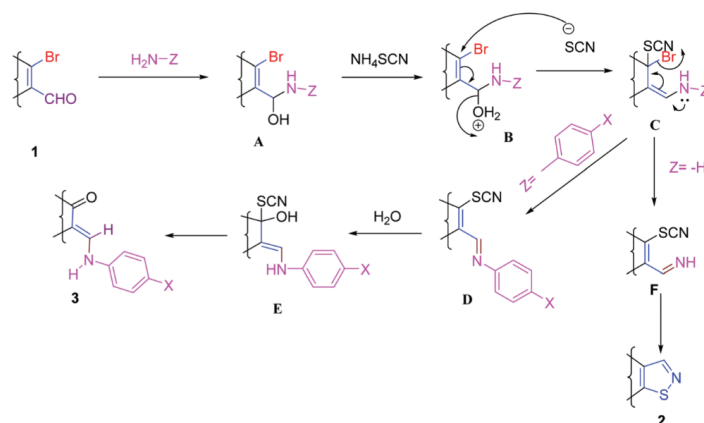
Considering the above findings, we have synthesized different β-enaminones **3a–f** *via* momentary changes (2–3 minutes) under solvent-free conditions (Table 3) and the structure of one of them (**3c**) was unambiguously confirmed by X-ray analysis, which established the best evidence for the formation of **3**. *N*-Aryl-β-enaminones of cyclohexanone, cycloheptanone, cyclooctanone and tetralone derivatives **3a–3f** were synthesized with good yields (62–76%). However, a diastereomeric mixture of **3f** (*E:Z* = 3:1) was obtained with a moderate yield when *p*-bromoaniline was taken as the coupling partner with **1**.

After synthesis of β-enaminones *via* momentary transformation, we wished to utilize the valuable intermediate in organic synthesis. Herein, we have achieved *N-p*-tolylformamide **3da** in the presence of potassium carbonate DMSO at 120 °C with the substrate **3d**. The formation of the product can be explained by base-mediated isomerization followed by hydrolysis to afford the desired formyl-substituted *p*-tolyl derivative with a 62% yield (Scheme 7).

Next, we concentrated on halogen functionalisation of isothiazole derivatives by considering the utility of chemical



Scheme 3 Synthesis of isothiazole from acyclic precursors.

Scheme 4 Series of control experiments for isothiazole/ β -enaminone formation.

Scheme 5 Mechanistic explanation of ammonium thiocyanate-promoted neat reaction.

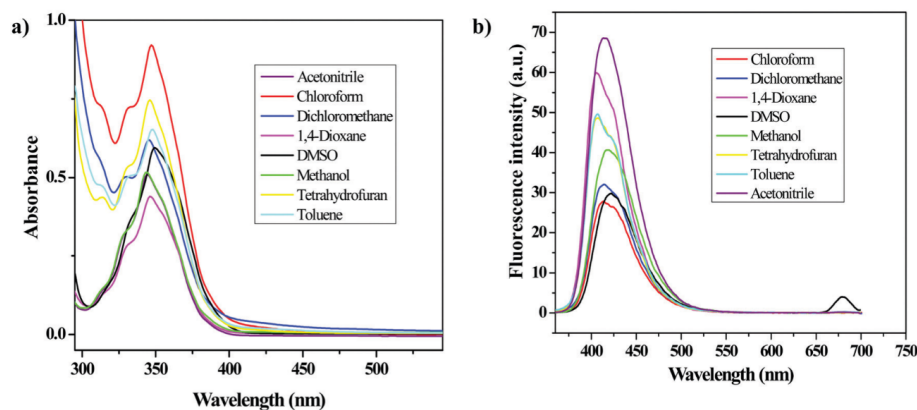
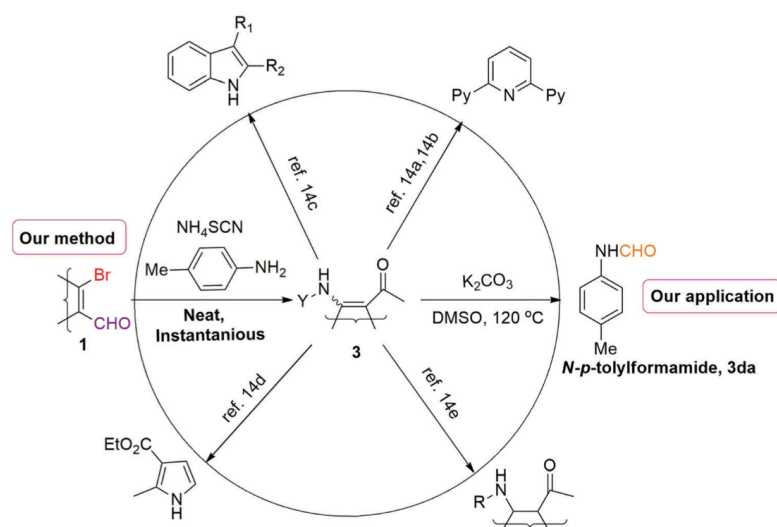
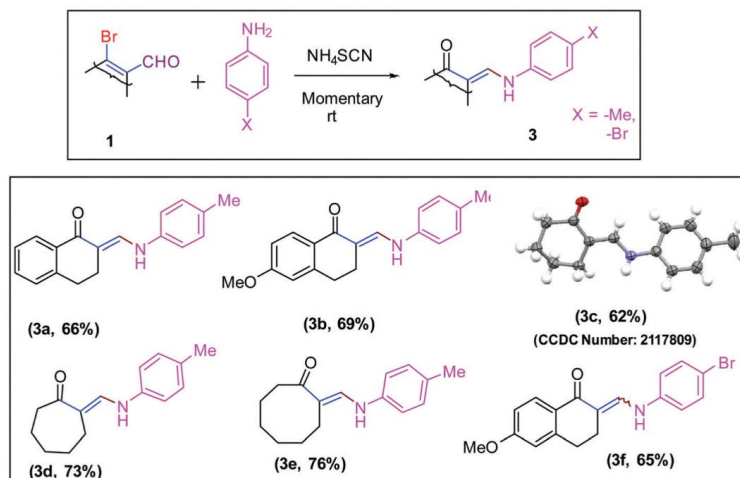


Fig. 3 Photophysical properties of **2p**. (a) Absorption and (b) fluorescence spectra of **2p** recorded at a concentration of 2.0×10^{-5} M in different solvents.

properties. Halogen-substituted isothiazoles are highly reactive synthetic building blocks, allowing the ability to obtain poly-functional isothiazoles with a wide variety of substituents. Hence, we wish to synthesize such a halogen-substituted isothiazole ring as our new tricyclic *d*-fused isothiazole derivative **2** and we anticipated that the 3-position is more susceptible for halogen-substitution as another position is blocked by ring substitution. Hence, we have used NBS for the said transformation. However, the reaction did not produce halogen-substituted isothiazole derivatives and surprisingly afforded complete aromatic compound **4** via the two-step mild oxidative reaction (Table 4). At first, halogenation occurred with NBS/

AcOH in dichloromethane at room temperature at the benzylic- sp^3 carbon atom and then elimination afforded highly aromatic tri-cyclic fused compounds with good yields within 6 h. To extend the scope for aromatization reactions, we have tested the reaction with a 4-methyl substituted β -bromo vinyl aldehyde derivative and found the formation of aromatized compound **4g** with a 61% yield. Previously, similar aromatic derivatives were obtained by refluxing the reaction mixture at high temperatures for 16 hours in a toluene medium in the presence of a stoichiometric amount of DDQ¹⁵ but we have achieved the synthesis of aromatic compounds efficiently by an NBS-promoted clean room temperature protocol.

Table 3 Momentary synthetic route of *N*-aryl β -enaminones

Reaction conditions: β -bromo vinyl aldehyde **1** (1 mmol), NH_4SCN (1 mmol), and ArNH_2 (1 mmol), at room temperature, 2–3 min.

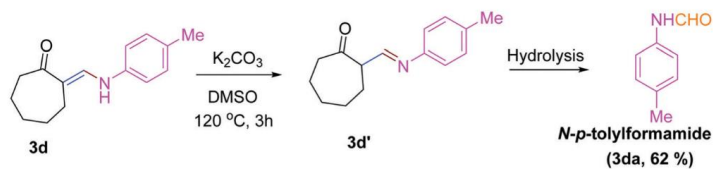
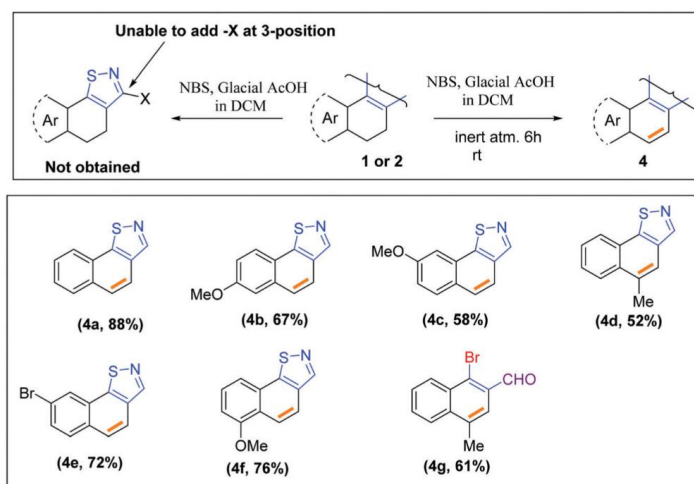
Scheme 7 Synthetic application of the β -enaminone intermediate.

Table 4 NBS-promoted aromatisation



Reaction conditions: substrate **1** or **2** (1 mmol), NBS (1 mmol), AcOH (1 drop), CH_2Cl_2 (3 mL), and room temperature.

Table 5 UV-Vis absorption and fluorescence data of **2p** in different solvents

Solvents	ϵ^a (25 °C)	λ_{max}^b (nm)	λ_{em}^c (nm)	ϵ_{max}^d ($10^3 \text{ M}^{-1} \text{ cm}^{-1}$)	Stokes shift ^e (nm)
1,4-Dioxane	2.25	346	408	2.07	62
Toluene	2.38	348	409	3.25	61
Chloroform	4.81	347	414	4.57	67
THF	7.58	346	409	3.71	63
DCM	8.93	346	415	3.09	69
MeOH	32.70	344	421	2.58	77
Acetonitrile	37.5	345	416	2.68	71
DMSO	46.68	349	424, 680	2.91	75

^a Dielectric constant at 25 °C. ^b Maximum absorption wavelength. ^c Molar absorption coefficient at maximum absorption wavelength. ^d Maximum emission wavelength. ^e Difference between absorption maximum and emission maximum.

Photophysical study

Pyrene-substituted fluorophores have received great attention in materials science, organic light-emitting diodes (OLEDs), light-emitting electrochemical materials, *etc.* due to them having different emissive properties in the functionalized form.¹⁶ Although a number of articles have been published regarding fluorescence properties of pyrene with different functionalities mainly at the 1/3/6 or 8-position, an isothiazole-substituted pyrene fluorophore is still not reported.¹⁷ In continuation of the application of the fluorescence properties of newly synthesized compounds,^{12,18} we have designed a new fluorophore that has not been synthesized as a pyrene substituent at the 1-position. To establish the photophysical properties of our synthesized pyrene fluorophore, we determined the absorption peaks in polar aprotic, polar protic, and nonpolar solvents (Fig. 3 and Table 5). It was found that the absorption maxima (λ_{max}) fall in the range of 349–344 nm in different solvents. Considering the absorption peak in the UV-vis spectra, we have also recorded the emission spectra excited at 344 nm in the same solvents and the emission maxima vary from 404–424 nm. Our study also revealed that the highest emission maximum along with an additional maximum will appear at 424 nm and 680 nm in DMSO and a greater Stokes shift (77 nm) is exhibited in the polar protic MeOH. The higher bathochromic shift in the emission spectra in the polar protic solvent (421 nm), compared to the nonpolar solvent toluene (409 nm), may be due to the specific interactions such as hydrogen bonding or molecular aggregations.¹⁹ In the viscous polar aprotic DMSO solvent, the higher bathochromic shift and lower emission intensity can be explained by the rigid rotation of the isothiazole unit in the pyrene group in the viscous solvent, which leads to the twisted conformation in the excited state and hence the dipole moment has been changed in the excited state.¹⁹ Hence, these initial observations in different solvents argue that our newly designed compound may be used for the detection of proton/metal/molecular sensing in due time.

Conclusions

In conclusion, we have developed an ammonium thiocyanate-promoted first neat synthetic approach of isothiazole to both

cyclic/acyclic precursors and the fate of the reaction with different equivalents of ammonium thiocyanate vs. temperature/time/yield was observed. The availability of various β -bromo vinyl aldehydes and the simplicity of the developed method can provide broad synthetic options for the synthesis of isothiazole derivatives. An instantaneous synthetic transformation to β -enaminones by the addition of aryl amine with ammonium thiocyanate to β -bromo vinyl aldehyde derivatives was also included during the mechanistic consideration of isothiazole formation. Further functionalization in fused isothiazoles *via* NBS-promoted aromatization is another application of our developed methodology. Also, we successfully investigated the emission properties of the newly synthesized isothiazole-substituted pyrene-based fluorophore and the investigation of other photophysical properties is in progress in our laboratory.

Conflicts of interest

There are no conflicts to declare.

Acknowledgements

We thank the Department of Science & Technology and Biotechnology under the Government of West Bengal (398 (Sanc.)/STBT-11012(25)/25/2021-ST SEC) & (368(Sanc.)/STBT-11012(25)/11/2020) for financial support.

References

- (a) D. Davyt and G. Serra, *Mar. Drugs*, 2010, **8**, 2755–2780; (b) R. E. Khidre, I. Ali and M. Radini, *Sci. Rep.*, 2021, **11**, 7846.
- (a) M. S.-C. Pedras and M. Suchy, *Org. Biomol. Chem.*, 2005, **3**, 2002–2007; (b) A. V. Kletskov, N. A. Bumagin, F. I. Zubkov, D. G. Grudinina and V. I. Potkin, *Synthesis*, 2020, 159–188.
- (a) Q. F. Wu, B. Zhao, Z. J. Fan, J. B. Zhao, X.-F. Guo, D.-Y. Yang, N.-L. Zhang, B. Yu, T. Kalinina and T. Glukhareva, *RSC Adv.*, 2018, **8**, 39593–39601; (b) G. N. Zong, F. Y. Li, Z. J. Fan, W. T. Mao, H. B. Song, L. Chen, Y. J. Zhu, J. H. Xu, Y. Q. Song and J. R. Wang, *Chin. J. Struct. Chem.*, 2015, **34**, 871; (c) R. Slack and K. R.-H. Wooldridge, *Adv. Heterocycl. Chem.*, 1965, **4**, 107; (d) M. Davis, *Adv. Heterocycl. Chem.*, 1972, **14**, 43; (e) European Patent Application EP0726268A1, 1996.
- (a) A. Adams, W. A. Freeman, A. Holland, D. Hossack, J. Inglis, J. Parkinson, H. W. Reading, K. Rivett, R. Slack, R. Sutherland and R. Wien, *Nature*, 1960, **186**, 221; (b) Z. Machoń, Z. Wiczorek and M. Zimecki, *Polym. J. Pharmacol.*, 2001, **53**, 377.
- (a) C. E. Blunt, C. Torcuk, Y. Liu, W. Lewis, D. Siegel, D. Ross and C. J. Moody, *Angew. Chem., Int. Ed.*, 2015, **54**, 8740–8745; (b) K. Stratmann, J. Belli, C. M. Jensen, R. E. Moore and G. M.-L. Patterson, *J. Org. Chem.*, 1994, **59**, 6279–6281.

- 6 (a) H. R. Howard, J. A. Lowe III, T. F. Seeger, P. A. Seymour, S. H. Zorn, P. R. Maloney, F. E. Ewing, M. Newman, A. W. Schmidt, J. S. Furman, G. L. Robinson, E. Jackson and C. J. Morrone, *J. Med. Chem.*, 1996, **39**, 143; (b) T. F. Seeger, P. A. Seymour, A. W. Schmidt, S. H. Zorn, D. W. Schulz, L. A. Lebel, S. McLean, V. Guanowsky, H. R. Howard, J. A. Lowe III and J. Heym, *J. Pharmacol. Exp. Ther.*, 1995, **275**, 101; (c) C. Prakash, A. Kamel and D. Cui, *Drug Metab. Dispos.*, 1997, **25**, 897.
- 7 (a) A. R. Rovira, A. Fin and Y. Tor, *Chem. Sci.*, 2017, **8**, 2983; (b) E. Krzyzak, M. Sliwinska and W. Malinka, *J. Fluoresc.*, 2015, **277**–282.
- 8 (a) G. Huang, J. Li, X. Ji, L. Chen, Q. Liu, X. Chen, Y. Huang and Y. Li, *Chem. Commun.*, 2020, **56**, 5763–5766; (b) M. J. Cabrera, S. Cembellín, A. H. Salem, M. Berton, L. Marzo, A. Miloudi, M. C. Maestro and J. Alemán, *Green Chem.*, 2020, **22**, 6792–6797; (c) H. Yuan and Z. Sun, *Synlett*, 2019, 1904–1908.
- 9 (a) N. O. Devarie-Baez and M. Xian, *Org. Lett.*, 2010, **12**, 752; (b) H. Xie, G. Li, F. Zhang, F. Xiao and G. J. Deng, *Green Chem.*, 2018, **20**, 827–831; (c) F. Xu, Y. Chen, E. Fan and Z. Sun, *Org. Lett.*, 2016, **18**(11), 2777–2779.
- 10 (a) P. Bezbaruah, J. Gogoi, K. S. Rao, P. Gogoi and R. C. Boruah, *Tetrahedron Lett.*, 2012, **53**, 4389–4392; (b) M. Scholz, H. K. Ulbrich, O. Soehnlein, L. Lindbom, A. Mattern and G. Dannhardt, *Bioorg. Med. Chem.*, 2009, **17**, 558–568.
- 11 (a) A. Bera, S. A. Ali, S. K. Manna, M. Ikbali, S. Misra, A. Saha and S. Samanta, *New J. Chem.*, 2020, **44**, 4324–4331; (b) A. Bera, S. K. Ali, A. Saha and S. Samanta, *Synth. Commun.*, 2021, **51**, 2377–2386.
- 12 (a) S. K. Manna, A. Mandal, S. K. Mondal, A. K. Adak, A. Jana, S. Das, S. Chattopadhyay, S. Roy, S. K. Ghorai, S. Samanta, M. Hossain and M. Baidya, *Org. Biomol. Chem.*, 2015, **13**, 8037; (b) S. K. Manna, S. K. Mondal, A. Ahmed, A. Mandal, A. Jana, M. Ikbali, S. Samanta and J. K. Ray, *RSC Adv.*, 2014, **4**, 2474; (c) S. K. Mondal, S. K. Manna, A. Mandal, S. Samanta and J. K. Ray, *Tetrahedron Lett.*, 2014, **55**, 6411; (d) A. Jana, S. K. Manna, S. K. Mondal, A. Mandal, A. Jana, B. K. Senapati, M. Jana and S. Samanta, *Tetrahedron Lett.*, 2016, **57**, 3722; (e) S. K. Mondal, A. Mandal, S. K. Manna, Sk.-A. Ali, M. Hossain, V. Venugopal, A. Jana and S. Samanta, *Org. Biomol. Chem.*, 2017, **15**, 2411; (f) S. K. Mondal, S. A. Ali, S. K. Manna, A. Mandal, B. K. Senapati, M. Hossain and S. Samanta, *ChemistrySelect*, 2017, **2**, 9312.
- 13 B. Govindh, B. S. Diwakar and Y. L.-N. Murthy, *Org. Commun.*, 2012, **5**(3), 105–119.
- 14 (a) M. H. Elnagdi, M. S. Moustafa, S. M. Al-Mousawi, R. A. Mekheimer and K. U. Sadek, *Mol. Diversity*, 2015, **19**, 625–651; (b) A. Livoreil, J. P. Sauvage, N. Armarolli, V. Balzani, L. Flamigni and B. Ventura, *J. Am. Chem. Soc.*, 1997, **119**, 12114–12124; (c) C. Caubere, P. Caubere, S. Ianelli, M. Nardelli and B. J. Gregoire, *Tetrahedron*, 1994, **50**, 11903–11920; (d) P. Jakobsen and S. O. Lawesson, *Tetrahedron*, 1968, **24**, 3671–3674; (e) D. Potin, F. Dumas and J. D'Angelo, *J. Am. Chem. Soc.*, 1990, **112**, 3483–3486.
- 15 F. Rammal, A. C. Gaumont and S. Lakhdar, *Eur. J. Org. Chem.*, 2020, 1482–1485.
- 16 (a) S. Tao, Z. Peng, X. Zhang, P. Wang, C. S. Lee and S. T. Lee, *Adv. Funct. Mater.*, 2005, **15**, 1716–1721; (b) J. Jayabharathi, P. Jeeva, V. Thanikachalam and S. Panimozhi, *J. Photochem. Photobiol., A*, 2017, **346**, 296–310; (c) M. T. Figueira-Duarte and K. Muillen, *Chem. Rev.*, 2011, **111**, 7260–7310.
- 17 M. M. Islam, Z. Hu, Q. Wang, C. Redshaw and X. Feng, *Mater. Chem. Front.*, 2019, **3**, 762–781.
- 18 S. A. Ali, S. Bhaumik, A. Jana, S. K. Manna, M. Ikbali, A. Mandal, A. Bera, A. Jana and S. Samanta, *ChemistrySelect*, 2018, **3**, 11950–11956.
- 19 (a) V. Kachwal, P. Alam, H. R. Yadav, S. S. Pasha, A. Roy Choudhury and I. R. Laska, *New J. Chem.*, 2018, **42**, 1133–1140; (b) A. Kathiravan, K. Sundaravel, M. Jacob, G. Dhinakaran, A. Rameshkumar, D. A. Ananth and T. Sivasudha, *J. Phys. Chem. B*, 2014, **118**, 13573–13581; (c) D. Kumar and K. R.-J. Thomas, *J. Photochem. Photobiol., A*, 2011, **218**, 162–163; (d) J.-Y. Hu, H. Hiyoshi, J.-H. Do and T. Yamato, *J. Chem. Res.*, 2010, **34**, 278–282.

Synthesis of Multifused Pyrrolo[1,2-*a*]quinoline Systems by Tandem Aza-Michael–Aldol Reactions and Their Application to Molecular Sensing Studies

Anirban Bera, Sk Abulkalam Azad, Prasanta Patra, Nayim Sepay, Rathin Jana, Tapas Das, Amit Saha,* and Shubhankar Samanta*

Cite This: *J. Org. Chem.* 2023, 88, 5622–5638

Read Online

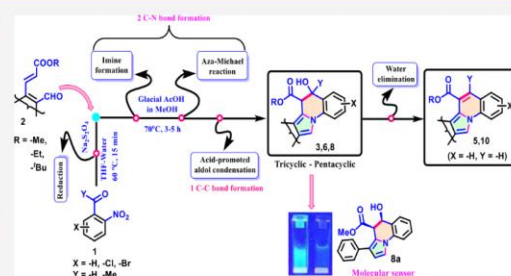
ACCESS |

Metrics & More

Article Recommendations

Supporting Information

ABSTRACT: Herein, we have presented a weak acid-promoted tandem aza-Michael–aldol strategy for the synthesis of diversely fused pyrrolo[1,2-*a*]quinoline (tricyclic to pentacyclic scaffolds) by the construction of both pyrrole and quinoline ring in one pot. The described protocol fabricated two C–N bonds and one C–C bond in the pyrrole–quinoline rings which have been sequentially formed under transition-metal-free conditions by the extrusion of eco-friendly water molecules. A ketorolac drug analogue has been synthesized following the current protocol, and one of the synthesized tricyclic pyrrolo[1,2-*a*]quinoline fluorophores has been used to detect highly toxic picric acid via the fluorescence quenching effect.



INTRODUCTION

Aza-Michael addition and aldol condensation are two well-documented reactions in organic synthesis as these reactions have been considerably used in the construction of C–N and C–C bond formation.¹ The combination of two reactions in a tandem fashion is an attractive tool for the construction of N-heterocycles in a single click reaction.² The transition-metal-free cascade Michael–aldol reactions have been considered as economical and environmentally friendly processes.³ The combination of these two reactions was applied to construct different N-bridged heterocycles and various natural products such as steroids (estradiol methyl ether) and pentacyclic anticancer agents (marmycin A and B).^{4,5} On the other hand, pyrrolo[1,2-*a*]quinolone scaffolds are important for their natural occurrences as well as their biological activities including antibacterial, antiviral, antioxidant, antihypoxia, anticancer, multidrug-resistance reversing, cytotoxic, and HIV-1 integrase inhibitory activities as depicted in Figure 1.⁶ Besides the biological applications, fluorescence properties of these heterocycles have received great attention in the past decades because of their applications in bioimaging, drug discovery, clinical diagnostics, and organic optoelectronic devices.⁷ Furthermore, multisubstitutions such as Ar–OH, carbonyl, and carboxyl groups in the fluorophore help in the manifestation of molecular sensing properties.⁸

Due to the tremendous biological and photophysical importance of pyrrolo[1,2-*a*]quinolone scaffolds, researchers have developed a large number of protocols for the synthesis of such compounds.^{9–11} However, there is no report on the

formation of tricyclic to pentacyclic rings in a single operation. There are some precedents (Scheme 1) to construct either pyridine,⁹ pyrrole,¹⁰ or both the moieties¹¹ for the synthesis of pyrrolo[1,2-*a*]quinolone from suitable precursors but in most of the cases either the pyridine or pyrrole moiety has been used as a starting material. However, in a few pieces of literature, it has been shown that both the rings of pyrrole and isoquinoline were formed in a one-pot methodology. However, in most of the cases, they used chlorinated solvents as the reaction media for a prolonged time. Herein, we have designed a protocol for the synthesis of pyrrolo[1,2-*a*]quinoline (tricyclic to pentacyclic) in a single-pot Michael–aldol reaction within a short reaction time under green conditions. The coupling reactions were performed with two substrates 2-nitrobenzaldehyde **1a** and 3-(2-formylcycloalkenyl)-acrylic ester derivatives **2** in the presence of the weak organic acid catalyst AcOH in MeOH. The generation of nontoxic byproducts is another attraction of this protocol.

3-(2-formylcycloalkenyl)-acrylic ester derivatives with two reactive functional groups (α,β -unsaturated ester and aldehyde) have been explored for the synthesis of heterocyclic

Received: January 16, 2023

Published: March 30, 2023



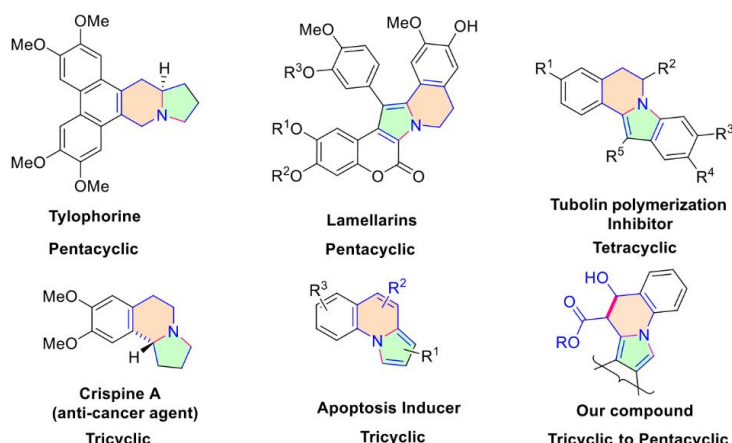
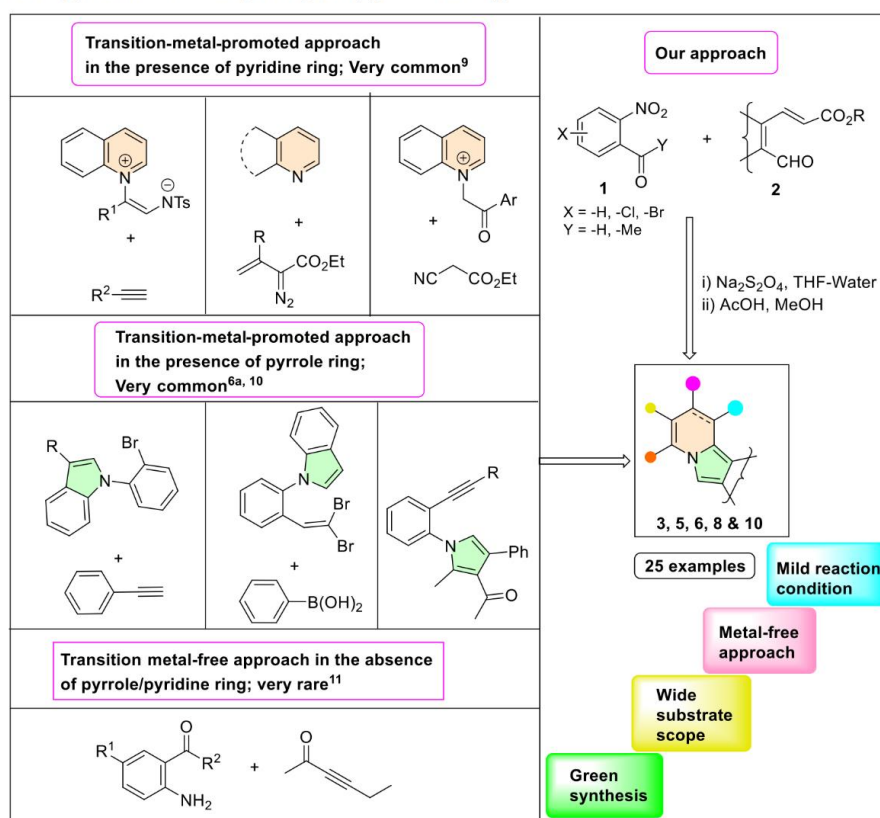


Figure 1. Naturally occurring bioactive molecules with a pyrrolo[1,2-*a*]quinoline moiety.

Scheme 1. Various Approaches of the Pyrrolo[1,2-*a*]quinoline Ring



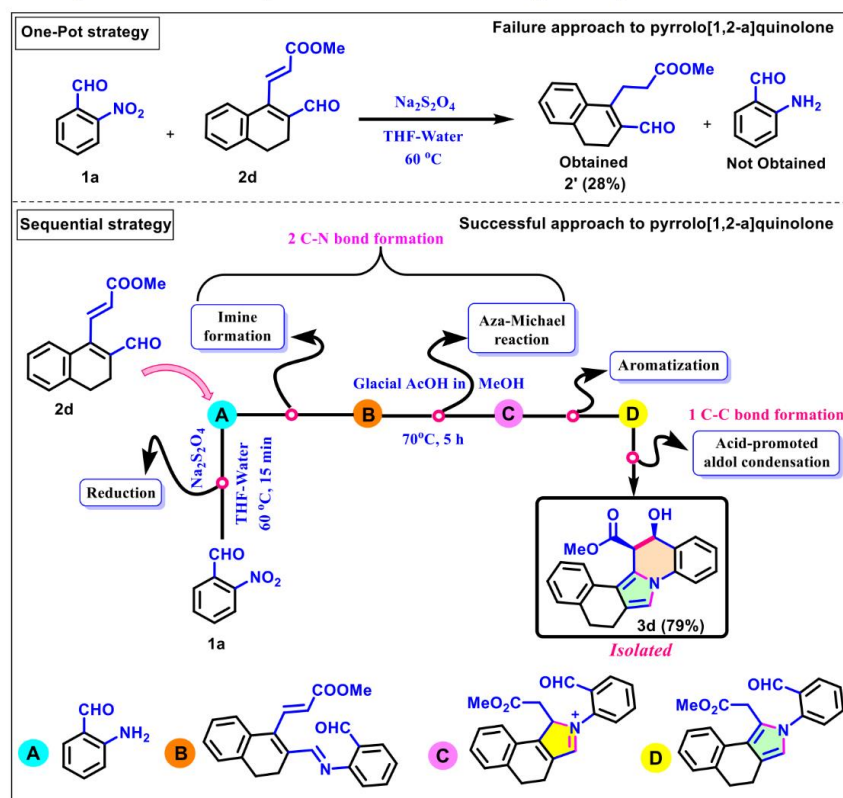
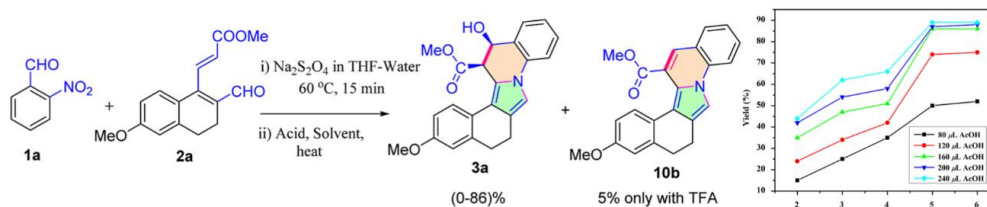
compounds by our research group.¹² In these consequences, we have taken two partners which underwent reduction/aza-Michael addition/aldol condensation smoothly to form multiple C–C and C–N bonds in a sequential reaction.

RESULTS AND DISCUSSION

From the retrosynthetic analysis, we have planned to synthesize the fused bicyclic ring structure of pyrroloquinoline

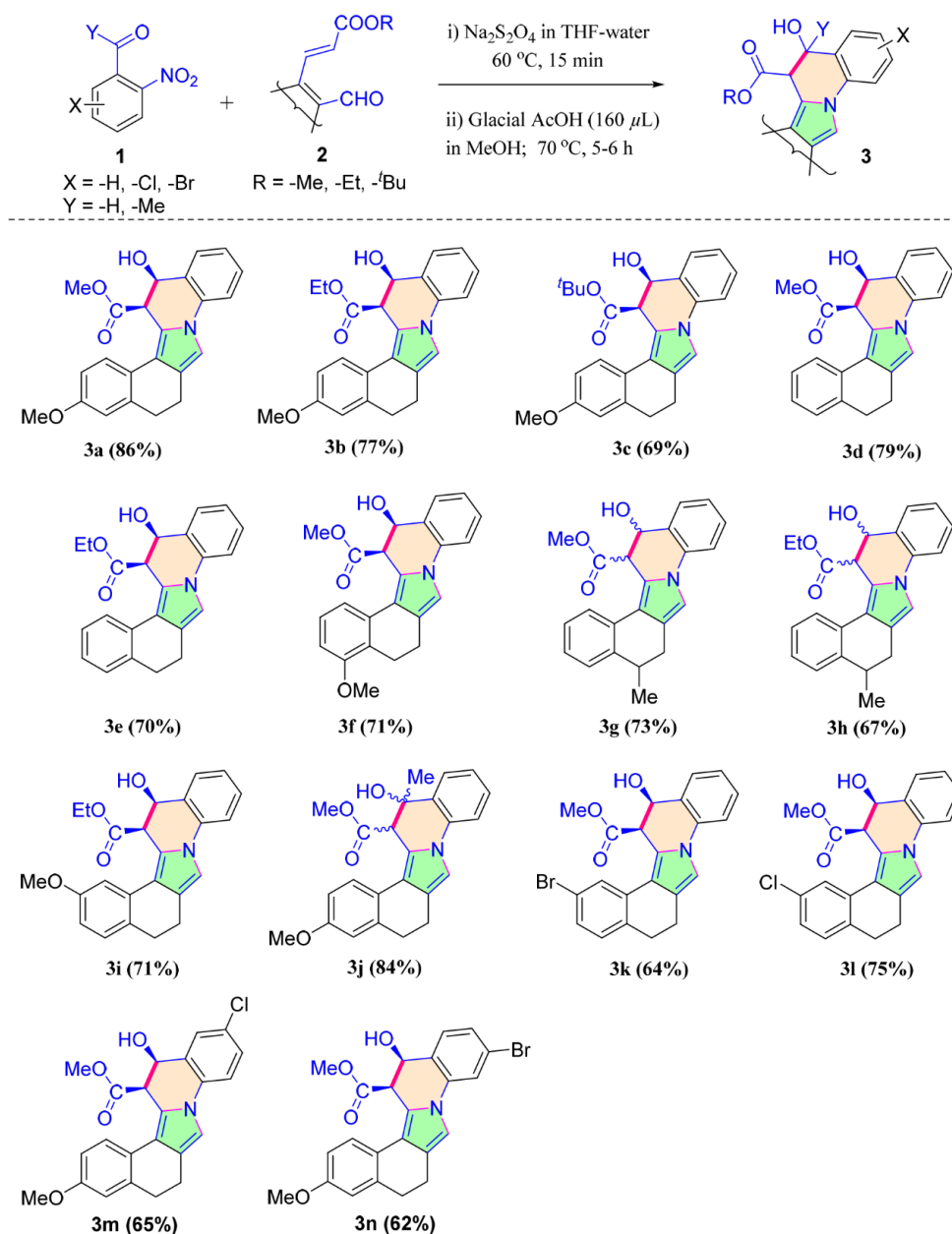
by the reaction of the easily available precursor 3-(2-formylcycloalkenyl)-acrylic ester derivative and 2-aminobenzaldehyde. However, 2-aminobenzaldehyde has a tendency for dimerization. So, we anticipated that 2-nitrobenzaldehyde could be taken as a good alternative to aminoaldehyde, and it can readily take part in reductive cyclization.¹³ Sodium dithionite is one of the popular transition-metal-free chemoselective reducing agents and it has been successfully used in the direct preparation of 2-aminoaldehyde from 2-nitro-

Scheme 2. Schematic Representation for Stepwise Formation of Our Target Compound

Table 1. Optimization of the Reaction Condition for the Synthesis of Pyrrolo[1,2-*a*]quinoline^a

sl. no	reaction conditions	temperature (°C)	time (h)	yield (%)
1	AcOH (40 μ L) in MeOH	40	8	NR
2	AcOH (40 μ L) in MeOH	70	8	NR
3	AcOH (120 μ L) in MeOH	70	6	75
4	AcOH (160 μ L) in MeOH	70	5	86
5	AcOH (240 μ L) in MeOH	70	5	87
6	AcOH (60 μ L) in neat	75	8	60
7	AcOH (160 μ L) in water	75	8	50
8	AcOH (160 μ L) in THF	70	10	45
9	AcOH (160 μ L) in 1,4-dioxane	70	7	25
10	AcOH (160 μ L) in DMF	70	12	NR
11	AcOH (160 μ L) in toluene	70	6	55
12	TFA (20 μ L) in MeOH	70	4	40
13	<i>p</i> -TsOH (0.5 equiv) in MeOH	70	6	65
14	Cu-triflate (0.5 equiv) in MeOH	70	6	54

^aReaction and conditions: substrate (i) 2-nitrobenzaldehyde **1a** (1 mmol, 1 equiv), Na₂S₂O₄ (6 mmol, 6 equiv), THF–water, 60 °C, 15 min; (ii) (*E*)-3-(2-formyl-6-methoxy-3,4-dihydronaphthalen-1-yl)acrylate **2a** (1 mmol, 1 equiv), solvent (4 mL), glacial AcOH (40–240 μ L).

Table 2. Substrate Scope of Pyrrolo[1,2-*a*]quinoline Synthesis^a

^aReaction conditions: (i) substituted 2-nitrobenzaldehyde **1** (1 mmol, 1 equiv), $\text{Na}_2\text{S}_2\text{O}_4$ (6 mmol, 6 equiv), THF–water, 60 °C, 15 min; (ii) 3-(2-formylcycloalkenyl)-acrylate derivatives **2** (1 mmol, 1 equiv), MeOH (4–5 mL), glacial AcOH (160 μL), 70 °C, 5–6 h.

benzaldehyde. Hence, we first started our mission with reductive cyclization via a tandem protocol in the presence of 2-nitrobenzaldehyde with substrate **2d** for the construction of two rings in one reaction vessel. The attempt failed to get the desired aminoaldehyde for aza-addition with substrate **2d**; instead, we have found the chemoselective reduction of the π -bond in the presence of sodium dithionite in boiling THF–H₂O to get **2'** (Scheme 2, one-pot strategy). This result further proves that sodium dithionite has a greater tendency for

reduction of the polar π -bond compared to the nitro group reduction. Next, we have planned an alternative pathway by two-pot sequential reactions where 2-nitrobenzaldehyde was first reduced to aminoaldehyde with sodium dithionite, and after aqueous work-up, it was added to the solution of substrate **2d** in methanol (Scheme 2, sequential strategy). Substrate **2d** could not be added to the reductive part of **1a** even after 24 h of reflux in methanol. However, reduction/aza-Michael/aldol reactions successfully occurred with **1a** and **2d**

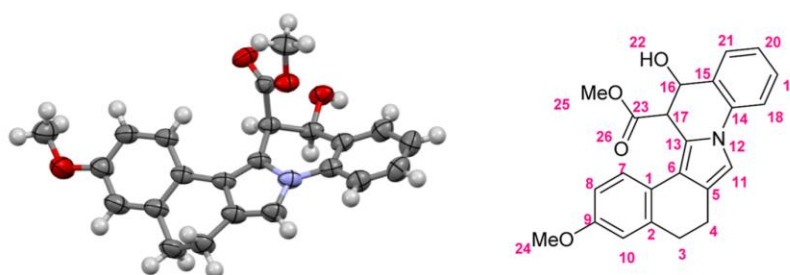
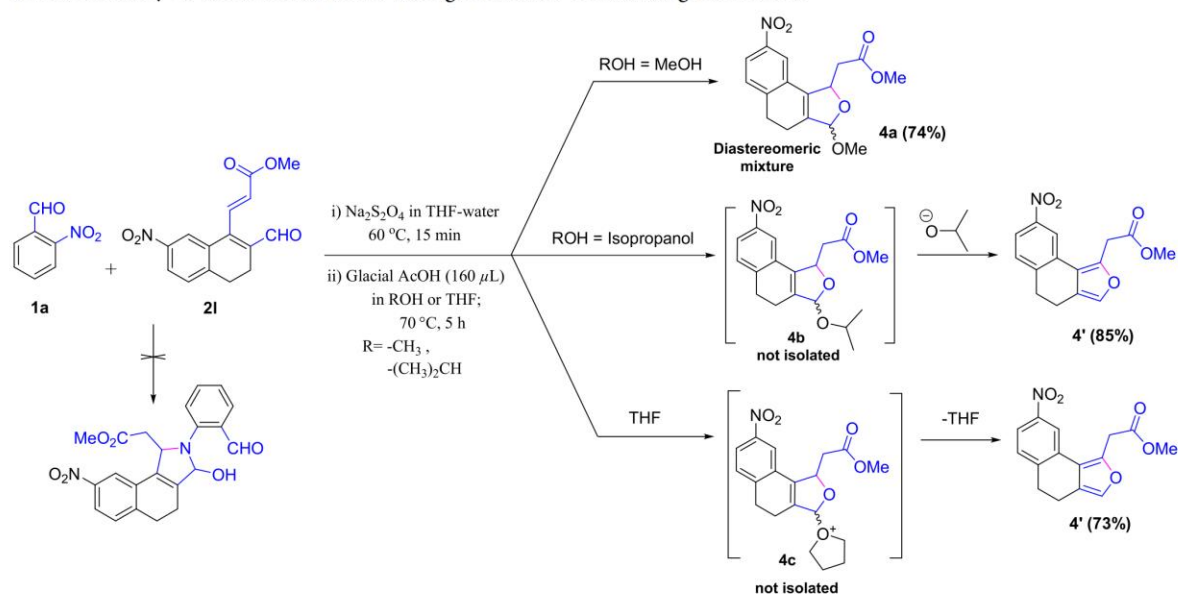


Figure 2. X-ray structure of 3a and its number-assigned structure.

Scheme 3. Study of the Reaction with a Stronger Electron-Withdrawing Substituent

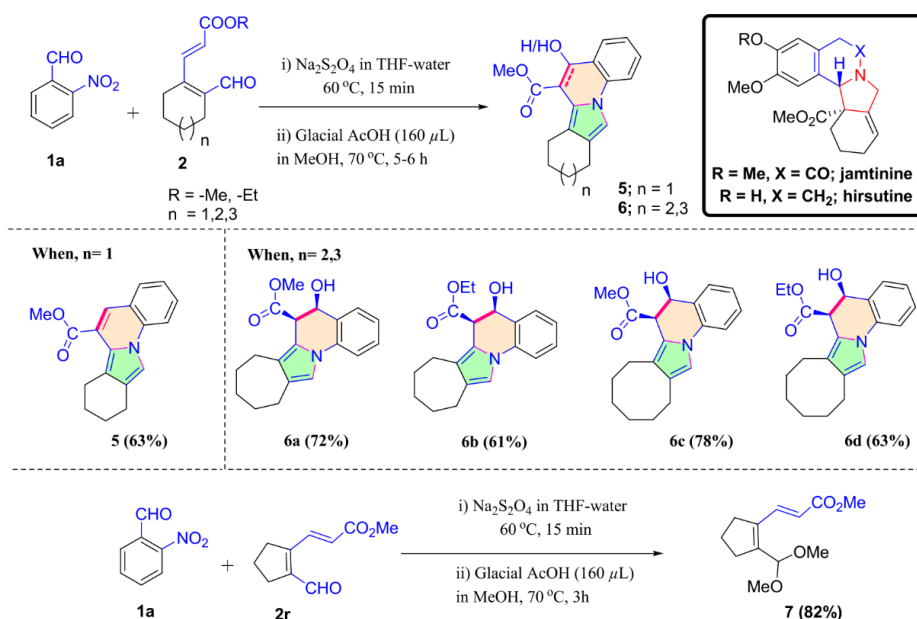


in the presence of AcOH in methanol under refluxing conditions. Hence, we have envisaged that direct construction of the pyrrole/isoindole ring along with the isoquinoline ring was carried out in a consecutive manner involving four steps (A-B-C-D) without the need for isolation and purification techniques and formed desired pyrrolo/isoindolo[1,2-*a*]-quinoline with excellent yield.

According to our hypothesis, initially, we planned to establish the tandem protocol by selecting the model substrates methyl (*E*)-3-(2-formyl-6-methoxy-3,4-dihydronaphthalen-1-yl)acrylate **2a** and 2-nitrobenzaldehyde as coupling partners. The coupling reaction was started with the addition of 40 μL of acetic acid at 40 $^{\circ}\text{C}$ or 70 $^{\circ}\text{C}$ in MeOH but did not achieve desired product **3a** (entries 1 and 2, Table 1). Interestingly, a pentacyclic angular multisubstituted isoindoloquinoline scaffold was formed with an 86% yield by the addition of 160 μL of AcOH (entry 4, Table 1). However, the yield of **3a** did not improve significantly even after the addition of 240 μL of AcOH (entry 5, Table 1). This has been confirmed by the study of the kinetics of the developed protocol with respect to the amount of AcOH (μL) used at a constant temperature (70 $^{\circ}\text{C}$) and found that the yield of the cyclized product was gradually increased up to 6 h (Table 1, graphical plot of yield vs time). With respect to the environmental concern, we

wanted to perform a reaction under solvent-free conditions by the addition of 60 μL of AcOH, but only a 60% yield of **3a** (entry 6, Table 1) was obtained. The comfortability of the developed protocol was also checked with protic, aprotic, and nonpolar solvents (e.g., water, THF, 1,4-dioxane, and toluene) in the presence of 160 μL of AcOH and found that the desired scaffolds were formed with a 25–55% yield except DMF (entry 7–11, Table 1). In the presence of trifluoroacetic acid (TFA) (20 μL) and *p*-TsOH (0.5 equiv) (entry 12–13, Table 1), the desired product was formed with 40 and 65% yields, respectively. However, in the case of TFA, a small amount of water elimination product was obtained along with **3a**. The efficiency of the cyclization reaction was also checked with the transition-metal catalyst $\text{Cu}(\text{OTf})_2$ in methanol to produce the product with a 54% yield after 6 h (entry 14, Table 1).

After the successful optimization studies, we examined the scope of the reaction using the reaction condition (entry 4, Table 1) which was supported by the corresponding kinetics study. The reactions were investigated in the presence of different substituents in the naphthyl ring of **2** using different Michael acceptors at position-1 (Table 2). The Michael and aldol addition both were unfavorable in presence of the $-\text{O}^t\text{Bu}$ group, but it becomes favorable with $-\text{OMe}$ and $-\text{OEt}$ in ester. The 5-OMe/7-OMe groups in **2** have no resonance

Table 3. Substrate Scope for the Synthesis of Tetracyclic Fused Pyrrolo[1,2-*a*]quinoline Systems^{a†}

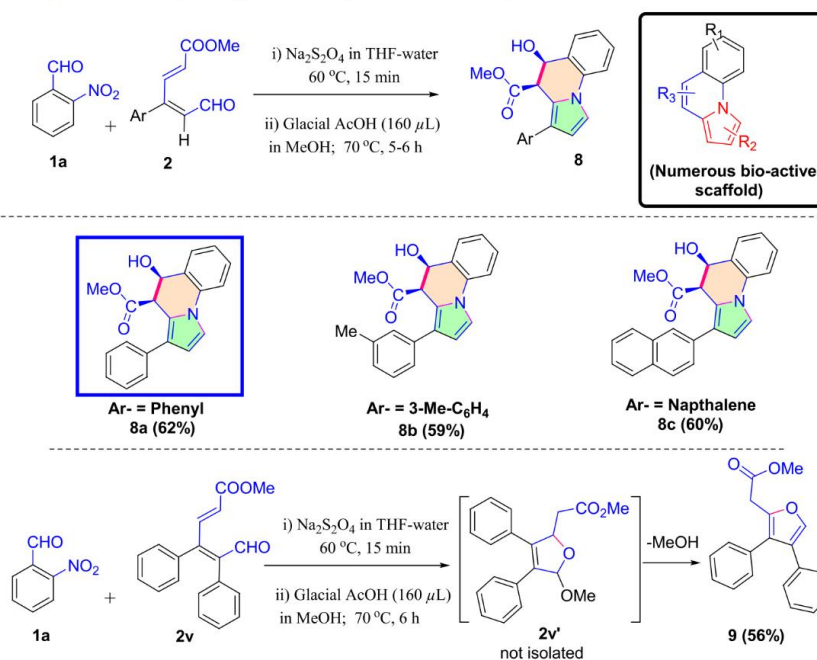
^{a†}Reaction conditions: (i) 2-nitrobenzaldehyde **1a** (1 mmol, 1 equiv), $\text{Na}_2\text{S}_2\text{O}_4$ (6 mmol, 6 equiv), THF–water, 60 °C, 15 min; (ii) 3-(2-formylcycloalkenyl)-acrylic ester derivatives **2** (1 mmol, 1 equiv), MeOH (4–5 mL), glacial AcOH (160 μL), 70 °C, 5–6 h.

effect with the C-1 substituent in the naphthyl ring, but it has an electron-withdrawing inductive effect, and hence, it shows a similar effect with 7-Br/7-Cl substituents (see the [Supporting Information](#)). They gave moderate yields of products **3f**, **3i**, **3k**, and **3l** (64–75%). This may be due to the lower rate of enolization during aldol addition in the presence of electron-withdrawing groups. Product **3** has two stereocenters which have been formed after aldol addition. Hence, there is a possibility of forming diastereoselective products during aldol addition. Our protocol exclusively furnishes only one diastereomer (see the [Supporting Information](#)) except **3g**, **3h**, and **3j**. In case of **3g** and **3h**, two diastereomeric mixtures have been observed with the ratios of 56:44 and 62:38, respectively, and it has been confirmed by NMR/HPLC analysis (see the [Supporting Information](#)). This may be due to the presence of another chiral center at the C-4 position. A diastereomeric ratio (74:26) of **3j** has been obtained due to the presence of the –COMe group instead of the –CHO group in substrate **1**. All the synthesized products are characterized by NMR and HRMS analysis. The structure of product **3a** was unambiguously confirmed by an X-ray crystallographic study ([Figure 2](#)), which reveals that two rings are formed via tandem aza-Michael–aldol reactions. From the X-ray analysis, it has been shown that **3a** compound was produced diastereoselectively. It has been further proven by HPLC analysis (see the [Supporting Information](#)). The *cis* orientation of two stereogenic centers was further supported by the series of 2D NMR (NOESY, HSQC, HMBC, and COSY; see the [Supporting Information](#)) experiments. For example, the NOESY spectrum exhibited a strong correlation between H-16 and H-17; hence, H-16/H-17 are *cis*-oriented. Spatial correlation was observed between H-7 and H-17 in NOESY; the HMBC experiment

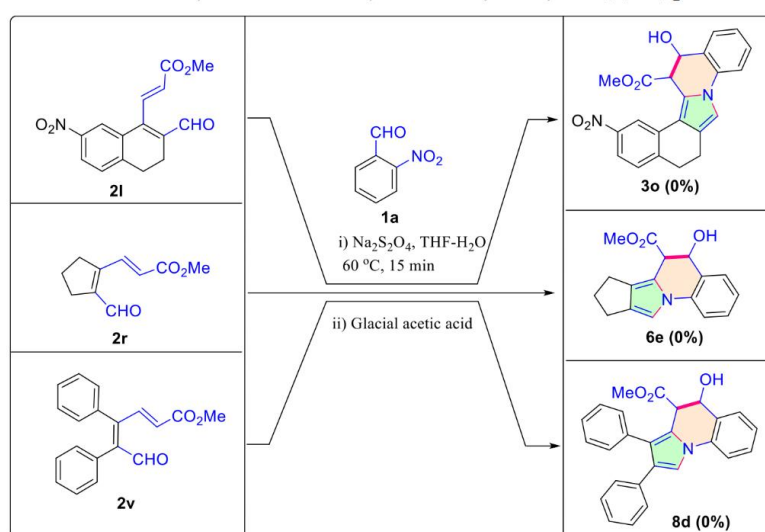
showed a strong correlation between H-17/C-16 and H-16/C-17.

To check the tolerance of our developed protocol with a stronger electron-withdrawing group, we took the –NO₂ group in the aryl ring in **2** under identical conditions, but it did not couple with **1a**; rather, it underwent intramolecular oxa-Michael addition by methanol molecules and furnished diastereomeric mixture (55:45) of dihydrofuran derivatives **4a** ([Scheme 3](#)). A similar diastereomeric mixture of **4b** and **4c** was also formed (not isolated) with the change of the solvent molecule from methanol to isopropanol or THF in the presence of AcOH which readily eliminate the added solvent molecule to form *c*-fused furan derivative **4'** with 85 and 73%, respectively. Hence, we think that the electronic effect is more prominent for inhibiting the formation of the desired product pyrrolo[1,2-*a*]quinoline, where the highly electrophilic carbonyl group of **2l** is readily attacked by the alcohol molecules compared to the less nucleophilic **1a** substrate.

To further explore the utility of our method, we wanted to examine the reaction in the cycloalkenyl system to get the tetracyclic fused pyrrolo[1,2-*a*]quinoline which has been found in biologically active natural alkaloids such as jantinine and hirsutine.¹⁴ These natural product analogues were successfully synthesized using the reductive/aza-Michael/aldol reaction under the optimized reaction condition as described in [Table 3](#). The yield of the cyclized products depends on the ring size as well as alkoxy substituents. A similar effect of the ester functionality (–OMe to –OEt) for the formation of **3** and **6** has been observed under optimized conditions (e.g., 72 to 61% for **6a–6b** and 78 to 63% for **6c–6d**) ([Table 3](#)). The cyclooctyl ring furnished better yields compared to the cycloheptyl rings, but the cyclohexyl ring deliberately eliminates the water molecules after sequential cyclization

Table 4. Substrate Scope of Pyrrolo[1,2-*a*]quinoline Synthesis from Acyclic Precursors^{a†}

^{a†}Reaction conditions: (i) 2-nitrobenzaldehyde **1a** (1 mmol, 1 equiv), $\text{Na}_2\text{S}_2\text{O}_4$ (6 mmol, 6 equiv), THF–water, 60 °C, 15 min; (ii) 3-(2-formylcycloalkenyl)-acrylic ester derivatives **2** (1 mmol, 1 equiv), MeOH (4–5 mL), glacial AcOH (160 μL), 70 °C, 5–6 h.

Scheme 4. Unsuccessful Results for the Synthesis of Pentacyclic to Tricyclic Pyrrolo[1,2-*a*]quinoline under Neat Conditions

and furnished **5** with 63% yields. From the series of results, it has been argued that lowering the ring size is uncomfortable for the aldol product formation, and hence, cyclohexyl leads to dissimilar results by the formation of stable geometry product **5** after extrusion of water. The formation of pyrrolo[1,2-*a*]quinoline became completely stopped in the case cyclopentenyl system, and it underwent acetal formation **7** in the presence of methanol and AcOH. Here, the destabilization

factor in the small ring is proven to inhibit the aza-Michael reaction with the aryl amine partner.

Besides the tetracyclic and pentacyclic scaffolds, we have further elaborated our methodology to the synthesis of tricyclic scaffolds of pyrrolo[2,1-*a*]isoquinolines which exist in different natural products and have been isolated from various sources and show diverse biological activities in the folk medicines of tropical and subtropical regions.¹⁵ These moieties have been synthesized from methyl (2*E*,4*E*)-4-aryl-6-oxohexa-2,4-dien-

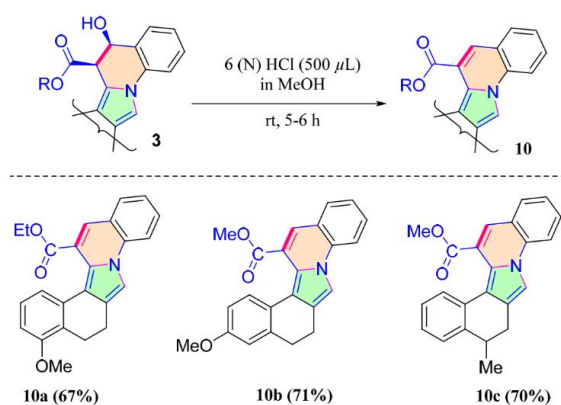
oate **2** under identical optimal conditions with 2-nitrobenzaldehyde **1a** as the coupling partner (Table 4). Yields of the tandem cyclized products were comparatively lowered than the tetracyclic or pentacyclic pyrrolo[1,2-*a*]quinoline analogues. Substrates containing Ar = Ph, 3-Me-C₆H₄, and 2-naphthyl furnished moderate yields of tricyclic derivatives (62–59%). Among them, an interesting blue fluorescence was observed for compound **8a**. Hence, a detailed photophysical study was carried out for further utilization of our product **8a**, and it is discussed in the later section. In case of substrate **2v** (4- and 5-positions are substituted with –Ph groups), oxa-Michael addition is preferable over the aza-Michael reaction and it gave 3,4-diphenyl-substituted furan **9** (56%) instead of a pyrroloquinoline derivative.

From the systematic substrate scope analysis, it has been found that substrates **2l**, **2r**, and **2v** fail to produce desired pyrrolo[1,2-*a*]quinolines under the optimized conditions (Table 1, entry 4). In all cases, MeOH takes part in the side reaction to form dihydrofuran/acetal/furan **4**, **7**, and **9** derivatives. Consequently, we anticipated that in the absence of MeOH, we may reach our goal. Hence, we applied neat conditions (Table 1, entry 6), but unfortunately, we did not get any pyrrolo[1,2-*a*]quinolines (Scheme 4).

After the successful synthesis of the pentacyclic to tricyclic embedded pyrrolo[1,2-*a*]quinoline ring, we tried to eliminate water molecules from the hydroxyl-substituted pyrroloquinoline derivatives under the standardized conditions using an increased amount of AcOH. The –OH group remains intact even after adding 600 μ L of AcOH. This result reveals that the acidity of AcOH is not sufficient to remove the water molecule. In order to obtain the dehydrated products, the hydroxyl-substituted pyrrolo[1,2-*a*]quinoline derivatives **3** were stirred at room temperature in the presence of 6 (N) HCl (500 μ L) in MeOH. It has been found that the unsaturated desired compounds **10** were obtained in 67–71% yields (Table 5).

We have added another useful feature to our developed protocol by synthesizing the ketorolac analogue. Ketorolac is a nonsteroidal anti-inflammatory drug (NSAID) that helps to reduce prostaglandin production by the cells of the immune system that causes fever and pain due to inflammation, and

Table 5. Synthetic Approach of Water-Eliminated Products of Pyrrolo[1,2-*a*]quinoline^a

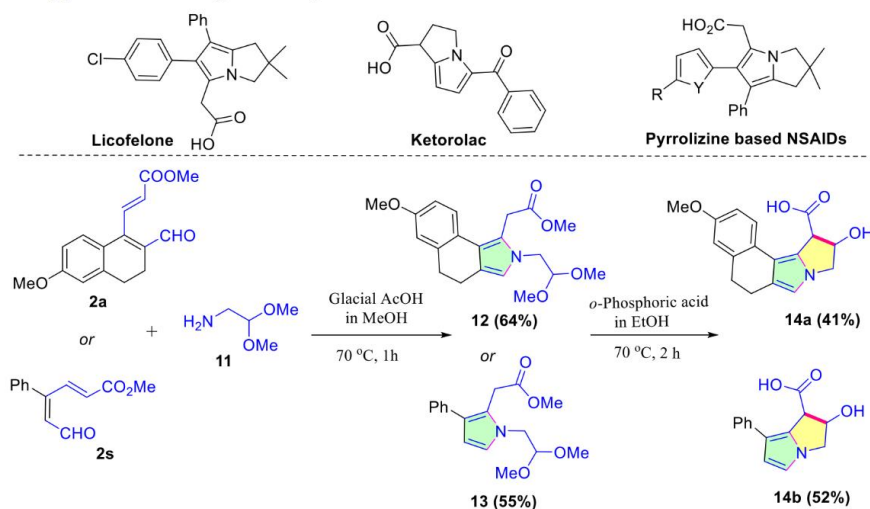


^aReaction conditions: substrate **3** (1 mmol, 1 equiv), MeOH (4–5 mL), 6 (N) HCl (500 μ L), rt, 5–6 h.

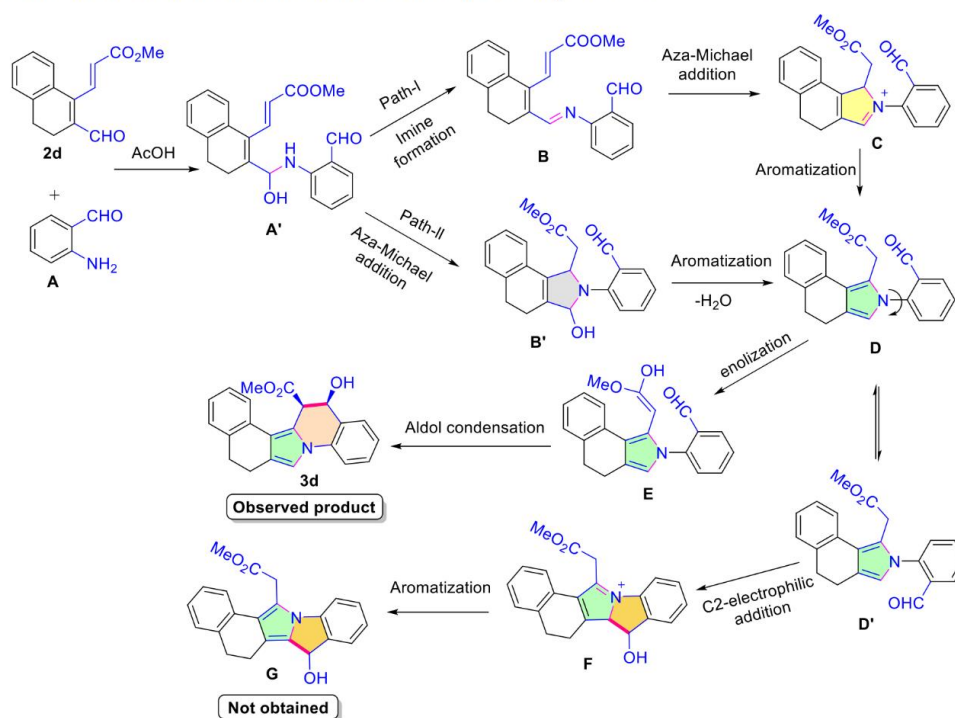
hence, it is enormously used as a pain reliever.¹⁶ However, these molecules have some adverse effects; consequently, there have been ongoing efforts to develop more effective and less toxic compounds. In this connection, we wish to synthesize such analogues by applying our developed protocol where aminoacetaldehyde dimethyl acetal is used instead of 2-nitrobenzaldehyde as the partner to react with substrate **2a**. Ketorolac is a pyrrolizine which contains one pyrrole ring attached at the C1–C2 position with another saturated analogue of the pyrrole ring. Hence, our target is to synthesize the pyrrolizine ring by the aza-Michael reaction followed by an aldol reaction using the aldehyde-protected amine partner **11** and substrate **2a** or **2s** in the presence of AcOH in MeOH at 70 °C. However, in the said conditions, we only got *c*-fused pyrrole **12** or **13** where *N*-alkyl contains aldehyde in the protected form (Table 6). The remaining aldol reaction succeeded in the presence of *o*-phosphoric acid in EtOH at 70 °C with moderate yields.

Theoretical Study of the Mechanism. The amine group of 2-aminobenzaldehyde attacks the aldehyde group of **2d** instead of at the β -position of α,β -unsaturated ester could produce the intermediate hemiaminal compound **A'**. Now, compound **A'** could convert into compound **D** in two pathways. In the first path, water elimination of **A'** gives imine **B** which can be converted to **D** through the aromatization of **C** (2*H*-pyrrol-1-ium compound) obtained from the intramolecular aza-Michael reaction of imine **B**. However, in the second path, it can be predicted that the intramolecular aza-Michael of **A'** can produce 2,5-dihydro-1*H*-pyrrole compound **B'** which could form pyrrole derivative **D** through aromatization by a water elimination reaction. It is interesting to note that compound **D** could exist in two diastereoisomeric forms (**D** and **D'**) in equilibrium by the rotation of the C–N bond. Aromatic electrophilic attack on the aldehyde group of **D'** by C2 of pyrrole produces **F** which could give the expected product **G** (not obtained). However, the obtained product **3d** could be formed through the intramolecular aldol reaction of enol **E** which was produced from **D**. The plausible mechanism is shown in Scheme 5.

A computational study on the production of the unexpected product **3d** from compounds 2-aminobenzaldehyde and **2d** has been performed here with the help of the DFT method. The reaction prefers only one reaction path and produces compound **3d** as the only product. The DFT calculation may help to understand the preference of the path. The formation of intermediate **A'** from 2-aminobenzaldehyde and **2d** is a low-energy process, and ΔG (change of free energy) involved in this process is –15.82 kcal/mol (Figure 3). From **A'**, either water elimination to give **B** ($\Delta G = 19.05$ kcal/mol) or the formation of **B'** ($\Delta G = 12.04$ kcal/mol) by intramolecular cyclization through the nucleophilic attack of an amine at the β -position of α,β -unsaturated ester is an endothermic reaction. Now, conversion of **B** to **C** ($\Delta G = -18.55$ kcal/mol) through the imine *N*-nucleophilic attack at the β -position of the α,β -unsaturated ester is favorable. Aromatization of the ionic intermediate **C** to form **D** ($\Delta G = 0.105$ kcal/mol) makes aldehyde and ester groups closer to each other. However, the same process (aromatization) of **B'** (where aldehyde and ester groups are already in close proximity) to give **D** is a favored process. Now, rotation of the N–C (phenyl) bond of **D** can produce **D'** ($\Delta G = -3.21$ kcal/mol) where the said groups are far apart from each other. Enol **E** ($\Delta G = -1.58$ kcal/mol) formation from **D** is favored

Table 6. Synthetic Approach of Analogous Compounds of Various Bioactive Natural Products^a

^aReaction conditions: (i) substrate **2a** or **2s** (1 mmol, 1 equiv), amino acetaldehyde dimethyl acetal **11** (1 mmol, 1 equiv), MeOH (4–5 mL), glacial AcOH (120 μ L), 70 $^{\circ}$ C, 1 h (ii) substrate **12** (229.8 mg) or **13** (166.7 mg), *o*-phosphoric acid (4 mL) in EtOH (4 mL), 70 $^{\circ}$ C, 2 h.

Scheme 5. Plausible Reaction Mechanism for the Formation of Compound **3d**

due to the formation of hydrogen bonds between enol hydrogen and aldehyde oxygen. Such hydrogen bonds in **E** make it susceptible to the aldol-type intramolecular attack by enol to the aldehyde which gives the product **3d** ($\Delta G = -28.02$ kcal/mol). However, the stable conformer **D'** of **D** does not undergo stabilization by hydrogen bond formation after enolization. Therefore, it can produce stable (with respect to **D'**) compound **F** ($\Delta G = -11.35$ kcal/mol) by an

intramolecular aromatic electrophilic substitution reaction at the C2 of the pyrrole ring of **D'**. The formation of **G** ($\Delta G = -0.165$ kcal/mol) from **F** is not favored, which may be due to the strain of the molecule having a reactive 1*H*-pyrrolizine ring.

Photophysical Studies. After the successful synthesis of pyrrolo[1,2-*a*]quinoline derivatives in different classes via the environmentally benign protocol, we wanted to investigate the photophysical properties of newly synthesized and highly

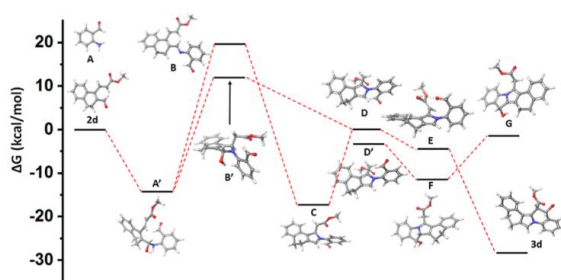


Figure 3. Energy profile diagram of the formation of 3d.

functionalized fluorescent molecules in correlation with the prevention of environmental pollution. Because of their explosive nature, nitroaromatic compounds are enormously used in chemical laboratories, mining units, chemical industries, and military training, and hence they are highly exposed to nature.¹⁷ Because of their extensive consumption, toxic nitrophenol compounds in industries regularly contaminate wastewater and eventually cause detrimental effects on living organisms even at their trace amounts. Hence, the specific recognition of such toxic materials has been developed using various methodologies based on several small-molecule sensors, nanoparticles, nanofibers, gels, polymers, metal-organic frameworks, and so forth.¹⁸ Though different techniques have been listed in the literature for the detection of nitroaromatic compounds at the micromolar level, fluorescence sensors have high demand due to their high sensitivity, cost efficiency, simple instrumentation, easy sample preparation, and quick response. Herein, we have synthesized a pyrrolo[1,2-*a*]quinoline-based sensor containing phenyl, hydroxyl, and ester functionalities which exhibited good fluorescence properties for the detection of picric acid via the quenching effect. Notably, most of the literature reports on picric acid/4-NP sensors are on their fluorescence quenching effect. To the best of our knowledge, there are no literature reports found where the fluorescence intensity of the fluorophore enhances with all analytes except picric acid which shows a quenching effect. To establish this effect, we first measured the UV-vis absorption spectra of the solution (2×10^{-5} M for **8a**; see the Supporting Information) in different solvents and found a λ_{max} around 276–293 nm, which are displayed in Table 7. Furthermore, we have measured the emission wavelength in different solvents from less-polar to highly polar solvents including the polar protic MeOH solvent (Table 7). We observed that the emission spectra are controlled by the viscosity of the solvents instead of the solvent polarity. Our synthesized fluorophore **8a** has the ability to show atropisomerism via C–C bond rotation (see the

Supporting Information), and hence, the emission intensity of the molecule was governed by the viscosity of solvents through fluorescence emission and nonradiative de-excitation.¹⁹ Restricted rotation of the C–C bond is inhibited with increasing viscosity of the solvents. Figure 4 shows the higher emission intensity of **8a** in DMSO ($\eta_{20} \text{ } ^\circ\text{C} = 1.99$ cP) and dioxane solvents ($\eta_{20} \text{ } ^\circ\text{C} = 1.17$ cP), and it exhibited similar observation in low-viscosity solvents (CHCl₃ for $\eta_{20} \text{ } ^\circ\text{C} = 0.51$ cP, CH₂Cl₂ for $\eta_{20} \text{ } ^\circ\text{C} = 0.44$ cP, MeOH for $\eta_{20} \text{ } ^\circ\text{C} = 0.54$ cP, and CH₃CN for $\eta_{20} \text{ } ^\circ\text{C} = 0.38$ cP).

Since the attached phenyl ring in pyrrolo[1,2-*a*]quinoline can freely rotate in a nonviscous solvent, in a DMSO solvent, the rotation becomes restricted and results in enhanced emission. With the addition of nonviscous toluene in a DMSO solution of **8a** (2×10^{-5} M), the emission intensity gradually decreased. This is attributed to the free rotation of the phenyl ring of the pyrrolo[1,2-*a*]quinoline derivative and the resulting nonradiative decay of the excited-state energy.

Our synthesized fluorophore has different functionalities for acid–base reactions, and the –OH group has a greater tendency to eliminate the water molecule to form a more stabilized α,β -unsaturated ester; hence, we choose some organic aromatic nitrophenol compounds that cause environmental pollution to a huge extent along with the aromatic carboxyl derivative for the acid–base interaction. To get an insight into the interaction of compounds with electron-deficient nitroaromatics and carboxylic acids, emission studies were carried out (Figure 5). The emission of **8a** displayed a significant change upon the addition of picric acid, thus making it an interesting sensor for the detection of toxic materials. The emission intensity of compound **8a** was significantly enhanced by the addition of 0.2 mL of 20 μM different nitrophenols, aromatic carboxylic acids, and TFA into a 2 mL solution of compound **8a** in CH₃CN (20 μM) except picric acid which quenched the fluorescence intensity. The disappearance of the bluish-green emission of compound **8a** was observed more effectively with picric acid, which could be visualized under a UV light of a long wavelength (lamp excitation: 365 nm) (Scheme 6).

This unusual phenomenon can be explained by the greater capability of picric acid to protonate the –OH group as well as the *N*-atom of fluorophore **8a** due to the lower pK_a (0.3) value compared to the other examined analytes. The eliminating tendency of the –OH group in the fluorophore makes it a more planar form which can strongly interact with the most electron-deficient aromatic compound via π – π interactions.²⁰ Furthermore, the higher acidity of picric acid also protonates the *N*-atom of **8a**, forming charge complexes. This also results in the excited-state energy transfer from **8a** to the picrate anion and accordingly radiation-less deactivation of the excited state

Table 7. UV-Vis Absorption and Emission Data of **8a** in Different Solvents

solvent	ϵ (25 $^\circ\text{C}$) ^a	viscosity (cP) ^b	λ_{max} (nm) ^c	λ_{emi} (nm) ^d	ϵ_{max} ($10^5 \text{ M}^{-1} \text{ cm}^{-1}$) ^e	Stokes shift (nm) ^f
1,4-dioxane	2.25	1.17	293	334	0.15	41
chloroform	4.81	0.51	277	353	1.82	76
DCM	8.93	0.449	279	337	1.67	58
MeOH	32.70	0.54	276	334	0.23	58
acetonitrile	37.5	0.38	281	333	0.16	52
DMSO	46.68	1.99	282	337	0.41	55

^aDielectric constant at 25 $^\circ\text{C}$. ^bViscosity of different solvents at 20 $^\circ\text{C}$. ^cMaximum absorption wavelength. ^dMaximum emission wavelength. ^eMolar absorption coefficient at the maximum absorption wavelength. ^fDifference between emission maxima and absorption maxima.

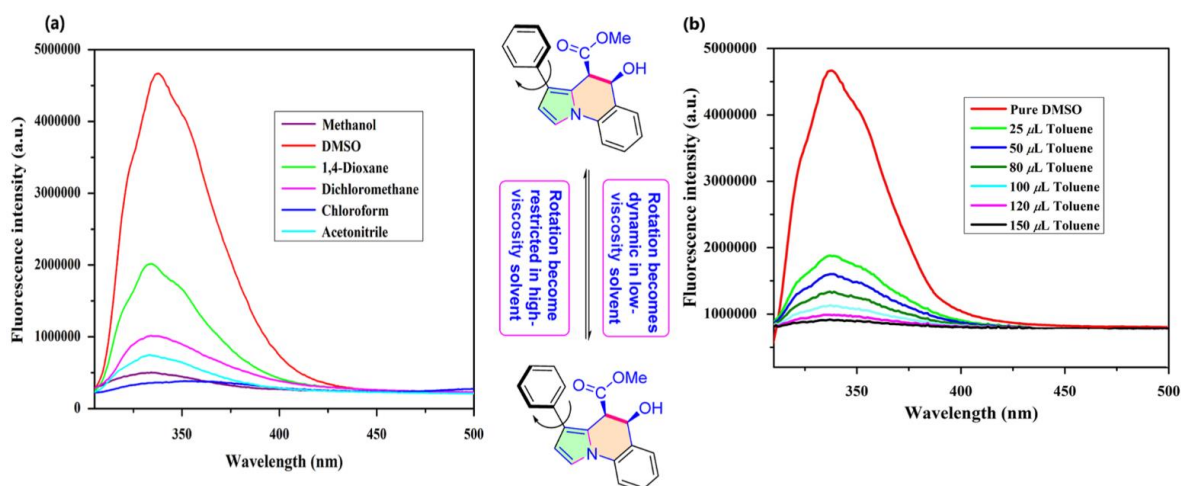


Figure 4. (a) Fluorescence spectra of **8a** recorded at a concentration of 2.0×10^{-5} M in different solvents. (b) Fluorescence quenching of **8a** by stepwise addition of toluene (μL) in a DMSO–toluene mixture.

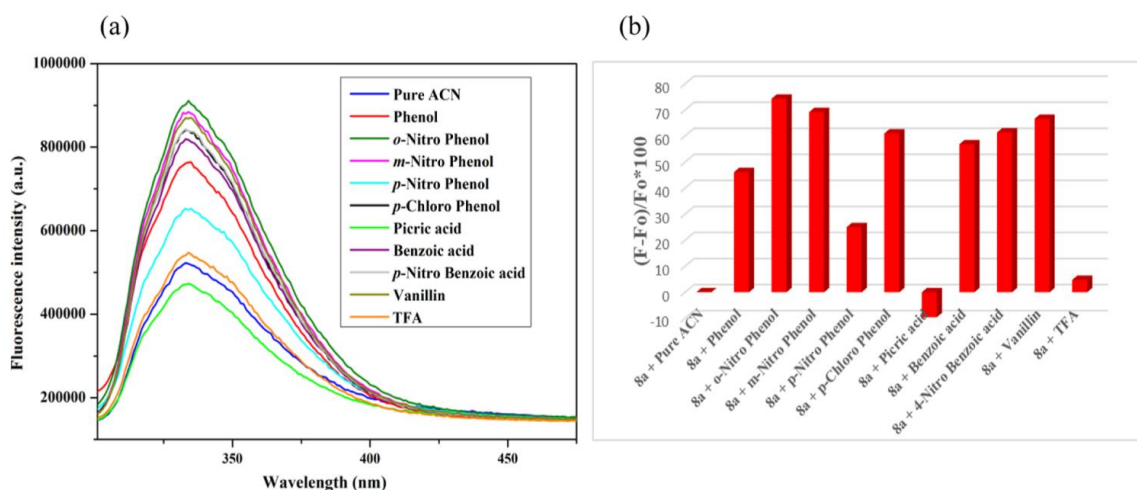


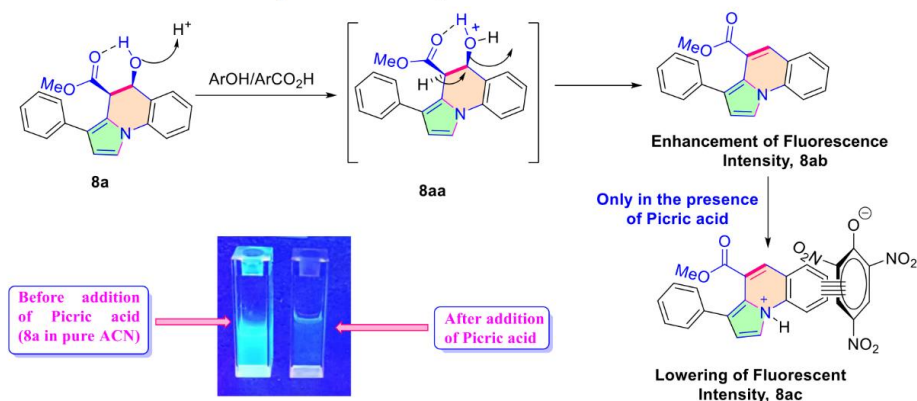
Figure 5. (a) Emission spectra of compound **8a** with different organic compounds ($\lambda_{\text{ext}} = 285$ nm) (concentration: 2×10^{-5} M solution in CH_3CN). (b) Changes in fluorescence intensity of the fluorophores **8a** [plotted as $(F - F_0)/F_0 \times 100$] observed upon the addition of various analytes.

to observe fluorescence quenching.^{12b} The acidic properties of other analytes are sufficient to interact with the $-\text{OH}$ group but not sufficient to protonate the N-atom of **8a**. Consequently, in the presence of other nitroaromatics/nitrocarboxylic acids, **8a** can form **8ab** which enhances the fluorescence intensity due to the planar and conjugated structure but cannot form **8ac** which quenches the fluorescence intensity. However, the pK_a of TFA (0.5) is very close to that of picric acid, so the enhancement of the fluorescence intensity is not so much as that of other acidic analytes. This can be attributed to the fact that picric acid has a lower pK_a value than TFA; hence, it has a stronger capability to protonate the N-atom of the pyrrole ring of **8ab** and picrate ion has extra π -electron in the aromatic ring which further interacts with the planar **8ab** and leads to the quenching effect. These observations indicate that our synthetic fluorophore **8a**

has a good capacity to detect picric acid in the presence of different nitrophenols, aromatic carboxylic acids, and TFA.

In summary, we have disclosed tandem cyclization using the Michael–aldol reaction between reductive partners of 2-nitrobenzaldehyde with 3-(2-formylcycloalkenyl)-acrylic ester derivatives with the formation of C–N and C–C bonds in one step by the elimination of the water molecule as the only byproduct. This process chronologically furnished highly substituted tri/tetra/pentacyclic pyrrolo[1,2-*a*]quinoline-embedded scaffolds with moderate to good yields. In addition, the target-oriented synthetic route of pyrrole-fused drug analogue, Toradol/Ketorol, has also been documented with the help of modified reacting aliphatic amine partners instead of 2-nitrobenzaldehyde. We have also included a detailed mechanistic observation via DFT studies with the comparison of reactivity to the addition of $-\text{CHO}$ at the C-2 position and C-5 substituents ($-\text{CH}_2\text{CO}_2\text{R}$) of the pyrrole ring. Further-

Scheme 6. Chemical Interaction of Fluorophores with Analytes



more, the photophysical application of new synthetic fluorophores and preliminary sensing properties adds a new era to our developed protocol. The broad substrate scope and the significant application of the cyclized products (drug analogue and photophysical study) reveal the potential value of this novel synthetic protocol.

EXPERIMENTAL SECTION

General Procedure for the Preparation of 3–9. The reaction was conducted in consecutive two-step procedures:

Step 1: At first 2-nitrobenzaldehyde **1** (1 mmol, 1 equiv) was reduced to 2-aminobenzaldehyde with sodium dithionite (6 mmol, 6 equiv) in THF–H₂O (1:1) at 60 °C within 15–20 min. The progress of the reaction was monitored by TLC. After completion of the reduction, the reaction mixture was diluted with EtOAc (20.0 mL) and washed with brine water (3 × 20.0 mL). The organic layer was dried (anhydrous Na₂SO₄), filtered, and concentrated under reduced pressure.

Step 2: The crude reduced product from step 1, that is, 2-aminobenzaldehyde, was added to substrate **2** (1 mmol, 1 equiv) in methanol (4–5 mL). Then, glacial AcOH (160 μL) was added to this reaction mixture. After that, the reaction mixture was allowed to stir for up to 5–6 h at 70 °C. The progress of the reaction was monitored by TLC. After the completion of the reaction, the crude mixture was neutralized with a NaHCO₃ solution (500 mg in 10 mL of water). Then, it was extracted with EtOAc (20.0 mL) followed by washing with brine water (2 × 10.0 mL), and then the solvent was removed under reduced pressure. The crude residue was purified by column chromatography (100–200 mesh of silica gel) using ethyl acetate and petroleum ether (1:5) as an eluent to get the desired products 3–9.

General Procedure for the Preparation of 10. Compound **3** (1 mmol, 1 equiv) was taken in methanol (4–5 mL), and 500 μL of 6 (N) HCl was added to this reaction mixture. The reaction mixture was allowed to stir for up to 5–6 h at room temperature. The progress of the reaction was monitored by TLC. After the formation of the desired product, the crude mixture was obtained by dilution with EtOAc (20.0 mL) followed by washing with brine water (2 × 10.0 mL). Then, it was concentrated under reduced pressure. The crude residue was purified by column chromatography (100–200 mesh of silica gel) using ethyl acetate and petroleum ether (1:10) as an eluent to get the desired product 10.

General Procedure for the Preparation of 14. This reaction was carried out in two-step procedures:

Step 1: Substrate **2a** or **2s** (1 mmol, 1 equiv) and amino acetaldehyde dimethyl acetal **11** (1 mmol, 1 equiv) in the presence of glacial AcOH (120 μL) in MeOH (4–5 mL) were taken in a reaction vessel. This reaction mixture was allowed to stir for 1 h at 70 °C. The reaction mixture was extracted with EtOAc (20 mL) followed by washing with brine water (2 × 10.0 mL). Then, the solvent was

evaporated under reduced pressure. After that, the pure *c*-fused pyrrole **12** (229.8 mg) or **13** (166.7 mg), respectively, was obtained by column chromatography (100–200 mesh of silica gel) using ethyl acetate and petroleum ether (1:5) eluents.

Step 2: Then, this *c*-fused pyrrole **12** (229.8 mg) or **13** (166.7 mg) was taken in ethanol (4 mL) and *o*-phosphoric acid (4 mL) was added into the reaction mixture. The reaction mixture was allowed to stir for up to 2 h at 70 °C. The progress of the reaction was monitored by TLC. Then, the resulting mixture was neutralized with a NaHCO₃ solution (500 mg in 10 mL of water) and it was extracted with EtOAc (20.0 mL) followed by washing with brine water (2 × 10.0 mL). After that, the solvent was removed under reduced pressure. The crude residue was purified by column chromatography (100–200 mesh silica gel) using ethyl acetate and petroleum ether (1:1) as eluents to get the desired product **14**.

Characterization of Spectral Data. *Methyl 3-(2-Formyl-3,4-dihydrobenzophthalen-1-yl)propanoate (2')*. Purified by silica gel column chromatography (eluent: petroleum ether/ethyl acetate = 20:1 to 8:1); yellow liquid, 28% yield, 68.3 mg. ¹H NMR (300 MHz, CDCl₃): δ 10.35 (s, 1H), 7.53–7.50 (m, 1H), 7.31–7.28 (m, 2H), 7.24–7.21 (m, 1H), 3.68 (s, 3H), 3.43–3.37 (m, 2H), 2.75–2.70 (m, 2H), 2.61–2.48 (m, 4H). ¹³C{¹H} NMR (76 MHz, CDCl₃): δ 190.5, 172.7, 150.5, 139.6, 134.8, 133.3, 130.3, 128.5, 127.1, 124.7, 52.0, 34.7, 27.8, 21.5, 20.2. HRMS (ESI) *m/z*: [M + H]⁺ calcd for C₁₅H₁₇O₃; 245.1179; found, 245.1181.

Methyl (13R,14R)-13-Hydroxy-3-methoxy-5,6,13,14-tetrahydrobenzo[6,7]isoindolo[2,1-a]quinoline-14-carboxylate (3a). Purified by silica gel column chromatography (eluent: petroleum ether/ethyl acetate = 20:1 to 5:1); yellow solid, 86% yield, 322.6 mg; mp 54–55 °C. ¹H NMR (300 MHz, CDCl₃): δ 7.58 (d, *J* = 7.6 Hz, 1H), 7.44 (d, *J* = 8.1 Hz, 1H), 7.23–7.19 (m, 2H), 7.13–7.08 (m, 1H), 6.91 (s, 1H), 6.74 (s, 1H), 6.73 (m, 1H), 5.02 (d, *J* = 6.0 Hz, 1H), 4.51 (d, *J* = 5.7 Hz, 1H), 3.72 (s, 3H), 3.50 (s, 3H), 2.82–2.71 (m, 2H), 2.69–2.54 (m, 2H). ¹³C{¹H} NMR (76 MHz, CDCl₃): δ 171.9, 157.8, 138.6, 134.9, 129.4, 128.4, 125.4, 124.9, 124.6, 124.4, 122.7, 120.1, 117.6, 114.9, 114.7, 112.1, 111.6, 68.0, 55.4, 52.7, 45.0, 31.5, 21.1. HRMS (ESI) *m/z*: [M + H]⁺ calcd for C₂₃H₂₂NO₄; 376.1551; found, 376.1548.

Ethyl (13R,14R)-13-Hydroxy-3-methoxy-5,6,13,14-tetrahydrobenzo[6,7]isoindolo[2,1-a]quinoline-14-carboxylate (3b). Purified by silica gel column chromatography (eluent: petroleum ether/ethyl acetate = 20:1 to 5:1); yellow solid, 77% yield, 299.6 mg; mp 52–54 °C. ¹H NMR (300 MHz, CDCl₃): δ 7.69 (d, *J* = 7.5 Hz, 1H), 7.61 (d, *J* = 8.1 Hz, 1H), 7.34–7.27 (m, 3H), 7.03 (s, 1H), 6.88–6.84 (m, 2H), 5.14–5.10 (m, 1H), 4.59 (d, *J* = 5.9 Hz, 1H), 4.06 (qd, *J* = 7.1, 1.4 Hz, 2H), 3.86 (s, 3H), 2.91–2.88 (m, 2H), 2.84–2.68 (m, 2H), 1.04 (t, *J* = 7.1 Hz, 3H). ¹³C{¹H} NMR (76 MHz, CDCl₃): δ 171.2, 157.7, 138.5, 135.1, 129.3, 128.3, 125.1, 124.6, 124.2, 122.6, 119.9, 117.7, 114.8, 114.6, 111.9, 111.5,

67.9, 61.5, 55.4, 45.4, 31.4, 21.1, 13.9. HRMS (ESI) m/z : $[M + H]^+$ calcd for $C_{24}H_{24}NO_4$, 390.1707; found, 390.1703.

tert-Butyl (13R,14R)-13-Hydroxy-3-methoxy-5,6,13,14-tetrahydrobenzo[6,7]isoindolo[2,1-a]quinoline-14-carboxylate (3c). Purified by silica gel column chromatography (eluent: petroleum ether/ethyl acetate = 15:1 to 5:1); yellow solid, 69% yield, 287.8 mg; mp 54–55 °C. 1H NMR (500 MHz, $CDCl_3$): δ 7.66 (d, J = 7.6 Hz, 1H), 7.58 (d, J = 8.2 Hz, 1H), 7.33–7.28 (m, 2H), 7.18 (td, J = 7.4, 1.4 Hz, 1H), 7.00 (s, 1H), 6.84–6.82 (m, 2H), 5.10–5.07 (m, 1H), 4.47 (d, J = 6.0 Hz, 1H), 3.84 (s, 3H), 2.89–2.67 (m, 4H), 1.20 (s, 9H). $^{13}C\{^1H\}$ NMR (126 MHz, $CDCl_3$): δ 170.3, 157.7, 138.5, 135.2, 129.6, 128.2, 125.3, 125.2, 124.8, 124.1, 122.7, 119.8, 118.4, 114.7, 114.6, 111.9, 111.2, 82.8, 68.0, 55.4, 46.4, 31.5, 27.9 (3C), 21.2. HRMS (ESI) m/z : $[M + H]^+$ calcd for $C_{26}H_{28}NO_4$, 418.2020; found, 418.2024.

Methyl (13R,14R)-13-Hydroxy-5,6,13,14-tetrahydrobenzo[6,7]isoindolo[2,1-a]quinoline-14-carboxylate (3d). Purified by silica gel column chromatography (eluent: petroleum ether/ethyl acetate = 15:1 to 5:1); yellow solid, 79% yield, 272.6 mg; mp 68–69 °C. 1H NMR (500 MHz, $CDCl_3$): δ 7.70 (d, J = 7.7 Hz, 1H), 7.61 (d, J = 7.6 Hz, 1H), 7.36–7.17 (m, 6H), 7.04 (s, 1H), 5.13–5.09 (m, 1H), 4.66 (d, J = 5.9 Hz, 1H), 3.88 (s, 1H), 3.60 (s, 3H), 2.93–2.84 (m, 3H), 2.75–2.69 (m, 1H). $^{13}C\{^1H\}$ NMR (126 MHz, $CDCl_3$): δ 171.9, 136.9, 134.9, 131.6, 129.5, 128.8, 128.5, 126.9, 125.8, 125.4, 124.6, 123.9, 123.2, 120.2, 118.7, 115.0, 111.7, 68.0, 52.7, 44.9, 31.1, 21.1. HRMS (ESI) m/z : $[M + H]^+$ calcd for $C_{22}H_{20}NO_3$, 346.1445; found, 346.1442.

Ethyl (13R,14R)-13-Hydroxy-5,6,13,14-tetrahydrobenzo[6,7]isoindolo[2,1-a]quinoline-14-carboxylate (3e). Purified by silica gel column chromatography (eluent: petroleum ether/ethyl acetate = 20:1 to 5:1); yellow solid, 70% yield, 251.4 mg; mp 66–68 °C. 1H NMR (400 MHz, $CDCl_3$): δ 7.67 (d, J = 7.6 Hz, 1H), 7.63 (d, J = 8.0 Hz, 1H), 7.34–7.27 (m, 4H), 7.18 (dt, J = 15.3, 7.4 Hz, 2H), 7.02 (s, 1H), 5.12 (s, 1H), 4.61 (d, J = 5.9 Hz, 1H), 4.05 (dt, J = 10.7, 7.1, 3.6 Hz, 2H), 3.79 (s, 1H), 2.92–2.66 (m, 4H), 1.02 (t, J = 7.1 Hz, 3H). $^{13}C\{^1H\}$ NMR (76 MHz, $CDCl_3$): δ 171.3, 136.9, 135.0, 131.7, 129.8, 129.4, 128.8, 128.4, 126.9, 125.7, 125.4, 124.5, 124.1, 123.2, 118.9, 114.9, 111.6, 68.0, 61.7, 45.2, 31.1, 21.1, 13.9. HRMS (ESI) m/z : $[M + H]^+$ calcd for $C_{23}H_{22}NO_3$, 360.1601; found, 360.1605.

Methyl (13R,14R)-13-Hydroxy-4-methoxy-5,6,13,14-tetrahydrobenzo[6,7]isoindolo[2,1-a]quinoline-14-carboxylate (3f). Purified by silica gel column chromatography (eluent: petroleum ether/ethyl acetate = 20:1 to 5:1); yellow solid, 71% yield, 266.3 mg; mp 73–75 °C. 1H NMR (500 MHz, $CDCl_3$): δ 7.69 (d, J = 7.6 Hz, 1H), 7.36–7.31 (m, 2H), 7.29–7.27 (m, 2H), 7.24–7.21 (m, 1H), 7.04 (s, 1H), 6.83–6.81 (m, 1H), 5.12–5.09 (m, 1H), 4.66 (d, J = 5.9 Hz, 1H), 3.90 (s, 3H), 3.60 (s, 3H), 3.33–3.29 (m, 1H), 2.87–2.83 (m, 1H), 2.66–2.55 (m, 2H). $^{13}C\{^1H\}$ NMR (126 MHz, $CDCl_3$): δ 171.9, 157.1, 134.9, 132.8, 129.5, 128.5, 127.1, 125.4, 124.5, 123.2, 120.2, 118.9, 117.6, 116.8, 115.1, 111.6, 108.4, 68.1, 55.7, 52.7, 45.0, 22.3, 20.4. HRMS (ESI) m/z : $[M + H]^+$ calcd for $C_{23}H_{22}NO_4$, 376.1551; found, 376.1549.

Methyl (14R)-13-Hydroxy-5-methyl-5,6,13,14-tetrahydrobenzo[6,7]isoindolo[2,1-a]quinoline-14-carboxylate (3g). Purified by silica gel column chromatography (eluent: petroleum ether/ethyl acetate = 18:1 to 5:1); yellow solid, 73% yield, 262.1 mg; mp 59–61 °C. 1H NMR (300 MHz, $CDCl_3$): δ major: 7.64 (d, J = 7.7 Hz, 2H), 7.34–7.21 (m, 6H), 6.99 (s, 1H), 5.10–5.07 (m, 1H), 4.59 (d, J = 5.9 Hz, 1H), 3.55 (s, 3H), 3.12–3.08 (m, 1H), 2.92–2.90 (m, 1H), 2.60 (dd, J = 14.8, 2.6 Hz, 1H), 1.36 (d, J = 7.1 Hz, 3H), minor: 7.56–7.54 (m, 2H), 7.18–7.11 (m, 6H), 6.98 (s, 1H), 5.05–5.02 (m, 1H), 4.63 (d, J = 5.9 Hz, 1H), 3.51 (s, 3H), 2.87–2.86 (m, 1H), 2.79 (dd, J = 14.5, 5.0 Hz, 1H), 2.42 (dd, J = 14.7, 10.9 Hz, 1H), 1.08 (d, J = 7.1 Hz, 3H). $^{13}C\{^1H\}$ NMR (76 MHz, $CDCl_3$): δ 171.9 (2C), 142.0, 141.2, 134.9 (2C), 131.3, 130.3, 129.4, 129.3 (2C), 128.5, 128.4, 128.3, 126.9, 126.7, 126.3, 126.1, 126.0, 125.5, 125.4, 124.5 (2C), 124.2, 123.9, 122.7, 121.1, 120.1, 119.4, 118.6, 118.5, 114.9, 113.0, 111.8, 67.9 (2C), 52.7 (2C), 45.1, 45.0, 35.3, 34.4, 29.5, 27.9, 21.5, 19.5. HRMS (ESI) m/z : $[M + H]^+$ calcd for $C_{23}H_{22}NO_3$, 360.1601; found, 360.1599.

Ethyl (14R)-13-Hydroxy-5-methyl-5,6,13,14-tetrahydrobenzo[6,7]isoindolo[2,1-a]quinoline-14-carboxylate (3h). Purified by silica gel column chromatography (eluent: petroleum ether/ethyl acetate = 15:1 to 5:1); yellow solid, 67% yield, 250.0 mg; mp 50–52 °C. 1H NMR (300 MHz, $CDCl_3$): δ major: 7.64 (d, J = 7.7 Hz, 2H), 7.28–7.15 (m, 6H), 7.03 (s, 1H), 5.12–5.07 (m, 1H), 4.61 (d, J = 5.9 Hz, 1H), 4.02–3.94 (m, 2H), 2.84 (dd, J = 14.5, 5.0 Hz, 1H), 2.65 (dd, J = 4.9, 2.6 Hz, 1H), 2.48 (dd, J = 14.0, 10.2 Hz, 1H), 1.13 (d, J = 7.1 Hz, 3H), 1.04 (t, J = 7.1 Hz, 3H). Minor: 7.68 (d, J = 7.1 Hz, 2H), 7.37–7.30 (m, 6H), 7.04 (s, 1H), 5.16–5.14 (m, 1H), 4.67 (d, J = 5.8 Hz, 1H), 4.09–4.04 (m, 2H), 3.16–3.12 (m, 1H), 2.93 (dd, J = 14.2, 5.2 Hz, 2H), 1.38 (d, J = 6.8 Hz, 3H), 0.97 (t, J = 7.1 Hz, 3H). $^{13}C\{^1H\}$ NMR (76 MHz, $CDCl_3$): δ 171.3 (2C), 141.9, 141.3, 135.1, 135.0, 131.4, 130.4, 129.5, 129.4, 128.4 (2C), 128.3, 126.8, 126.6, 126.4, 126.0, 125.9, 125.4 (2C), 124.5, 124.4 (2C), 124.0, 122.6, 121.0, 120.0, 119.4, 118.8, 118.7, 114.9 (2C), 112.9, 111.7, 68.1, 68.0, 61.7, 61.6, 45.3, 45.2, 35.3, 34.5, 29.4, 27.9, 21.6, 19.6, 14.0, 13.9. HRMS (ESI) m/z : $[M + H]^+$ calcd for $C_{24}H_{24}NO_3$, 374.1758; found, 374.1756.

Ethyl (13R,14R)-13-Hydroxy-2-methoxy-5,6,13,14-tetrahydrobenzo[6,7]isoindolo[2,1-a]quinoline-14-carboxylate (3i). Purified by silica gel column chromatography (eluent: petroleum ether/ethyl acetate = 20:1 to 5:1); yellow solid, 71% yield, 276.3 mg; mp 55–57 °C. 1H NMR (300 MHz, $CDCl_3$): δ 7.63 (d, J = 7.5 Hz, 1H), 7.29–7.14 (m, 5H), 6.99 (s, 1H), 6.70 (dd, J = 8.3, 2.6 Hz, 1H), 5.08–5.04 (m, 1H), 4.58 (d, J = 6.0 Hz, 1H), 4.02 (q, J = 4.8 Hz, 2H), 3.82 (s, 3H), 2.81–2.65 (m, 4H), 1.00 (t, J = 7.1 Hz, 3H). $^{13}C\{^1H\}$ NMR (76 MHz, $CDCl_3$): δ 170.9, 158.7, 134.9, 132.5, 129.8, 129.4, 129.3, 129.1, 128.3, 125.3, 124.4, 123.2, 118.8, 114.9, 111.7, 110.9, 110.1, 67.8, 61.6, 55.5, 45.4, 30.1, 21.3, 13.9. HRMS (ESI) m/z : $[M + H]^+$ calcd for $C_{24}H_{24}NO_4$, 390.1707; found, 390.1705.

Methyl (13S,14R)-13-Hydroxy-3-methoxy-13-methyl-5,6,13,14-tetrahydrobenzo[6,7]isoindolo[2,1-a]quinoline-14-carboxylate (3j). Purified by silica gel column chromatography (eluent: petroleum ether/ethyl acetate = 15:1 to 5:1); yellow solid, 84% yield, 326.8 mg; mp 44–46 °C. 1H NMR (500 MHz, $CDCl_3$): δ major: 7.55 (d, J = 8.5 Hz, 1H), 7.49 (d, J = 7.8 Hz, 1H), 7.38 (m, 2H), 7.14–7.12 (m, 1H), 7.05 (s, 1H), 6.86 (m, 2H), 4.43 (s, 1H), 3.83 (s, 3H), 3.56 (s, 3H), 2.87–2.80 (m, 4H), 1.83 (s, 3H), minor: 7.69 (d, J = 8.0 Hz, 1H), 7.62 (d, J = 8.4 Hz, 1H), 7.30–7.28 (m, 2H), 7.20–7.18 (m, 1H), 6.99 (s, 1H), 6.83 (s, 2H), 4.34 (s, 1H), 3.84 (s, 3H), 3.59 (s, 3H), 2.71–2.61 (m, 4H), 1.32 (s, 3H). $^{13}C\{^1H\}$ NMR (126 MHz, $CDCl_3$): δ 172.3, 170.4, 157.8, 138.6, 138.5, 135.4, 134.4, 133.9, 129.6, 129.5, 128.3, 125.5, 125.4, 125.0, 124.8, 124.7, 124.6, 124.5, 124.1, 122.9, 122.7, 121.6, 120.5, 118.1, 117.3, 116.9, 115.6, 115.0, 114.7 (2C), 114.1, 112.1, 111.5 (2C), 71.9, 69.7, 55.4 (2C), 52.9 (2C), 52.7, 52.4, 52.3, 50.8, 31.5, 31.4, 24.3, 21.1. HRMS (ESI) m/z : $[M + H]^+$ calcd for $C_{24}H_{24}NO_4$, 390.1707; found, 390.1705.

Methyl (13R,14R)-2-Bromo-13-hydroxy-5,6,13,14-tetrahydrobenzo[6,7]isoindolo[2,1-a]quinoline-14-carboxylate (3k). Purified by silica gel column chromatography (eluent: petroleum ether/ethyl acetate = 20:1 to 10:1); yellow solid, 64% yield, 270.7 mg; mp 114–116 °C. 1H NMR (300 MHz, $CDCl_3$): δ 7.78 (d, J = 2.1 Hz, 1H), 7.70 (d, J = 7.5 Hz, 1H), 7.35–7.24 (m, 4H), 7.13 (d, J = 8.1 Hz, 1H), 7.03 (s, 1H), 5.13 (dd, J = 10.4, 5.7 Hz, 1H), 4.61 (d, J = 5.8 Hz, 1H), 3.81 (d, J = 10.5 Hz, 1H), 3.64 (s, 3H), 2.88–2.65 (m, 4H). $^{13}C\{^1H\}$ NMR (76 MHz, $CDCl_3$): δ 171.5, 135.6, 134.6, 133.7, 130.2, 129.6, 128.5, 128.4, 126.8, 125.5, 124.9, 122.9, 120.5, 119.2, 119.1, 115.1, 111.9, 67.9, 52.8, 44.8, 30.6, 20.8. HRMS (ESI) m/z : $[M + H]^+$ calcd for $C_{22}H_{19}BrNO_3$, 424.0550; found, 424.0550.

Methyl (13R,14R)-2-Chloro-13-hydroxy-5,6,13,14-tetrahydrobenzo[6,7]isoindolo[2,1-a]quinoline-14-carboxylate (3l). Purified by silica gel column chromatography (eluent: petroleum ether/ethyl acetate = 20:1 to 8:1); yellow solid, 75% yield, 284.3 mg; mp 119–121 °C. 1H NMR (300 MHz, $CDCl_3$): δ 7.72 (d, J = 7.7 Hz, 1H), 7.64 (d, J = 2.1 Hz, 1H), 7.37–7.21 (m, 4H), 7.15 (dd, J = 8.1, 2.1 Hz, 1H), 7.06 (s, 1H), 5.15 (dd, J = 10.0, 5.9 Hz, 1H), 4.64 (d, J = 5.9 Hz, 1H), 3.87 (d, J = 10.7 Hz, 1H), 3.66 (s, 3H), 2.89–2.81 (m, 3H), 2.73–2.68 (m, 1H). $^{13}C\{^1H\}$ NMR (76 MHz, $CDCl_3$): δ 171.5, 135.1, 134.7, 133.2, 132.4, 129.9, 129.5, 128.5, 125.5 (2C), 124.9,

123.9, 122.9, 119.3, 119.1, 115.1, 111.9, 67.9, 52.7, 44.8, 30.5, 20.9. HRMS (ESI) m/z : $[M + H]^+$ calcd for $C_{22}H_{19}ClNO_3$, 380.1055; found, 380.1053.

Methyl (13R,14R)-11-Chloro-13-hydroxy-3-methoxy-5,6,13,14-tetrahydrobenzo[6,7]isoindolo[2,1-a]quinoline-14-carboxylate (3m). Purified by silica gel column chromatography (eluent: petroleum ether/ethyl acetate = 20:1 to 6:1); off-white solid, 65% yield, 265.9 mg; mp 172–173 °C. 1H NMR (300 MHz, $CDCl_3$): δ 7.66 (s, 1H), 7.52 (d, $J = 7.5$ Hz, 1H), 7.29–7.18 (m, 2H), 6.96 (s, 1H), 6.85–6.82 (m, 2H), 5.09–5.04 (m, 1H), 4.59 (d, $J = 5.9$ Hz, 1H), 3.84 (s, 3H), 3.80 (s, 1H), 3.61 (s, 3H), 2.90–2.64 (m, 4H). $^{13}C\{^1H\}$ NMR (76 MHz, $CDCl_3$): δ 171.7, 157.9, 138.7, 133.6, 131.2, 129.9, 128.4, 125.9, 125.0, 124.3, 123.1, 120.4, 117.3, 116.2, 114.7, 112.1, 111.7, 67.7, 55.4, 52.8, 44.8, 31.4, 21.1. HRMS (ESI) m/z : $[M + H]^+$ calcd for $C_{23}H_{21}ClNO_4$, 410.1161; found, 410.1158.

Methyl (13R,14R)-10-Bromo-13-hydroxy-3-methoxy-5,6,13,14-tetrahydrobenzo[6,7]isoindolo[2,1-a]quinoline-14-carboxylate (3n). Purified by silica gel column chromatography (eluent: petroleum ether/ethyl acetate = 20:1 to 5:1); yellow solid, 62% yield, 280.8 mg; mp 153–155 °C. 1H NMR (300 MHz, $CDCl_3$): δ 7.53 (t, $J = 7.2$ Hz, 2H), 7.42 (s, 1H), 7.30 (d, $J = 8.2$ Hz, 1H), 6.96 (s, 1H), 6.85–6.82 (s, 2H), 5.06–5.01 (m, 1H), 4.58 (d, $J = 5.9$ Hz, 1H), 3.84 (s, 3H), 3.77 (d, $J = 10.3$ Hz, 1H), 3.61 (s, 3H), 2.88–2.64 (m, 4H). $^{13}C\{^1H\}$ NMR (76 MHz, $CDCl_3$): δ 171.8, 158.0, 138.7, 136.1, 128.4, 127.2 (2C), 125.1, 124.2, 123.4, 121.9, 120.6, 118.1, 117.6, 114.7, 112.2, 111.7, 67.8, 55.4, 52.8, 44.8, 31.3, 21.0. HRMS (ESI) m/z : $[M + H]^+$ calcd for $C_{23}H_{21}BrNO_4$, 454.0656; found, 454.0652.

Methyl 2-(3-Methoxy-8-nitro-2,3,4,5-tetrahydro-1H-cyclopenta[*a*]naphthalen-1-yl)acetate (4a). Purified by silica gel column chromatography (eluent: petroleum ether/ethyl acetate = 10:1 to 3:1); brown liquid, 74% yield, 236.1 mg. 1H NMR (300 MHz, $DMSO-d_6$): δ major: 8.08 (d, $J = 1.9$ Hz, 1H), 7.81 (d, $J = 2.4$ Hz, 1H), 7.54–7.53 (m, 1H), 5.83 (d, $J = 4.0$ Hz, 1H), 5.63 (s, 1H), 3.61 (s, 3H), 3.20 (s, 3H), 3.06–2.98 (m, 3H), 2.49–2.44 (m, 3H). minor: 8.05 (d, $J = 2.1$ Hz, 1H), 7.79 (d, $J = 2.3$ Hz, 1H), 7.52–7.51 (m, 1H), 5.68–5.65 (m, 1H), 5.51–5.47 (m, 1H), 3.64 (s, 3H), 3.31 (s, 3H), 2.95–2.90 (m, 3H), 2.42–2.40 (m, 3H). $^{13}C\{^1H\}$ NMR (76 MHz, $DMSO-d_6$): δ 170.6 (2C), 146.6, 144.2, 137.5 (2C), 135.9, 135.8, 130.2, 130.1, 129.2 (2C), 122.9, 122.8, 117.3, 117.2, 108.4, 108.2, 80.4, 79.7, 78.8, 75.3, 53.7, 52.6, 51.6 (2C), 40.9, 39.9, 27.9, 27.8, 19.4, 19.0. HRMS (ESI) m/z : $[M + Na]^+$ calcd for $C_{16}H_{17}NO_6Na$, 342.0954; found, 342.0956.

Methyl 2-(8-Nitro-4,5-dihydronaphtho[1,2-*c*]furan-1-yl)acetate (4'). Purified by silica gel column chromatography (eluent: petroleum ether/ethyl acetate = 30:1 to 10:1); yellow liquid, 85% yield, 244.0 mg and 73% yield, 209.5 mg for 2-propanol and THF respectively. 1H NMR (300 MHz, $CDCl_3$): δ 8.39 (d, $J = 2.5$ Hz, 1H), 8.04 (dd, $J = 8.3, 2.5$ Hz, 1H), 7.41 (d, $J = 8.3$ Hz, 1H), 7.27 (s, 1H), 3.99 (s, 2H), 3.81 (s, 3H), 2.99–2.95 (m, 2H), 2.76–2.72 (m, 2H). $^{13}C\{^1H\}$ NMR (76 MHz, $CDCl_3$): δ 169.4, 147.4, 144.3, 143.4, 136.2, 131.1, 129.6, 122.3, 121.5, 119.1, 118.6, 52.8, 34.3, 30.8, 18.8. HRMS (ESI) m/z : $[M + H]^+$ calcd for $C_{15}H_{14}NO_5$, 288.0874; found, 288.0874.

Methyl 7,8,9,10-Tetrahydroisoindolo[2,1-*a*]quinoline-6-carboxylate (5). Purified by silica gel column chromatography (eluent: petroleum ether/ethyl acetate = 30:1 to 20:1); yellow solid, 63% yield, 175.8 mg; mp 84–86 °C. 1H NMR (300 MHz, $CDCl_3$): δ 7.76 (d, $J = 8.4$ Hz, 1H), 7.67–7.61 (m, 2H), 7.53 (ddd, $J = 8.5, 7.2, 1.5$ Hz, 1H), 7.37 (s, 1H), 7.28–7.23 (m, 1H), 3.97 (s, 3H), 2.84–2.82 (m, 4H), 1.85–1.81 (m, 4H). $^{13}C\{^1H\}$ NMR (76 MHz, $CDCl_3$): δ 167.6, 134.1, 129.6 (2C), 125.8, 123.4, 123.3, 122.7, 121.9, 121.5, 114.6, 113.9, 109.3, 52.3, 24.2, 23.9, 23.5, 22.9. HRMS (ESI) m/z : $[M + H]^+$ calcd for $C_{18}H_{18}NO_2$, 280.1339; found, 280.1337.

Methyl (5R,6R)-5-Hydroxy-6,7,8,9,10,11-hexahydro-5H-cyclohepta[3,4]pyrrolo[1,2-*a*]quinoline-6-carboxylate (6a). Purified by silica gel column chromatography (eluent: petroleum ether/ethyl acetate = 25:1 to 10:1); yellow solid, 72% yield, 224.0 mg; mp 110–112 °C. 1H NMR (300 MHz, $CDCl_3$): δ 7.67 (d, $J = 7.6$ Hz, 1H), 7.31–7.28 (m, 1H), 7.22–7.12 (m, 2H), 6.91 (s, 1H), 5.12–5.06 (m, 1H), 4.26 (d, $J = 5.9$ Hz, 1H), 3.82–3.76 (m, 1H), 3.58 (s, 3H), 2.63–2.59 (m, 4H), 1.89–1.82 (m, 3H), 1.69–1.68 (m, 3H).

$^{13}C\{^1H\}$ NMR (76 MHz, $CDCl_3$): δ 172.1, 134.9, 128.9, 128.3, 128.2, 125.6, 125.4, 123.9, 119.4, 114.4, 112.4, 67.8, 52.4, 43.5, 33.1, 30.1, 29.6, 28.4, 26.7. HRMS (ESI) m/z : $[M + H]^+$ calcd for $C_{19}H_{22}NO_3$, 312.1601; found, 312.1599.

Ethyl (5R,6R)-5-Hydroxy-6,7,8,9,10,11-hexahydro-5H-cyclohepta[3,4]pyrrolo[1,2-*a*]quinoline-6-carboxylate (6b). Purified by silica gel column chromatography (eluent: petroleum ether/ethyl acetate = 25:1 to 10:1); yellow solid, 61% yield, 198.3 mg; mp 116–118 °C. 1H NMR (500 MHz, $CDCl_3$): δ 7.66 (d, $J = 7.7$ Hz, 1H), 7.29–7.27 (m, 1H), 7.20 (d, $J = 7.9$ Hz, 1H), 7.14 (t, $J = 7.5$ Hz, 1H), 6.90 (s, 1H), 5.08 (dd, $J = 10.1, 5.7$ Hz, 1H), 4.24 (d, $J = 6.0$ Hz, 1H), 4.10–3.94 (m, 2H), 3.74 (d, $J = 11.1$ Hz, 1H), 2.62–2.61 (m, 5H), 1.86–1.84 (m, 2H), 1.70–1.64 (m, 3H), 1.12 (t, $J = 7.1$ Hz, 3H). $^{13}C\{^1H\}$ NMR (126 MHz, $CDCl_3$): δ 171.6, 134.9, 129.0, 128.3, 128.2, 125.6, 125.4, 123.8, 119.6, 114.3, 112.3, 67.8, 61.3, 43.7, 33.2, 30.1, 29.7, 28.4, 26.7, 14.0. HRMS (ESI) m/z : $[M + H]^+$ calcd for $C_{20}H_{24}NO_3$, 326.1758; found, 326.1760.

Methyl (5R,6R)-5-Hydroxy-5,6,7,8,9,10,11,12-octahydrocycloocta[3,4]pyrrolo[1,2-*a*]quinoline-6-carboxylate (6c). Purified by silica gel column chromatography (eluent: petroleum ether/ethyl acetate = 20:1 to 5:1); yellow solid, 78% yield, 253.6 mg; mp 108–109 °C. 1H NMR (500 MHz, $CDCl_3$): δ 7.64 (d, $J = 7.5$ Hz, 1H), 7.29–7.28 (m, 1H), 7.22 (d, $J = 8.1$ Hz, 1H), 7.14 (t, $J = 7.5$ Hz, 1H), 6.90 (s, 1H), 5.05 (s, 1H), 4.22 (d, $J = 5.8$ Hz, 1H), 3.82 (m, 1H), 3.55 (s, 3H), 2.65–2.56 (m, 4H), 1.65–1.58 (m, 4H), 1.47 (s, 4H). $^{13}C\{^1H\}$ NMR (126 MHz, $CDCl_3$): δ 172.2, 135.0, 128.9, 128.3, 126.4, 125.5, 123.9, 123.4, 119.5, 114.4, 112.5, 67.9, 52.3 (2C), 43.7, 32.3, 30.5, 25.9, 24.3, 22.6. HRMS (ESI) m/z : $[M + H]^+$ calcd for $C_{20}H_{24}NO_3$, 326.1758; found, 326.1755.

Ethyl (5R,6R)-5-Hydroxy-5,6,7,8,9,10,11,12-octahydrocycloocta[3,4]pyrrolo[1,2-*a*]quinoline-6-carboxylate (6d). Purified by silica gel column chromatography (eluent: petroleum ether/ethyl acetate = 30:1 to 20:1); pale-yellow liquid, 63% yield, 213.6 mg. 1H NMR (300 MHz, $CDCl_3$): δ 7.64 (d, $J = 7.6$ Hz, 1H), 7.28–7.20 (m, 2H), 7.13 (td, $J = 7.5, 1.4$ Hz, 1H), 6.89 (s, 1H), 5.04 (dd, $J = 10.8, 5.7$ Hz, 1H), 4.18 (d, $J = 5.7$ Hz, 1H), 4.08–3.92 (m, 2H), 3.81 (d, $J = 10.8$ Hz, 1H), 2.63–2.54 (m, 4H), 1.62 (s, 4H), 1.47–1.46 (m, 4H), 1.07 (t, $J = 7.1$ Hz, 3H). $^{13}C\{^1H\}$ NMR (76 MHz, $CDCl_3$): δ 171.8, 135.1, 129.2, 128.3, 126.4, 125.5, 123.8, 123.2, 119.7, 114.4, 112.4, 68.1, 61.4, 43.8, 32.4, 30.5, 25.9 (2C), 24.4, 22.6, 14.0. HRMS (ESI) m/z : $[M + H]^+$ calcd for $C_{21}H_{26}NO_3$, 340.1914; found, 340.1910.

Methyl (E)-3-(2-(Dimethoxymethyl)cyclopent-1-en-1-yl)acrylate (7). Purified by silica gel column chromatography (eluent: petroleum ether/ethyl acetate = 30:1 to 20:1); pale-yellow liquid, 82% yield, 185.4 mg. 1H NMR (300 MHz, $CDCl_3$): δ 7.75 (d, $J = 15.6$ Hz, 1H), 5.79 (d, $J = 15.6$ Hz, 1H), 5.14 (s, 1H), 3.72 (s, 3H), 3.31 (s, 6H), 2.55–2.54 (m, 4H), 1.92–1.81 (m, 2H). $^{13}C\{^1H\}$ NMR (76 MHz, $CDCl_3$): δ 167.8, 146.7, 137.6, 137.5, 119.4, 100.6, 53.9 (2C), 51.6, 33.7, 33.1, 21.5. HRMS (ESI) m/z : $[M + Na]^+$ calcd for $C_{12}H_{18}O_4Na$, 249.1102; found, 249.1104.

Methyl (4R,5R)-5-Hydroxy-3-phenyl-4,5-dihydropyrrolo[1,2-*a*]quinoline-4-carboxylate (8a). Purified by silica gel column chromatography (eluent: petroleum ether/ethyl acetate = 15:1 to 5:1); yellow solid, 62% yield, 197.8 mg; mp 41–43 °C. 1H NMR (300 MHz, $CDCl_3$): δ 7.70 (dd, $J = 7.6, 1.0$ Hz, 1H), 7.51–7.27 (m, 9H), 6.53 (d, $J = 3.1$ Hz, 1H), 5.09–5.07 (m, 1H), 4.44 (d, $J = 5.6$ Hz, 1H), 3.58 (s, 3H). $^{13}C\{^1H\}$ NMR (76 MHz, $CDCl_3$): δ 172.2, 135.4, 135.0, 129.8, 128.8 (2C), 128.6, 127.8 (2C), 126.5, 125.8, 125.0, 124.9, 120.5, 116.6, 115.2, 110.7, 68.4, 52.7, 44.3. HRMS (ESI) m/z : $[M + H]^+$ calcd for $C_{20}H_{18}NO_3$, 320.1288; found, 320.1282.

Methyl (4R,5R)-5-Hydroxy-3-(*m*-tolyl)-4,5-dihydropyrrolo[1,2-*a*]quinoline-4-carboxylate (8b). Purified by silica gel column chromatography (eluent: petroleum ether/ethyl acetate = 15:1 to 5:1); yellow liquid, 59% yield, 196.5 mg. 1H NMR (300 MHz, $CDCl_3$): δ 7.70 (d, $J = 8.3$ Hz, 1H), 7.38–7.37 (m, 2H), 7.33–7.31 (m, 3H), 7.27–7.25 (m, 3H), 6.53 (d, $J = 3.0$ Hz, 1H), 5.09 (s, 1H), 4.45 (d, $J = 5.6$ Hz, 1H), 3.58 (s, 3H), 2.43 (s, 3H). $^{13}C\{^1H\}$ NMR (76 MHz, $CDCl_3$): δ 172.2, 138.3, 135.3, 134.9, 129.8, 129.3, 128.7, 128.6, 127.2, 125.7, 124.9 (2C), 120.4, 120.2, 116.6, 115.2, 110.8,

68.3, 52.7, 44.3, 21.7. HRMS (ESI) m/z : $[M + H]^+$ calcd for $C_{21}H_{20}NO_3$, 334.1445; found, 334.1444.

Methyl (R)-5-Hydroxy-3-(naphthalen-2-yl)-4,5-dihydropyrrolo[1,2-a]quinoline-4-carboxylate (8c). Purified by silica gel column chromatography (eluent: petroleum ether/ethyl acetate = 15:1 to 7:1); yellow liquid, 60% yield, 221.4 mg. 1H NMR (300 MHz, $CDCl_3$): δ 7.95 (d, J = 5.4 Hz, 1H), 7.91–7.88 (m, 2H), 7.74–7.66 (m, 2H), 7.56–7.50 (m, 2H), 7.42–7.40 (m, 1H), 7.33 (d, J = 3.1 Hz, 1H), 7.30–7.27 (m, 3H), 6.66 (d, J = 3.0 Hz, 1H), 5.11 (s, 1H), 4.55 (d, J = 5.6 Hz, 1H), 3.61 (s, 3H). $^{13}C\{^1H\}$ NMR (76 MHz, $CDCl_3$): δ 172.1, 134.9, 133.8, 129.8, 129.3 (2C), 128.9, 128.7, 128.2, 127.8, 127.2, 126.3, 125.9, 125.1, 124.5, 124.4, 124.2, 120.2, 117.6, 115.3, 110.9, 68.3, 52.7, 44.5. HRMS (ESI) m/z : $[M + H]^+$ calcd for $C_{24}H_{20}NO_3$, 370.1445; found, 370.1444.

Methyl 2-(3,4-Diphenylfuran-2-yl)acetate (9). Purified by silica gel column chromatography (eluent: petroleum ether/ethyl acetate = 15:1 to 5:1); yellow solid, 56% yield, 163.5 mg; mp 45–47 °C. 1H NMR (300 MHz, $CDCl_3$): δ 7.60 (s, 1H), 7.38–7.35 (m, 3H), 7.30–7.23 (m, 5H), 7.18 (dd, J = 7.2, 2.6 Hz, 2H), 3.79 (s, 3H), 3.75 (s, 2H). $^{13}C\{^1H\}$ NMR (76 MHz, $CDCl_3$): δ 170.2, 145.4, 139.0, 132.3, 132.1, 129.9 (2C), 128.5 (2C), 128.4 (2C), 128.3 (2C), 127.3, 127.1, 126.9, 123.6, 52.5, 32.8. HRMS (ESI) m/z : $[M + H]^+$ calcd for $C_{19}H_{17}O_3$, 293.1179; found, 293.1175.

Ethyl 4-Methoxy-5,6-dihydrobenzo[6,7]isoindolo[2,1-a]quinoline-14-carboxylate (10a). Purified by silica gel column chromatography (eluent: petroleum ether/ethyl acetate = 40:1 to 20:1); brown liquid, 67% yield, 248.6 mg. 1H NMR (500 MHz, $CDCl_3$): δ 7.82 (d, J = 8.4 Hz, 1H), 7.77 (s, 1H), 7.70 (d, J = 7.9 Hz, 1H), 7.58–7.54 (m, 2H), 7.31 (t, J = 7.5 Hz, 1H), 7.17 (t, J = 8.0 Hz, 1H), 6.82 (d, J = 7.7 Hz, 1H), 6.76 (d, J = 8.1 Hz, 1H), 4.10 (q, J = 7.1 Hz, 2H), 3.89 (s, 3H), 3.00–2.98 (m, 2H), 2.84–2.81 (m, 2H), 0.85 (t, J = 7.1 Hz, 3H). $^{13}C\{^1H\}$ NMR (126 MHz, $CDCl_3$): δ 168.1, 156.5, 134.3, 134.1, 130.2, 129.9, 127.8, 125.9, 124.8, 124.3, 124.2, 123.7, 122.3, 122.2, 118.8, 116.2, 114.1, 108.7, 107.9, 61.8, 55.8, 21.9, 21.4, 13.4. HRMS (ESI) m/z : $[M + H]^+$ calcd for $C_{24}H_{22}NO_3$, 372.1601; found, 372.1602.

Methyl 3-Methoxy-5,6-dihydrobenzo[6,7]isoindolo[2,1-a]quinoline-14-carboxylate (10b). Purified by silica gel column chromatography (eluent: petroleum ether/ethyl acetate = 25:1 to 10:1); orange solid, 71% yield, 253.5 mg; mp 151–152 °C. 1H NMR (300 MHz, $CDCl_3$): δ 7.82–7.76 (m, 2H), 7.69 (d, J = 7.9 Hz, 1H), 7.58–7.50 (m, 2H), 7.32–7.27 (m, 1H), 7.03 (d, J = 8.4 Hz, 1H), 6.87–6.77 (m, 2H), 3.84 (s, 3H), 3.68 (s, 3H), 2.94–2.91 (m, 2H), 2.88–2.85 (m, 2H). $^{13}C\{^1H\}$ NMR (76 MHz, $CDCl_3$): δ 168.5, 157.4, 138.4, 134.4, 130.2, 129.8, 127.1, 126.4, 125.7, 124.1, 123.9, 123.6, 122.2, 121.3, 115.9, 114.0, 113.8, 111.3, 108.8, 55.4, 52.5, 31.4, 21.9. HRMS (ESI) m/z : $[M + H]^+$ calcd for $C_{23}H_{20}NO_3$, 358.1445; found, 358.1448.

Methyl 5-Methyl-5,6-dihydrobenzo[6,7]isoindolo[2,1-a]quinoline-14-carboxylate (10c). Purified by silica gel column chromatography (eluent: petroleum ether/ethyl acetate = 25:1 to 10:1); yellow liquid, 70% yield, 238.7 mg. 1H NMR (300 MHz, $CDCl_3$): δ 7.84–7.78 (m, 2H), 7.72–7.69 (m, 2H), 7.60–7.54 (m, 2H), 7.34–7.29 (m, 2H), 7.22–7.11 (m, 2H), 3.62 (s, 3H), 3.14–3.07 (m, 1H), 2.98 (dd, J = 14.9, 5.0 Hz, 1H), 2.68–2.61 (m, 1H), 1.00–0.96 (m, 3H). $^{13}C\{^1H\}$ NMR (76 MHz, $CDCl_3$): δ 168.5, 141.1, 134.3, 132.0, 131.1, 130.2, 129.9, 128.9, 126.4, 126.2, 125.8, 125.6, 125.5, 124.2, 124.1, 123.7, 122.2, 114.1, 109.4, 52.3, 34.5, 29.6, 19.5. HRMS (ESI) m/z : $[M + H]^+$ calcd for $C_{23}H_{20}NO_2$, 342.1496; found, 342.1497.

(10R,11R)-10-Hydroxy-3-methoxy-5,9,10,11-tetrahydro-6H-benzo[g]pyrrolo[2,1-a]isoindole-11-carboxylic Acid (14a). Purified by silica gel column chromatography (eluent: petroleum ether/ethyl acetate = 10:1 to 2:1); yellow liquid, 41% yield, 78.4 mg. 1H NMR (300 MHz, $CDCl_3$): δ 7.99 (d, J = 8.6 Hz, 1H), 6.84–6.80 (m, 2H), 6.68–6.67 (m, 1H), 4.17–4.07 (m, 2H), 3.85 (s, 3H), 3.82–3.80 (m, 2H), 3.67 (br s, 1H), 2.99–2.95 (m, 2H), 2.50–2.45 (m, 2H). $^{13}C\{^1H\}$ NMR (76 MHz, $CDCl_3$): δ 167.8, 157.5, 151.0, 138.5, 131.0 (2C), 128.9 (2C), 124.4, 114.8, 112.0, 65.7, 55.4, 53.6, 38.9, 32.1,

22.8. HRMS (ESI) m/z : $[M]^+$ calcd for $C_{17}H_{17}NO_4$, 299.1158; found, 299.1155.

(1R,2R)-2-Hydroxy-7-phenyl-2,3-dihydro-1H-pyrrolizine-1-carboxylic Acid (14b). Purified by silica gel column chromatography (eluent: petroleum ether/ethyl acetate = 10:1 to 2:1); brown liquid, 52% yield, 69.5 mg. 1H NMR (400 MHz, $CDCl_3$): δ 7.40–7.34 (m, 5H), 6.70 (d, J = 3.0 Hz, 1H), 6.39 (d, J = 3.0 Hz, 1H), 4.31 (t, J = 6.7 Hz, 2H), 4.09 (d, J = 6.8 Hz, 1H), 3.73–3.72 (m, 1H), 3.68 (br s, 1H). $^{13}C\{^1H\}$ NMR (101 MHz, $CDCl_3$): δ 167.9, 131.0, 128.9, 128.6 (2C), 128.5 (2C), 128.3, 126.2, 122.1, 109.8, 65.7, 56.7, 32.1. HRMS (ESI) m/z : $[M + H]^+$ calcd for $C_{14}H_{14}NO_3$, 244.0975; found, 244.0975.

■ ASSOCIATED CONTENT

Data Availability Statement

The data underlying this study are available in the published article and its Supporting Information.

Supporting Information

The Supporting Information is available free of charge at <https://pubs.acs.org/doi/10.1021/acs.joc.3c00109>.

General information, X-ray crystallographic data, outlook of our starting materials and synthesized derivatives, NMR and HRMS spectra of all compounds, 2D NMR spectra, report of chiral Pak column, explanation for the diastereomeric mixture of **3g** and **3h**, photo-physical data, and coordinates of the energy-minimized structure of the compounds (PDF)

Accession Codes

CCDC 2114554 contains the supplementary crystallographic data for this paper. These data can be obtained free of charge via www.ccdc.cam.ac.uk/data_request/cif, or by emailing data_request@ccdc.cam.ac.uk, or by contacting The Cambridge Crystallographic Data Centre, 12 Union Road, Cambridge CB2 1EZ, UK; fax: +44 1223 336033.

■ AUTHOR INFORMATION

Corresponding Authors

Amit Saha – Department of Chemistry, Jadavpur University, Kolkata 700032, India; Email: amit.saha@jadavpuruniversity.in

Shubhankar Samanta – Department of Chemistry, Bidhannagar College, Kolkata 700064, India; orcid.org/0000-0002-7173-8681; Phone: 919775550193; Email: chemshubha@gmail.com; Fax: (9133) 2337 4782

Authors

Anirban Bera – Department of Chemistry, Bidhannagar College, Kolkata 700064, India; Department of Chemistry, Jadavpur University, Kolkata 700032, India

Sk Abulkalam Azad – Department of Chemistry, Bidhannagar College, Kolkata 700064, India

Prasanta Patra – Jhargram Raj College, Jhargram, West Bengal 721507, India

Nayim Sepay – Department of Chemistry, Lady Brabourne College, Kolkata 700 017, India; orcid.org/0000-0001-7702-3989

Rathin Jana – Department of Chemistry, Shahid Matangini Hazra Govt. General Degree College for Women, Kulberia, West Bengal 721649, India

Tapas Das – Department of Chemistry, National Institute of Technology, Jamshedpur 831014, India; orcid.org/0000-0002-3194-0340

Complete contact information is available at:

<https://pubs.acs.org/10.1021/acs.joc.3c00109>

Notes

The authors declare no competing financial interest.

ACKNOWLEDGMENTS

We thank the Department of Science Technology and Biotechnology under the Government of West Bengal (398(Sanc.)/STBT-11012(25)/25/2021-ST SEC) and (368(Sanc.)/STBT-11012(25)/11/2020) and also thank the SERB TAR/2022/000070 and SRG/2020/000326 for financial support.

REFERENCES

- (1) (a) Sharma, P.; Gupta, R.; Bansal, R. K. Recent advances in organocatalytic asymmetric aza-Michael reactions of amines and amides. *Beilstein J. Org. Chem.* **2021**, *17*, 2585–2610. (b) Mandal, S.; Mandal, S.; Ghosh, S. K.; Ghosh, A.; Saha, R.; Banerjee, S.; Saha, B. Review of the aldol reaction. *Synth. Commun.* **2016**, *46*, 1327–1342. (c) Trost, B. M.; Brindle, C. S. The direct catalytic asymmetric aldol reaction. *Chem. Soc. Rev.* **2010**, *39*, 1600–1632. (d) Okino, T.; Hoashi, Y.; Takemoto, Y. Enantioselective Michael Reaction of Malonates to Nitroolefins Catalyzed by Bifunctional Organocatalysts. *J. Am. Chem. Soc.* **2003**, *125*, 12672–12673.
- (2) (a) Yamamoto, Y.; Momiyama, N.; Yamamoto, H. Enantioselective Tandem *o*-Nitroso Aldol/Michael Reaction. *J. Am. Chem. Soc.* **2004**, *126*, 5962–5963. (b) Wang, W.; Li, H.; Wang, J.; Zu, L. Enantioselective organocatalytic tandem Michael-Aldol reactions: one-pot synthesis of chiral thiochromenes. *J. Am. Chem. Soc.* **2006**, *128*, 10354–10355. (c) Halland, N.; Aburel, P. S.; Jørgensen, K. A. Highly Enantio- and Diastereoselective Organocatalytic Asymmetric Domino Michael–Aldol Reaction of β -Ketoesters and α,β -Unsaturated Ketones. *Angew. Chem., Int. Ed.* **2004**, *43*, 1272–1277.
- (3) (a) Yang, P.; Xu, W.; Wang, R.; Zhang, M.; Xie, C.; Zeng, X.; Wang, M. Potassium tert-Butoxide-Mediated Condensation Cascade Reaction: Transition Metal-Free Synthesis of Multisubstituted Aryl Indoles and Benzofurans. *Org. Lett.* **2019**, *21*, 3658–3662. (b) Satpathi, B.; Dutta, L.; Ramasastry, S. S. V. Metal- and Hydride-Free Pentannulative Reductive Aldol Reaction. *Org. Lett.* **2019**, *21*, 170–174. (c) Maezono, S. M. B.; Poudel, T. N.; Lee, Y. R. One-pot construction of sterically challenging and diverse poly-arylphenols via transition-metal-free benzannulation and their potent in vitro antioxidant activity. *Org. Biomol. Chem.* **2017**, *15*, 2052–2062.
- (4) (a) Gummidli, L.; Muddassar, A.; Sharma, G. V. M.; Muruges, V.; Suresh, S. Tandem aza-Michael addition–vinylogous aldol condensation: synthesis of N-bridged pyridine fused quinolones. *Org. Biomol. Chem.* **2022**, *20*, 773–777. (b) Obulesu, O.; Muruges, V.; Harish, B.; Suresh, S. Tandem Aza Michael Addition–Vinylogous Nitroaldol Condensation: Construction of Highly Substituted N-Fused 3-Nitropyrzoloopyridines. *J. Org. Chem.* **2018**, *83*, 6454–6465.
- (5) (a) Bourcet, E.; Bröhmer, M. C.; Nieger, M.; Brase, S. Synthetic studies towards marmycins A and B: development of the vinylogous aldol–aza-Michael domino reaction. *Org. Biomol. Chem.* **2011**, *9*, 3136. (b) Koshino, S.; Kwon, E.; Hayashi, Y. Total Synthesis of Estradiol Methyl Ether and Its Five-Pot Synthesis with an Organocatalyst. *Eur. J. Org. Chem.* **2018**, *2018*, 5629–5638.
- (6) (a) Baumann, M.; Baxendale, I. R. Batch and Flow Synthesis of Pyrrolo[1,2-*a*]quinolines via an Allene-Based Reaction Cascade. *J. Org. Chem.* **2015**, *80*, 10806–10816. (b) Lahm, G.; Stoye, A.; Opatz, T. A Five-Step Synthesis of (\pm)-Tylophorine via a Nitrile-Stabilized Ammonium Ylide. *J. Org. Chem.* **2012**, *77*, 6620–6623. (c) Wu, F. S.; Zhao, H. Y.; Xu, Y. L.; Hu, K.; Pan, Y. M.; Ma, X. L. Catalyst-Free Synthesis of Pyrrolo[1,2-*a*]quinolines via Dehydration/[3+2] Cycloaddition Directly from 2-Methylquinolines, Aldehydes, and Alkynoates. *J. Org. Chem.* **2017**, *82*, 4289–4296. (d) Mohan, C.; Krishna, R. B.; Sivanandan, S. T.; Ibnusaud, I. Cover Feature: Synthesis of Pyrrolo[2,1-*a*]isoquinoline Class of Natural Product Crispine A. *Eur. J. Org. Chem.* **2021**, *2021*, 4911–4926. (e) Cui, H.-L. Recent progress in the synthesis of pyrrolo[2,1-*a*]isoquinolines. *Org. Biomol. Chem.* **2022**, *20*, 2779–2801. (f) Aggarwal, T.; Kumar, S.; Dhaked, D. K.; Tiwari, R. K.; Bharatam, P. V.; Verma, A. K. Site-Selective Electrophilic Cyclization and Subsequent Ring-Opening: A Synthetic Route to Pyrrolo[1,2-*a*]quinolines and Indolizines. *J. Org. Chem.* **2012**, *77*, 8562–8573.
- (7) (a) Sarkar, S.; Bera, K.; Jalal, S.; Jana, U. Synthesis of Structurally Diverse Polyfunctional Pyrrolo[1,2-*a*]quinolines by Sequential Iron-Catalyzed Three-Component Coupling and Gold-Catalyzed Hydroarylation Reactions. *Eur. J. Org. Chem.* **2013**, *2013*, 6055–6061. (b) Tatu, M. L.; Georgescu, E.; Boscornea, C.; Popa, M. M.; Ungureanu, E. M. Synthesis and fluorescence of new 3-biphenylpyrrolo[1,2-*c*]pyrimidines. *Arabian J. Chem.* **2017**, *10*, 643–652. (c) Park, S.; Kwon, D. I.; Lee, J.; Kim, I. When Indolizine Meets Quinoline: Diversity-Oriented Synthesis of New Polyheterocycles and Their Optical Properties. *ACS Comb. Sci.* **2015**, *17*, 459–469. (d) Karpe, A.; Parab, A.; Ganesan, G.; Walke, P.; Chaskar, A. Highly conjugated carbazole and pyrrolo[1,2-*a*]quinoxaline based small molecules for fluorescent detection of nitro explosives. *J. Photochem. Photobiol., A* **2022**, *431*, 114004.
- (8) (a) Nath, S.; Pathak, S. K.; Pradhan, B.; Gupta, R. K.; Reddy, K. A.; Krishnamoorthy, G.; Achalkumar, A. S. A sensitive and selective sensor for picric acid detection with a fluorescence switching response. *New J. Chem.* **2018**, *42*, 5382–5394. (b) Mishra, A.; Dheepika, R.; Parvathy, P. A.; Imran, P. M.; Bhuvanesh, N. S. P.; Nagarajan, S. Fluorescence quenching based detection of nitroaromatics using luminescent triphenylamine carboxylic acids. *Sci. Rep.* **2021**, *11*, 19324. (c) Dai, H.; Deng, Z.; Zeng, Y.; Zhang, J.; Yang, Y.; Ma, Q.; Hu, W.; Guo, L.; Li, L.; Wan, S.; Liu, H. Highly sensitive determination of 4-nitrophenol with coumarin-based fluorescent molecularly imprinted poly (ionic liquid). *J. Hazard. Mater.* **2020**, *398*, 122854.
- (9) (a) Xu, Y. W.; Wang, J.; Wang, G.; Zhen, L. Diethyl Azodicarboxylate-Promoted Oxidative [3+2] Cycloaddition for the Synthesis of Pyrrolo[2,1-*a*]isoquinolines. *J. Org. Chem.* **2021**, *86*, 91–102. (b) Wu, F. S.; Zhao, H. Y.; Xu, Y. L.; Hu, K.; Pan, Y. M.; Ma, X. L. Catalyst-Free Synthesis of Pyrrolo[1,2-*a*]quinolines via Dehydration/[3+2] Cycloaddition Directly from 2-Methylquinolines, Aldehydes, and Alkynoates. *J. Org. Chem.* **2017**, *82*, 4289–4296. (c) Aggarwal, T.; Kumar, S.; Dhaked, D. K.; Tiwari, R. K.; Bharatam, P. V.; Verma, A. K. Site-Selective Electrophilic Cyclization and Subsequent Ring-Opening: A Synthetic Route to Pyrrolo[1,2-*a*]quinolines and Indolizines. *J. Org. Chem.* **2012**, *77*, 8562–8573.
- (10) (a) Chai, D. I.; Lautens, M. Tandem Pd-Catalyzed Double C–C Bond Formation: Effect of Water. *J. Org. Chem.* **2009**, *74*, 3054–3061. (b) Verma, A. K.; Shukla, S. P.; Singh, J.; Rustagi, V. Synthesis of 5-Iodopyrrolo[1,2-*a*]quinolines and Indolo[1,2-*a*]quinolines via Iodine-Mediated Electrophilic and Regioselective 6-endo-dig Ring Closure. *J. Org. Chem.* **2011**, *76*, 5670–5684. (c) Sansom, G. N.; Semken, J.; Kelso, M. J.; Richardson, C. A novel and unexpected one pot synthesis of pyrrolo[1,2-*a*]quinolines. *Tetrahedron Lett.* **2022**, *98*, 153794. (d) Nayak, M.; Kim, I. Construction of benzo-fused indolizines, pyrrolo[1,2-*a*]quinolines via alkyne–carbonyl metathesis. *Org. Biomol. Chem.* **2015**, *13*, 9697–9708. (e) Thanetchaiyakup, A.; Rattanarat, H.; Chuanopparat, N.; Ngermmeesri, P. One-pot synthesis of substituted indolo[1,2-*a*]quinolines under transition-metal-free conditions. *Tetrahedron Lett.* **2018**, *59*, 1014–1018.
- (11) (a) Luo, Z.; Han, X.; Liu, C.; Liu, Q.; Li, R.; Liu, P.; Xu, X. Catalyst-Free Synthesis of 1,4-Dihydroquinolines and Pyrrolo[1,2-*a*]quinolines via Intermolecular [4+2]/[3+2] Radical Cyclization of N-Methylanilines with Alkynoates. *Synthesis* **2020**, *52*, 1067–1075. (b) Zhang, Y.; Sun, Y.; Wei, Y.; Shi, M. Phosphine-Catalyzed Intermolecular Annulations of Fluorinated *ortho*-Aminophenones with Alkynones – The Switchable [4+2] or [4+2]/[3+2] Cycloaddition. *Adv. Synth. Catal.* **2019**, *361*, 2129–2135. (c) Arisawa, M.; Fujii, Y.; Kato, H.; Fukuda, H.; Matsumoto, T.; Ito, M.; Abe, H.; Ito, Y.; Shuto, S. One-Pot Ring-Closing Metathesis/1,3-Dipolar Cycloaddition through Assisted Tandem Ruthenium Catalysis: Synthesis of

a Dye with Isoindolo[2,1-a]quinoline Structure. *Angew. Chem.* **2013**, *125*, 1037–1041. (d) Joshi, D. R.; Kim, I. Michael-Aldol Double Elimination Cascade to Make Pyridines: Use of Chromone for the Synthesis of Indolizines. *J. Org. Chem.* **2021**, *86*, 10235–10248.

(12) (a) Jana, A.; Manna, S. K.; Mondal, S. K.; Mandal, A.; Manna, S. K.; Jana, A.; Senapati, B. K.; Jana, M.; Samanta, S. An efficient synthesis of pyrrole and fluorescent isoquinoline derivatives using $\text{NaN}_3/\text{NH}_4\text{Cl}$ promoted intramolecular aza-annulation. *Tetrahedron Lett.* **2016**, *57*, 3722–3726. (b) Mondal, S. K.; Mandal, A.; Manna, S. K.; Ali, S. A.; Hossain, M.; Venugopal, V.; Jana, A.; Samanta, S. Intramolecular macrolactonization, photophysical and biological studies of new class of polycyclic pyrrole derivatives. *Org. Biomol. Chem.* **2017**, *15*, 2411–2421. (c) Ray, J.; Yasmin, N. A New Facile Approach to Isoindole and Pyrrole Derivatives. *Synlett* **2010**, *2010*, 924–930. (d) Ali, S. A.; Mondal, S. K.; Das, T.; Manna, S. K.; Bera, A.; Dafadar, D.; Naskar, S.; Molla, M. R.; Samanta, S. One-pot tandem cyclisation to pyrrolo[1,2-a] [1,4]-benzodiazepines: a modified approach to the Pictet–Spengler reaction. *Org. Biomol. Chem.* **2019**, *17*, 4652–4662. (e) Bera, A.; Patra, P.; Azad, A.; Ali, S. A.; Manna, S. K.; Saha, A.; Samanta, S. Neat synthesis of isothiazole compounds, and studies on their synthetic applications and photophysical properties. *New J. Chem.* **2022**, *46*, 11685–11694. (f) Samanta, S.; Ali, S. A.; Bera, A.; Giri, S.; Samanta, K. Transition metal-free advanced synthetic approaches for isoindolinones and their fused analogues. *New J. Chem.* **2022**, *46*, 7780–7830. (g) Bera, A.; Ali, S. A.; Saha, A.; Samanta, S. Neat synthesis of *c*-fused pyrroles and its application to macrolactamization. *Synth. Commun.* **2021**, *51*, 2377–2386. (h) Ali, S. A.; Bera, A.; Manna, S. K.; Santra, S.; Molla, M. R.; Samanta, S. First Example of Copper(I) Catalyzed Decarboalkoxymethylation of Alkyl 2-[1-(Pyridin-2-yl)-1H-pyrrol-2-yl]acetates. *Eur. J. Org. Chem.* **2020**, *2020*, 2754–2760. (i) Bera, A.; Ali, S. A.; Manna, S. K.; Ikbal, M.; Misra, S.; Saha, A.; Samanta, S. A solvent- and catalyst-free tandem reaction: synthesis, and photophysical and biological applications of isoindoloquinazolinones. *New J. Chem.* **2020**, *44*, 4324–4331.

(13) (a) Fouad, M. A.; Ferretti, F.; Formenti, D.; Milani, F.; Ragaini, F. Synthesis of Indoles by Reductive Cyclization of Nitro Compounds Using Formate Esters as CO Surrogates. *Eur. J. Org. Chem.* **2021**, *2021*, 4876–4894. (b) Naeimi, H.; Alishahi, N. An efficient and one-pot reductive cyclization for synthesis of 2-substituted benzimidazoles from *o*-nitroaniline under microwave conditions. *J. Ind. Eng. Chem.* **2014**, *20*, 2543–2547. (c) Ferretti, F.; Ramadan, D. R.; Ragaini, F. Transition Metal Catalyzed Reductive Cyclization Reactions of Nitroarenes and Nitroalkenes. *ChemCatChem* **2019**, *11*, 4450–4488.

(14) (a) Rasheed, T.; Khan, M. N. I.; Zhadi, S. S. A.; Durrani, S. Hirsutine: A New Alkaloid from *Cocculus Hirsutus*. *J. Nat. Prod.* **1991**, *54*, 582–584. (b) Huang, Z.; Meng, Y.; Wu, Y.; Song, C.; Chang, J. Synthesis of isoindolo[1,2-a]isoquinoline and isoindolo[2,1-a]quinoline derivatives via trifluoroacetic acid-mediated cascade reactions. *Tetrahedron* **2021**, *93*, 132280–132289.

(15) (a) Wei, L.-L.; Hsung, R. P.; Sklenicka, H. M.; Gerasuto, A. I. A Novel and Highly Stereoselective Intramolecular Formal [3+3] Cycloaddition Reaction of Vinylogous Amides Tethered with α,β -Unsaturated Aldehydes: A Formal Total Synthesis of (+)-Gephyrotoxin. *Angew. Chem., Int. Ed.* **2001**, *40*, 1516–1518. (b) Santarem, M.; Vanucci-Bacqué, C.; Lhomme, G. Formal Total Synthesis of (+)-Gephyrotoxin. *J. Org. Chem.* **2008**, *73*, 6466–6469. (c) Ikeda, T.; Yaegashi, T.; Matsuzaki, T.; Hashimoto, S.; Sawada, S. Asymmetric synthesis of phenanthroindolizidine alkaloids with hydroxyl group at the C14 position and evaluation of their antitumor activities. *Bioorg. Med. Chem. Lett.* **2011**, *21*, 342–345. (d) Hazra, A.; Mondal, S.; Maity, A.; Naskar, S.; Saha, P.; Paira, R.; Sahu, K. B.; Paira, P.; Ghosh, S.; Sinha, C.; Samanta, A.; Banerjee, S.; Mondal, N. B. Amberlite-IRA-402 (OH) ion exchange resin mediated synthesis of indolizines, pyrrolo [1,2-a] quinolines and isoquinolines: Antibacterial and antifungal evaluation of the products. *Eur. J. Med. Chem.* **2011**, *46*, 2132–2140. (e) Leontie, L.; Druta, I.; Danac, R. G.; Rusu, G. On the electronic transport properties of pyrrolo[1,2-a] [1,10]phenanthroline derivatives in thin films. *Synth. Met.* **2005**, *155*, 138–145.

(16) Madrigal, D. A.; Escalante, C. H.; Gutiérrez-Rebolledo, G. A.; Cristobal-Luna, J. M.; Gómez-García, O.; Hernández-Benitez, R. I.; Esquivel-Campos, A. L.; Pérez-Gutiérrez, S.; Chamorro-Cevallos, G. A.; Delgado, F.; Tamariz, J. Synthesis and highly potent anti-inflammatory activity of licofelone- and ketorolac-based 1-arylpyrrolizin-3-ones. *Bioorg. Med. Chem.* **2019**, *27*, 115053.

(17) (a) Perez, G. V.; Perez, A. L. Organic Acids without a Carboxylic Acid Functional Group. *J. Chem. Educ.* **2000**, *77*, 910–915. (b) Nipper, M.; Carr, R. S.; Biedenbach, J. M.; Hooten, R. L.; Miller, K. Fate and effects of picric acid and 2,6-DNT in marine environments: Toxicity of degradation products. *Mar. Pollut. Bull.* **2005**, *50*, 1205–1217. (c) Beyer, C.; Bohme, U.; Pietzsch, C.; Roewer, G. Preparation, characterization and properties of dipolar 1,2-N, N-dimethylaminomethylferrocenylsilanes. *J. Organomet. Chem.* **2002**, *654*, 187–201.

(18) (a) Junqueira, J. R.; de Araujo, W. R.; Salles, M. O.; Paixão, T. R. Flow injection analysis of picric acid explosive using a copper electrode as electrochemical detector. *Talanta* **2013**, *104*, 162–168. (b) Shanmugaraju, S.; Mukherjee, P. S. Self-Assembled Discrete Molecules for Sensing Nitroaromatics. *Chem.—Eur. J.* **2015**, *21*, 6656–6666. (c) Jiang, Y.; Zhao, H.; Zhu, N.; Lin, Y.; Yu, P.; Mao, L. A Simple Assay for Direct Colorimetric Visualization of Trinitrotoluene at Picomolar Levels Using Gold Nanoparticles. *Angew. Chem., Int. Ed.* **2008**, *47*, 8601–8604. (d) Yang, Y.; Wang, H.; Su, K.; Long, Y.; Peng, Z.; Li, N.; Liu, F. A facile and sensitive fluorescent sensor using electrospun nanofibrous film for nitroaromatic explosive detection. *J. Mater. Chem.* **2011**, *21*, 11895–11900. (e) Bhalla, V.; Gupta, A.; Kumar, M.; Rao, D. S. S.; Prasad, S. K. Self-Assembled Pentacenequinone Derivative for Trace Detection of Picric Acid. *ACS Appl. Mater. Interfaces* **2013**, *5*, 672–679.

(19) Zheng, C.; Zhai, W.; Hong, J.; Zhang, X.; Zhu, Z.; Wang, L. Synthesis of two 6-aza-uridines modified by benzoheterocycle as environmentally sensitive fluorescent nucleosides. *Tetrahedron Lett.* **2017**, *58*, 3008–3013.

(20) Shanmugaraju, S.; Joshi, S. A.; Mukherjee, P. S. Fluorescence and visual sensing of nitroaromatic explosives using electron rich discrete fluorophores. *J. Mater. Chem.* **2011**, *21*, 9130.

Annexure III

*Copyright Permission from
Journals*

A solvent- and catalyst-free tandem reaction: synthesis, and photophysical and biological applications of isoindoloquinazolinones

A. Bera, S. A. Ali, S. K. Manna, M. Ikbal, S. Misra, A. Saha and S. Samanta, *New J. Chem.*, 2020, **44**, 4324 DOI: 10.1039/C9NJ05808G

To request permission to reproduce material from this article, please go to the [Copyright Clearance Center request page](#).

If you are **an author contributing to an RSC publication, you do not need to request permission** provided correct acknowledgement is given.

If you are **the author of this article, you do not need to request permission to reproduce figures and diagrams** provided correct acknowledgement is given. If you want to reproduce the whole article in a third-party publication (excluding your thesis/dissertation for which permission is not required) please go to the [Copyright Clearance Center request page](#).

Read more about [how to correctly acknowledge RSC content](#).



Home



Help ▾



Live Chat



ANIRBAN BERA ▾

Neat synthesis of c-fused pyrroles and its application to macrolactamization

Author: Anirban Bera, , Sk Asraf Ali, et al



Publication: Synthetic Communications

Publisher: Taylor & Francis

Date: Aug 3, 2021

Rights managed by Taylor & Francis

Thesis/Dissertation Reuse Request

Taylor & Francis is pleased to offer reuses of its content for a thesis or dissertation free of charge contingent on resubmission of permission request if work is published.

BACK

CLOSE

Neat synthesis of isothiazole compounds, and studies on their synthetic applications and photophysical properties

A. Bera, P. Patra, A. Azad, S. A. Ali, S. K. Manna, A. Saha and S. Samanta, *New J. Chem.*, 2022, **46**, 11685 DOI: 10.1039/D2NJ01962K

To request permission to reproduce material from this article, please go to the [Copyright Clearance Center request page](#).

If you are **an author contributing to an RSC publication**, you do not need to request permission provided correct acknowledgement is given.

If you are **the author of this article**, you do not need to request permission to reproduce figures and diagrams provided correct acknowledgement is given. If you want to reproduce the whole article in a third-party publication (excluding your thesis/dissertation for which permission is not required) please go to the [Copyright Clearance Center request page](#).

Read more about [how to correctly acknowledge RSC content](#).



Home



Help ▾



Live Chat



ANIRBAN BERA ▾



Synthesis of Multifused Pyrrolo[1,2-a]quinoline Systems by Tandem Aza-Michael-Aldol Reactions and Their Application to Molecular Sensing Studies

Author: Anirban Bera, Sk Abulkalam Azad, Prasanta Patra, et al

Publication: The Journal of Organic Chemistry

Publisher: American Chemical Society

Date: May 1, 2023

Copyright © 2023, American Chemical Society

PERMISSION/LICENSE IS GRANTED FOR YOUR ORDER AT NO CHARGE

This type of permission/license, instead of the standard Terms and Conditions, is sent to you because no fee is being charged for your order. Please note the following:

- Permission is granted for your request in both print and electronic formats, and translations.
- If figures and/or tables were requested, they may be adapted or used in part.
- Please print this page for your records and send a copy of it to your publisher/graduate school.
- Appropriate credit for the requested material should be given as follows: "Reprinted (adapted) with permission from {COMPLETE REFERENCE CITATION}. Copyright {YEAR} American Chemical Society." Insert appropriate information in place of the capitalized words.
- One-time permission is granted only for the use specified in your RightsLink request. No additional uses are granted (such as derivative works or other editions). For any uses, please submit a new request.

If credit is given to another source for the material you requested from RightsLink, permission must be obtained from that source.

[BACK](#)

[CLOSE WINDOW](#)

Recent development of solvent-free synthesis of heterocycles

N. Dey, A. Mandal, R. Jana, A. Bera, S. A. AZAD, S. Giri, M. Iqbal and S. Samanta, *New J. Chem.*, 2023, Accepted Manuscript , DOI: 10.1039/D3NJ01991H

To request permission to reproduce material from this article, please go to the [Copyright Clearance Center request page](#).

If you are **an author contributing to an RSC publication, you do not need to request permission** provided correct acknowledgement is given.

If you are **the author of this article, you do not need to request permission to reproduce figures and diagrams** provided correct acknowledgement is given. If you want to reproduce the whole article in a third-party publication (excluding your thesis/dissertation for which permission is not required) please go to the [Copyright Clearance Center request page](#).

Read more about [how to correctly acknowledge RSC content](#).

Annexure IV

*Presentation/Participation in
International/National Symposium/Conferences*

Presentation/Participation in International/National/Symposium/ Conferences:

- (1) **Oral presentation** entitled “*Green synthetic approach of isoindoloquinazolinones, studies on their photophysical, and biological applications*” in the celebration of the 99th Foundation Day Celebration of the Indian Chemical Society & International Research Scholars’ Meet held on May 09, 2022, was selected for the “**Indian Chemical Society Award of Excellence**”.



- (2) **Poster presentation** entitled “*Environmentally benign synthetic routes to fused heterocycles and their photophysical studies*” in the virtual “International Conference on Recent Trends in Green Chemistry (ICRTGC-2021)” organized jointly by the Department of Chemistry, Akal University, Punjab and Indian Chemical Society, Kolkata, during September 28th -30th, 2021.



- (3) **Poster presentation** entitled “Solvent and catalyst-free tandem reaction: synthesis, photophysical, and biological applications of isoindoloquinazolinones” and was selected as **best presentation** in the National Seminar on “Modern Trends in Chemistry for Sustainable Development” organized by the Department of Chemistry, Vijaygarh Jyotish Ray College, Kolkata, and the Indian Chemical Society, Kolkata, on March 03, 2020.

